- -

Anion-π Catalysis with Peptides and Synthesis of Thiol-Mediated Uptake Inhibitors

- -

Pham, Anh Tuan

UNIVERSITÉ DE GENÈVE   FACULTÉ DES SCIENCES

Section de chimie et biochimie

Département de chimie organique   Professeur Stefan Matile

Anion-π Catalysis with Peptides and Synthesis of Thiol-Mediated Uptake Inhibitors

THÈSE

présentée à la Faculté des sciences de l'Université de Genève
pour obtenir le grade de Docteur ès sciences, mention chimie

par

Anh Tuan PHAM

de

Ninh Binh (Vietnam)

Thèse N° 5593

GENÈVE

Atelier Repromail – Uni Mail

2021

**UNIVERSITÉ
DE GENÈVE**

FACULTÉ DES SCIENCES

DOCTORAT ÈS SCIENCES, MENTION CHIMIE

Thèse de Monsieur Anh Tuan PHAM

intitulée :

«Anion-π Catalysis with Peptides and Synthesis of Thiol-Mediated Uptake Inhibitors»

La Faculté des sciences, sur le préavis de Monsieur S. MATILE, professeur ordinaire et directeur de thèse (Département de chimie organique), Monsieur C. MAZET, professeur ordinaire (Département de chimie organique), Monsieur K. TIEFENBACHER, professeur (Department of chemistry, and Department of Biosystems Science and Engineering, University of Basel, Basel), autorise l'impression de la présente thèse, sans exprimer d'opinion sur les propositions qui y sont énoncées.

Genève, le 27 septembre 2021

Thèse - 5593 -

Le Doyen

Acknowledgements

List of Publications

(1)   Zhang, X.; Hao, X.; Liu, L.; **Pham, A.-T.**; López-Andarias, J.; Frontera, A.; Sakai, N.; Matile, S. Primary Anion-π Catalysis and Autocatalysis, *J. Am. Chem. Soc.* **2018**, *140*, 17867-17871.

(2)   **Pham, A.-T.**; Matile, S. Peptide Stapling with Anion-π Catalysts, *Chem. Asian J.* **2020**, *15*, 1562-1566.

(3)   Cheng, Y.; **Pham, A.-T.**; Kato, T.; Lim, B.; Moreau, D.; López-Andarias, J.; Zong, L.; Sakai, N.; Matile, S. Inhibitors of Thiol-Mediated Uptake *Chem. Sci.* **2021**, *12*, 626-631.

(4)   Laurent, Q.; Martinent, R.; Lim, B.; **Pham, A.-T.**; Kato, T.; López-Andarias, J.; Sakai, N.; Matile, S. Thiol-Mediated Uptake, *JACS Au* **2021**, *1*, 710–728.

(5)   Lim, B.; Cheng, Y.; Kato, T.; **Pham, A.-T.**; Du, E. L.; Mishra, A. K., Grinhagena, E.; Moreau, D.; Sakai, N.; Waser, J.; Matile, S. Irreversible Inhibition of Thiol-Mediated Uptake with Hypervalent Iodine Reagent, *Helv. Chim. Acta* **2021**, *104*, e2100085.

Summary

Despite being the youngest in the noncovalent interaction family, anion-π interaction has found its applications in the last decade. From the early applications in anion recognition and transport, anion-π interaction has found its way to potential utilization in self-assembly and catalysis. Together with other older interactions such as π-π stacking and cation-π interaction, anion-π interaction somewhat completed the picture of organocatalysis based on aromatic scaffolds. The new concept of catalysis - anion-π catalysis has been employed successfully in many chemical transformations.

As anion-π catalysis is developing, the need of having new efficient catalytic systems is urgent. Finding the correlation between catalyst structures and their activities is very important for rational design of advanced catalytic systems. In the first topic of this thesis, peptide secondary structure was explored to produce novel anion-π catalysts with defined conformations. Naphthalenediimides (NDIs) – highly electron-deficient aromatic surfaces were chosen as the central platform to build the new catalysts. They provide not only anion-π interactions for catalysis, but also act as covalent linkers to stabilize one turn of an α-helix. The rigid peptide skeleton allows fine control of the positions of each amino acid residue above the NDI surface. Introducing a tertiary amine to amino acid side chain triggers the formation of anionic reactive intermediate close to the π-acidic surface of catalyst **S1**, thus, enable anion-π catalysis (Figure S1b).
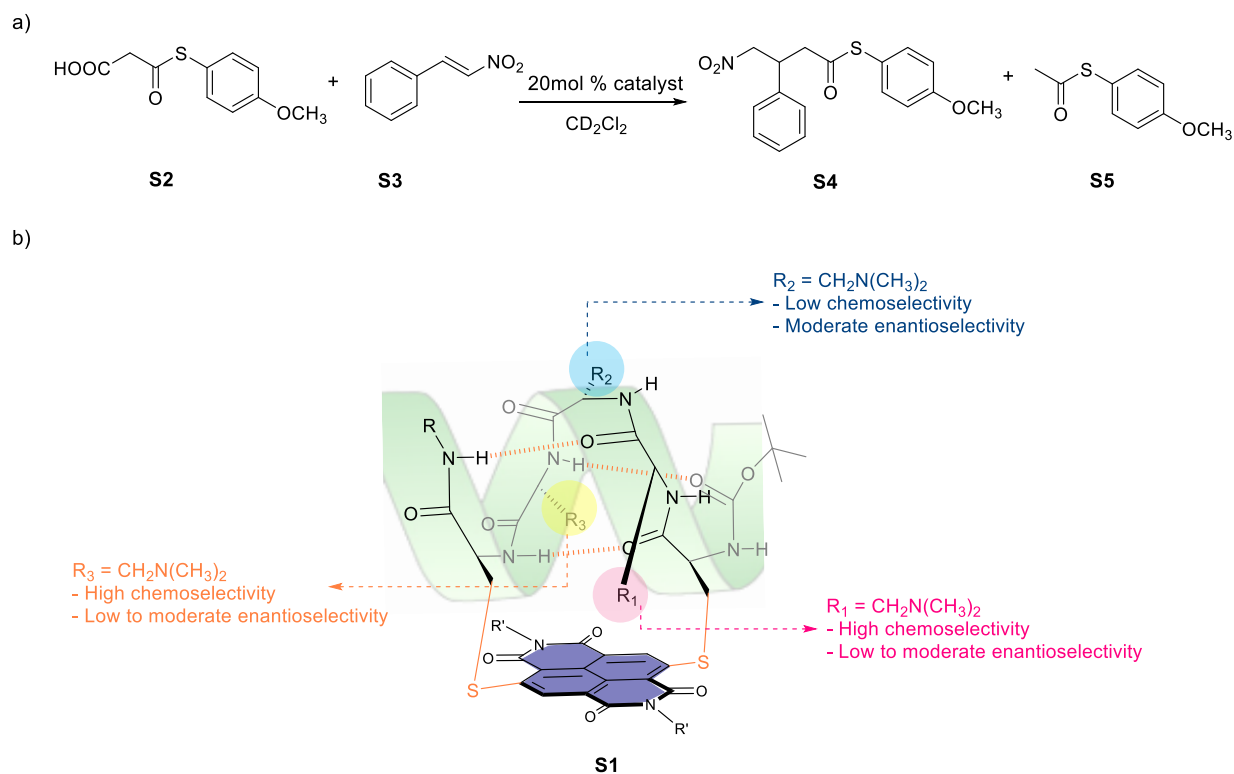
Figure S1. (a) MAHT reaction between substrates **S2** and **S3** that results addition product **S4** and decarboxylation product **S5**. (b) General structure of novel anion-π catalysts **S1** with their peptide backbone in the formal α-helix conformation. Dashed arrows show catalytic activities observed when the tertiary amine was placed in the side chain of different amino acid residues.

By moving the tertiary amine along the peptide chain, the catalytic activity of catalysts could be modulated in a predictable manner. The catalytic activity was evaluated using the addition of a malonic acid half thioester **S2** to a nitro olefin **S3** (MAHT reaction) (Figure S1a). Different chemoselectivity observed with different catalysts could be rationalized by the helix-like conformation of the peptide backbone above NDI surface. When the tertiary amine was put at the optimal position for anion-π catalysis, excellent selectivity for the formation of addition product **S4** was found. The decrease in selectivity between **S4** and **S5** when the peptides were modified to disrupt helix turn confirmed the importance of secondary structure

to the performance of catalysts. Elongation of peptide turn to a short α-helix, on the other hand, greatly enhanced chemoselectivity due to improving structure organization.

Encouraged by these results, the scope of electron-poor aromatic surface was extended to perylenediimides (PDIs). The larger PDI surface enables anion-π catalysis for the tertiary amine in the position which was inactive with NDIs. The secondary structure of catalysts has been studied using 2D NMR spectroscopy, which indicated a helix-like conformation for the peptide backbone. The contribution of twisted PDI surface to enantioselectivity has also been considered. The peptide backbones were effective in blocking the twisting motion of PDI core. Thus, two atropo-diastereomers of PDI catalysts could be separated. Overall performance of PDI catalysts was significantly improved in comparison with the NDI analogs.

In the second topic of this thesis, the application of peptide secondary structures was examined in a more biorelevant process – thiol-mediated uptake. Highly reactive macrocyclic disulfide bridged γ-turn peptides were synthesized as potential thiol-mediated uptake inhibitors. Even though thiol-mediated uptake has been proven to be an excellent tool to transport impermeable molecules across the cellular membrane, its mechanism has not been fully understood. The lack of reliable inhibitors hinders the contribution of thiol-mediated uptake in a lot of biological events. With the intention to identify more efficient inhibitors, a large library of thiol-reactive reagents has been synthesized. Encouraging results from disulfide bridged γ-turn peptides **S6** called for the extension of the library to other reactive cyclic disulfides such as ETP **S7** (Figure S2). Different oxidation levels of disulfide bonds were addressed with thiosulfinates **S8** and thiosulfonates **S9** inhibitors. As one of the most potent families among synthesized inhibitors, cyclic thiosulfonate scaffolds have been extensively modified to access better reactivity. Their potential application as a thiol-mediated uptake

transporter was also considered with the synthesis of fluorescently-labelled thiosulfonate probe for future uptake experiments in cells. Except for reversible thiol-mediated uptake inhibitors, excellent reactivities of irreversible thiol-reactive reagents were also taken into account. Heteroaromatic sulfones like 2-(methylsulfonyl)benzooxazole **S10** and Michael acceptor **S11** efficiently inhibited thiol-mediated uptake.
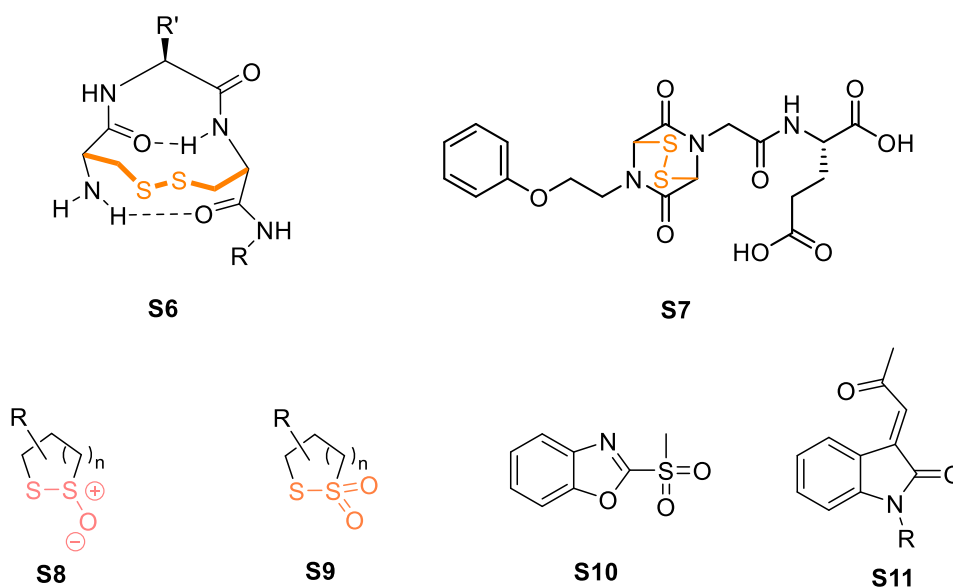
Figure S2. Structure of the most active thiol-mediated uptake inhibitors.

Résumé

Bien qu'elle soit la plus jeune de la famille des interactions non covalentes, l'interaction anion-π a trouvé ses applications au cours de la dernière décennie. Depuis les premières applications dans la reconnaissance et le transport des anions, l'interaction anion-π a trouvé son chemin vers des utilisations potentielles dans l'auto-assemblage et la catalyse. Avec d'autres interactions plus anciennes telles que l'empilement π-π et l'interaction cation-π, l'interaction anion-π a quelque peu complété le tableau de l'organocatalyse basée sur des superpositions aromatiques. Le nouveau concept de catalyse - la catalyse anion-π a été utilisé avec succès dans de nombreuses transformations chimiques.

Alors que la catalyse anion-π se développe, les besoins de disposer de nouveaux systèmes catalytiques efficaces sont urgents. Trouver la corrélation entre les structures catalytiques et leurs activités est très important pour la conception rationnelle de systèmes catalytiques avancés. Dans le premier sujet de cette thèse, la structure secondaire des peptides a été explorée pour produire de nouveaux catalyseurs anion-π avec des conformations définies. Naphtalènediimides (NDIs) – des surfaces aromatiques fortement déficientes en électrons ont été choisies comme plate-forme principale pour construire les nouveaux catalyseurs. Ils fournissent non seulement des interactions anion-π pour la catalyse, mais agissent également en tant que lieurs covalents pour stabiliser un tour d'une hélice. Le squelette peptidique rigide permet un contrôle fin des positions de chaque résidu d'acide aminé au-dessus de la surface NDI. L'introduction d'une amine tertiaire à la chaîne latérale d'acides aminés déclenche la formation d'un intermédiaire réactif anionique à proximité de la surface π-acide du catalyseur **S1**, ainsi, permet la catalyse anion-π (Figure S1b).
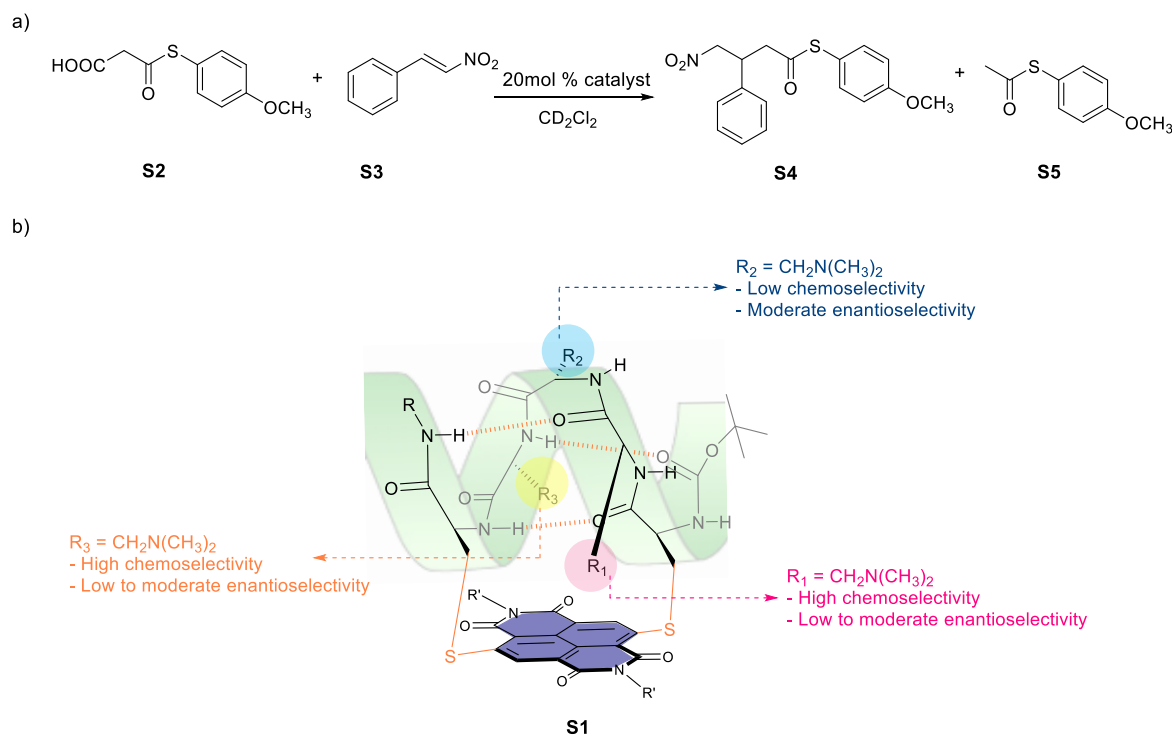
Figure S1. (a) Réaction MAHT entre les substrats **S2** et **S3** qui entraîne l'addition du produit **S4** et du produit de décarboxylation **S5**. (b) Structure générale des nouveaux catalyseurs anion-π **S1** avec leur squelette peptidique dans la conformation formelle de α-hélice. Les flèches en pointillés montrent les activités catalytiques observées lorsque l'amine tertiaire a été placée dans la chaîne latérale de différents résidus d'acides aminés.

En déplaçant l'amine tertiaire le long de la chaîne peptidique, l'activité catalytique des catalyseurs pourrait être modulée de manière prévisible. L'activité catalytique a été évaluée en utilisant l'ajout d'un demi-thioester d'acide malonique **S2** à une nitro-oléfine **S3** (réaction MAHT) (Figure S1a). La chimiosélectivité différente observée avec différents catalyseurs pourrait être rationalisée par la conformation en hélice du squelette peptidique au-dessus de la surface NDI. Lorsque l'amine tertiaire a été placée à la position optimale pour la catalyse anion-π, une excellente sélectivité pour la formation du produit d'addition **S4** a été trouvée. La

diminution de la sélectivité entre **S4** et **S5** lorsque les peptides ont été modifiés pour perturber le tour d'hélice a confirmé l'importance de la structure secondaire pour les performances des catalyseurs. L'allongement du peptide se transforme en une courte hélice, d'autre part, une chimiosélectivité grandement améliorée en raison de l'amélioration de l'organisation de la structure.

Fort de ces résultats, le domaine de la surface aromatique pauvre en électrons a été étendu aux pérylènediimides (PDIs). La plus grande surface PDI permet la catalyse anion-π pour l'amine tertiaire dans la position qui était inactive avec les NDI. La structure secondaire des catalyseurs a fait l'objet d'études utilisant la spectroscopie RMN 2D qui a indiqué une conformation en hélice pour le squelette peptidique. La contribution de la surface PDI torsadée à l'énantiosélectivité a également été considérée. Les squelettes peptidiques étaient efficaces pour bloquer le mouvement de torsion du noyau PDI. Ainsi, deux atropo-diastéréomères de catalyseurs PDI ont pu être séparés. Les performances globales des catalyseurs PDI ont été significativement améliorées par rapport aux analogs NDI.

Dans le deuxième sujet de cette thèse, l'application des structures secondaires peptidiques a été examinée dans un processus plus bio-pertinent – thiol-mediated uptake. Des peptides à γ-tour pontés par disulfure macrocyclique hautement réactifs ont été synthétisés en tant qu'inhibiteurs potentiels de l'absorption médiée par les thiols. Même si thiol-mediated uptake s'est avérée être un excellent outil pour transporter des molécules imperméables à travers la membrane cellulaire, son mécanisme n'a pas été entièrement compris. Le manque d'inhibiteurs fiables entrave la contribution de l'absorption médiée par les thiols dans de nombreux événements biologiques. Dans le but d'identifier des inhibiteurs plus efficaces, une grande bibliothèque de réactifs réactifs aux thiols a été synthétisée. Les résultats encourageants des

peptides à γ-tour pontés par disulfure **S6** ont nécessité l'extension de la bibliothèque à d'autres disulfures cycliques réactifs tels que l'ETP **S7** (Figure S2). Différents niveaux d'oxydation de la liaison disulfure ont été traités avec des inhibiteurs de thiosulfinates **S8** et de thiosulfonates **S9**. En tant que l'une des familles les plus puissantes parmi les inhibiteurs synthétisés, les échafaudages de thiosulfonate cycliques ont été largement modifiés pour accéder à une meilleure réactivité. Leur application potentielle en tant que transporteur thiol-mediated uptake a également été envisagée avec la synthèse d'une sonde thiosulfonate marquée par fluorescence pour de futures expériences d'absorption dans les cellules. À l'exception des inhibiteurs d'absorption réversibles médiés par les thiols, d'excellentes réactivités des réactifs irréversibles réactifs aux thiols ont également été prises en compte. Les sulfones hétéroaromatiques comme le 2-(méthylsulfonyl)benzooxazole **S10** et l'accepteur de Michael **S11** ont inhibé efficacement l'absorption médiée par les thiols.
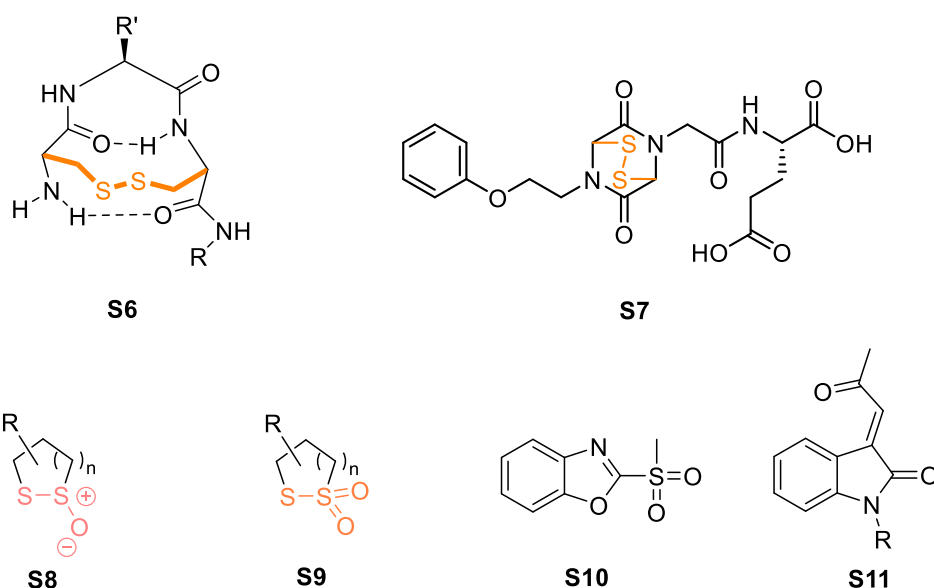
Figure S2. Structure des inhibiteurs thiol-mediated uptake les plus actifs.

Contents

CHAPTER 1:

INTRODUCTION

Noncovalent interactions are essential in all biological systems. While a typical covalent bond is on the order of 400 kJmol^{-1} – 800 kJmol^{-1}, most noncovalent interactions lie in the range of 10 kJmol^{-1} – 80 kJmol^{-1}.[1] The weak nature of noncovalent interactions in comparison with covalent bonds allows them to be switched on or off with energies that are relatively low. This means that processes base on noncovalent interactions could be easily modulated at life temperatures.[2] Therefore, nature has chosen noncovalent interactions to control the dynamic character of living systems. For example, noncovalent interactions involve in molecular recognition and catalytic activity of enzymes. Also, the directionality and specificity of noncovalent interactions make them responsible for determining the shapes of macromolecules like proteins, DNA or RNA.[1–5] These weak interactions could be illustrated as small muscles that hold the covalent skeleton together so that the functions of the whole body could be maintained.

1.1. Anion-π Interactions

1.1.1. The Origins of Anion-π Interactions

The history of anion-π interactions could be dated back to 1980s when one of the first evidence was reported by Hiraoka *et al.*[6,7] The gas-phase clustering reactions of electron-poor C_6F_6 with halide anions were investigated by the pulsed electron-beam high-pressure mass spectrometer and computational calculations. This study showed the noncovalent nature of the interactions observed in C_6F_6 – halide complexes, which were characterized by geometry of these complexes and the location of halide anions above the center of C_6F_6 moiety. In the 90s, Schneider *et al.* found attractive interactions between negative charges and polarizable aryl moieties.[8] However, not until 2002, the question ''Anion–π interactions. Do they exist?'' was first addressed by Deyà *et al.*[9] Looking at the Cambridge Structural Database allowed the authors to find π interactions between anions and pentafluorobenzene derivatives. Computational calculations were also performed to analyze the physical nature of the anion-π interactions. Three terms were found to contribute to the interaction energy, included electrostatic, dispersion-repulsion and polarization.[9] In the same year, theoretical studies from Mascal and Alkorta came up with the same conclusion about the existence of interactions between anions and π-acidic rings.[10,11] At the first glance these findings were controversial because the electron clouds of aromatic systems tend to attract cations rather anions.[12] A debate concerned the existence of anion-π interactions was published by Hay *et al.*[13] When they applied their criteria for searching in Cambridge Structural Database, no clear example of anion-π interactions could be found. Nonetheless, with more and more experimental evidence and functional systems based on anion-π interactions being discovered recently, this noncovalent interaction is now well accepted.[7,12,14–17] To date, anion-π interactions could be defined as the interaction between an electron-deficient π system and an anionic moiety.[14]

Crystallographic and computational evidence suggested that the physical nature of anion-π interactions is similar to its complementary counterpart – cation-π interactions. Electrostatic

forces and ion-induced polarization contribute mainly to the interactions between anions and π-systems.[18–23] The electrostatic term could be explained by the quadrupole moment of the arene Q_{zz}, which is the charge distribution of the aromatic system perpendicular to the plane.[7,16] In benzene **1**, negative Q_{zz} (–8.5 B) causes repulsion between aromatic surface and anion. However, attractive interactions with anions could be achieved by putting electro-withdrawing groups to the benzene core in order to invert Q_{zz} (Q_{zz} = +9.5 B for C_6F_6 **2**, Figure 1a). When an anion approaches the π system, it induces a dipole in the system, which enhances the interactions in return (Figure 1b). Thus, for molecules with high polarizability, the contribution of ion-induced polarization to the total interaction energy is significant.[7]
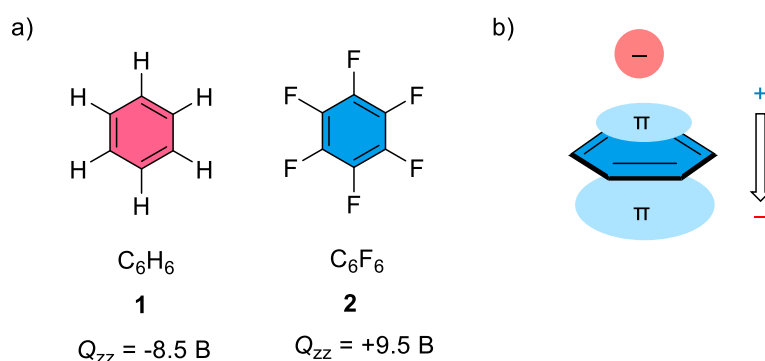
Figure 1. (a) Quadrupole moments of benzene **1** and hexafluorobenzene **2**. (b) Schematic representation of the ion-induced dipole. Adapted from reference.[16]

Using anion photoelectron spectroscopy and high-level electronic structure theory, Verlet *et al.* confirmed the nature of anion-π interactions.[24] The bond has an approximately 40% correlation interaction contribution. The electrostatic term provides about 20% to the strength of the interactions. The rest comes from polarization. The dissociation energy measured for $I^-.C_6F_6$ complex is 51 kJmol^{-1}, which is comparable with other noncovalent interactions.

1.1.2.   Applications

Following the pioneer works which proved the existence of anion-π interaction as well as described its nature, in the last decades, more efforts could be seen in finding potential applications for this young, underappreciated noncovalent interaction. Plenty of sophisticated supramolecular systems have been designed for anion recognition, sensing and transport. Anion-π interactions have also been shown to be powerful in catalysis and self-assembly of supramolecular structures.

1.1.2.1.   Anion Recognition, Sensing and Transport

The first example of anion channel exploited the advantages of anion-π interactions was reported in 2006.[25] Being highly electron-deficient with a global quadrupole moment Q_{zz} = +19.4 B, NDI appeared as an ideal module for constructing anion channels. Upon insertion into lipid bilayer membrane, oligo-NDI rods **3**-**5** formed bundles of anion-π slides with a rare halide VI selectivity in transport experiments (Figure 2). Strong anomalous mole fraction effect supported the presence of multiple binding sites in the supramolecular structure.[25]
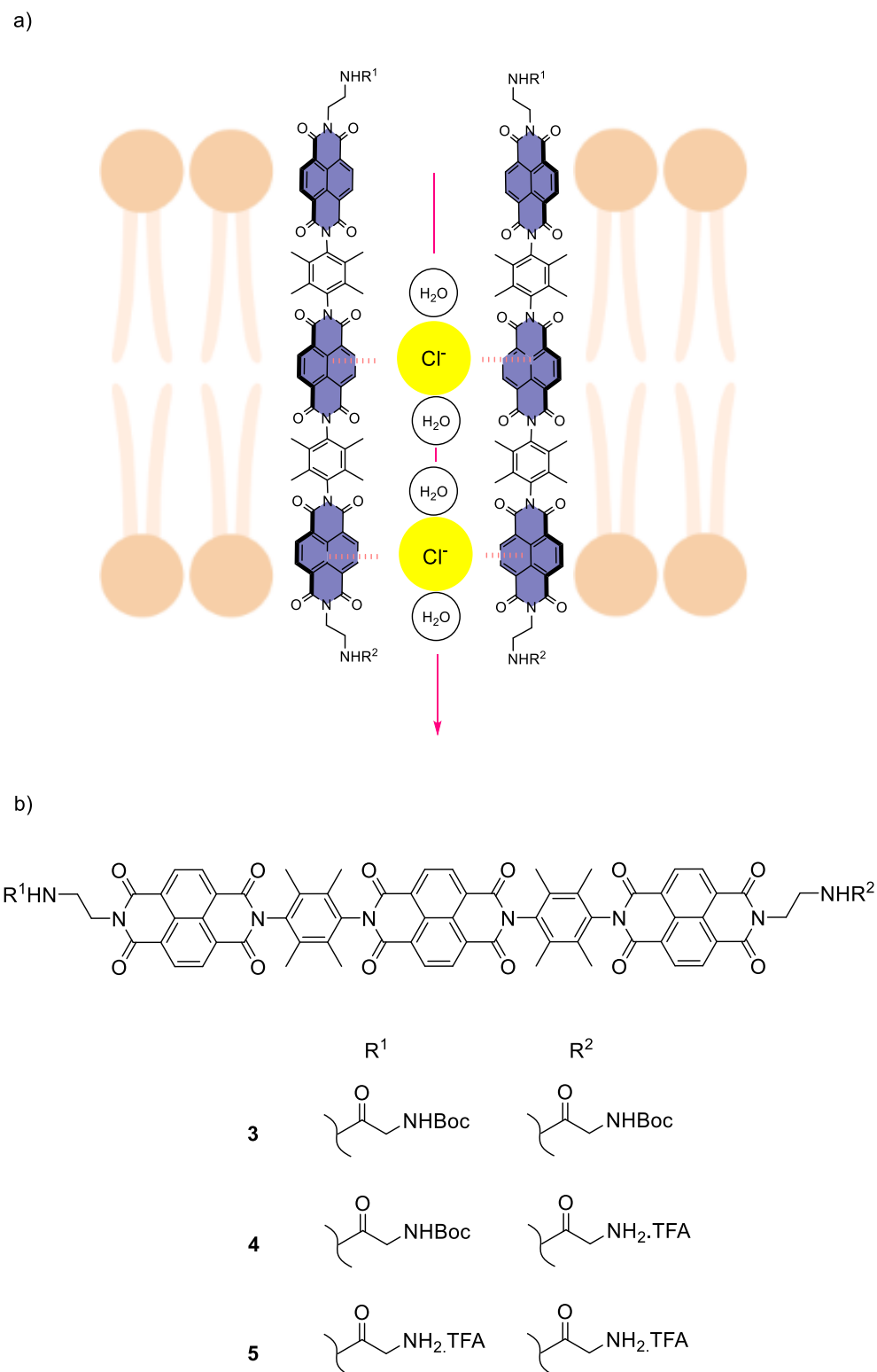
Figure 2. (a) Representative mode of action of anion-π slides in lipid bilayers. (b) Structure of anion-π slides **3-5**. Adapted from reference.[25]

Replacing NDI with a larger aromatic surface like PDI was able to combine ion-channel and photosynthetic activity for anion-π slides.[26] PDI rods such as **6** operated by active electron influx and passive anion efflux (Figure 3). This electron–anion antiport mechanism of action yielded significant photosynthetic activity for designed systems.

Figure 3. Anion transport and photo-synthetic activity of PDI rods. Adapted from reference.[26]

Based on electron-deficient triazines, Wang *et al.* designed tetraoxacalix[2]arene[2]triazine host molecules **7-9**, which could recognize halides and other polyatomic anions in both solution and in the solid state (Figure 4a).[27,28] The V-shaped π-deficient cleft created by the two triazine rings allowed the macrocycle to bind different anions in 1:1 stoichiometry through multiple noncovalent interactions, included anion-π, lone pair-π interactions and hydrogen bonding. Moreover, this binding pocket could adapt to different cavity size while complexing with different guests. The self-tuning ability of the macrocycles provided better interactions between host and guest in the complexes. The substitution effect at the triazine rings was also examined. The trend followed the expected behavior for anion-π interactions with electron-withdrawing groups improved the complexations and *vice versa*.
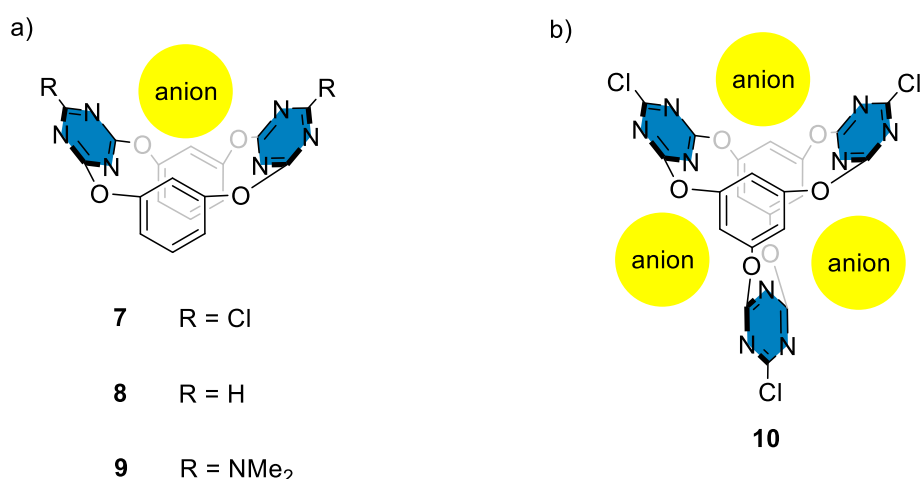
Figure 4. (a) V-shaped tetraoxacalix[2]arene[2]triazine host molecules **7-9**. (b) bis(tetraoxacalix[2]arene[2]triazine) cage **10** as multidentate anion binder. Adapted from reference.[27–29]

Multiple anion-π interactions could be accessed with tridentate anion binder **10** (Figure 4b).[29] Having three electron-deficient V-shaped binding pockets, conformationally rigid cage

10 formed various anion-π complexes with halides in both solution and in solid state. The interactions were directed by anion-π interactions together with other noncovalent bonds like hydrogen bonding, halogen bonding and lone pair-π interactions. The application of these anion binders could be extended to transport. Fine-tuning of lipophilicity of V-shaped tetraoxacalix[2]arene[2]triazines allowed them to pass through lipid bilayer membranes and act as ion carriers (Figure 5).[30,31]

a)

b)

R

11 Me

12 OMe

13 CF$_3$
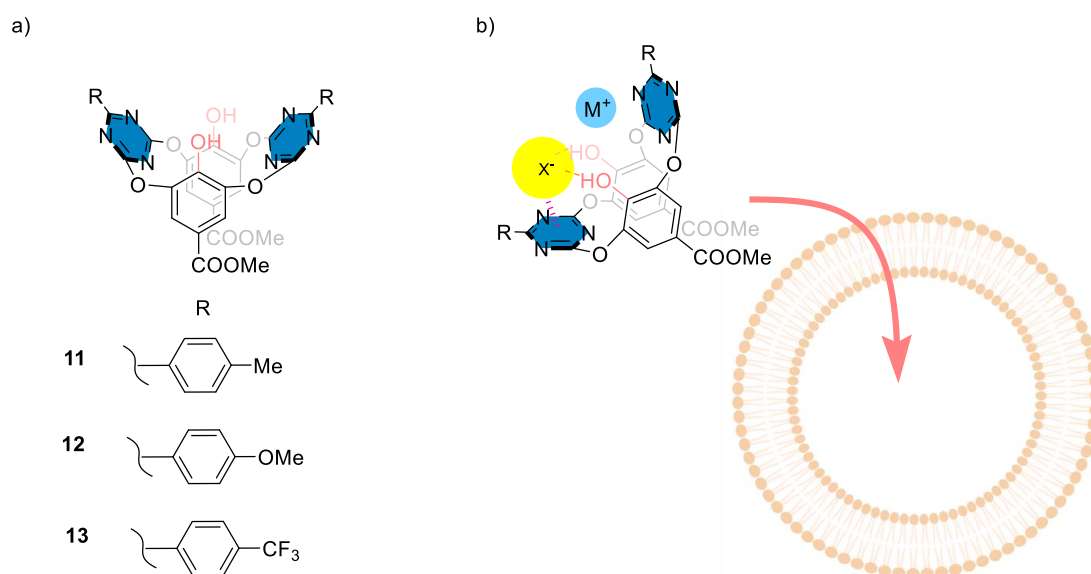
Figure 5. (a) Structures of tetraoxacalix[2]arene[2]triazine ion carriers **11**-**13**. (b) Ion-pair transport model of ion carriers **11**-**13**. Adapted from reference.[30,31]

Hydroxy groups attached to the benzene rings of transporter **11**-**13** are important to enable cooperative hydrogen bonding and anion-π interactions with halide and improve overall transport activity. Hydrophobic substituents in triazine rings increase partition of the probes into lipid bilayer. Besides, these substituents change the electron density of the heteroaromatic rings, thus, alter anion-π interactions. With electron-withdrawing substituents, **13** shows the

highest transport activity corresponds with strongest anion-π interactions. Electron-donating substituents in **12** reduces its activity to lower than **11** with weaker electron-donating groups. Mechanistic studies reveal that the ion transporters operate as X^-/M^+ ion-pair carriers (Figure 5b). Introducing substituents containing halogen-bonding sites to triazine rings adds another type of noncovalent interactions to facilitate halide transport.[31] Combination of multiple weak interactions results transporters with effective concentrations fall in the range of μM. These molecules also have good anticancer activity.

Based on calixarene scaffold, molecular hourglass **14** was designed to mimic structure and functions of chloride channels (Figure 6).[32] High chloride selectivity was accomplished by a size-exclusion mechanism. With a defined size and shape, the calixarene core of **14** excludes larger anions during transport process. The V-shaped of the core calixarene in combination with proper length of the arms allows the probe to partition to the lipid bilayers and form a channel-like structure. Moreover, the rigid electron-poor imide motif presented on the arms maintains the shape of the channel and assists the transport via anion-π interactions.
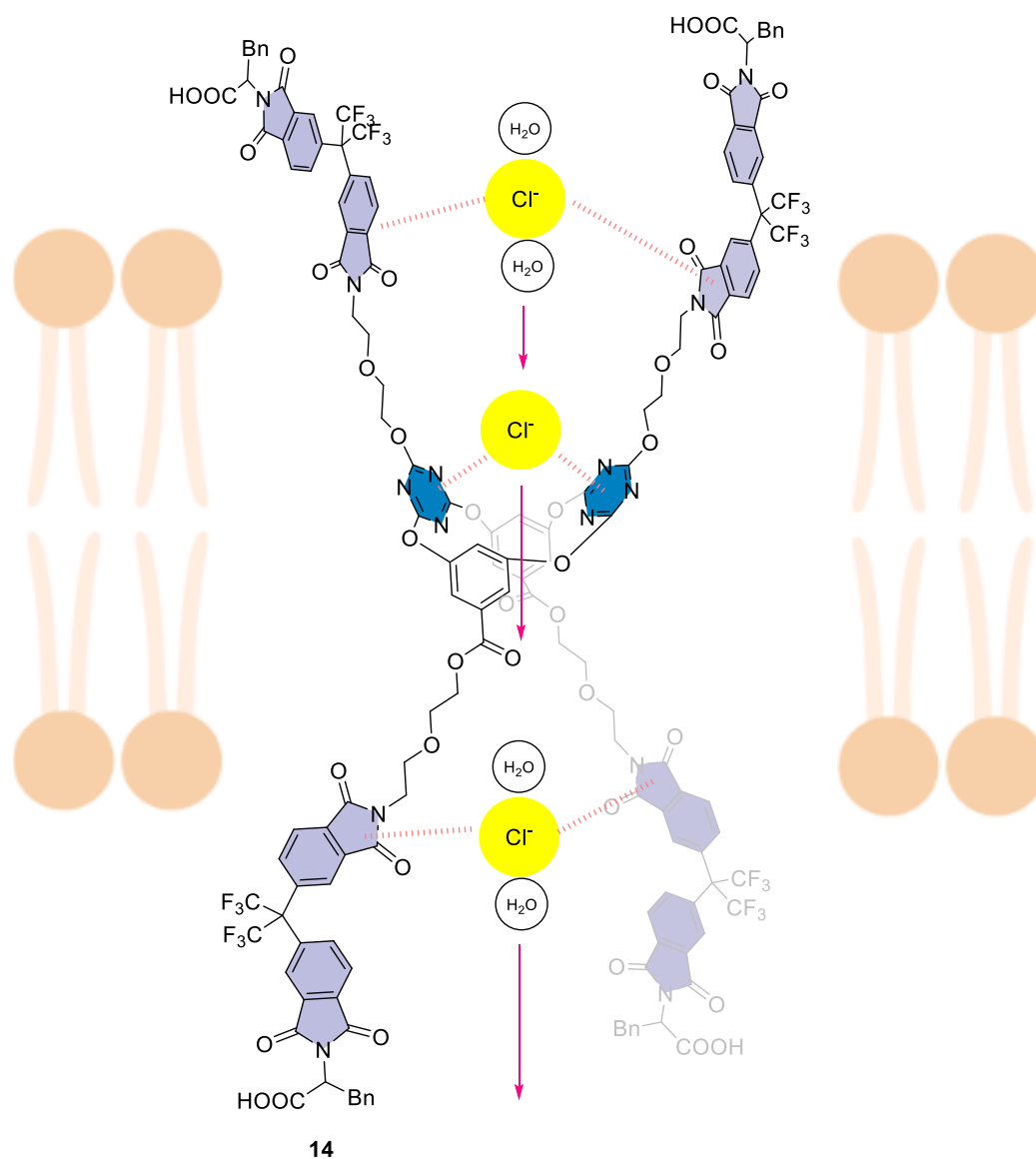
Figure 6. Molecular hourglass **14** forms chloride channel in lipid bilayers. Adapted from reference.[32]

Stoddard *et al.* used enantiopure *trans*-1,2-cyclohexanediamine as linkers to connect three NDI units in order to construct NDI prism **15** (Figure 7a).[33] Geometry of the linker renders a macrocycle with efficient orbital overlap between NDI units, thus, creates an electron-deficient cavity, which is suitable for exploring anion-π interactions. Molecular prism **15** was able to encapsulate linear I_3^- anion. Interestingly, the binding triggered π-π stacking of the

prisms in solid state to form one-handed supramolecular helices (Figure 7b). This anion-induced self-assembly could be of interest for developing new type of materials, ion channels, etc.

a)   b)
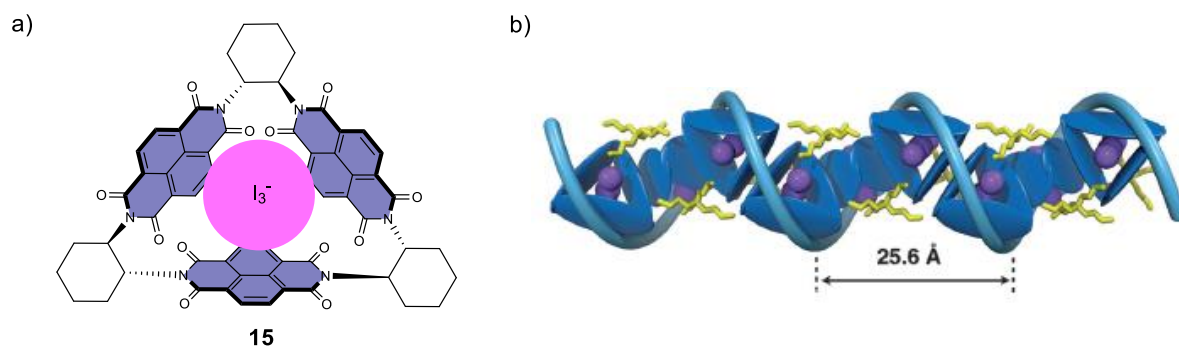
Figure 7. (a) Structure of molecular prism **15** and I_3^- anion in its cavity. (b) Graphical representations of the right-handed, π-stacked supramolecular *(P)*-helices present in the solid state of (-)-**15**. Adapted from reference.[33]

1.1.2.2. Self-Assembly

One of the first examples of applying anion-π interactions in supramolecular self-assembly was reported by Kochi *et al.*[34] While co-crystalizing various anions with π-acidic compounds such as **16**-**19**, they noticed the formation of linear 1D molecular chains (Figure 8). The 1D wires were constructed from repeated anion/π-acid units. This behavior was surprising since simple ionic salts usually do not form cocrystals with uncharged organic compounds. The observation of charge transfer suggested that anion-π interactions were the driving forces to generate these supramolecular structures. Larger π systems such as $HAT(CN)_6$ (1,4,5,8,9,12-hexaazatriphenylene-hexacarbonitrile) could bind several anions to form supramolecular columns in the similar manner.[35]
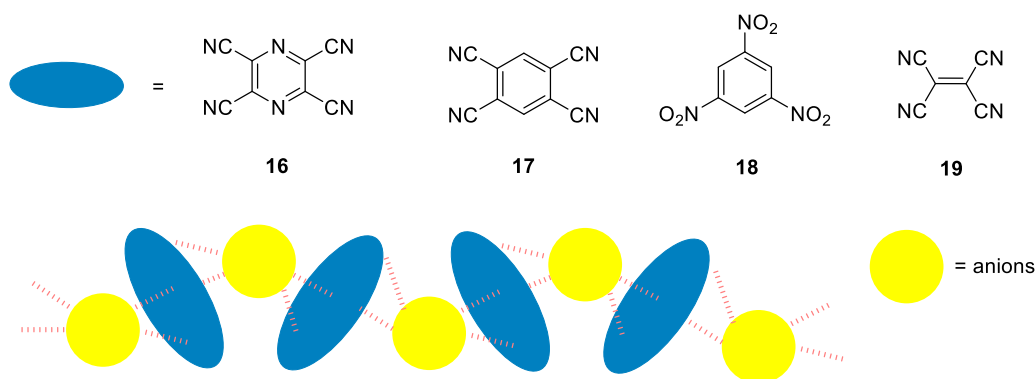
Figure 8. Representation of the 1D π-stacking of anion/π-acid cocrystals. Adapted from reference.[34]

To target amphiphilic macrocyclic molecules, Wang *et al.* introduced long alkyl chains to calixarene structure (Figure 9).[36] As expected, macrocycles **20** formed bilayer vesicles in aqueous media with narrow size distribution. Crystal structures and changes in activities upon modifications at the tail of these molecules suggested the important role of amide groups in vesicle formation. The intermolecular hydrogen-bond network between amide groups and water bridges together with hydrophobic effect of the alkyl chains provided necessary forces for self-assembly. Surprisingly, upon addition of various anions into the media, the size of formed vesicles increased. The effect of anions on the size of vesicles was in good agreement with the order of binding constants between anions and the host. In this case, regulation of anion-π interactions allowed to control self-assembly of amphiphilic calixarenes.
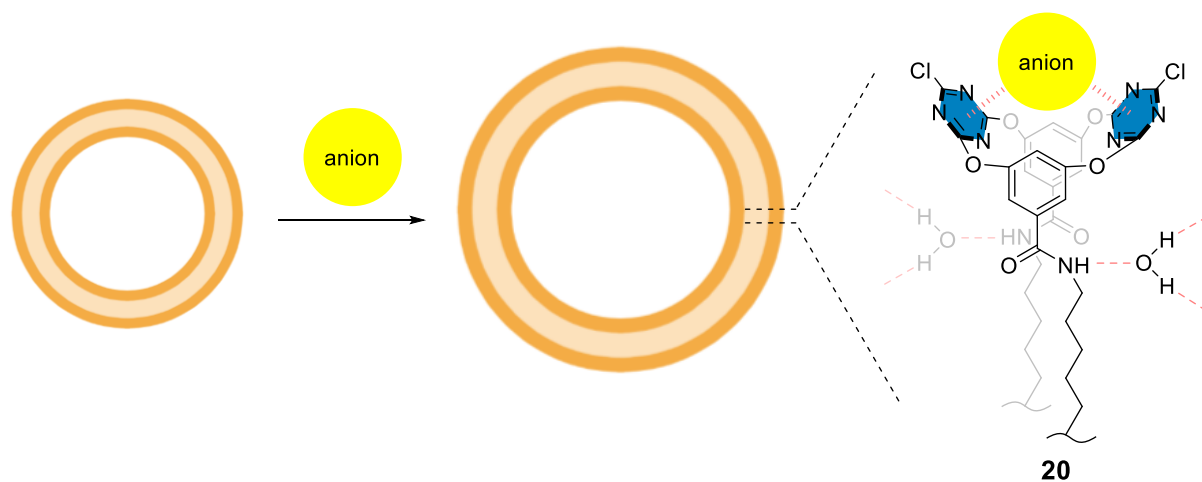
Figure 9. Control vesicles size by anion-π interactions. Adapted from reference.[36]

More complex self-assembled structures could be accessed using anion-π interactions with bidentate hosts **21**-**25** and dianion **26** (Figure 10).[37] In solution, host **21**-**25** could form aggregates. In the presence of the guest, dianion **26**, the oligomeric host-guest complexes appear. The guest molecules act as glue to link the host particles together through anion-π interactions. Changing the structure of the linkers between two anion binding sites of hosts leads to alternation of host-guest complexes morphology.
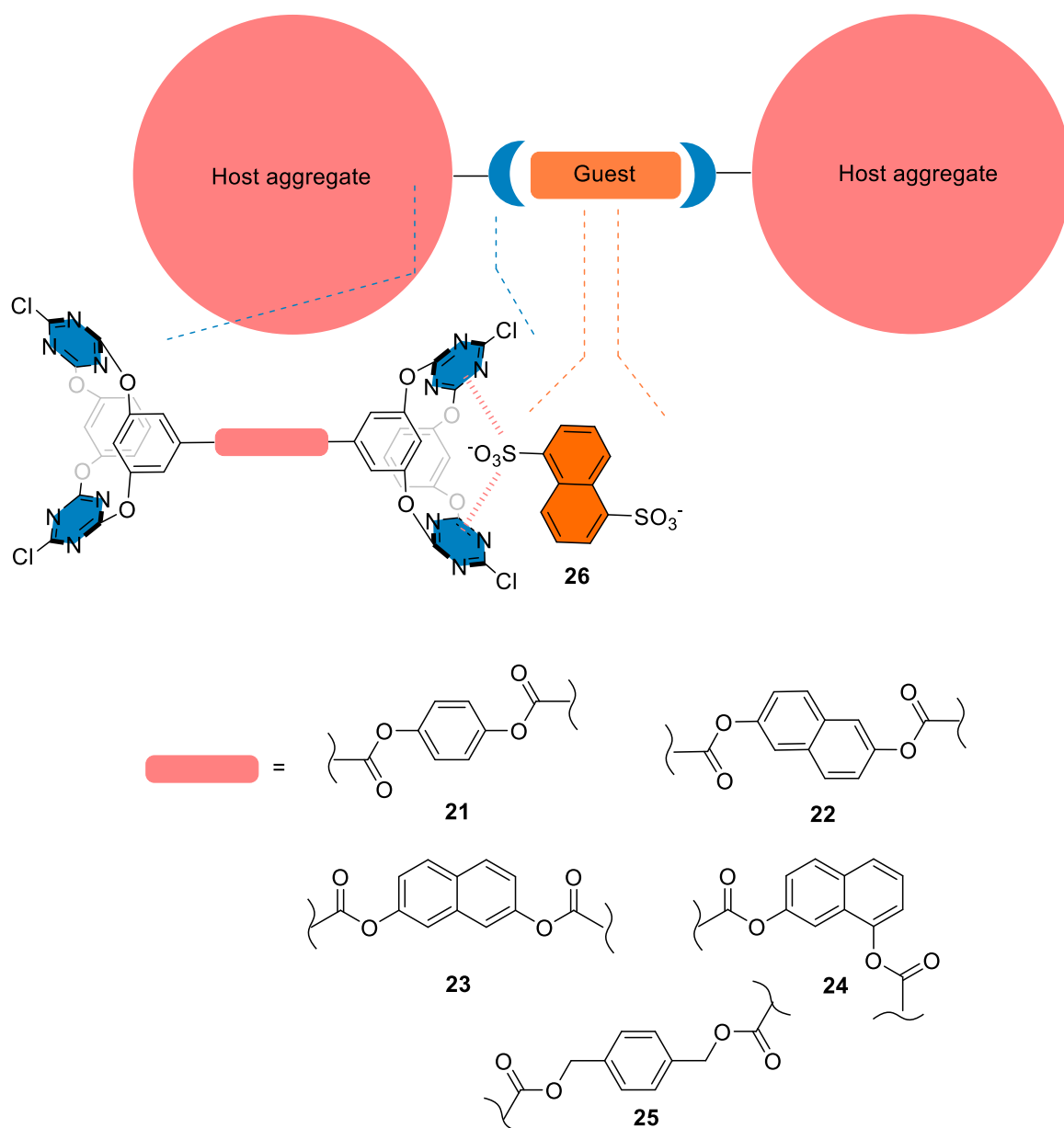
Figure 10. Anion-π interactions between bidentate hosts **21-25** and guest naphathalene-1,5-disulfonate **26** result host-guest self-assembled coherent particles. Adapted from reference.[37]

1.1.2.3. Catalysis

As anion-π interactions are evolving, more and more potential applications have been discovered. Realizing that anion- π interactions could be used to stabilize anionic transition

states, Matile *et al.* first introduced the concept of anion-π catalysis in 2013.[38] Proceeding with a single anionic transition state, Kemp elimination was an ideal reaction to develop a new concept of catalysis based on anion-π interactions (Figure 11).[38,39]
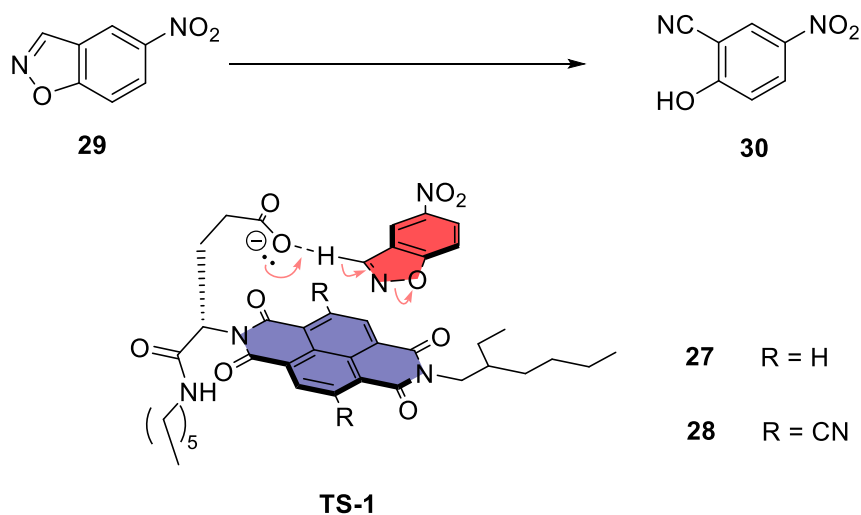
Figure 11. Kemp elimination with anionic transition state stabilized by anion-π interactions. Adapted from reference.[38]

The key to trigger anion-π catalysis is the generation of anionic transition state in close proximity with a π-acidic scaffold. For this purpose, catalysts **27** and **28** were designed with an NDI, equipped with one carboxylate group and one solubilizing group. A proper linker allowed the carboxylate to sit on top of the electron-deficient NDI surface. The catalyst cycle started by deprotonation of substrate **29** by the basic carboxylate above the π-acidic surface (**TS-1**). Upon formation, the anionic transition state was stabilized by anion-π interactions with NDI surface. Following proton transfer between the carboxylic group and the anionic intermediated afforded product **29** and liberated the catalyst. As the results, impressive rate enhancement was observed. Increasing rate enhancement together with increasing π-acidity in the NDI core when cyano-substituents were introduced to NDI confirmed the contribution of anion-π interactions

in catalytic activities. In order to increase π-acidity of catalysts without significant changes in catalyst conformation, sulfides were introduced into NDI core.[39] Oxidation at sulfur atoms could turn the donors into sulfoxide and sulfone acceptors. Similar to previous study, increasing π-acidity led to better catalyst performance. More structure reactivity relationship studies revealed that the correct positioning of the carboxylate base above NDI surface mainly governed the catalytic activity. Whereas, the structure of solubilizing groups was irrelevant. The decrease in activity observed when NDI was replaced by a larger, but less π-acidic PDI surface suggested that the contribution of π-π interactions to anion-π catalysis was negligible.[39]

The contribution of anion-π interactions to anionic transition state stabilization was strongly confirmed in enolate chemistry.[40] To directly generate enolate above π-acidic surface, model compound **31** was designed (Figure 12).
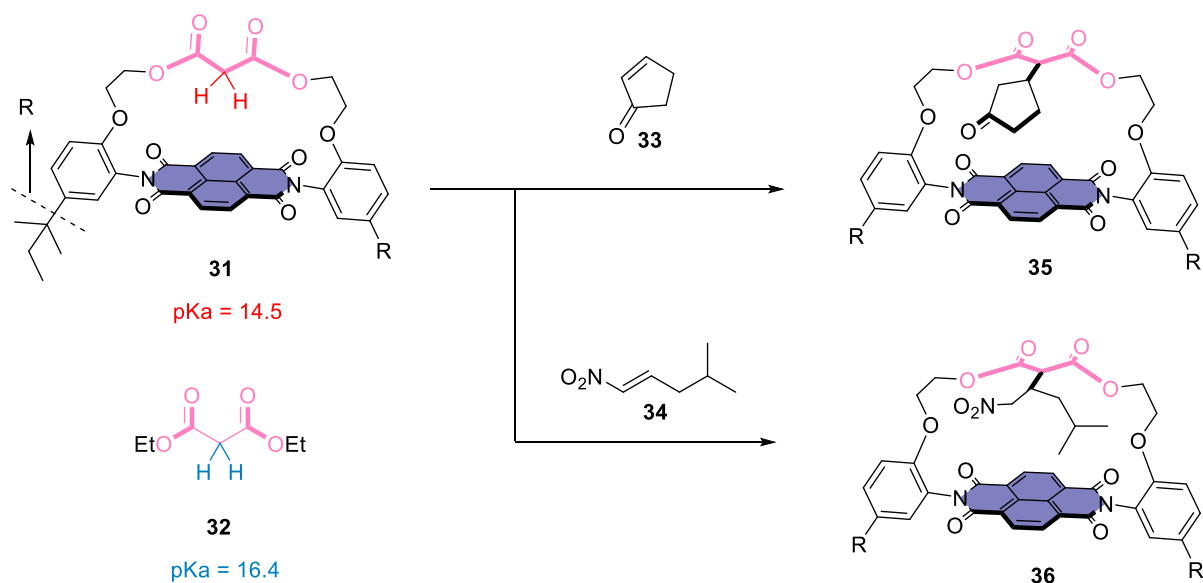
Figure 12. Michael additions of macrocycle **31** to acceptors **33** and **34** result products **35** and **36**, respectively. Adapted from reference.[40]

In comparison with a standard malonate such as **32**, almost two unit of pKa increase was found for the macrocycle **31**. The increasing in acidity of malonic protons demonstrated that the conjugated enolate anion was more stable above NDI surface. This behavior could be translated to significant rate enhancement observed for reactions between **31** and enone **33** or nitroolefin **34** in comparison with standard malonate control **32** (Figure 12).

Asymmetric anion-π catalysis was first addressed in enamine addition to nitroolefins.[41] To construct catalysts for this reaction, π-acidic surface likes NDI was inserted between the proline residue and the carboxylic acid of Wennemers catalysts (Figure 13).[41–43]
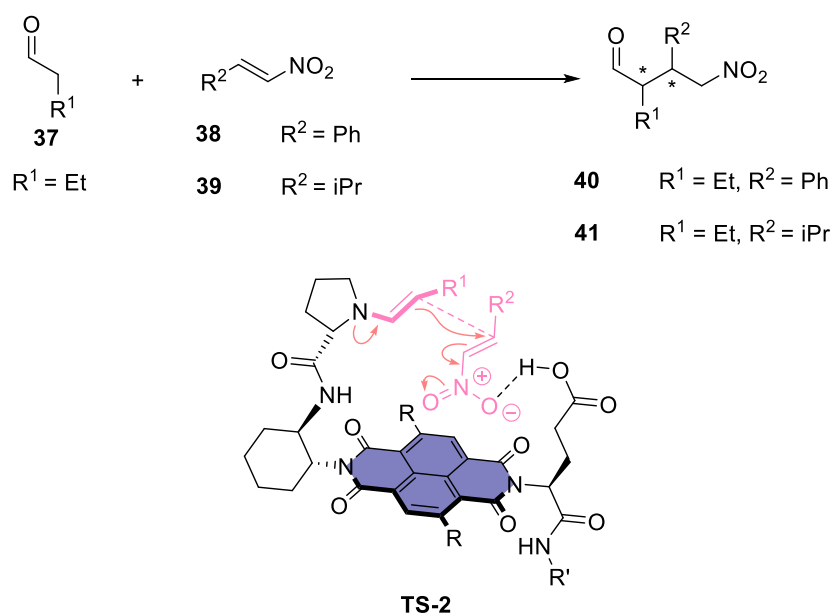
Figure 13. The additions of enamine (from aldehyde **37**) to nitroolefins **38** and **39** result products **40** and **41**, respectively. Adapted from reference.[41]

Newly synthesized catalysts had at one side a proline derivative to yield the enamine with substrate **37**. The carboxylic acid at the other side of NDI protonated the nitronate intermediate

and released the product from the aromatic surface (**TS-2**). This design also allowed the stereo-information to be transferred from imide head groups to the products. Thus, right combination of point chirality of the catalysts led to excellent enantioselectivity in the final products.

Extending the π-surface by replacing ethyl groups with phenyl together with introducing more chiral centers close to the core NDI by oxidation of sulfides to sulfoxides provided core-expanded chiral surfaces.[44] These new chiral π-boxes offered better stereoselectivity for asymmetric anion-π catalysts. Approaching this strategy from a different perspective by replacing NDI with a larger π-surface PDI also gave better stereoselectivity for the former reactions.[45] However, with core substituents at the bay area, the PDI surface twisted. Thus, rate enhancement decreased together with quadrupole moment.

The next step in the development of anion-π catalysis focused on finding its special features. Owning a large and flat aromatic surface, anion-π catalysts are excellent in distinguishing different anionic transition states. The first reaction that demonstrated the exceptional chemoselectivity of anion-π catalysts was the addition of malonic acid half thioesters **42**, **43** (MAHTs) to enolate acceptors **44**, **45** to yield products **46** and **47** (MAHT reaction, Figure 14a).[46] Using conventional bases as the catalysts, MAHT reactions proceed mostly through decarboxylation pathway to yield **47** as the main product. The more important addition product **46**, in general, is not favored. To control the selectivity of two possible products, discrimination between two MAHT tautomers (**RI-1** and **RI-2**) should be achieved. This task is ideal for anion-π catalysts since the more relevant planar charge delocalized tautomer **RI-1** should be favored when the anionic intermediate is sandwiched between two NDI surfaces of the tweezer catalysts. In contrast, the tetrahedral sp^3 carbon in **RI-2** disrupts anion-π interactions (Figure 14b). In other words, as soon as the MAHT anion is formed by

deprotonation of the tertiary amine base in the tweezer linker, anion recognition on flat π-acid aromatic surfaces shifts the equilibrium of two MAHT tautomers toward the planar **RI-1**. Thus, anion-π catalysts are able to control chemoselectivity for this particular reaction. Increasing selectivity together with increasing π-acidity of NDI again confirms the involvement of anion-π interactions in catalysis.[46]
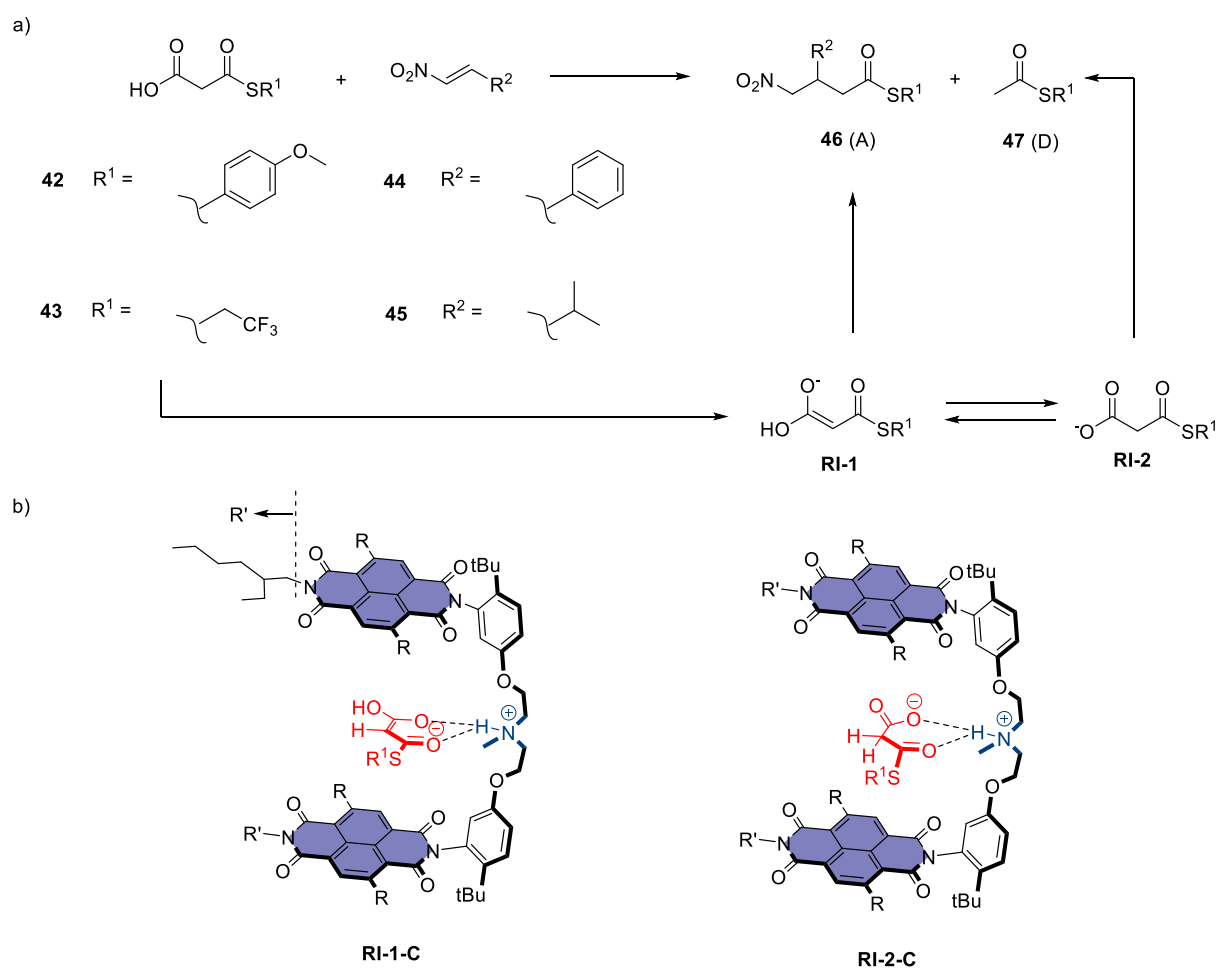
Figure 14. (a) MAHT reactions. (b) Planar MAHT tautomer **RI-1** is better stabilized between two NDI surfaces in tweezer catalysts in comparison with non-planar **RI-2**. Adapted from reference.[46]

Based on the same principle, Diels-Alder reactions were also performed by anion-π catalysis with excellent control over the ratio between *endo-* and *exo*-products.[47] [4+2] cycloadditions in mild conditions usually favor *endo*-products because of secondary orbitals interactions between the diens and dienophiles. Inverting this chemoselectivity is a big challenge in organic chemistry. Conventional organic bases mostly deliver poor chemoselecvity. However, with anion-π catalysts, the reactions proceeded with exceptional *exo*-selectivity and high enantioselectivity.
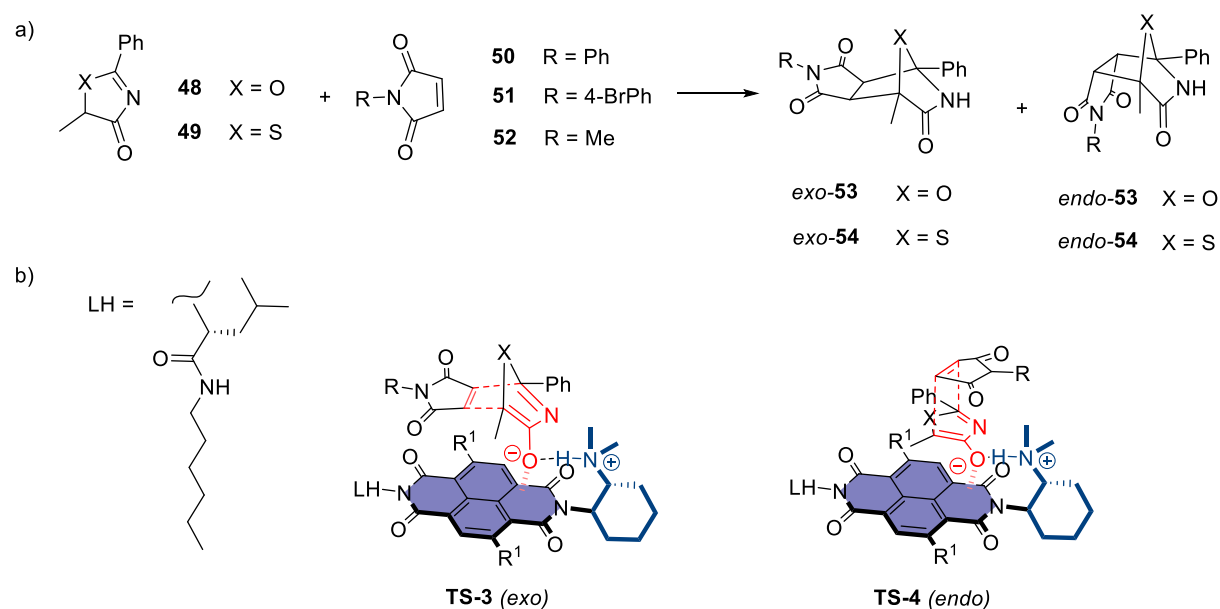
Figure 15. (a) Base-catalyzed Diels-Alder reactions between oxazolone **48** or thiazolone **49** and maleimides **50**-**52** result products **53** or **54**. (b) Proposed anionic transition states **TS-3** for *exo*-products and **TS-4** for *endo*-products. Adapted from reference.[47]

Anion-π interactions allow NDI to stabilize the conjugated base of oxazolone **48** or thiazolone **49** on top of the aromatic surface. The formation of *exo-* or *endo*-products depends on how the dienophiles approach the reactive intermediates. In **TS-3**, the maleimides **50**-**52**

attack oxazolone **48** from the side of NDI surface (Figure 15). Not only more accessible, this movement should also be directed by π-π interactions between substrate and catalysts. In other words, the large and flat aromatic surfaces of anion-π catalysts act as a template for the formation of *exo*-product. On the other hand, the "top-down" approach of the dienophiles in **TS-4** is less favored because the stabilization of the entire transition state with anion-π interactions should not be possible. Thus, the corresponding *endo*-products are diminished.

The specificity of anion-π catalysis was emphasized in epoxide opening reactions (Figure 16).[48,49] Different from previous studies, multifunctionality was not necessary for catalyst design. Catalysts like **55-57** were able to operate just by primary anion-π interactions. Interestingly, the reaction profile shows autocatalytic behavior, which is unique for anion-π catalysis. The addition of product at the beginning of the reaction greatly increased initial rates. Computational studies reveal that transition state and product were forming a hydrogen-bonded macrocycle (**CPS‡**). The initial lone pair-π interactions of substrate **58a-c** with π acidic surfaces turned into anion-π interactions to stabilize the alcoholate leaving group. Also, chemoselectivity in this reaction shifts to the direction which breaks the well-established Baldwin rule in comparison with standard Brønsted acids.

a)

58a: $R^1 = R^2 = H$
58b: $R^1 = CH_3$, $R^2 = H$
58c: $R^1 = R^2 = CH_3$

TS-5

59a-c
(anti-Baldwin product)

TS-6

60a-c
(Baldwin product)

b)

LH =

55: R = Et
56: R = C_6H_5
57: R = C_6F_6

c)

CPS‡
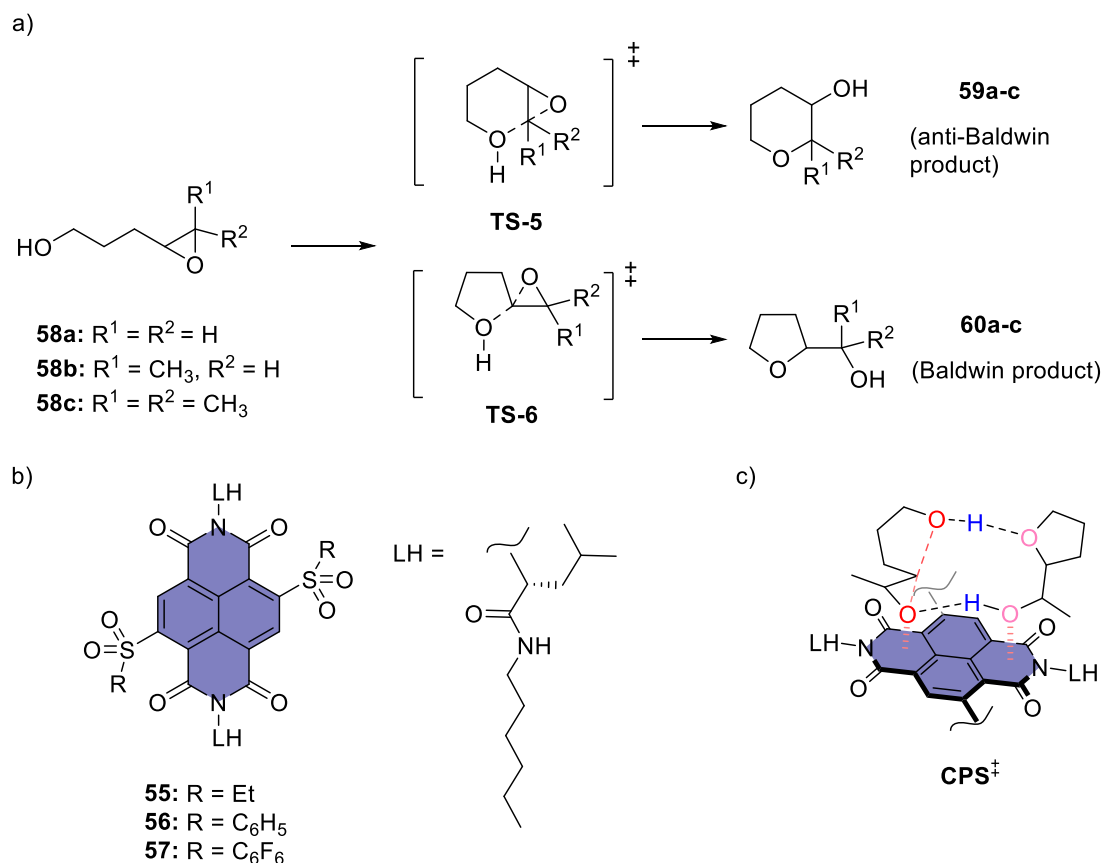
Figure 16. (a) Epoxide opening reactions of **58a-c** yield two possible anti-Baldwin **59a-c** and Baldwin **60a-c** products. (b) Structure of NDI catalysts **55-57**. (c) Activation of **58b** by product **60b** and anion-π catalysts. Adapted from reference.[48,49]

The delocalized nature of anion-π interactions over large aromatic surface appears to be ideal for long-distance charge displacements.[50–52] Utilizing this advantage, several cascade reactions have been developed with anion-π catalysis, include iminium/nitroaldol,[51] Michael–Henry reaction,[52] or epoxide opening cascade cyclizations.[50]

Except for new reactions, novel catalytic systems operating by anion-π interactions were also extensively explored. For this purpose, MAHT reaction is chosen as a benchmark to prove anion-π catalysis. With this reaction, structures of anion-π catalysts have been optimized with

a more rigid head group to fix the organic base on top of the aromatic surface.[53] The influence of axial chirality created by blocking free rotation of substituents at imides position of NDI was also studied.[54] Further, more advanced supramolecular systems have been introduced, for instance, anion-π enzyme or electric-field-assisted anion-π catalysts.[55,56] Equipped with a biotin, anion-π catalysts could easily bind to streptavidin because of the high binding affinity of biotin with the former protein (Figure 17a).[55] Proper linker length allowed the NDI surface to be fully located in the binding pocket of streptavidin, thus yielded a chiral environment around the active center of NDI co-factor. Screening a big library of streptavidin mutants afforded the best artificial enzyme with excellent chemo- and stereoselectivity for MAHT reactions.

As described in section 1.1.1, the nature of anion-π interactions mainly consists of electrostatic forces and ion-induced polarization. While the importance of electrostatic forces in catalysis has been shown clearly by the increase in catalytic activity with more π-acidic catalysts, the contribution of ion-induced polarization to anion-π interactions got less attention. The impact of induced polarization on catalysis as well as possible remote control was addressed by the immobilization of anion-π catalysts on conductive indium tin oxide surfaces (Figure 17b).[56]

a)

61

b)

62
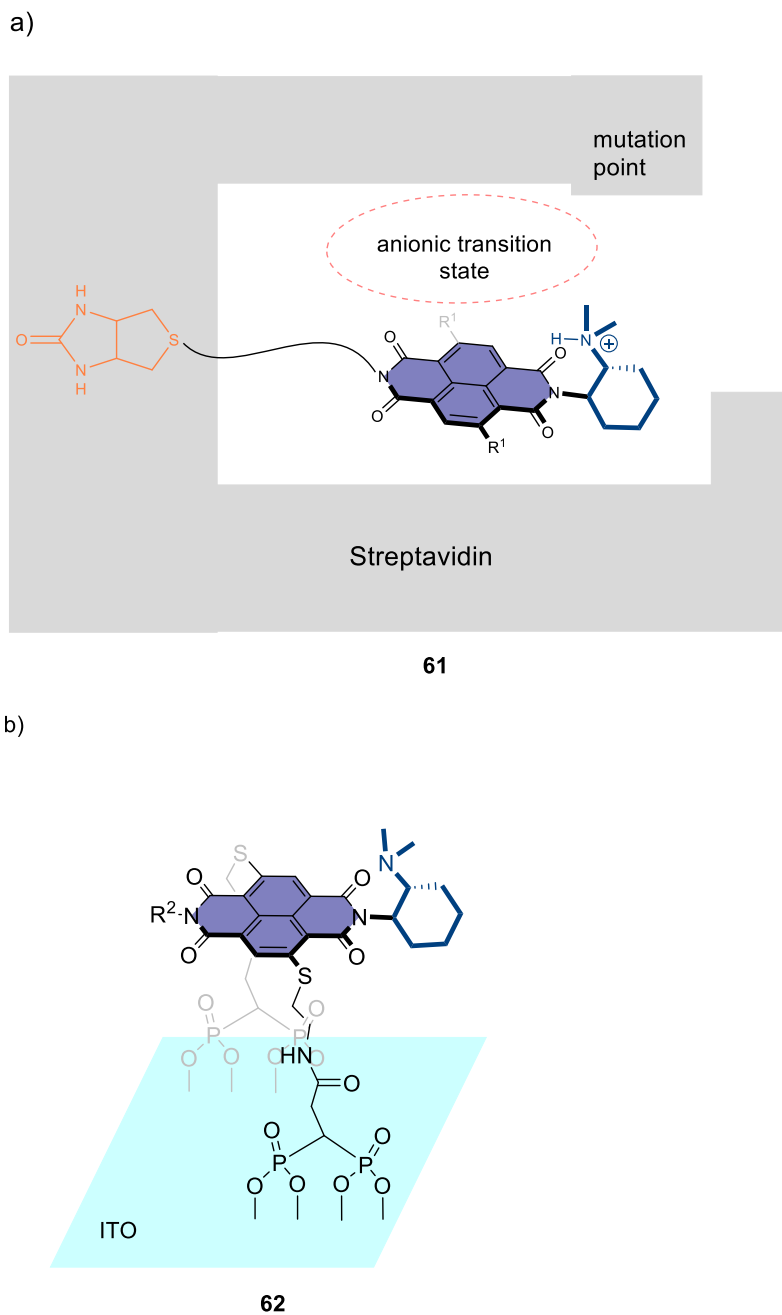
Figure 17. (a) Structure of anion-π enzyme **61**. (b) Anion-π catalyst **62** on ITO surface. Adapted from reference.[55,56]

Applied increasing electric fields to the electrode catalyst **62** led to increase in activity and selectivity toward addition product of MAHT reaction. This behavior was in agreement with systems operated by anion-π interactions. Therefore, these results demonstrated that the

polarization of the π-acidic NDI surface played important roles in anion-π catalysis. In homogenous catalysis, the effect of ion-induced polarization was confirmed when NDI was replaced by a larger, more polarizable aromatic surface such as fullerene.[57,58] Record chemoselectivity in MAHT reaction was observed for fullerene dimer.[58] Overall better performance of fullerene catalysts in comparison with the NDI ones encouraged the extension of anion-π catalysis on even larger, more polarizable aromatic systems. For this purpose, carbon nanotubes have been used for designing of a new class of anion-π catalysts.[59] Even though low solubility of carbon nanotube catalysts classified them as heterogeneous catalysts, their comparable activity in comparison with homogenous systems highlighted the importance of ion-induced polarization in anion-π interactions.

Most anion-π catalysts reported to date employ a large aromatic surface. This choice gives the advantages in increasing ion-induced polarization as well as provides enough space for cascade reactions. However, for some reactions, a more confined environment is necessary to achieve high selectivity. Also, smaller π-acidic systems should not be ignored since they are relatively easy to construct and modify. To overcome the low π-acidity of small aromatic surfaces, Wang *et al.* have designed molecular cages which exploited cooperative anion-π interactions between multiple small aromatic surfaces for catalysis.[60] Three V-shaped electron-deficient cavities in the prism-like cages could activate the imine substrate **63** in the decarboxylate Mannich reactions through lone pair-π interactions (**TS-7**, Figure 18b). These interactions could turn into anion-π interactions to stabilize the anionic sulfamate group in the transition state. The organic base on the sides of the cages generates the enolate species from **42** close to the cyclic aldimines for further nucleophilic addition. With this design, molecular cages were very efficient in catalyzing decarboxylative Mannich reaction. Products **64** were yielded quantitatively with high enantioselectivity.

a)

b)

TS-7
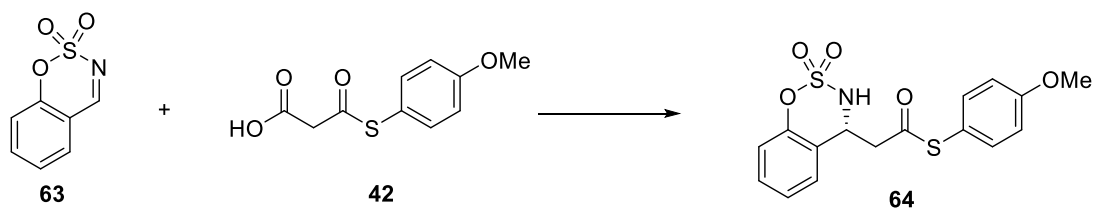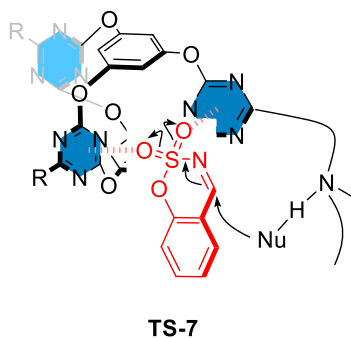
Figure 18. (a) Decarboxylate Mannich reactions of cyclic aldimine **63** and malonic acid half thioester **42**. (b) Proposed transition state in presence of molecular cages. Adapted from reference.[60]

1.2.   Cysteine-Cysteine Peptide Stapling Techniques via Aromatic Nucleophilic Substitution

Peptide stapling is defined as a method to force short peptides to a stable conformation.[61] Typically, it is done by introducing a covalent linker between the side chains of two amino acids to form a peptide macrocycle with an α-helical backbone.[61–63] Since the helical structure is one of the two main peptide secondary structures, it plays important roles in protein functions. A great number of α-helices has been found at the binding interface between two proteins. Thus, developing molecules which adapt helical structure is important in finding inhibitors of protein-protein interactions (PPIs). Even though small molecules have been used

widely for protein inhibitions, some PPIs require large interfaces, which can only be achieved with rather long peptides. In comparison with native peptides, stapled peptides have many advantages such as higher stability, selectivity and better membrane permeability. Structure rigidity of stapled peptide also simplify synthetic routes since usually shorter peptide sequence is needed to achieve the same secondary structure.

The importance of stapled peptides in drug discovery leads to massive efforts in finding and optimizing peptide stapling techniques. Well-established stapling techniques include lactam formation between Lys and Glu/Asp residues, hydrocarbon stapling using ring-closing metathesis or introducing unnatural amino acids for click chemistry.[61–64] One remained popular approach is Cysteine-Cysteine stapling. High nucleophilicity of the thiol side chain and the low-abundance of Cysteine make the Cys-Cys stapling strategy highly selective and easy to handle.[63] Most Cysteine stapling techniques rely on two-component approach using an appropriate bifunctional linker to crosslink the side chains of two Cysteines.[65] To stabilize peptide secondary structure, in general α-helices, the Cysteine pair must be located in the same face of the helix to facilitate macrocyclization. Therefore (i, i+4), (i, i+7) or (i, i+11) stapling are preferred. Based on the chemistry utilized during stapling, Cys-Cys stapling could be classified into S-Alkylation, thiol-ene coupling, disulfide formation or S_N-Arylation. While the first three methods have been reviewed elsewhere, the last more relevant method will be discussed in more detail.[63,65]

One of the first mild, biocompatible arylations of Cysteine was reported by Pentelute *et al.*[64] They found the optimal conditions for coupling Cysteine thiols and perfluorinated compounds such as hexafluorobenzene **2** and decafluorobiphenyl **65** (Figure 19). In polar organic solvent at room temperature with the presence of base, hexafluorobenzene reacts with

thiol groups to give exclusively 1,4-disubstitution products. The same result was found even when hexafluorobenezene was used in excess. The unique regioselectivity of this reaction was explained by steric hindrance of ortho substituents and simultaneous activation of the para position by thioether moiety. Being highly selective for Cysteine, this method could be easily applied for longer peptides or even large proteins. Interestingly, the rigidity of the aromatic system could enhance helicity in some peptides. The hexafluorobenzene is better matched for stapling one turn of α-helices. Although the distance in decafluorobiphenyl moiety is much longer, improvement in helicity is also noticeable. In general, stapled peptides using this method experience better proteolytic stability and cell permeability. Introducing perfluoronated linker into affibodies did not alter their conformations and functions. Thus, this method could be applied to improve the properties of biomolecules that contain Cysteines. Some potential applications could be listed. For instance, significant improvement in the ability to cross the blood-brain barrier was observed for stapled peptides.[66] Frédérick *et al.* used this stapling technique to develop macrocyclic peptides that disrupted and destabilized Lactacte Dehydrogenases tetramers, one of cancer therapy targets.[67] Tackling this stapling strategy from a different perspective, Coxon *et al.* examined the compatibility of several Cysteine analogs. As expected, replacement of one or more L-Cysteine residues resulting significant changes in activity and selectivity of model peptides. This could be of interest for the development of protein inhibitors.[68]
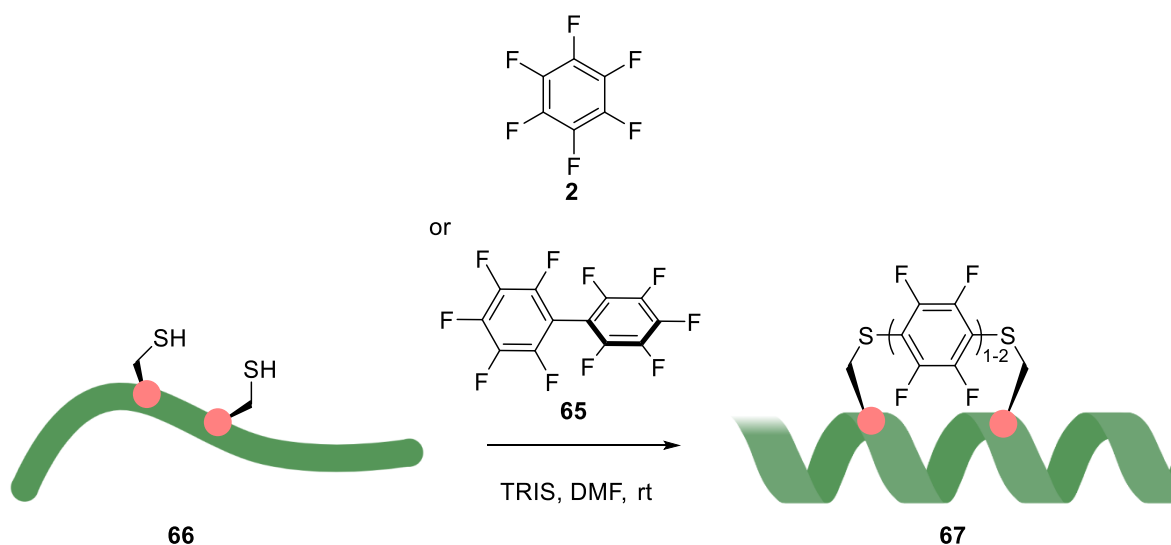
Figure 19. Peptide stapling using perfluoroaromatic linkers. Adapted from reference.[63,64]

Taking the high reactivity of perfluoroaromatic compounds into consideration, other perfluoroaromatic scaffolds have been chosen for the mildest stapling conditions. Derda *et al.* introduced decafluoro-diphenylsulfone (DFS) **68** as one of the most reactive S_NAr electrophiles (Figure 20).[69] With superior reactivity in comparison with previously reported perfluoroarenes, DFS was able to react with Cysteine residue in conditions that required minimal amount of organic cosolvent. Therefore, it could be used in macrocyclization of peptide libraries displayed on bacteriophages, which are usually sensitive to chemical modification. Besides, the exceptional oxidative stability of the resulting thioethers allowed the stapled peptides to be further modified. Wu *et al.* was successful to use 2,3,5,6-tetrafluoroterephthalonitrile (4F-2CN) **69** as covalent linkers to access more complex multicyclic topologies through a one-pot reaction.[70] Under mild aqueous conditions, 4F-2CN reacts with four thiolate groups via a highly controllable pathway. The first two thiolates react selectively with the two *para*-C-F sites. The reactivity of the remaining *ortho*-C-F is significantly weaker due to steric hindrance. Moreover, the second and the fourth substitutions are greatly enhanced by sulfur atoms after the first and

the third substitutions. Therefore, in combination with modulating thiolate reactivities using Penicillamines instead of Cysteines, reactions of 4F-2CN with peptides are highly programable with much fewer isomers in comparison with traditional stapling methods. Using this method, some of the stapled peptides experienced better binding affinity to Ubiquitin ligase and Tripsin. These results suggested its potential application in locking the conformation of peptides to improve their activity in inhibition studies. Wilson *et al.* reported dibromomaleimide **70** as a promising reversible stapling linker.[71] Upon treatment with **70**, peptides containing two Cysteine residues at position i and i+4 rapidly and completely crosslink. The resulting constrained peptides show significant improvement in helicity in comparison with linear peptide controls. More importantly, exposing stapled peptides with high concentration of thiol regenerates the initial linear peptides. In addition, alkyne group could be introduced at the imide position of **70** for further click-functionalization.
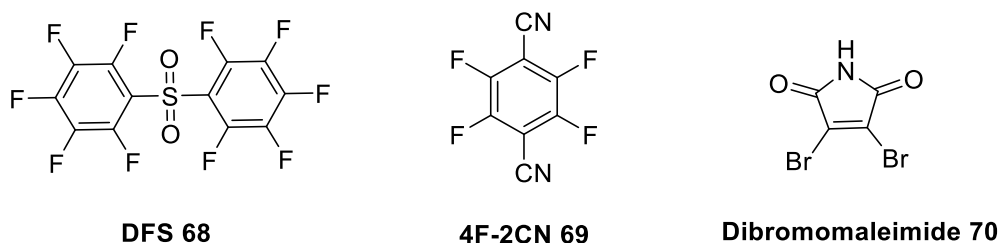
Figure 20. Some highly reactive scaffolds for Cys-Cys crosslinking.

Another approach to reversibly staple and unstaple peptides using S-tetrazine moiety was discovered by Smith group in collaboration with Hochstrasser group.[72–74] In biphasic system, peptides containing two Cysteines **71** could easily react with 1,4-dichlorotetrazine **72** to yield the designed macrocyclic peptides **73** (Figure 21). After irradiation of the S,S-tetrazine chromophore with light (355 or 410 nm), ultrafast degradation of the tetrazine moiety releases

the thiocyanate peptides **74** and unlocks molecular restriction. The sulfhydryl groups in Cysteine side chains could be restored after treatment with Cysteine. Thus, the initial unstapled peptides are recovered. This stapling method tolerates a wide variety of short peptides and even large proteins such as Thioredoxin. In addition, the presence of tetrazine allows the incorporation of inverse electron demand Diels-Alder reactions to orthogonally functionalize the stapled peptides.[74]
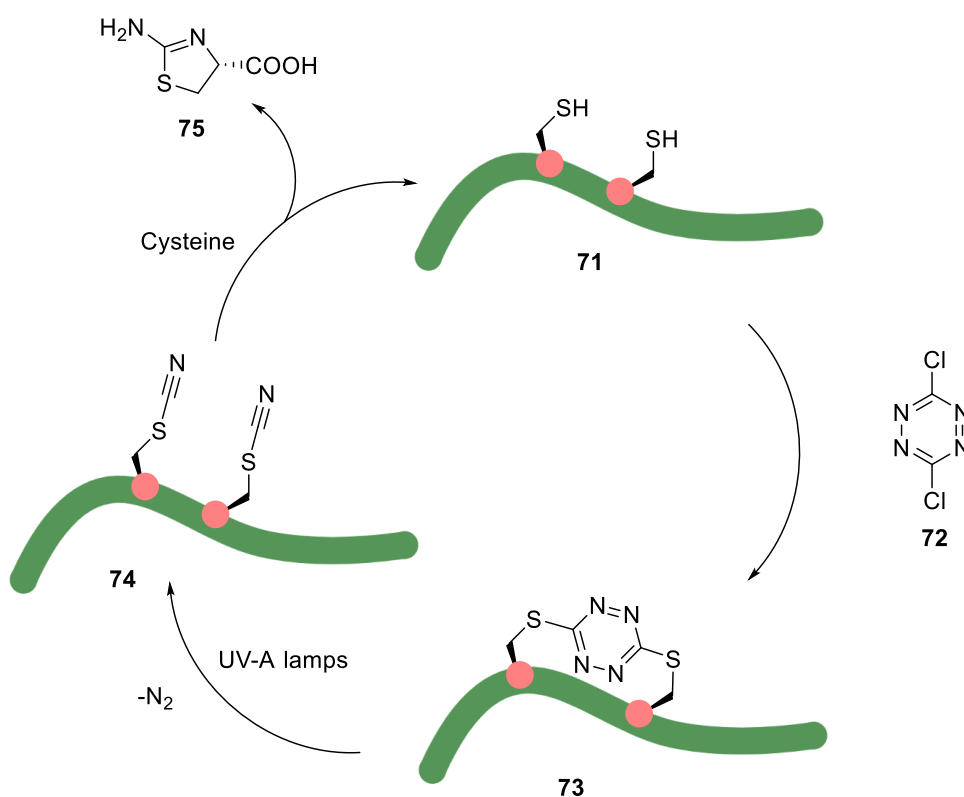
Figure 21. Reversible stapling of peptides using 1,4-dichlorotetrazine **72**. Adapted from reference.[74]

1.3. Stapled Peptides in Catalysis

As described previously, stapled peptides have many advantages over unstapled ones. However, they were mostly used for only biological applications. Even though peptide-based catalysts get more and more attention recently, strategies for catalyst development usually center on screening a big library of catalytic peptides. Despite the fact that peptide secondary structure has been known to be important in the catalytic activity of many reactions, examples of rigidifying peptide catalysts using stapling techniques are extremely rare.[75–82] The only study that examined the benefit of stapling catalytic peptides came from Kurihara *et al.*[83] In this study, a series of unstapled and stapled peptides were used to catalyze Juliá−Colonna epoxidation. Since mechanistic studies suggest that for this chiral epoxidation, helicity of catalytic peptides is essential for high yield and stereoselectivity, this reaction could be ideal to evaluate the effect of conformation constrain induced by stapling on catalytic activity.[82] Four L-Leucine based heptapeptides were designed and synthesized with different stereochemistry of the Serine residues at the 3rd and 7th positions (Figure 22). To improve overall helicity of the linear peptide, 2-Aminoisobutyric acid (Aib) residue was put in the middle of the peptide sequence. Allyl protecting groups at the side chains of Serine residues allowed ring-closing metathesis to be performed for stapling. Conformations of resulting peptides were analyzed using CD spectra and X-ray crystallography. Linear peptides (3S-7S), (3S-7R) and (3R-7S)-**76** adopted right-handed 3_{10}-helical structure in solution. Upon stapling, structures of the corresponding cyclic peptides remained unchanged. These results explained the almost identical catalytic activity in epoxidation reactions for each pair of peptides. In contrast, stapling shifted the conformation of (3R,7R)-**76** from 3_{10}-helix to α-helix in the cyclic (3R-7R)-**77**. This change led to a significant improvement in enantioselectivity. These promising results demonstrated that stapling techniques could be applied to designed peptide-based catalysts with higher efficiency.
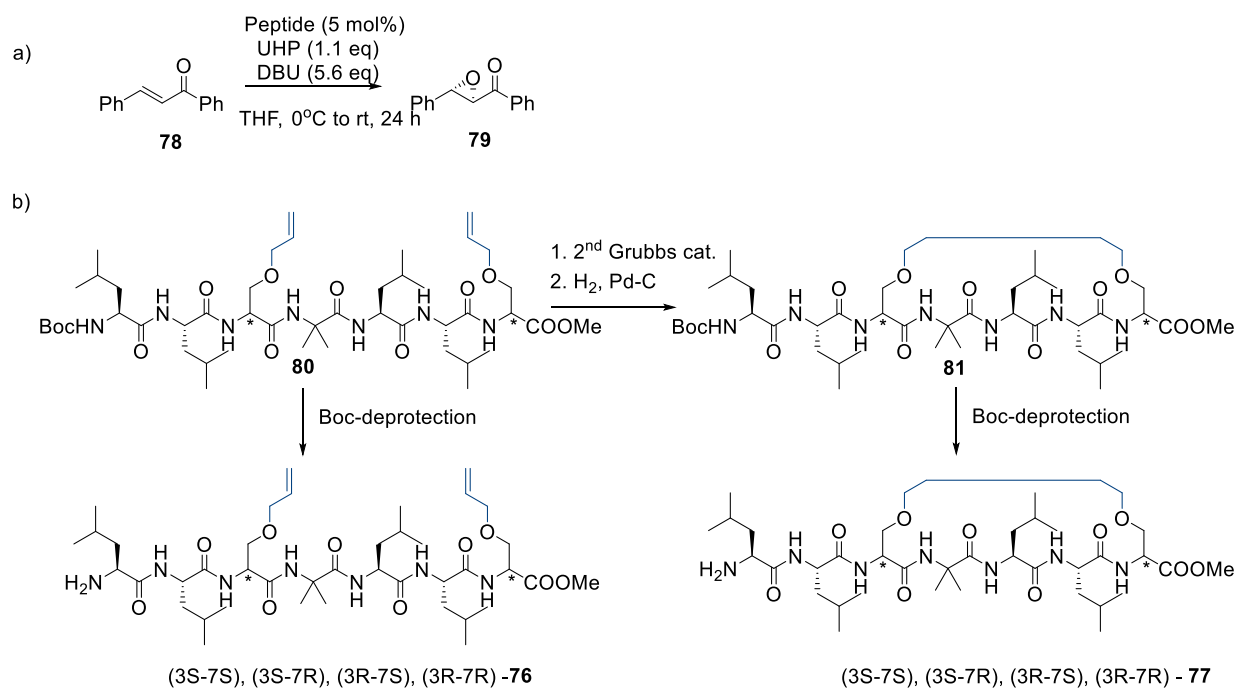
Figure 22. (a) Juliá−Colonna epoxidations catalyzed by peptides. (b) Synthesis of linear and cyclic peptide catalysts (stereo chemistry of 3rd and 7th Serine residues were given inside parenthesis). Adapted from reference.[83]

1.4. Planar Chirality in Twisted Perylenediimides

Since the molecular basis of chirality was proposed by Louis Pasteur almost two centuries ago, chirality has always been one of the most intriguing phenomena of organic chemistry. While chirality created by a stereocenter has been well studied, the outbreak of discoveries in axial chirality was started just a few decades ago. Together with the development of organometallic chemistry, a lot of axial chiral compounds have found their applications in asymmetric catalysis. One influential scaffold could be named during this period is BINAP developed by Noyori *et al.* in 1980s.[84] The importance of such chiral ligands in asymmetric catalysis encouraged the exploration of novel chiral motifs in organic chemistry. Moving from axial

chirality created by restriction in rotation around a single bond, in the last decades, the attention shifts more toward planar chirality in polyaromatic systems.[85,86] Substantial amounts of new chiral polyaromatic systems have been reported. However, these studies focused more on the synthesis and resolution of such compounds rather than their applications. This trend could be understood since the racemization barriers of polyaromatic systems are usually low and the difficulty in their preparation prevented modifications suitable for potential usage. The only scaffold that has been used more frequently for designing functional systems was helicene.[87–90] The applications of other classes of strain-induced chiral polyarenes, on the other hand, were very limited. Among these compounds, considering the relatively small size and high photo- and redox-stabilities, twisted acenes (or twistacenes) appear as the most promising class for future applications in supramolecular chemistry and asymmetric catalysis.[85,91,92]

As a polyarene, perylenediimides (PDIs) could be easily transferred to twisted acenes by introduction of substituents at bay-region (Figure 23).[93–95] Except for cyano groups, even the smallest substituent like fluorine atoms causes the deplanarization of the PDI core.[96,97] The twisting angles of the π-systems strongly depends on the size of substituents and might vary significantly (from 4º in difluoro-PDIs to 35º in tetrachloro-PDIs).[98] The twisting of the core PDI leads to the formations of two atropo-enantiomers (Figure 23b).[100] However, the isolation of these isomers for common PDIs usually are not possible since the inversion barriers are quite low (around 60 kJmol^{-1}). Thus, rapid interconversion between *M* and *P* occurs at room temperature.[97]

a)

Compound	82	83	84	85	86
$\Delta\theta$ (deg)	0°	14°	23°	25°	37°

R = TEG :

b)

(*M*)-enantiomer   (*P*)-enantiomer

83-86   83-86
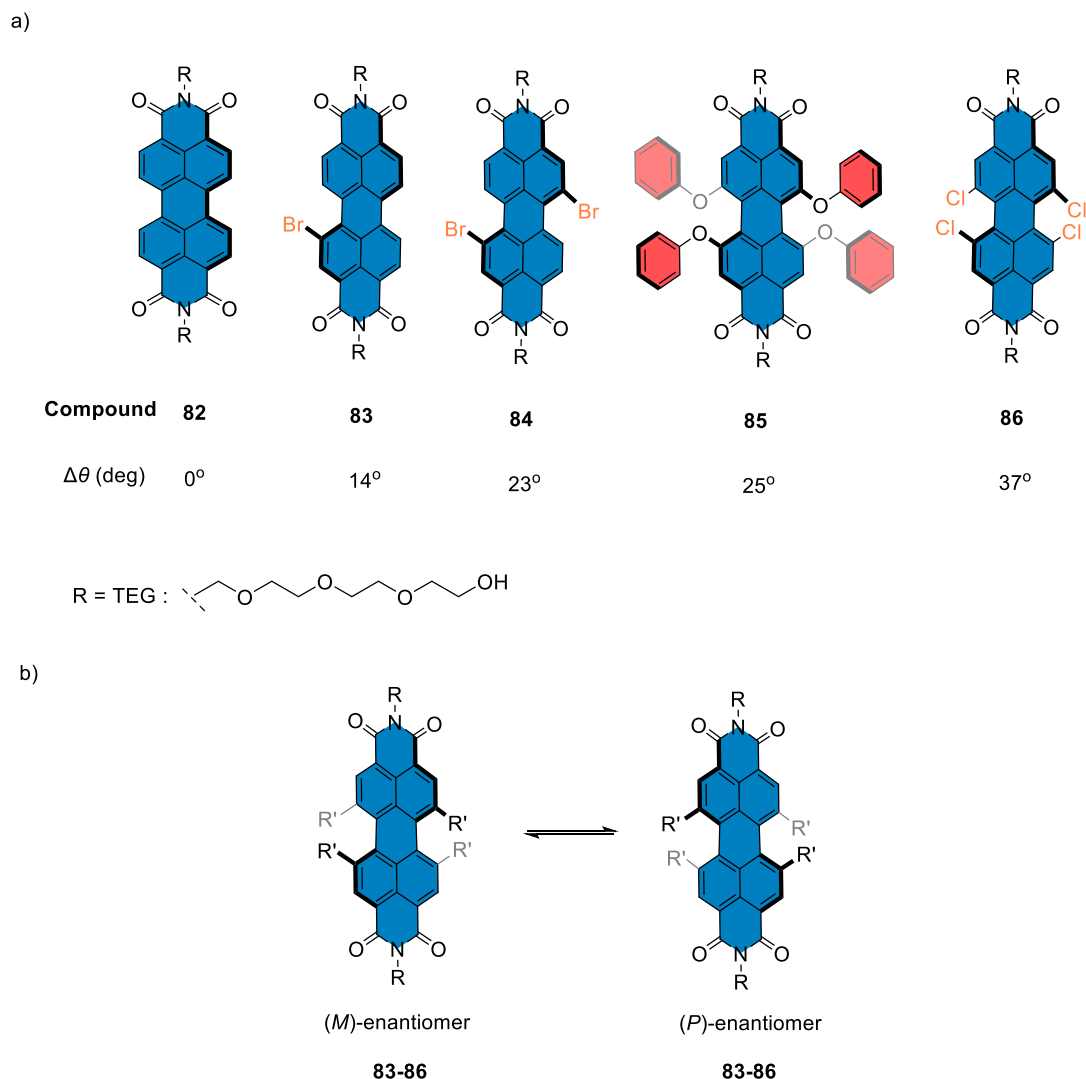
Figure 23. (a) Twisting angles of some bay-substituted PDIs. (b) *M* to *P* interconversion process of bay-substituted PDIs. Adapted from reference.[100,102]

As one of the first attempts to exploit the chirality of PDIs, Würthner *et al.* have systematically studied the racemization process of PDIs.[98] For this purpose, activation barriers for racemization of a series of PDI derivatives with different core substituents were measured by dynamic NMR spectroscopy and time- and temperature-dependent CD spectroscopy. For PDI bearing four aryloxy substituents in bay positions, free enthalpy of activation was calculated to be 60 kJmol^{-1}. This corresponded with a half-life of only 10 s for the pure atropo-

enantiomer at 270 K. Therefore, the resolution of isomers was clearly not possible at room temperature. For smaller substituents, it was obvious that the barriers were even lower. Similar to tetrafluoro-PDI derivatives, 1,7-dihalogenated PDIs own the free enthalpy of activation $\Delta G^{\ddagger}$ around 40 kJmol^{-1} at 180 K. With very big core substituents, atropo-enantiomers of tetrachloro- and tetrabromo-PDIs could be separated using chiral HPLC. For the tetrachloro-derivatives, the half-lifetime could be more than one day at room temperature. However, as temperature increases, their half-lifetimes drop significantly to less than one hour. Although without special techniques to increase the racemization barriers, core substituted PDIs present in their racemate form, the distortion of the π-surface in bay-substituted PDIs could be highly desirable for designing organic dyes and supramolecular systems. It provides dyes with high solubility even in nonpolar solvents. The larger distance between each PDI units in their supramolecular structures could be maintained for reducing fluorescence quenching in dye aggregates. Moreover, different twisting angles could tun the strength of π-π stacking in supramolecular assemblies with the higher associate constant corresponds to more planar structures.[97] Realized these advantages, Li *et al.* were the pioneers in using PDIs to drive reaction pathways in complex environments.[101,102] The impact of specific chiral self-assembly of PDIs to reaction mechanism was demonstrated by the deacetylation of the racemate of twisted chiral monomer **87** in basic condition (Figure 24).[101] After deprotection of thiolates, homochiral cyclic product **88-Homo** and heterochiral linear dimer **89-Hetero** could be found in the reaction mixture. In this condition, no formation of homochiral linear dimer **89-Homo** or heterochiral macrocycle **88-Hetero** was observed. When the reaction was allowed to proceed to completion, **88-Homo** was the only major product. These results could be explained by the following reaction pathway. Firstly, monomer **87** underwent self-assembly by homo or hetero manners. In homo-self-assembly, a better fit of π-π stacking between PDI monomer brought reactive thiolates in close proximity and led to the spontaneous formation of two disulfide bonds, which resulted

homochiral cyclic product **88-Homo**. On the other hand, π-π stacking in hetero assembly could not be able to keep two pairs of thiolates close at the same time. Therefore, the formation of cyclic dimer, in this case, went through a stepwise mechanism with heterochiral linear dimer **89-Hetero** as an intermediate. In order to undergo ring closure, **89-Hetero** needed to be transformed to homochiral linear dimer **89-Homo**, in which reactive centers are closer. Thus, heterochiral cyclic dimer **88-Hetero** could not be found despite the reaction was quenched shortly after starting. However, since **88-Hetero** and **88-Homo** are thermodynamically equaled, during storage **88-Homo** slowly transferred to a mixture of 1:1 **88-Homo**: **88-Hetero**. This example beautifully demonstrated how planar chirality in bay-substituted PDIs could be used to create molecular codes that controlled self-assembly of building blocks and translated them into a more favored reaction pathway.
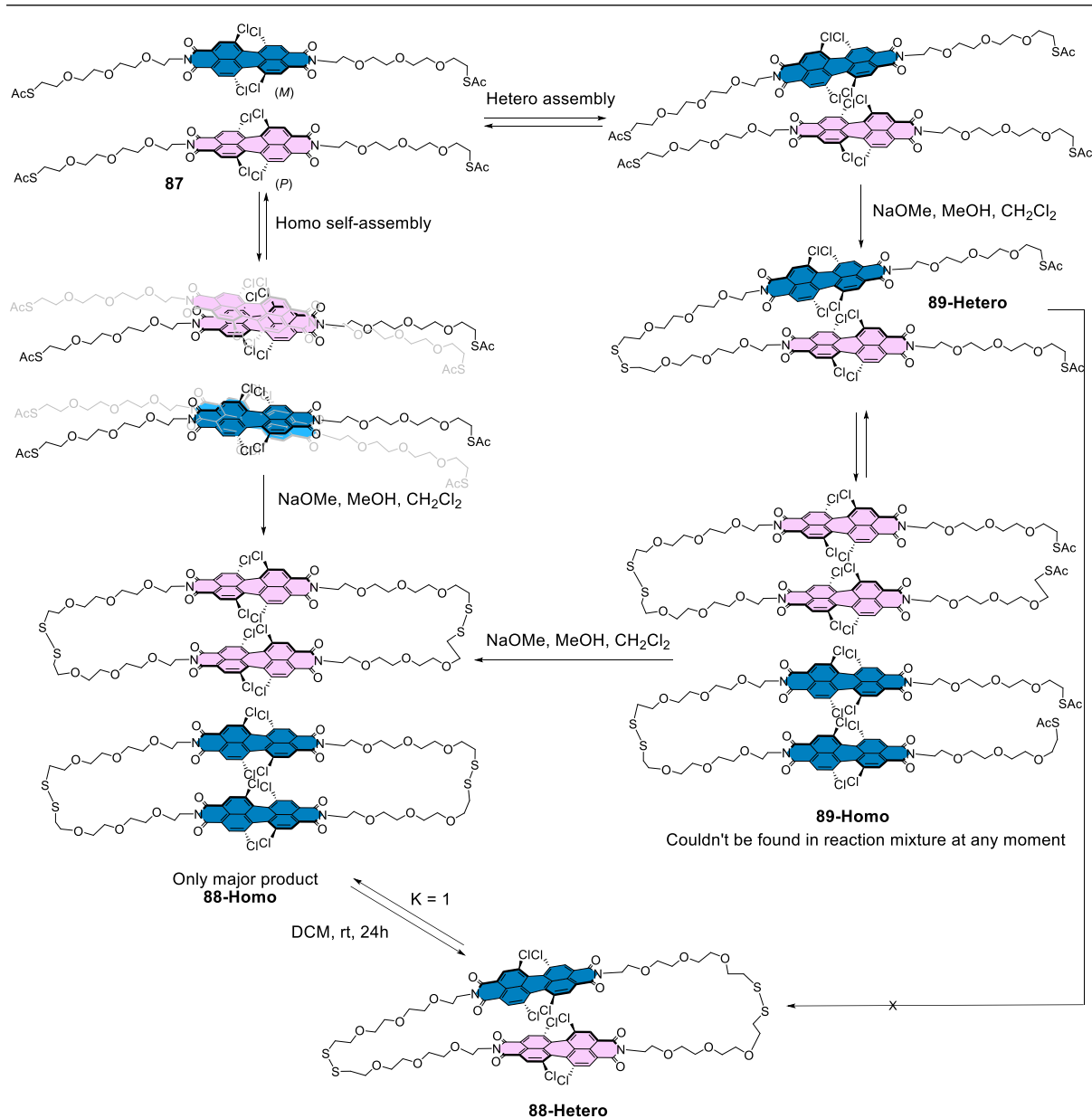
Figure 24. Possible reaction pathways to form cyclic dimer **88** from monomer **87**. Adapted from reference.[101]

The former principle could be applied for even more complex system containing several reactive monomers.[102] In a mixture of several monomers **82-86** owning different twist angles of PDI core, each monomer preferentially self-assembles into PDI stacks with very minimal

cross stacking (Figure 25a). This surprising observation could be rationalized by the different

aggregation rates for each monomer created by different levels of twisting.
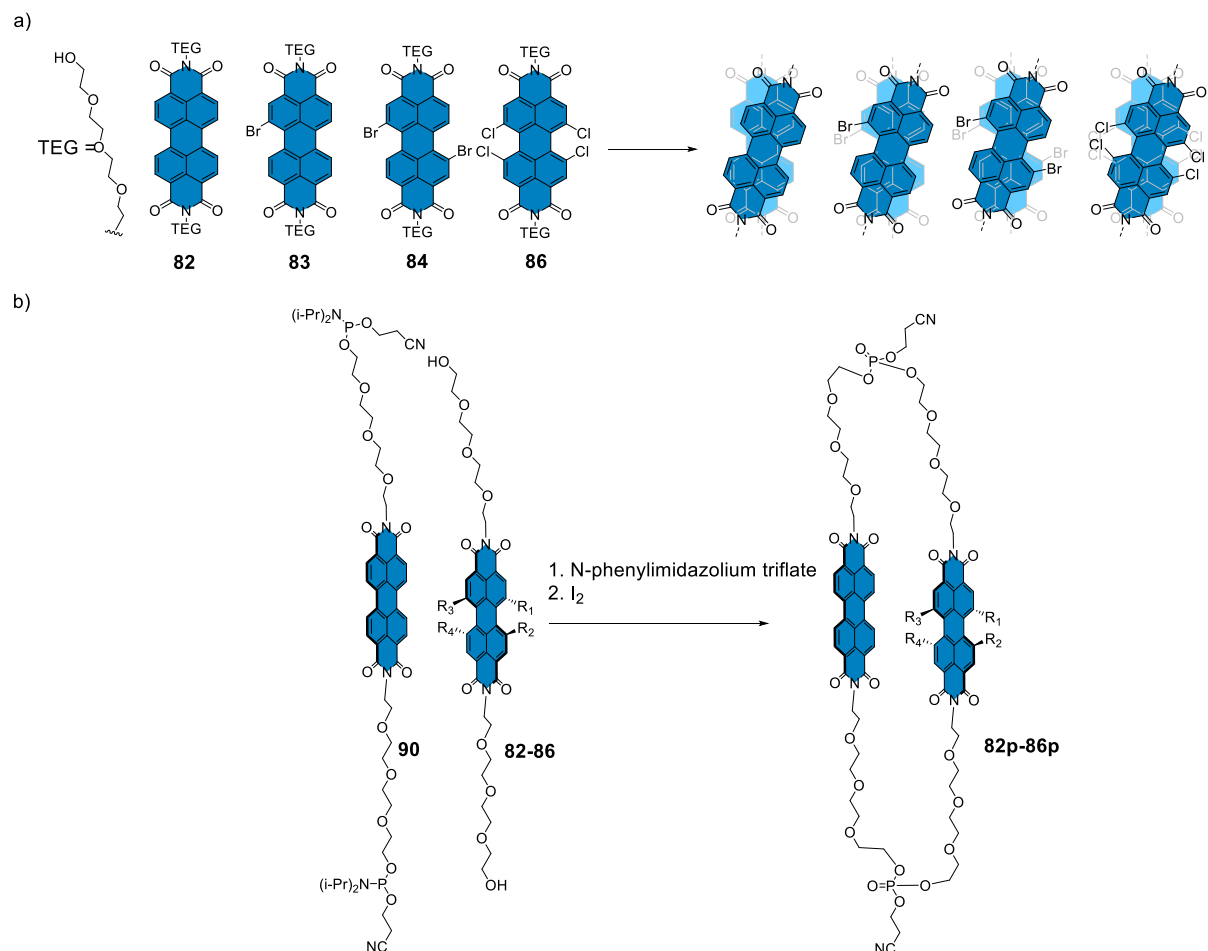
Figure 25. (a) Self-assembly of monomers **82**-**86**. (b) The formation of cyclic dimer **82p-86p** from **90** and monomer **82**-**86**. Adapted from reference.[102]

While planar monomer **82** could experience significant π-π interactions between each

molecule and stack at low concentration, π-π interactions in twisted PDIs like **83**-**86** were

clearly less favored. Therefore, they would form aggregates at higher concentrations. In other

words, the non-interchangeable molecular codes created by the distortion of PDI core directed

the assembly of monomers toward self-assembly. These unique properties of twisted PDI

should be considered in the design of functional systems since they could greatly affect the formation of designed products. It could be seen via the reaction of **90** with different monomers **82**-**86** to yield cyclic dimers **82p**-**86p** (Figure 25b). As the twist angle of the starting materials increased, the reaction yields dropped quickly. The more the molecular codes unmatched, the lower the formation of dimeric product was obtained. Thus, understanding factors that direct self-assembly is crucial for designing functional systems and could be of interest for developing more efficient synthesis in complex environments.

1.5.   Bridged Naphthalenediimides and Perylendiimides

Having excellent photo- and electronic properties, NDIs have been employed widely in chemistry and biology. Their electron-poor nature makes them one of the most attractive building blocks in supramolecular chemistry.[103–105] NDIs have been incorporated into plenty of macrocyclic structures. Most of the bridged NDIs use a tether linker between two imide positions. However, hash imide formation conditions usually prevent them from being directly linked to peptides.[104] Introducing NDIs into peptides usually requires two steps. Firstly, the commercially available 1,4,5,8-Naphthalenetetracarboxylic dianhydride (NDA) is transformed to NDIs bearing other functional groups. Following modifications rely on other milder reactions rather than imide formations. The first example of peptide bridged NDIs was reported by Mallouk *et al.*[106] With the intention to construct a chiral host molecule for indole derivatives, a tripeptide was integrated into structure of macrocycle NDI **91** (Figure 26a). Together with NDI surface, tripeptide Valine-Leucine-Alanine created an electron-deficient hydrophobic chiral pocket that is capable of binding to suitable guests. Despite being a strong π-donating guest, indole was weakly bound to the host NDI. A surprisingly low association constant of 13 $\pm$ 1 M^{-1} was determined.[106]
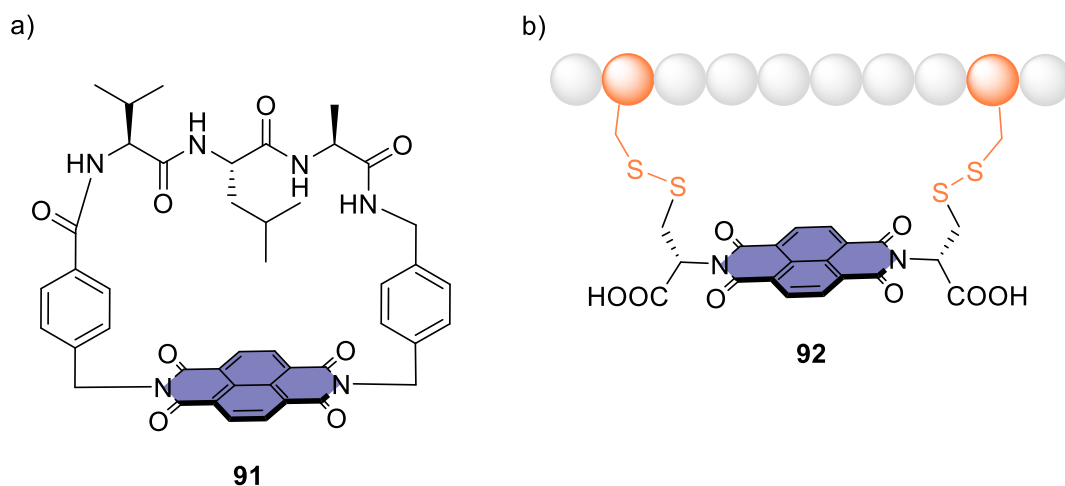
Figure 26. (a) NDI-peptide host **91** for indole guest. (b) Disulfide-bridged conjugation with NDI for stabilization of peptides against proteolysis. Adapted from reference.[106,107]

Wu *et al.* have used NDI for peptide stapling.[107] Having two Cysteine moieties at imide positions, NDI linker could easily form two disulfide bonds with Cysteine residues in the peptides (Figure 26b). When two Cysteines located at i and i+7 positions in peptide sequence, this strategy allowed to stabilize two turns of an α-helix. Thus, overall helicity was improved for stapled peptides **92**. At the same time, stapled peptides experienced remarkable proteolytic stability as a result of steric effect from NDI linker and π-π interactions between NDI and aromatic side chains of amino acid residues.[107] Even though the idea of incorporating NDI into peptide structure has been around, bridging NDI with peptide through imide positions required indirect methods which might complicate the synthesis. On the other hand, the approach of bridging NDI diagonally by covalent linker at core-substituted positions has not been explored.

As described in previous section, even with very big substituents at bay area of PDI, the interconversion between two atropo-enantiomers could be very fast at elevated temperatures. To exploit the planar chirality of PDIs, it is necessary to develop methods for locking PDI conformations. Würthner *et al.* were successful to employ tethered linker for increasing

racemization barriers of core-substituted PDIs. Introduction of such linkers to connect bay

positions of PDIs could be done using etherification of **93** with ditosilates **94a-d** at high dilution

(Scheme 1).[108]
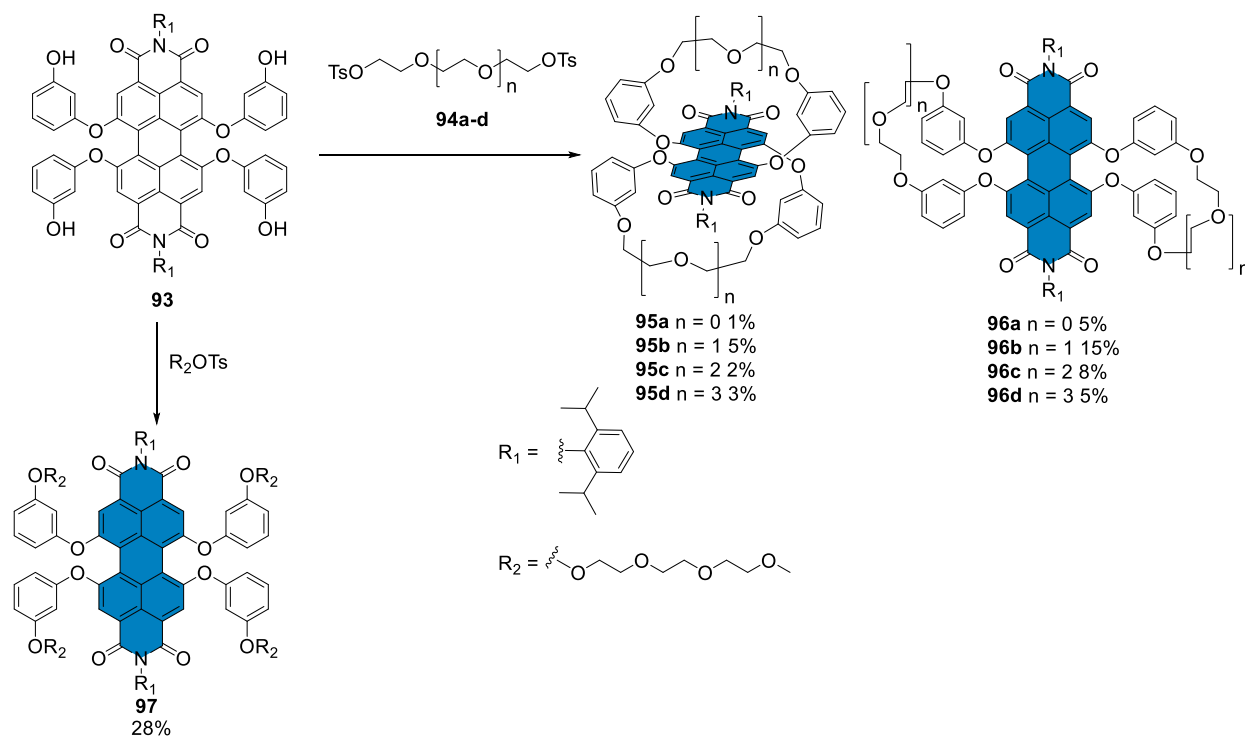
Scheme 1. Synthesis of bridged PDIs. Adapted from reference.[108]

After purification the diagonally bridged PDIs **95a-d** and their laterally bridge isomers

96a-d were obtained in low yields. Different linker lengths were used to control the twisting

angles of the PDI core. For the diagonally linked systems **95a-d**, interconversion between two

atropo-isomers was not possible since racemization required breaking the covalent linker. This

type of structure was of interest since their spectroscopic properties were significantly altered

in comparison with non-bridged PDIs **97**. A substantial hypsochromic shift in absorption

spectra and decreasing of fluorescent quantum yields were noticed for **95a-d**. Covalent linkers

in **95** could change the conjugation between phenoxy groups and PDI chromophore and led to

special features in spectroscopic properties. The energy barrier for the interconversion between 2 atropo-enantiomers (*P*) and (*M*) of **96** was determined using temperature-dependent ^{1}H NMR. The results showed a higher barrier for **96a** with a short linker. For **96b-d** there are only slightly higher energy barriers than acyclic reference **97**. Therefore, to achieve PDI with permanent planar chirality, diagonally bridged linkers are more desired.[95]

The first example of isolation of two stable atropisomers of core twisted PDIs was presented in 2007.[109] To restrict the interconversion of the two twisted enantiomeric conformers of PDI (*P* ↔ *M*), two macrocycles were introduced using oligo(ethelene glycol) bridges **98** following previously developed procedure to yield **99** (Scheme 2). Then, (*P*) and (*M)* isomers could be separated on chiral HPLC column. Even though both imide substituents of **99** were (R)-configured, two epimers showed a mirror image relation in CD spectra. This pseudo-enantiomeric behavior indicated that the CD signals came mostly from the planar chirality of PDI surface. In agreement with CD study, the optical rotation values of +6600 and -6600 were obtained for two diastereomers. Thus, chirality along the polyaromatic system greatly dominated point chirality. By comparison of experimental and simulated CD spectra, conformation of both diastereomers of **99** could be assigned. Conformational properties of these diastereomers were also studied using temperature-dependent ^{1}H NMR, with the results showed strongly restricted inversion of the core PDI.
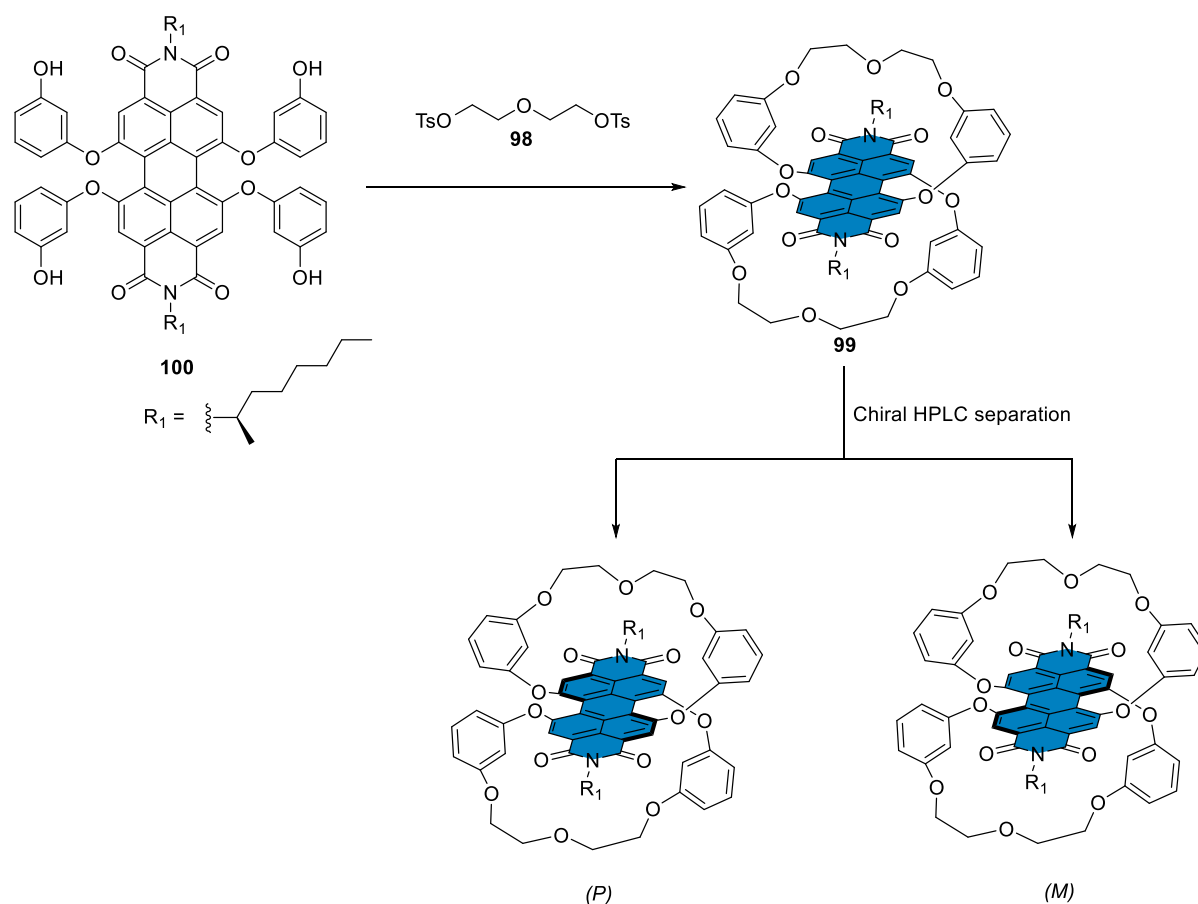
Scheme 2. Synthesis and separation of atropo-diastereomers of PDI **99**. Adapted from reference.[109]

Stabilization of PDI atropo-enantiomers could be achieved with a simpler approach. Using only one covalent linker in 1,7-substituted PDIs, Würthner *et al.* were able to separate two stable enantiomers or macrocycle **101** (Figure 27a).[110] Their chiral self-recognition and self-discrimination were realized using concentration-dependent UV-Vis absorption spectra and ^{1}H NMR. The association constant for the recognition of two molecules owning the same stereochemistry was estimated to be one order of magnitude higher than molecules with different chirality. Having the same configuration, the π-π stacking in the case of homochiral

dimer was much greater. Thus, in racemic mixture of **101**, monomer tend to form homochiral aggregate rather than heterochiral one (Figure 27b).

a)

b)

Homochiral dimeric aggregate Heterochiral dimeric aggregate
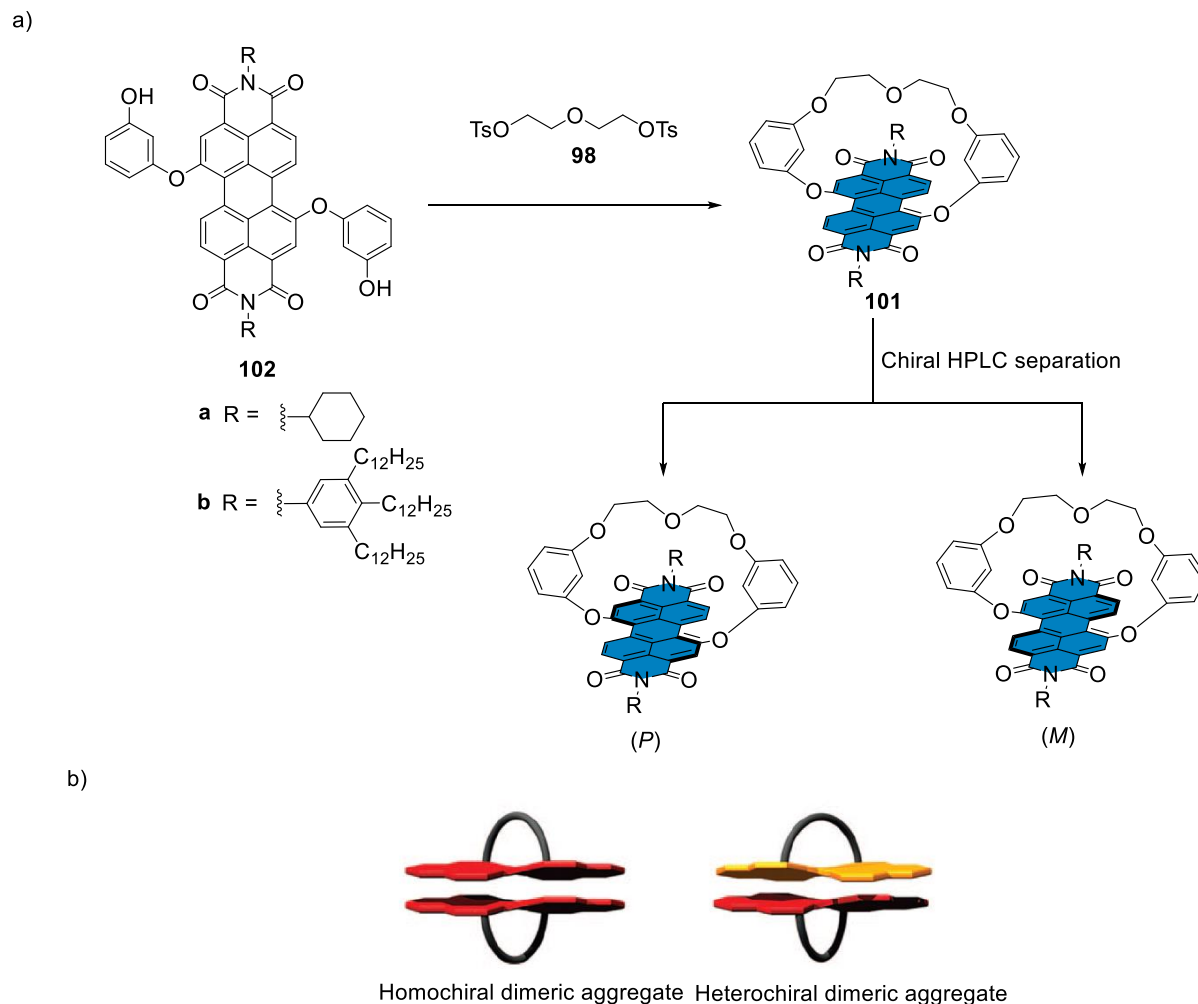
Figure 27. (a) Synthesis and separation of atropo-enantiomers of PDI **101**. (b) Dimeric assembly of **101**. Adapted from reference.[110]

Taking advantages of this self-recognition, supramolecular structures with different properties have been prepared using chiral pure or racemic starting monomers.[111] In racemic homochiral dimers, building block formed a soft columnar crystalline phase of higher thermodynamic stability, whereas for enantio-pure monomer, a lamellar liquid crystalline

phase was observed. Force field calculations supported that nano segregation and interaction between the bridges were important for the difference of condensed phase. Alternation of *MM* and *PP* homochiral dimers in racemic mono-bridged PDIs allowed better nanosegregation as well as more dense packing of building blocks. In contrast, for enantio-pure mono-bridged PDIs, steric shielding of the bridges prevented nanosegregation, resulting a lamellar organization with high fluidity.[111]

The influence of bridge linker length on the assembly of chiral PDIs was also examined.[112] Upon increasing the length of the linker, CD signal decreased in intensity, which indicated the decrease in average twisting angle of PDI core. The larger Stockes shifts in fluorescence spectra observed for compounds with longer linkers also suggested more relaxation in these molecules during excitation. Dimerization constants increased with increasing linker length was in good agreement with increasing π-π stacking in less twisted PDI derivatives. However, the difference between $K_{D \text{ (homochiral)}}$ and $K_{D \text{ (heterochiral)}}$ decreased dramatically. This behavior could be explained by induced-fit dimerization mechanism as well as the possible interconversion between two atropo-enantiomers for compounds with longer linkers.[112]

The applications of chiral PDIs could be extended to deracemization of carbohelicenes when twisted PDI was incorporated into the design of cyclophane.[113] With aliphatic tethered linker to block the configuration of PDI monomer, chiral PDI cyclophane **103**-*MM* and **103**-*PP* could be synthesized. The electron-poor nature of PDIs rendered the cavity of cyclophane **103** to an excellent host to electron-rich helicenes. The binding affinity of **103** for [4]-helicene could reach nanomolar range. For [5]-helicene, its racemization barrier is higher than 100 kJmol^{-1}. Therefore, enantiomers could be separated and stable at room temperature for several

hours. Since the [5]-helicene guest was sandwiched between two PDI surfaces, the cyclophane host would prefer to bind to the helicene with the same helical chirality. The enantiomer with the opposite configuration would be left in solution. Separation of the mixture containing guest and host-guest complex allowed enantiomeric excess (*ee*) of the guest to be enriched.
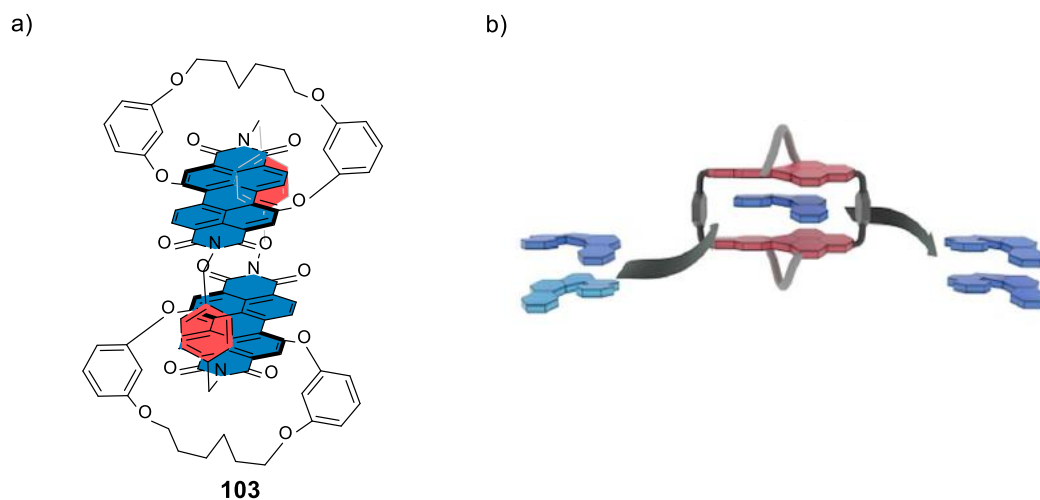
Figure 28. (a) Structure of homochiral PDI cyclophane **103**. (b) Deracemization of [5]-helicene using cyclophane **103**. Adapted from reference.[113]

Even though the tethered covalent bridge is excellent in maintaining the conformation of twisted PDIs, this strategy suffers from the difficulty in further chemical functionalization of the PDI core.[114] To overcome this challenge, a rigid 2,2'-biphenol bridge has been used to block one bay area of PDIs (Scheme 3). The racemate of **104** could be separated with chiral HPLC to yield enantiopure product. Two positions left at bay area were easily further functionalized by aromatic nucleophilic substitution of chlorines. The free activation enthalpy for the racemization of **104** was estimated to be 98.5 kJmol^{-1} at 323K. Although this method did not completely block the interconversion, the rotation barrier of the core PDI was significantly increased in comparison with previously reported PDIs bearing large substituents.

Using this strategy for disubstituted PDIs, Nuckolls *et al.* was successful in synthesizing chiral PDI cyclophane.[115]
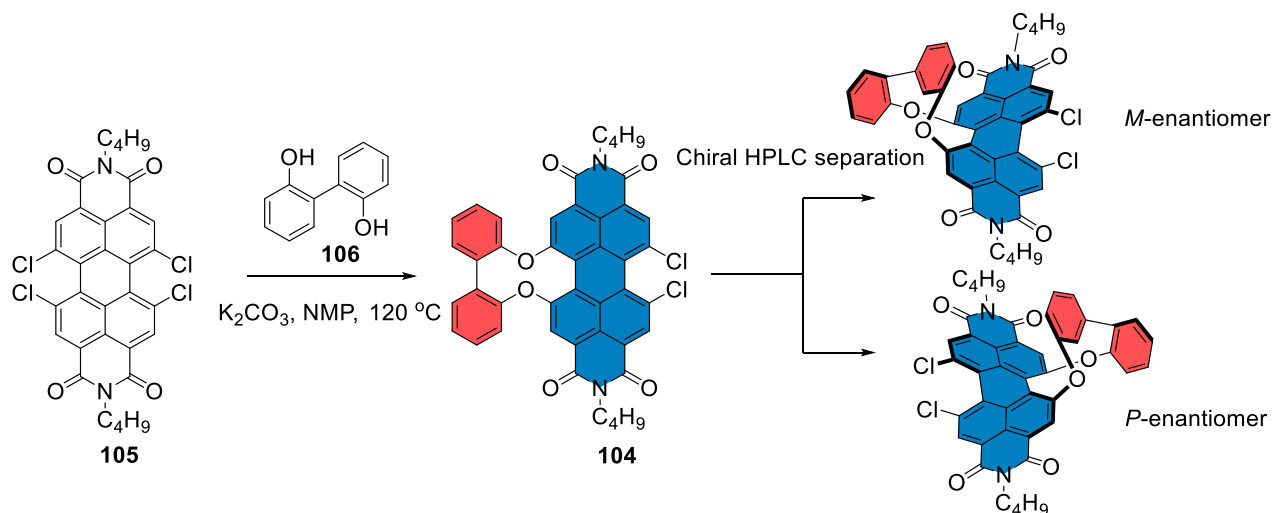
Scheme 3. Synthesis and separation of atropo-diastereomers of PDI **104**. Adapted from reference.[109]

Despite the fact that methods for preparation of enantiopure PDIs have been developed, their applications are barely studied. Most of the examples are limited in the context of supramolecular chemistry. Therefore, other potential applications of chiral PDIs, especially in asymmetric catalysis, could be of interest to be explored in the future.

1.6.   Thiol-Mediated Uptake

Being one of the most important organelles of cell, cellular membrane plays vital roles in cell metabolism. Its primary functions include protection of cells from their outer environment and regulation of cell signaling. These functions relate to controlling the exchange of matter and

information between the cell and its surrounding.[116] Cellular uptake, therefore, is a very important function of cell membrane. Cellular uptake or transport of substances through the cell membrane might take place under different mechanisms. While most small nonpolar compounds can simply diffuse through the phospholipid bilayer by hydrophobic effect, transport of polar and big molecules requires energy and mostly is taken care of by transmembrane proteins. For some small cargos like ions or carbohydrates, transport occurs through transmembrane protein channels. Transportation of larger molecules usually goes through endocytosis, which may involve receptor recognition in the first place. Due to the diversity and complexity of transmembrane protein structures, to date, there is still a lot of missing information to complete the picture of cellular uptake.[117–119] Recent reports have shown that membrane proteins could participate in cellular uptake of various cargos using disulfide bonds or free thiols present in their structure.[120] Even though the abundance of disulfide and sulfhydryl groups in protein structures has been noticed, their main functions were considered to only relate to protein folding and maintaining protein integrity for a long time.[121] Not until the functions of some Thiol-disulfide Oxidoreductases were discovered, the disulfide bonds are believed to have significant roles in protein functions. The disulfide bonds and free thiols of membrane proteins have been proved to be the critical element in cellular uptake of various viruses and biomolecules.[122–130] These observations inspired the designing of artificial systems taking the advantages of cell surface thiols to internalize into cytoplasm.[120,131] Thus, a totally new research direction based on this novel cellular uptake mechanism refers as "Thiol-mediated uptake" has been developed in the last decade. The most recent definition considers "Thiol-mediated uptake" as the observation that "(i) cellular uptake reliably and often dramatically increases in the presence of chalcogenides (or mimics) capable of dynamic covalent exchange, usually disulfides, and that (ii) this uptake can be inhibited with thiol-reactive agents."[131] Despite more and more functional systems based on this uptake mechanism

have been exploited to deliver a wide range of cargos into the inner cellular environment (section 1.6.2), there are very little detailed information at the molecular level about how thiol-mediated uptake takes place. In a review covering early studies on this topic, Gait *et al.* proposed three models for the interactions of thiolated biomolecules with exofacial thiols and subsequent uptake process (Figure 29).[120]
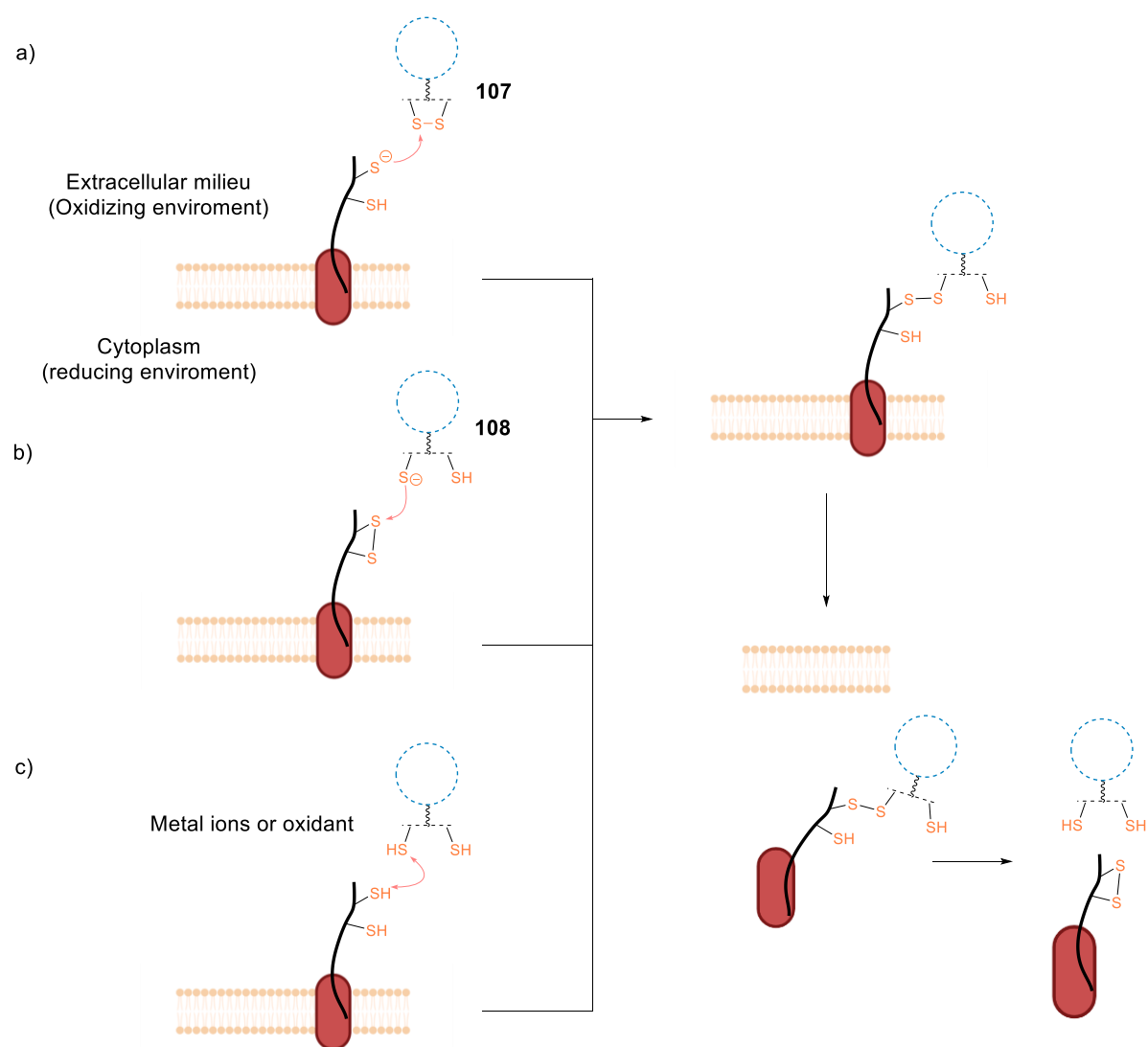
Figure 29. Proposed mechanisms of thiol-mediated uptake of biomolecules (blue circles) upon interactions with exofacial thiols of membrane proteins (red rods). (a) Reactive thiolates at the cell surface cleave disulfide bonds in biomolecules. (b) Thiol-reactive functional groups in

biomolecules could attack disulfide bonds within cell surface proteins. (c) Reactive thiols in biomolecules and membrane proteins could form a disulfide bridge assisted by metal ions or other oxidizing agents in the media. The mixed disulfide complex could further internalize and be reduced in the inner cellular compartment to release the biomolecules. Adapted from reference.[120]

The most likely mechanism starts with the nucleophilic attack of Cysteine side chain in membrane protein on a disulfide bond within the cargos to form a covalent conjugate (Figure 29a). If the free thiol presents in structure of cargo, similar reactions with disulfide groups at cell surface will take place (Figure 29b). Another possibility is the formation of a disulfide bridge between cargo and target protein from free thiolates under the present of metal ions or oxidative agents (Figure 29c). Either process would result a cargo-protein complex which could further internalize into cytoplasm by endocytosis, fusion or direct translocation.[120,132]

To shed light on this complex mechanism, Adibekian *et al.* performed proteomic analysis to identify target proteins of thiol-mediated uptake.[133] With a CSSC dihedral angle of 27°, the disulfide ring tension in Asparagusic acid (AspA) is significant. Therefore, AspA is highly reactive toward exofacial thiols on cell membrane and was known to be one efficient thiol-mediated uptake transporter (section 1.6.2).[134] Equipped with an Asparagusic acid ring, probe **109** could internalize into cytoplasm via thiol-mediated uptake (Figure 30). As described previously, the first step in uptake mechanism required the formation of transporter-target proteins complexes. To identify these complexes, the cell lysates were treated with biotin azide. Click products were enriched over streptavidin beads and subjected to LC-MS/MS analysis after digestion (Figure 30b).

a)

109

b)

1. Cell lysis and Click reaction with biotin azide
2. Enrichment with streptavidin beads
3. Tryptic digest and LC-MS/MS analysis

Target proteins
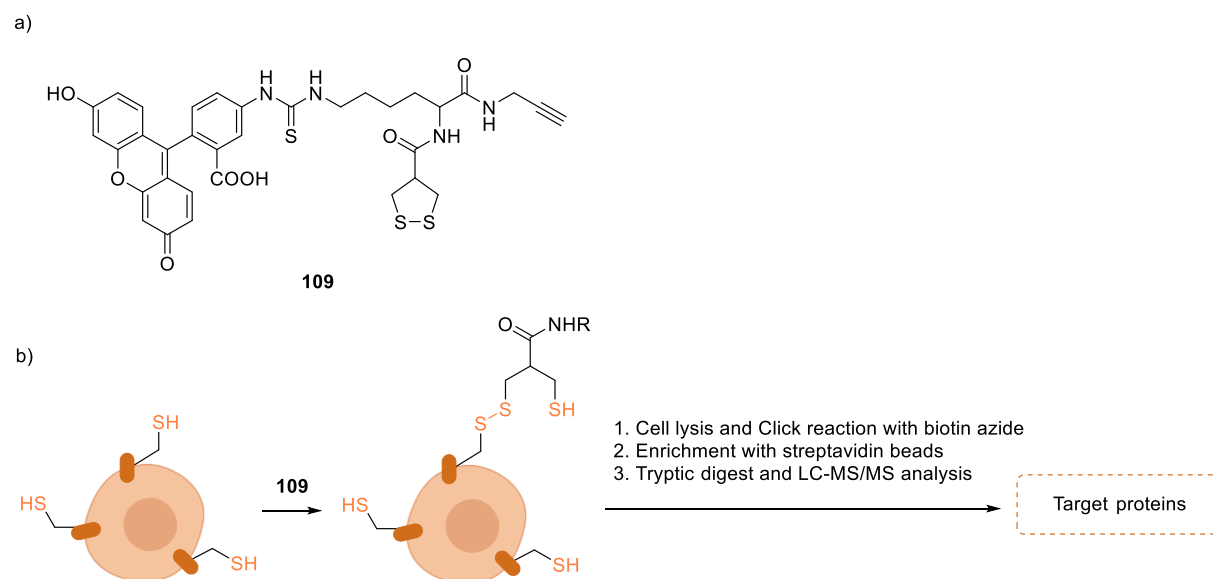
Figure 30. (a) Structure of AspA probe **109** for proteomic studies. (b) Layout of the chemical enrichment experiment coupled with protein identification by LC-MS/MS. Adapted from reference.[133]

Five hit proteins were identified, included Transferrin receptor protein 1 (TFRC), Cytosekeleton-associated protein 4 (CKAP4), Scavenger receptor class B member 1 (SCARB1), Chloride intracellular channel protein 1 (CLIC1) and Vesicle-associated membrane protein-associated protein A (VAPA). Among these targets, TFRC was considered the most important because of its abundance on cellular membranes. To confirm the results obtained from proteomic studies, TFRC was knocked down or overexpressed in cells. As expected, TFRC knockdown led to a >75% decrease in uptake efficiency in comparison with wild-type cells. In contrast, overexpression resulted about 45% increase in uptake. Finally, the binding site of AspA was determined to be C556 and C558 located on the surface of TFRC.[133]

After the identification of some potential target proteins, understanding of uptake mechanism was not easier due to the dynamic nature of thiol-mediated uptake.[131] The

complexity of thiol-disulfide exchange involving in thiol-mediated uptake makes this process extremely difficult to follow in real-time. However, with data obtained from thiol-exchange affinity columns and exchange kinetics, each step of thiol-mediated uptake could be partially revealed. For selenium-based thiol-mediated uptake transporter, a more detailed uptake mechanism has been proposed inspiring by molecular walkers.[135,136] Diseleno lipoic acid (DiSeL) transporter could act as a molecular walker to internalize into cytosol by moving along transmembrane disulfide tracks in membrane proteins through a cascade of exchange reactions (Figure 31). Micellar pore formation next to target proteins could facilitate the uptake of large cargos.
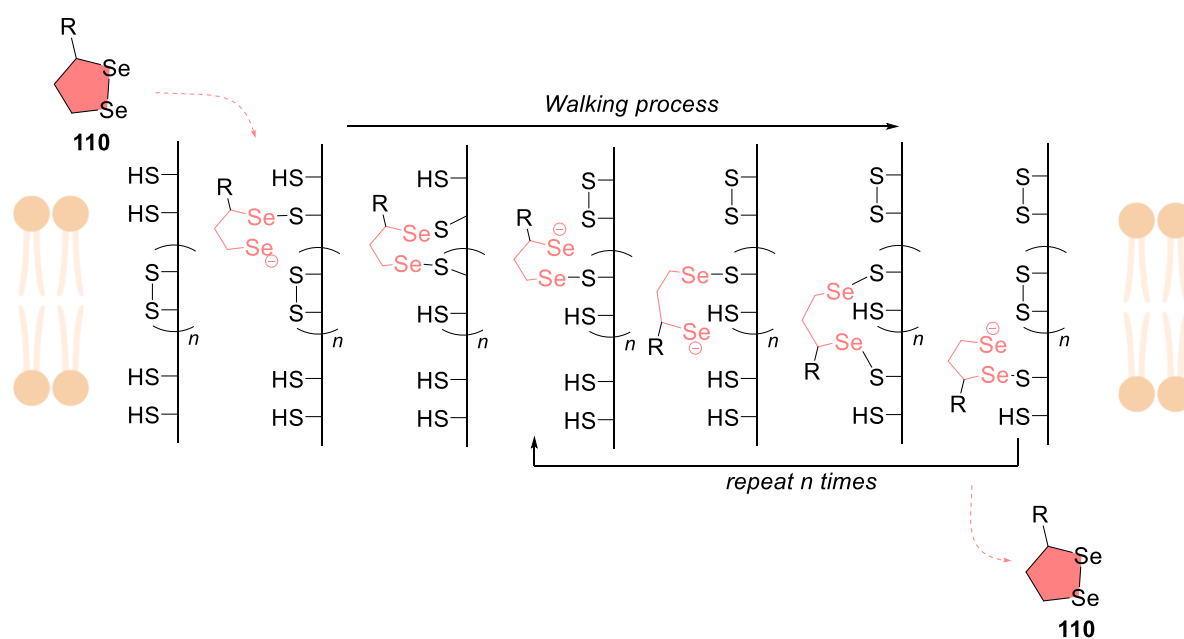
Figure 31. The hypothesized uptake mechanism of DiSeL-transporter **110**, with **110** as molecular walker walking along transmembrane disulfide tracks in membrane proteins. Adapted from reference.[135,136]

While this mechanism could perfectly explain the activity of selenium-based transporters, with dithiolane transporter likes AspA this process is not likely since the acidity of thiols is much less than selenols. It was proposed that transporters like AspA would be covalently linked to the membrane proteins and accumulated in endosomes with partial release afterward.[135]

Based on available data of thiol-mediated uptake in biology and synthetic transport systems, a recent perspective on this topic suggested possible cellular targets for this uptake mechanism.[131] Except already mentioned TFRC and CLIC1, other potential membrane proteins with disulfide tracks or free thiols at accessible positions included TMEM16F, TRPA1, $Ca_v1.1$, EGFR or Protein Disulfide Isomerases (PDIases). Even though these early studies have put some basic for thiol-mediated uptake, there are still a lot of questions should be answered to understand this appealing process at molecular level.

1.6.1. Thiol-Mediated Uptake in Biological Processes

As mentioned previously, thiol-mediated uptake was inspired by early observations of the contribution of thiol-disulfide exchange to different biological processes. The majority of thiol-mediated uptake evidence in biology links to the internalizations of viruses into cells with the most well-established example is cell-entry of HIV virus.[137] The envelope glycoprotein gp120 of HIV virus is responsible to attach the virus to the host cell by binding to CD4 receptor (Figure 32A).
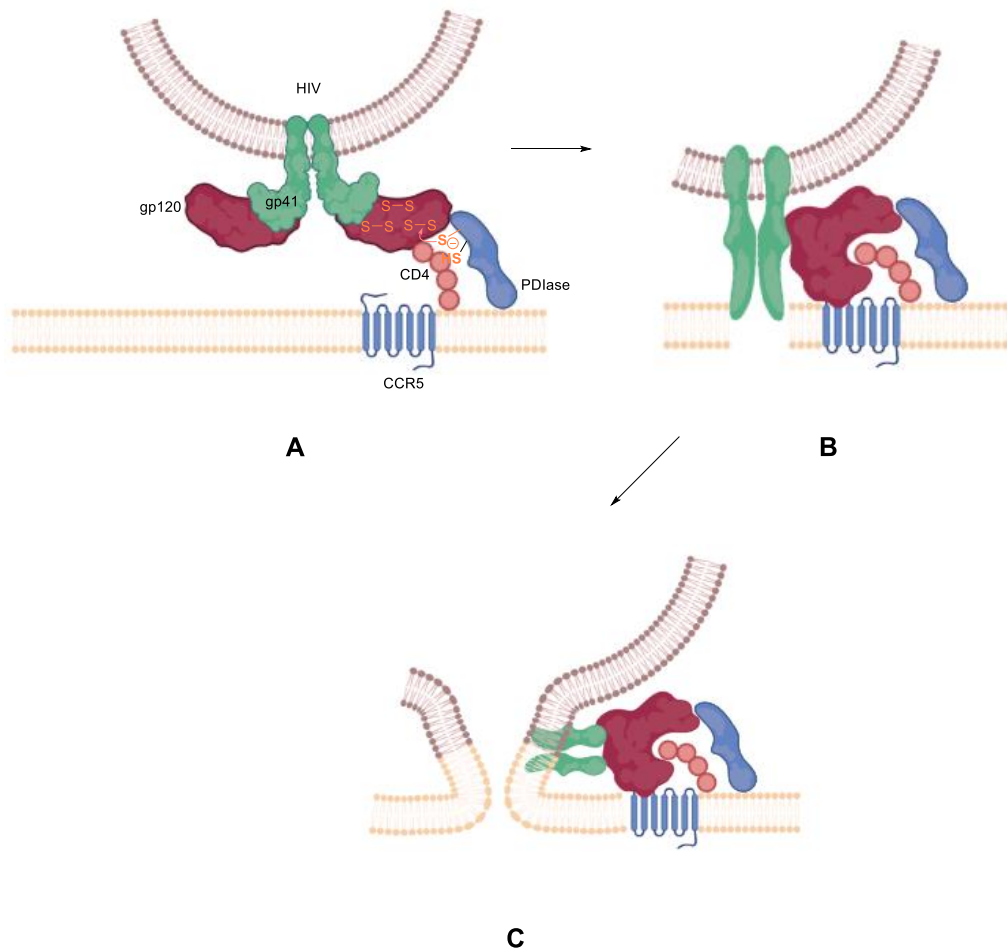
Figure 32. Cell-entry mechanism of HIV virus by thiol-disulfide exchange between PDIase and gp120 (A, B) and subsequent membrane fusion (C). Adapted from reference.[131]

CD4 also has a binding site for PDIase. Thus, the interactions of these proteins during infection lead to the formation of PDIase-CD4-gp120 complex. In this complex, PDIase reduces disulfide bonds which stabilize structure of gp120 and induces conformational changes in gp120. These changes increase the interaction of gp120 with co-receptors and with a small loop of gp41. As the results, gp41 is elongated and the small loop forms the N-terminal fusion peptide that inserts into the cell membrane (Figure 32B). The distance between virus and host

cells decreases and their membranes are fused by helix bundle formation. Since PDIase plays a key role in this mechanism, inhibition of PDIase activity with thiol blockers such as 5,5-dithio-bis(2-nitrobenzoic acid) (DTNB) efficiently reduces infection.[131,137]

Similar to HIV virus, Sindbis virus (SIN) membrane fusion is also mediated by reduction of glycoprotein disulfides at the cell surface.[125,130] When SIN is binding to cell membrane receptors, the conformation of viral spike protein changes and its key disulfide bonds are exposed to thiol-disulfide exchange reactions. As a result, the structure of spike protein is reorganized to facilitate membrane fusion. Again, treatment of the host cells with thiol blocking reagent DTNB reduces cell-entry of SIN while infection increases in the presence of disulfide reducing agents like 2-mercaptoethanol.[125] Thiol-mediated uptake has been found to be responsible for cell-entry of many other viruses, such as Newcastle disease virus,[124] Baculovirus,[138] Murine Leukemia virus,[139] Lactate Dehydrogenase-Elevating virus,[140] and Hepatitis viruses.[141] Therefore, utilization of thiol blocking reagents could be a solution for the treatment of viral diseases.[131]

Cell surface sulfhydryls and thiol-disulfide exchange were also believed to be important for cytotoxicity of some toxins. Using some membrane-impermeable sulfhydryl inhibitors, Ghani *et al.* have shown that the uptake of Diphtheria toxin (DT) was mediated by exofacial thiols.[122] Diphtheria toxin is a 62 kDa protein exotoxin produced by *Corynebacterium diphtheriae.*[142] It has been used widely in cancer therapy in the context of immunotoxins.[143] DT is a single chain peptide constructed from two functional fragments. The A-chain at the N-terminus contained a catalytic domain that blocks protein synthesis in cells. The B-chain at the C-terminus is responsible for binding to cell receptors. It also plays an essential function in the translocation of the A-chain across the membrane of early endosomes. To enable the

translocation of the A-chain, the interchain disulfide bonds of DT should be cleaved. The reduction of this disulfide bond was proposed to be catalyzed by free thiol on cell surface. Thus, blocking sulfhydryls by thiol reactive reagents should abolish DT toxicity. As expected, when the cells were treated with DTNB or p-chloromecuriphenylsulfonic acid, cytotoxicity of DT was remarkably reduced.[122,143]

These examples are just the tip of the iceberg. There are probably many more biological events related to thiol-mediated uptake. However, the complex structures of proteins involved in these processes and the dynamic nature of thiol-disulfide exchange make it difficult to reveal the role of exofacial thiols and disulfides. In order to prove thiol-mediated uptake, most studies rely on the inhibition experiment with cell-impermeable thiol blocking reagent like DTNB **111** (Figure 33).
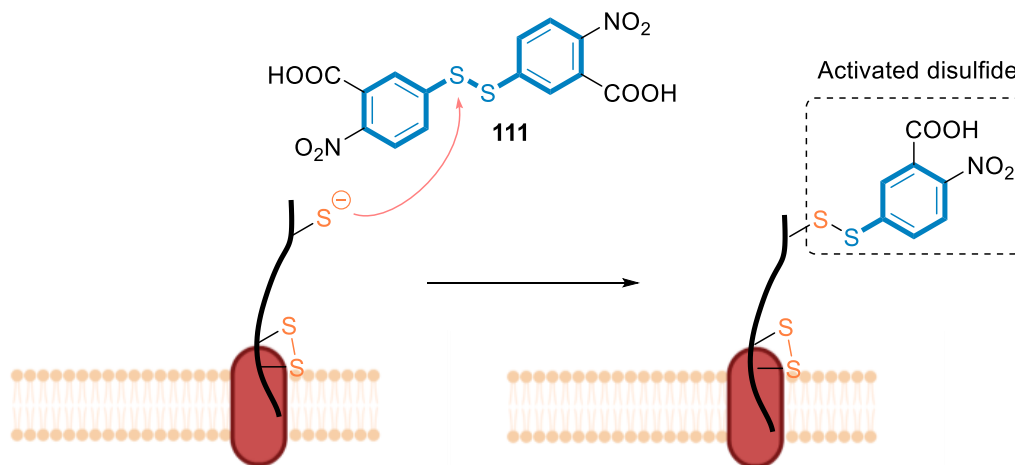
Figure 33. Reaction of cell membrane thiols with DTNB which results product with an activated disulfide bond.

Despite being the only well-established thiol-mediated uptake inhibitor, DTNB has poor reactivity and usually shows effect only at high concentrations. Besides, the disulfide products obtained after the exchange reactions are highly reactive and could easily participate in further thiol-disulfide exchange (Figure 33). Therefore, the results from DTNB inhibition are not always trustworthy, especially in cases when thiol-mediated uptake couples with several other uptake mechanisms.[132,144] For these reasons, to have better understanding of thiol-mediated uptake, the need of developing more efficient inhibitors is highly desired.

1.6.2. Thiol-Mediated Uptake Transport Systems

The development of thiol-mediated uptake transporters started from a general observation that molecules are easier to be uptaken when a thiol reactive functionality was integrated into their structures. One of the first studies was reported by Ryser *et al.* in 1990.[145] An undegradable polylysine was covalently linked to a radioiodinated tyramine through a disulfide bridge and its cellular uptake was monitored over time. Uptake kinetic showed that the uptake of the conjugate was very rapid and efficient. The missing of the lag phase in the release of radioiodinated residue proved that disulfide cleavage occurred spontaneously at the cell surface. This observation was consistent with inhibition experiment, when the cleavage of disulfide bonds was significantly suppressed after treatment of the cells with DTNB.[145] Behr *et al.* introduced the first thiol-mediated uptake delivery system for gene transfection in 1995.[146] Transfecting particles were prepared by mixing lipospermine, DNA and a thiol-reactive derivative of phosphatodylethanolamine (PEA). This novel system led to several order of magnitude increasing in transfection yields. Transfection efficiency was correlated well with the reactivities of thiol-reactive fragments of PEA derivatives. The contribution of thiol-mediated uptake, in this case, was believed to be the reactions between the thiol-reactive

functions of the particles with the sulfhydryls to attach them to the cell surfaces. Subsequent absorptive endocytosis allowed the particles to internalize into cells.[146] While examined the cellular uptake of some cell-penetrating peptides (CPPs) containing disulfide bridges, Sagan *et al.* found that these CPPs could react with thiols of membrane proteins and form covalent bonds.[147] This reactivity increased the amount of peptides which bound to cell membrane and facilitated their internalization.

These early studies were followed up by more rational designs of delivery systems utilizing thiol-mediated uptake. One of the most promising thiol-mediated uptake transporters is cell-penetrating poly(disulfide)s (CPDs). CPDs like **112** could be synthesized under the mildest conditions (Figure 34).[148] Easily to prepare, various cargos could be attached to the polymer chain shortly before delivery. A thiol group in the structure of the cargos **113** would initiate a disulfide exchange cascade of monomer **114** to grow the disulfide polymer chain. The polymerization was terminated with a thiol blocking reagent such as **115**. The structure of the polymers could be modified by simply applying modification at monomer level.[149–151] For monomer **114**, a guanidinium functionality was introduced to couple CPPs uptake mechanism with thiol-mediated uptake. CPDs **112** was shown to be very efficiently uptaken by cells. The polydisulfide chain allowed **112** to be degraded and release cargos upon entering the cytoplasm due to high concentration of glutathione (GSH) inside cells. Thus, cytotoxicity was significantly lower in comparison with standard CPPs.[148] Using this transporter, cargos as big as streptavidin could be delivered to the cytosol with minimal endosomal capture.[149,152] CPDs were also tolerated for delivery of other advanced systems such as artificial metalloenzyme,[153] quantum dots,[154] nanoparticles and proteins.[155–160]
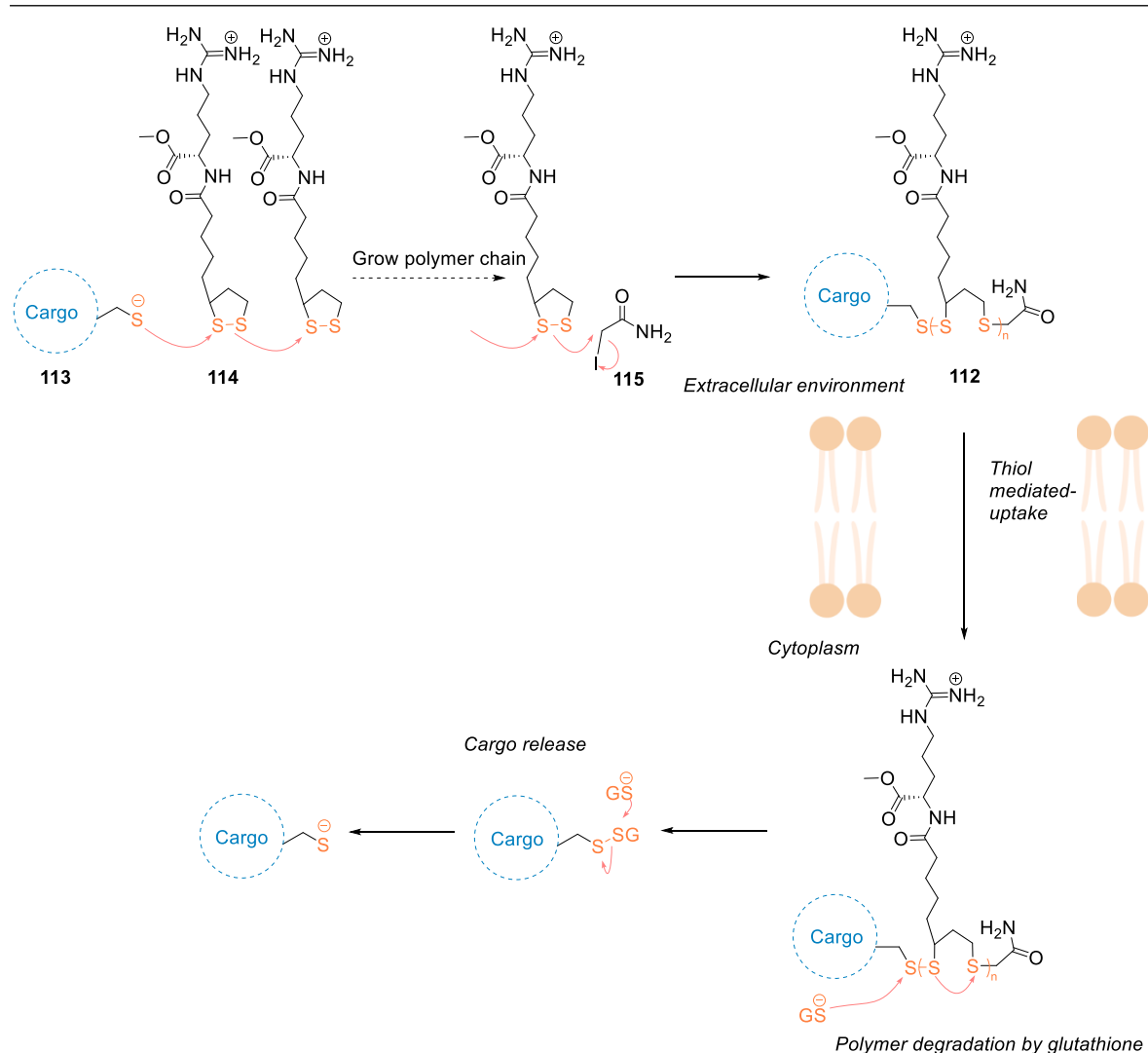
Figure 34. Polymerization of monomer **114** to form CPD **112** and CPD degradation inside the cytoplasm. Adapted from reference.[148]

The power of thiol-mediated uptake was demonstrated through a series of small molecule transporters. Even though they are much smaller in comparison with CPDs, their uptake activities have been shown to be as good as or even superior. The attention was first focused on the correlation between ring strain in cyclic disulfide compounds and their uptake efficiency. A fluorescent probe was equipped with cyclic disulfides with different tension (Figure 35).[134,161] As expected, cellular uptake increased with increasing ring tension in the

disulfide rings. From dithiane ring **116** with the CSSC dihedral angle 62º to 35º in lipoic acid derivatives **117**, almost double fluorescent intensity was recorded. Even a small increase in ring tension of AspA derivative **118** caused significant improvement in cellular uptake.[134] This trend was very consistent with Epidithiodiketopiperazine **119** (ETP) was the best transporter in this series. Having the CSSC dihedral angle close to 0º, the ring tension in ETPs reach the maximum. Ring-opening disulfide exchange in ETPs occurs much faster and results more than 20 times increase in uptake compared with AspA transporter.[161]
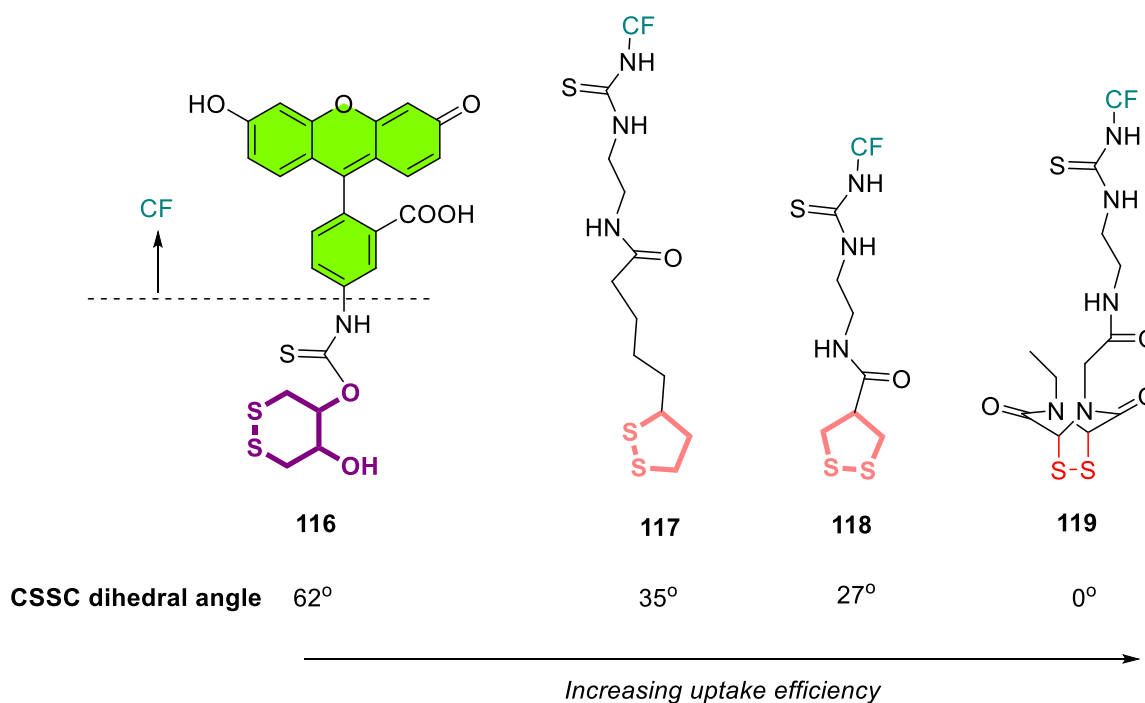
Figure 35. Cyclic disulfide transporters and their CSSC dihedral angle. Adapted from reference.[131,134,161]

Considering faster thiolate-diselenide exchange reactions compared with thiolate-disulfide, replacement of sulfur by selenium has been employed to improve the activity of existed thiol-mediated uptake transporters.[136] Even for the relaxed linear diselenides, their

uptake activity surpassed ETPs. Not surprisingly, decrease CSeSeC dihedral angle in diselenolipoic acid (DiSeL) further improved uptake efficiency.[136,162] Tackling the ring tension from a different perspective, Wu *et al.* introduce CXC cyclic γ-turn peptides as potential thiol-mediated uptake transporters (Figure 36).[163,164] The 11-membered ring in cyclic γ-turn peptides **120** experienced significant Prelog strain. Thus, the linear CXC motif was more oxidation resistant to form the ring-closed disulfide in comparison with other popular Cysteine-rich peptide motifs in biology such as CXXC or CC. Because of that, upon ring-opening, cyclic CXC tended to form mixed disulfide bonds with other thiols. The doubly bridged disulfides created between transporter and transmembrane proteins could explain the superior transport activity of cyclic CXC γ-turn peptides since the attachment of transporter to cell membrane for further translocation was greatly enhanced.[163,164]

120
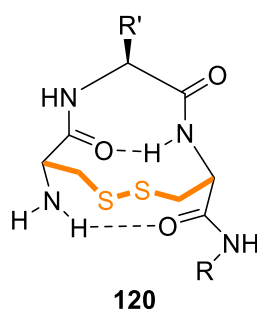
Figure 36. General structure of cyclic disulfide CXC γ-turn peptides.

The dynamic nature of thiol-disulfide exchange in thiol-mediated uptake was exploited to its maximum with the introduction of benzopolysulfane (BPS) transporter.[165] In solution, BPS **121** created a library of BPSs having different sulfur ring sizes, with pentasulfide **121** is the most stable, followed by trisulfide **122**. In the presence of thiolates and disulfides, the

library could be extended to the extreme with the formation of BPS oligomers together with acyclic members (Figure 37).
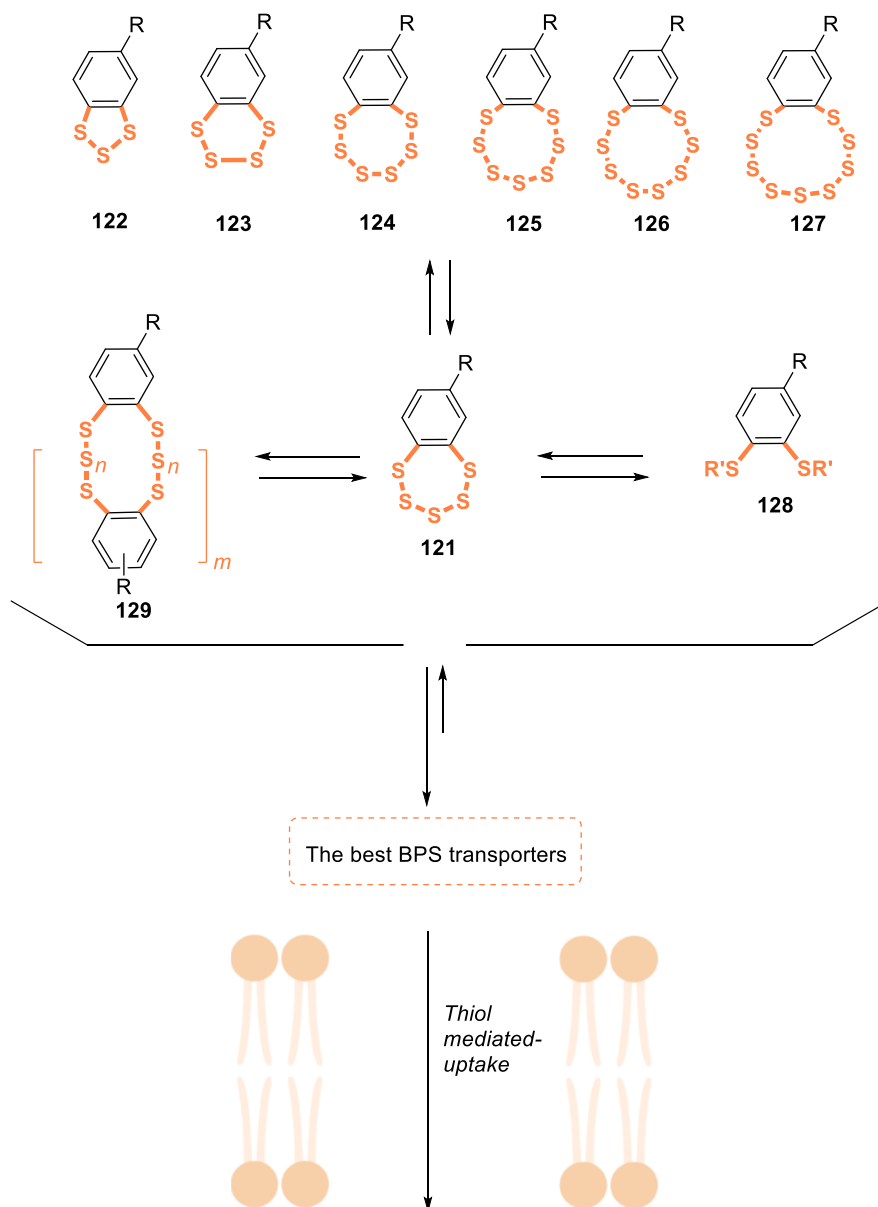
Figure 37. Library of transporters created by dynamic covalent exchange of BPS **121**, with selection for the best transporters to be uptaken. Adapted from reference.[131]

This rich dynamic covalent network allowed cells to select the best transporter within the library for uptake. Re-equilibrium of the whole system pushed for the amplification of the best transporter. This reactivity made BPS **121** the best small molecule thiol-mediated uptake transporter known to date.[131,165]

Based on these small transporters, more advanced delivery systems have been developed. For example, cell-penetrating streptavidin bearing BPSs has been introduced for delivery of multiple cargos at the same time.[166] The potential of using multivalency to transport giant cargos through lipid bilayer membrane was also addressed with versicles containing small transporter at their surface or oligomers of cyclic oligochalcogenides.[167,168] Being non-toxic and very versatile, thiol-mediated uptake is one of the best methods so far to cross the cellular membrane.

1.7. Thiol-Reactive Reagents

The roles of Cysteines in living organisms are essential. As mentioned previously, thiol-disulfide exchange helps to maintain protein structures. Cysteine derivatives such as glutathione protect cells from oxidative stress. The presence of Cysteines in enzymes is critical for their functions. In addition, Cysteines participate in complexing various metals in a broad range of proteins.[169–171] Since the functions of Cysteine are mostly based on the nucleophilicity of the sulfur atom at the side chain, a wide variety of thiol-reactive reagents has been developed in the last decades to selectively and efficiently target sulfhydryl group of Cysteines. These probes have been extensively used to detect and modulate Cysteines which resulted various useful protein inhibitors, sensors or chemical proteomic probes. Numerous reactions have been employed to access Cysteine reactivities in mildest conditions, for instances, Michael addition,

cyclization, disulfide cleavage, metal complexation or oxidations.[170] Some popular probes are listed in Figure 38. Since the utilization of such probes has been review recently,[169–171] In this section, only some probes related to the content of this thesis would be discussed.

130

Haloacetamides

131

Ethynyl benziodoxolones

132

Chloromethyl triazoles

133

Asparagusic acid

134

Michael acceptors

135

Maleimides

136

Vinyl sulfones

137

Vinyl sulfones

138

Propargyl amides

139

Acyloxymethyl ketones

140

Halomethyl ketones

141

Sulfonate esters

142

Activated aryl halides

143

Alkylsulfonyl benzothiazole

144

Bromobenzylphosphonate

145

Palladium reagents

Figure 38. Some common thiol-reactive reagents. Adapted from reference.[171]

As an attempt to find a less toxic reagent for Cysteines cross-linking in proteins which could avoid "dead-end" modification of lone thiols, Agar *et al.* introduced cyclic thiosulfinates in 2018.[172] A thiolate could trigger ring cleavage in cyclic thiosulfinate **146** to yield a disulfide

bond and a sulfenic acid moiety (Figure 39b). The resulting terminal sulfenic acid could participate in further disulfide formation after condensation with another thiolate in close proximity. In comparison with the more popular cyclic disulfide **147**, the cross-linking process with the alternative thiosulfinate was much favored. For **147**, after ring opening, oxidation of sulfhydryl group to sulfenic acid was required for disulfide formation (Figure 39a).
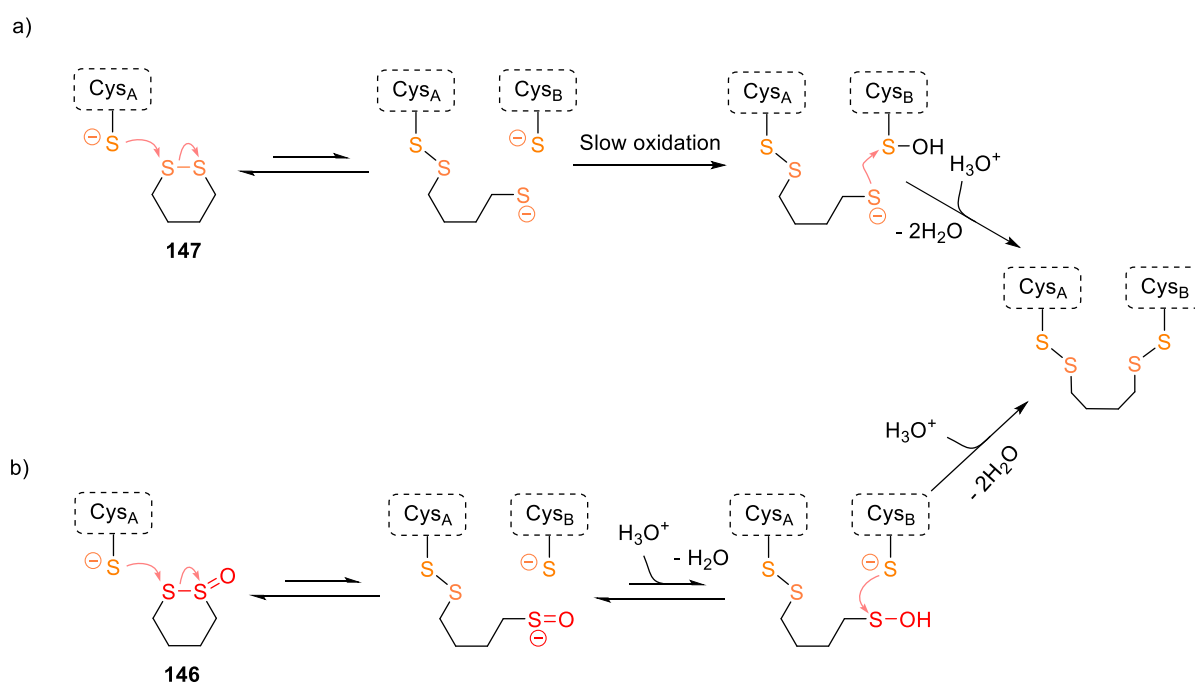
Figure 39. Reaction of (a) cyclic disulfide **147** and (b) cyclic thiosulfinate **146** with two adjacent Cysteines. Adapted from reference.[172]

Since the oxidation step was the rate-determining step and extremely slow ($t_{1/2} = 10$ days), cyclic thiosulfinate was expected to be more than 10^4 times efficient to cross-link adjacent Cysteines. Applying this novel thiol-reactive probe, the authors were successfully to cross-linked Cu/Zn-superoxide dismutase (SOD1) monomers to form dimeric structure with minimal side reactions. This method could be used even in living cells. The most important advantage

for cyclic thiosulfinates was that the new covalent bridges were formed based on disulfide bonds which could easily participate in thiol-disulfide exchange. Thus, the initial structure could be restored and led to low cytotoxicity.[172]

Moving from cyclic thiosulfinate to cyclic thiosulfonate – the more oxidized derivative of cyclic disulfide, Law *et al.* have shown that they were excellent probes for disturbing disulfide bonds in proteins.[173] Similar to the less oxidized alternatives, cyclic thiosulfonates like **148** could react with thiolate to form a disulfide bond and release sulfinate functionality (Figure 40). The nucleophilicity of sulfinate group allows it to attack nearby disulfide bonds to yield a linear thiosulfonate and a free thiolate which could continue to exchange with other disulfides. Anticancer activity of sulfinate derivatives was believed to relate to its ability to cleave disulfide bonds in Epidermal Growth Factor Receptor (EGFR) which disrupted EGFR structure.[173]
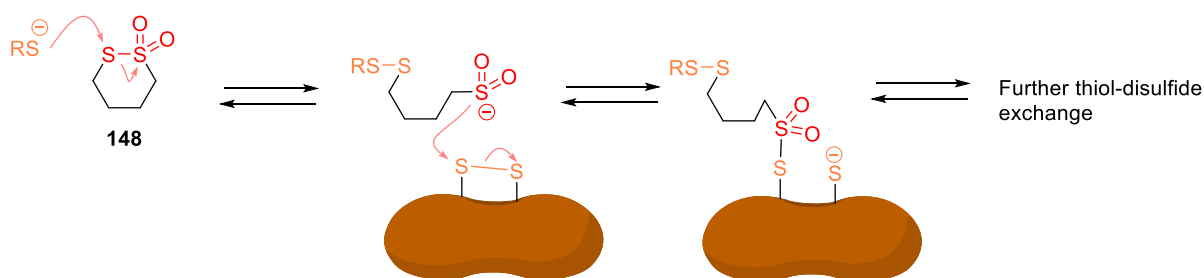
Figure 40. Reaction of cyclic thiosulfonate **148** and thiolate results sulfinate group which could disrupt disulfide bonds in proteins. Adapted from reference.[173]

Apart from reversible thiol-reactive reagents, irreversible thiol-blocking agents have also been actively used to modify Cysteines in proteins. Even though "dead-end" modification of proteins usually leads to high toxicity in living systems, the great reactivity of such probes is

undeniable. Most of them show activity at concentrations much lower than toxic concentration. One class of highly selective irreversible thiol-blocking reagents for proteins modification is heteroaromatic sulfones which was first reported by Xian *et al.* in 2012.[174] In biologically relevant conditions, heteroaromatic sulfone such as methylsulfonyl benzothiazole (MSBT) selectively reacts with free thiol via nucleophilic aromatic substitution. Reactions could be completed within minutes without signs of any side reactions. Other functional groups which are popular in protein structure like amino or hydroxy groups remained inactive. In addition, the resulting product shows excellent stability toward different reductants and oxidants over a long time. MSBT was also shown to be extremely efficient in blocking free thiol residues in Glyceraldehyde 3-phosphate dehydrogenase (GAPDH).[174] Following this study, Barbas *et al.* extended the family of heteroaromatic sulfones by varying structures of the heterocycles.[175] Replacing benzothiazole ring in MSBT by phenyltetrazine or phenyloxadiazole greatly enhanced the reactivity of the probe. They were applied to couple fluorophore or polyethylene glycol (PEG) into protein structure. More detailed studies concerned other factors which could affect heteroaromatic sulfones properties such as substituents at the aromatic ring, nature of the sulfone leaving group were addressed by Martin *et al.*[176] Different modifications were utilized to access a big library of heteroaromatic sulfones with reactivity differences spread across several order of magnitudes. The best probes could be used in Cysteine proteomic studies.

Even though thiol-reactive reagents have been considered as a very important tool in chemical biology, in the context of thiol-mediated uptake, thiol-reactive reagents have been scarcely explored for developing new transporters. Their roles as universal thiol-mediated uptake inhibitors are almost untouched. Therefore, it could be of interest to repurpose existed highly reactive probes for inhibiting thiol-mediated uptake or use them for other applications.

CHAPTER 2:

OBJECTIVES

For anion-π catalysis project, the first objective is to apply peptide secondary structure to anion-π catalyst design. The rigid helical structure of α-helices will create precise relative positions between amino acid residues in peptide sequence and anion-π catalyst. A high level of conformation control will provide better understanding of structure activity relationship. On the other hand, the chiral environment of peptides around anion-π catalyst will contribute to asymmetric anion-π catalysis. For this purpose, NDI will be used as covalent linker to stabilize one turn of an α-helix. Introduction of a tertiary amine to a side chain of one amino acid residue in peptide sequence will turn on anion-π catalysis above NDI surface. Modifications in peptide backbone will give access to a library of catalysts. The structure of catalysts will be studied by various spectroscopic techniques. Their catalytic activity will be evaluated using MAHT reaction (a benchmark reaction to probe anion-π catalysis). Information obtained for catalyst structures and their catalytic activities will allow rationalizing catalyst design.

To provide a more versatile stapling method to integrate anion-π catalysts into peptide structure, PDI will also be chosen to stabilize one helix peptide turn. A larger PDI surface will enable anion-π catalysis for peptide sequences that could not operate effectively with NDI. Besides, planar chirality created by twisting PDI surface could be advantageous to improve enantioselectivity of the systems. A library of PDI-peptide conjugate catalysts will be

synthesized following the developed method for NDI. Their secondary structures will be studied by different spectroscopic techniques. To get a direct comparison with NDI catalysts, PDI catalysts will be tested using MAHT reaction. Their catalytic performance together with catalyst secondary structure will again allow rationalizing structure reactivity relationship. Finally, highly electron-deficient additives will be added to catalytic system to examine the influence of induced polarization to catalyst activities.

For thiol-mediated uptake inhibitor project, a big library of reversible and irreversible inhibitors will be developed. A wide range of thiol-reactive reagents will be chosen for the library. For reversible inhibitors, the focus will be kept on thiosulfonates and disulfide bridged γ-turn peptides because of their selective reactivity toward free thiol and low cytotoxicity. Various modifications will be applied for these scaffolds to tun their reactivity. Among irreversible inhibitors, heteroaromatic sulfones will be the major class since their reactivity could be change significantly by simply utilizing different heteroaromatic cycles. The potential application of thiosulfonates as thiol-mediated uptake transporters will be addressed by synthesizing fluorescently labelled derivatives.

CHAPTER 3:

RESULTS AND DISCUSSION

3.1.   NDI-Peptide Conjugates for Anion-π Catalysis

3.1.1.   Design of Catalysts

It was shown theoretically and experimentally that anion-π interactions depend on electrostatic quadrupole-charge interaction, polarization and correlation interaction.[7,15,24,177] Therefore, to ensure strong interactions between catalyst and substrates, a big and electron-deficient aromatic surface must be chosen as the main platform to build the designed catalysts. NDIs are the best candidates because of their high intrinsic quadrupole moments (Q_{zz} = +19.4 B).[25] On the other hand, NDIs are very versatile scaffold which can be easily modified at the imide positions as well as at the core positions. Base on NDIs structure, a big number of anion-π catalysts has been reported.[38,39,41,44,46–56,178–180] Peptides could be introduced to the structure of the catalysts at imide or core positions of NDIs. For better control of catalyst conformation, a stable peptide secondary structure will be ideal. Among popular secondary structure motifs of peptide, helical structure is the most attractive since there are variety of methods have been reported for building helical structure from short peptides. Remarkably, one turn of an α helix could be stabilized by covalent linkers to form a stable helix-like structure in water with as short as pentapeptides.[181] By looking at reported crystal structures of some NDIs and α-helices, we realized that the dimension of core substituted NDIs matches well with one turn of an α helices.

The distance between two hydrogen atoms at positions 2 and 6 of NDIs is 6.9 Å.[182] Although

the pitch of one turn of an α-helix is 5.4 Å, the distance between two C_γ of two amino acid

residues at the ends of one helix turn can reach 8.5 Å.[183,184] (Figure 41). Based on this

information, NDIs could be used as a covalent linker to stabilize one turn of an α-helix. This

design allowed us to precisely control the catalyst conformation using peptide secondary

structure. The peptide could be linked to the NDI core by aromatic nucleophilic substitution of

Cysteine residues and dibromo-NDIs following similar reported syntheses.[46,53,185]

a)

b)

149

150
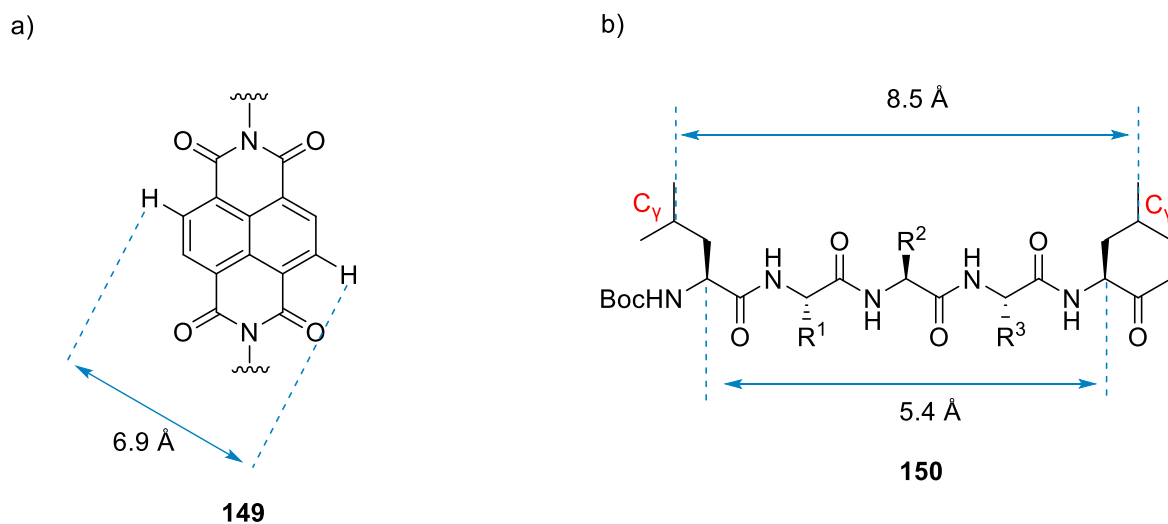
Figure 41. Distances base on reported crystal structures. (a) Distance between two hydrogen

atoms at positions 2 and 6 of NDI. (b) Distance between two C_γ of two amino acid residues at

the ends of one helix turn and the pitch of one α-helix turn (3D structures are not shown for

clarity).

The expected conformation of designed catalysts is shown in Figure 42. In the "active

center" of the catalysts, NDI was used to provide anion-π interactions. It also serves as a

covalent linker to stabilize one turn of an α-helix. To generate anionic transition state during

catalytic reaction by substrate deprotonation, an organic base should be integrated into catalyst structure. Amino acid side chains could be the ideal positions to modify, since the rigid conformation of peptide backbone should allow precisely control the positions of each amino acid residues. Thus, the position of the amine in the side chain above the aromatic surface could be predicted.
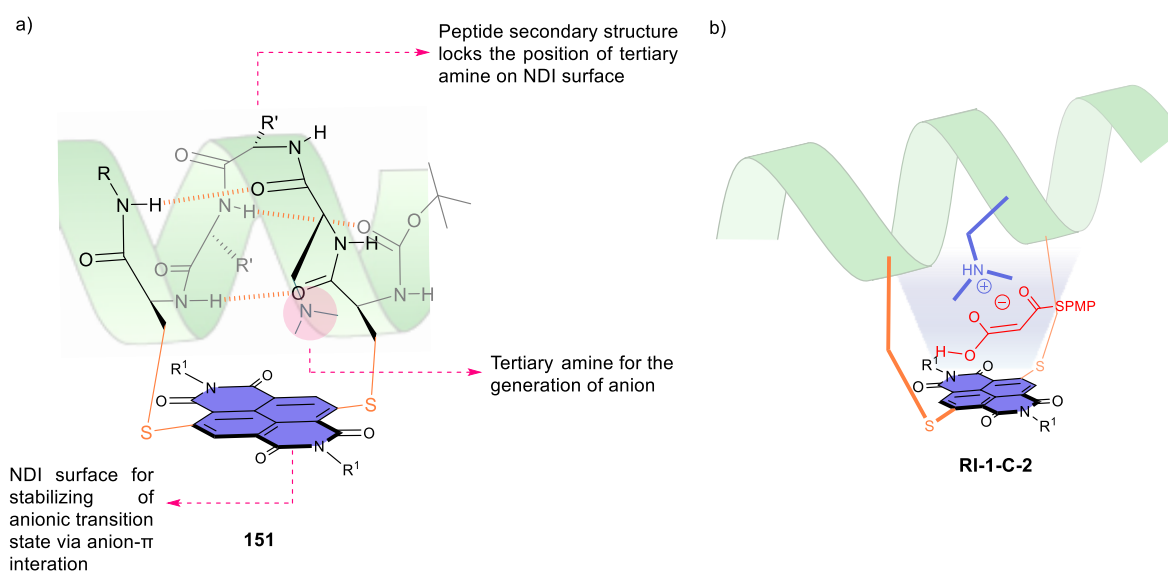
Figure 42. Representative model of designed catalysts. (a) NDI catalysts with peptide backbone in α-helical conformation. (b) Deprotonation of MAHT substrate above the NDI surface.

3.1.2. Synthesis of Catalysts

The synthesis of NDI-Peptide conjugates was carried out following scheme 4. The dibromo-NDI **152**, was synthesized by first treating commercially available NDA **153** with DBH in concentrated sulfuric acid at 50°C for 2 days. The solubilizing group in amine **154** was introduced into formed dibromo-NDA **155** via imide formation. The peptide backbone **156** was

synthesized by conventional solution phase peptide synthesis using EDC as coupling reagent.

For peptide structure, two protected Cysteine are needed for further linking with dibromo-NDI.

Three amino acid residues were placed between two Cysteines to create an α-helix turn after

stapling. A tertiary amine was engaged into peptide structure by using an artificial amino acid

S-3-dimethylamino-2-aminopropionic acid at corresponding coupling step. Leucine was

chosen for non-functionalized positions in peptide sequence to promote helicity and improve

solubility of the catalysts in organic solvent.[186,187] After deprotection by disulfide cleavage,

nucleophilic aromatic substitution of the bromines in **152** with the two thiols in pentapeptide

157 at high dilution afforded the cyclic peptides **158** in 14% yield.
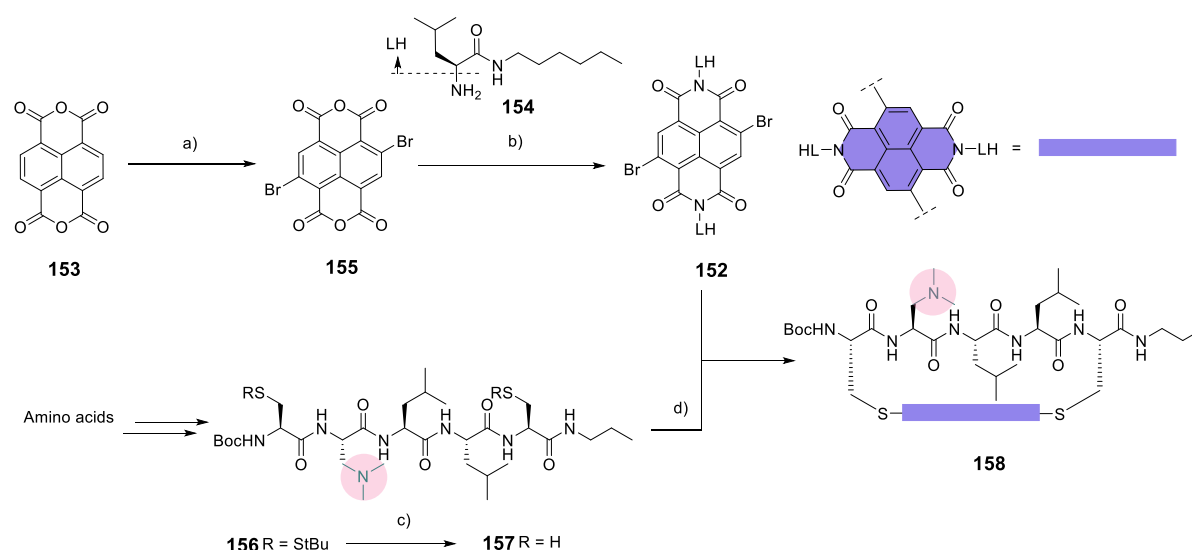
Scheme 4. (a) DBH, 98% H_2SO_4, 50 $^\circ$C, 46%; (b) AcOH, μW, 125 $^\circ$C, 20 min, 91%; (c) PBu_3,

TEA, H_2O, TFE, rt, overnight; (d) TCEP.HCl, CH_3CN /NH_4HCO_3 buffer 3:1, 65 $^\circ$C, overnight,

14% (2 steps).

Following this synthetic procedure, a library of catalysts could be made simply by

changing structure of peptide backbone (Figure 43). More detail synthetic procedures are

described in section 5.2.2. For simplification, single letter abbreviations were used for describing peptide sequences (L, L-Leucine, C, L-Cysteine; ^hC, L-Homocysteine; ^pC, protected C (StBu); B, S-3-dimethylamino-2-aminopropionic acid; R^N, protecting group at the N terminus, R^C, protecting group at the C terminus, sequences of cyclic peptides are underlined).

159: <u>CLLBC</u>, X = CH, Y = CH, Z = NH, R^c = NHnPr
162: <u>CLLBC</u>, X = CH, Y = CH, Z = NH, R^c = NHAd
160: <u>CLBLC</u>, X = CH, Y = NH, Z = CH, R^c = NHnPr
163: <u>CLBLC</u>, X = CH, Y = NH, Z = CH, R^c = NHAd
158: <u>CBLLC</u>, X = NH, Y = CH, Z = CH, R^c = NHnPr
161: <u>CBLLC</u>, X = NH, Y = CH, Z = CH, R^c = NHAd

164: <u>CBLC</u>, R^N = Boc, n = 0, m = 1, l = 1
172: <u>LCBLC</u>, R^N = Boc-L, n = 0, m = 1, l = 1
165: <u>CBLLLC</u>, R^N = Boc, n = 2, m = 1, l = 1
166: <u>CBLL^{h}C</u>, R^N = Boc, n = 1, m = 2, l = 1
167: <u>^{h}CBLL^{h}C</u>, R^N = Boc, n = 1, m = 2, l = 2

168: <u>CBLLCL</u>, n = 1
169: <u>CBLLCLL</u>, n = 2
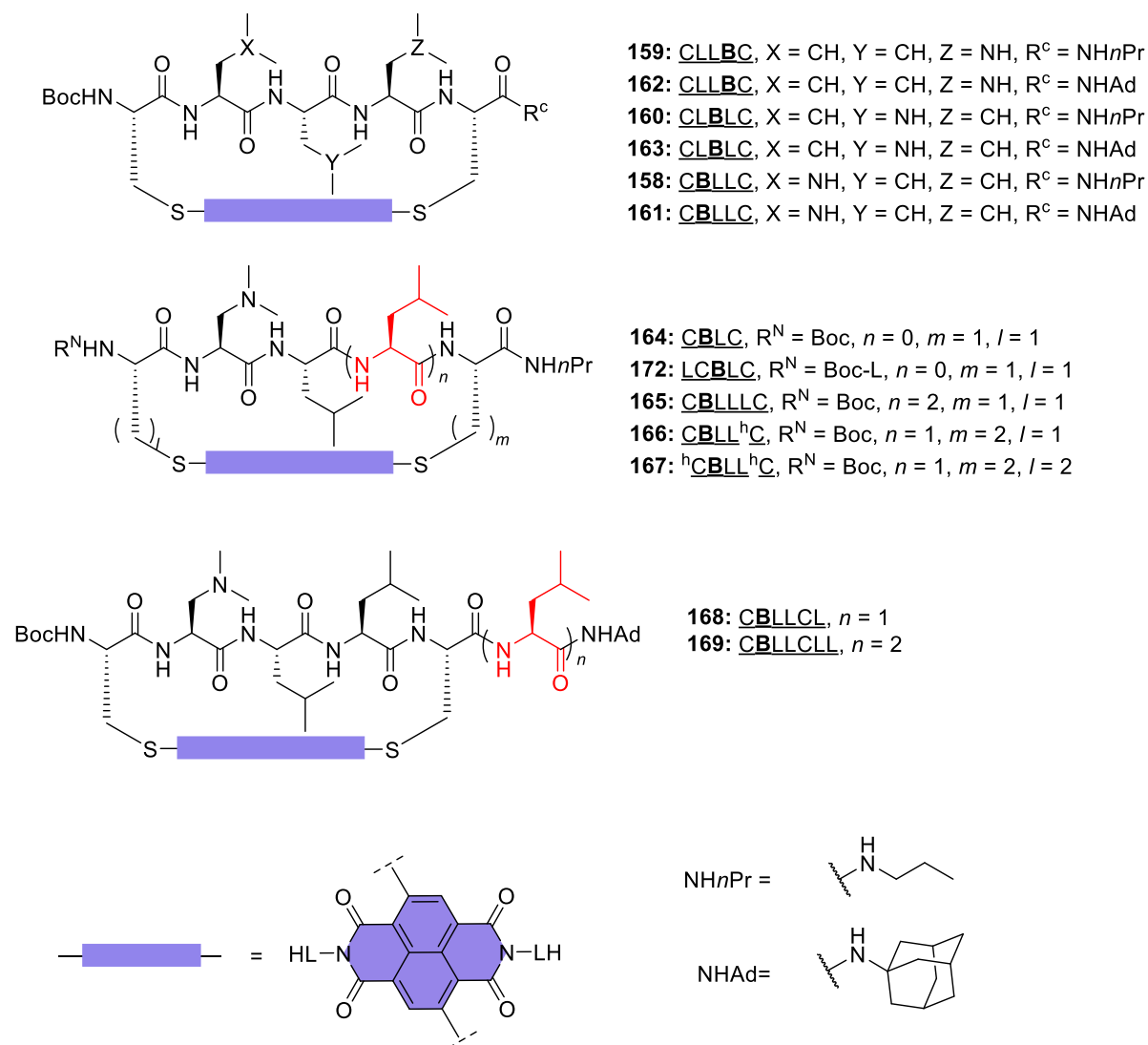
Figure 43. Structure of NDI catalysts in the library.

To examine the relative position of the amino acid side chains with NDI surface, the tertiary amine could be placed at different amino acids as in catalysts **158**, **159**, **160**. Solubility

of this series could be improved by replacing *n*-propyl protecting group at the C terminus by adamantly as in **161**, **162**, **163**. To rationalize the importance of secondary structure to catalytic activity, the peptide turn could be tightened or loosened by removing or adding one amino acid residue in the turn as in **164**, **165**, respectively. The distance between the peptide backbone and electron-poor aromatic surface could be adjusted by replacing Cysteine by Homocysteine with longer side chain as in **166**, **167**. Finally, peptide elongation as in **168**, **169** should give valuable information about the relationship between structure stability and catalytic activity. Potentially, the effect of increasing peptide macro dipole on catalyst reactivity could be also revealed. For the catalysts with pentapeptide backbone, in their formal α-helix-like conformation, there could be three possible Hydrogen bonds to stabilize secondary structure. One Hydrogen bond was created between NH group of the first Cysteine and carbonyl group of the lastest. Protecting groups at the C and N terminus allowed the formation of two additional Hydrogen bonds. These three Hydrogen bonds with the NDI covalent linker could be able to define the structure of one α-helix turn (Figure 42).[181] By increasing the number of amino acids in peptide sequence, the number of potential Hydrogen bonds for structure stabilization could be increased up to five Hydrogen bonds in heptapeptide NDI conjugate **169**.

3.1.3.   Circular Dichroism

For some prepared NDI-Peptide conjugates (**159**, **167**), two stable atropisomers could be separated (Figure 44). The peptide backbone close to the NDI prevented the aromatic surface from flipping through the macrocycle, thus, created a pair of diastereomers. The restricted rotation of the NDI surface contributed strongly to the CD spectra of **159** (Figure 45). In CD spectra, an asymmetric bisignated signal was observed with a positive first Cotton effect and a negative second one for **159a** and *vice versa* for **159b** in the region related to optical transitions

of NDI (300-600 nm). CD signals with opposite signs of two diastereomers indicated the dominant contribution of chiral chromophore to optical activity. In other words, the role of point chirality of peptide backbone is not pronounced. For this reason, it is not possible to extract useful information about peptide conformation from CD spectra. This behavior was also previously observed in similar systems with planar chirality of aromatic surfaces.[109,187]

151

Figure 44. General structure of a pair of atropisomers of NDI-peptide conjugates. Red: Peptide backbone in formal α-helical conformation.

Figure 45. Circular Dichroism spectra of **159a** (red) and **159b** (blue).

3.1.4.   Catalyst Evaluation

3.1.4.1.   MAHT Reaction

In order to evaluate catalytic activity of newly synthesized library of NDI-peptide conjugates, MAHT reaction was chosen (section 1.1.2.3, Figure 14a). MAHT reaction has been used as bench mark reaction to prove the contribution of anion-π interactions to catalytic activity of various systems.[46,53–59,189] Despite the fact that MAHT reaction could be catalyzed by Cinchona-based catalysts with high chemo- and enantioselectivities, the important of this reaction in biosynthesis of fatty acids and polyketides still called for discovering new efficient catalytic systems.[190–193] Catalyzed by polyketide synthases, in nature, the addition of malonic acid half thioesters **42** to enolate acceptors such as **44** affords addition product **46** as the sole product.[192–194] Without the active pocket of enzyme, using conventional organic bases as catalysts delivered decarboxylation product **47** as the major one. The possibility to distinguish

the planar, charge-delocalized enol tautomers **RI-1** and bent, charge-localized keto tautomers

RI-2 of the conjugate base of **42** on flat electron-deficient aromatic surfaces by anion-π

interaction leads to reversed chemoselectivity with favoring of addition product **46**. Thus, the

ratio between two products of this reaction (A/D value) could serve as a universal scale to

reflect anion-π interactions in different systems.[46,53,58,189]
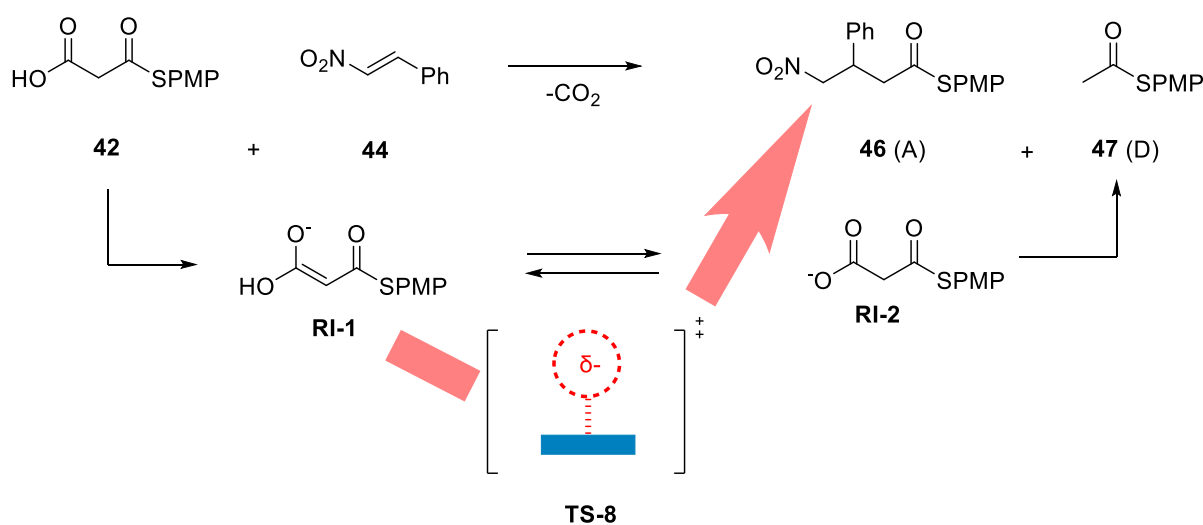
Figure 46. MAHT reaction to probe for anion-π catalysis.

To determine the reactivity of synthesized catalysts, solutions comprising substrates **42**

(200 mM) and **44** (2000 mM) and desired catalyst (20 mol%, i.e. 40 mM) were prepared in

CD_2Cl_2 and stirred at 20 °C. ^1H NMR spectra of the mixture in $CDCl_3$ were recorded at

different times after the start of the reaction until the reaction was completed (for more details,

see section 5.3). CD_2Cl_2 was chosen because such aprotic solvent should improve anion-π

interactions as well as promote helicity of peptide backbone by favoring Hydrogen bonds

formation. Under this condition, an A/D = 35 was obtained for catalyst <u>CBLLC</u> **158**. Moving

the tertiary amine to the middle of peptide sequence in <u>CLBLC</u> **160** dramatically reduced

chemoselectivity with an A/D value of 4.0 similar to TEA. The changes at high A/D could be

overappreciated in comparison with low A/D. For better comparison in catalytic activity, qAD - the log of the measured A/D minus the log of the intrinsic A/D_0 with TEA was also used. Thus, for catalyst <u>CBLLC</u> **158**, qAD = 0.94, which is much higher than qAD = 0 for <u>CLBLC</u> **160**. The catalytic activity of <u>CLBLC</u> **160** is even lower than the corresponding acyclic peptide [P]CLBL[P]C **170** with qAD = 0.18. Because of that, the reactivity of catalysts came probably from correctly positioning of the tertiary amine above NDI surface rather cyclization. When the tertiary amine was placed in the middle of peptide sequence, the helical peptide turn should force it away from NDI surface, thus, anion-π interactions could not be achieved after substrate deprotonation (Figure 44). Moving the tertiary amine one more position closer to the C terminus in <u>CLLBC</u> **159** restored part of catalytic reactivity with qAD = 0.68, 0.60. However, the acyclic control [P]CLLB[P]C **171** was also more selective than [P]CBLL[P]C **156** with qAD = 0.30 against qAD = -0.12 (Table 1, Figure 47). Therefore, the effect from anion-π interaction of NDI surface was more dominant in case of <u>CBLLC</u> catalyst. Even though the amine group in **158** and **159** should be quite close to the NDI surface according to the model in Figure 44, ^{1}H NMR analysis revealed only the amine group in <u>CBLLC</u> **158** is properly located above the NDI surface. In ^{1}H NMR spectrum of <u>CBLLC</u> **158**, the signal from methyl groups in the tertiary amine shifted upfield in comparison with acyclic peptide [P]CBLL[P]C (from 2.25 ppm to 2.08 ppm). In contrast, for <u>CLLBC</u> **159**, the signal shifted downfield slightly (from 2.28 ppm to 2.33/2.31 ppm). These behaviors demonstrated that the optimal position of the tertiary amine for having significant anion-π interactions could be achieved only in <u>CBLLC</u> catalyst series. The same trends in catalytic activity could be observed when replacing *n*-propyl protecting groups with more soluble adamantyl in **161**, **162** and **163**. Slightly weaker catalytic activity in this series could be generated by steric effect of bulky adamantyl group.

Table 1. Characteristic of NDI catalysts.[a]

Cat[b]	Sequence[c]	R^C[d]	qAD[e]	A/D[f]	er[g]
158	<u>C**BL**LC</u>	NHnPr	0.94	35	65:35
156	^{P}C**BL**L^{P}C	NHnPr	–0.12	3	41:59
166	<u>C**BL**L^{h}C</u>	NHnPr	0.40	10	54:46
167	^{h}<u>C**BL**L^{h}C</u>	NHnPr	0.18	6	55:45
			0.51	13	54:46
164	<u>C**B**LC</u>	NHnPr	0.18	6	46:54
172	L<u>C**B**LC</u>	NHnPr	0.35	9	45:55
165	<u>C**B**LLLC</u>	NHnPr	0.30	8	52:48
161	<u>C**BL**LC</u>	NHAd	0.72	21	61:39
173	^{P}C**BL**L^{P}C	NHAd	0.10	5	43:57
168	<u>C**BL**LCL</u>	NHAd	0.97	37	58:42
174	^{P}C**BL**L^{P}CL	NHAd	–0.12	3	43:57
169	<u>C**BL**LCLL</u>	NHAd	1.20	63	56:44
175	^{P}C**BL**L^{P}CLL	NHAd	–0.12	3	43:57
160	<u>C**LB**LC</u>	NHnPr	0.00	4	66:34
170	^{P}C**LB**L^{P}C	NHnPr	0.18	6	49:51
163	<u>C**LB**LC</u>	NHAd	0.25	7	61:39
159	<u>C**LLB**C</u>	NHnPr	0.68	19	48:52
			0.60	16	49:51
171	^{P}C**LLB**^{P}C	NHnPr	0.30	8	49:51
162	<u>C**LLB**C</u>	NHAd	0.70	20	36:64
TEA			0.00	4	50:50

[a] Reactions were conducted as in Figure 45 and followed by ^{1}H NMR spectroscopy. See Figure 42 for pertinent examples of full structures. [b] Catalysts; two data sets for one compound indicates that two atropisomers have been isolated and characterized. [c] Peptide sequences. [d] C-terminal substituents. [e] qAD = log (A/D) – log $(A/D)_0$. [f] Yield of addition product **46** divided by yield of decarboxylation product **47** at full substrate conversion. $(A/D)_0$: A/D with TEA as catalyst (A/D = 4.0, $\log(A/D)_0 = 0.60$). [g] Enantiomeric ratio.
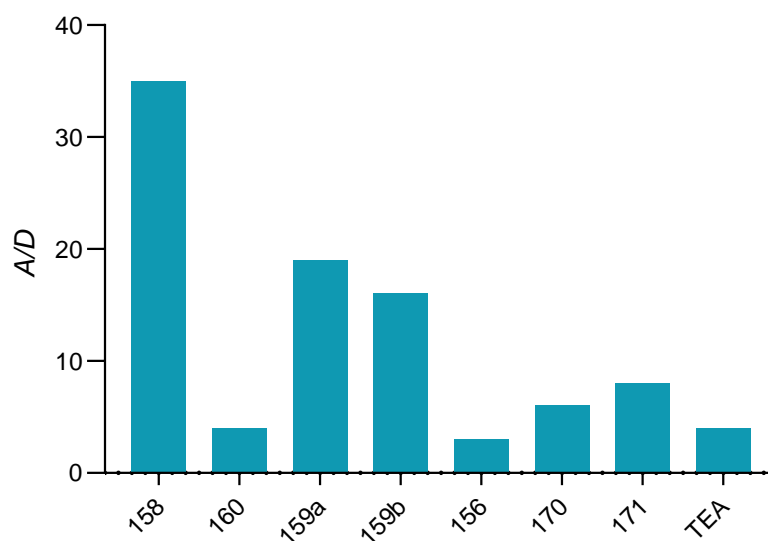
Figure 47. A/D values of MAHT reaction obtained with different catalysts.

Other modifications in peptide backbone, which violated the helical like structure in CBLLC **158**, lead to reduction of catalytic activity. Increasing the distance between NDI and peptide as in CBLL[h]C **166** and [h]CBLL[h]C **167** gave qAD values of 0.40 and 0.51, respectively. Tightening peptide turn as in CBLC **164** and LCBLC **172** clearly removed the activity of **158**. qAD = 0.18 for **164** and 0.35 for **172** are much lower than 0.94 for **158**. Similarly, loosening the peptide turn in CBLLLC **165** resulted equally poor activity (qAD = 0.30) (Table 1, Figure 48). Strong dependence between peptide structure and catalytic activity indicates the importance of α-helix-like conformation in providing powerful anion-π catalysis.
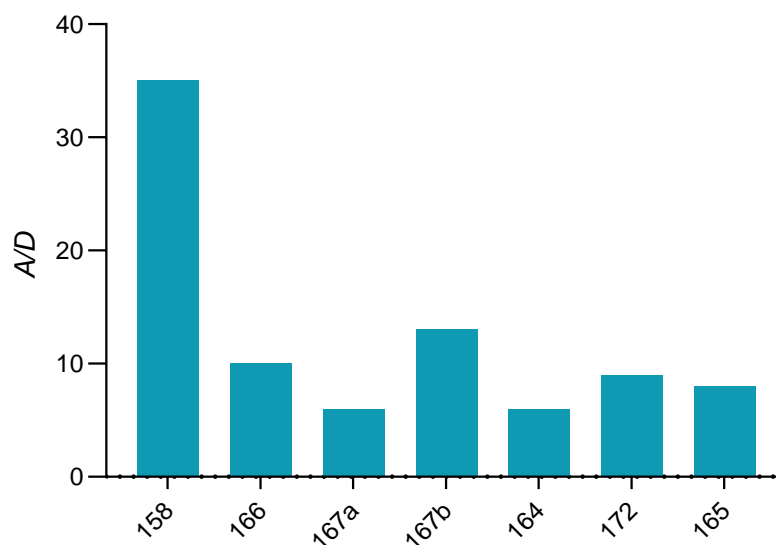
Figure 48. A/D values of MAHT reaction obtained with **158** compared to other catalysts with modifications in peptide backbone.

Elongation of peptide sequence at C terminus of <u>CBLLC</u> **161** strongly increased catalytic activity, qAD = 0.97 was observed for hexapeptide <u>CBLLCL</u> **168**. And continued to increase for heptapeptide <u>CBLLCLL</u> **169** (qAD = 1.2) (Table 1, Figure 49). At the same time, corresponding acyclic peptide control remained weakly active (qAD = -0.12 for both ᴾCBLLᴾCL **174** and ᴾCBLLᴾCLL **175**). Higher chemoselectivity probably came from increasing structure stabilization of peptide backbone above the NDI surface. Elongation of peptides provided potential additional Hydrogen bonds for better organization of α-helix turn. Thus, the position of the tertiary amine could be locked at more optimal position for anion-π catalysis.
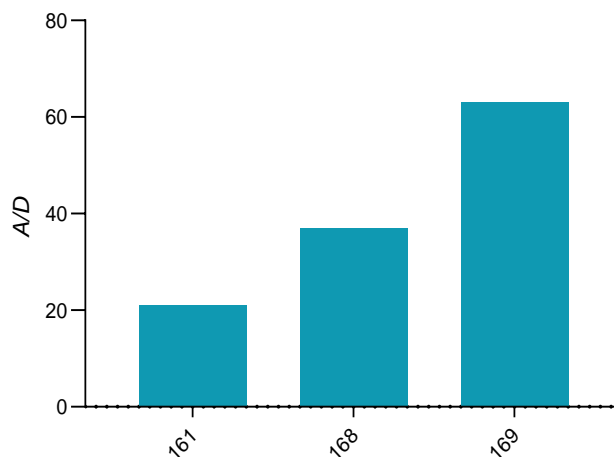
Figure 49. A/D values of MAHT reaction obtained with catalysts with increasing the number of amino acid residues in peptide backbone.

In organic solvents, anion-π catalysis of MAHT reaction usually occurred with weak enantioselectivity. Point chirality close to the tertiary amine base failed to deliver any enantioselectivity.[53] Axial chirality nearby NDI surface gained enantioselectivity only up to 22% *ee*. To obtain this result, performing reaction at low temperature and introduction of strong electron-withdrawing groups to NDI core to strengthen anion-π interactions were required.[54] High enantioselectivity was observed only with artificial enzyme in water. However, the presence of big protein is essential for this high reactivity.[55] Asymmetric catalysis of MAHT reaction could be observed with NDI-peptide conjugates even though the reactivity is weak. For catalysts operated by anion-π interactions, *er* of 65:35 was found for <u>CBLLC</u> **158**. Interestingly, acyclic control ᴾCBLLᴾC **156** inverted the enantioselectivity with *er* = 41:49 (Table 1, Figure 50). Enantioselectivity seemed to come not only from point chirality at peptide backbone, but also from relative position of the tertiary amine with NDI surface. With catalyst <u>CLBLC</u> **160** low A/D value has indicated that **160** did not operate by anion-π interactions. However, enantioselectivity of **160** was as good as **158**. Placing the

tertiary amine in the middle of the peptide seemed to create a good sequence for improving enantioselectivity. When the tertiary amine close to the C terminus as in <u>CLLBC</u> **159**, both catalysts and acyclic control gave the same preference for the same enantiomer with quite similar *er* value. Elongation of peptide backbone unfortunately did not improve enantioselectivity.
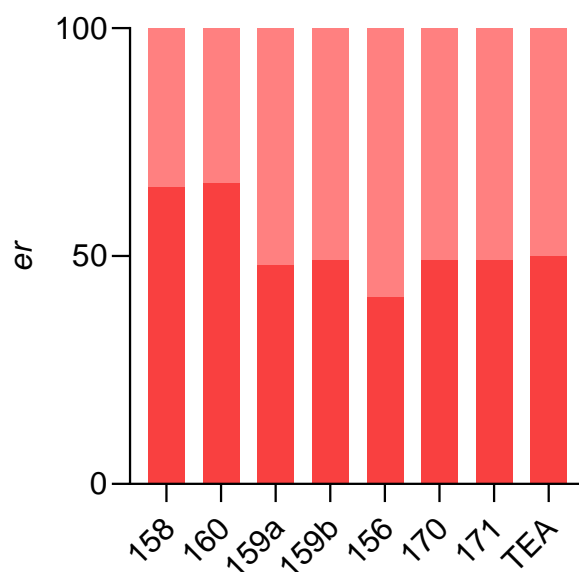
Figure 50. Enantiomeric ratio values of MAHT reaction obtained with different catalysts.

Finally, reaction kinetics were measured for cyclic catalysts **158**, **159** and **160** against their corresponding acyclic controls **156**, **171** and **170**. For catalyst <u>CBLLC</u> **158**, which previously shown to adapt the best conformation for anion-π catalysis, acceleration in initial rate of addition product was observed in comparison with acyclic control ^{P}CBLL^{P}C **156**. k^A increased more than three folds. Meanwhile, decarboxylation process was decelerated with $k_c^D/k_o^D = 0.2$ (Table 2, Figure 51). This corresponded with a -6.9 kJmol^{-1} selective transition-state stabilization by anion-π interactions. In contrast, <u>CLBLC</u> catalyst **160** increased reaction

rates for both addition and decarboxylation reactions with the preference of less relevant decarboxylation process in comparison with its acyclic control ^{P}CL**BL**^{P}C **170** (k_c^A/k_o^A = 1.9, k_c^D/k_o^D = 3.6). Not operating by anion-π interactions, <u>CL**B**LC</u> **160** thus destabilized the transition state of addition reactions by +1.5 kJmol^{-1}. For catalysts <u>CLL**B**C</u> **159**, even though the position of the tertiary amine is not ideal above NDI surface, close proximity to π-acidic surface still delivered -1.5 kJmol^{-1} of stabilization to reaction of interest. Rate enhancements were obtained for both processes, however, higher for addition (k_c^A/k_o^A = 2.3, k_c^D/k_o^D = 1.3).
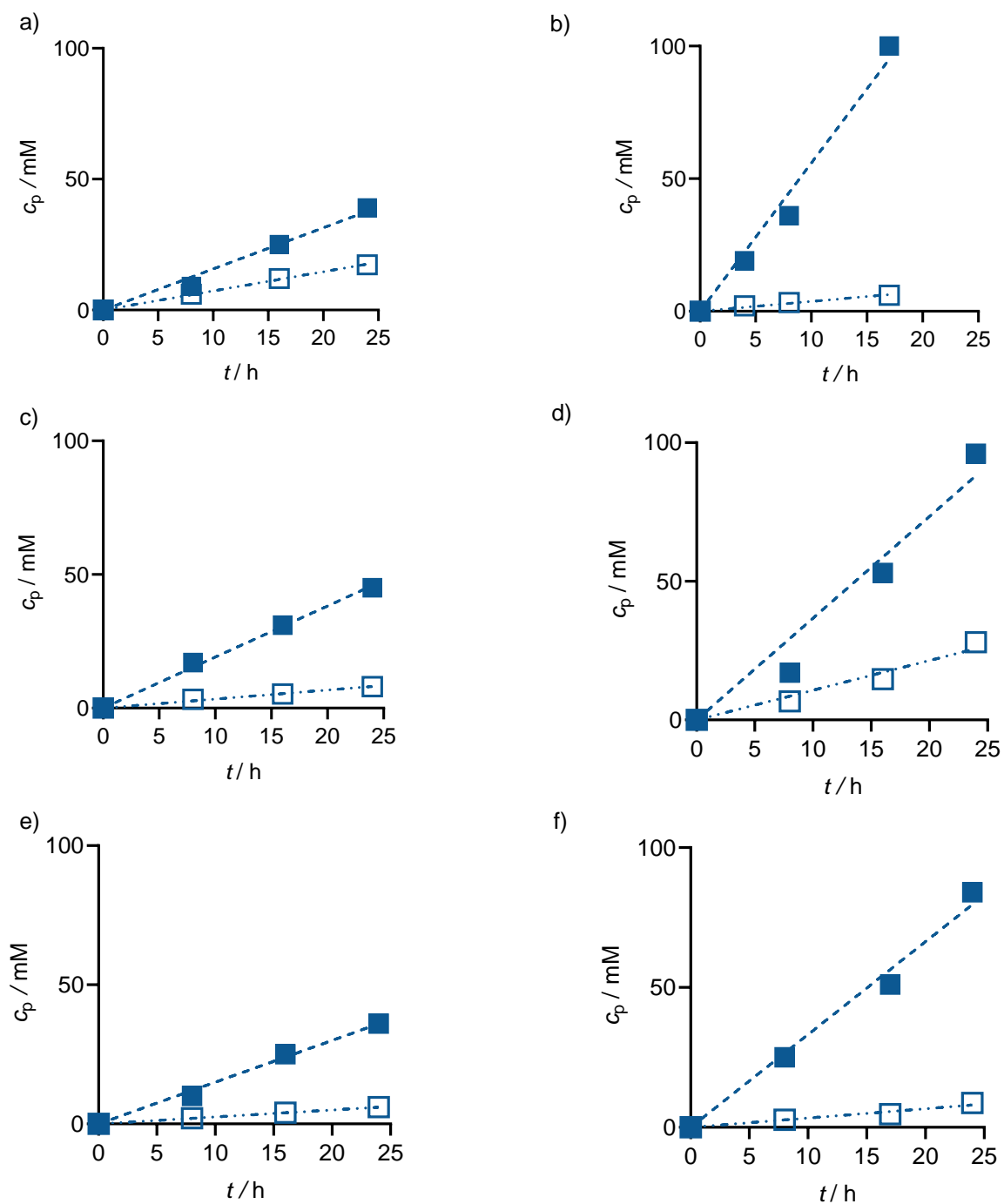
Figure 51. Reaction kinetics for addition (filled squares) and decarboxylation (empty circles) reaction of **42** (200 mM), **44** (2000 mM) and catalyst **156** (a), **158** (b), **170** (c), **160** (d), **171** (e), **159b** (f) (40 mM) in CD$_2$Cl$_2$ at 20 °C as an example.

Table 2. Kinetic analysis of selected NDI catalysts.[a]

Entry	Cat[b]	Sequence[c]	$k_C^A/k_O^{A[d]}$	$k_C^D/k_O^{D[e]}$	$\Delta\Delta E_a$ [kJmol^{-1}][f]
1	**158/156**	CBLLC	3.3	0.2	−6.9
2	**160/170**	CLBLC	1.9	3.6	+1.5
3	**159b/171**	CLLBC	2.3	1.3	−1.5

[a] Conditions as in Figure 46. [b] Catalysts, see Figure 43 and Table 1. [c] Peptide sequences. [d] Rate enhancement for formation of addition (A) product **46**: Initial rate constant of the cyclic (C) catalyst divided by that for the acyclic (O) control, from NMR kinetics (Figure 50). [e] Same for decarboxylation (D) product **47**. [f] Difference in activation energy ΔE_a of cyclic peptide compared to open control for addition product formation minus ΔE_a for decarboxylation product formation.

3.1.5. Conclusion

Using rational catalysts design, this study showed the possibility of using peptide secondary structures for precisely control conformation of functional systems. By screening a library of catalysts with various modifications in peptide backbone using MAHT reaction, a good structure reactivity relationship was established. Peptide backbones above NDI surface adapted a helix-like conformation. Relative positions between the tertiary amine in amino acid residues side chain and NDI surface were defined by rigid catalyst conformations. High chemoselectivity was observed for catalysts with the tertiary amine placed in the position for

optimal anion-π interactions. Other modifications in peptide backbone, which violated helical motif, led to dramatically decrease in activity. On the other hand, exocyclic elongation promoted catalytic activity as a result of improving structure organization. Although being weak, enantioselectivity was improved for MAHT reaction in comparison with other small anion-π catalysts.[54] These results bring new opportunities to use peptide secondary structures for catalyst design or other functional systems, including ion channels.

3.2.　　PDI-Peptide Conjugates for Anion-π Catalysis

Stapling peptides by NDI has shown excellent chemoselectivity for MAHT reaction. However, enantioselectivity is rather weak. Interestingly, catalyst CLBLC **160**, which did not allow anion-π interactions, gave enantioselectivity as good as catalyst CBLLC **158** ($er = 66{:}34$ versus $er = 65{:}35$).[195] This behavior brought possibility of improving enantioselectivity in the system by changing catalyst design to turn on anion-π interactions for the tertiary amine at the middle of the peptide. Cooperative effect between anion-π catalysis and good enantioselective peptide sequence could allow enhancement of enantioselectivity without the need of screening a big library of peptide sequences. The distance between two nitrogens in amides groups of NDIs was estimated to be 7.0 Å, which is only three times longer than the diameter of an α-helix (Figure 52a).[181–184] Therefore, it is impossible to achieve a substrate binding site between NDI and the tertiary amine in the middle of a peptide sequence without changing stapling motif. However, with a larger aromatic surface, a potential binding pocket could be created as shown in Figure 52b.

a)

b)
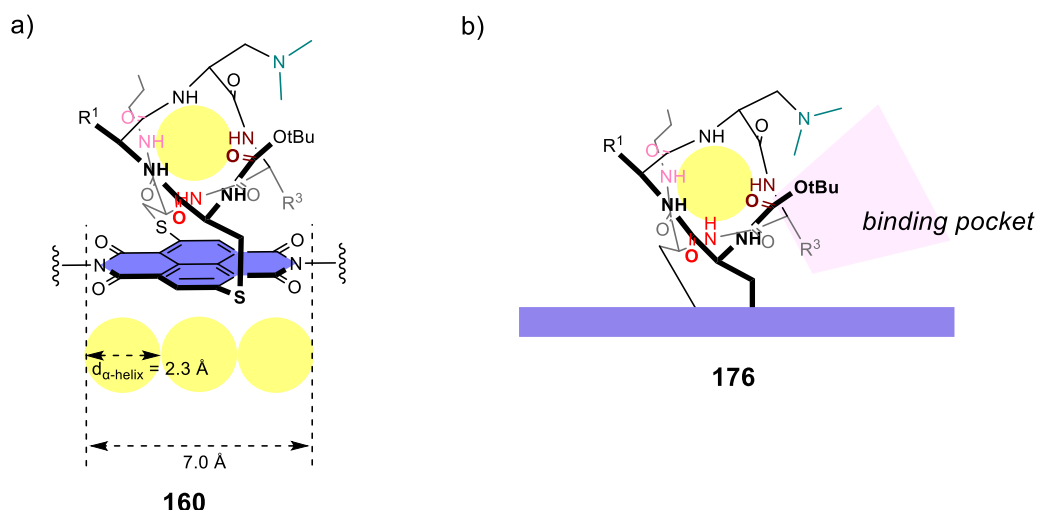
Figure 52. (a) Structure of catalyst <u>CLBLC</u> **160**. (b) The tertiary amine in the middle of peptide sequence and larger aromatic surface could create a binding pocket.

Larger than NDIs, perylenediimides (PDIs) was chosen as the most appealing candidate for replacing NDIs because of its electron-deficient nature (Q_{zz} = +23.2 B).[45] Besides, well-studied aromatic nucleophilic substitution of the bromines in 1,7-dibromo-PDIs allowed applying the developed stapling method for the synthesis of PDI-peptide conjugates.[195–203]

3.2.1. Bridged PDIs and their Planar Chirality

3.2.1.1. Design of Alkyl-Bridged PDIs

Introduction of substituents at bay positions of PDIs twists the PDI surface.[93–95] This twisting creates planar chirality of the aromatic surface. However, twisted aromatic systems usually do not have stable conformations. Interconversion between enantiomers could happen even at low temperature, thus prevents their potential applications as optical pure materials. To stabilize

twisted conformations, covalent linker was commonly introduced to block the rotation.[204–208]

Also, for PDIs, the same strategy has been applied resulting stable atropo-enantiomers, which could be separated by semipreparative HPLC on a chiral column. The reported synthesis of bridged PDIs usually goes through three steps. First, nucleophilic substitution of halogen atoms at bay positions in PDIs by 3-methoxyphenol. Then the methyl ether groups are cleaved. And finally, Williamson ether synthesis affords desired macrocycles (Scheme 1, 2).[108–113] In contrast, stapling methods developed for NDIs could be used to result bridged PDIs with stable conformations in only one step.

3.2.1.2. Synthesis of Alkyl-Bridged PDIs

We first examined the synthetic route by synthesizing a simple alkyl-bridged PDI model following scheme 5. PDI **177** was synthesis by treatment of commercially available PDA **178** with amine **179** in melted imidazole at 170°C overnight. It was then subjected to bromination in reflux CH_2Cl_2. Bromination of PDIs resulted a mixture of 1,6-dibromo-PDIs and 1,7-dibromo-PDIs. 1,7-dibromo-derivaties could be separated from its regioisomer by recrystallization. Aromatic nucleophilic substitution of bromines in PDI **180** by 1,8-octanedithiol **181** at high dilution gave PDI **182** as a mixture of two stable atropo-enantiomers. Attempt to shorten the alkyl bridge by replacing 1,8-octanedithiol with 1,6-octanedithiol failed to give designed macrocycle. Only oligomers and bis(6-mercaptohexylthio)-derivative were obtained. Two enantiomers of PDI **182** could be separated using preparative HPLC on a chiral column. Separated enantiomers are stable at room temperature, and could be further transferred to a more electron-deficient sulfone PDIs **183** by *m*-CPBA oxidation without the loss of chirality. Thus, from halogenated PDI **180**, stabilization of conformation could be achieved

with only one synthetic step, which is more convenient in comparison with reported procedures.[108–111,113]
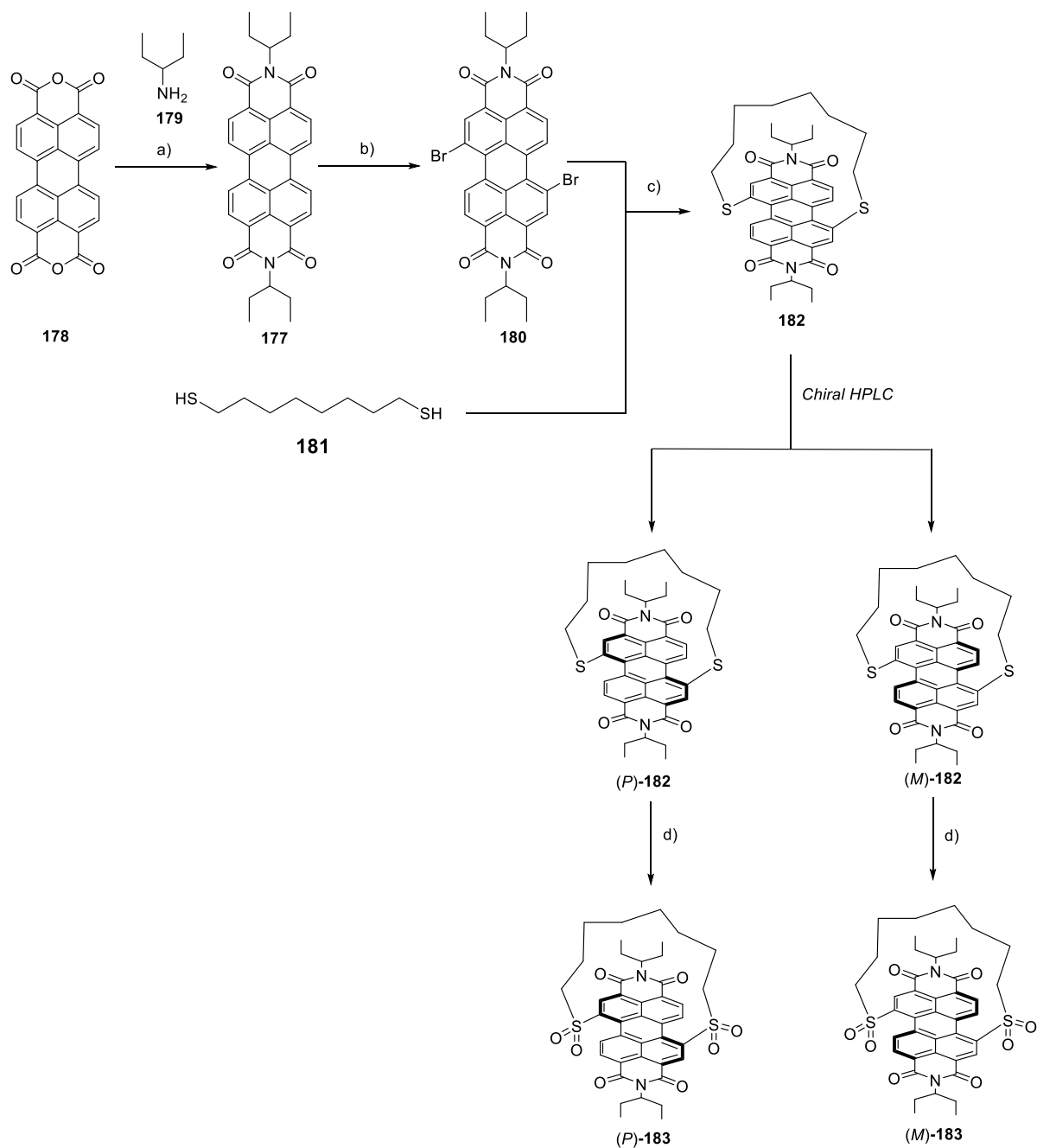
Scheme 5. (a) Imidazole, 170 °C, overnight, 96%; (b) Br$_2$, CH$_2$Cl$_2$, reflux, 2 d, 77%; (c) TCEP.HCl, CH$_3$CN /NH$_4$HCO$_3$ buffer 3:1, 65 °C, overnight, 17%; (d) *m*-CPBA, CH$_2$Cl$_2$, rt, overnight, 45%.

3.2.1.3. Circular Dichroism

Separation of racemate **182** by chiral HPLC afforded **182a** and **182b** in high ee (95% and 78%, respectively). Their CD spectra are mirror images indicated their enantiomeric relationship (Figure 53).
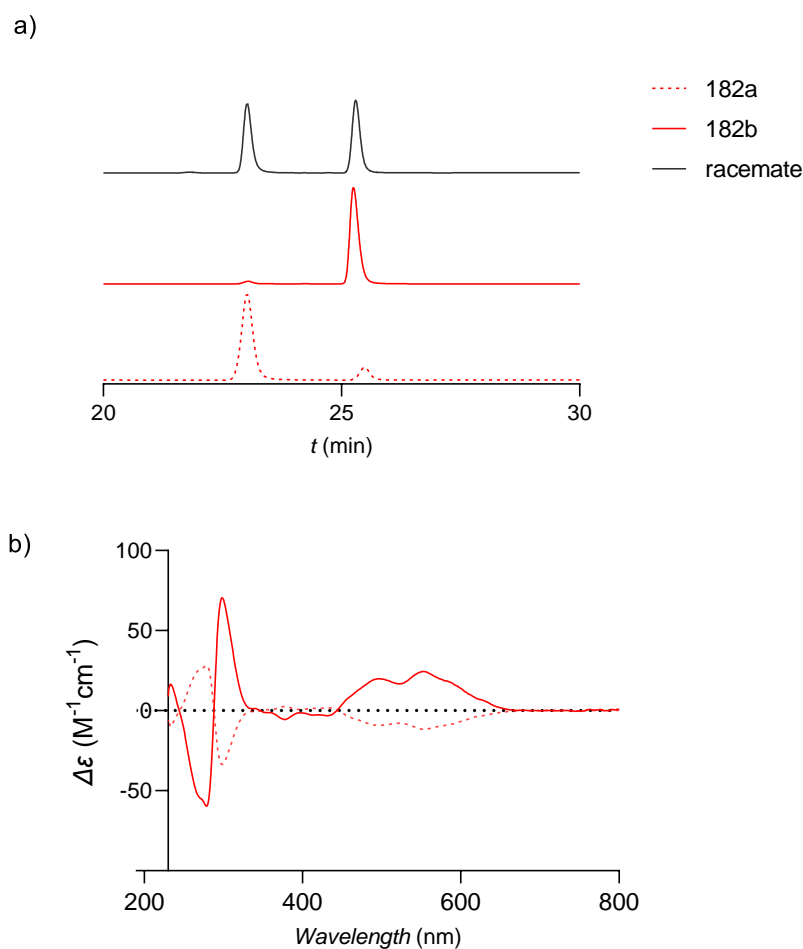
Figure 53. (a) Chiral HPLC chromatograms obtained using chiralpak IA column (CH_2Cl_2/*n*–hexane gradient from 0% of CH_2Cl_2 at 0 min to 100% of CH_2Cl_2 at 90 min, 1 mL/min, 25 °C; detection: 544 nm) of **182a**, **182b** and their racemate. (b) CD spectra of **182a** (dotted line) and **182b** (solid line).

The absolute configurations of these atropo-enantiomers could be assigned by comparison of CD spectra with reported data of other bridged PDIs. In visible region (400-640 nm), a broad monosignated peak was observed. In the UV region (250 – 400 nm), a symmetric bisignated signal was found with a positive first Cotton effect and a negative second one for the first eluted isomer **182a**. Similar signals have been seen in CD spectra of PDI with *(P)* conformation.[109] Thus, the first eluted isomer **182a** should be *(P)*-configured. Therefore, the conformation of second eluted isomer **182b** could be assigned to *(M)*-configuration.

After oxidation of the sulfurs in **182** to sulfones, PDIs **183** still gave mirror images of CD spectra. Characteristic features of newly obtained CD spectra still retained indicating stable conformation of **183** after further chemical transformation (Figure 54).
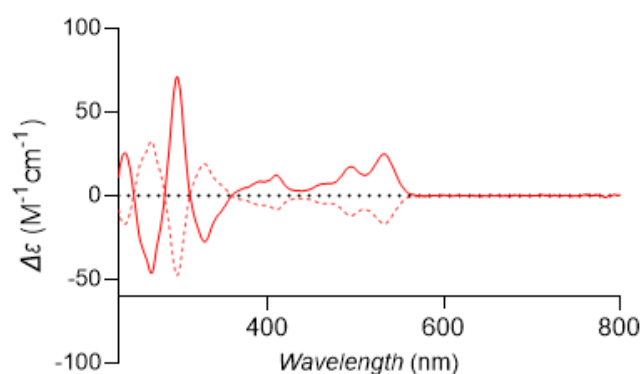
Figure 53. CD spectra of **183a** (dotted line) and **183b** (solid line).

3.2.2. PDI-Peptide Conjugates

3.2.2.1. Design of Catalysts

Even though PDI surface is larger than NDI, the distance between two substituents at positions 1 and 7 of PDIs still allows for using PDI as covalent linker to stabilize one turn of an α-helix. The distance was estimated to be around 7.5 Å which is smaller than the distance between two C_γ of two amino acid residues at the ends of one helix turn (8.5 Å) (Figure 41).[110,184,209] However, this close fit may stretch the peptide turn and create some deviation from a perfect α-helical structure. Following catalyst design of NDI, a library of peptide with different modification in peptide backbone could be stapled by PDIs to form a library of macrocycles having stable conformation. Moving the tertiary amine in amino acid residues side chain again allows to reveal structure reactivity relationship. It is worth to remind that substitution at bay areas of PDIs formed atropo-enantiomers, and peptide backbone could potentially block the interconversion between these isomers.

3.2.2.2.   Synthesis of Catalysts

The synthesis of PDI-peptide conjugates was carried out using the same condition which was developed for NDI-peptide conjugates (Section 3.1.2, Scheme 4). After removing StBu protecting groups of two Cysteines in pentapeptide **171**, aromatic nucleophilic substitution at bromines in PDI **180** resulted macrocycles **184** as a mixture of two atropo-diasteremers. These two diastereomers could be separated by PTLC or flash chromatography on a chiral column (Scheme 6). They exhibited very distinct physical properties with different colors (**184a** – purple, **184b** – red).
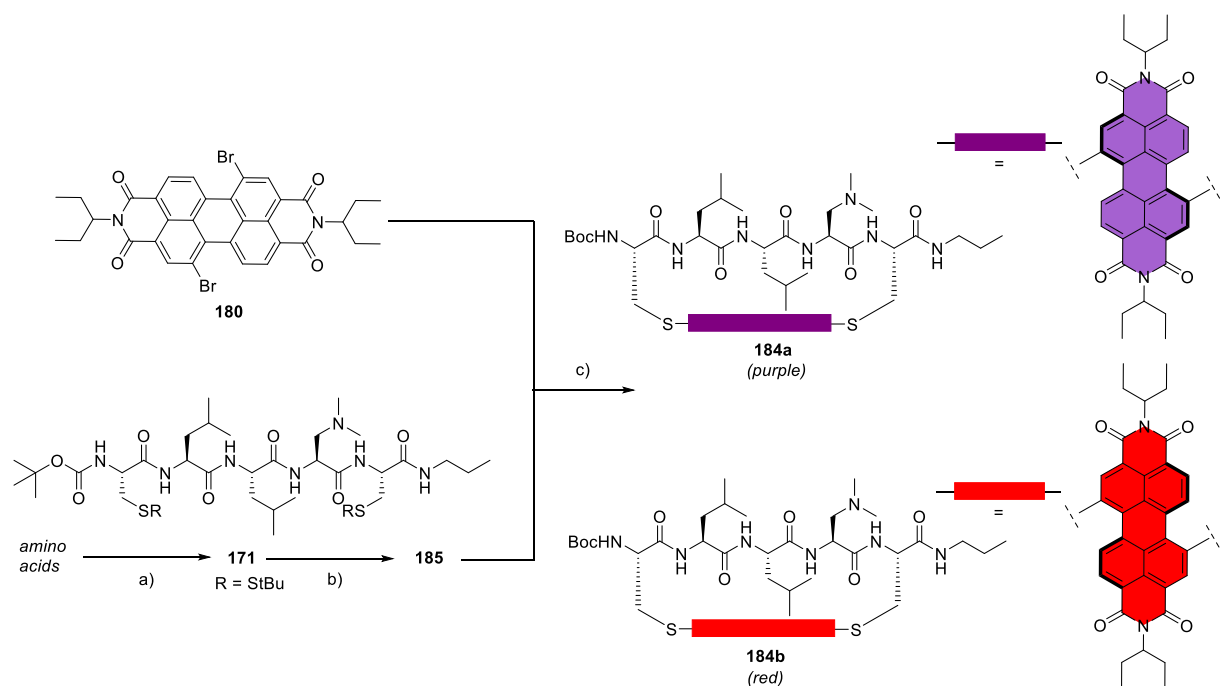
Scheme 6. (a) Standard solution phase peptide synthesis; (b) PBu$_3$, TEA, H$_2$O, TFE, rt, overnight; (c) TCEP.HCl, CH$_3$CN /NH$_4$HCO$_3$ buffer 3:1, 65 °C, overnight, 10% (**184a**), 8% (**184b**) (2 steps)

Following this synthetic procedure, a library of catalysts was developed by changing structure of peptide backbone (Figure 55). Rationalization of peptide modifications has been explained in section 3.1.2. In most cases, two diastereomers could be easily resolved.

184: <u>CLLBC</u>, X = CH, Y = CH, Z = NH, R^c = NHnPr
188: <u>CLLBC</u>, X = CH, Y = CH, Z = NH, R^c = NHAd
186: <u>CLBLC</u>, X = CH, Y = NH, Z = CH, R^c = NHnPr
190: <u>CLBLC</u>, X = CH, Y = NH, Z = CH, R^c = NHAd
187: <u>CBLLC</u>, X = NH, Y = CH, Z = CH, R^c = NHnPr
192: <u>CBLLC</u>, X = NH, Y = CH, Z = CH, R^c = NHAd

195: <u>CBLC</u>, R^N = Boc, n = 0, m = 1
197: <u>LCBLC</u>, R^N = Boc-L, n = 0, m = 1
199: <u>CBLLLC</u>, R^N = Boc, n = 2, m = 1
200: <u>CBLL^{h}C</u>, R^N = Boc, n = 1, m = 2

201: <u>CLLBCL</u>, X = CH, Y = CH, Z = NH
203: <u>CLBLCL</u>, X = CH, Y = NH, Z = CH
205: <u>CBLLCL</u>, X = CH, Y = NH, Z = CH
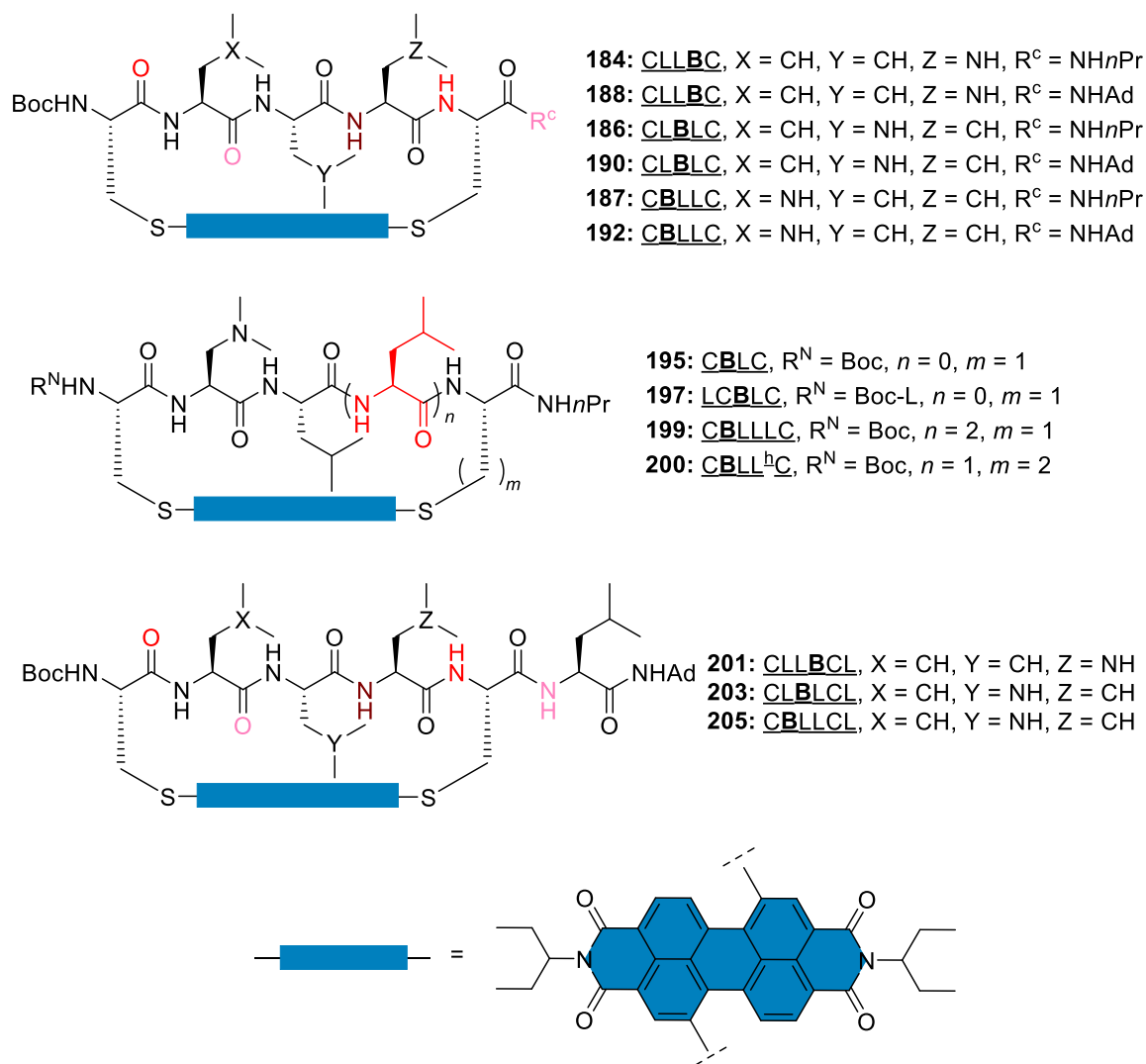
Figure 55. Structure of peptide-PDI conjugated catalysts.

3.2.2.3. Characterization of Catalysts

3.2.2.3.1. 1D NMR Characterization

Comparison of ^{1}H NMR spectra of linear control peptide with their corresponding PDI-peptide conjugates brought fruitful information about catalyst conformation. For catalysts <u>CLLBC</u> **184**, upon stapling, ^{1}H NMR spectra of **184a** and **184b** changed dramatically in comparison with

the parent peptide **171** (Figure 56). The signals of peptide backbone mostly shifted upfield because of strong ring current effect of PDI. This observation confirmed that peptide backbone indeed lied on top of PDI surface. For two Leucines (L) and S-3-dimethylamino-2-aminopropionic acid (**B**) residues in the middle of the helix turn, C_α-H protons shifted upfield clearly. The multiplet corresponds with C_α-H of **B** residue shifted from 4.32 – 4.12 ppm in **171** to 3.91 – 3.84 ppm in **184a** and 4.23 – 4.16 ppm in **184b**. A larger change was found for the singlet of the methyl groups in the tertiary amine at the side chain of **B**. The singlet moved from 2.28 ppm in **171** to 1.64 ppm in **184a** and 1.57 ppm in **184b**. Located above the PDI surface, the tertiary amine in amino acid residue close to the C terminus is able to turn on anion-π interactions after substrate deprotonation. The different in chemical shifts of similar protons in two diastereomers indicated the different in their conformations. For the adjacent L residue, C_α-H signal located at 4.32 – 4.12 ppm in **171** jumped to 3.67 – 3.58 ppm in **184a** and 3.71 - 3.62 ppm in **184b**. An impressive change was noticed for the C_α-H of L residue close to the N terminus. Relocation of the signal from 4.32 – 4.12 ppm in **171** to 2.18 – 2.10 ppm in **184a** and 1.78 – 1.72 ppm in **184b** corresponded to a Δ_δ =2.1 ppm and Δ_δ =2.5 ppm, respectively. This huge change was probably caused by very close proximity between this amino acid residue and PDI surface.[210,211] The big difference in Δ_δ of C_α-H observed for two amino acid residues close to Cysteines of peptide turn suggested that the axis of the helix turn was tilted rather parallel with aromatic surface. Similar to C_α-H signals, signals from CH_3 groups in Leucine side chains also shifted upfield. Each CH_3 group experienced different ring current effect with the most noticeable change from 1.00 – 0.84 ppm in **171** to 0.48 ppm in **184a** and 0.53 ppm in **184b**. C_α-H signal of Cysteine residue at the N terminus of peptide sequence also moved upfield upon cyclization, the multiplet at 4.43 – 4.34 ppm in **171** relocated at 4.03 – 3.94 ppm in **184a** and 4.24 – 4.17 ppm in **184b**. On the other hand, two diastereotopic protons close to the sulfur atom in this Cysteine moved downfield, from 3.08/2.99 ppm in **171** to 3.54/3.40 ppm in **184b**. In

184a, only one of these two protons shifted downfield, chemical shifts of 3.97 ppm was found for the first one. The other shifted upfield to 2.78 ppm. While the CH_2 group of Cysteine residue in **184b** was located in deshielding environment of PDI, the one in **184a** seemed to fall into the border of shielding and deshielding areas of PDI. Chemical shift changes in Cysteine residue at the C terminus of peptide backbone were also significant. C_α-H signal moved downfield from 4.76 – 4.65 ppm in **171** to 5.24 – 5.14 ppm in **184a**, while slightly upfield in **184b** (4.68 – 4.56 ppm). Two diastereotopic protons in CH_2 group shifted downfield, from 3.36/3.13 ppm in **171** to 4.24/3.92 ppm in **184a**. In **184b**, only one of these two protons shifted downfield to 4.74 ppm while the same value of 3.13 ppm was observed for the other. Contrary ring current effects found for adjacent protons in two Cysteines indicated that they were located at the edge of PDI surface. Interestingly, CH_2 group close to the amide group in *n*-propyl protecting group of the C terminus changed from a quartet at 3.20 ppm in **171** to a multiplet at 3.20 – 3.05 ppm in **184a**. Changing coupling patent of this CH_2 was caused probably by the new diastereotopic relationship of these two protons in **184a**. Located close to the PDI surface, this CH_2 group was affected by chirality of PDI surface. This behavior was even more pronounced in **184b**, two multiplets at 3.34 – 3.25 ppm and 3.09 – 3.01 ppm was observed for the first CH_2 group in *n*-propyl residue. Chirality caused by twisting of aromatic surface seemed to be quite strong and could be interesting for improving enantioselectivity in catalytic reactions.
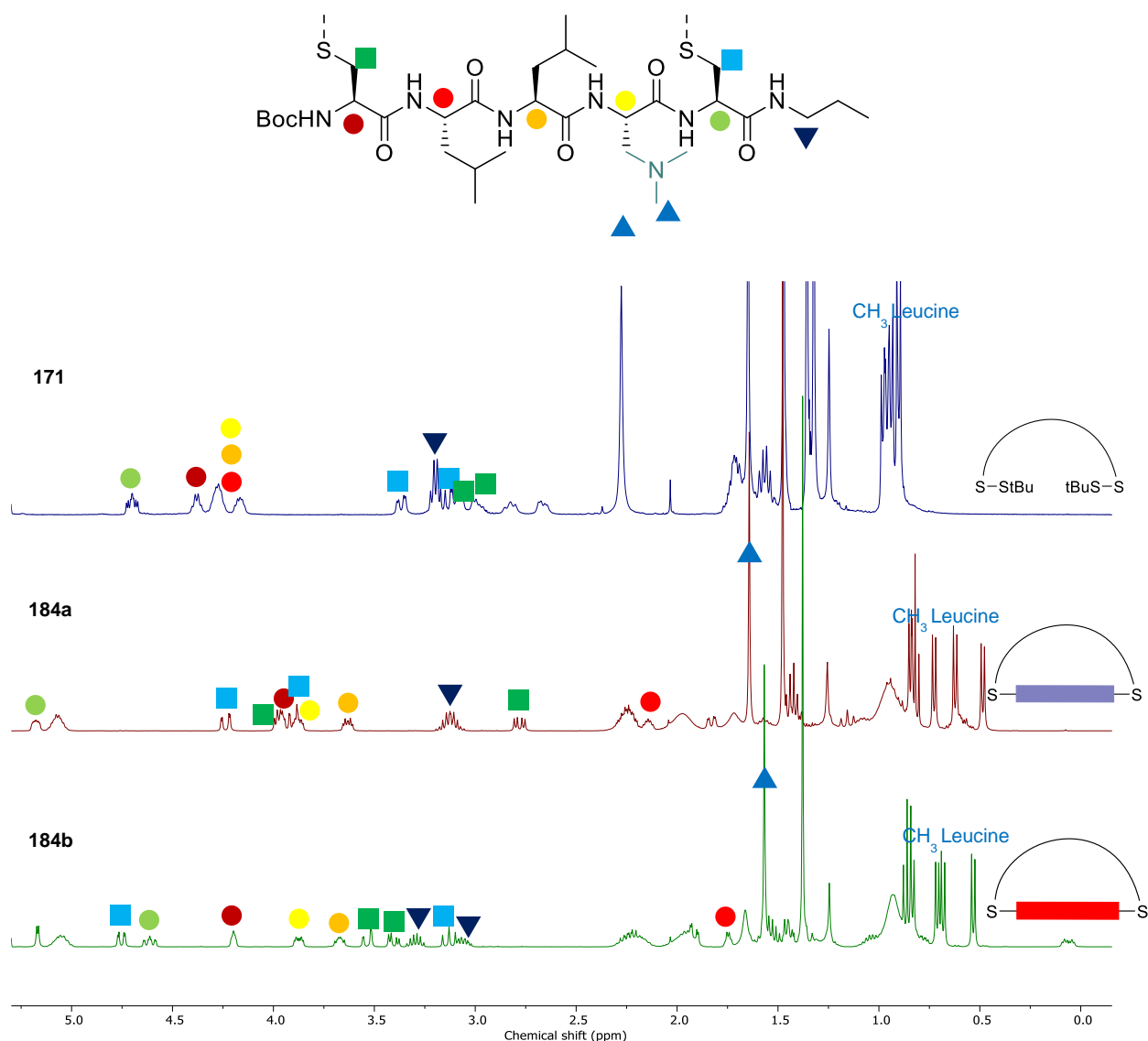
Figure 56. Zoom in ¹H NMR of **171** (top), **184a** (middle) and **184b** (bottom).

When the tertiary amine was moved to the middle of peptide sequence as in <u>CLBLC</u> **186**, very similar changes in chemical shifts of peptide backbone in comparison with <u>CLLBC</u> catalyst **184** were found (Figure 57). Brought the tertiary amine one more position closer to the N terminus as in <u>CBLLC</u> **187** gave the same results (Figure 58). Despite the position of the tertiary amine in the peptide sequence, peptide conformations did not change significantly. However, the relative position of the tertiary amine and PDI varied following modifications in peptide backbone. For catalysts <u>CLBLC</u> **186**, the singlet of methyl groups in the organic base

relocated from 2.23 ppm in **170** to 2.06 ppm and 2.05 ppm in **186a** and **186b**, respectively. Δ_δ = 0.17/0.18 ppm clearly smaller than Δ_δ = 0.64/0.71 ppm in <u>CLLBC</u> **184**. Upfield shifting of Δ_δ = 0.35/0.37 ppm was found for corresponding methyl groups in catalyst <u>CBLLC</u> **187**.
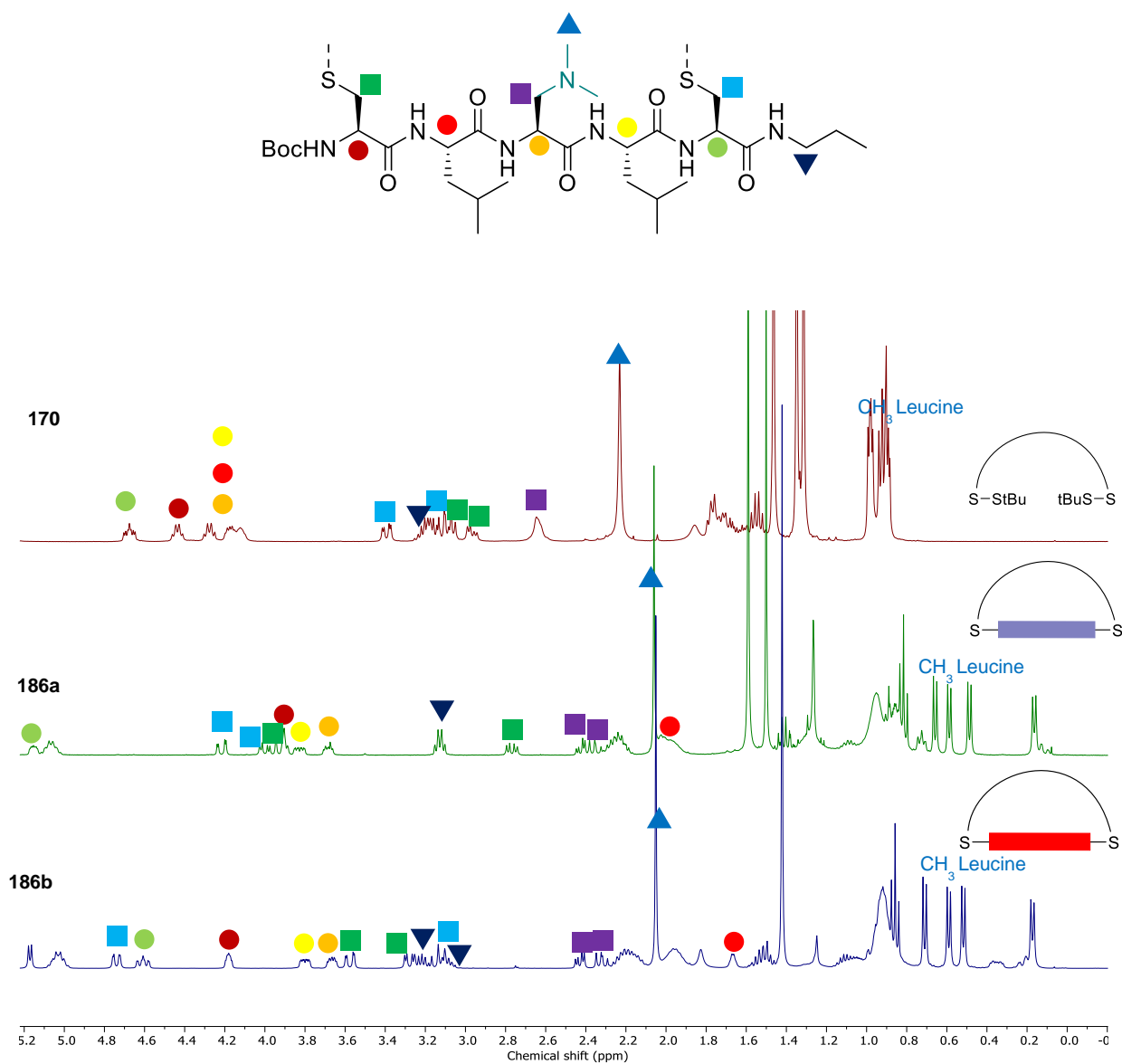
Figure 57. Zoom in ^{1}H NMR of **170** (top), **186a** (middle) and **186b** (bottom).
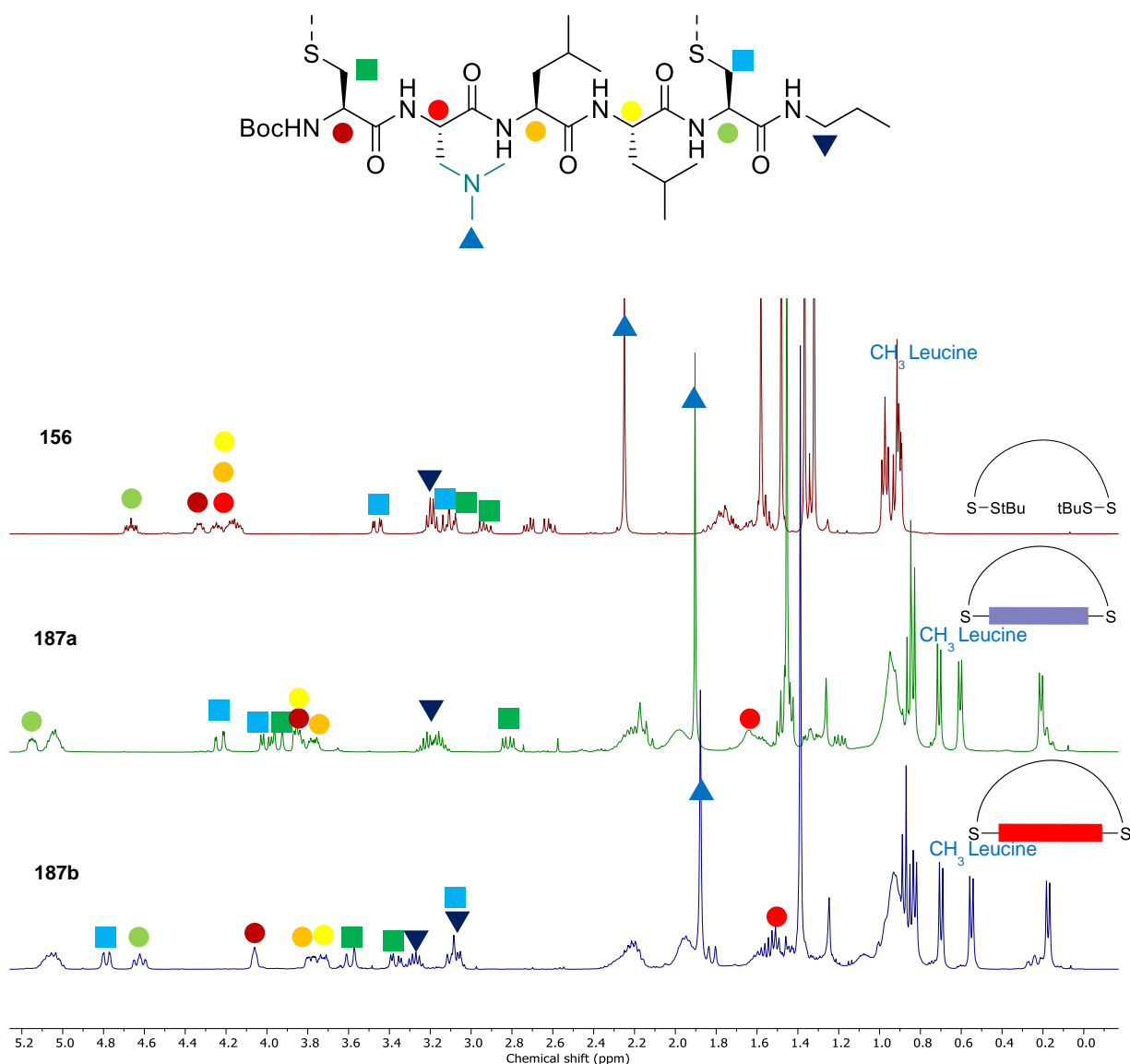
Figure 58. Zoom in ¹H NMR of **156** (top), **187a** (middle) and **187b** (bottom).

To have a good prediction of catalyst activities, determining position of the nitrogen atom in the tertiary amine is important since its lone pair is the key element to create anionic intermediate above the PDI surface. Even though ¹H NMR spectra could be used to access useful information of catalyst conformations, using ¹³C NMR spectra allowed more precise prediction. In the side chain of **B** residue, nitrogen atom is located between CH$_2$ group and CH$_3$ groups. Therefore, knowing the locations of the carbon atoms in these groups could reveal position of nitrogen atom above the aromatic surface. This approach is clearly better than using

^{1}H NMR spectra since the distances from hydrogen atoms in adjacent groups to nitrogen is greater than the ones for nearby carbon atoms. For catalyst <u>CLLBC</u> **184**, low solubility of its acyclic peptide **171** in CDCl$_3$ prevented obtaining a good ^{13}C NMR spectrum for comparison. However, the more soluble adamantyl protected analogue <u>CLLBC</u> **188** could be used. Although <u>CLLBC</u> **188** was obtained as inseparable mixture of two diastereomers, signals from each diastereomer could be assigned without any problems. Both signals corresponded to the CH$_3$ groups and CH$_2$ group near by the basic nitrogen atom shifted upfield (Figure 59).
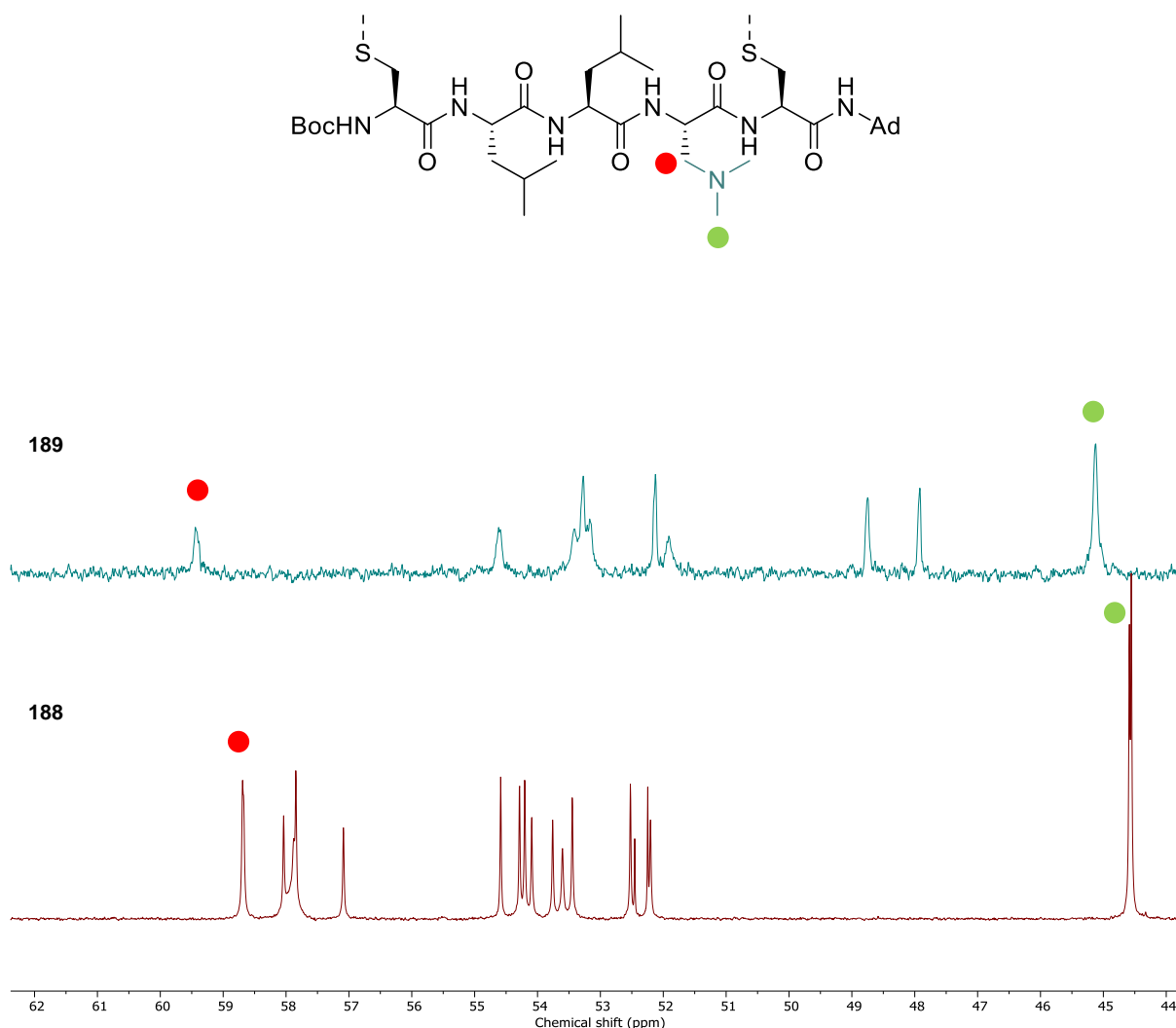
Figure 59. Zoom in ^{13}C NMR of **189** (top) and **188** (bottom).

Signal of CH_2 group moved from 59.4 ppm in **189** to 58.71/58.69 ppm in **188**. Also, CH_3 groups relocated from 45.1 ppm in **189** to 44.61/44.57 ppm in **188**. Thus, the lone pair of the tertiary amine was likely located above aromatic surface.

When the tertiary amine was placed in the middle of the peptide backbone, the nitrogen atom in the tertiary amine clearly was above PDI surface. For catalysts <u>CLBLC</u> **186**, CH_2 signal moved from 58.8 ppm to 58.5 ppm in **186a** and 58.1 ppm in **186b**. (Figure 60).
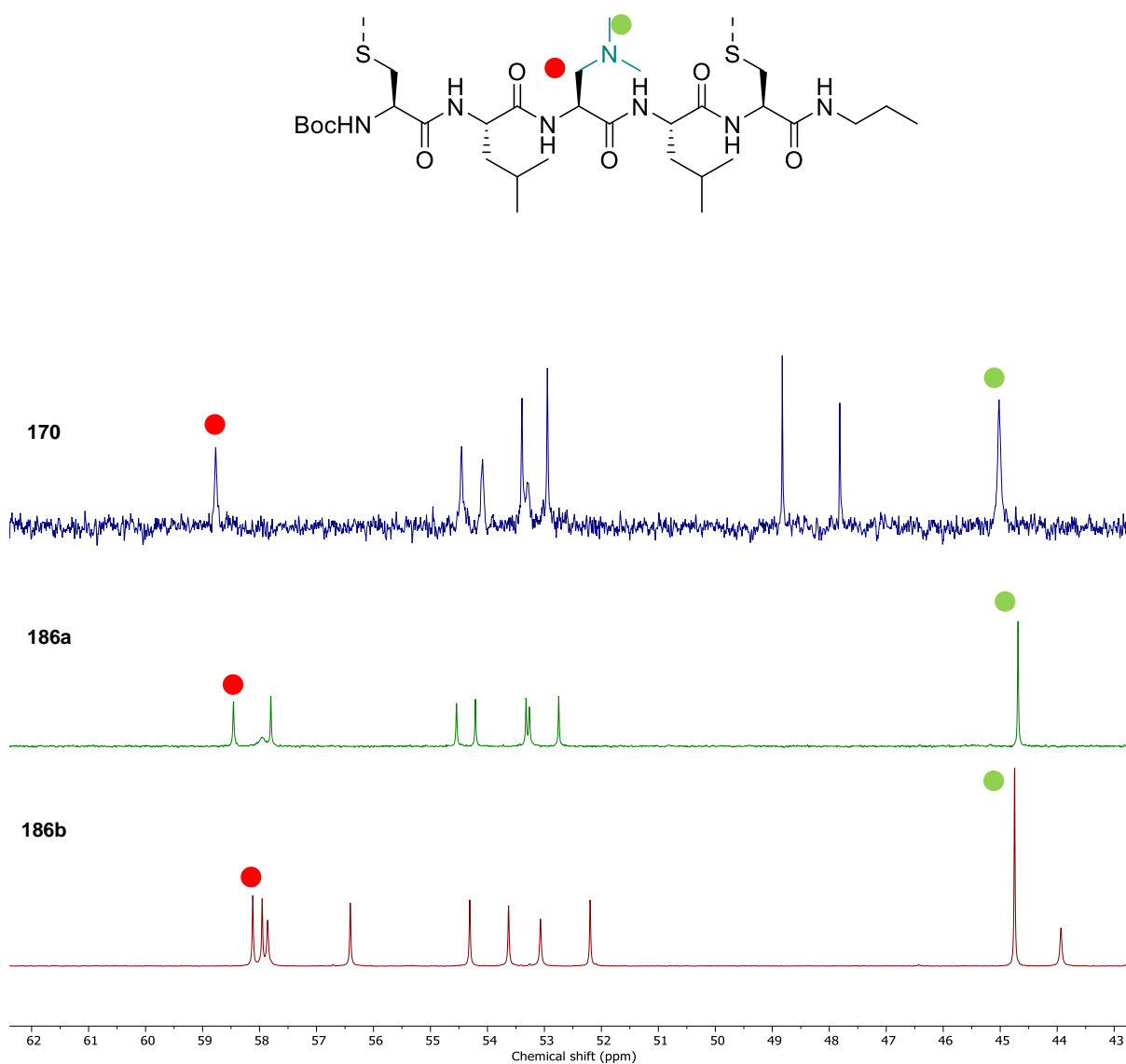
Figure 60. Zoom in ^{13}C NMR of **170** (top), **186a** (middle) and **186b** (bottom).

CH$_3$ signal changed from 45.0 ppm in **170** to 44.5 ppm in **186a** and 44.8 ppm in **186b** The same trend was found for the adamantyl analogue <u>CL**B**LC</u> **190** (Figure 61). Also, almost identical chemical shifts of methyl and methylene groups in <u>CL**B**LC</u> **186** in comparison with <u>CL**B**LC</u> **190** indicating that there are minimal structure changes when replacing *n*-propyl protecting group with much bulkier adamantyl.
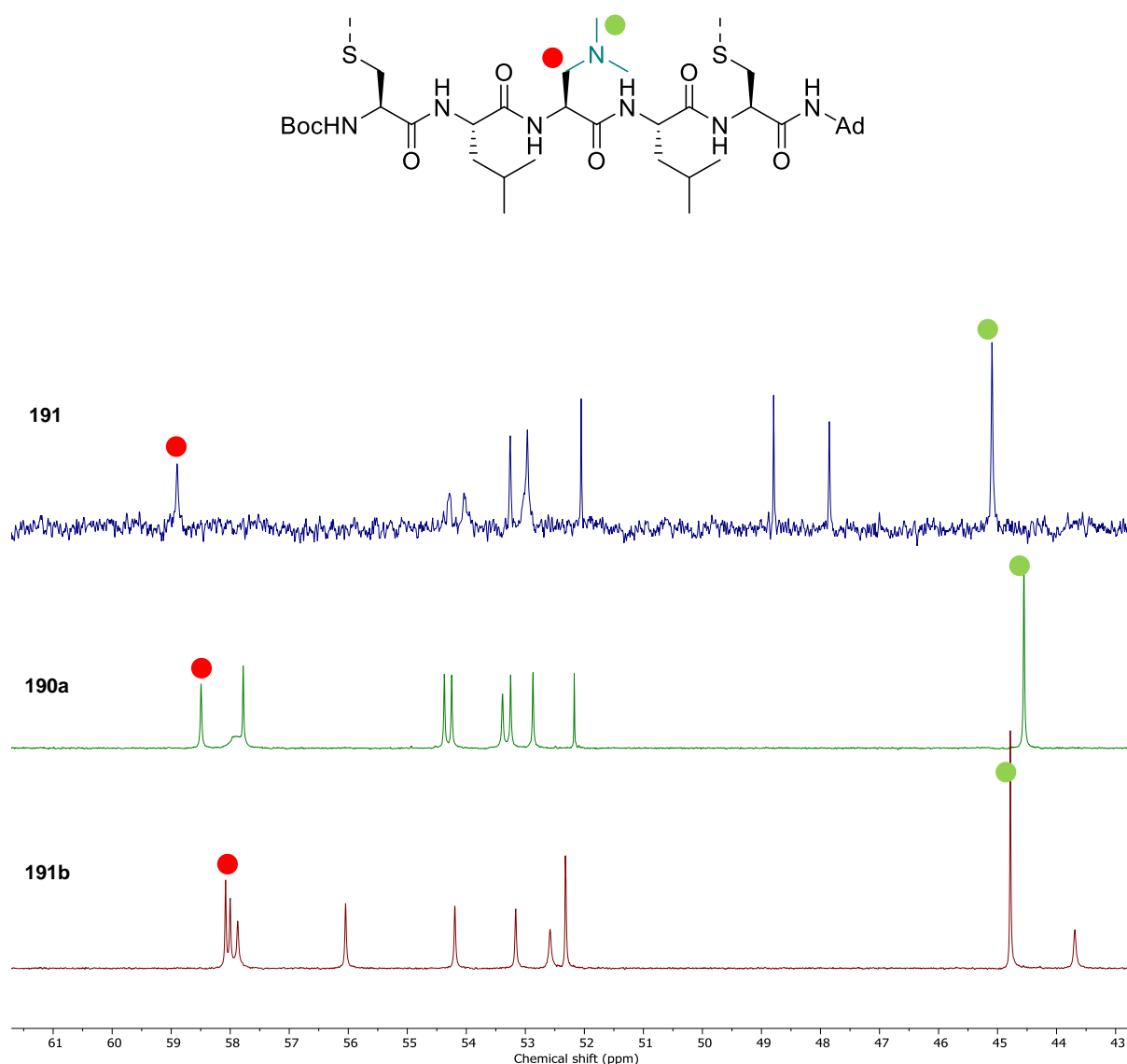
Figure 61. Zoom in ^{13}C NMR of **191** (top), **190a** (middle) and **190b** (bottom).

For the series <u>CBLLC</u>, CH$_2$ groups of **B** residues shifted upfield in both **187** (58.5 ppm to 57.0/56.8 ppm in **187a** and **187b**, respectively) and **192** (58.5 ppm to 57.1/56.7 ppm in **192a** and **192b**, respectively) (Figure 62, Figure 63).
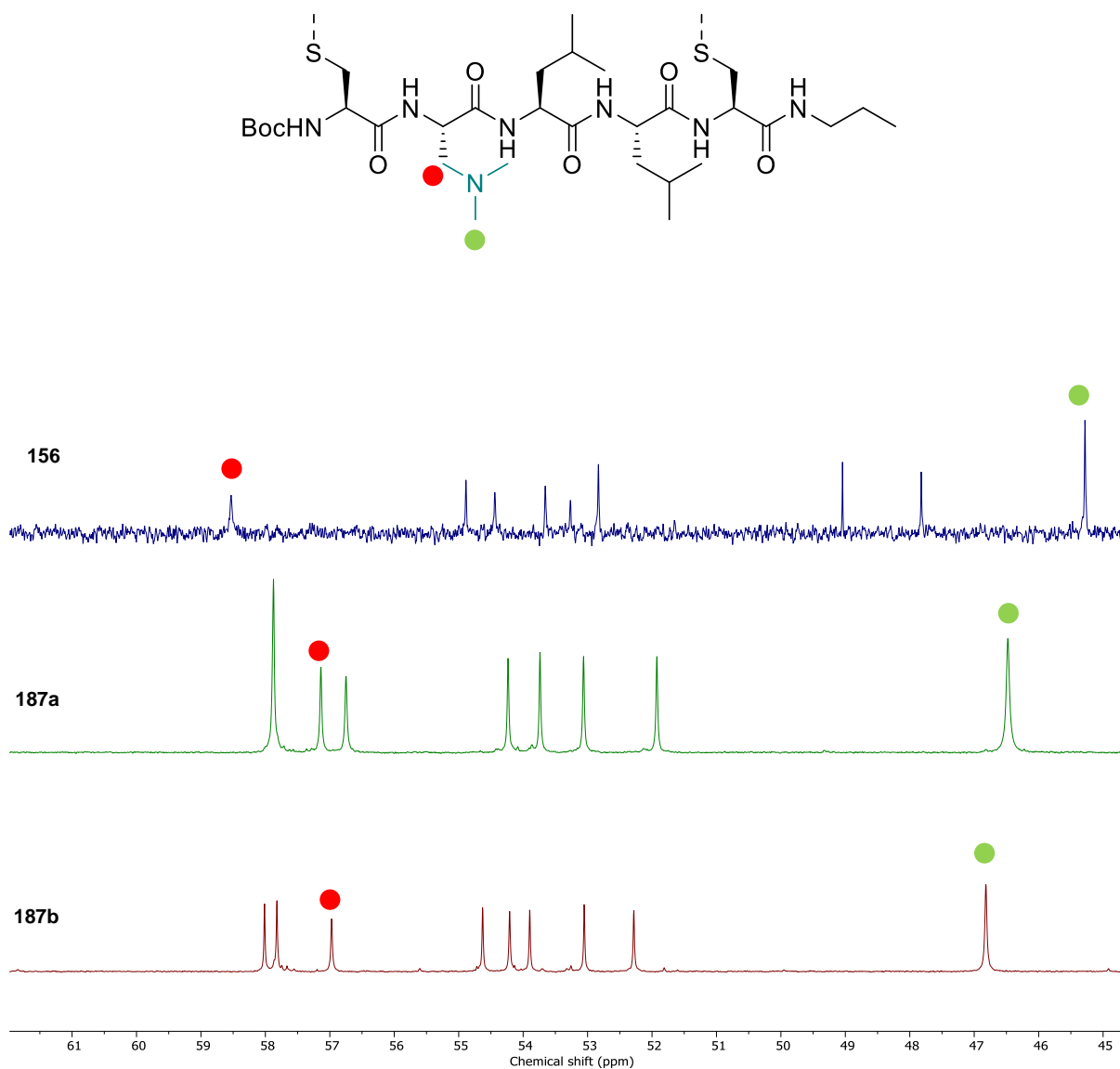
Figure 62. Zoom in ^{13}C NMR of **156** (top), **187a** (middle) and **187b** (bottom).

In contrast, CH$_3$ signals shifted downfield from 45.3 ppm in the acyclic peptide **156** to 46.9 ppm in catalyst <u>CBLLC</u>, **187a** and 46.5 ppm in **187b**. The same phenomenon was observed for adamantyl protected catalyst <u>CBLLC</u> **192**. Despite the hydrogen atoms in CH$_3$

groups of **CBLLC** series were found to be upfield shifted in ^{1}H NMR spectra, moving only one bond from hydrogen atoms put this methyl carbon fell into deshielding region of PDI. In this situation, nitrogen atom in the tertiary amine should be in the border of shielding and deshielding areas of aromatic system. In other words, it could be located on the edge of PDI rather perfectly above.
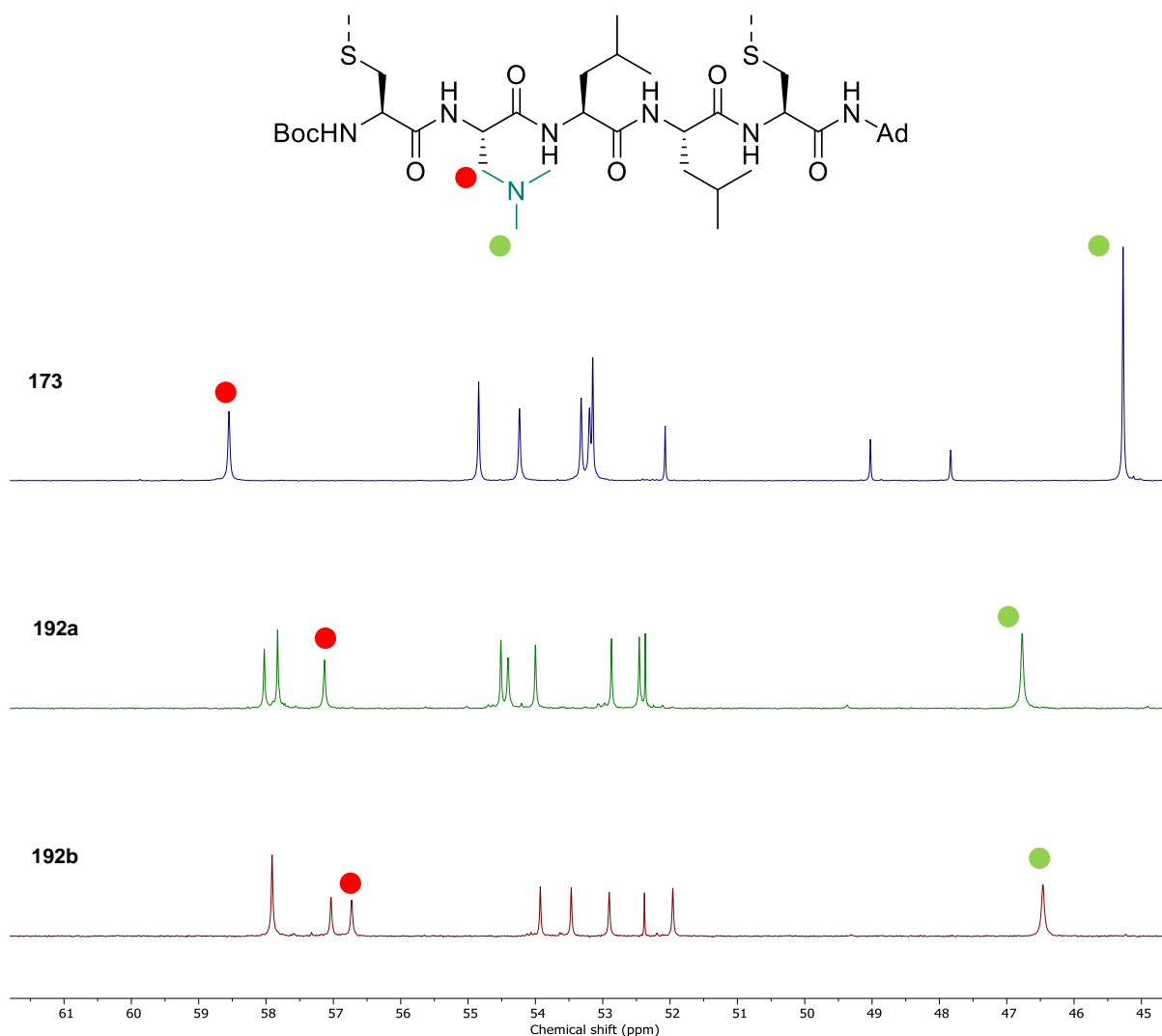
Figure 63. Zoom in ^{13}C NMR of **173** (top), **192a** (middle) and **192b** (bottom).

3.2.2.3.2. 2D NMR Characterization

Secondary structure of stapled peptides above aromatic surface could be accessed by 2D NOE NMR spectra. ROESY spectrum of <u>CLLBC</u> catalyst **184** showed characteristic H-H correlations for helical structure. Correlations between two neighboring protons of amide groups could be observed over the whole peptide backbone (Figure 64-66). These strong correlations were in good agreement with their short distance of 2.8 Å in an α-helix.[211] C_α-H protons of amino acid residues within peptide sequence also had interactions with amide protons. Except the obvious cross peaks between C_α-H proton of amino acid i with N-H proton of i+1 residue ($d_{\alpha N}$ (i, i+1)), other long-range correlations could be found on ROESY spectrum. The $d_{\alpha N}$ (i, i+2), $d_{\alpha N}$ (i, i+3) correlations featured a helix-like conformation for PDI-peptide conjugates. Although the distance between C_α-H proton of amino acid i and N-H proton of i+4 residue is smaller than the one between C_α-H proton of amino acid i and N-H proton of i+2 residue in an α-helix (4.2 Å vs 4.4 Å), $d_{\alpha N}$ (i, i+4) correlations were not visible. It suggested some deviation in conformation of peptide turn in <u>CLLBC</u> **184** from a perfect α-helix. Since the stapling linker PDI is larger than NDI, the peptide turn could be stretched, most likely, to a 3_{10} helix-like conformation. Because the pitch of 3_{10} helix is longer than α-helix (6.0 Å vs 5.4 Å), the distance between C_α-H proton of amino acid i and N-H proton of i+4 residue is now longer than the one between C_α-H proton of amino acid i and N-H proton of i+2 residue.[211] The absence of $d_{\alpha N}$ (i, i+4) correlations could be explained by this change. Moreover, mostly $^3J_{\text{H}\alpha-\text{HN}}$ measured in ^{1}H NMR spectra were rather small (< 5.0 Hz). Based on Karplus equation, the dihedral angle H-N-Cα-H could be estimated to have the absolute value close to 60°. In accordance, C-N-Cα-C angle φ fell into the region of helical conformations on Ramanchandran plot.[211–214] Taken all together, NMR data strongly suggested a helix-like conformation for peptide above PDI surface in <u>CLLBC</u> **184**. However, clear differentiation between α-helix and 3_{10}-helix could be a challenge especially within short peptide sequences. As discussed in

previous section, changing positions of the tertiary amine did not gave any significant changes in peptide secondary structure. Similar ROESY spectra were found for other catalyst series C**B**LLC, CL**B**LC.
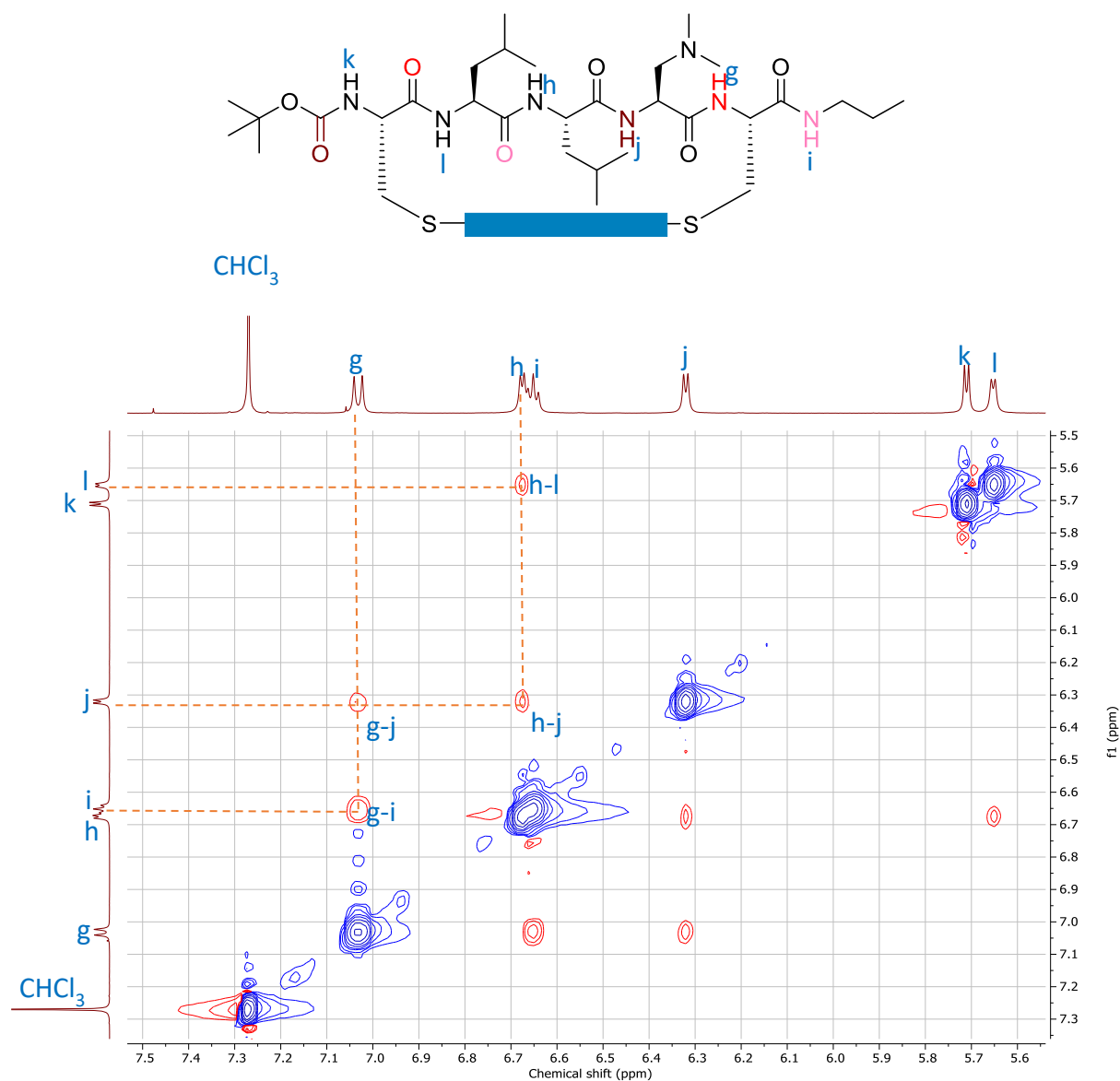
Figure 64. Zoom in 2D ROESY NMR of **184a** at NH region. d_{NN} (i, i+1) correlations were marked by dotted line.
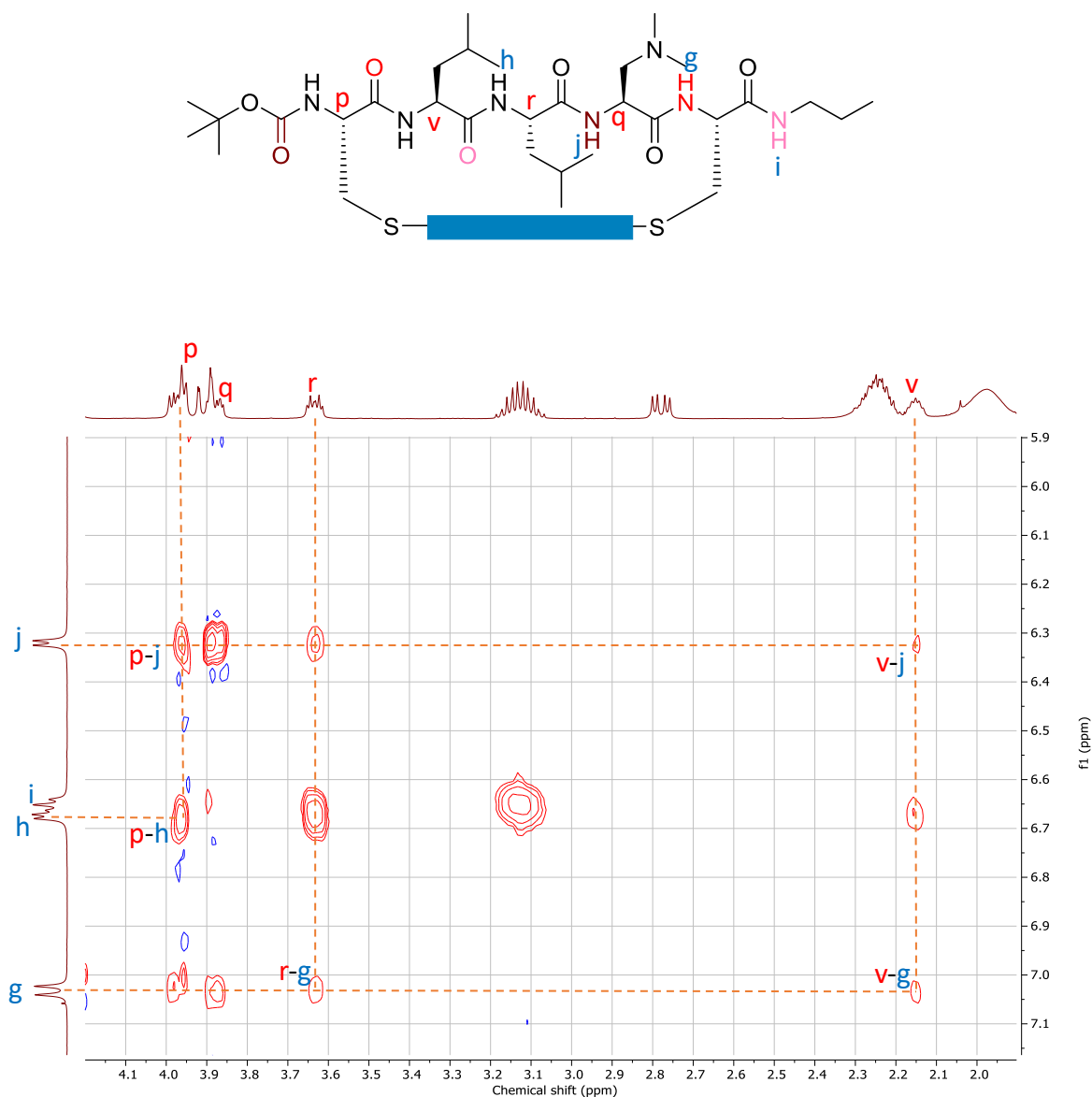
Figure 65. Zoom in 2D ROESY NMR of **184a** at NH-C$_\alpha$H region. d$_{\alpha N}$ (i, i+2) and d$_{\alpha N}$ (i, i+3) correlations were marked by dotted line.
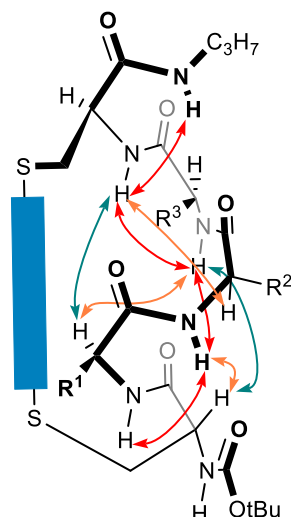
Figure 66. NOE contact map of **184a** from 2D ROESY NMR (Figure 64, 65) (3_{10}-helix model). Arrows: red: d_{NN} (i, i+1) correlations, orange: $d_{\alpha N}$ (i, i+2) correlations, green: $d_{\alpha N}$ (i, i+3) correlations. (Only characteristic correlations of helical structure were shown).

3.2.2.3.3.   Circular Dichroism

In analogy to NDI-peptide conjugates, two atropo-diastereomers of <u>CLLBC</u> **184a** and **184b** exhibited semi-pseudo enantiomeric behavior (Figure 67b). Their CD spectra had opposite sign of $\Delta\varepsilon$. In visible region (400-650 nm), **184a** showed a monosignated peak with two maxima at 597 nm and 477 nm. These maxima corresponded to S_{0-0} transition at 587 nm and S_{0-2} transition at 425 nm in UV-Vis absorption spectra (Figure 67a). S_{0-1} and S_{0-3} vibrational bands of PDI chromophore were not well resolved. They appeared as shoulders centered at 552 nm and 402 nm, respectively. In the UV region (200 – 400 nm), an asymmetric bisignated signal was found with a positive first Cotton effect and a negative second one. Comparison of CD spectra of **184a** with reported data of other bridged-PDIs allowed to assign (*P*) conformation for **184a**.[109] Therefore, PDI surface of **184b** should have (*M*)-configuration.
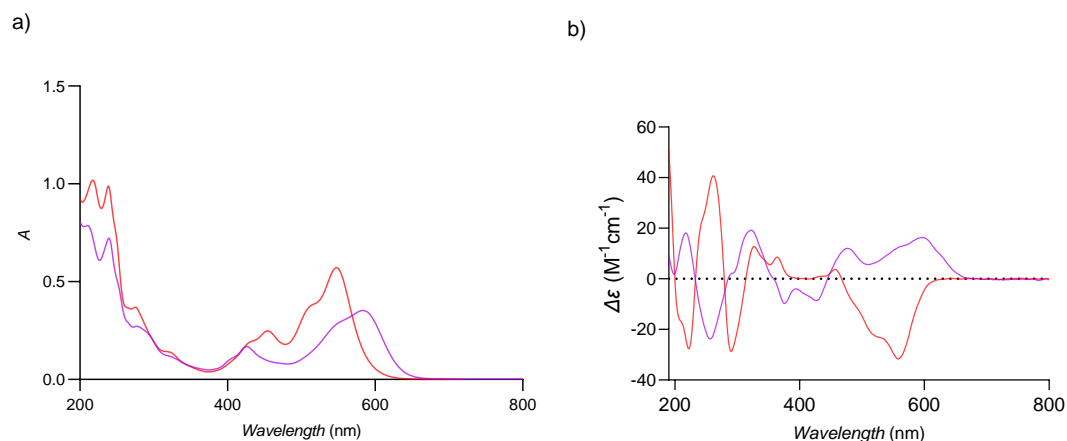
Figure 67. (a) UV-Vis and (b) CD spectra of **184a** (purple) and **184b** (red).

For **184b**, a broad monosignated peak with maximum at 557 nm and shoulder around 517 nm could be observed in visible region. They corresponded with S_{0-0} and S_{0-1} transitions of PDI core at 547 nm and 510 nm in UV-Vis absorption spectrum. In the UV region, an asymmetric bisignated signal was found with opposite signs in comparison with **184a**. Again, dominant contribution of PDI over peptide backbone to optical properties of the conjugates limited the possibility to study peptide conformation using CD.

3.2.2.4.   Synthesis of Additives

Addition of other species which can assemble with anion-π catalysts has been showed to have great influence to catalytic reactions.[58,59] In order to improve catalyst activity, it is important to have a scaffold which promotes anion-π interactions of catalysts and anionic transition states. Self-assembly ability of PDI has been extensively exploited for building supramolecular oligomers.[99,110,112,215–220] Therefore, using an electron-poor PDI as an activator for PDI-peptide

conjugates in catalysis was an appealing approach to increase catalyst performance. In solution, PDI activator could assembly with PDI catalysts by π-π interactions. Electron-deficient nature of activator would polarize PDI surface of catalysts, thus enhances anion-π interactions on catalyst surface. A more electron-poor PDI could be achieved by simply introducing two strong electron-withdrawing sulfone groups at its bay positions. The synthesis of PDI sulfone **193** was done following scheme 7. Aromatic nucleophilic substitution at bromine atoms in PDI **180** by 1-octanethiol afforded PDI sulfide **194** in good yield. Subsequent oxidation in CH_2Cl_2 with excess amount of *m*-CPBA gave the designed PDI sulfone **193**.
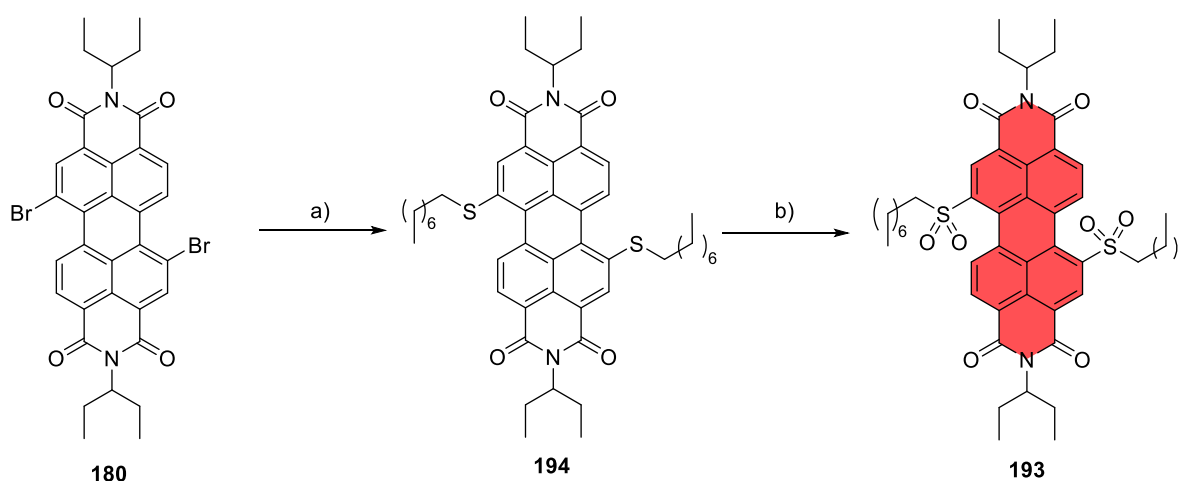
Scheme 7. (a) 1-octanethiol, K_2CO_3, 18-Crown-6, THF, rt, overnight, 84%; (b). *m*-CPBA, CH_2Cl_2, 86%.

3.2.2.5.   Catalyst Evaluation

3.2.2.5.1. MAHT Reaction

MAHT reaction was chosen to evaluate catalytic activities of PDI-peptide conjugates in order to have a direct comparison with their NDI analogs. For catalyst <u>CLLBC</u> **184**, high chemoselectivity was observed for both diastereomers. qAD = 0.90 for **184a** and qAD = 0.92 for **184b** were clearly better than qAD = 0.68 and qAD = 0.60 of the corresponding NDI catalysts <u>CLLBC</u> **159** (Table 1, Table 3, Figure 68). This result was in good agreement with the positions of the tertiary amine determined for each catalyst in previous sections. While the amine in PDI catalyst <u>CLLBC</u> **184** was located above and close to aromatic surface, in NDI catalyst <u>CLLBC</u> **159**, it fell to deshielding area of NDI. Even though, the anionic transition state was still close to aromatic surface to be stabilized in NDI catalyst, the effect of anion-π catalysis was clearly less pronounced in comparison with PDIs. Replacement of stapling linker from NDI to PDI did not cause major changes in the motif of peptide secondary structure as described by NMR studies previously. However, using a larger π-acidic surface indeed changed the relative positions of the amine to anion acceptor aromatic surface. Enantioselectivity was also much better for PDI series, *er* of 62:38 and 47:53 was observed for **184a** and **184b**, respectively. Their different enantiomeric preferences in MAHT reaction suggested the contribution of chiral PDI surface to enantioselectivity. In case of NDI analogue <u>CLLBC</u> **159**, no enantioselectivity was found. Replacement of *n*-propyl protecting group by bulkier adamantyl group led to slightly decrease in reactivity. qAD = 0.70 was obtained for <u>CLLBC</u> **188**. *Er* was also low because two diastereomers were not separable.

As expected, larger PDI surface enables anion-π catalysis for PDIs having the tertiary amine in the middle of the peptide sequence. High values of qAD were found for catalysts <u>CLBLC</u> **186a** (0.85) and **186b** (0.80). Chemoselectivity was less impressive in comparison with catalysts <u>CLLBC</u> **184** since the tertiary amine should be located further from PDI surface. However, enantioselectivity was improved. Similar to NDI-peptide conjugates, having the

amine in the peptide sequence gave the best *er* ratio (*er* = 33:67 and 38:62 for **186a** and **186b**, respectively). Preference of the same enantiomer of addition products, observed with these two PDIs, indicated decrease in the influence of axial chirality to enantioselectivity. In adamantyl analogue <u>CLLBC</u> **190**, while reactivity of (*M*)-configured catalyst **190b** was almost the same in comparison with *n*-propyl protected **186b**, reactivity of the (*P*)-isomer **190a** dropped slightly (qAD = 0.65, *er* = 41:59). In contrast with NDI catalysts, tertiary amine at position close to the N terminus in peptide sequence of PDI catalysts had very low reactivity. For catalyst <u>CBLLC</u> **187**, qAD = 0.24 for **187a** and qAD = 0.18 for **187b** were observed, which were only slightly better than the acyclic control ^{P}**CBLL**^{P}C **156** (qAD = -0.12). As described in section 3.2.2.3.1, the tertiary amine at this position located at the border of shielding and deshielding areas of PDIs, which was probably not ideal for anion-π interactions. Besides, since the amino acid residue close to the N terminus had been proven to be very closed to PDI surface, potential lone pair-π interactions could hinder the basicity of nitrogen atom. Thus, reactivity observed for the library of catalysts seemed to follow structure elucidation. Various attempts to restore anion-π interactions of the tertiary amine at this position by structure modifications failed. Changing protecting group at the C terminus from *n*-propyl to adamantyl gave equally bad chemoselectivity (qAD = 0.30 for **192a** and qAD = 0.10 for **192b**). Taking consideration that the adamantyl protected acyclic control ^{P}**CBLL**^{P}C **173** was better than the *n*-propyl one (qAD = 0.10 vs qAD = - 0.12), the effect of anion-π interactions in the case of <u>CBLLC</u> **192** was negligible. Enantioselectivity was in same range with the *n*-propyl predecessor.
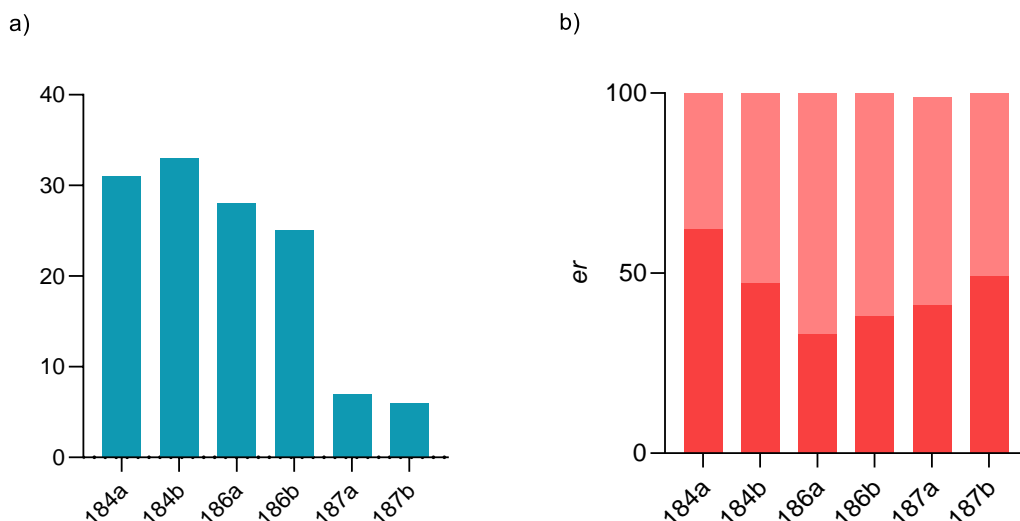
Figure 68. Catalytic activity of some PDI catalysts in MAHT reaction. (a) A/D ratio; (b) enantiomeric ratio.

Tightening peptide turn by removing one Leucine residue between two Cysteines as in <u>CBLC</u> **195** did not improve catalyst performance. qAD = 0.24 for **195a** and qAD = 0.10 for **195b** were not superior qAD = 0.10 of the corresponding acyclic control ^{p}CBL^{p}C **196**. Elongation of <u>CBLC</u> by adding one more Leucine residue at the N terminus as in <u>LCBLC</u> **197** increased reactivity (qAD = 0.48 and 0.76 for **197a** and **197b**, respectively). However, the acyclic control L^{p}CBL^{p}C **198** also became more active (qAD = 0.24). Catalytic activity remained low in <u>CBLLLC</u> **199** (qAD = 0.40 for **199a** and 0.24 for **199b**). Similarly, increasing the distance between PDI and peptide backbone by replacing one Cysteine by Homocysteine in <u>CBLL^{h}C</u> **200** worsened chemoselectivity (qAD = 0.00 for **200a** and 0.3 for **200b**). Overall, when the tertiary amine was placed close to the C terminus or in the middle of peptide backbone, high catalytic activity was observed because of the effect generated from anion-π interactions. On the other hand, tertiary amine close to the N terminus was not able to turn on anion-π interactions. Located at the edge of PDI surface rather above, tertiary amine at this position was not ideal for anion-π catalysis.

In accordance with NDI studies, when catalysts operated by anion-π interactions, exocyclic elongation of peptide backbone greatly enhances catalytic activity. For catalyst CLLBCL **201**, qAD = 1.0 and qAD = 1.3 were found for **201a** and **201b**, respectively. Even though the acyclic control ^{P}CLL**B**^{P}CL **202** was also became more active, this record activity is remarkable. Only trace of decarboxylation product was obtained. For (*P*)-configurated isomer **201a**, *er* was slightly improved (*er* = 62:38). Interestingly, (*M*)-configurated isomer **201b** prefered the same enantiomer of addition product (*er* = 56:44). In contrast with shorter catalyst CLLBL, contribution of chiral PDI surface to enantioselectivity was reduced. Similar results were found for CLBLCL catalyst **203**. Chemoselectivity was excellent (qAD = 1.4 for **203a** and qAD = 1.0 for **203b**), while catalytic activity of the acyclic peptide ^{P}CLBL^{P}CL **204** did not change significantly (qAD = 0.35). For **203a**, enantioselectivity was also increased up to -50% *ee* (*er* = 25:75). At the same time, *er* of **203b** remained unchanged (*er* = 39:61). The series CBLLC has been showed to not function by anion-π interactions. Thus, there was no increase in activity upon elongation. Catalyst CBLLCL **205** gave low chemoselectivity (qAD = 0.10 for **205a** and qAD = 0.44 for **205b**). Enantioselectivity was also not impressive (*er* = 48:52 and 40:60 for **205a** and **205b**, respectively).

Table 3. Characteristics of PDI catalysts.[a]

Cat[b]	Sequence[c]	R$^{C[d]}$	qAD[e]	A/D[f]	*er*[g]
184a	CLLBC	NH*n*Pr	0.90	31	62:38
184b	CLLBC	NH*n*Pr	0.92	33	47:53
188a, b (mixture)	CLLBC	NHAd	0.70	20	56:44
189	^{P}CLL**B**^{P}C	NHAd	0.44	11	50:50

201a	<u>CLLBCL</u>	NHAd	1.0	40	65:35
201b	<u>CLLBCL</u>	NHAd	1.3	74	56:44
202	$^{\text{P}}$CLL**B**$^{\text{P}}$CL	NHAd	0.51	13	51:49
186a	<u>CLBLC</u>	NH*n*Pr	0.85	28	33:67
186b	<u>CLBLC</u>	NH*n*Pr	0.80	25	38:62
190a	<u>CLBLC</u>	NHAd	0.65	18	41:59
190b	<u>CLBLC</u>	NHAd	0.80	25	32:68
191	$^{\text{P}}$CL**B**L$^{\text{P}}$C	NHAd	0.40	10	46:54
203a	<u>CLBLCL</u>	NHAd	1.4	97	25:75
203b	<u>CLBLCL</u>	NHAd	1.0	41	39:61
204	$^{\text{P}}$CL**B**L$^{\text{P}}$CL	NHAd	0.35	9	45:55
187a	<u>C**B**LLC</u>	NH*n*Pr	0.24	7	41:58
187b	<u>C**B**LLC</u>	NH*n*Pr	0.18	6	49:51
192a	<u>C**B**LLC</u>	NHAd	0.30	8	44:56
192b	<u>C**B**LLC</u>	NHAd	0.10	5	47:53
205a	<u>C**B**LLCL</u>	NHAd	0.10	5	48:52
205b	<u>C**B**LLCL</u>	NHAd	0.44	11	40:60
195a	<u>C**B**LC</u>	NH*n*Pr	0.24	7	47:53
195b	<u>C**B**LC</u>	NH*n*Pr	0.10	5	39:61
196	$^{\text{P}}$C**B**L$^{\text{P}}$C	NH*n*Pr	0.10	5	43:57
197a	<u>LC**B**LC</u>	NH*n*Pr	0.48	12	48:52
197b	<u>LC**B**LC</u>	NH*n*Pr	0.76	23	56:44
198	L$^{\text{P}}$C**B**L$^{\text{P}}$C	NH*n*Pr	0.24	7	48:52
199a	<u>C**B**LLLC</u>	NH*n*Pr	0.40	10	48:52
199b	<u>C**B**LLLC</u>	NH*n*Pr	0.24	7	38:62

206	^{P}**CBLLL**^{P}**C**	NHnPr	-0.12	3	44:56
200a	**CBLL**^{h}**C**	NHnPr	0	4	44:56
200b	**CBLL**^{h}**C**	NHnPr	0.3	8	35:65
207	^{P}**CBLL**^{ph}**C**	NHnPr	-0.12	3	38:62

[a] Reactions were conducted as in Figure 46 and followed by ^{1}H NMR spectroscopy. See Figure 55 for pertinent examples of full structures. [b] Catalyst abbreviation structures. [c] Peptide sequences. [d] C-terminal substituents. [e] qAD = log (A/D) – log (A/D)$_0$. [f] Yield of addition product **46** divided by yield of decarboxylation product **47** at full substrate conversion. (A/D)$_0$: A/D with TEA as catalyst (A/D = 4.0, log(A/D)$_0$ = 0.60). [g] Enantiomeric ratio.

3.2.2.5.2. Catalysis with Additives

As described previously, PDI is an excellent building block for construction of supramolecular oligomers. Strong π-π interactions between PDI molecules allowed them to stack together. Standing alone, PDI-peptide conjugates could only form a dimeric structure since one face of PDI was blocked by peptide back bone. Dimerization constants obtained for similar bridged-PDI usually fall in the range of $10^3\,M^{-1}$, suggesting that at mM concentration they prefer to stay in dimeric form.[110,112] In MAHT reaction, where the concentrations of catalysts were kept at 40 mM, catalysts would probably operate as a dimer. When activator **193** was introduced to the catalytic reaction, its strong electron-deficient nature would allow it to intercalate into PDI dimer stack (Figure 69a). Following this intercalation, activator induced polarization of PDI catalysts, thus, improved anion-π interactions. While activator did not have any influence to chemo and enantioselectivity, initial velocity of MAHT reaction increased significantly for catalysts which operated by anion-π interaction. For CLLBC **188**, almost two folds increasement of initial velocity was observed upon addition of activator (Figure 69b). This

behavior, however, was not found for the acyclic control ^{P}CLL**B**^{P}C **189**. The same trend could be reproduced for <u>CL**B**LC</u> **190a** and its acyclic control ^{P}CL**B**L^{P}C **191**. Not only improved overall performance of catalytic systems, the effect of the activator also showed that anion-π interactions were the main mode of action for PDI-peptide conjugates in MAHT reaction.
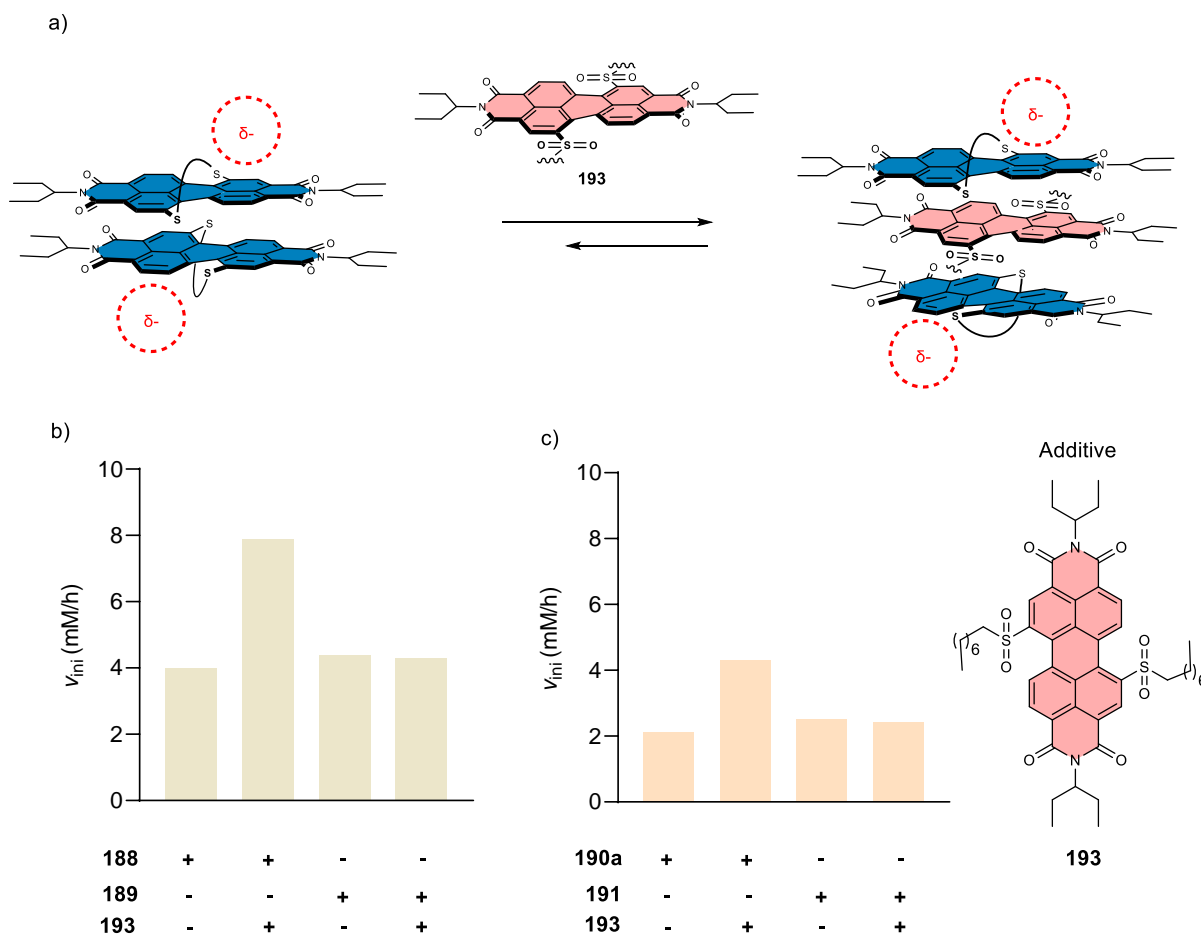
Figure 69. (a) Intercalation of activator **193** to PDI dimer. (b), (c) Initial velocities of MAHT reactions with different combination of catalysts and activator.

3.2.3.   Conclusion

Extending aromatic surface from NDI to PDI opens new possibility to design anion-π catalysts-peptide conjugates. While keeping helical motif of peptide backbone in catalyst secondary

structure, larger PDI surface is able to turn on anion-π catalysis for the tertiary amine at position which was unactive for NDI. Moreover, twisting PDI surface adds planar chirality to catalytic systems, which maybe the reason for better enantioselectivity in new library of catalysts. NMR studies revealed the positions of amino acid residue side chains above aromatic surface. Best catalytic activity was found for catalysts with optimal positions of the tertiary amine for anion-π interactions. Exocyclic elongation of peptide backbone gave significant improvement in both chemo- and enantioselectivities. On the other hand, different modifications in peptide turn failed to restore reactivity when the amine located at the edge of PDI. Increasement of initial velocities for PDI-catalyzed reactions upon addition of activator supported the contribution of anion-π interactions to catalyst performance. These results encouraged applying different electron-poor aromatic scaffolds as covalent linker to stabilize peptide secondary structures for catalysis, supramolecular assembly, etc. Also, application of chiral PDI surface in catalysis remained unexplored.

3.3.   Thiol-Mediated Uptake Inhibitors

3.3.1.   Design of Inhibitors

Although targets of thiol-mediated uptake are not totally clear, it was known that thiol-mediated uptake transporters did react with free thiol or disulfides of membrane proteins.[131,133] High reactivity of transporters as well as possible dynamic covalent exchange of resulted disulfide bonds lead to a wide range of target proteins identified in proteomic studies.[133] Therefore, inhibitions of thiol-mediated uptake required highly thiol-reactive probes which can react and block free thiol or disulfide bonds on cell membrane (Figure 70). Derivatives of thiol-mediated uptake transporters should be ideal to develop thiol-mediated uptake inhibitors

because they would react with the same target proteins of transporters. To minimize cytotoxicity, impermeable probes were desired since they could not react with other important proteins within cells. For this purpose, a library of inhibitors was developed based on reported thiol-mediated uptake inhibitors bearing anionic functional groups. Also, other neutral thiol-reactive reagents were not excluded since some of them was known to exhibit minimal toxicity in cells.
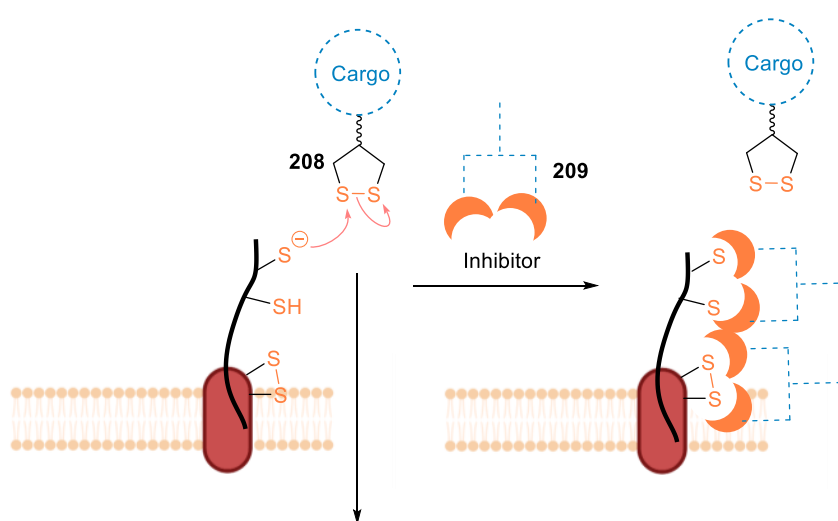
Figure 70. Thiol-mediated uptake and its inhibition by removal of exofacial thiols and disulfides.

3.3.2.   Synthesis of Inhibitors

3.3.2.1.   Synthesis of Thiosulfonate Derivatives

Thiosulfonate derivatives were chosen as promising candidates for thiol-mediated uptake inhibitions because of their high reactivity toward free thiol. In physiological conditions,

nucleophilic attack of free thiolate to thiosulfonate is ultrafast. Resulted disulfide bond could participate to further exchange with other free thiolates. Besides, newly generated sulfinate could cleave nearby disulfide bonds (Figure 71).[173]
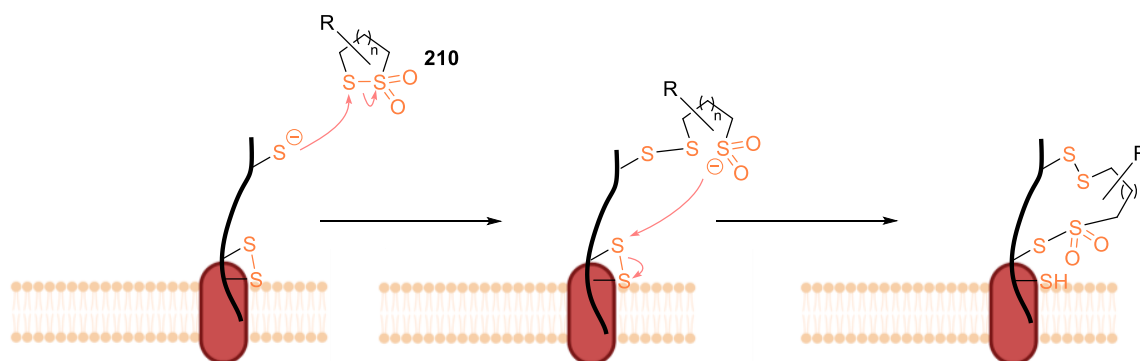
Figure 71. Reaction of thiosulfonates with free thiols of membrane proteins results sulfinate group which could cleave nearby disulfide bonds.

A big library of thiosulfonates was developed based on two synthetic pathways in scheme 8. Following synthetic pathway A, nucleophilic substitution at leaving groups of starting materials **211** allows two acetylthio groups to be installed. Deprotection of acetyl groups of **212** in acidic condition affords dithiol products **213**. Oxidative cyclization using H_2O_2 in acetic acid gives desired thiosulfonates **210**. Alternatively, synthetic pathway B could be used for substrates which were not compatible with previous synthetic route. Oxidative cyclization in mild condition using air yields cyclic disulfide products **214**. Subsequently oxidation with *m*-CPBA in CH_2Cl_2 gives final thiosulfonates.

Synthetic pathway A:
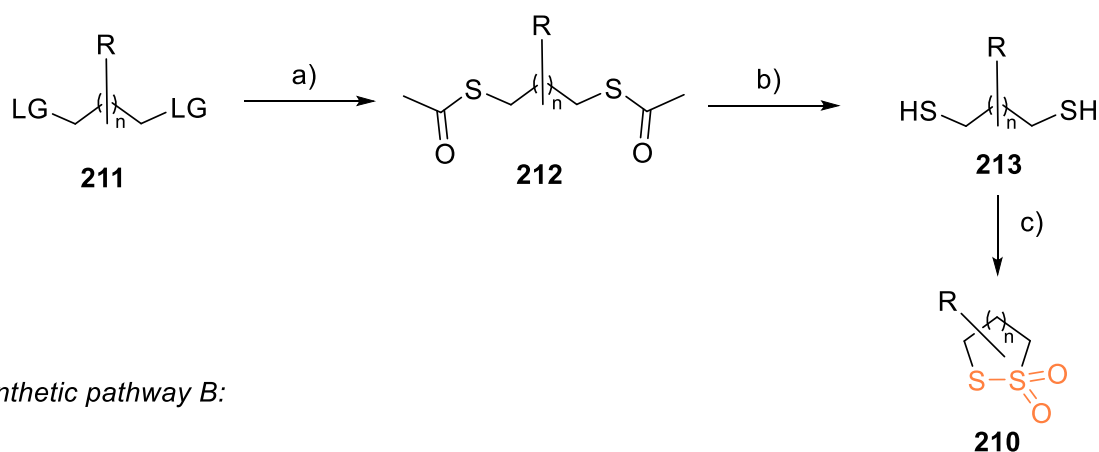
Synthetic pathway B:
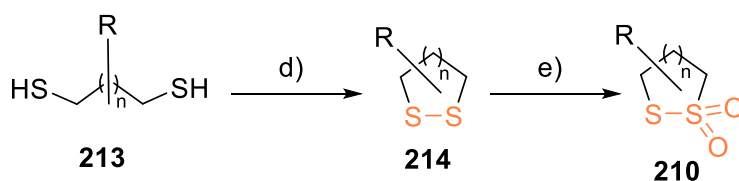
Scheme 8. General synthetic procedures for thiosulfonates. (a) KSAc, 18-crown-6-ether, DMF, rt, overnight; (b) 1.25 M HCl in MeOH; (c) H_2O_2, AcOH; (d) bubbling air, KOH, MeOH; (e) *m*-CPBA, CH_2Cl_2.

Various modifications were applied to tun the reactivity of the probes, such as changing ring size, modification of ring skeletons, installation of different functional groups. Structures of synthesized thiosulfonates were listed in Figure 72. More detail synthetic procedures can be found in section 5.2.6.1.

5-Membered Cyclic Thiosulfonates Derivatives

215

216 *(mixture of regioisomers)*

217 *(mixture of regioisomers)*
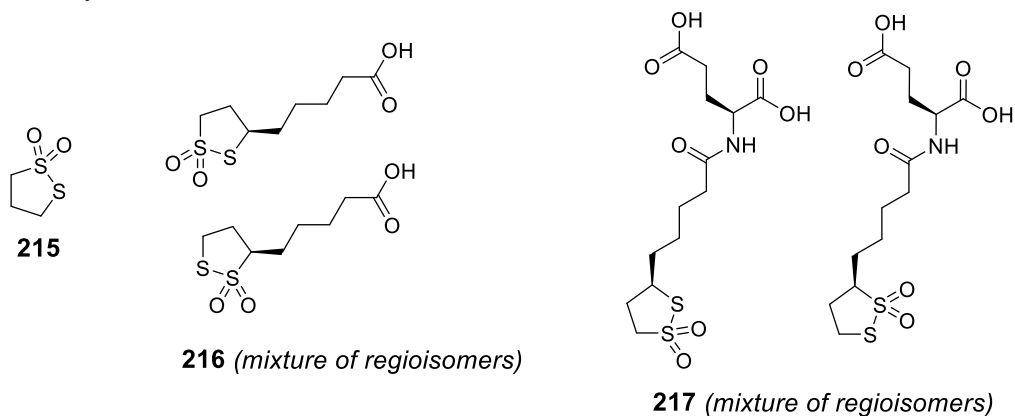
6-Membered Cyclic Thiosulfonates Derivatives

Monocyclic Derivatives

148

218

219 *(mixture of regioisomers and enantiomers)*

220 *(mixture of regioisomers)*

221 *(mixture of regioisomers)*

Bicyclic Derivatives

222

223 *(mixture of diastereomers)*

224

225 *(mixture of diastereomers)*
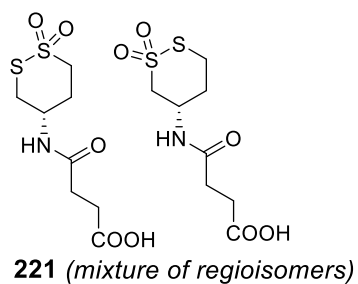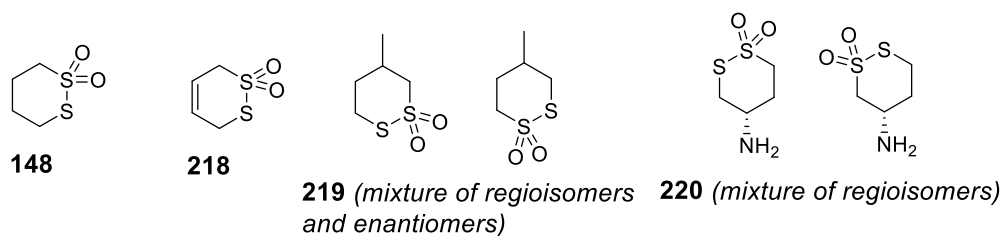
226 *(mixture of diastereomers)*
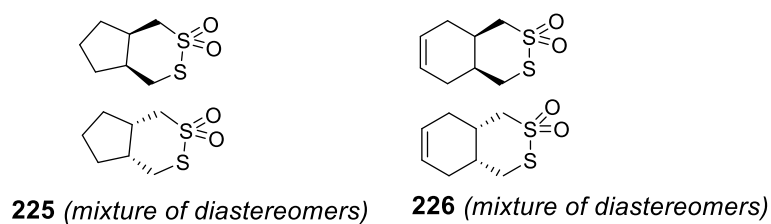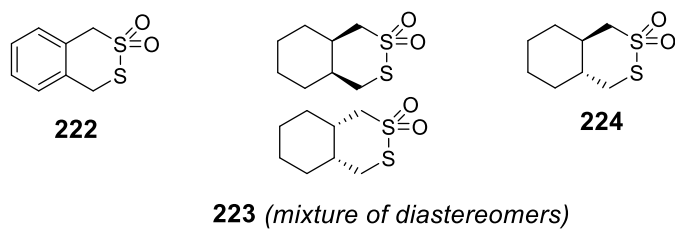
Dimeric Derivatives
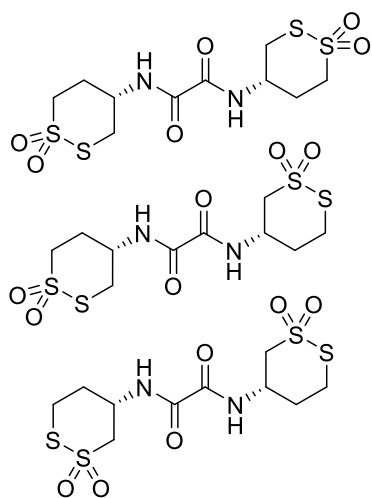
227 *(mixture of regioisomers)*
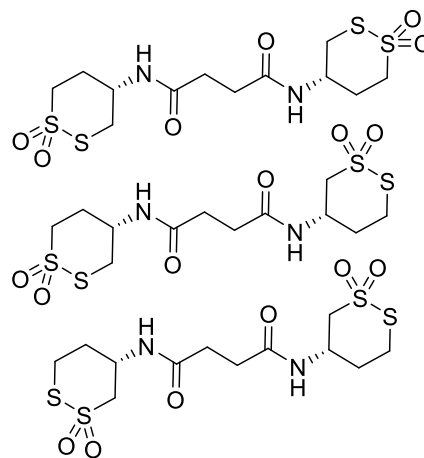
228 *(mixture of regioisomers)*
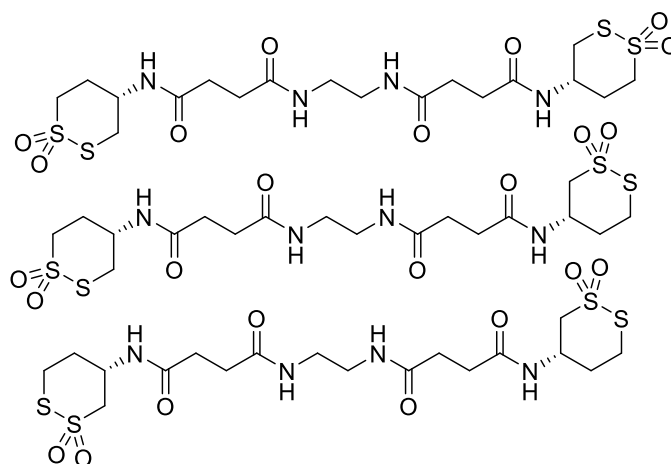
229 *(mixture of regioisomers)*

7 and 8-Membered Cyclic Thiosulfonates

230
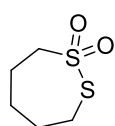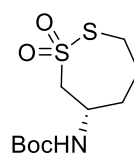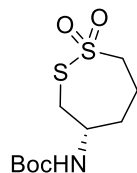
231 *(mixture of regioisomers)*
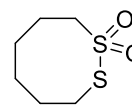
232

Figure 72. Structure of thiosulfonate inhibitors.

3.3.2.2. Synthesis of Disulfide Bridged γ-turn Peptides

Disulfide-bridged γ-turn CXC peptides have been shown to be efficiently uptaken into cells by thiol-mediate uptake.[163,164] An 11-memberred ring creates by disulfide bond between two Cysteines in CXC motif induces significant Prelog strain to the macrocycle. Thus, disulfide-bridged γ-turn CXC peptides are highly reactive toward free thiols. Structure of chosen CXC candidates were shown in Figure 73. Free N terminus at the Cysteine residue allows the thiolate formed after disulfide cleavage to be stabilized by ion paring. Therefore, rate of ring opening reactions by nucleophilic attack should increase. At the same time, carboxylic group at the C terminus in **233** could destabilize the thiolate in opened form of CXC peptide.[222] To overcome this problem, anionic groups were moved further from the Cysteine residue as in **234** and **235**. Removing substituent at X residue as in CGCE **234** reduces the Thorpe–Ingold effect, thus, increases ring strain and reactivity of the peptide. Synthesis of CXC cyclic peptides were conducted following standard solution phase peptide synthesis using EDC as coupling reagent. More detailed procedures could be found in section 5.2.6.2.

233

234 R^1 = H, R^2 = -CH$_2$CH$_2$COOH

235 R^1 = -CH$_2$CH$_2$COOH, R^2 = H
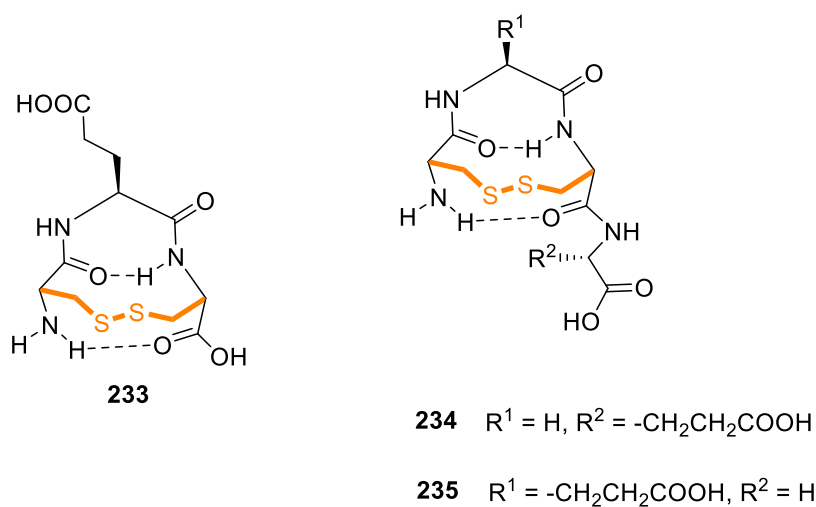
Figure 73. Structure of disulfide-bridged γ-turn CXC peptides.

3.3.2.3.   Heteroaromatic Sulfones

Heteroaromatic sulfones have been used widely in Cysteine proteomic studies and protein modifications. Their tunable reactivity is attractive for repurposing them as irreversible inhibitors for thiol-mediated uptake. By simply changing the nature of heteroaromatic component, probes with various range of activity toward nucleophiles could be obtained. The difference up to 1000 folds in reactivity has been found for a big library of heteroaromatic sulfones.[176] Aromatic nucleophilic substitution at sulfone groups in heteroaromatic sulfones caps free thiols presented in cell proteins and prevents them from participating in exchange process with thiol-mediated uptake transporters (Figure 74).
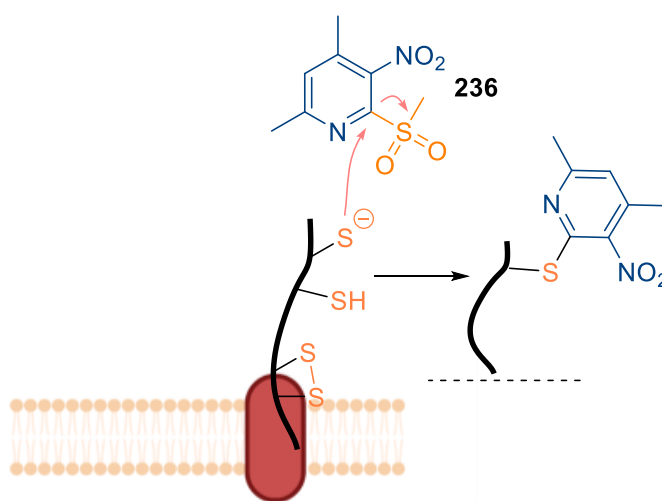
Figure 74. Reaction of heteroaromatic sulfone **236** with free thiol in membrane proteins.

Even though irreversible inhibition could cause cytotoxicity, the high reactivity of heteroaromatic sulfones and their easily synthetic accessibility could not be ignored. Some heteroaromatic sulfones were chosen for preliminary inhibition studies considering they covered a big range of reactivity. Their syntheses followed synthetic pathway in scheme 9.

Free thiol group in heteroaromatic rings **237** was capped with methyl group using CH$_3$I in basic condition to form thioether intermediate **238** in good yield. Oxidation of the sulfur atom afforded desired sulfone derivatives **239**. Probes **240**-**245** and **236** were arranged by their reactivity toward nucleophiles. More detail synthetic procedures could be found in section 5.2.6.3.
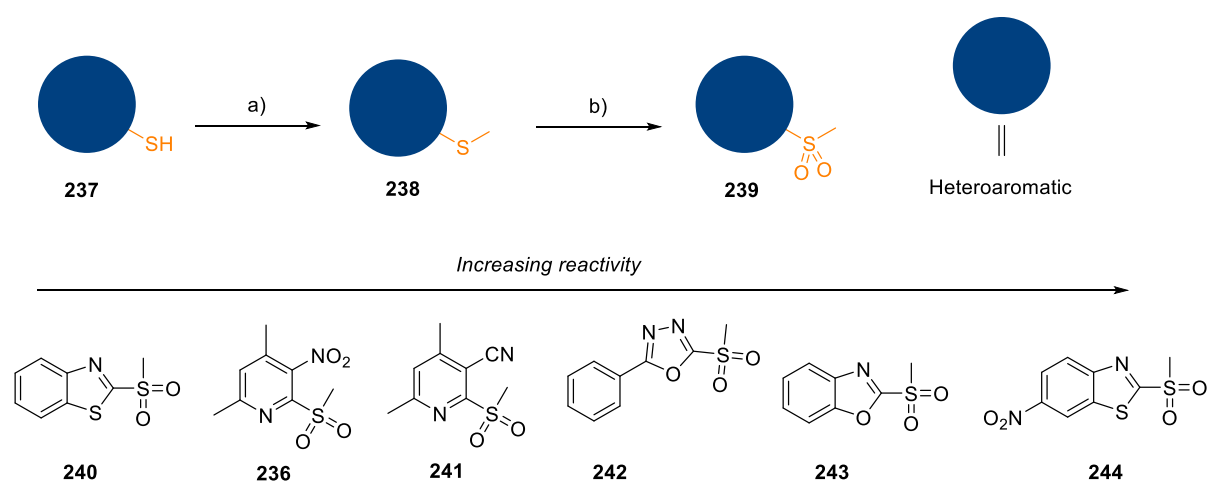
Scheme 9. Synthesis of heteroaromatic sulfones and their relative reactivity. (a) CH$_3$I, CH$_2$Cl$_2$, TEA, 15 min; (b) Oxidation (*m*-CPBA or KMnO$_4$).

3.3.2.4.   Synthesis of Other Inhibitors

Other thiol reactive reagents were also considered as promising inhibitors. ETPs, for instance, have been used as one of the most active thiol-mediated uptake inhibitors.[161,165] Minimal CSSC dihedral angle ($\theta \approx 0°$) created maximum disulfide ring tension in ETPs. Thus, their reactivity toward free thiol is excellent. ETP **245** was equipped with two carboxylic groups by standard peptide coupling with glutamic acid residue to improve its retention on cell membrane (Figure 75). Cyclic thiosulfinates have been used to selectively crosslink proteins. Upon ring opening,

cyclic thiosulfinates generated free terminal sulfenic acid, which participated rapidly to disulfide formation.[172] Cyclic thiosulfinate **246** could be accessed by oxidation of commercially available lipoic acid using H_2O_2 in acetone. Coupling with glutamic acid residue gave dicarboxylic probe **247**. Dynamic-covalent benzopolysulfane networks on cell membrane could be recognized with PBS_3 **248**. While PBS_5 was proven to be the best thiol-mediated uptake transporter, application of PBS_3 in thiol-mediated uptake was scarcely studied.[165] Its high bioactivity, however, encouraged inclusion of PBS_3 **248** to inhibitor library.[223] Polydisulfide sulfinates **249** and **250** were effective in destabilized Epidermal Growth Factor Receptor (EGFR) by disrupting disulfide bonds in protein structure.[173] Activated Michael acceptors such as **251** and **252** were shown to be highly reactive toward Cysteine in Transient receptor potential ankyrin 1 ion channel (TRPA1).[224] Since EGFR and TRPA1 have been considered as potential targets of thiol-mediated uptake, probes targeted these membrane proteins should not be excluded from the inhibitor library.[131] Mimicking reactivity of Protein Disulfide Isomerase, (±)-trans-1,2-bis(2-mercaptoacetamido)cyclohexane (BMC) **253** and its oxidation form **254** could also be interesting to include to this study.[225] Finally, antimony derivatives were synthesized. The dynamic covalent exchanges of thiols at pnictogen center also provided possibility to inhibit thiol-mediated uptake. More detail synthetic procedures of these compounds could be found in section 5.2.6.4.
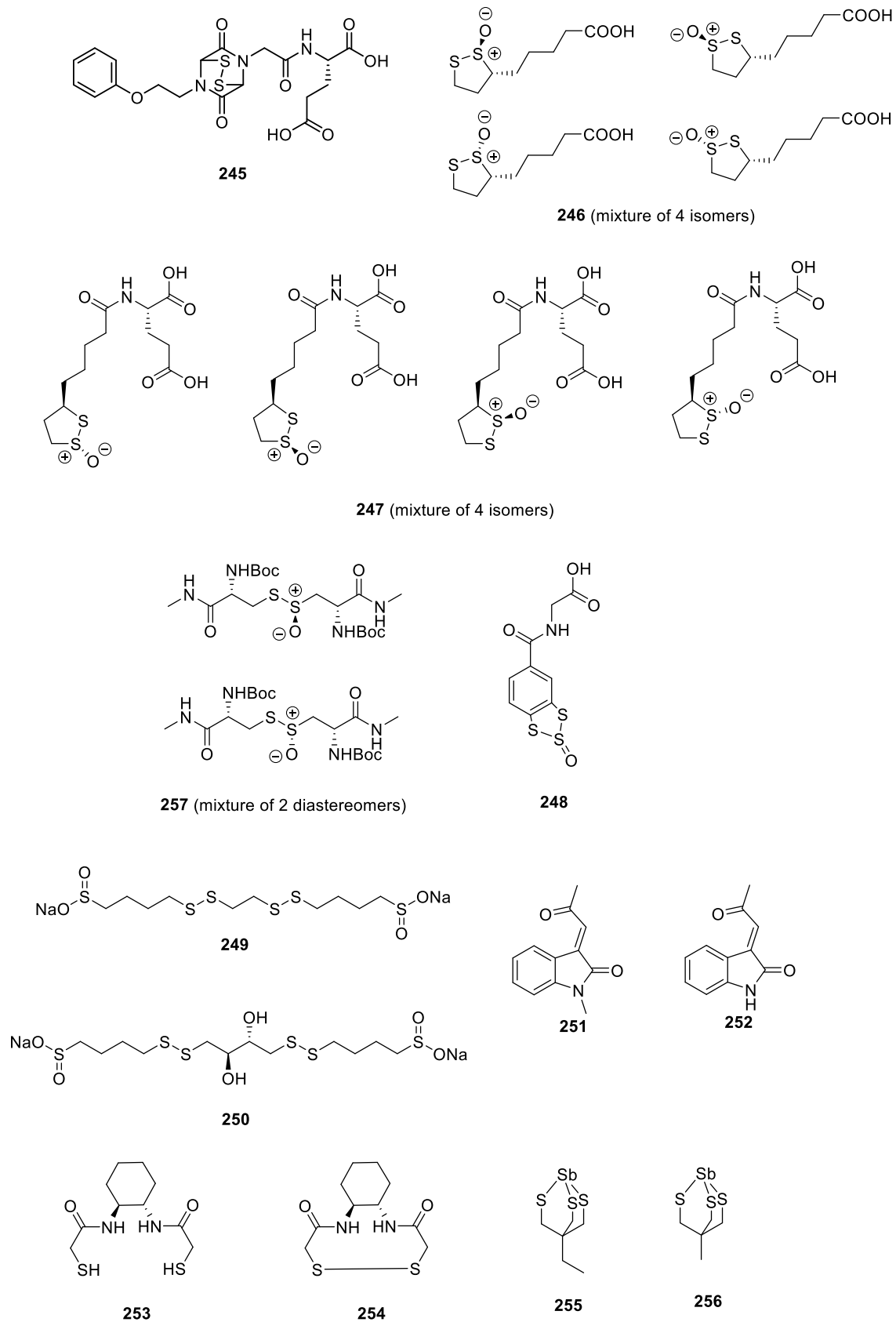
Figure 75. Structures of other potential thiol-mediated uptake inhibitors.

3.3.3. Synthesis of Fluorescently-Labelled Thiosulfonate

Cyclic thiosulfonates were ranked among the best inhibitors for thiol-mediated uptake.[132] In aqueous media, thiosulfonates quickly and selectively reacted with free thiols. Other nucleophiles such as amino, hydroxyl groups were unreactive in the same conditions. This highly selective reactivity and low toxicity of thiosulfonates suggested that they could also be promising thiol-mediated uptake transporters. To quantify uptake efficiency of these scaffolds, fluorescently labelled thiosulfonate **258** was prepared following scheme 10. From racemate **259**, treatment with *N*-Hydroxysuccinimide in presence of EDC afforded activated ester **260**. Oxidation of **260** using *m*-CPBA gave thiosulfonate activated esters **261**. Since it was not possible to control chemoselectivity, this oxidation gave mixture of regioisomers. Activated esters **261** were coupled with Fluorescein labelled amine **262** to yield fluorescently labelled probe **263**. Finally, TBS protecting group could be removed in acidic condition to give desired product 2**58**.
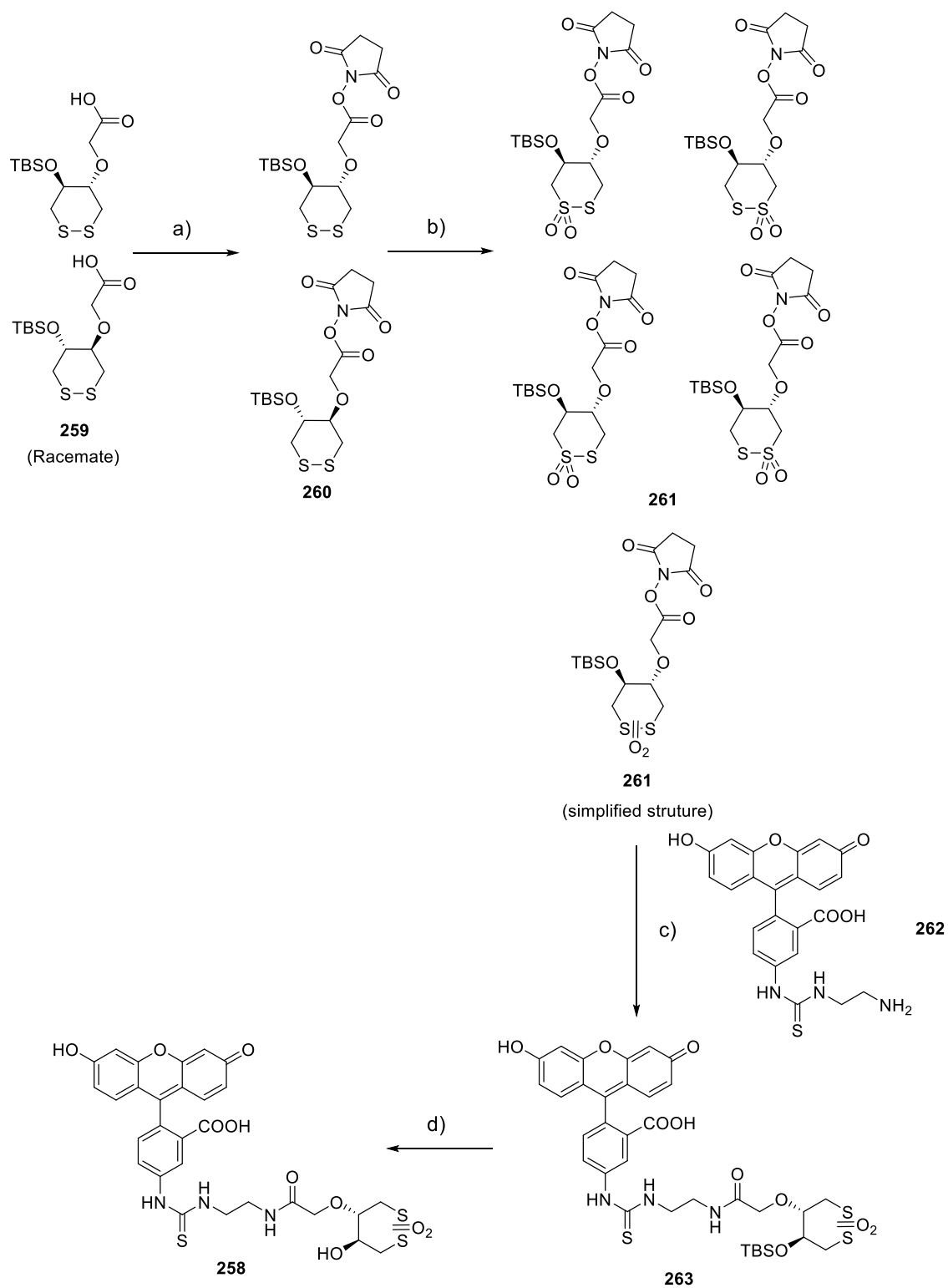
Scheme 10. (a) *N*-Hydroxysuccinimide, EDC, CH₂Cl₂, rt, overnight, 29%; (b) *m*-CPBA, rt, 2

d, 47%; (c) DMF, rt, 4 h, 31%; (d) 1.25 M HCl in MeOH, rt, 1 h, 33%.

3.3.4. Conclusion

A big library of reversible and irreversible covalent inhibitors for thiol-mediated uptake has been developed. Different functional groups with their various reactivity were taken into consideration. Since thiol-mediated uptake is a multiple targets process with complex mechanism, possibility of screening a wide range of thiol reactive reagents provided good inhibitions and better understanding of uptake mechanism. Modifications of thiol reactive probes within their class allowed their reactivities to be tuned. To access potential application of cyclic thiosulfonates as thiol-mediated uptake transporter, fluorescently labelled probes have been prepared.

CHAPTER 4

PERSPECTIVES

In this thesis, it was shown that rigid peptide secondary structures could be utilized to design catalysts with predictable reactivities. However, for MAHT reaction, enantioselectivity so far was not impressive. Solving this problem could be achieved by screening a big library of peptides. On-bead screening could be ideal for this purpose since it reduces synthetic effort significantly. However, a new stapling method, which is compatible with automated solid-phase peptide synthesis, needs to be developed. Replacing Cysteine with other staple-able amino acids could be also attractive in this regard since it would allow improving diversity of the library. From a different perspective, the content of this thesis was limited to helical peptide structures. To reach the ultimate goal of designing highly effective catalytic systems for more reactions based on peptide skeleton, more information on other peptide secondary motifs needs to be acquired. Adopting the developed stapling methods, stabilization of non-regular secondary structures like peptide turns using anion-π catalysts could be easily achieved. On the other hand, other peptide secondary structures may require redesign of the whole system. The second most popular peptide secondary motif – β sheet could be promising to develop foldamers and stacked π system for anion-π catalysis (Figure 76). Various levels of stacking or folding could be controlled by changing solvents polarity. Thus, potential control of catalyst reactivity could be achieved.

a)

b)
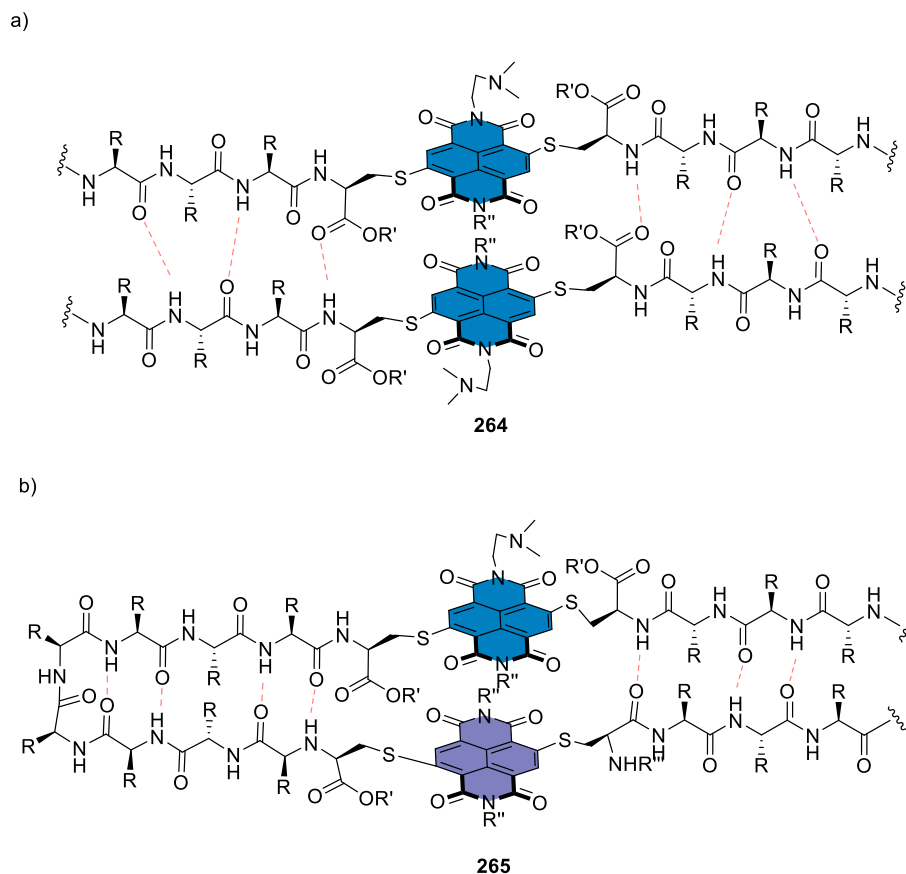
Figure 76. Possible anion-π catalysts based on β-sheet structure. (a) Stacked NDI system **264**; (b) NDI foldamer **265**.

The next goal for future development could be centered on developing more sophisticated structures for application in biology and living systems. For this purpose, the integration of anion-π catalysts into big proteins to create anion-π enzymes should not be excluded. However, this direction could be challenged since a milder stapling condition should be developed. Besides, reengineering of the active pocket would probably be necessary to afford high selectivity for a reaction of interest. On the other hand, extending the application of anion-π catalyst-peptide conjugates to other areas should be more reasonable. A helix long enough to span lipid bilayer membrane with multiple anion binding surfaces along its axis could be used to form ion channel (Figure 77). This scaffold could also be used to perform reaction in

membrane. Operating in a highly order and hydrophobic environment, anion-π catalysis in this case could lead to exceptional selectivity.
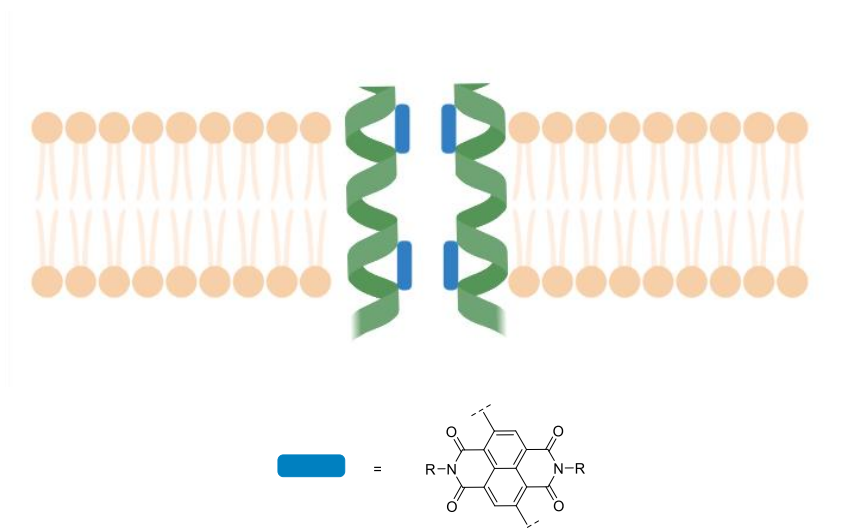
Figure 77. Possible system for ion transport.

For anion-π catalysts based on PDI platform, even though chiral PDI surface could participate in enantioselectivity, quantification of this contribution was complicated because of the presence of point chirality at peptide backbone. Since the application of chiral PDI surface in asymmetric catalysis has not been explored, it could be of interest to examine the pure effect of chiral PDI on enantioselectivity using catalysts shown in Figure 78.
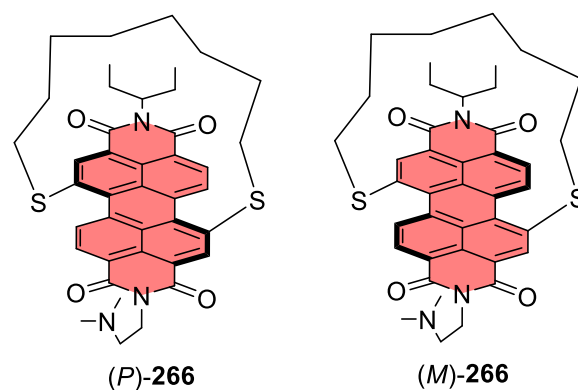
Figure 78. Possible chiral PDI catalysts **266**.

Going further from anion-π catalyst-peptide conjugates, developing more advanced systems for anion-π catalysis is appealing. One attractive direction is remotely controlling of anion-π catalysts. Except for electric field, other potential stimuli have not been applied for this purpose.[56] Light is probably the most advantageous stimulus because of its non-invasive nature. Besides, precise control of light could be easily achieved with modern optical equipment.[226,227] Due to the supramolecular character of anion-π catalysis, developing photo-controllable anion-π catalysts based on photoswitches could be the most reasonable approach. Getting inspiration from the accuracy movement of molecular shuttles, photoswitchable anion-π catalysts could be designed as rotaxane **267** (Figure 79). Similar structures have been successfully utilized for designing molecular shutters which operate by external stimuli.[228–231] In **267a** the macrocycle rests over the strongly macrocycle binding fumaramide station of the thread. Thus, NDI catalyst would operate normally by anion-π interactions. This conformation corresponds to the "on-state" of the system. Irradiating the catalyst with UV light triggers photoisomerization, intramolecular Hydrogen bond and changing in conformation reduces binding affinity of the olefin station. The weaker binding station-NDI in initial state now becomes more favorable for the macrocycle. When the ring moves to the NDI-station in **267b**, its electron-rich aromatic

unit will mask the NDI surface. Therefore, anion-π interactions and catalyst activity could be shut down. Restoration of catalyst activity could be done by irradiating visible light to the system.
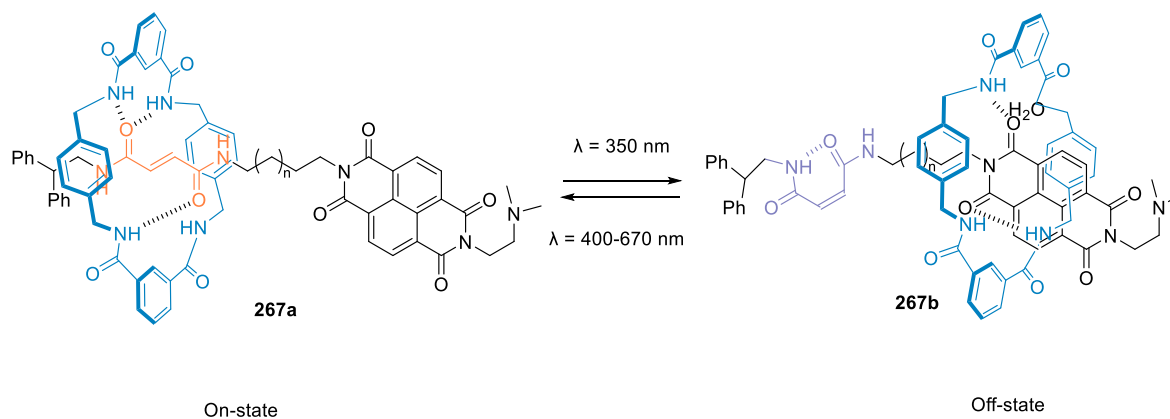
Figure 79. "On" and "Off" states of photoswitchable anion-π catalyst.

The idea of photoswitchable anion-π catalysts could be considered under a different perspective. For instance, synergistic effects between anion-π interactions and π-π stacking for anion-$(\pi)_n$-π catalysis could be controlled by azobenzene photoswitch as shown in Figure 80. In formal *E* conformation, **268** does function by anion-π interactions. However, upon switching from *E* to *Z* conformation, the second NDI surface could be able to stack to the first one. Thus, catalytic activity should be improved. To explore the contribution of polarizability in anion-π interactions, the second NDI unit in **268** could be replaced by an organic cation. Engineering of a photoswitchable organic base at imide position of NDI could also be interesting to turn on or off the effect of anion-π interactions.
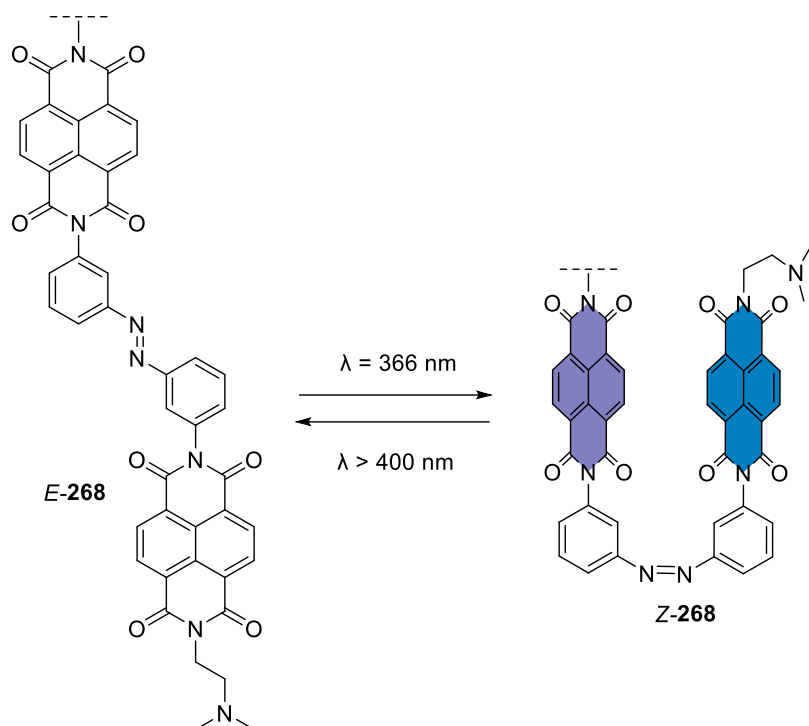
Figure 80. Azobenzene photoswitch anion-π catalyst.

Related to the thiol-mediated uptake inhibitors part of this thesis, even though a lot of chemical modifications have been applied, the information obtained was still insufficient to rationalize structure reactivity relationship. The multitarget and dynamic nature of thiol-mediated uptake could be one of the reasons. To develop better inhibitors, uptake mechanism needs to be investigated in more detail. Systematic proteomics analysis with different inhibitors could reveal the overlap protein targets. In other words, the determination of the most important proteins involved in thiol-mediated uptake would allow a more rational design for future inhibitors based on molecular recognition. Also, utilization of these inhibitors for other purposes should also be considered. Their highly selective reactivity toward thiols could be applied to develop new thiol-mediated uptake transporters or antivirals.

CHAPTER 5

EXPERIMENTAL SECTION

5.1.   General

5.1.1.   Reagents, Solvents and Equipment for Synthesis

As in reference [195] and [132]. Reagents for synthesis were purchased from Brunschwig, Fluka, Sigma–Aldrich, Apollo Scientific and Acros. Analytical grade organic solvents were used for all syntheses.

Reactions were carried out in closed flasks without special cautions (unless specified) with magnetic stirring.

Solvents were evaporated using a Büchi R-200 rotavapor equipped with a vacuum controller (PVK 610 from MLT Labortechnik AG or vacuum MZ 2C model) and a Büchi heating bath.

The glassware used for synthesis and experiments was washed with a soap solution, water, and acetone and was dried in an oven at 120 ºC for at least one hour.

Microwave reactions were performed on a CEM Microwave Synthesis System Discover SP.

5.1.2.   Chromatographic Methods

Column chromatography was carried out on silica gel (SiliaFlash® P60, SILICYCLE, 230 – 400 mesh). Analytical thin layer chromatography (TLC) was performed on silica gel 60 F254 (Merck). Preparative thin layer chromatography (PTLC) was performed on silica gel (SiliCycle, 1000 µm). Reverse phase flash chromatography (column: SNAP Ultra C18 12 g, 25 g or 60 g), hydrophilic interaction chromatography (BGB Scorpius Diol column 20 g), chiral flash chromatograghy (column: Chiralflash® IF particle size 20 µm, 30 mm x 100 mm) were performed on Biotage IsoleraTM Four.

Chiral HPLC were performed on a LC–4000 from JASCO. HPLC–MS were recorded using a Thermo Scientific Accela HPLC equipped with a Thermo C18 Hypersil GOLD column (50 × 2.1 mm, 1.9 µm particles size) coupled with a LCQ Fleet three–dimensional ion trap mass spectrometer (ESI, Thermo Scientific) with a linear elution gradient from 70% H_2O/30% CH_3CN + 0.01% TFA to 10% H_2O/90% CH_3CN + 0.01% TFA in 4.0 minutes at a flow rate of 0.75 mL/min. Retention times R_t are reported in minutes.

5.1.3.   Equipment for Compound Characterization

Melting points (Mp) were measured on a Melting Point M–565 (BUCHI). IR spectra were recorded on a Perkin Elmer Spectrum One FTERT–IR spectrometer (ATR, Golden Gate) and are reported as wavenumbers v in cm^{-1} with band intensities indicated as s (strong), m

(medium), w (weak). ^{1}H and ^{13}C NMR spectra were recorded (as indicated) either on a Bruker

300 MHz, 400 MHz or 500 MHz spectrometer and are reported as chemical shifts (δ) in ppm

relative to TMS ($\delta = 0$). Spin multiplicities are reported as a broad (br), singlet (s), doublet (d),

triplet (t) and quartet (q), with coupling constants (J) given in Hz, or multiplet (m). ESI–MS

were performed on a ESI API 150EX and are reported as m/z (%). Accurate mass

determinations using ESI (HR ESI–MS) were performed on a Sciex QSTAR Pulsar mass

spectrometer. MALDI MS analysis for the characterization of new compounds was performed

using Bruker MALDI Autoflex Speed TOF/TOF and is reported as mass-per-charge ratio m/z

(matrix solution: DCTB (0.5 mg/0.2 mL) in CHCl$_3$). Specific rotations were measured on a

Polarimeter P–1030 from JASCO. Circular dichroism spectra were obtained using JASCO J–

815 spectropolarimeter and are reported as extremum wavelength λ in nm ($\Delta\varepsilon$ in M^{-1}cm^{-1}). UV–

vis spectra were recorded on a JASCO V–650 spectrophotometer equipped with a stirrer and a

temperature controller (20 ℃) and are reported as maximal absorption wavelength λ in nm.

5.2. Synthesis

5.2.1.   General Procedures

Solution Phase Peptide Synthesis

General Procedure A for Removing Boc Protecting Group with TFA

Boc–protected peptide (or amino acid) was dissolved in a mixture of TFA/CH$_2$Cl$_2$ 1:1 (more

than 20 eq of TFA) to make 0.40 M solution. The resulting solution was stirred at rt for 1 h.

The solvents were removed *in vacuo*. The residue was used for the coupling reaction without further purification.

General Procedure B for Removing Fmoc Protecting Group

Fmoc-protected peptide (or amino acid) was dissolved in a mixture of diethylamine/CH_2Cl_2 1:1 (more than 20 eq of diethylamine) to make 0.2 M solution. The resulting solution was stirred at rt for 1 h. The solvents were removed in vacuo. The residue was dried under vacuum for 30 min and then used for the coupling reaction without further purification.

General Procedure C for Removing Boc and tBu Protecting Group with HCl Gas

HCl gas was bubbled through a solution of protected peptide in EtOAc during stirring for 1 h. Then solvent was removed *in vacuo*. The residue was washed with Et_2O 3 times, dried under vacuum to yield desired product.

General Procedure D for Amide Formation with EDC

To a 0.20 M solution of *N*–deprotected peptide (or amino acid) in CH_2Cl_2, DIPEA (5.0 eq) was added, followed by DMAP (1.2 eq), *N*–Boc–amino acid–OH (1.2 eq) and EDC (1.2 eq). The resulting mixture was stirred at rt overnight. The reaction mixture was diluted with CH_2Cl_2 and washed with 10% aqueous solution of citric acid, water, saturated aqueous solution of $NaHCO_3$ and brine. The organic phase was dried over Na_2SO_4 and concentrated *in vacuo*. The residue was purified by flash column chromatography (CH_2Cl_2/MeOH) to yield the desired product.

General Procedure E for Cyclization of Peptide using I$_2$

To a 2.8 mM solution of I$_2$ (2 eq) in methanol, 3.5 mM solution of peptide (1 eq) in methanol was added dropwise. Reaction mixture was stirred at rt for another 4 h. Then, reaction mixture was diluted with CH$_2$Cl$_2$. The organic solution was washed 3 times with 10% aqueous solution of KI to remove the excess I$_2$. The organic layer was dried over Na$_2$SO$_4$, filtered and concentrated in vacuo. The residue was purified by flash chromatography (CH$_2$Cl$_2$/MeOH) to yield desired product.

Synthesis of Peptide–Bridged NDIs and PDIs

General Procedure F for Cysteine Deprotection

To a 50 mM solution of peptide in TFE/water 6:1, PBu$_3$ (4.0 eq) was added, followed by TEA (2.5 eq). The resulting mixture was stirred at rt overnight under N$_2$ atmosphere. The solvents and resulting *tert*–butylthiol were removed under vacuum. The residue was used for the next step without further purification.

General Procedure G for Cyclization

The residue after Cysteine deprotection was dissolved in CH$_3$CN/buffer 3:1 (buffer: 60 mM aqueous solution of NH$_4$HCO$_3$ pH 8.0) to make 1.0 mM solution of peptide. To the resulting solution, TCEP·HCl (1.1 eq) was added, followed by **152** or **180** (1.0 eq). The reaction mixture was stirred at rt for 30 min, then at 65 °C overnight under N$_2$ atmosphere. The reaction mixture was allowed to cool to rt and concentrated *in vacuo*. The residue was dissolved in CH$_2$Cl$_2$ and

washed with water. The organic phase was dried over Na_2SO_4 and concentrated *in vacuo*. The residue was purified by flash column chromatography (CH_2Cl_2/MeOH) to yield the desired product. Two isomers were separated by PTLC (CH_2Cl_2/MeOH) or chiral flash chromatograghy (column: Chiralflash® IF particle size 20 μm, 30 mm x 100 mm, eluent: CH_2Cl_2/MeOH).

Synthesis of Thiosulfonate derivatives

General Procedure H for the Introduction of SAc Groups

Di-halogeno or di-OTs substances (1.0 eq) were dissolved in DMF (0.10 M solution). Then 18-crown-6-ether (1.0 eq) was added, followed by 4.0 eq of KSAc. The reaction mixture was kept stirring at rt, under N_2 overnight. Then the solvent was removed under vacuum. To the residue, water was added. And CH_2Cl_2 was used to extract the product. The organic layer was washed with water, brine and dried over anhydrous Na_2SO_4. The solvent was removed under vacuum. The residue was purified by flash chromatography to yield the desired product.

General Procedure I for the Deprotection of SAc Groups

Di-SAc substances were dissolved in 1.25 M solution of HCl in MeOH to form 0.30 M solution. The reaction mixture was stirred at rt, under N_2 for 4 h. Then the solvent was removed under vacuum. The residue was purified by flash chromatography to yield the desired product.

General Procedure J for the Formation of Cyclic Thiosulfonates

To a solution of dithiol in AcOH at 0 °C, H_2O_2 (3.5 eq) was added dropwise. The reaction mixture was warmed up to rt and kept stirring overnight. The solvent was removed under vacuum. The residue was purified by flash chromatography to yield the desired product.

General Procedure K for Tosylation of Hydroxy Groups

In a round bottom flask, TsCl (4.0 eq) was dissolved in pyridine (2.2 M solution) at 0 °C. To the reaction mixture was added dropwise a 1.85 M solution of alcohol in $CHCl_3$ (1.0 eq). The reaction mixture was warmed up to rt and stirred for 2 h. The reaction mixture was poured into ice. 1.0 M aqueous solution of HCl was added until pH lower than 5.0. The mixture was extracted using CH_2Cl_2. The organic layer was dried over anhydrous Na_2SO_4. The solvent was removed under vacuum. The residue was purified by flash chromatography to yield the desired product.

5.2.2.   NDI-Peptide Conjugates
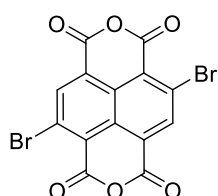
Compound 155. To a suspension of **153** (15 g, 56 mmol) in 98% H_2SO_4 (150 mL), DBH (24 g, 84 mmol) was added. The reaction mixture was kept stirring at 100 °C for 2 d. The reaction mixture was allowed to cool down to rt and then centrifuged to separate the precipitate. The precipitate was washed with cold water and dried to yield **155** as a bright yellow solid (11 g, 46%). Spectroscopic data were consistent with those reported in the literature.[232]

Compound 154 was synthesized as described previously. [233]
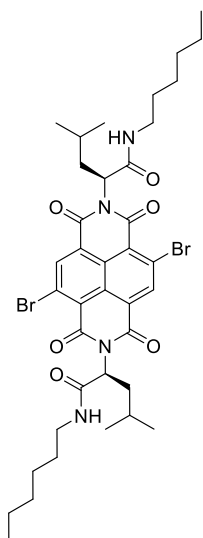
Compound 152 was synthesized following a modified procedure adapted from reference.[48] A mixture of **153** (2.0 g, 4.7 mmol) and **154** (2.0 g, 9.8 mmol) in AcOH (40 mL) was stirred in a pressured tight tube at 130 °C under μW irradiation for 20 min. The resulting mixture was cooled down to rt then poured into water. The precipitate was filtered, dried and washed with CH_2Cl_2 (20 mL). The residue was purified by flash column chromatography (CH_2Cl_2/MeOH 30:1) to yield **152** as a pale yellow solid (1.2 g, 31%). R_f (CH_2Cl_2/MeOH 25:1): 0.43; Mp: 273 – 274 °C (decomp); IR (neat): 3269 (w), 3073 (w), 2956 (m), 2981 (m), 2868 (w), 1714 (m), 1672 (s), 1649 (s), 1550 (m), 1465 (w), 1421 (s), 1363 (m), 1305 (s), 1264 (w), 1228 (s), 1212 (s), 1173 (w), 1129 (w), 919 (w), 887 (w), 840 (w), 788 (w), 761 (w), 731 (w), 651 (w), 621 (w); ^{1}H NMR (400 MHz, CDCl$_3$): 8.97 (s, 2H), 5.82 (t, $^3J_{H-H}$ = 5.7 Hz, 2H), 5.70 (dd, $^3J_{H-H}$ = 9.8 Hz, 5.2 Hz, 2H), 3.36 – 3.22 (m, 4H), 2.31 (ddd, $^2J_{H-H}$ = 14.0 Hz, $^3J_{H-H}$ = 9.8, 4.7 Hz, 2H), 1.92 (ddd, $^2J_{H-H}$ = 14.0 Hz, $^3J_{H-H}$ = 9.1, 5.2 Hz, 2H), 1.59 – 1.46 (m, 6H), 1.36 – 1.25 (m, 12H), 1.00 (d, $^3J_{H-H}$ = 6.5 Hz, 6H), 0.95 (d, $^3J_{H-H}$ = 6.6 Hz, 6H), 0.91 – 0.84 (m, 6H); ^{13}C NMR (100 MHz, CDCl$_3$): 168.6 (C), 161.1 (C), 160.8 (C), 139.5 (CH), 128.7 (C), 127.9 (C), 125.2 (C), 124.2 (C), 54.5 (CH), 40.1 (CH$_2$), 37.7 (CH$_2$), 31.5 (CH$_2$), 29.5 (CH$_2$), 26.6 (CH$_2$), 25.9 (CH), 23.4 (CH$_3$), 22.6 (CH$_2$), 22.1 (CH$_3$), 14.1 (CH$_3$); MS (ESI, MeOH): 817.2/818.8/819.4/821.5 (56/100/65/62, [M+H]$^+$).
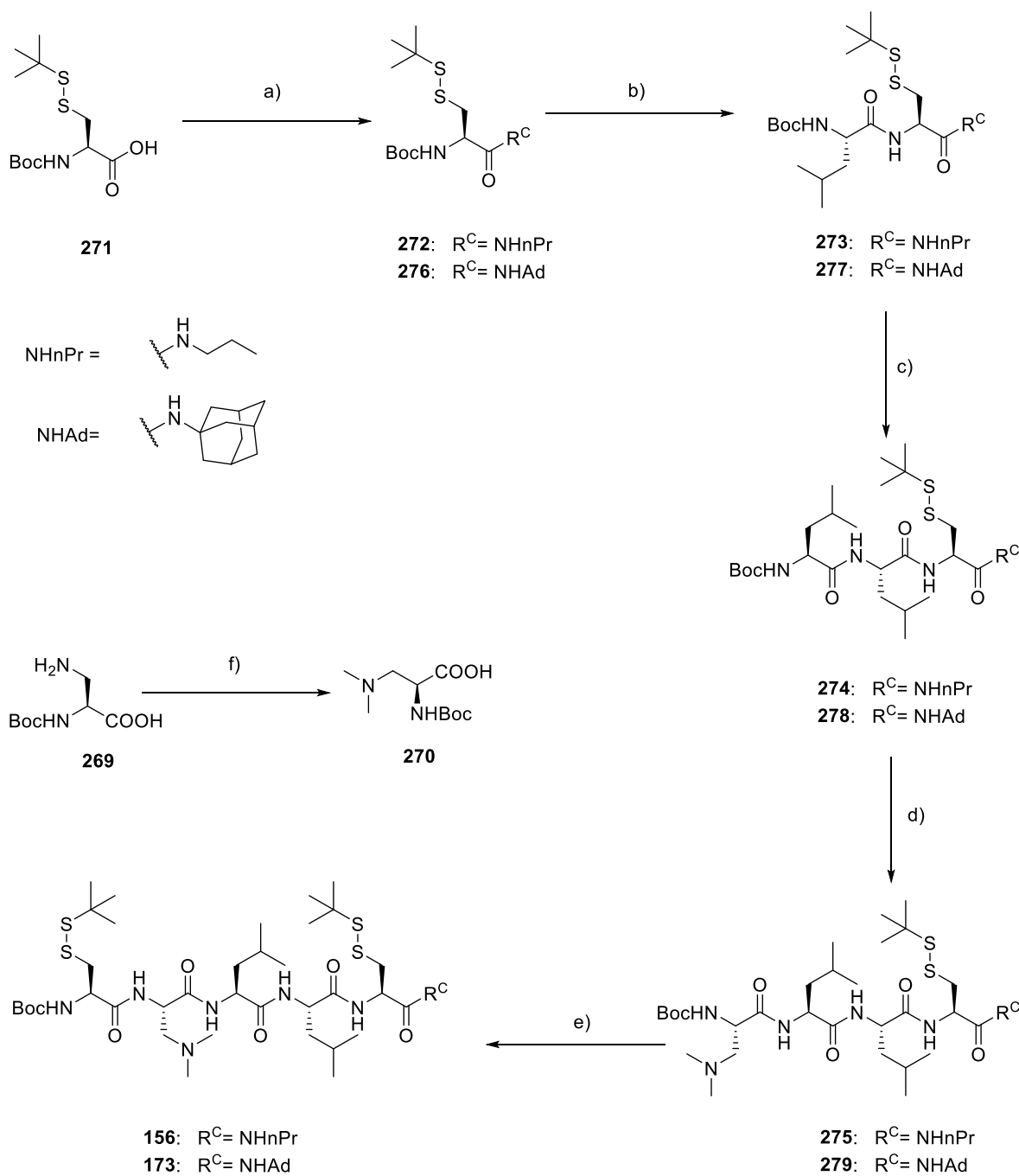
Scheme 11. (a) EDC, DMAP, CH₂Cl₂, rt, overnight, *n*–propylamine, 48% (**272**), 1–adamantylamine, 17% (**276**); (b) 1. TFA/CH₂Cl₂ 1:1, rt, 1 h; 2. Boc–L–Leu–OH, EDC, DMAP, DIPEA, CH₂Cl₂, rt, overnight, 77% (**273**), 43% (**277**); (c) 1. TFA/CH₂Cl₂ 1:1, rt, 1 h; 2. Boc–L–Leu–OH, EDC, DMAP, DIPEA, CH₂Cl₂, rt, overnight, 81% (**274**), 85% (**278**); (d) 1. TFA/CH₂Cl₂ 1:1, rt, 1 h; 2. **270**, EDC, DMAP, DIPEA, CH₂Cl₂, rt, overnight, 38% (**275**), 91%

(**279**); (e) 1. TFA/CH$_2$Cl$_2$ 1:1, rt, 1 h; 2. **271**, EDC, DMAP, DIPEA, CH$_2$Cl$_2$, rt, overnight, 64% (**156**), 36% (**173**); (f) formaldehyde, NaBH$_3$CN, EtOH, overnight, 94%.
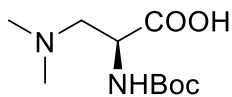
Compound 270. To a cold solution (0 °C) of Boc–L–Dap–OH (1.1 g, 5.3 mmol) in EtOH (50 mL), formaldehyde (1.6 mL, 16 mmol, 37% aqueous solution) was added. The resulting mixture was stirred at 0 °C for 10 min, then NaBH$_3$CN (1.3 g, 21 mmol) was added. Reaction mixture was stirred at rt overnight. The solvent was removed *in vacuo*. The residue was dissolved in water (50 mL). The aqueous layer was washed with CHCl$_3$ (50 mL) and then concentrated *in vacuo*. The residue was purified by reverse–phase flash column chromatography (100% H$_2$O + 0.1% TFA/0% CH$_3$CN + 0.1% TFA to 60% H$_2$O + 0.1% TFA/40% CH$_3$CN + 0.1% TFA) and then lyophilized to yield **270** as a colorless solid (1.2 g, 94%). Mp: 73 – 74 °C; [α]$_D^{20}$ +9.80 (*c* 1.00, DMSO); IR (neat): 3272 (w), 2978 (w), 2829 (w), 2782 (w), 1688 (m), 1640 (m), 1461 (w), 1392 (m), 1365 (s), 1251 (w), 1204 (w), 1164 (s), 1133 (m), 1051 (w), 1019 (w), 971 (w), 861 (w), 836 (w), 800 (w), 779 (w), 720 (w), 669 (w); ^{1}H NMR (300 MHz, DMSO–d_6): 6.26 (d, $^3J_{H–H}$ = 7.4 Hz, 1H), 3.92 – 3.77 (m, 1H), 2.64 (d, $^3J_{H–H}$ = 6.9 Hz, 2H), 2.33 (s, 6H), 1.39 (s, 9H); ^{13}C NMR (75 MHz, DMSO–d_6): 173.9 (C), 155.5 (C), 78.1 (C), 60.6 (CH$_2$), 52.5 (CH), 45.0 (2xCH$_3$), 28.7 (3xCH$_3$); MS (ESI, MeOH): 255 (100, [M+Na]$^+$).
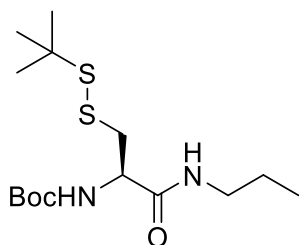
Compound 272 (269 mg, 48%, colorless solid) was prepared from **271** (500 mg, 1.61 mmol) and *n*-propylamine (265 µL, 3.22 mmol) following the general procedure D. R_f (CH$_2$Cl$_2$/MeOH 15:1): 0.64; Mp: 81 – 82 °C; [α]$_D^{20}$ –38.3 (*c* 1.00, CHCl$_3$); IR (neat): 3312 (w), 3260 (w), 3077 (w), 2967 (w), 2939 (w), 2876 (w), 1682 (s), 1651 (s), 1529 (s), 1456 (w), 1389 (w), 1364 (m), 1316 (w), 1281 (m), 1249 (m), 1167 (s), 1076 (w), 1049

(m), 1025 (w), 956 (w), 874 (w), 843 (w), 782 (w), 752 (w), 720 (w), 645 (m); ^{1}H NMR (300 MHz, CDCl$_3$): 6.38 (br s, 1H), 5.35 (d, $^3J_{H-H}$ = 8.1 Hz, 1H), 4.42 – 4.28 (m, 1H), 3.21 (dt, $^3J_{H-H}$ = 7.8, 6.1 Hz, 2H), 3.13 – 2.95 (m, 2H), 1.59 – 1.47 (m, 2H), 1.43 (s, 9H), 1.32 (s, 9H), 0.90 (t, $^3J_{H-H}$ = 7.4 Hz, 3H); ^{13}C NMR (75 MHz, CDCl$_3$): 170.2 (C), 155.4 (C), 80.3 (C), 54.3 (CH), 48.3 (C), 42.6 (CH$_2$), 41.3 (CH$_2$), 29.8 (3xCH$_3$), 28.3 (3xCH$_3$), 22.7 (CH$_2$), 11.3 (CH$_3$); MS (ESI, MeOH): 251 (100, [M–Boc+H]$^+$).
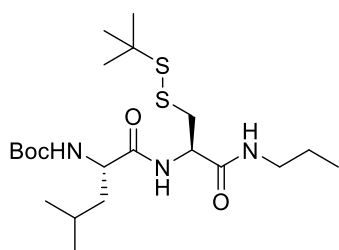
Compound 273 (276 mg, 77%, colorless solid) was prepared from **272** (269 mg, 0.767 mmol) and Boc–L–Leu–OH (213 mg, 0.921 mmol) following the general procedures A and D. R_f (CH$_2$Cl$_2$/MeOH 15:1): 0.53; Mp: 84 – 85 °C; [α]$_D^{20}$ –93.2 (c 1.00, CHCl$_3$); IR (neat): 3296 (w), 3080 (w), 2962 (w), 2874 (w), 1689 (m), 1643 (s), 1516 (m), 1457 (w), 1388 (w), 1364 (m), 1322 (w), 1247 (m), 1164 (s), 1046 (w), 1020 (w), 955 (w), 872 (w), 778 (w), 665 (w); ^{1}H NMR (300 MHz, DMSO–d_6): 7.98 – 7.84 (m, 2H), 7.00 (d, $^3J_{H-H}$ = 7.6 Hz, 1H), 4.47 – 4.35 (m, 1H), 3.98 – 3.80 (m, 1H), 3.12 – 2.87 (m, 4H), 1.70 – 1.51 (m,1H), 1.47 – 1.32 (m, 13H), 1.27 (s, 9H), 0.90 – 0.74 (m, 9H); ^{13}C NMR (75 MHz, DMSO–d_6): 172.9 (C), 169.6 (C), 156.0 (C), 78.7 (C), 53.8 (CH), 52.7 (CH), 48.1 (C), 42.9 (CH$_2$), 41.1 (CH$_2$), 40.9 (CH$_2$), 30.0 (3xCH$_3$), 28.6 (3xCH$_3$), 24.7 (CH), 23.3 (CH$_3$), 22.6 (CH$_2$), 22.1 (CH$_3$), 11.7 (CH$_3$); MS (ESI, MeOH): 464 (100, [M+H]$^+$).
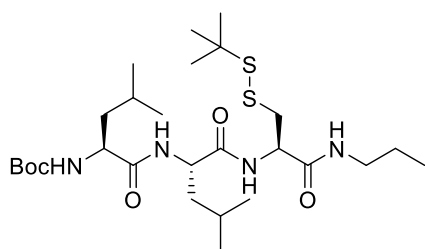
Compound 274 (278 mg, 81%, colorless solid) was prepared from **273** (276 mg, 0.596 mmol) and Boc–L–Leu–OH (165 mg, 0.713 mmol) following the general procedures A and D. R_f (CH$_2$Cl$_2$/MeOH 15:1): 0.51; Mp: 188 – 189 °C; [α]$_D^{20}$ –56.0 (c 1.00, DMSO); IR (neat): 3276 (w), 3071 (w), 2959 (w), 2871

(w), 1638 (s), 1525 (s), 1456 (m), 1388 (m), 1364 (m), 1321 (w), 1239 (m), 1165 (s), 1121 (w), 1046 (w), 1020 (w), 953 (w), 873 (w), 778 (w), 657 (m); ^{1}H NMR (400 MHz, DMSO–d_6): 8.08 (d, $^3J_{H–H}$ = 8.0 Hz, 1H), 7.91 (t, $^3J_{H–H}$ = 5.7 Hz, 1H), 7.86 (d, $^3J_{H–H}$ = 7.9 Hz, 1H), 6.95 (d, $^3J_{H–H}$ = 8.2 Hz, 1H), 4.45 – 4.34 (m, 1H), 4.32 – 4.22 (m, 1H), 3.99 – 3.87 (m, 1H), 3.08 – 2.87 (m, 4H), 1.64 – 1.52 (m, 2H), 1.46 – 1.32 (m, 15H), 1.27 (s, 9H), 0.90 – 0.74 (m, 15H); ^{13}C NMR (75 MHz, DMSO–d_6): 173.0 (C), 172.3 (C), 169.5 (C), 155.8 (C), 78.5 (C), 53.3 (CH), 52.8 (CH), 51.6 (CH), 48.1 (C), 42.8 (CH$_2$), 41.3 (2xCH$_2$), 40.9 (CH$_2$), 30.0 (3xCH$_3$), 28.6 (3xCH$_3$), 24.7 (CH), 24.5 (CH), 23.5 (CH$_3$), 23.4 (CH$_3$), 22.6 (CH$_2$), 22.1 (2xCH$_3$), 11.8 (CH$_3$); MS (ESI, MeOH): 577 (100, [M+H]$^+$).
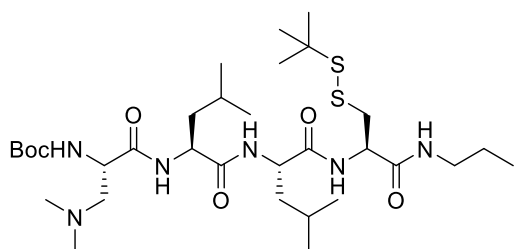
Compound 275 (0.5 g, 38%, colorless solid) was prepared from **274** (1.1 g, 1.8 mmol) and **270** (0.51 g, 2.5 mmol) following the general procedures A and D. R_f (CH$_2$Cl$_2$/MeOH 15:1): 0.36; Mp: 209 – 210 °C (decomp); $[\alpha]_D^{20}$ –101 (*c* 1.00, CHCl$_3$); IR (neat): 3271 (w), 3084 (w), 2959 (w), 1719 (w), 1630 (s), 1535 (m), 1457 (m), 1388 (w), 1364 (m), 1249 (m), 1165 (m), 1050 (w), 1019 (w), 864 (w), 778 (w), 700 (m); ^{1}H NMR (400 MHz, CDCl$_3$): 7.34 (d, $^3J_{H–H}$ = 6.4 Hz, 1H), 7.22 (d, $^3J_{H–H}$ = 8.0 Hz, 1H), 7.12 (br s, 1H), 6.81 (d, $^3J_{H–H}$ = 5.6 Hz, 1H), 5.72 (s, 1H), 4.74 – 4.61 (m, 1H), 4.34 – 4.21 (m, 1H), 4.20 – 4.12 (m, 1H), 4.08 – 4.00 (m, 1H), 3.40 (dd, $^2J_{H–H}$ = 13.4 Hz, $^3J_{H–H}$ = 3.7 Hz, 1H), 3.27 – 3.04 (m, 3H), 2.64 (dd, $^2J_{H–H}$ = 12.3 Hz, $^3J_{H–H}$ = 6.5 Hz, 1H), 2.50 (dd, $^2J_{H–H}$ = 12.3 Hz, $^3J_{H–H}$ = 9.0 Hz, 1H), 2.28 (s, 6H), 1.86 – 1.61 (m, 5H), 1.61 – 1.53 (m, 3H), 1.47 (s, 9H), 1.32 (s, 9H), 1.01 – 0.84 (m, 15H); ^{13}C NMR (100 MHz, CDCl$_3$): 173.2 (C), 172.9 (C), 172.4 (C), 170.2 (C), 156.9 (C), 81.2 (C), 59.5 (CH$_2$), 54.0 (CH), 53.3 (2xCH), 52.9 (CH), 48.0 (C), 45.1 (2xCH$_3$), 41.9 (CH$_2$), 41.5 (CH$_2$), 40.2 (CH$_2$), 39.5

(CH$_2$), 30.0 (3xCH$_3$), 28.2 (3xCH$_3$), 25.2 (CH), 25.0 (CH), 23.2 (CH$_3$), 23.1 (CH$_3$), 22.5 (CH$_2$), 21.7 (CH$_3$), 21.0 (CH$_3$), 11.4 (CH$_3$); MS (ESI, MeOH): 691 (100, [M+H]$^+$).
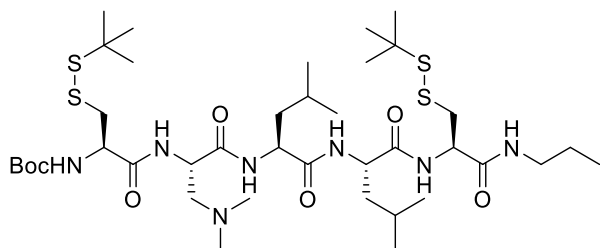
Compound 156 (400 mg, 64%, colorless solid) was prepared from **275** (488 mg, 0.707 mmol) and **271** (262 mg, 1.13 mmol) following the general procedures A and D. R_f (CH$_2$Cl$_2$/MeOH 15:1): 0.46; Mp: 226 – 227 $^\circ$C; [α]$_D^{20}$ –101 (*c* 1.00, CHCl$_3$); IR (neat): 3263 (w), 3088 (w), 2961 (w), 1717 (w), 1690 (w), 1631 (s), 1548 (m), 1471 (m), 1388 (w), 1364 (m), 1303 (w), 1252 (w), 1216 (w), 1163 (m), 1060 (w), 1023 (w), 917 (w), 877 (w), 780 (w), 715 (m); ^{1}H NMR (400 MHz, CDCl$_3$): 7.53 (s, 1H), 7.46 (d, $^3J_{H-H}$ = 6.3 Hz, 1H), 7.40 (d, $^3J_{H-H}$ = 5.5 Hz, 1H), 7.16 (d, $^3J_{H-H}$ = 8.1 Hz, 1H), 6.86 (t, $^3J_{H-H}$ = 5.7 Hz, 1H), 5.46 (d, $^3J_{H-H}$ = 4.3 Hz, 1H), 4.71 – 4.62 (m, 1H), 4.38 – 4.11 (m, 4H), 3.46 (dd, $^2J_{H-H}$ = 13.3 Hz, $^3J_{H-H}$ = 3.6 Hz, 1H), 3.27 – 3.06 (m, 4H), 3.00 – 2.92 (m, 1H), 2.72 (dd, $^2J_{H-H}$ = 12.6 Hz, $^3J_{H-H}$ = 5.9 Hz, 1H), 2.62 (dd, $^2J_{H-H}$ = 12.6 Hz, $^3J_{H-H}$ = 8.4 Hz, 1H), 2.25 (s, 6H), 1.89 – 1.71 (m, 4H), 1.70 – 1.62 (m, 2H), 1.46 (s, 9H), 1.40 – 1.28 (m, 18H), 1.01 – 0.84 (m, 15H); ^{13}C NMR (100 MHz, CDCl$_3$): 173.9 (C), 172.8 (C), 172.5 (C), 172.0 (C), 170.3 (C), 156.2 (C), 81.4 (C), 58.5 (CH$_2$), 54.9 (CH), 54.4 (CH), 53.7 (CH), 53.3 (CH), 52.8 (CH), 49.0 (C), 47.8 (C), 45.3 (2xCH$_3$), 42.0 (CH$_2$), 41.5 (CH$_2$), 40.1 (CH$_2$), 39.7 (CH$_2$), 39.3 (CH$_2$), 30.0 (CH$_3$), 29.9 (CH$_3$), 28.2 (CH$_3$), 25.2 (CH), 24.9 (CH), 23.4 (CH$_3$), 23.1 (CH$_3$), 22.5 (CH$_2$), 21.0 (CH$_3$), 20.9 (CH$_3$), 11.4 (CH$_3$); MS (ESI, MeOH): 882 (100, [M+H]$^+$); HRMS (ESI, +ve) calcd for C$_{39}$H$_{75}$N$_7$O$_7$S$_4$ ([M+H]$^+$): 882.4684, found: 882.4673.
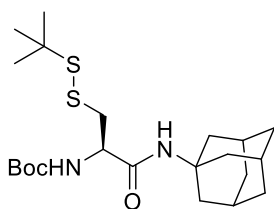
Compound 276 (1.8 g, 17%, colorless solid) was prepared from **271** (7.3 g, 29 mmol) and adamantyl–1–amine (7.1 g, 47 mmol) following the general procedure D. R_f (CH$_2$Cl$_2$/MeOH 100:1): 0.33; Mp: 68 – 69 °C; $[\alpha]_D^{20}$ –20.0 (c 1.00, CHCl$_3$); IR (neat): 3314 (w), 2908 (m), 2852 (w), 1658 (s), 1528 (m), 1454 (w), 1362 (m), 1312 (w), 1273 (w), 1247 (m), 1164 (s), 1094 (w), 1048 (w), 1020 (w), 989 (w), 870 (w), 778 (w); ^{1}H NMR (300 MHz, CDCl$_3$): 5.91 (br s, 1H), 5.25 (br s, 1H), 4.32 – 4.14 (m, 1H), 3.10 (dd, $^2J_{H-H}$ = 13.6 Hz, $^3J_{H-H}$ = 6.0 Hz, 1H), 2.95 (dd, $^2J_{H-H}$ = 13.6 Hz, $^3J_{H-H}$ = 6.7 Hz, 1H), 2.17 – 2.01 (m, 3H), 1.99 (d, $^3J_{H-H}$ = 2.9 Hz, 6H), 1.67 (t, $^3J_{H-H}$ = 3.1 Hz, 6H), 1.45 (s, 9H), 1.34 (s, 9H); ^{13}C NMR (75 MHz, CDCl$_3$): 169.0 (C), 155.2 (C), 80.4 (C), 54.5 (CH), 52.2 (C), 48.4 (C), 42.8 (CH$_2$), 41.5 (3xCH$_2$), 36.3 (3xCH$_2$), 29.9 (3xCH$_3$), 29.4 (CH), 28.3 (3xCH); MS (ESI, MeOH): 443 (100, [M+H]$^+$).
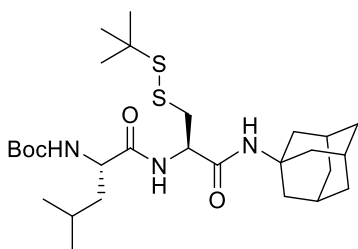
Compound 277 (0.7 g, 43%, colorless solid) was prepared from **276** (1.3 g, 2.9 mmol) and Boc–L–Leu–OH (0.82 g, 3.3 mmol) following the general procedures A and D. R_f (CH$_2$Cl$_2$/MeOH 25:1): 0.31; Mp: 142 – 143 °C; $[\alpha]_D^{20}$ –57.7 (c 1.00, CHCl$_3$); IR (neat): 3300 (w), 3073 (w), 2909 (m), 2853 (w), 1694 (m), 1641 (s), 1516 (s), 1454 (m), 1388 (w), 1373 (s), 1311 (w), 1273 (w), 1254 (m), 1165 (s), 1102 (w), 1046 (w), 1021 (w), 953 (w), 872 (w), 778 (w), 612 (m); ^{1}H NMR (300 MHz, CDCl$_3$): 6.97 (d, $^3J_{H-H}$ = 7.8 Hz, 1H), 6.11 (s, 1H), 4.88 (d, $^3J_{H-H}$ = 6.8 Hz, 1H), 4.61 – 4.48 (m, 1H), 4.15 – 4.00 (m, 1H), 3.18 (dd, $^2J_{H-H}$ = 13.4 Hz, $^3J_{H-H}$ = 5.9 Hz, 1H), 2.95 (dd, $^2J_{H-H}$ = 13.4 Hz, $^3J_{H-H}$ = 6.5 Hz, 1H), 2.12 – 2.03 (m, 3H), 2.03 – 1.95 (m, 6H), 1.78 – 1.62 (m, 8H), 1.52 – 1.39 (m, 10H), 1.34 (s, 9H), 1.02 – 0.88 (m, 6H); ^{13}C NMR (100 MHz, CDCl$_3$): 172.4 (C), 168.3 (C), 155.2 (C), 80.5 (C), 53.7 (CH), 53.3 (CH), 52.4 (C), 48.5 (C), 42.0 (CH$_2$), 41.4 (3xCH$_2$), 41.0 (CH$_2$), 36.3

(3xCH$_2$), 29.9 (3xCH$_3$), 29.4 (CH), 28.3 (3xCH$_3$), 24.9 (CH), 23.0 (CH$_3$), 21.8 (CH$_3$); MS (ESI, MeOH): 556 (100, [M+H]$^+$).
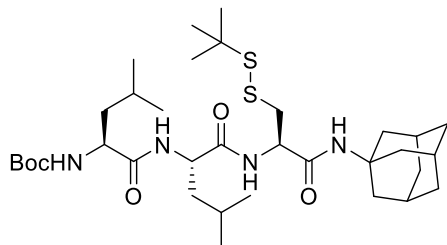
Compound 278 (0.7 g, 85%, colorless solid) was prepared from **277** (0.71 g, 1.3 mmol) and Boc–L–Leu–OH (0.35 g, 1.5 mmol) following the general procedures A and D. R_f (CH$_2$Cl$_2$/MeOH 15:1): 0.61; Mp: 162 – 163 ^{o}C; [α]$_D^{20}$ –97.5 (*c* 1.00, CHCl$_3$); IR (neat): 3298 (w), 3075 (w), 2956 (w), 2910 (m), 2854 (w), 1719 (w), 1638 (s), 1515 (m), 1455 (m), 1389 (w), 1363 (m), 1312 (w), 1273 (w), 1246 (m), 1164 (s), 1103 (w), 1046 (w), 1019 (w), 935 (w), 872 (w), 777 (w), 665 (w); ^{1}H NMR (400 MHz, DMSO–d_6): 7.99 – 7.83 (m, 2H), 7.29 (s, 1H), 6.92 (d, $^3J_{H-H}$ = 8.2 Hz, 1H), 4.45 – 4.19 (m, 2H), 4.04 – 3.89 (m, 1H), 3.04 (dd, $^2J_{H-H}$ = 12.6 Hz, $^3J_{H-H}$ = 5.8 Hz, 1H), 2.93 (dd, $^2J_{H-H}$ = 12.6 Hz, $^3J_{H-H}$ = 7.6 Hz, 1H), 2.06 – 1.96 (m, 3H), 1.95 – 1.87 (m, 6H), 1.71 – 1.52 (m, 8H), 1.52 – 1.32 (m, 13H), 1.28 (s, 9H), 0.95 – 0.73 (m, 12H); ^{13}C NMR (100 MHz, DMSO–d_6): 172.9 (C), 172.2 (C), 168.6 (C), 155.8 (C), 78.5 (C), 53.2 (CH), 53.0 (CH), 51.7 (CH), 51.5 (C), 48.1 (C), 43.4 (CH$_2$), 41.3 (3xCH$_2$), 40.9 (CH$_2$), 36.5 (3xCH$_2$), 30.0 (3xCH$_3$), 29.2 (3xCH$_3$), 28.6 (CH), 24.67 (CH), 24.50 (CH), 23.5 (CH$_3$), 23.4 (CH$_3$), 22.1 (2xCH$_3$); MS (ESI, MeOH): 669 (100, [M+H]$^+$).
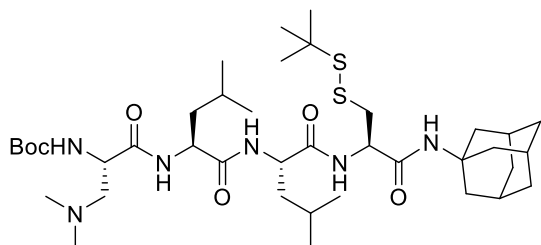
Compound 279 (770 mg, 91%, colorless solid) was prepared from **278** (722 mg, 1.08 mmol) and **270** (301 mg, 1.30 mmol) following the general procedures A and D. R_f (CH$_2$Cl$_2$/MeOH 25:1): 0.2; Mp: 198 – 199 ^{o}C (decomp); [α]$_D^{20}$ –82.8 (*c* 1.00, CHCl$_3$); IR (neat): 3285 (w), 3083 (w), 2912 (w), 2854 (w), 1633 (s), 1533 (m), 1456 (m), 1389 (w), 1363 (m),

1310 (w), 1246 (w), 1165 (m), 1098 (w), 1050 (w), 1020 (w), 911 (w), 865 (w), 778 (w), 730 (w), 689 (w), 619 (w); ^{1}H NMR (400 MHz, CDCl$_3$): 7.28 – 7.15 (m, 3H), 6.25 (s, 1H), 5.69 (s, 1H), 4.59 – 4.53 (m, 1H), 4.36 – 4.29 (m, 1H), 4.21 – 4.14 (m, 1H), 4.09 – 4.02 (m, 1H), 3.29 (dd, $^2J_{H–H}$ = 13.3 Hz, $^3J_{H–H}$ = 4.3 Hz, 1H), 3.07 (dd, $^2J_{H–H}$ = 13.3 Hz, $^3J_{H–H}$ = 9.7 Hz, 1H), 2.72 – 2.44 (m, 2H), 2.29 (s, 6H), 2.11 – 1.94 (m, 9H), 1.82 – 1.61 (m, 11H), 1.58 – 1.50 (m, 1H), 1.46 (s, 9H), 1.31 (s, 9H), 1.03 – 0.81 (m, 12H); ^{13}C NMR (100 MHz, CDCl$_3$): 172.7 (C), 172.5 (C), 172.3 (C), 169.1 (C), 156.8 (C), 81.1 (C), 59.6 (CH$_2$), 53.8 (CH), 53.2 (CH, 2xCH), 52.9 (CH), 52.1 (C), 48.0 (C), 45.1 (2xCH$_3$), 42.0 (CH$_2$), 41.1 (3xCH$_2$), 40.2 (CH$_2$), 39.6 (CH$_2$), 36.4 (3xCH$_2$), 30.0 (CH), 29.5 (3xCH$_3$), 28.2 (3xCH$_3$), 25.2 (CH), 25.0 (CH), 23.2 (CH$_3$), 23.1 (CH$_3$), 21.8 (CH$_3$), 21.0 (CH$_3$); MS (ESI, MeOH): 783 (100, [M+H]$^+$).
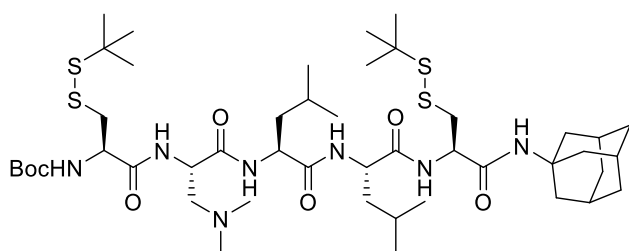
Compound 173 (344 mg, 36%, colorless solid) was prepared from **279** (770 mg, 0.984 mmol) and **271** (365 mg, 1.18 mmol) following the general procedures A and D. R_f (CH$_2$Cl$_2$/MeOH 15:1): 0.36; Mp: 210 – 211 °C (decomp); $[\alpha]_D^{20}$ –88.7 (c 1.00, CHCl$_3$); IR (neat): 3279 (w), 2958 (w), 2911 (w), 1633 (s), 1528 (m), 1455 (m), 1390 (w), 1363 (m), 1311 (w), 1248 (m), 1164 (s), 1048 (w), 1015 (w), 936 (w), 871 (w), 612 (w); ^{1}H NMR (300 MHz, CDCl$_3$): 7.54 (s, 1H), 7.46 – 7.35 (m, 2H), 7.15 (d, $^3J_{H–H}$ = 8.0 Hz, 1H), 6.32 (s, 1H), 5.47 (d, $^3J_{H–H}$ = 4.4 Hz, 1H), 4.66 – 4.49 (m, 1H), 4.39 – 4.09 (m, 4H), 3.39 (dd, $^2J_{H–H}$ = 13.3 Hz, $^3J_{H–H}$ = 3.7 Hz, 1H), 3.14 – 2.87 (m, 3H), 2.78 – 2.58 (m, 2H), 2.26 (s, 5H), 2.10 – 1.98 (m, 9H), 1.90 – 1.56 (m, 12H), 1.48 (s, 9H), 1.37 (s, 9H), 1.32 (s, 9H), 1.05 – 0.86 (m, 12H); ^{13}C NMR (125 MHz, CDCl$_3$): 173.3 (C), 172.7 (C), 172.3 (C), 172.0 (C), 169.4 (C), 156.1 (C), 81.3 (C), 58.6 (CH$_2$), 54.8 (CH), 54.2 (CH), 53.3 (CH), 53.20 (CH), 53.15 (CH), 52.1 (C), 49.0 (C), 47.8 (C), 45.3 (2xCH$_3$), 42.0 (CH$_2$), 41.1 (3xCH$_2$), 40.2 (CH$_2$), 39.7 (CH$_2$),

39.3 (CH$_2$), 36.5 (3xCH$_2$), 30.0 (CH), 29.9 (3xCH$_3$), 29.5 (3xCH$_3$), 28.2 (3xCH$_3$), 25.2 (CH), 24.9 (CH), 23.5 (CH$_3$), 23.1 (CH$_3$), 21.0 (CH$_3$), 20.9 (CH$_3$); MS (ESI, MeOH): 974 (100, [M+H]$^+$); HRMS (ESI, +ve) calcd for C$_{46}$H$_{83}$N$_7$O$_7$S$_4$ ([M+H]$^+$): 974.5310, found: 974.5303.

156: R^C= NHnPr
173: R^C= NHAd

158: R^C= NHnPr
161: R^C= NHAd
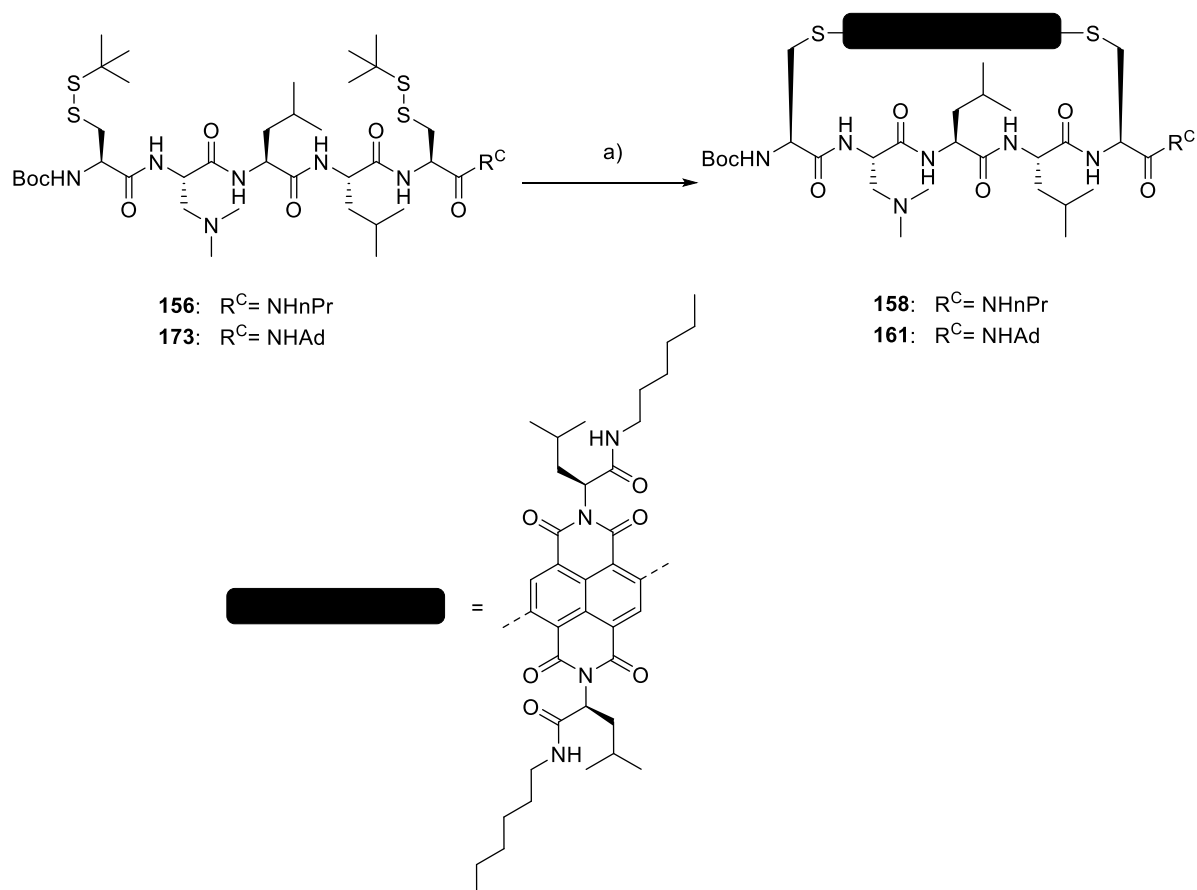
Scheme 12. (a) 1. PBu$_3$, TEA, H$_2$O, TFE, rt, overnight; 2. **152**, TCEP·HCl, CH$_3$CN/buffer 3:1, 65 $^\circ$C, overnight, 14% (**158**), 11% (**161**).
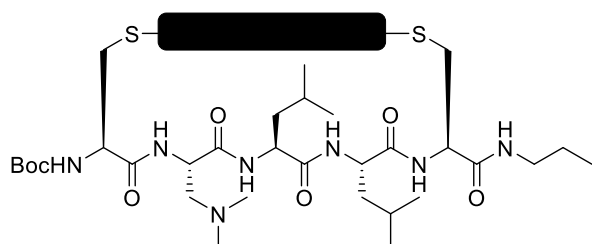
Compound 158 (32 mg, 14%, atropisomers not detectable, red solid) was prepared from **156** (150 mg, 0.170 mmol) following the general procedures F and G. R_f (CH$_2$Cl$_2$/MeOH 15:1): 0.35;

Mp: 171 – 172 °C; UV-Vis (TFE): 517 (15.3), 373 (12.3), 294 (36.4); CD (TFE): 531 (–1.4), 366 (+1.9), 298 (+2.2), 241 (–0.9), 209 (+7.7); IR (neat): 3312 (w), 2930 (m), 2871 (w), 1652 (s), 1528 (m), 1439 (m), 1367 (m), 1314 (m), 1214 (m), 1159 (m), 1049 (w), 906 (w), 791 (w), 732 (w); ^{1}H NMR (400 MHz, CDCl$_3$): 8.93 (s, 1H), 8.69 (d, $^3J_{H–H}$ = 8.8 Hz, 1H), 8.64 (s, 1H), 6.95 (s, 1H), 6.80 (s, 1H), 6.72 – 6.56 (m, 2H), 6.04 (d, $^3J_{H–H}$ = 6.3 Hz, 1H), 5.82 (s, 1H), 5.72 (dd, $^3J_{H–H}$ = 9.2 Hz, 4.7 Hz, 1H), 5.63 (dd, $^3J_{H–H}$ = 9.2 Hz, 5.7 Hz, 1H), 5.57 (s, 1H), 4.96 – 4.88 (m, 1H), 4.85 – 4.76 (m, 1H), 4.52 – 4.42 (m, 1H), 4.11 – 3.98 (m, 3H), 3.88 – 3.78 (m, 1H), 3.54 – 3.45 (m, 1H), 3.37 – 3.27 (m, 1H), 3.21 – 3.03 (m, 3H), 2.50 – 2.38 (m, 1H), 2.18 – 2.04 (m, 12H), 2.03 – 1.94 (m, 10H), 1.89 (m, 6H), 1.84 – 1.72 (m, 6H), 1.72 – 1.64 (m, 6H), 1.54 – 1.35 (m, 5H), 1.35 – 1.16 (m, 19H), 1.03 – 0.79 (m, 18H); ^{13}C NMR (100 MHz, CDCl$_3$): 178.6 (C), 171.2 (C), 170.7 (C), 169.1 (2xC), 168.74 (C), 168.68 (C), 168.1 (C), 163.9 (C), 162.9 (C), 162.1 (C), 158.9 (C), 146.5 (C, 2xC), 129.5 (CH), 128.8 (CH), 125.2 (C), 125.1 (C), 123.8 (C), 122.5 (C), 121.3 (C), 119.7 (C), 84.0 (C), 60.8 (CH$_2$), 57.2 (CH), 54.3 (CH), 54.1 (CH), 51.3 (CH), 49.1 (CH), 48.9 (CH), 47.3 (CH), 44.7 (2xCH$_3$), 41.5 (CH$_2$), 40.1 (CH$_2$), 40.0 (CH$_2$), 39.1 (CH$_2$), 38.2 (CH$_2$), 37.9 (CH$_2$), 36.4 (CH$_2$), 36.2 (CH$_2$), 34.4 (CH$_2$), 33.6 (CH$_2$), 31.5 (CH$_2$), 31.4 (CH$_2$), 29.6 (CH$_2$), 29.4 (CH$_2$), 29.4 (3xCH$_3$), 28.0 (2xCH), 26.7 (CH$_2$), 26.6 (CH$_2$), 25.9 (CH), 25.7 (CH), 23.2 (CH$_3$), 23.1 (CH$_3$), 22.63 (CH$_2$), 22.56 (CH$_2$), 22.16 (CH$_3$), 22.14 (CH$_3$), 19.8 (2xCH$_3$), 17.6 (2xCH$_3$), 14.1 (CH$_3$); HPLC–MS: R_t = 2.63 min, 1363 (100, [M+H]$^+$); HRMS (ESI, +ve) calcd for C$_{69}$H$_{107}$N$_{11}$O$_{13}$S$_2$ ([M+H]$^+$): 1362.7565, found: 1362.7565.
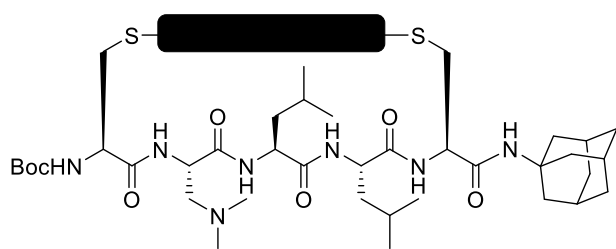
Compound 161 (26 mg, 11%, atropisomers not detectable, red solid) was prepared from **173** (150 mg, 0.154 mmol) following the general procedures F and G. R_f (CH$_2$Cl$_2$/MeOH 15:1): 0.40; Mp: 185 – 186 °C; UV-Vis (TFE): 519 (15.1), 373 (11.7), 294 (37.9); CD (TFE): 537 (–5.3), 359 (+8.5), 319 (–0.4), 295 (+7.1), 240 (–7.9), 210 (+20.8); IR (neat): 3327 (w), 2913 (m), 1658 (s), 1529 (s), 1440 (m), 1367 (w), 1315 (m), 1217 (m), 1165 (m); ^{1}H NMR (400 MHz, CDCl$_3$): 9.67 (br s, 1H), 8.90 (s, 1H), 8.83 (s, 1H), 6.82 – 6.67 (m, 1H), 6.12 (br s, 1H), 5.92 (br s, 1H), 5.85 (br s, 1H), 5.81 – 5.68 (m, 1H), 5.67 –5.59 (m, 1H), 5.55 (br s, 1H), 5.21 – 5.10 (m, 1H), 4.99 – 4.80 (br s, 1H), 4.35 – 4.26 (m, 1H), 4.17 – 3.98 (m, 3H), 3.96 – 3.82 (m, 1H), 3.68 – 3.54 (m, 1H), 3.39 – 3.11 (m, 5H), 3.03 – 2.85 (m, 1H), 2.83 – 2.69 (m, 1H), 2.37 – 2.23 (m, 7H), 2.11 – 2.05 (m, 4H), 2.02 – 1.99 (m, 5H),1.95 – 1.90 (m, 6H), 1.50 – 1.45 (m, 6H), 1.44 – 1.40 (m, 6H), 1.32 – 1.25 (m, 16H), 1.03 – 0.99 (m, 6H), 0.97 – 0.85 (m, 27H), 0.67 – 0.54 (m, 3H), 0.47 – 0.32 (m, 3H); ^{13}C NMR (125 MHz, CDCl$_3$): 173.1 (C), 172.6 (C), 172.3 (C), 169.5 (C), 168.9 (C), 168.4 (C), 168.3 (C), 163.9 (C), 163.0 (C), 162.5 (C), 161.8 (C), 154.1 (C), 149.0 (C), 143.1 (C), 130.0 (CH), 127.3 (CH), 126.0 (C), 125.8 (C), 125.4 (C), 124.9 (C), 123.7 (C), 119.4 (C), 80.3 (C), 58.4 (CH$_2$), 54.3 (CH), 54.1 (CH), 54.0 (CH), 53.44 (CH), 53.37 (CH), 52.5 (C), 52.0 (CH), 51.7 (CH), 48.8 (CH), 44.4 (2xCH$_3$), 41.34 (CH$_2$), 41.26 (CH$_2$), 41.14 (CH$_2$), 41.1 (CH$_2$), 40.3 (CH$_2$), 40.1 (CH$_2$), 38.6 (CH$_2$), 38.2 (CH$_2$), 37.7 (CH$_2$), 36.3 (CH$_2$), 33.1 (CH$_2$), 32.5 (CH$_2$), 31.9 (CH$_2$), 31.6 (CH$_2$), 31.5 (CH$_2$), 30.1 (CH$_2$), 29.7 (CH$_2$), 29.5 (CH$_2$), 29.4 (CH), 28.2 (CH$_3$), 26.8 (CH$_2$), 26.6 (CH$_2$), 25.9 (CH), 25.7 (CH), 24.6 (CH), 24.5 (CH), 23.5 (CH$_3$), 23.3 (2xCH$_3$), 23.0 (CH$_3$), 22.63 (CH$_2$), 22.56 (CH$_2$), 22.3 (CH$_3$), 22.0 (2xCH$_3$), 20.3 (CH$_3$), 14.1 (CH$_3$), 14.0 (CH$_3$); HPLC–MS: R_t = 3.19 min, 1455 (100,

[M+H]$^+$); HRMS (ESI, +ve) calcd for $C_{76}H_{115}N_{11}O_{13}S_2$ ([M+H]$^+$): 1454.8191, found: 1454.8213.
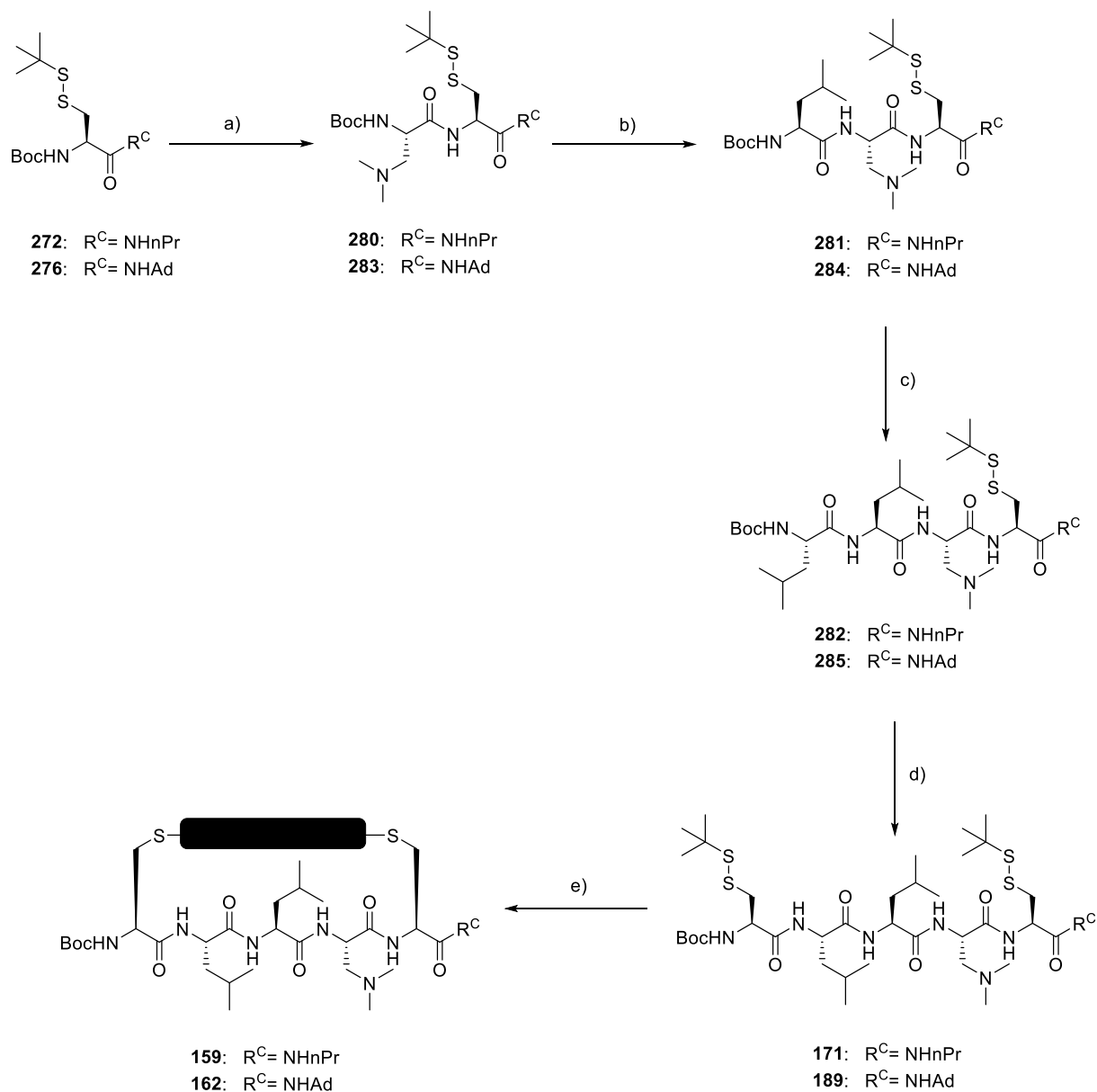
Scheme 13. (a) 1. TFA/CH$_2$Cl$_2$ 1:1, rt, 1 h; 2. **270**, EDC, DMAP, DIPEA, CH$_2$Cl$_2$, rt, overnight, 27% (**280**), 83% (**283**); (b) 1. TFA/CH$_2$Cl$_2$ 1:1, rt, 1 h; 2. Boc–L–Leu–OH, EDC, DMAP, DIPEA, CH$_2$Cl$_2$, rt, overnight, 63% (**281**), 61% (**284**); (c) 1. TFA/CH$_2$Cl$_2$ 1:1, rt, 1 h; 2. Boc–L–Leu–OH, EDC, DMAP, DIPEA, CH$_2$Cl$_2$, rt, overnight, 87% (**282**), 84% (**285**); (d) 1.

TFA/CH$_2$Cl$_2$ 1:1, rt, 1 h; 2. **271**, EDC, DMAP, DIPEA, CH$_2$Cl$_2$, rt, overnight, 54% (**171**), 48%

(**189**); (e) 1. PBu$_3$, TEA, H$_2$O, TFE, rt, overnight; 2. **152**, TCEP·HCl, CH$_3$CN/buffer 3:1, 65

$^\circ$C, overnight, 15% (**159**), 15% (**162**).
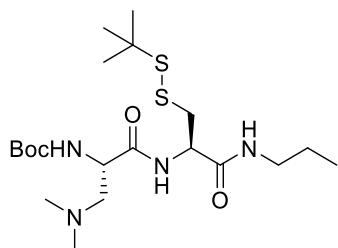
Compound 280 (0.7 g, 27%, colorless oil) was prepared from **272** (2.1 g, 6.0 mmol) and **270** (1.7 g, 7.3 mmol) following the general procedures A and D. R_f (CH$_2$Cl$_2$/MeOH 15:1): 0.34; $[\alpha]_D^{20}$ −98.0 (*c* 1.00, CHCl$_3$); IR (neat): 3288 (w), 2966 (w), 1650 (s), 1529 (m), 1458 (m), 1389 (w), 1364 (m), 1248 (m), 1164 (s), 1050 (w), 1013 (m), 858 (w), 778 (w); ^{1}H NMR (300 MHz, CDCl$_3$): 8.26 (br s, 1H), 6.94 (br s, 1H), 5.61 (s, 1H), 4.75 − 4.63 (m, 1H), 4.12 − 3.99 (m, 1H), 3.37 − 2.95 (m, 4H), 2.62 − 2.50 (m, 2H), 2.31 (s, 6H), 1.60 − 1.50 (m, 2H), 1.45 (s, 9H), 1.33 (s, 9H), 0.97 − 0.83 (m, 3H); ^{13}C NMR (100 MHz, CDCl$_3$): 171.4 (C), 169.6 (C), 156.3 (C), 80.5 (C), 60.4 (CH$_2$), 53.3 (CH), 52.1 (CH), 48.5 (C), 45.2 (2xCH$_3$), 42.0 (CH$_2$), 41.5 (CH$_2$), 29.8 (3xCH$_3$), 28.3 (3xCH$_3$), 22.6 (CH$_2$), 11.4 (CH$_3$); MS (ESI, MeOH): 465 (100, [M+H]$^+$).
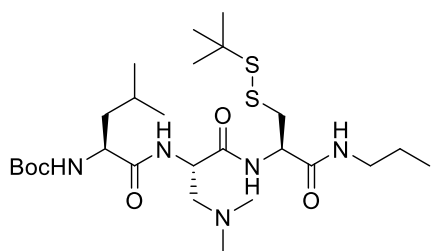
Compound 281 (580 mg, 63%, colorless solid) was prepared from **280** (743 mg, 1.60 mmol) and Boc–L– Leu–OH (444 mg, 1.92 mmol) following the general procedures A and D. R_f (CH$_2$Cl$_2$/MeOH 15:1): 0.30; Mp: 162 − 163 $^\circ$C; $[\alpha]_D^{20}$ −102 (*c* 1.00, CHCl$_3$); IR (neat): 3276 (w), 3096 (w), 2963 (w), 2871 (w), 2825 (w), 2775 (w), 1715 (w), 1688 (w), 1629 (s), 1528 (m), 1455 (m), 1390 (w), 1364 (m), 1331 (w), 1251 (m), 1165 (s), 1044 (w), 1021 (w), 915 (w), 877 (w), 854 (w), 831 (w), 767 (w), 732 (m), 648 (m); ^{1}H NMR (400 MHz, DMSO–d_6): 8.53 (d, $^3J_{H-H}$ = 7.9 Hz, 1H), 8.03 (t, $^3J_{H-H}$ = 5.8 Hz, 1H), 7.76 (d, $^3J_{H-H}$ = 7.5 Hz, 1H), 6.99 (d, $^3J_{H-H}$ = 8.3 Hz, 1H), 4.53 − 4.35

(m, 2H), 4.02 – 3.87 (m, 1H), 3.23 – 2.82 (m, 4H), 2.61 – 2.54 (m, 1H), 2.38 – 2.28 (m, 1H), 2.22 (s, 6H), 1.72 – 1.51 (m, 1H), 1.46 – 1.32 (m, 13H), 1.29 (s, 9H), 0.93 – 0.72 (m, 9H); ^{13}C NMR (100 MHz, DMSO–d_6): 173.0 (C), 171.3 (C), 169.6 (C), 155.8 (C), 78.6 (C), 61.5 (CH$_2$), 53.3 (CH), 53.0 (CH), 51.0 (CH), 48.1 (C), 46.0 (2xCH$_3$), 42.3 (CH$_2$), 41.1 (2xCH$_2$), 41.0 (CH$_2$), 30.1 (3xCH$_3$), 28.7 (3xCH$_3$), 24.7 (CH), 23.5 (CH$_3$), 22.8 (CH$_2$), 22.0 (CH$_3$), 11.7 (CH$_3$); MS (ESI, MeOH): 578 (100, [M+H]$^+$).
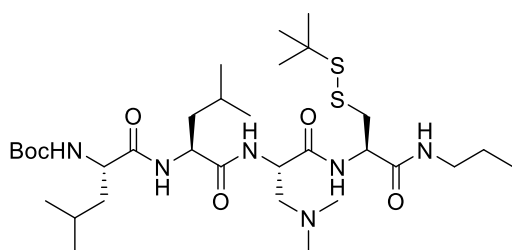
Compound 282 (601 mg, 87%, colorless solid) was prepared from **281** (580 mg, 1.00 mmol) and Boc–L–Leu–OH (279 mg, 1.21 mmol) following the general procedures A and D. R_f (CH$_2$Cl$_2$/MeOH 15:1): 0.34; Mp: 218 – 219 °C (decomp); $[\alpha]_\mathrm{D}^{20}$ –119 (*c* 1.00, CHCl$_3$); IR (neat): 3273 (w), 3086 (w), 2959 (w), 2872 (w), 2825 (w), 2773 (w), 1719 (w), 1689 (w), 1628 (s), 1531 (m), 1458 (w), 1388 (w), 1364 (m), 1249 (m), 1165 (s), 1045 (w), 1021 (w), 955 (w), 875 (w), 852 (w), 776 (w), 699 (m); ^{1}H NMR (300 MHz, CDCl$_3$): 8.04 (d, $^3J_{\text{H–H}}$ = 8.3 Hz, 1H), 7.28 (br s, 1H), 7.02 (s, 1H), 6.82 (br s, 1H), 4.91 (d, $^3J_{\text{H–H}}$ = 7.5 Hz, 1H), 4.77 – 4.65 (m, 1H), 4.36 – 4.04 (m, 3H), 3.31 – 3.07 (m, 4H), 2.72 – 2.54 (m, 2H), 2.28 (s, 6H), 1.87 – 1.76 (m, 2H), 1.77 – 1.61 (m, 2H), 1.61 – 1.49 (m, 4H), 1.44 (s, 9H), 1.33 (s, 9H), 1.01 – 0.86 (m, 15H); ^{13}C NMR (100 MHz, CDCl$_3$): 173.8 (C), 172.8 (C), 170.9 (C), 170.0 (C), 156.1 (C), 80.6 (C), 59.3 (CH$_2$), 53.2 (CH), 53.0 (CH), 52.9 (CH), 51.5 (CH), 48.2 (C), 45.3 (2xCH$_3$), 42.2 (CH$_2$), 41.5 (CH$_2$), 40.7 (CH$_2$), 40.4 (CH$_2$), 29.9 (3xCH$_3$), 28.3 (3xCH$_3$), 24.79 (CH), 24.76 (CH), 23.0 (2xCH$_3$), 22.6 (CH$_2$), 21.9 (CH$_3$), 21.7 (CH$_3$), 11.4 (CH$_3$); MS (ESI, MeOH): 691 (100, [M+H]$^+$).
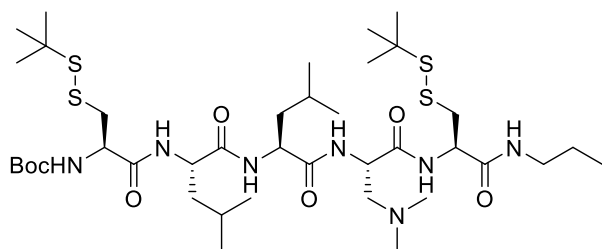
Compound 171 (412 mg, 54%, colorless solid) was prepared from **282** (601 mg, 0.871 mmol) and **271** (323 mg, 1.04 mmol) following the general procedures A and D. R_f (CH$_2$Cl$_2$/MeOH 15:1): 0.29; Mp: 188 – 189 °C (decomp); $[\alpha]_D^{20}$ –60.5 (*c* 1.00, CHCl$_3$); IR (neat): 3271 (w), 3102 (w), 2959 (w), 2872 (w), 2772 (w), 2822 (w), 1721 (w), 1691 (w), 1627 (s), 1540 (s), 1456 (w), 1410 (w), 1388 (w), 1350 (m), 1324 (w), 1276 (w), 1256 (w), 1235 (w), 1165 (m), 1122 (w), 1042 (w), 1021 (w), 873 (w), 835 (w), 773 (w), 698 (m), 637 (m); ^{1}H NMR (400 MHz, DMSO–d_6): 8.43 (d, $^3J_{H-H}$ = 7.9 Hz, 1H), 8.05 – 7.79 (m, 4H), 7.15 (d, $^3J_{H-H}$ = 8.3 Hz, 1H), 4.50 – 4.08 (m, 5H), 3.23 – 2.86 (m, 6H), 2.61 – 2.53 (m, 1H), 2.34 (dd, $^2J_{H-H}$ = 12.1 Hz, $^3J_{H-H}$ = 6.4 Hz, 1H), 2.21 (s, 6H), 1.70 – 1.54 (m, 2H), 1.50 – 1.33 (m, 15H), 1.29 (s, 18H), 0.97 – 0.76 (m, 15H); ^{13}C NMR (100 MHz, DMSO–d_6): 172.2 (C), 172.1 (C), 171.1 (C), 170.4 (C), 169.6 (C), 157.1 (C), 78.9 (C), 61.3 (CH$_2$), 54.4 (CH), 52.9 (CH), 51.4 (2xCH), 51.2 (CH), 48.1 (C), 45.9 (2xCH$_3$), 42.9 (CH$_2$), 42.4 (CH$_2$), 41.3 (CH$_2$), 41.1 (CH$_2$), 40.9 (CH$_2$), 30.1 (3xCH$_3$), 28.6 (3xCH$_3$), 24.50 (CH), 24.45 (CH), 23.57 (CH$_3$), 23.55 (CH$_3$), 22.8 (CH$_2$), 22.2 (CH$_3$), 22.1 (CH$_3$), 11.7 (CH$_3$); MS (ESI, MeOH): 882 (100, [M+H]$^+$); HRMS (ESI, +ve) calcd for C$_{39}$H$_{75}$N$_7$O$_7$S$_4$ ([M+H]$^+$): 882.4684, found: 882.4673.
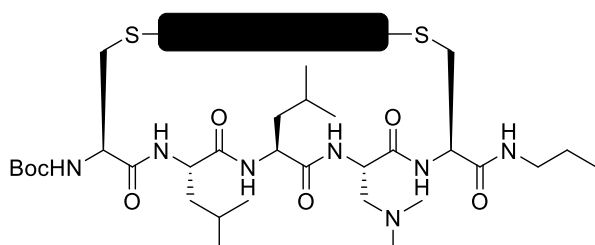
Compound 159 (35 mg, 15%, mixture of two atropisomers **159a** and **159b**, red solid) was prepared from **171** (150 mg, 0.170 mmol) following the general procedures F and G. R_f (CH$_2$Cl$_2$/MeOH 15:1): 0.34. **159a** and **159b** were separated using PTLC (CH$_2$Cl$_2$/MeOH 18:1) **159a** (24 mg), **159b** (10 mg). **159a**. R_f (CH$_2$Cl$_2$/MeOH 18:1): 0.30; Mp:

188 – 189 °C; UV-Vis (TFE): 522 (10.0), 374 (7.9), 295 (23.7); CD (TFE): 529 (–6.7), 376 (+8.7), 317 (–3.1), 299 (+3.4), 248 (–0.7), 207 (+25.6), IR (neat): 3313 (w), 2958 (w), 1651 (s), 1530 (m), 1438 (m), 1367 (m), 1314 (m), 1214 (s), 1159 (m), 907 (w); ^{1}H NMR (400 MHz, CDCl$_3$): 8.91 (s, 1H), 8.59 (s, 1H), 7.16 (br s, 1H), 7.06 (br s, 1H), 6.41 (br s, 1H), 6.02 (d, $^3J_{H-H}$ = 8.1 Hz, 1H), 5.93 – 5.79 (m, 2H), 5.74 – 5.64 (m, 2H), 5.57 (br s, 1H), 4.92 – 4.79 (m, 1H), 4.75 – 4.61 (m, 1H), 4.09 – 3.90 (m, 4H), 3.75 – 3.44 (m, 2H), 3.34 – 3.14 (m, 5H), 3.08 – 2.94 (m, 1H), 2.39 – 2.29 (m, 8H), 2.23 – 2.08 (m, 2H), 2.07 – 1.92 (m, 2H), 1.78 – 1.73 (m, 3H), 1.72 – 1.62 (m, 2H), 1.56 – 1.47 (m, 12H), 1.42 – 1.38 (m, 1H), 1.31 – 1.20 (m, 18H), 1.05 – 0.98 (m, 3H), 0.95 – 0.90 (m, 9H), 0.88 – 0.82 (m, 15H), 0.71 – 0.58 (m, 6H); ^{13}C NMR (125 MHz, CDCl$_3$): 171.9 (C), 170.4 (C), 170.2 (C), 169.4 (C), 169.2 (2xC), 168.8 (C), 168.7 (C), 164.2 (C), 162.7 (C), 162.6 (C), 162.4 (C), 154.9 (C), 146.9 (C), 145.3 (C), 130.2 (CH), 128.8 (CH), 125.5 (C), 125.3 (C), 124.1 (C), 122.5 (C), 122.0 (C), 120.0 (C), 81.0 (C), 61.8 (CH$_2$), 56.6 (CH), 54.6 (CH), 54.3 (CH), 54.0 (CH), 53.1 (CH), 51.1 (CH), 48.7 (CH), 45.7 (2xCH$_3$), 42.5 (CH$_2$), 41.9 (CH$_2$), 40.1 (CH$_2$), 40.0 (CH$_2$), 39.1 (CH$_2$), 38.2 (CH$_2$), 34.9 (CH$_2$), 33.4 (CH$_2$), 31.50 (CH$_2$), 31.47 (CH$_2$), 29.7 (CH$_2$), 29.5 (CH$_2$), 28.2 (3xCH$_3$), 26.7 (CH$_2$), 26.6 (CH$_2$), 26.0 (CH), 25.7 (CH), 25.4 (CH), 24.5 (CH), 24.2 (CH$_3$), 23.2 (CH$_3$), 23.1 (CH$_3$), 22.99 (CH$_3$), 22.96 (CH$_2$), 22.7 (CH$_2$), 22.6 (CH$_2$), 22.2 (CH$_3$), 22.0 (CH$_3$), 21.6 (CH$_3$), 21.5 (CH$_3$), 14.1 (CH$_3$), 14.0 (CH$_3$), 11.4 (CH$_3$); HPLC–MS: R_t = 2.83 min, 1363 (100, [M+H]$^+$); HRMS (ESI, +ve) calcd for C$_{69}$H$_{107}$N$_{11}$O$_{13}$S$_2$ ([M+H]$^+$): 1362.7565, found: 1362.7565. **159b**. R_f (CH$_2$Cl$_2$/MeOH 18:1): 0.28; Mp, IR spectrum, HRMS were identical with **159a**; UV-Vis (TFE): 516 (12.7), 375 (12.6), 294 (29.8); CD (TFE): 515 (+5.4), 379 (–4.5), 283 (–0.4), 271 (–2.4), 256 (+0.3), 235 (–8.2), 210. (0.0); ^{1}H NMR (400 MHz, CDCl$_3$) : 9.60 (s, 1H), 8.71 (s, 1H), 8.65 (d, $^3J_{H-H}$ = 8.2 Hz, 1H), 7.32 (s, 1H), 7.12 (s, 1H), 6.64 – 6.47 (m, 1H), 5.83 (s, 1H), 5.80 – 5.60 (m, 2H), 5.28 (d, $^3J_{H-H}$ = 9.1 Hz, 1H), 5.00 – 4.89 (m, 1H), 4.52 – 4.40 (m, 1H), 4.38 – 4.23 (m, 1H), 4.22 – 4.09 (m, 1H), 4.07 – 3.92 (s, 1H), 3.74 – 3.57 (m, 1H), 3.37 – 3.11

(m, 5H), 3.09 – 2.94 (m, 1H), 2.73 – 2.62 (m, 1H), 2.40 – 2.22 (m, 7H), 2.21 – 2.10 (m, 1H), 2.10 – 1.91 (m, 2H), 1.91 – 1.70 (m, 6H), 1.67 – 1.42 (m, 18H), 1.39 – 1.15 (m, 17H), 1.08 – 0.66 (m, 30H), 0.65 – 0.55 (m, 3H); ^{13}C NMR (100 MHz, CDCl$_3$): 172.3 (C), 171.4 (C), 170.4 (C), 170.0 (C), 169.4 (C), 169.3 (C), 168.7 (C), 165.8 (C), 163.3 (C), 161.9 (C), 161.6 (C), 155.3 (C), 148.0 (C), 144.5 (C), 136.7 (CH), 129.8 (CH), 126.4 (C), 125.5 (C), 125.2 (C), 124.2 (C), 123.9 (C), 118.8 (C), 81.4 (C), 61.5 (CH$_2$), 55.5 (CH), 54.9 (CH), 54.2 (CH), 51.3 (CH), 50.7 (CH), 40.3 (CH), 49.2 (CH), 45.7 (2xCH$_3$), 43.5 (CH$_2$), 42.0 (CH$_2$), 41.6 (CH$_2$), 40.1 (CH$_2$), 40.0 (CH$_2$), 38.3 (CH$_2$), 38.0 (CH$_2$), 37.6 (CH$_2$), 36.3 (CH$_2$), 31.52 (CH$_2$), 31.48 (CH$_2$), 29.7 (CH$_2$), 29.4 (CH$_2$), 28.2 (3xCH$_3$), 26.7 (CH$_2$), 26.6 (CH$_2$), 25.9 (CH), 25.6 (CH), 24.4 (CH), 24.2 (CH), 23.3 (CH$_3$), 23.2 (CH$_3$), 23.1 (CH$_3$), 22.9 (CH$_2$), 22.8 (CH$_3$), 22.64 (CH$_2$), 22.57 (CH$_2$), 22.2 (CH$_3$), 21.80 (CH$_3$), 21.77 (CH$_3$), 21.5 (CH$_3$), 14.1 (CH$_3$), 14.0 (CH$_3$), 11.3 (CH$_3$); HPLC–MS: R_t = 2.79 min, 1363 (100, [M+H]$^+$).
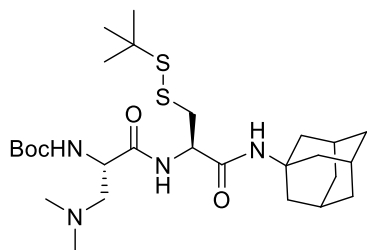
Compound 283 (1.8 g, 83%, colorless solid) was prepared from **276** (1.8 g, 4.0 mmol) and **270** (1.1 g, 4.7 mmol) following the general procedures A and D. R_f (CH$_2$Cl$_2$/MeOH 15:1): 0.50; Mp: 80 – 81 °C; [α]$_D^{20}$ –67.9 (*c* 1.00, CHCl$_3$); IR (neat): 3305 (w), 2908 (m), 2854 (w), 1651 (s), 1515 (m), 1456 (m), 1362 (m), 1246 (m), 1175 (s), 1099 (w), 1049 (m), 1015 (m), 862 (m), 778 (w); ^{1}H NMR (300 MHz, CDCl$_3$): 8.74 (s, 1H), 6.12 (s, 1H), 5.59 (s, 1H), 4.55 – 4.48 (m, 1H), 4.12 – 3.99 (m, 1H), 3.22 (dd, $^2J_{H-H}$ = 13.5 Hz, $^3J_{H-H}$ = 6.2 Hz, 1H), 2.94 (dd, $^2J_{H-H}$ = 13.5 Hz, $^3J_{H-H}$ = 6.0 Hz, 1H), 2.69 – 2.42 (m, 2H), 2.33 (s, 6H), 2.1 – 2.02 (m, 3H), 1.99 (d, $^3J_{H-H}$ = 2.9 Hz, 6H), 1.75 – 1.57 (m, 6H), 1.46 (s, 9H), 1.33 (s, 9H); ^{13}C NMR (100 MHz, CDCl$_3$): 171.5 (C), 168.6 (C), 155.9 (C), 80.1 (C), 60.6 (C), 53.6 (CH), 52.3 (C), 51.4 (CH), 48.4 (C), 45.1 (2xCH$_3$), 42.4 (CH$_2$), 41.4

(3xCH$_2$), 36.3 (3xCH$_2$), 29.9 (CH), 29.4 (3CH$_3$), 28.4 (3xCH$_3$); MS (ESI, MeOH): 557 (100, [M+H]$^+$).
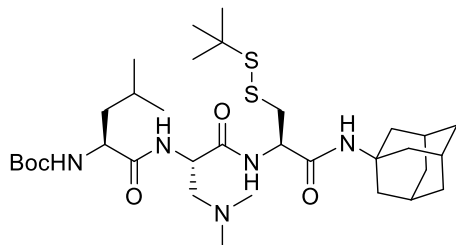
Compound 284 (1.4 g, 61%, colorless solid) was prepared from **283** (1.8 g, 3.2 mmol) and Boc–L–Leu–OH (0.92 g, 4.0 mmol) following the general procedures A and D. R_f (CH$_2$Cl$_2$/MeOH 15:1): 0.50; **72** was a colorless oil; $[\alpha]_D^{20}$ –80.5 (*c* 1.00, CHCl$_3$); IR (neat): 3300 (w), 2910 (m), 1854 (w), 2786 (w), 1643 (s), 1516 (s), 1455 (m), 1389 (w), 1363 (m), 1311 (w), 1272 (m), 1274 (m), 1165 (s), 1103 (w), 1045 (w), 1024 (w), 909 (m), 873 (w), 730 (s), 645 (m); ^{1}H NMR (300 MHz, CDCl$_3$): 8.54 (d, $^3J_{H–H}$ = 8.3 Hz, 1H), 7.47 (d, $^3J_{H–H}$ = 4.6 Hz, 1H), 6.36 (s, 1H), 5.06 (d, $^3J_{H–H}$ = 7.1 Hz, 1H), 4.66 – 4.57 (m, 1H), 4.34 – 4.1 (m, 2H), 3.14 – 2.90 (m, 2H), 2.70 – 2.41 (m, 2H), 2.29 (s, 6H), 2.07 – 1.87 (m, 9H), 1.77 – 1.54 (m, 8H), 1.49 – 1.33 (m, 10H), 1.28 (s, 9H), 0.94 – 0.80 (m, 6H); ^{13}C NMR (75 MHz, CDCl$_3$): 173.2 (C), 171.0 (C), 168.9 (C), 155.8 (C), 80.2 (C), 59.8 (CH$_2$), 53.5 (CH), 53.4 (CH), 52.1 (C), 50.6 (CH), 48.1 (C), 45.1 (2xCH$_3$), 42.7 (CH$_2$), 41.7 (CH$_2$), 41.3 (3xCH$_2$), 36.3 (3xCH$_2$), 29.9 (3xCH$_3$), 29.4 (3xCH$_3$), 28.4 (CH), 24.8 (CH), 23.0 (CH$_3$), 21.9 (CH$_3$); MS (ESI, MeOH): 670 (100, [M+H]$^+$).
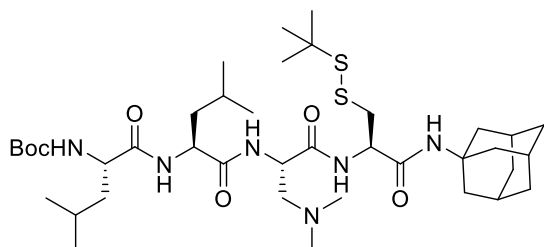
Compound 285 (1.3 g, 84%, colorless solid) was prepared from **284** (1.4 g, 2.1 mmol) and Boc–L–Leu–OH (0.56 g, 2.4 mmol) following the general procedures A and D. R_f (CH$_2$Cl$_2$/MeOH 15:1): 0.49; Mp: 153 – 154 °C; $[\alpha]_D^{20}$ –114 (*c* 1.00, CHCl$_3$); IR (neat): 3293 (w), 2911 (w), 1634 (s), 1515 (m), 1363 (m), 1247 (w), 1164 (m), 1045 (w); ^{1}H NMR (300 MHz, CDCl$_3$): 8.43 (br s, 1H), 7.37 (br s, 1H), 6.91 (br s, 1H), 6.40 (s, 1H), 5.01 (d, $^3J_{H–H}$ = 6.9

Hz, 1H), 4.67 – 4.56 (m, 1H), 4.49 – 4.36 (m, 1H), 4.36 – 4.25 (m, 1H), 4.22 – 4.06 (m, 1H), 3.19 – 2.96 (m, 2H), 2.71 – 2.46 (m, 2H), 2.29 (s, 6H), 2.11 – 1.92 (m, 9H), 1.79 – 1.49 (m, 12H), 1.42 (s, 9H), 1.30 (s, 9H), 1.00 – 0.78 (m, 12H); ^{13}C NMR (75 MHz, CDCl$_3$): 173.4 (C), 172.4 (C), 170.9 (C), 168.9 (C), 80.3 (C), 59.7 (CH$_2$), 53.4 (CH), 53.1 (CH), 52.6 (CH), 52.1 (C), 50.7 (CH), 48.1 (C), 45.2 (2xCH$_3$), 42.8 (CH$_2$), 41.3 (3xCH$_2$), 40.7 (CH$_2$), 36.4 (3xCH$_2$), 29.9 (3xCH$_3$), 29.4 (3xCH$_3$), 28.3 (CH), 24.75 (CH), 24.73 (CH), 23.1 (CH$_3$), 23.0 (CH$_3$), 22.0 (2xCH$_3$); MS (ESI, MeOH): 784 (100, [M+H]$^+$).
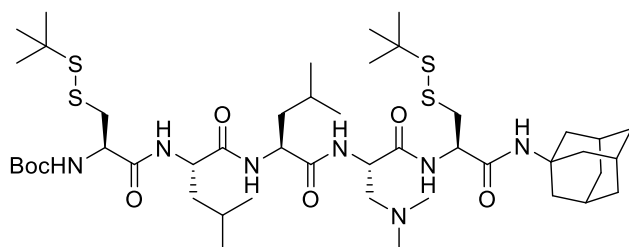
Compound 189 (0.8 g, 48%, colorless solid) was prepared from **285** (1.3 g, 1.7 mmol) and **271** (0.63 g, 2.0 mmol) following the general procedures A and D. R_f (CH$_2$Cl$_2$/MeOH 15:1): 0.42; Mp: 203 – 204 $^{\circ}$C; [α]$_D^{20}$ –107 (*c* 1.00, CHCl$_3$); IR (neat): 3271 (w), 3083 (w), 2956 (w), 2911 (w), 2856 (w), 1721 (w), 1631 (s), 1527 (m), 1456 (m), 1389 (w), 1362 (m), 1311 (w), 1273 (w), 1246 (w), 1164 (s), 1101 (w), 1047 (w), 872 (w), 701 (w), 648 (w); ^{1}H NMR (400 MHz, CDCl$_3$): 7.87 (br s, 1H), 7.26 (br s, 1H), 7.06 (s, 1H), 6.63 (d, $^3J_{H–H}$ = 5.4 Hz, 1H), 6.36 (s, 1H), 5.42 (d, $^3J_{H–H}$ = 5.7 Hz, 1H), 4.67 – 4.57 (m, 1H), 4.45 – 4.19 (m, 4H), 3.27 (dd, $^2J_{H–H}$ = 13.4, $^3J_{H–H}$ = 4.2 Hz, 1H), 3.15 – 2.96 (m, 3H), 2.79 (dd, $^2J_{H–H}$ = 12.5, $^3J_{H–H}$ = 8.4 Hz, 1H), 2.64 (dd, $^2J_{H–H}$ = 12.5, $^3J_{H–H}$ = 5.9 Hz, 1H), 2.28 (s, 6H), 2.10 – 2.03 (m, 9H), 1.76 – 1.59 (m, 12H), 1.47 (s, 9H), 1.35 (s, 9H), 1.32 (s, 9H), 0.99 – 0.89 (m, 12H); ^{13}C NMR (75 MHz, CDCl$_3$): 172.8 (C, 2xC), 171.3 (C), 171.0 (C), 169.1 (C), 156.0 (C), 81.1 (C), 59.4 (CH$_2$), 54.6 (CH), 53.3 (2xCH), 52.1 (CH), 51.9 (CH), 48.8 (C), 47.9 (C), 45.1 (2xCH$_3$), 42.4 (2xCH$_2$), 41.2 (3xCH$_2$), 40.4 (CH$_2$), 40.2 (CH$_2$), 36.4 (3xCH$_2$), 29.94 (3xCH$_3$), 29.85 (3xCH$_3$), 29.5 (3xCH$_3$), 28.2 (CH), 24.9 (2xCH), 23.1 (CH$_3$), 22.9 (CH$_3$), 21.8 (CH$_3$),

21.6 (CH$_3$); MS (ESI, MeOH): 974 (100, [M+H]$^+$); HRMS (ESI, +ve) calcd for C$_{46}$H$_{83}$N$_7$O$_7$S$_4$ ([M+H]$^+$): 974.5310, found: 974.5303.
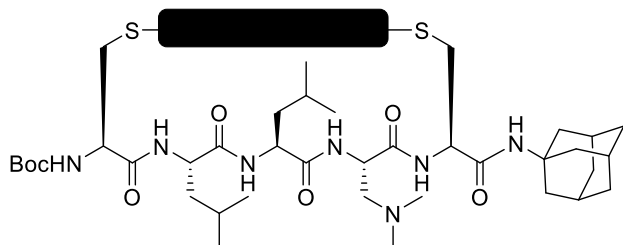
Compound 162 (32 mg, 15%, atropisomers not detectable) was prepared from **189** (100 mg, 0.103 mmol) following the general procedures F and G. R_f (CH$_2$Cl$_2$/MeOH 15:1): 0.4; Mp: 181 – 182 °C; UV-Vis (TFE): 520 (9.5), 374 (7.6), 295 (22.5); CD (TFE): 531 (–12.2), 378 (+15.2), 318 (–3.7), 300 (+9.1), 241 (–6.2), 209 (+47.2); IR (neat): 3324 (w), 2926 (w), 1652 (s), 1527 (m), 1438 (m), 1366 (m), 1313 (m), 1214 (m), 1160 (m), 1044 (w), 907 (w), 851 (w), 791 (w); ^{1}H NMR (400 MHz, CDCl$_3$): 9.00 (s, 1H), 8.90 (br s, 1H), 8.57 (s, 1H), 7.20 (br s, 1H), 6.46 (br s, 1H), 6.04 (d, $^3J_{H–H}$ = 8.4 Hz, 1H), 5.82 (s, 1H), 5.77 – 5.66 (m, 3H), 5.64 – 5.52 (m, 2H), 4.78 – 4.63 (m, 2H), 4.20 – 3.99 (m, 3H), 3.97 – 3.90 (m, 1H), 3.88 – 3.74 (m, 2H), 3.50 – 3.40 (m, 1H), 3.33 – 3.24 (m, 4H), 3.11 – 2.97 (m, 1H), 2.41 – 2.27 (m, 9H), 2.14 – 2.09 (m, 4H), 2.05 – 1.97 (m, 9H), 1.71 – 1.67 (m, 16H), 1.36 – 1.30 (m, 9H), 1.26 – 1.21 (m, 9H), 1.03 (d, $^3J_{H–H}$ = 6.5 Hz, 3H), 0.97 – 0.93 (m, 6H), 0.91 – 0.84 (m, 18H), 0.71 – 0.65 (m, 6H); ^{13}C NMR (125 MHz, CDCl$_3$): 172.1 (C), 170.3 (C), 170.2 (C), 169.3 (2xC), 168.7 (C), 167.9 (C), 163.7 (C), 162.8 (C), 162.7 (C), 162.2 (C), 160.2 (C), 154.9 (C), 147.3 (C), 144.9 (C), 130.0 (CH), 128.6 (CH), 125.5 (C), 125.3 (C), 124.9 (C), 122.5 (C), 122.1 (C), 120.8 (C), 81.8 (C), 61.5 (CH$_2$), 57.7 (CH), 54.5 (CH), 54.14 (CH), 54.09 (CH), 53.2 (CH), 52.6 (C), 50.8 (CH), 48.3 (CH), 45.6 (2xCH$_3$), 41.4 (3xCH$_2$), 40.1 (CH$_2$), 40.0 (CH$_2$), 38.9 (CH$_2$), 38.1 (CH$_2$), 37.7 (CH$_2$), 36.2 (3xCH$_2$), 34.9 (CH$_2$), 34.8 (CH$_2$), 31.5 (CH$_2$), 29.71 (CH$_2$), 29.67 (CH$_2$), 29.62 (CH$_2$), 29.5 (CH$_2$), 29.4 (CH), 28.2 (3xCH$_3$), 26.7 (CH$_2$), 26.6 (CH$_2$), 25.9 (CH), 25.7 (CH), 25.4 (CH), 24.5 (CH), 24.2 (CH$_3$), 23.22 (CH$_3$), 23.15 (CH$_3$), 23.1 (CH$_3$), 22.7 (CH$_2$), 22.6 (CH$_2$), 22.3 (CH$_3$), 22.0 (CH$_3$), 21.6

(CH$_3$), 21.4 (CH$_3$), 14.1 (2xCH$_3$); HPLC–MS: R_t = 3.02 min, 1455 (100, [M+H]$^+$); HRMS

(ESI, +ve) calcd for C$_{76}$H$_{115}$N$_{11}$O$_{13}$S$_2$ ([M+H]$^+$): 1454.8191, found: 1454.8213.
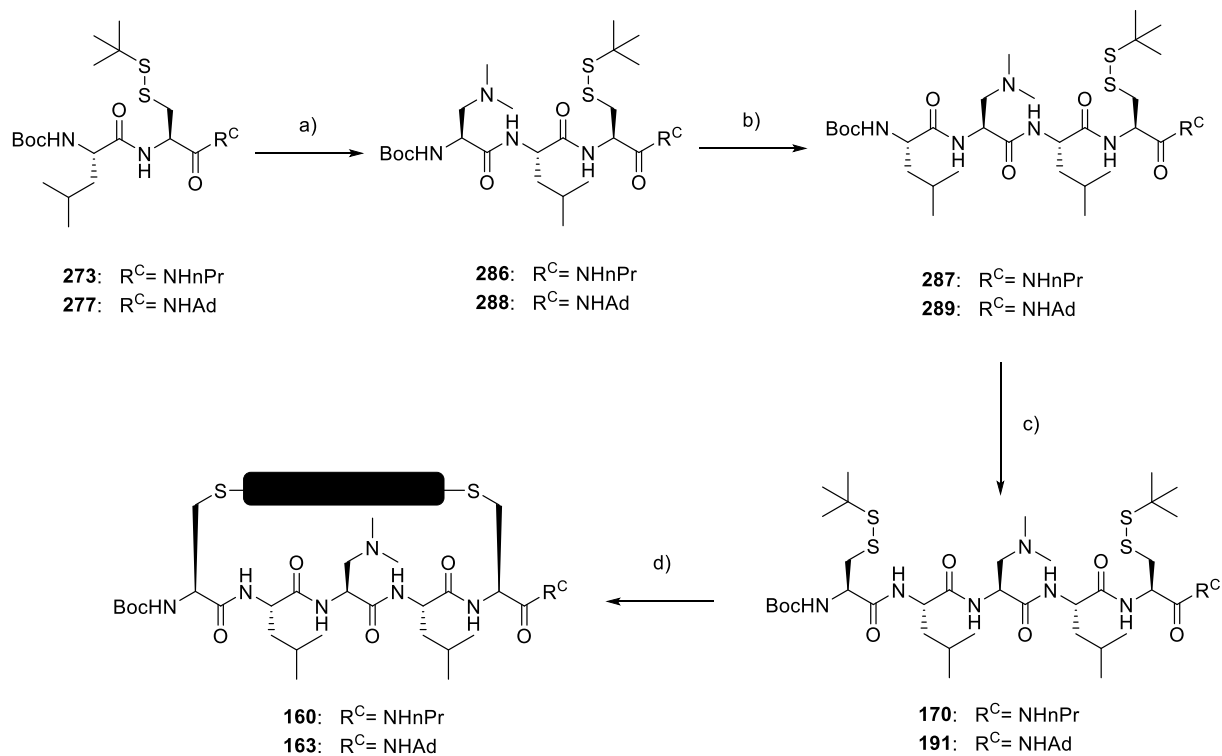
Scheme 14. (a) 1. TFA/CH$_2$Cl$_2$ 1:1, rt, 1 h; 2. **270**, EDC, DMAP, DIPEA, CH$_2$Cl$_2$, rt, overnight, 42% (**286**), 62% (**288**); (b) 1. TFA/CH$_2$Cl$_2$ 1:1, rt, 1 h; 2. Boc–L–Leu–OH, EDC, DMAP, DIPEA, CH$_2$Cl$_2$, rt, overnight, 85% (**287**), 59% (**289**); (c) 1. TFA/ CH$_2$Cl$_2$ 1:1, rt, 1 h; 2. **271**, EDC, DMAP, DIPEA, CH$_2$Cl$_2$, rt, overnight, 49% (**170**), 44% (**191**); (d) 1. PBu$_3$, TEA, H$_2$O, TFE, rt, overnight; 2. **152**, TCEP·HCl, CH$_3$CN/buffer 3:1, 65 ºC, overnight, 27% (**160**), 15% (**163**).
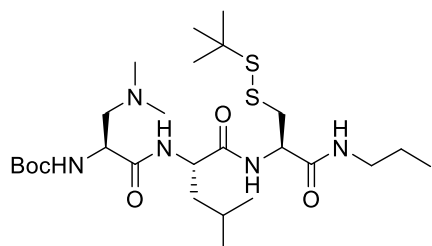
Compound 286 (0.6 g, 42%, colorless solid) was prepared from **273** (1.1 g, 2.4 mmol) and **270** (0.66 g, 2.8 mmol) following the general procedures A and D.

R_f (CH$_2$Cl$_2$/MeOH 15:1): 0.47; Mp: 167 – 168 °C; $[\alpha]_D^{20}$ –82.7 (c 1.00, CHCl$_3$); IR (neat): 3277 (w), 3107 (w), 2964 (w), 2872 (w), 2823 (w), 2770 (w), 1692 (w), 1631 (s), 1524 (s), 1463 (m), 1388 (w), 1365 (m), 1324 (w), 1250 (m), 1167 (s), 1099 (w), 1052 (w), 1008 (w), 912 (m), 863 (w), 779 (w), 730 (s), 647 (m); ^{1}H NMR (300 MHz, CDCl$_3$): 8.10 (br s, 1H), 7.21 (d, $^3J_{H-H}$ = 8.3 Hz, 1H), 6.74 (s, 1H), 5.55 (s, 1H), 4.76 – 4.60 (m 1H), 4.33 – 4.18 (m, 1H), 4.05 – 3.90 (m, 1H), 3.34 – 2.94 (m, 4H), 2.66 (dd, $^2J_{H-H}$ = 12.3 Hz, $^3J_{H-H}$ = 8.7 Hz, 1H), 2.51 (dd, $^2J_{H-H}$ = 12.3 Hz, $^3J_{H-H}$ = 6.7 Hz, 1H), 2.30 (s, 6H), 1.83 – 1.45 (m, 5H), 1.41 (s, 1H), 1.30 (s, 9H), 1.03 – 0.82 (m, 9H); ^{13}C NMR (75 MHz, CDCl$_3$): 172.4 (C), 171.9 (C), 169.8 (C), 156.3 (C), 80.7 (C), 60.2 (CH$_2$), 53.1 (CH), 52.6 (CH), 51.9 (CH), 48.2 (C), 45.0 (2xCH$_3$), 41.7 (CH$_2$), 41.5 (CH$_2$), 40.1 (CH$_2$), 29.9 (3xCH$_3$), 28.3 (3xCH$_3$), 25.1 (CH), 23.1 (CH$_3$), 22.5 (CH$_2$), 21.7 (CH$_3$), 11.4 (CH$_3$); MS (ESI, MeOH): 578 (100, [M+H]$^+$).
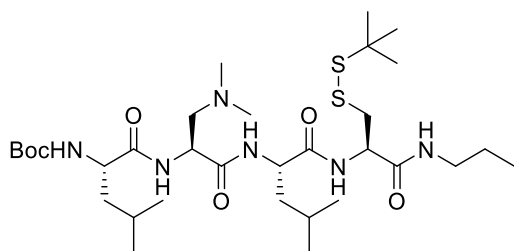
Compound 287 (585 mg, 85%, colorless solid) was prepared from **286** (573 mg, 0.993 mmol) and Boc–L–Leu–OH (276 mg, 1.19 mmol) following the general procedures A and D. R_f (CH$_2$Cl$_2$/MeOH 15:1): 0.41; Mp: 211 – 212 °C (decomp); $[\alpha]_D^{20}$ –104 (c 1.00, CHCl$_3$); IR (neat): 3270 (w), 3095 (w), 2961 (w), 2872 (w), 2824 (w), 2773 (w), 1720 (w), 1689 (w), 1628 (s), 1534 (s), 1457 (m), 1389 (w), 1364 (m), 1251 (m), 1165 (s), 1043 (w), 1021 (w), 918 (w), 874 (w), 777 (w), 699 (m); ^{1}H NMR (300 MHz, CDCl$_3$): 7.62 (d, $^3J_{H-H}$ = 6.6 Hz, 1H), 7.44 – 7.28 (m, 2H), 6.73 (d, $^3J_{H-H}$ = 6.0 Hz, 1H), 4.95 (d, $^3J_{H-H}$ = 3.9 Hz, 1H), 4.71 – 4.54 (m, 1H), 4.35 – 4.20 (m, 1H), 4.13 – 3.92 (m, 2H), 3.34 (dd, $^2J_{H-H}$ = 13.5 Hz, $^3J_{H-H}$ = 4.0 Hz, 1H), 3.23 – 2.98 (m, 3H), 2.76 – 2.51 (m, 2H), 2.21 (s, 6H), 1.94 – 1.46 (m, 8H), 1.43 (s, 9H), 1.28 (s, 9H), 0.98 – 0.77 (m, 15H); ^{13}C NMR (75 MHz, CDCl$_3$): 174.1 (C), 172.5 (C), 172.1 (C), 170.3 (C), 155.2 (C), 81.0 (C), 59.0 (CH$_2$), 54.6 (CH), 53.3 (CH), 52.9 (CH), 52.8 (CH), 47.9 (CH),

45.3 (2xCH$_3$), 41.7 (CH$_2$), 41.4 (CH$_2$), 40.5 (CH$_2$), 39.8 (CH$_2$), 30.0 (3xCH$_3$), 28.2 (3xCH$_3$), 25.0 (CH), 24.9 (CH), 23.2 (CH$_3$), 23.0 (CH$_3$), 22.5 (CH$_2$), 21.7 (CH$_3$), 21.0 (CH$_3$), 11.4 (CH$_3$); MS (ESI, MeOH): 691 (100, [M+H]$^+$).
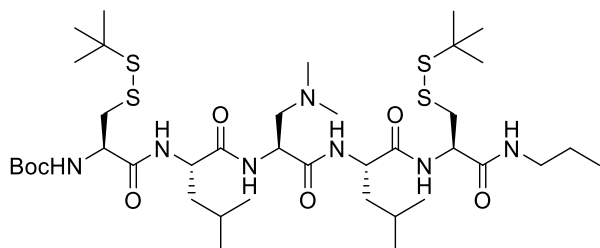
Compound 170 (363 mg, 49%, colorless solid) was prepared from **287** (585 mg, 0.847 mmol) and **271** (315 mg, 1.02 mmol) following the general procedures A and D. R_f (CH$_2$Cl$_2$/MeOH 15:1): 0.4; Mp: 214 – 215 °C (decomp); [α]$_D^{20}$ –93.7 (c 0.25, DMSO); IR (neat): 3269 (w), 3101 (w), 2961 (w), 1724 (w), 1690 (w), 1627 (s), 1542 (m), 1462 (w), 1409 (w), 1363 (m), 1278 (w), 1251 (w), 1166 (m), 1046 (w), 1021 (w), 868 (w), 776 (w), 704 (m), 639 (w); ^{1}H NMR (400 MHz, CDCl$_3$): 7.55 (d, $^3J_{H-H}$ = 6.5 Hz, 1H), 7.35 (d, $^3J_{H-H}$ = 8.0 Hz, 1H), 7.25 (s, 1H), 6.87 (s, 1H), 6.81 (d, $^3J_{H-H}$ = 5.8 Hz, 1H), 5.27 (d, $^3J_{H-H}$ = 7.0 Hz, 1H), 4.73 – 4.59 (m, 1H), 4.51 – 4.37 (m, 1H), 4. 33 – 4.21 (m, 1H), 4.20 – 4.06 (m, 2H), 3.39 (dd, $^2J_{H-H}$ = 13.4 Hz, $^3J_{H-H}$ = 3.8 Hz, 1H), 3.26 – 2.91 (m, 5H), 2.70 – 2.55 (m, 2H), 2.23 (s, 6H), 1.92 – 1.50 (m, 8H), 1.46 (s, 9H), 1.40 – 1.22 (m, 18H), 1.05 – 0.83 (m, 15H); ^{13}C NMR (100 MHz, CDCl$_3$): 173.3 (C, 2xC), 172.6 (C), 172.0 (C), 170.3 (C), 157.4 (C), 81.3 (C), 58.8 (CH$_2$), 54.5 (CH), 54.1 (CH), 53.4 (CH), 53.3 (CH), 53.0 (CH), 48.8 (C), 47.8 (C), 45.0 (2xCH$_3$), 41.9 (CH$_2$), 41.4 (CH$_2$), 40.3 (CH$_2$), 40.0 (CH$_2$), 39.6 (CH$_2$), 30.0 (3xCH$_3$), 29.8 (3xCH$_3$), 28.2 (3xCH$_3$), 25.1 (CH), 24.9 (CH), 23.4 (CH$_3$), 23.0 (CH$_3$), 22.5 (CH$_2$), 21.5 (CH$_3$), 20.9 (CH$_3$), 11.4 (CH$_3$); MS (ESI, MeOH): 882 (100, [M+H]$^+$); HRMS (ESI, +ve) calcd for C$_{39}$H$_{75}$N$_7$O$_7$S$_4$ ([M+H]$^+$): 882.4684, found: 882.4673.
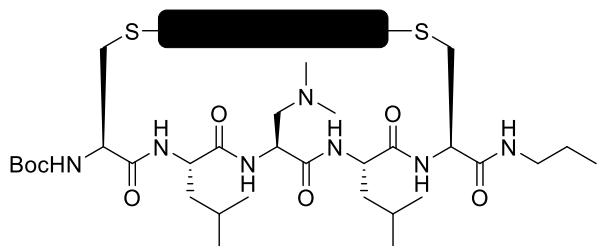
Compound 160 (63 mg, 27%, mixture of two atropisomers **160a** and **160b**, red solid) was prepared from **170** (150 mg, 0.170 mmol) following the general procedures F and G. R_f (CH$_2$Cl$_2$/MeOH 15:1): 0.40; Mp: 168 – 169 °C; UV-Vis (TFE): 522 (15.1), 372 (12.2), 296 (36.1); CD (TFE): 529 (–9.4), 376 (+12.0), 317 (–4.3), 298 (+8.0), 245 (–1.2), 207 (+41.0); IR (neat): 3312 (w), 2957 (w), 2933 (w), 2871 (w), 1651 (s), 1535 (m), 1439 (m), 1367 (m), 1314 (m), 1238 (m), 1214 (m), 1160 (m), 1030 (w), 907 (w), 851 (w), 791 (w), 731 (w); ^{1}H NMR (400 MHz, CDCl$_3$): 8.99 – 8.90 (m, 2H), 8.64 (s, 1H), 6.93 (s, 1H), 6.71 (d, $^3J_{H-H}$ = 9.5 Hz, 1H), 6.49 (br s, 1H), 6.18 (br s, 1H), 6.08 (d, $^3J_{H-H}$ = 6.4 Hz, 1H), 5.85 (t, $^3J_{H-H}$ = 5.7 Hz, 1H), 5.71 (dd, $^3J_{H-H}$ = 9.1, 5.5 Hz, 1H), 5.65 (dd, $^3J_{H-H}$ = 9.3, 4.6 Hz, 1H), 5.38 (d, $^3J_{H-H}$ = 7.3 Hz, 1H), 4.97 – 4.82 (m, 1H), 4.49 – 4.35 (m, 2H), 4.30 – 4.17 (m, 2H), 4.09 (dd, $^2J_{H-H}$ = 16.4, $^3J_{H-H}$ = 10.1 Hz, 1H), 3.73 – 3.59 (m, 1H), 3.51 (dd, $^2J_{H-H}$ = 13.3, $^3J_{H-H}$ = 3.8 Hz, 1H), 3.38 – 3.18 (m, 5H), 3.12 – 3.01 (m, 1H), 2.99 – 2.88 (m, 1H), 2.42 (ddd, $^2J_{H-H}$ = 14.2, $^3J_{H-H}$ = 9.3, 4.6 Hz, 1H), 2.26 – 2.13 (m, 7H), 2.12 – 2.09 (m, 3H), 2.00 (ddd, $^2J_{H-H}$ = 14.2, $^3J_{H-H}$ = 9.3, 4.9 Hz, 2H), 1.91 – 1.72 (m, 2H), 1.71 – 1.60 (m, 1H), 1.57 – 1.50 (m, 5H), 1.48 – 1.44 (m, 11H), 1.32 – 1.21 (m, 13H), 1.02 – 0.84 (m, 35H); ^{13}C NMR (125 MHz, CDCl$_3$): 171.8 (C), 171.1 (C), 171.0 (C), 169.5 (C), 169.2 (C), 168.9 (C), 168.8 (C), 164.0 (C), 162.9 (C), 162.3 (C), 162.0 (C), 155.3 (C), 146.4 (C), 145.7 (C), 129.7 (CH), 129.0 (CH), 125.5 (C), 125.4 (C), 123.8 (C), 122.7 (C), 121.8 (C), 119.7 (C), 81.1 (C), 60.6 (CH$_2$), 56.8 (CH), 54.2 (CH), 54.1 (CH), 52.7 (CH), 51.8 (CH), 50.5 (CH), 48.9 (CH), 44.6 (2xCH$_3$), 42.7 (CH$_2$), 41.7 (CH$_2$), 41.5 (2xCH$_2$), 40.1 (CH$_2$), 40.0 (CH$_2$), 38.1 (CH$_2$), 38.0 (CH$_2$), 33.1 (CH$_2$), 31.5 (CH$_2$), 31.4 (CH$_2$), 29.7 (CH$_2$), 29.5 (CH$_2$), 28.3 (3xCH$_3$), 26.8 (CH$_2$), 26.6 (CH$_2$), 25.9 (CH), 25.6 (CH), 25.1 (CH), 24.4 (CH), 23.23 (CH$_3$), 23.18 (CH$_3$), 23.14 (CH$_3$), 23.09 (CH$_3$), 22.69 (CH$_2$), 22.65 (CH$_2$), 22.6 (CH$_2$), 22.2 (CH$_3$), 22.1 (CH$_3$), 21.7 (CH$_3$), 21.6 (CH$_3$), 14.08 (CH$_3$),

14.06 (CH$_3$), 11.3 (CH$_3$); HPLC–MS: R_t -= 2.78 min (**160b**), 1363 (100, [M+H]$^+$), R_t = 2.81 min (**160a**), 1363 (100, [M+H]$^+$); HRMS (ESI, +ve) calcd for C$_{69}$H$_{107}$N$_{11}$O$_{13}$S$_2$ ([M+H]$^+$): 1362.7565, found: 1362.7565.
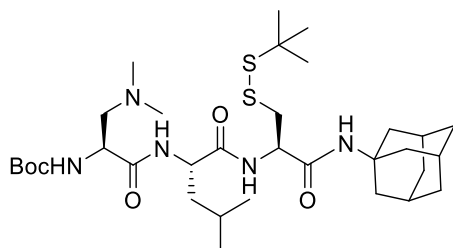
Compound 288 (476 mg, 62%, colorless solid) was prepared from **277** (635 mg, 1.14 mmol) and **277** (318 mg, 1.37 mmol) following the general procedures A and D. R_f (CH$_2$Cl$_2$/MeOH 15:1): 0.30; Mp: 87 – 88 °C; [α]$_D^{20}$ –76.0 (c 1.00, CHCl$_3$); IR (neat): 3304 (w), 2908 (w), 1636 (s), 1529 (m), 1390 (w), 1363 (m), 1246 (w), 1166 (s), 1099 (w), 1050 (w), 1017 (w), 909 (w), 865 (w), 731 (s), 647 (m); ^{1}H NMR (300 MHz, CDCl$_3$): 8.19 (br s, 1H), 7.08 (d, $^3J_{H-H}$ = 8.2 Hz, 1H), 6.10 (s, 1H), 5.54 (br s, 1H), 4.65 – 4.48 (m, 1H), 4.39 – 4.25 (m, 1H), 4.11 – 3.94 (m, 1H), 3.20 – 2.93 (m, 2H), 2.70 – 2.47 (m, 2H), 2.32 (s, 6H), 2.11 – 2.02 (m, 3H), 1.99 (d, $^3J_{H-H}$ = 2.9 Hz, 6H), 1.76 – 1.50 (m, 9H), 1.44 (s, 9H), 1.32 (s, 9H), 1.00 – 0.83 (m, 6H); ^{13}C NMR (100 MHz, CDCl$_3$): 171.9 (C), 171.8 (C), 168.7 (C), 156.2 (C), 80.4 (C), 60.4 (CH$_2$), 52.8 (CH), 52.6 (CH), 52.3 (C), 51.5 (CH), 48.3 (C), 45.1 (2xCH$_3$), 41.9 (CH$_2$), 41.3 (3xCH$_2$), 40.2 (CH$_2$), 36.3 (3xCH$_2$), 29.9 (CH), 29.4 (3xCH$_3$), 28.4 (3xCH$_3$), 25.1 (CH), 23.1 (CH$_3$), 21.8 (CH$_3$); MS (ESI, MeOH): 670 (100, [M+H]$^+$).
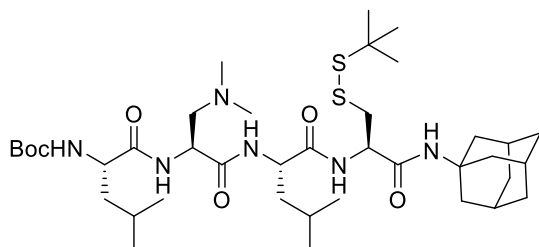
Compound 289 (328 mg, 59%, colorless solid) was prepared from **288** (476 mg, 0.710 mmol) and Boc–L–Leu–OH (197 mg, 0.852 mmol) following the general procedures A and D. R_f (CH$_2$Cl$_2$/MeOH 15:1): 0.36; Mp: 197 – 198 °C (decomp); [α]$_D^{20}$ –97.0 (c 1.00, CHCl$_3$); IR (neat): 3275 (w), 3084 (w), 2911 (w), 1720 (w), 1631 (s), 1529 (m), 1455 (w), 1389

(w), 1363 (m), 1311 (w), 1274 (w), 1247 (w), 1165 (s), 1101 (w), 1044 (w), 919 (w), 871 (w), 655 (m); ^{1}H NMR (300 MHz, CDCl$_3$): 7.65 (d, $^3J_{H-H}$ = 7.1 Hz, 1H), 7.40 – 7.30 (m, 2H), 6.22 (s, 1H), 4.95 (d, $^3J_{H-H}$ = 4.3 Hz, 1H), 4.63 – 4.51 (m, 1H), 4.42 – 4.29 (m, 1H), 4.19 – 3.98 (m, 2H), 3.28 (dd, $^2J_{H-H}$ = 13.5 Hz, $^3J_{H-H}$ = 4.3 Hz, 1H), 3.05 (dd, $^2J_{H-H}$ = 13.5 Hz, $^3J_{H-H}$ = 10.0 Hz, 1H), 2.75 – 2.56 (m, 2H), 2.25 (s, 6H), 2.11 – 1.93 (m, 9H), 1.84 – 1.55 (m, 12H), 1.45 (s, 9H), 1.31 (s, 9H), 1.08 – 0.79 (m, 12H); ^{13}C NMR (75 MHz, CDCl$_3$): 173.9 (C), 172.4 (C), 171.6 (C), 169.3 (C), 156.1 (C), 80.8 (C), 59.1 (CH$_2$), 54.5 (CH), 53.2 (CH), 52.9 (CH), 52.5 (CH), 52.1 (C), 47.9 (C), 45.3 (2xCH$_3$), 41.8 (CH$_2$), 41.2 (3xCH$_2$), 40.7 (CH$_2$), 39.8 (CH$_2$), 36.4 (3xCH$_2$), 30.0 (CH), 29.5 (3xCH$_3$), 28.2 (3xCH$_3$), 24.95 (CH), 24.91 (CH), 23.2 (CH$_3$), 23.0 (CH$_3$), 21.7 (CH$_3$), 21.0 (CH$_3$); MS (ESI, MeOH): 783 (100, [M+H]$^+$).
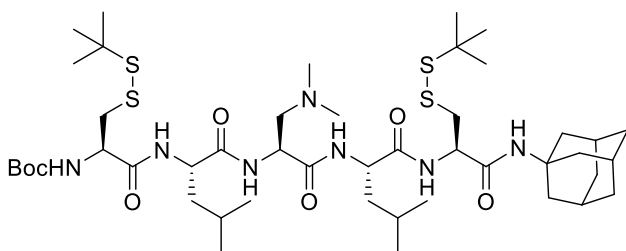
Compound 191 (178 mg, 44%, colorless solid) was prepared from **289** (328 mg, 0.419 mmol) and **271** (155 mg, 0.501 mmol) following the general procedures A and D. R_f (CH$_2$Cl$_2$/MeOH 15:1): 0.43; Mp: 213 – 214 °C (decomp); $[\alpha]_D^{20}$ –64.5 (c 1.00, CHCl$_3$); IR (neat): 3276 (w), 3089 (w), 2910 (w), 1720 (w), 1630 (s), 1531 (s), 1455 (m), 1390 (w), 1362 (m), 1311 (w), 1273 (w), 1248 (w), 1164 (s), 1101 (w), 1046 (w), 909 (w), 872 (w), 779 (w), 731 (s), 645 (m); ^{1}H NMR (300 MHz, CDCl$_3$): 7.54 (d, $^3J_{H-H}$ = 7.0 Hz, 1H), 7.31 (d, $^3J_{H-H}$ = 7.9 Hz, 1H), 7.23 (d, $^3J_{H-H}$ = 4.3 Hz, 1H), 6.84 (s, 1H), 6.26 (s, 1H), 5.24 (d, $^3J_{H-H}$ = 7.1 Hz, 1H), 4.62 – 4.50 (m, 1H), 4.50 – 4.37 (m, 1H), 4.36 – 4.27 (m, 1H), 4.26 – 4.09 (m, 2H), 3.32 (dd, $^2J_{H-H}$ = 13.4 Hz, $^3J_{H-H}$ = 4.1 Hz, 1H), 3.16 – 2.91 (m, 3H), 2.73 – 2.57 (m, 2H), 2.23 (s, 6H), 2.08 – 1.93 (m, 9H), 1.93 – 1.81 (m, 2H), 1.79 – 1.58 (m, 11H), 1.46 (s, 9H), 1.38 – 1.26 (m, 18H), 1.07 – 0.80 (m, 12H); ^{13}C NMR (75 MHz, CDCl$_3$): 173.0 (C), 172.6 (C), 171.8 (C), 171.5 (C), 169.4 (C), 155.8 (C), 81.2 (C), 58.9 (CH$_2$), 54.3 (CH), 54.0 (CH), 53.3

(CH), 53.0 (2xCH), 52.1 (C), 48.8 (C), 47.9 (C), 45.1 (2xCH$_3$), 41.8 (CH$_2$), 41.1 (3xCH$_2$), 40.4 (CH$_2$), 40.2 (CH$_2$), 39.6 (CH$_2$), 36.4 (3xCH$_2$), 30.0 (CH), 29.8 (3xCH$_3$), 29.5 (3xCH$_3$), 28.2 (3xCH$_3$), 25.1 (CH), 24.9 (CH), 23.5 (CH$_3$), 23.0 (CH$_3$), 21.6 (CH$_3$), 20.9 (CH$_3$); MS (ESI, MeOH): 974 (100, [M+H]$^+$).
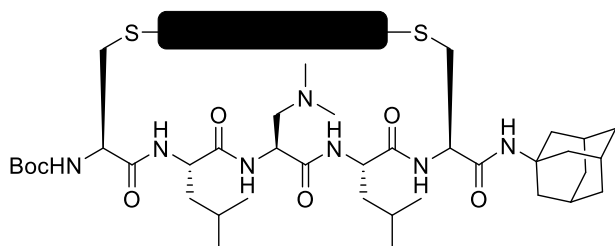
Compound 163 (36 mg, 15%, atropisomers not detectable, red solid) was prepared from **191** (150 mg, 0.154 mmol) following the general procedures

F and G. R_f (CH$_2$Cl$_2$/MeOH 15:1): 0.19; Mp: 193 – 194 ºC; UV-Vis (TFE): 523 (15.3), 372 (11.7), 296 (35.0); CD (TFE): 531 (–10.2), 376 (+12.7), 319 (–4.3), 299 (+5.1), 244 (–0.9), 207 (+41.4); IR (neat): 3324 (w), 2925 (m), 2869 (w), 1653 (s), 1527 (m), 1439 (m), 1366 (m), 1313 (m), 1237 (m), 1214 (m), 1162 (m), 1031 (w), 908 (w), 852 (w), 791 (w), 731 (w), 632 (w); ^{1}H NMR (400 MHz, CDCl$_3$): 8.94 (s, 1H), 8.91 – 8.77 (m, 1H), 8.62 (s, 1H), 6.98 (s, 1H), 6.79 – 6.61 (m, 2H), 6.09 (d, $^3J_{H–H}$ = 6.7 Hz, 1H), 5.93 (s, 1H), 5.86 – 5.74 (m, 1H), 5.73 – 5.60 (m, 2H), 5.50 (d, $^3J_{H–H}$ = 7.4 Hz, 1H), 4.86 – 4.73 (m, 1H), 4.54 – 4.34 (m, 2H), 4.24 – 4.14 (m, 1H), 4.08 – 3.94 (m, 2H), 3.74 – 3.61 (m, 1H), 3.55 – 3.45 (m, 1H), 3.37 – 3.17 (m, 3H), 3.15 – 2.99 (m, 1H), 2.99 – 2.86 (m, 1H), 2.82 – 2.60 (m, 2H), 2.44 – 2.34 (m, 1H), 2.24 – 2.08 (m, 8H), 2.03 – 1.88 (m, 8H), 1.80 – 1.62 (m, 6H), 1.58 – 1.35 (m, 18H), 1.35 – 1.14 (m, 16H), 1.10 – 0.72 (m, 30H); ^{13}C NMR (125 MHz, CDCl$_3$): 171.7 (C), 171.0 (C), 170.9 (C), 169.1 (C), 169.0 (C), 168.8 (C), 168.4 (C), 164.0 (C), 162.9 (C), 162.3 (C), 162.1 (C), 155.2 (C), 146.6 (C), 145.7 (C), 129.6 (CH), 129.0 (CH), 125.5 (C), 125.4 (C), 123.8 (C), 122.6 (C), 121.7 (C), 119.6 (C), 81.1 (C), 60.6 (CH$_2$), 57.4 (CH), 54.2 (CH), 54.0 (CH), 52.7 (2xCH), 51.9 (CH), 50.4 (CH), 48.8 (C), 44.5 (2xCH$_3$), 42.9 (CH$_2$), 41.7 (CH$_2$), 41.5 (CH$_2$), 40.2 (CH$_2$), 40.0 (CH$_2$), 38.1 (CH$_2$), 38.0 (CH$_2$), 36.2 (CH$_2$), 33.2 (CH$_2$), 31.5 (CH$_2$), 31.4 (CH$_2$), 29.7

(CH$_2$), 29.4 (CH$_2$), 29.3 (CH), 28.3 (3xCH$_3$), 26.8 (CH$_2$), 26.6 (CH$_2$), 25.9 (CH), 25.6 (CH),

25.1 (CH), 24.4 (CH), 23.3 (CH$_3$), 23.2 (CH$_3$), 23.14 (CH$_3$), 23.08 (CH$_3$), 22.7 (CH$_2$), 22.6

(CH$_2$), 22.2 (CH$_3$), 22.1 (CH$_3$), 21.7 (CH$_3$), 21.6 (CH$_3$), 14.1 (2xCH$_3$); HPLC–MS: R_t = 3.31

min, 1453 (100, [M+H]$^+$); HRMS (ESI, +ve) calcd for C$_{76}$H$_{115}$N$_{11}$O$_{13}$S$_2$ ([M+H]$^+$): 1454.8191,

found: 1454.8213.
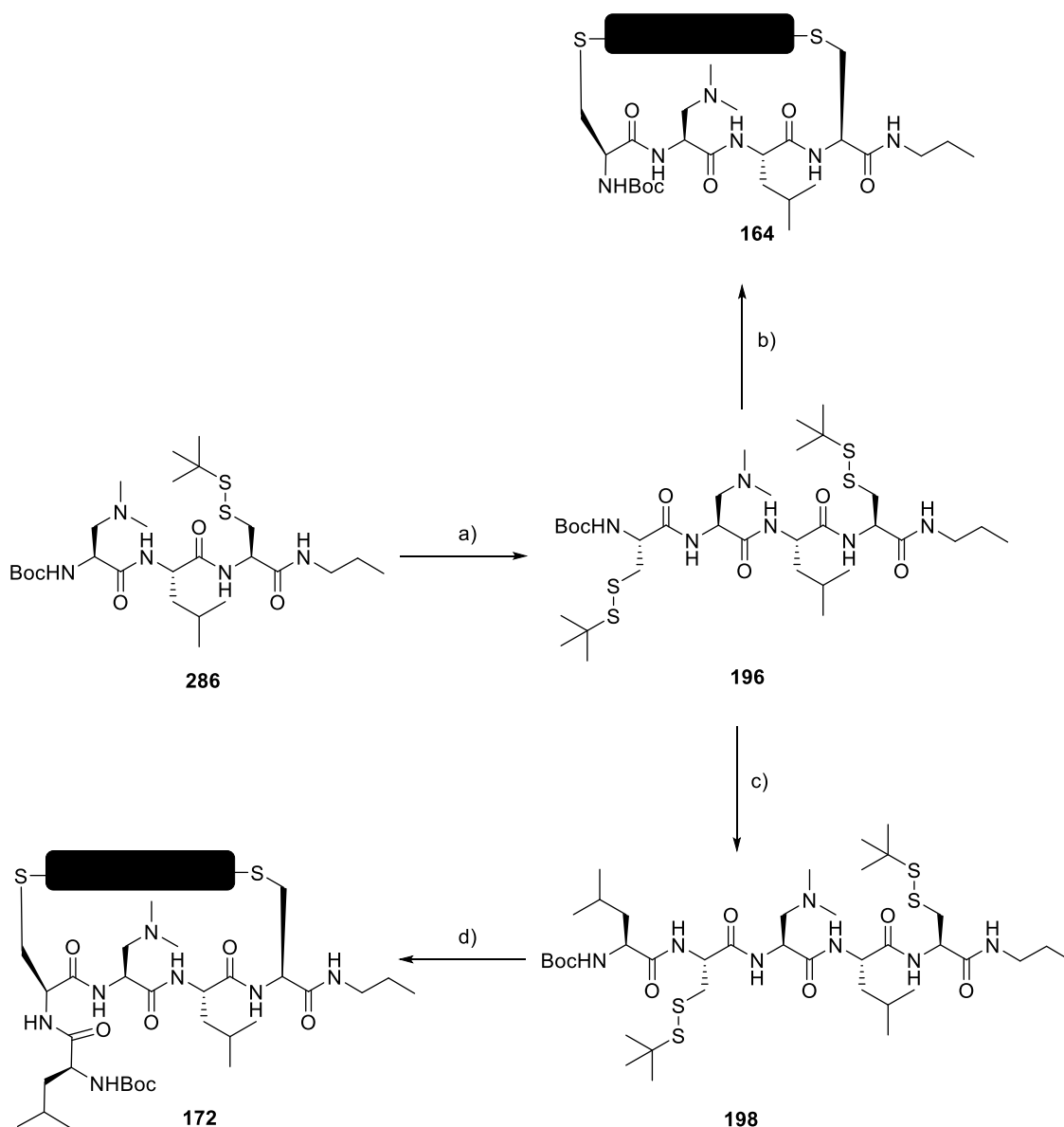
Scheme 15. (a) 1. TFA/CH$_2$Cl$_2$ 1:1, rt, 1 h; 2. **271**, EDC, DMAP, DIPEA, CH$_2$Cl$_2$, rt, overnight,

69%; (b) 1. PBu$_3$, TEA, H$_2$O, TFE, rt, overnight; 2. **152**, TCEP·HCl, CH$_3$CN/buffer 3:1, 65 °C,

overnight, 3%; (c) 1. TFA/CH$_2$Cl$_2$ 1:1, rt, 1 h; 2. Boc–L–Leu–OH, EDC, DMAP, DIPEA, CH$_2$Cl$_2$, rt, overnight, 75%; (d) 1. PBu$_3$, TEA, H$_2$O, TFE, rt, overnight; 2. **152**, TCEP·HCl, CH$_3$CN/buffer 3:1, 65 °C, overnight, 3%.
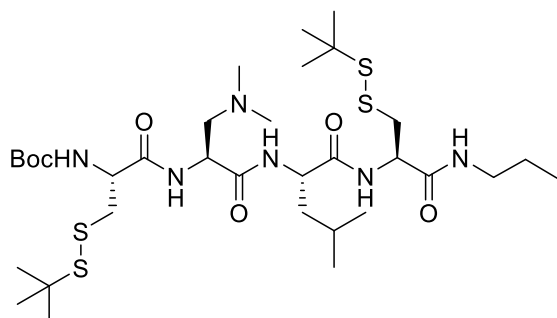
Compound 196 (0.9 g, 69%, colorless solid) was prepared from **286** (1.0 g, 1.7 mmol) and **271** (0.67 g, 2.2 mmol) following the general procedures A and D. R_f (CH$_2$Cl$_2$/MeOH 15:1): 0.35; Mp: 201 – 202 °C (decomp); [α]$_D^{20}$ –65.5 (c 1.00, CHCl$_3$); IR (neat): 3272 (w), 2964 (w), 1630 (s), 1533 (m), 1390 (w), 1362 (m), 1250 (m), 1163 (m), 1045 (w), 872 (w), 776 (w), 700 (w); ^{1}H NMR (400 MHz, CDCl$_3$): 7.53 (br s, 1H), 7.43 (d, $^3J_{H-H}$ = 6.5 Hz, 1H), 7.33 (d, $^3J_{H-H}$ = 8.1 Hz, 1H), 6.74 (s, 1H), 5.41 (d, $^3J_{H-H}$ = 5.8 Hz, 1H), 4.74 – 4.63 (m, 1H), 4.51 – 4.42 (m, 1H), 4.33 – 4.23 (m, 1H), 4.14 – 4.05 (m, 1H), 3.47 – 2.99 (m, 6H), 2.80 – 2.55 (m, 2H), 2.27 (s, 6H), 1.89 – 1.60 (m, 3H), 1.60 – 1.51 (m, 2H), 1.46 (s, 9H), 1.38 – 1.31 (m, 18H), 0.99 – 0.83 (m, 9H); ^{13}C NMR (100 MHz, CDCl$_3$): 172.3 (C), 172.2 (C), 171.7 (C), 170.2 (C), 155.7 (C), 81.1 (C), 58.8 (CH$_2$), 54.4 (CH), 53.4 (CH), 53.3 (CH), 52.7 (CH), 49.1 (C), 48.0 (C), 45.2 (2xCH$_3$), 41.7 (CH$_2$), 41.4 (CH$_2$), 40.2 (CH$_2$), 39.7 (CH$_2$), 30.0 (3xCH$_3$), 29.9 (3xCH$_3$), 28.2 (3xCH$_3$), 25.0 (CH), 23.2 (CH$_3$), 22.5 (CH$_2$), 20.8 (CH$_3$), 11.4 (CH$_3$); MS (ESI, MeOH): 769 (100, [M+H]+).
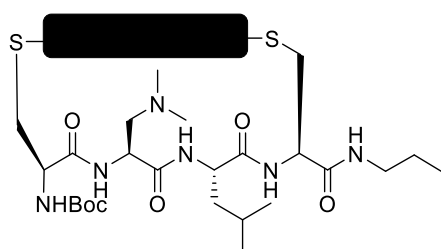
Compound 164 (7 mg, 3%, atropisomers not detectable, red solid) was prepared from **196** (150 mg, 0.195 mmol) following the general procedures F and G. R_f (CH$_2$Cl$_2$/MeOH 15:1): 0.28; Mp: 204 – 205 °C; UV-Vis (TFE): 515 (11.9), 376 (12.7), 298 (26.5); CD (TFE): 525 (–8.4), 378 (+9.3), 316 (–

2.2), 298 (+3.7), 259 (–2.1), 236 (+4.5), 208 (+26.5); IR (neat): 3300 (w), 2957 (w), 2931 (w), 2870 (w), 1652 (s), 1528 (m), 1464 (m), 1439 (m), 1367 (m), 1314 (m), 1215 (s), 1157 (m), 1046 (w), 905 (w), 850 (w), 789 (w), 730 (w); ^{1}H NMR (400 MHz, CDCl$_3$): 9.26 (d, $^3J_{H-H}$ = 8.1 Hz, 1H), 8.90 (s, 1H), 8.79 (s, 1H), 6.93 (br s, 1H), 6.44 (d, $^3J_{H-H}$ = 9.2 Hz, 1H), 6.11 – 6.03 (m, 1H), 5.98 (br s, 1H), 5.80 – 5.62 (m, 3H), 5.50 (s, 1H), 4.88 – 4.75 (m, 1H), 4.49 – 4.25 (m, 1H), 4.13 – 3.99 (m, 1H), 3.94 – 3.82 (m, 2H), 3.81 – 3.68 (m, 1H), 3.39 – 3.09 (m, 8H), 3.06 – 2.95 (m, 1H), 2.38 – 2.30 (m, 1H), 2.27 – 2.18 (m, 2H), 2.17 – 2.01 (m, 8H), 1.97 – 1.89 (m, 2H), 1.59 – 1.52 (m, 5H), 1.47 – 1.40 (m, 11H), 1.33 – 1.25 (m, 14H), 1.01 – 0.86 (m, 27H); ^{13}C NMR (100 MHz, CDCl$_3$): 171.6 (C), 170.2 (C), 169.4 (C), 169.2 (C), 169.1 (C), 169.0 (C), 164.0 (C), 162.8 (C), 162.2 (C), 162.0 (C), 143.5 (C), 133.3 (2xC), 129.8 (2xCH), 126.4 (C), 125.75 (C), 125.66 (C), 123.7 (C), 123.3 (C), 120.3 (C), 80.8 (C), 58.6 (CH$_2$), 56.5 (CH), 54.2 (CH), 54.1 (CH), 51.25 (CH), 51.21 (CH), 49.1 (CH), 44.6 (2xCH$_3$), 41.6 (CH$_2$), 40.1 (CH$_2$), 40.0 (CH$_2$), 38.2 (CH$_2$), 37.9 (CH$_2$), 35.6 (CH$_2$), 33.2 (CH$_2$), 31.6 (CH$_2$), 31.5 (CH$_2$), 29.8 (CH$_2$), 29.4 (CH$_2$), 28.3 (3xCH$_3$), 26.8 (CH$_2$), 26.6 (2xCH$_2$), 25.9 (CH), 25.7 (CH), 25.0 (CH), 23.25 (CH$_3$), 23.24 (CH$_3$), 22.8 (CH$_3$), 22.7 (CH$_2$), 22.57 (CH$_2$), 22.56 (CH$_2$), 22.2 (CH$_3$), 22.1 (CH$_3$), 22.0 (CH$_3$), 14.1 (CH$_3$), 14.0 (CH$_3$), 11.30 (CH$_3$); HPLC–MS: R_t = 2.72 min, 1250 (100, [M+H]$^+$); HRMS (ESI, +ve) calcd for C$_{63}$H$_{96}$N$_{10}$O$_{12}$S$_2$ ([M+H]$^+$): 1249.6724, found: 1249.6733.
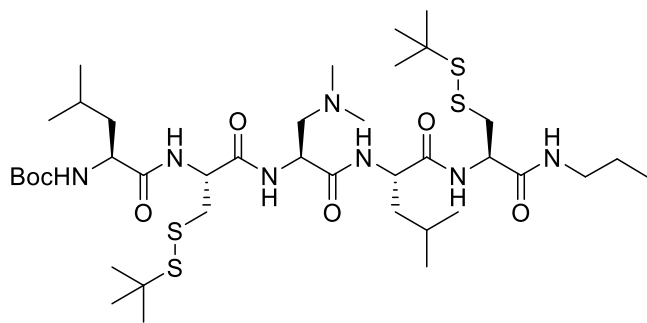
Compound 198 (680 mg, 75%, colorless solid) was prepared from **196** (789 mg, 1.03 mmol) and Boc–L–Leu–OH (285 mg, 1.23 mmol) following the general procedures A and D. R_f (CH$_2$Cl$_2$/MeOH 15:1): 0.38; Mp: 216 – 217 °C (decomp); [α]$_D^{20}$ –78.3 (c 1.00,

DMSO); IR (neat): 3275 (w), 3095 (w), 2961 (w), 1725 (w), 1692 (w), 1630 (s), 1532 (m), 1457 (w), 1363 (m), 1252 (w), 1166 (m), 1045 (w), 1016 (w), 873 (w), 777 (w), 701 (m); ^{1}H NMR (400 MHz, CDCl$_3$): 7.70 – 7.50 (m, 2H), 7.37 – 7.29 (m, 2H), 6.82 (s, 1H), 4.94 (d, $^3J_{H-H}$ = 5.3 Hz, 1H), 4.76 – 4.59 (m, 2H), 4.38 – 4.12 (m, 2H), 4.10 – 4.03 (m, 1H), 3.54 – 3.34 (m, 1H), 3.29 – 3.03 (m, 5H), 2.80 – 2.67 (m, 1H), 2.32 (s, 6H), 1.95 – 1.65 (m, 7H), 1.61 – 1.54 (m, 2H), 1.49 (s, 9H), 1.38 (s, 9H), 1.35 (s, 9H), 1.01 – 0.90 (m, 15H); ^{13}C NMR (100 MHz, CDCl$_3$): 173.9 (2xC), 172.5 (C), 171.7 (C), 170.3 (C), 156.2 (C), 81.1 (C), 58.5 (CH$_2$), 54.5 (CH), 54.0 (CH), 53.6 (CH), 52.8 (2xCH), 49.1 (C), 48.0 (C), 45.1 (2xCH$_3$), 41.6 (CH$_2$), 41.5 (CH$_2$), 40.7 (CH$_2$), 39.8 (CH$_2$), 39.5 (CH$_2$), 30.0 (3xCH$_3$), 29.9 (3xCH$_3$), 28.3 (3xCH$_3$), 25.0 (CH), 24.9 (CH), 23.3 (CH$_3$), 23.0 (CH$_3$), 22.5 (CH$_2$), 21.7 (CH$_3$), 20.9 (CH$_3$), 11.4 (CH$_3$); MS (ESI, MeOH): 882 (100, [M+H]$^+$).
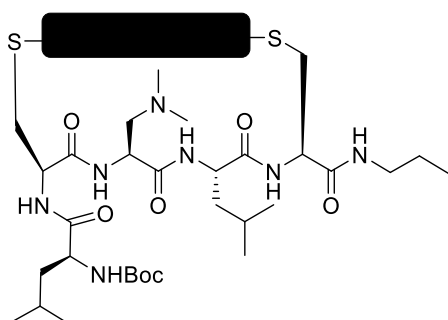
Compound 172 (18 mg, 8%, atropisomers not detectable, red solid) was prepared from **198** (150 mg, 0.170 mmol) following the general procedures F and G. R_f (CH$_2$Cl$_2$/MeOH 15:1): 0.31; Mp: 151 – 152 ^{o}C (decomp); UV-Vis (TFE): 519 (11.2), 377 (11.8), 298 (24.1); CD (TFE): 526 (–13.6), 381 (+11.9), 314 (–5.0), 283 (+2.0), 229 (–5.0), 209 (+24.8); IR (neat): 3320 (w), 2957 (w), 2932 (w), 2871 (w), 1651 (s), 1534 (m), 1438 (m), 1367 (m), 1314 (m), 1240 (m), 1213 (m), 1163 (m), 1026 (w), 907 (w), 849 (w), 792 (w); ^{1}H NMR (400 MHz, CDCl$_3$): 9.42 (d, $^3J_{H-H}$ = 7.7 Hz, 1H), 8.86 (s, 1H), 8.82 (s, 1H), 6.83 (d, $^3J_{H-H}$ = 8.0 Hz, 1H), 6.53 (br s, 1H), 6.36 (d, $^3J_{H-H}$ = 9.1 Hz, 1H), 6.24 (t, $^3J_{H-H}$ = 5.9 Hz, 1H), 5.97 (t, $^3J_{H-H}$ = 5.7 Hz, 1H), 5.80 – 5.73 (m, 1H), 5.69 – 5.60 (m, 1H), 5.42 (d, $^3J_{H-H}$ = 6.6 Hz, 1H), 5.00 (s, 1H), 4.76 – 4.66 (m, 1H), 4.61 – 4.48 (m, 1H), 4.08 – 3.97 (m, 3H), 3.92 – 3.80 (m, 2H), 3.37 – 3.09 (m, 7H), 3.00 – 2.90 (m, 1H), 2.35 – 2.29 (m, 2H), 2.24 – 2.15 (m, 9H), 2.00 – 1.89

(m, 1H), 1.63 – 1.49 (m, 8H), 1.47 – 1.42 (m, 11H), 1.36 – 1.24 (m, 16H), 0.99 – 0.86 (m, 33H); ^{13}C NMR (100 MHz, CDCl$_3$): 172.2 (C), 172.0 (C), 170.5 (C), 169.8 (C), 169.3 (C), 169.1 (C), 168.0 (C), 164.2 (C), 162.7 (C), 162.4 (C), 162.3 (C), 155.5 (C), 145.3 (C), 143.4 (C), 131.9 (CH), 130.1 (CH), 126.6 (C), 126.2 (C), 125.6 (C), 123.63 (C), 123.57 (C). 121.0 (C), 80.1 (C), 58.8 (CH$_2$), 56.8 (CH), 54.1 (CH), 54.0 (CH), 53.1 (CH), 52.3 (CH), 51.3 (CH), 48.5 (CH), 44.5 (2xCH$_3$), 41.7 (CH$_2$), 41.5 (CH$_2$), 41.0 (CH$_2$), 40.2 (CH$_2$), 40.0 (CH$_2$), 38.1 (CH$_2$), 37.8 (CH$_2$), 33.8 (CH$_2$), 32.8 (CH$_2$), 31.6 (CH$_2$), 31.5 (CH$_2$), 29.8 (CH$_2$), 29.4 (CH$_2$), 28.4 (3xCH$_3$), 26.8 (CH$_2$), 26.6 (CH$_2$), 25.9 (CH), 25.7 (CH), 25.1 (CH), 24.7 (CH), 23.33 (CH$_3$), 23.29 (CH$_3$), 23.0 (CH$_3$), 22.9 (CH$_3$), 22.7 (CH$_2$), 22.61 (CH$_2$), 22.57 (CH$_2$), 22.2 (CH$_3$), 22.0 (CH$_3$), 21.9 (CH$_3$), 21.7 (CH$_3$), 14.1 (CH$_3$), 14.0 (CH$_3$), 11.3 (CH$_3$); HPLC–MS: R_t = 2.81 min, 1363 (100, [M+H]$^+$); HRMS (ESI, +ve) calcd for C$_{69}$H$_{107}$N$_{11}$O$_{13}$S$_2$ ([M+H]$^+$): 1362.7565, found: 1362.7565.
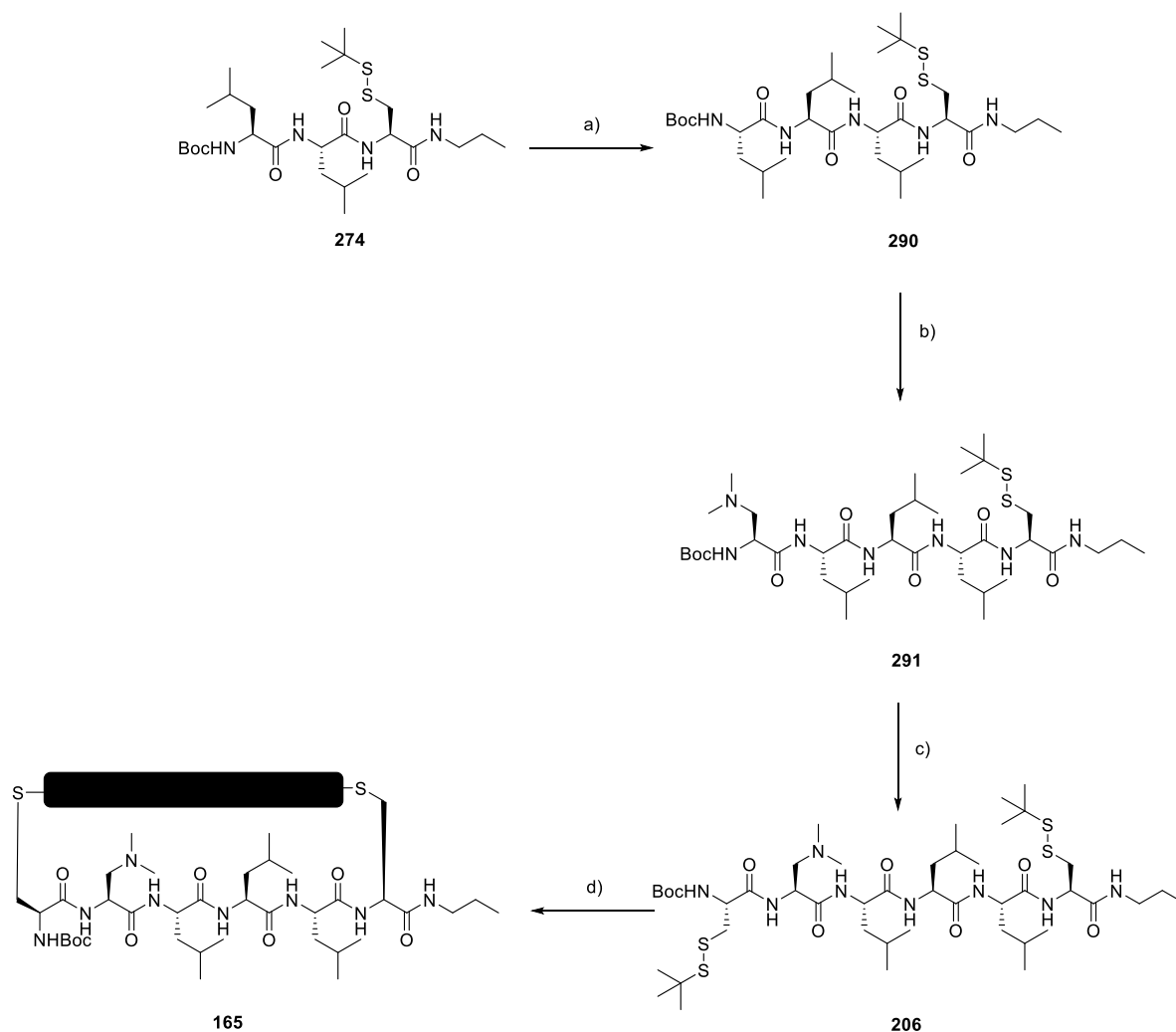
Scheme 16. (a) 1. TFA/CH$_2$Cl$_2$ 1:1, rt, 1 h; 2. Boc–L–Leu–OH, EDC, DMAP, DIPEA, CH$_2$Cl$_2$, rt, overnight, 80%; (b) 1. TFA/CH$_2$Cl$_2$ 1:1, rt, 1 h; 2. **270**, EDC, DMAP, DIPEA, CH$_2$Cl$_2$, rt, overnight, 27%; (c) 1. TFA/CH$_2$Cl$_2$ 1:1, rt, 1 h; 2. **271**, EDC, DMAP, DIPEA, CH$_2$Cl$_2$, rt, overnight, 34%; (d) 1. PBu$_3$, TEA, H$_2$O, TFE, rt, overnight; 2. **152**, TCEP·HCl, CH$_3$CN/buffer 3:1, 65 °C, overnight, 10%.
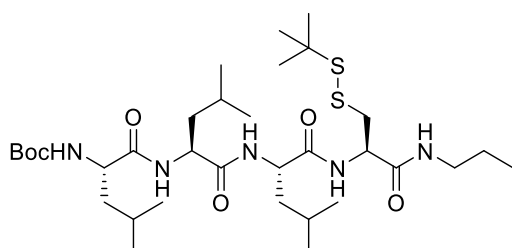
Compound 290 (267 mg, 80%, colorless solid) was prepared from **274** (278 mg, 0.482 mmol) and Boc–L–Leu–OH (134 mg, 0.579 mmol) following the general procedures A and D. R_f

(CH$_2$Cl$_2$/MeOH 15:1): 0.47; Mp: 239 – 240 °C; IR (neat): 3265 (w); 3077 (w), 2959 (w), 1720 (w), 1687 (w), 1628 (s), 1534 (m), 1468 (w), 1388 (w), 1365 (m), 1250 (m), 1166 (m), 1045 (w), 1019 (w), 874 (w), 779 (w), 698 (m), 649 (m); ^{1}H NMR (300 MHz, CDCl$_3$): 7.22 (br s, 1H), 7.16 (d, $^3J_{H-H}$ = 6.4 Hz, 1H), 6.81 (br s, 1H), 6.55 (d, $^3J_{H-H}$ = 5.0 Hz, 1H), 4.88 (s, 1H), 4.78 – 4.64 (m, 1H), 4.39 – 3.95 (m, 3H), 3.51 – 3.02 (m, 4H), 1.89 – 1.42 (m, 20H), 1.32 (s, 9H), 1.06 – 0.79 (m, 21H); MS (ESI, MeOH): 690 (100, [M+H]$^+$).
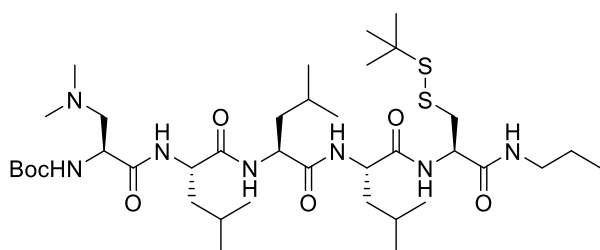
Compound 291 (0.5 g, 27%, colorless solid) was prepared from **290** (1.7 g, 2.5 mmol) and **270** (1.1 g, 4.7 mmol) following the general procedures A and D. R_f (CH$_2$Cl$_2$/MeOH 15:1): 0.36; Mp: 237 – 238 °C (decomp); [α]$_D^{20}$ –69.1 (*c* 0.50, DMSO); IR (neat): 3259 (w), 3088 (w), 2958 (w), 2933 (w), 2871 (w), 2823 (w), 2774 (w), 1717 (w), 1691 (w), 1628 (s), 1546 (m), 1490 (m), 1458 (m), 1388 (w), 1364 (m), 1279 (w), 1247 (w), 1218 (w), 1167 (m), 1049 (w), 1020 (w), 942 (w), 869 (w), 784 (w), 714 (m), 638 (w); ^{1}H NMR (400 MHz, DMSO–d_6): 8.14 (d, $^3J_{H-H}$ = 7.9 Hz, 1H), 8.09 – 7.95 (m, 1H), 7.94 – 7.81 (m, 3H), 6.81 (d, $^3J_{H-H}$ = 7.6 Hz, 1H), 4.44 – 4.17 (m, 4H), 4.11 – 4.01 (m, 1H), 3.12 – 2.90 (m, 4H), 2.48 – 2.40 (m, 1H), 2.36 – 2.28 (m, 1H), 2.16 (s, 6H), 1.74 – 1.52 (m, 3H), 1.48 – 1.36 (m, 17H), 1.28 (s, 9H), 0.89 – 0.81 (m, 21H); ^{13}C NMR (100 MHz, DMSO–d_6): 172.3 (2xC), 172.2 (C), 171.7 (C), 169.5 (C), 155.6 (C), 78.6 (C), 60.9 (CH$_2$), 52.9 (CH), 52.8 (CH), 51.8 (CH), 51.3 (2xCH), 48.1 (C), 45.7 (2xCH$_3$), 42.7 (CH$_2$), 41.2 (CH$_2$), 40.9 (3xCH$_2$), 30.0 (3xCH$_3$), 28.6 (3xCH$_3$), 24.51 (2xCH), 21.48 (CH), 23.6 (CH$_3$), 23.5 (2xCH$_3$), 22.6 (CH$_2$), 22.1 (3xCH$_3$), 11.8 (CH$_3$); MS (ESI, MeOH): 804 (100, [M+H]$^+$).
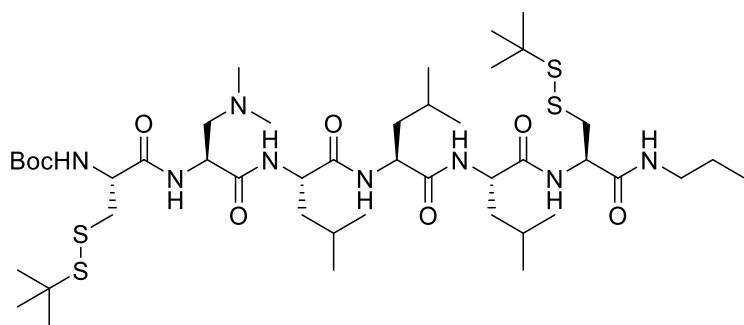
Compound 206 (224 mg, 34%, colorless solid) was prepared from **291** (532 mg, 0.662 mmol) and **270** (246 mg, 0.795 mmol) following the general procedures A and D. R_f (CH$_2$Cl$_2$/MeOH 15:1): 0.35; Mp: 233 – 234 °C (decomp); IR (neat): 3266 (w), 3093 (w), 2959 (w), 2872 (w), 1719 (w), 1691 (w), 1628 (s), 1534 (s), 1469 (m), 1388 (m), 1364 (m), 1250 (m), 1219 (m), 1164 (s), 1046 (w), 1022 (w), 914 (w), 872 (w), 781 (w), 712 (m), 643 (m); ^{1}H NMR (400 MHz, CDCl$_3$): 7.64 (br s, 1H), 7.52 (s, 1H), 7.42 (br s, 1H), 7.31 (s, 1H), 7.27 (s, 1H), 6.95 (t, $^3J_{H-H}$ = 5.6 Hz, 1H), 5.54 (br s, 1H), 4.76 – 4.62 (m, 1H), 4.42 – 4.28 (m, 1H), 4.28 – 4.19 (m, 2H), 4.18 – 4.01 (m, 2H), 3.45 (dd, $^2J_{H-H}$ = 13.5 Hz, $^3J_{H-H}$ = 3.6 Hz, 1H), 3.29 – 3.05 (m, 4H), 3.02 – 2.88 (m, 1H), 2.84 – 2.4 (m, 2H), 2.28 (s, 6H), 2.10 – 1.44 (m, 18H), 1.44 – 1.17 (m, 20H), 1.13 – 0.67 (m, 21H); MS (ESI, MeOH): 995 (100, [M+H]$^+$).
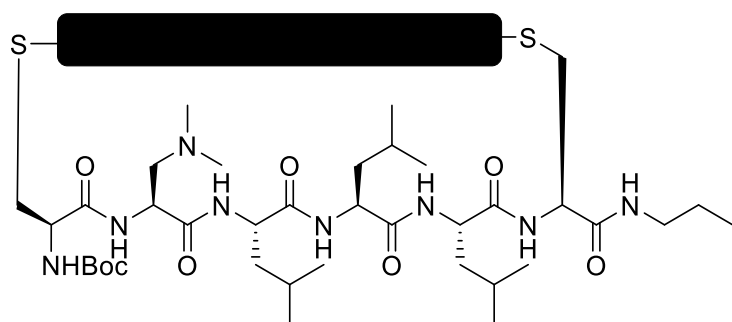
Compound 165 (21 mg, 10%, atropisomers not detectable, red solid) was prepared from **206** (150 mg, 0.151 mmol) following the general procedures F and G. R_f (CH$_2$Cl$_2$/MeOH 15:1): 0.26; Mp: 183 – 184 °C; UV-Vis (TFE): 517 (9.6), 373 (8.6), 294 (22.4); CD (TFE): 526 (–5.9); 376 (+8.0), 316 (+0.2), 297 (+8.5), 258 (+0.2), 206 (+32.3); IR (neat): 3315 (w), 2958 (w), 2932 (w), 2871 (w), 1651 (s), 1527 (m), 1439 (m), 1367 (m), 1315 (m), 1214 (m), 1159 (m), 1027 (w), 906 (w), 851 (w), 790 (w); ^{1}H NMR (400 MHz, CDCl$_3$): 8.87 (s, 1H), 8.73 (s, 1H), 7.75 (br s, 1H), 7.34 (s, 1H), 5.99 (br s,

1H), 5.79 – 5.60 (m, 2H), 5.19 (br s, 1H), 4.30 – 3.87 (m, 4H), 3.84 – 3.58 (m, 1H), 3.53 – 3.37 (m, 1H), 3.35 – 3.04 (m, 5H), 3.00 – 2.80 (m, 1H), 2.77 – 2.49 (m, 2H), 2.35 – 1.94 (m, 8H), 1.91 – 1.69 (m, 6H), 1.69 – 1.45 (m, 12H), 1.38 – 1.22 (m, 18H), 1.09 – 0.53 (m, 46H); ^{13}C NMR (125 MHz, CDCl$_3$): 173.1 (C), 172.8 (C), 172.4 (C), 171.2 (C), 169.52 (C), 169.47 (C), 169.3 (C), 168.7 (C), 162.9 (C), 162.5 (C), 162.2 (C), 161.9 (C), 154.8 (C), 149.3 (C), 145.0 (C), 131.0 (CH), 129.6 (CH), 125.7 (C), 125.6 (2xC), 124.3 (C) 123.2 (C), 122.0 (C), 80.8 (C), 60.0 (CH$_2$), 55.0 (2xCH), 54.6 (CH), 54.1 (3xCH), 51.9 (2xCH), 45.9 (2xCH$_3$), 41.5 (CH$_2$), 40.42 (CH$_2$), 40.35 (CH$_2$), 40.0 (CH$_2$), 39.7 (CH$_2$), 38.6 (CH$_2$), 38.0 (CH$_2$), 35.9 (CH$_2$), 32.4 (CH$_2$), 31.6 (CH$_2$), 31.5 (2xCH$_2$), 29.7 (CH$_2$), 29.5 (2xCH$_2$), 28.2 (3xCH$_3$), 26.7 (CH$_2$), 26.6 (CH$_2$), 26.0 (CH), 25.7 (CH), 24.8 (CH), 24.5 (2xCH), 23.5 (CH$_3$), 23.3 (CH$_3$), 23.2 (CH$_3$), 23.1 (CH$_3$), 23.0 (CH$_3$), 22.60 (CH$_2$), 22.58 (CH$_2$), 22.31 (2xCH$_3$), 22.25 (CH$_3$), 20.9 (2xCH$_3$), 14.2 (CH$_3$), 14.0 (CH$_3$), 11.4 (CH$_3$); HPLC–MS: R_t = 2.72 min, 1476 (100, [M+H]$^+$); HRMS (ESI, +ve) calcd for C$_{75}$H$_{118}$N$_{12}$O$_{14}$S$_2$ ([M+H]$^+$): 1475.8406, found: 1475.8371.
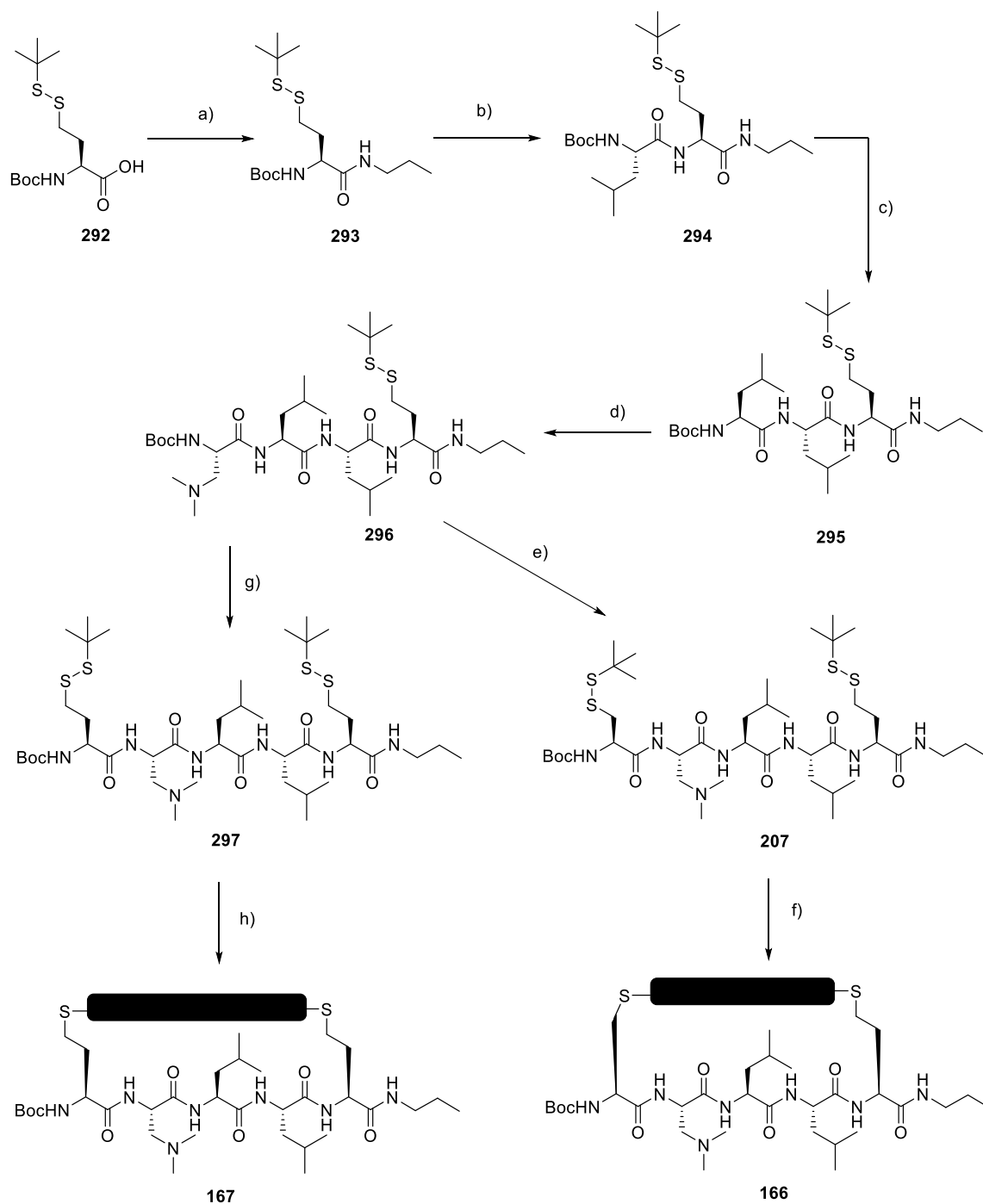
Scheme 17. (a) EDC, DMAP, CH₂Cl₂, rt, overnight, *n*–propylamine, 85%; (b) 1. TFA/CH₂Cl₂ 1:1, rt, 1 h; 2. Boc–L–Leu–OH, EDC, DMAP, DIPEA, CH₂Cl₂, rt, overnight, 84%; (c) 1. TFA/CH₂Cl₂ 1:1, rt, 1 h; 2. Boc–L–Leu–OH, EDC, DMAP, DIPEA, CH₂Cl₂, rt, overnight, 80%; (d) 1. TFA/CH₂Cl₂ 1:1, rt, 1 h; 2. **270**, EDC, DMAP, DIPEA, CH₂Cl₂, rt, overnight, 68%; (e) 1. TFA/CH₂Cl₂ 1:1, rt, 1 h; 2. **271**, EDC, DMAP, DIPEA, CH₂Cl₂, rt, overnight, 54%; (f)

1. PBu$_3$, TEA, H$_2$O, TFE, rt, overnight; 2. **152**, TCEP·HCl, CH$_3$CN/buffer 3:1, 65 °C, overnight, 7%; (g) 1. TFA/CH$_2$Cl$_2$ 1:1, rt, 1 h; 2. **292**, EDC, DMAP, DIPEA, CH$_2$Cl$_2$, rt, overnight, 15%; (h) 1. PBu$_3$, TEA, H$_2$O, TFE, rt, overnight; 2. **152**, TCEP·HCl, CH$_3$CN/buffer 3:1, 65 °C, overnight, 14%.

Compound 292 was synthesized as described previously.[234]
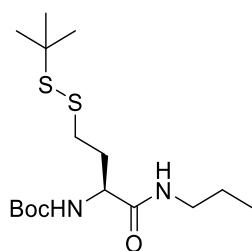
Compound 293 (2.9 g, 85%, colorless oil) was prepared from **292** (3.0 g, 9.3 mmol) and *n*–propylamine (1.5 mL, 18 mmol) following the general procedure D. R_f (CH$_2$Cl$_2$/MeOH 15:1): 0.56; $[\alpha]_D^{20}$ –29.7 (*c* 1.00, CHCl$_3$); IR (neat): 3305 (w), 2967 (w), 1656 (s), 1530 (m), 1365 (m), 1249 (m), 1168 (s), 1048 (w); ^{1}H NMR (300 MHz, CDCl$_3$): 6.36 (s, 1H), 5.25 (d, $^3J_{H-H}$ = 8.3 Hz, 1H), 4.27– 4.10 (m, 1H), 3.32 – 3.13 (m, 2H), 2.85 – 2.63 (m, 2H), 2.30 – 1.87 (m, 2H), 1.60 – 1.45 (m, 2H), 1.42 (s, 9H), 1.30 (s, 9H), 0.90 (t, $^3J_{H-H}$ = 7.4 Hz, 3H); ^{13}C NMR (75 MHz, CDCl$_3$): 171.4 (C), 155.7 (C), 80.1 (C), 53.4 (CH), 48.0 (C), 41.2 (CH$_2$), 36.4 (CH$_2$), 32.3 (CH$_2$), 30.0 (3xCH$_3$), 28.3 (3xCH$_3$), 22.8 (CH$_2$), 11.4 (CH$_3$); MS (ESI, MeOH): 265 (100, [M–Boc+H]$^+$).
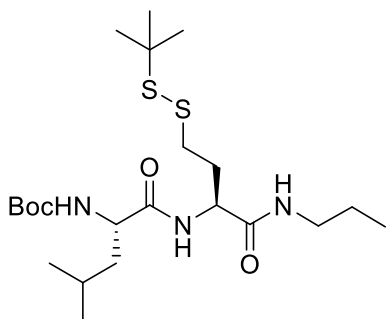
Compound 294 (3.2 g, 84%, colorless solid) was prepared from **293** (2.9 g, 8.0 mmol) and Boc–L–Leu–OH (2.2 g, 9.5 mmol) following the general procedures A and D. R_f (CH$_2$Cl$_2$/MeOH 15:1): 0.53, Mp: 101–102 °C; $[\alpha]_D^{20}$ –74.8 (*c* 1.00, CHCl$_3$); IR (neat): 3290 (w), 3088 (w), 2962 (w), 2873 (w), 1690 (m), 1624 (s), 1520 (m), 1455 (m), 1389 (m), 1364 (m), 1319 (w), 1275 (m), 1241 (m), 1165 (s), 1121 (w), 1046 (w), 1021 (w), 953 (w), 873 (w), 778 (w), 663 (m); ^{1}H

NMR (400 MHz, CDCl$_3$): 7.03 (d, $^3J_{H-H}$ = 8.1 Hz, 1H), 6.72 (d, $^3J_{H-H}$ = 6.1 Hz, 1H), 5.06 (d, $^3J_{H-H}$ = 6.8 Hz, 1H), 4.60 – 4.47 (m, 1H), 4.14 – 4.00 (m, 1H), 3.25 – 3.07 (m, 2H), 2.75 – 2.59 (m, 2H), 2.31 – 1.94 (m, 2H), 1.71 – 1.57 (m, 2H), 1.57 – 1.46 (m, 3H), 1.42 (s, 9H), 1.29 (s, 9H), 0.99 – 0.67 (m, 9H); ^{13}C NMR (100 MHz, CDCl$_3$): 172.7 (C), 170.6 (C), 155.9 (C), 80.4 (C), 53.6 (CH), 52.3 (CH), 48.0 (C), 41.3 (CH$_2$), 41.1 (CH$_2$), 36.3 (CH$_2$), 31.4 (CH$_2$), 30.0 (3xCH$_3$), 28.3 (3xCH$_3$), 24.8 (CH), 23.0 (CH$_3$), 22.7 (CH$_2$), 21.8 (CH$_3$), 11.4 (CH$_3$); MS (ESI, MeOH): 478 (100, [M+H]$^+$).
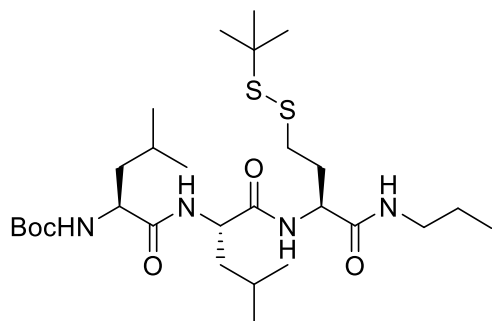
Compound 295 (3.2 g, 80%, colorless solid) was prepared from **294** (3.2 g, 6.7 mmol) and Boc–L–Leu–OH (1.9 g, 8.2 mmol) following the general procedures A and D. R_f (CH$_2$Cl$_2$/MeOH 15:1): 0.44; Mp: 201 – 202 ºC; [α]$_D^{20}$ –56.3 (c 1.00, CHCl$_3$); IR (neat): 3283 (w), 3086 (w), 2959 (w), 2872 (w), 1638 (s), 1535 (s), 1456 (m), 1389 (m), 1364 (m), 1319 (w), 1239 (m), 1165 (s), 1121 (w), 1045 (w), 1023 (w), 953 (w), 874 (w), 779 (w), 666 (m); ^{1}H NMR (400 MHz, CDCl$_3$): 7.12 (d, $^3J_{H-H}$ = 8.5 Hz, 1H), 6.78 – 6.63 (m, 2H), 4.98 (d, $^3J_{H-H}$ = 5.1 Hz, 1H), 4.61 – 4.47 (m, 1H), 4.40 – 4.29 (m, 1H), 4.12 – 3.99 (m, 1H), 3.32 – 3.12 (m, 2H), 2.85 – 2.63 (m, 2H), 2.50 – 2.30 (m, 1H), 2.08 – 1.91 (m, 1H), 1.83 – 1.63 (m, 4H), 1.63 – 1.53 (m, 4H), 1.48 (s, 9H), 1.33 (s, 9H), 1.04 – 0.76 (m, 15H); ^{13}C NMR (100 MHz, CDCl$_3$): 173.3 (C), 171.8 (C), 170.6 (C), 156.4 (C), 81.2 (C), 54.1 (CH), 52.8 (CH), 52.6 (CH), 48.0 (C), 41.4 (CH$_2$), 40.6 (CH$_2$), 40.5 (CH$_2$), 37.1 (CH$_2$), 31.5 (CH$_2$), 30.0 (3xCH$_3$), 28.3 (3xCH$_3$), 25.0 (CH), 24.9 (CH), 23.1 (CH$_3$), 23.0 (CH$_3$), 22.6 (CH$_2$), 21.8 (CH$_3$), 21.7 (CH$_3$), 11.4 (CH$_3$); MS (ESI, MeOH): 591 (100, [M+H]$^+$).
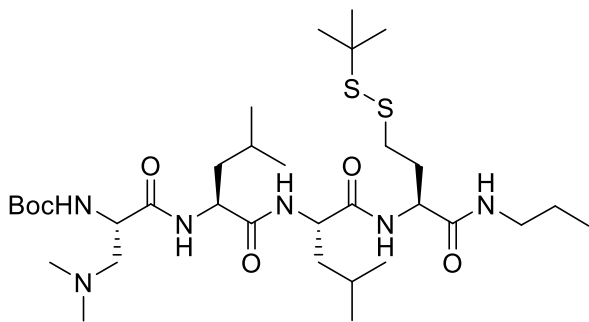
Compound 296 (2.6 g, 68%, colorless solid) was prepared from **295** (3.2 g, 5.4 mmol) and **270** (1.5 g, 6.5 mmol) following the general procedures A and D. R_f (CH$_2$Cl$_2$/MeOH 15:1): 0.32; Mp: 206 –

207 °C (decomp); $[\alpha]_D^{20}$ –21.1 (*c* 1.00, CHCl$_3$); IR (neat): 3271 (w), 3090 (w), 2959 (w), 2872

(w), 2825 (w), 2774 (w), 1717 (w), 1687 (w), 1628 (s), 1546 (m), 1458 (m), 1388 (w), 1364

(m), 1279 (w), 1247 (w), 1218 (w), 1165 (m), 1051 (w), 1020 (w), 912 (w), 864 (w), 780 (w),

727 (m), 647 (w); ^{1}H NMR (400 MHz, CDCl$_3$): 7.38 (d, $^3J_{H-H}$ = 6.1 Hz, 1H), 7.26 – 7.15 (m,

2H), 6.74 (s, 1H), 5.83 (s, 1H), 4.52 – 4.28 (m, 2H), 4.21 – 4.10 (m, 1H), 4.02 – 3.91 (m, 1H),

3.27 – 3.07 (m, 2H), 2.77 – 2.39 (m, 5H), 2.27 (s, 6H), 2.09 – 1.94 (m, 1H), 1.86 – 1.72 (m,

1H), 1.75 – 1.59 (m, 4H), 1.59 – 1.51 (m, 3H), 1.45 (s, 9H), 1.27 (s, 9H), 0.99 – 0.75 (m, 15H);

^{13}C NMR (100 MHz, CDCl$_3$): 173.0 (C), 172.9 (C), 172.5 (C), 171.0 (C), 157.1 (C), 81.2 (C),

59.5 (CH$_2$), 54.1 (CH), 53.8 (CH), 53.1 (CH), 52.9 (CH), 47.8 (C), 45.1 (2xCH$_3$), 41.3 (CH$_2$),

40.3 (CH$_2$), 39.7 (CH$_2$), 37.5 (CH$_2$), 31.7 (CH$_2$), 29.9 (3xCH$_3$), 28.2 (3xCH$_3$), 25.2 (CH), 25.0

(CH), 23.2 (CH$_3$), 23.0 (CH$_3$), 22.5 (CH$_2$), 21.8 (CH$_3$), 20.9 (CH$_3$), 11.4 (CH$_3$); MS (ESI,

MeOH): 705 (100, [M+H]$^+$).
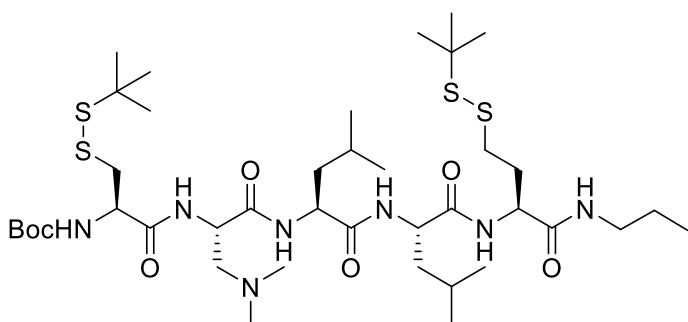
Compound 207 (0.6 g, 54%, colorless solid) was prepared from **296** (0.92 g, 1.2 mmol) and **271** (0.45 g, 1.4 mmol) following the general procedures A and D. R_f

(CH$_2$Cl$_2$/MeOH 15:1): 0.3; Mp: 228 – 229 °C (decomp); $[\alpha]_D^{20}$ –48.8 (*c* 1.00, CHCl$_3$); IR (neat):

3266 (w), 3090 (w), 2960 (w), 1717 (w), 1691 (w), 1627 (s), 1546 (m), 1488 (m), 1390 (w),

1364 (m), 1277 (w), 1250 (w), 1165 (m), 1057 (w), 878 (w), 781 (w), 712 (m), 645 (w); ^{1}H NMR (400 MHz, CDCl$_3$): 7.67 (br s, 1H), 7.47 – 7.29 (m, 2H), 7.11 (d, $^3J_{H-H}$ = 8.5 Hz, 1H), 6.74 (t, $^3J_{H-H}$ = 5.6 Hz, 1H), 5.52 (d, $^3J_{H-H}$ = 4.0 Hz, 1H), 4.50 – 4.37 (m, 1H), 4.37 – 4.21 (m, 2H), 4.21 – 4.01 (m, 2H), 3.25 – 2.40 (m, 8H), 2.28 (s, 6H), 2.14 – 1.51 (m, 10H), 1.48 (s, 9H), 1.41 – 1.25 (m, 18H), 1.07 – 0.82 (m, 15H); ^{13}C NMR (100 MHz, CDCl$_3$): 173.8 (C), 172.8 (C), 172.4 (C), 171.6 (C), 171.0 (C), 156.3 (C), 81.4 (C), 58.5 (CH$_2$), 55.0 (CH), 54.5 (CH), 53.6 (CH), 53.3 (CH), 53.2 (CH), 49.1 (C), 47.7 (C), 45.2 (2xCH$_3$), 41.4 (CH$_2$), 40.1 (CH$_2$), 39.7 (CH$_2$), 39.5 (CH$_2$), 37.7 (CH$_2$), 31.6 (CH$_2$), 30.0 (3xCH$_3$), 29.9 (3xCH$_3$), 28.2 (3xCH$_3$), 25.2 (CH), 24.9 (CH), 23.6 (CH$_3$), 23.1 (CH$_3$), 22.5 (CH$_2$), 20.94 (CH$_3$), 20.89 (CH$_3$), 11.4 (CH$_3$); MS (ESI, MeOH): 896 (100, [M+H]$^+$).
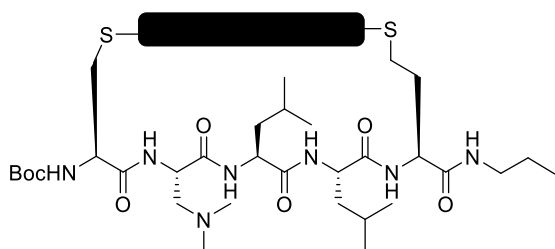
Compound 166 (16 mg, 7%, atropisomers not detectable, red solid) was prepared from **207** (150 mg, 0.168 mmol) following the general procedures F and G. R_f (CH$_2$Cl$_2$/MeOH 15:1): 0.23; Mp: 114 – 115 ^{o}C; UV-Vis (TFE): 523 (12.5), 372 (9.9), 295 (33.4); CD (TFE): 543 (+5.0), 374 (–3.5), 313 (+2.6), 289 (–6.4), 238 (–5.1), 209 (+9.3); IR (neat): 3300 (w), 2957 (w), 2930 (w), 2870 (w), 1651 (s), 1534 (m), 1438 (m), 1367 (w), 1315 (m), 1215 (s), 1150 (s), 904 (w); ^{1}H NMR (400 MHz, CDCl$_3$): 9.43 (s, 1H), 8.57 (s, 1H), 7.38 (s, 1H), 7.19 – 6.92 (m, 2H), 6.78 (br s, 1H), 6.49 (br s, 1H), 5.90 (br s, 1H), 5.74 (dd, $^3J_{H-H}$ = 9.4 Hz, 4.9 Hz, 1H), 5.68 – 5.58 (m, 1H), 5.33 – 5.08 (m, 1H), 4.8 (s, 1H), 4.56 – 4.41 (m, 1H), 4.36 – 4.18 (m, 1H), 4.18 – 3.92 (m, 3H), 3.55 – 3.46 (m, 1H), 3.37 – 3.14 (m, 8H), 3.01 – 2.85 (m, 1H), 2.81 – 2.68 (m, 1H), 2.34 – 2.24 (m, 3H), 2.13 (s, 6H), 2.09 – 2.03 (m, 2H), 1.69 – 1.62 (m, 2H), 1.58 – 1.52 (m, 5H), 1.49 – 1.46 (m, 10H), 1.32 – 1.22 (m, 14H), 0.98 – 0.83 (m, 35H), 0.56 – 0.47 (m, 6H); ^{13}C NMR (100 MHz, CDCl$_3$): 171.2 (C), 170.8 (C), 169.4

(3xC), 168.6 (2xC), 164.4 (C), 163.3 (2xC), 162.1 (C), 155.0 (C), 147.1 (2xC), 128.4 (CH), 126.7 (CH), 126.1 (C), 125.3 (C), 124.2 (C), 123.7 (C), 122.2 (C), 121.4 (C), 81.2 (C), 57.2 (CH$_2$), 55.9 (2xCH), 54.3 (CH), 53.9 (CH), 52.6 (CH), 51.5 (CH), 50.7 (CH), 45.4 (2xCH$_3$), 42.8 (2xCH$_2$), 42.5 (CH$_2$), 41.3 (2xCH$_2$), 40.1 (2xCH$_2$), 38.2 (CH$_2$), 37.8 (CH$_2$), 31.54 (CH$_2$), 31.51 (CH$_2$), 29.48 (CH$_2$), 29.45 (CH$_2$), 28.3 (3xCH$_3$), 28.0 (CH$_2$), 26.8 (CH$_2$), 26.6 (CH$_2$), 25.9 (CH), 25.6 (CH), 24.9 (CH), 24.4 (CH), 24.3 (CH$_3$), 23.8 (CH$_3$), 23.3 (CH$_3$), 23.1 (CH$_3$), 22.9 (CH$_2$), 22.61 (CH$_2$), 22.57 (CH$_2$), 22.3 (CH$_3$), 22.2 (CH$_3$), 22.1 (CH$_3$), 21.8 (CH$_3$), 14.1 (CH$_3$), 13.6 (CH$_3$), 11.3 (CH$_3$); HPLC–MS: R_t = 2.61 min, 1377 (100, [M+H]$^+$); HRMS (ESI, +ve) calcd for C$_{70}$H$_{109}$N$_{11}$O$_{13}$S$_2$ ([M+H]$^+$): 1376.7721, found: 1376.7694.
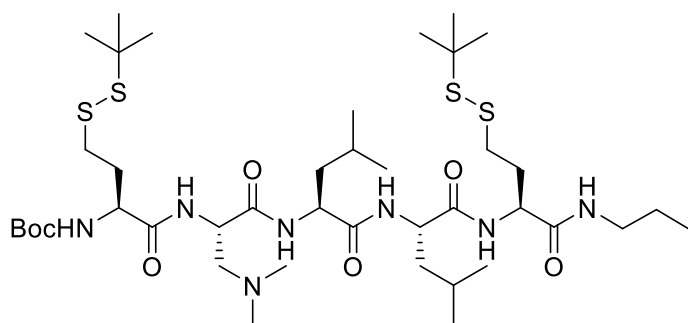
Compound 297 (0.2 g, 15%, colorless solid) was prepared from **296** (0.92 g, 1.2 mmol) and **292** (0.47 g, 1.4 mmol) following the general procedures A and D. R_f (CH$_2$Cl$_2$/MeOH 15:1): 0.36; Mp: 224 – 225 °C; [α]$_D^{20}$ –9.00 (c 1.00, CHCl$_3$); IR (neat): 3265 (w), 3087 (w), 2960 (w), 2871 (w), 2774 (w), 1715 (w), 1689 (w), 1627 (s), 1530 (s), 1456 (m), 1406 (w), 1388 (w), 1363 (m), 1277 (w), 1284 (m), 1166 (s), 1047 (w), 871 (w), 782 (w), 706 (m); ^{1}H NMR (400 MHz, CDCl$_3$): 7.71 – 7.46 (m, 2H), 7.41 (d, $^3J_{H-H}$ = 6.6 Hz, 1H), 7.12 (d, $^3J_{H-H}$ = 8.5 Hz, 1H), 6.76 (t, $^3J_{H-H}$ = 5.6 Hz, 1H), 5.41 (s, 1H), 4.48 – 3.95 (m, 5H), 3.26 – 3.08 (m, 2H), 2.83 – 2.72 (m, 4H), 2.68 – 2.42 (m, 2H), 2.28 (s, 6H), 2.12 – 1.98 (m, 2H), 1.92 – 1.52 (m, 10H), 1.48 (s, 9H), 1.36 – 1.26 (m, 18H), 1.06 – 0.82 (m, 15H); ^{13}C NMR (100 MHz, CDCl$_3$): 173.9 (C), 173.3 (C), 172.9 (C), 172.6 (C), 171.1 (C) 156.5 (C), 81.4 (C), 58.7 (CH$_2$), 55.8 (CH), 54.5 (CH), 53.4 (2xCH), 53.2 (CH), 48.4 (C), 47.8 (C), 45.5 (2xCH$_3$), 41.4 (CH$_2$), 39.8 (CH$_2$), 39.4 (CH$_2$), 37.7 (CH$_2$), 36.2 (CH$_2$), 31.6 (CH$_2$), 30.8 (CH$_2$), 29.97 (3xCH$_3$), 29.95

(3xCH$_3$), 28.2 (3xCH$_3$), 25.2 (CH), 24.9 (CH), 23.4 (CH$_3$), 23.1 (CH$_3$), 22.5 (CH$_2$), 21.0 (CH$_3$), 20.9 (CH$_3$), 11.4 (CH$_3$); MS (ESI, MeOH): 910 (100, [M+H]$^+$).
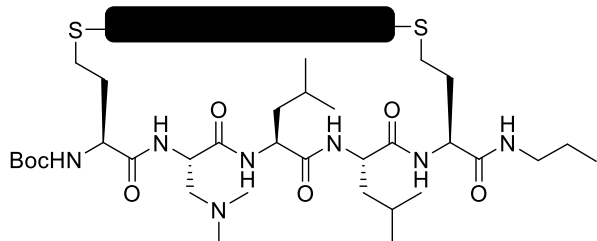
Compound 167 (30 mg, 14%, mixture of two atropisomers **167a** and **167b**, red solid) was prepared from **297** (136 mg, 0.150 mmol) following the general procedures F and G. R_f (CH$_2$Cl$_2$/MeOH 15:1): 0.42. **167a** and **167b** were separated using PTLC (CH$_2$Cl$_2$/MeOH 18:1) **167a** (13 mg), **167b** (17 mg). **167a**. R_f (CH$_2$Cl$_2$/MeOH 18:1): 0.35; Mp: 158 – 159 °C; UV-Vis (TFE): 525 (12.7), 371 (12.5), 296 (33.4); CD (TFE): 539 (+11.9), 376 (–6.5), 309 (+5.7), 274 (–8.0), 253 (–1.8), 238 (–8.4), 207 (+18.3); IR (neat): 3314 (w), 2957 (w), 2871 (w), 1651 (s), 1527 (m), 1466 (w), 1434 (m), 1368 (w), 1315 (m), 1238 (m), 1212 (s), 1159 (m), 1026 (w), 905 (w), 849 (w), 791 (w), 732 (w); ^{1}H NMR (400 MHz, CDCl$_3$): 8.71 (s, 1H), 8.53 (s, 1H), 7.51 – 7.27 (m, 2H), 7.17 – 7.09 (m, 1H), 6.91 (br s, 1H), 6.52 (br s, 1H), 6.27 (br s, 1H), 6.02 (br s, 1H), 5.79 (dd, $^3J_{H-H}$ = 9.9 Hz, 5.1 Hz, 1H), 5.72 (dd, $^3J_{H-H}$ = 9.9 Hz, 6.0 Hz, 1H), 5.25 (d, $^3J_{H-H}$ = 8.3 Hz, 1H), 4.73 – 4.60 (m, 1H), 4.30 – 4.12 (m, 3H), 3.54 – 3.07 (m, 11H), 2.54–2.39 (m, 2H), 2.34 – 2.25 (m, 2H), 2.18 (s, 6H), 2.15 – 2.08 (m, 2H), 2.02 – 1.93 (m, 3H), 1.91 – 1.73 (m, 2H), 1.70 – 1.62 (m, 3H), 1.60 – 1.51 (m, 6H), 1.47 – 1.41 (m, 13H), 1.33 – 1.30 (m, 4H), 1.28 – 1.24 (m, 6H), 0.99 – 0.93 (m, 13H), 0.91 – 0.83 (m, 16H), 0.74 – 0.64 (m, 3H), 0.54 – 0.36 (m, 3H); ^{13}C NMR (100 MHz, CDCl$_3$): 172.4 (C), 172.2 (C), 171.7 (C), 170.9 (C), 169.7 (C), 169.2 (C), 169.1 (C), 163.8 (C), 162.6 (C), 162.4 (C), 161.7 (C), 155.4 (C), 147.0 (2xC), 127.5 (2xCH), 126.7 (C), 125.8 (C), 125.2 (C), 123.7 (C), 122.9 (C), 120.3 (C), 80.0 (C), 59.3 (CH$_2$), 53.8 (CH), 53.7 (CH), 52.9 (CH), 52.7 (CH), 51.7 (CH), 51.5 (CH), 49.8 (CH), 45.3 (2xCH$_3$), 41.4 (CH$_2$), 40.4 (CH$_2$), 40.1 (CH$_2$), 37.6 (CH$_2$), 37.3 (CH$_2$), 31.53 (CH$_2$), 31.47 (CH$_2$), 29.6 (CH$_2$), 29.4 (CH$_2$), 28.6 (CH$_2$), 28.3 (3xCH$_3$), 28.0

(CH$_2$), 27.4 (CH$_2$), 26.7 (CH$_2$), 25.9 (CH), 25.6 (CH), 24.9 (CH), 24.4 (CH$_2$), 24.2 (CH$_2$), 24.1 (CH), 23.82 (CH$_2$), 23.78 (CH$_2$), 23.4 (CH$_3$), 23.3 (CH$_3$), 23.0 (2xCH$_3$), 22.7 (CH$_2$), 22.58 (CH$_2$), 22.56 (CH$_2$), 22.1 (CH$_3$), 22.0 (CH$_3$), 21.3 (CH$_3$), 21.0 (CH$_3$), 14.0 (CH$_3$), 13.6 (CH$_3$), 11.3 (CH$_3$); HPLC–MS: R_t = 2.77 min, 1391 (100, [M+H]$^+$); HRMS (ESI, +ve) calcd for C$_{71}$H$_{111}$N$_{11}$O$_{13}$S$_2$ ([M+H]$^+$): 1390.7877, found: 1390.7853. **167b**. R_f (CH$_2$Cl$_2$/MeOH 18:1): 0.33; Mp; IR and HRMS were identical with **167a**; UV-Vis (TFE): 522 (7.5), 372 (8.0), 295 (18.9); CD (TFE): 529 (–6.4), 377 (+5.2), 311 (–2.8), 271 (+4.0), 249 (+0.3), 209 (+14.8); ^{1}H NMR (400 MHz, CDCl$_3$): 8.82 – 8.66 (m, 2H), 7.85 (br s, 1H), 7.13 – 6.80 (m, 2H), 6.62 – 6.35 (m, 1H), 6.26 (br s, 1H), 6.03 (br s, 1H), 5.79 – 5.68 (m, 2H), 5.46 (br s, 1H), 4.67 – 4.56 (m, 1H), 4.51 – 4.39 (m, 1H), 4.04 – 3.88 (m, 1H), 3.53 – 2.94 (m, 9H), 2.66 – 2.35 (m, 1H), 2.32 – 2.14 (m, 10H), 2.10 – 1.92 (m, 2H), 1.79 – 1.71 (m, 4H), 1.58 – 1.40 (m, 19H), 1.35 – 1.23 (m, 16H), 0.99 – 0.84 (m, 25H), 0.83 – 0.63 (m, 10H); ^{13}C NMR (125 MHz, CDCl$_3$): 172.4 (C), 171.7 (C), 171.5 (C), 171.0 (C), 170.1 (C), 169.1 (C), 169.0 (C), 163.4 (C), 162.8 (2xC), 162.5 (C), 155.4 (C), 147.8 (2xC), 132.7 (CH), 130.6 (CH), 126.1 (C), 125.5 (C), 124.2 (2xC), 123.4 (C), 120.9 (C), 80.6 (C), 59.2 (CH$_2$), 54.2 (CH), 54.1 (CH), 53.4 (CH), 52.2 (CH), 51.6 (CH), 50.6 (2xCH), 45.0 (2xCH$_3$), 41.4 (CH$_2$), 40.4 (CH$_2$), 40.2 (CH$_2$), 39.1 (CH$_2$), 38.0 (CH$_2$), 37.9 (CH$_2$), 37.7 (CH$_2$), 36.4 (CH$_2$), 36.3 (CH$_2$), 31.6 (CH$_2$), 31.5 (CH$_2$), 31.1 (CH$_2$), 30.7 (CH$_2$), 29.7 (CH$_2$), 29.6 (CH$_2$), 29.4 (CH$_2$), 28.3 (3xCH$_3$), 26.70 (CH$_2$), 26.67 (CH$_2$), 26.0 (CH), 25.8 (CH), 24.9 (CH), 24.4 (CH), 23.3 (3xCH$_3$), 23.0 (CH$_3$), 22.7 (CH$_2$), 22.6 (CH$_2$), 22.14 (CH$_3$), 22.06 (CH$_3$), 21.8 (CH$_3$), 21.3 (CH$_3$), 14.0 (2xCH$_3$), 11.4 (CH$_3$); HPLC–MS: R_t = 2.75 min, 1391 (100, [M+H]$^+$).
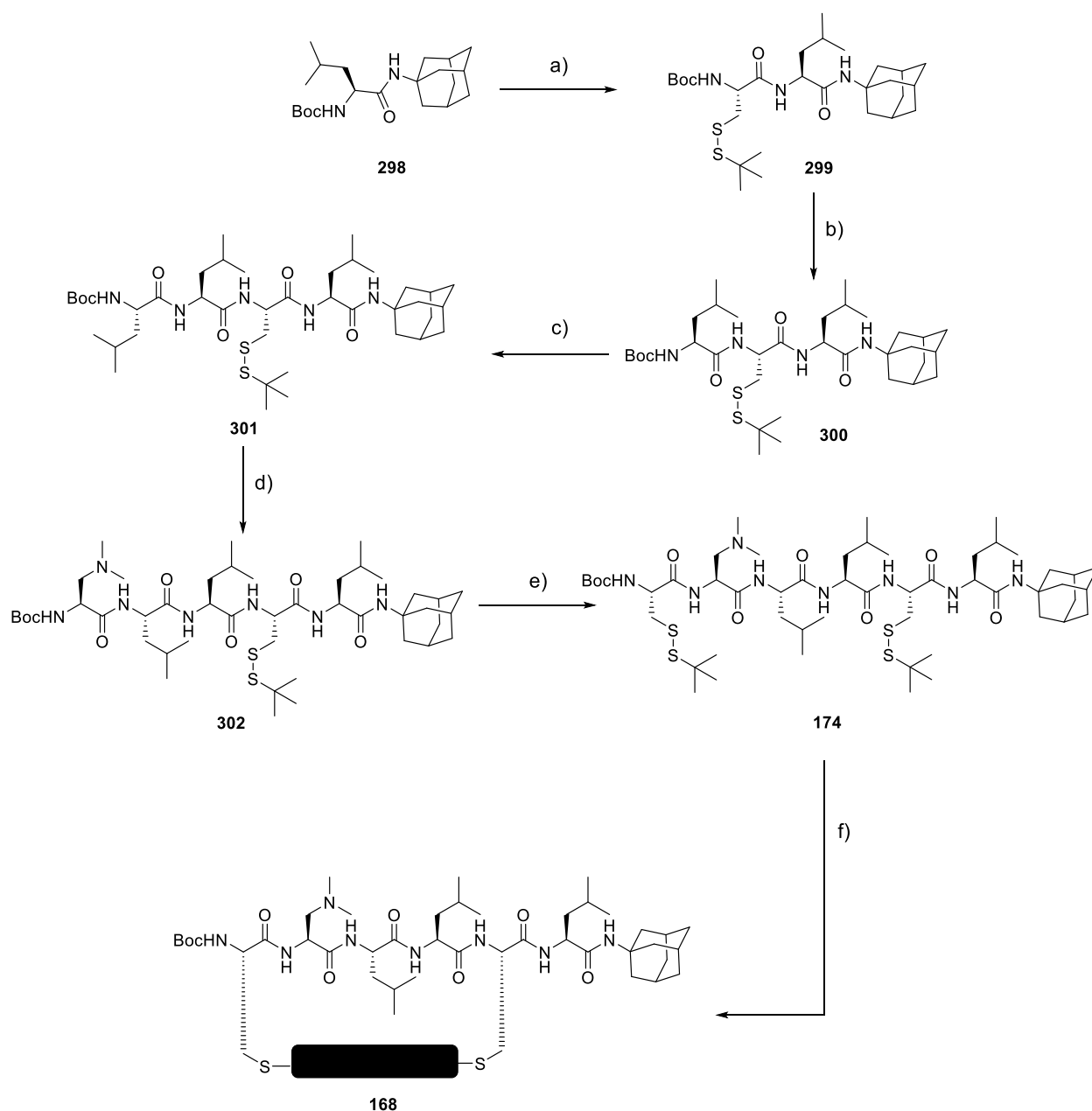
Scheme 18. (a) 1. TFA/CH₂Cl₂ 1:1, rt, 1 h; 2. **271**, EDC, DMAP, DIPEA, CH₂Cl₂, rt, overnight, 51%; (b) 1. TFA/CH₂Cl₂ 1:1, rt, 1 h; 2. Boc–L–Leu–OH, EDC, DMAP, DIPEA, CH₂Cl₂, rt, overnight, 86%; (c) 1. TFA/CH₂Cl₂ 1:1, rt, 1 h; 2. Boc–L–Leu–OH, EDC, DMAP, DIPEA, CH₂Cl₂, rt, overnight, 82%; (d) 1. TFA/CH₂Cl₂ 1:1, rt, 1 h; 2. **270**, EDC, DMAP, DIPEA, CH₂Cl₂, rt, overnight, 38%; (e) 1. TFA/CH₂Cl₂ 1:1, rt, 1 h; 2. **271**, EDC, DMAP, DIPEA, CH₂Cl₂, rt, overnight, 40% (f) 1. PBu₃, TEA, H₂O, TFE, rt, overnight; 2. **152**, TCEP·HCl, CH₃CN/buffer 3:1, 65 °C, overnight, 4%.

Compound 298 was synthesized as described previously.[235]
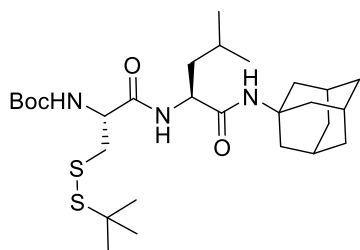
Compound 299 (1.9 g, 51%, colorless solid) was prepared from **298** (2.0 g, 5.5 mmol) and **271** (2.0 g, 6.4 mmol) following the general procedures A and D. R_f (CH$_2$Cl$_2$/MeOH 25:1): 0.47; Mp: 128 – 129 °C; $[\alpha]_D^{20}$ –53.0 (*c* 1.00, CHCl$_3$); IR (neat): 3320 (w), 2908 (m), 2853 (w), 1693 (w), 1643 (s), 1524 (m), 1454 (w), 1388 (w), 1363 (m), 1313 (w), 1273 (w), 1246 (m), 1164 (s), 1095 (w), 1047 (w), 1021 (w), 872 (w), 778 (w), 622 (w); ^{1}H NMR (400 MHz, DMSO–d_6): 7.74 (d, $^3J_{H–H}$ = 8.6 Hz, 1H), 7.25 (s, 1H), 7.19 (d, $^3J_{H–H}$ = 8.3 Hz, 1H), 4.33 – 4.04 (m, 2H), 3.09 – 2.84 (m, 2H), 2.10 – 1.96 (m, 3H), 1.90 (d, $^3J_{H–H}$ = 3.0 Hz, 6H), 1.66 – 1.49 (m, 7H), 1.47 – 1.33 (m, 11H), 1.29 (s, 9H), 0.93 – 0.77 (m, 6H); ^{13}C NMR (100 MHz, DMSO–d_6): 171.2 (C), 170.1 (C), 155.6 (C), 79.0 (C), 54.6 (CH), 52.0 (CH), 51.2 (C), 48.1 (C), 42.7 (CH$_2$), 42.0 (CH$_2$), 41.4 (3xCH$_2$), 36.5 (3xCH$_2$), 30.0 (CH), 29.3 (3xCH$_3$), 28.6 (3xCH$_3$), 24.6 (CH), 23.5 (CH$_3$), 22.3 (CH$_3$); MS (ESI, MeOH): 556 (100, [M+H]$^+$).
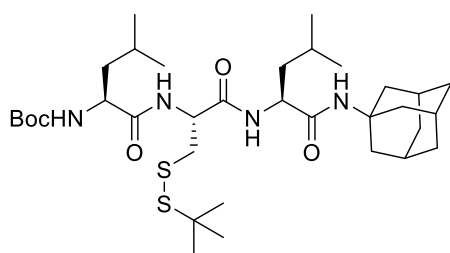
Compound 300 (1.9 g, 86%, colorless solid) was prepared from **299** (1.9 g, 3.4 mmol) and Boc–L–Leu–OH (0.94 g, 3.9 mmol) following the general procedures A and D. R_f (CH$_2$Cl$_2$/MeOH 25:1): 0.49; Mp: 183 – 184 °C; $[\alpha]_D^{20}$ –102 (*c* 1.00, CHCl$_3$); IR (neat): 3277 (w), 3080 (w), 2956 (w), 2909 (m), 1640 (s), 1515 (m), 1454 (w), 1388 (w), 1363 (m), 1313 (w), 1241 (m), 1165 (s), 1046 (w), 1021 (w), 872 (w), 780 (w), 665 (w); ^{1}H NMR (400 MHz, DMSO–d_6): 8.09 (d, $^3J_{H–H}$ = 7.9 Hz, 1H), 7.89 (d, $^3J_{H–H}$ = 8.5 Hz, 1H), 7.11 (s, 1H), 6.98 (d, $^3J_{H–H}$ = 7.9 Hz, 1H), 4.56 – 4.43 (m, 1H), 4.28 – 4.14 (m, 1H), 4.01 – 3.88 (m, 1H), 3.09 (dd, $^2J_{H–H}$ = 12.8 Hz, $^3J_{H–H}$ = 6.2 Hz,

1H), 2.95 (dd, $^2J_{H-H}$ = 12.8 Hz, $^3J_{H-H}$ = 7.6 Hz, 1H), 2.07 – 1.95 (m, 3H), 1.90 (d, $^3J_{H-H}$ = 2.9 Hz, 6H), 1.72 – 1.48 (m, 8H), 1.48 – 1.33 (m, 13H), 1.29 (s, 9H), 0.94 – 0.66 (m, 12H); ^{13}C NMR (100 MHz, DMSO–d_6): 173.1 (C), 171.0 (C), 169.5 (C), 155.8 (C), 78.6 (C), 53.5 (CH), 52.7 (CH), 52.2 (CH), 51.3 (C), 48.2 (C), 42.8 (CH$_2$), 41.7 (CH$_2$), 41.3 (3xCH$_2$), 41.1 (CH$_2$), 36.5 (3xCH$_2$), 30.0 (CH), 29.3 (3xCH$_3$), 28.6 (3xCH$_3$), 24.7 (CH), 24.6 (CH), 23.5 (CH$_3$), 23.4 (CH$_3$), 22.2 (CH$_3$), 22.0 (CH$_3$); MS (ESI, MeOH): 669 (100, [M+H]$^+$).
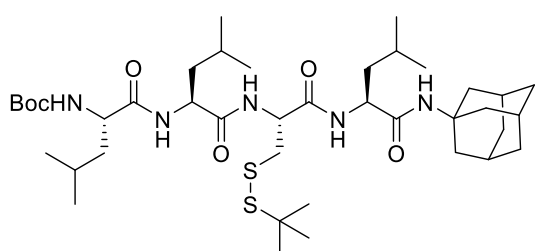
Compound 301 (1.9 g, 82%, colorless solid) was prepared from **300** (1.9 g, 2.8 mmol) and Boc–L–Leu–OH (0.81 g, 3.5 mmol) following the general procedures A and D. R_f (CH$_2$Cl$_2$/MeOH 25:1): 0.49; Mp: 224 – 225 °C (decomp); [α]$_D^{20}$ –138 (*c* 1.00, CHCl$_3$); IR (neat): 3288 (w), 3084 (w), 2956 (w), 2910 (w), 1634 (s), 1530 (m), 1455 (w), 1389 (w), 1363 (w), 1313 (w), 1247 (w), 1164 (m), 1046 (w), 1019 (w), 873 (w), 676 (w); ^{1}H NMR (400 MHz, DMSO–d_6): 8.25 (d, $^3J_{H-H}$ = 7.9 Hz, 1H), 7.82 (d, $^3J_{H-H}$ = 8.1 Hz, 2H), 7.12 (s, 1H), 6.92 (d, $^3J_{H-H}$ = 8.3 Hz, 1H), 4.52 – 4.42 (m, 1H), 4.36 – 4.28 (m, 1H), 4.25 – 4.14 (m, 1H), 4.05 – 3.75 (m, 1H), 3.13 – 3.05 (m, 1H), 2.91 (dd, $^2J_{H-H}$ = 12.9 Hz, $^3J_{H-H}$ = 7.8 Hz, 1H), 2.04 – 1.93 (m, 3H), 1.90 (d, $^3J_{H-H}$ = 3.0 Hz, 6H), 1.70 – 1.48 (m, 9H), 1.48 – 1.32 (m, 15H), 1.29 (s, 9H), 0.98 – 0.69 (m, 18H); ^{13}C NMR (100 MHz, DMSO–d_6): 172.9 (C), 172.5 (C), 171.1 (C), 169.4 (C), 155.8 (C), 78.5 (C), 53.3 (CH), 52.8 (CH), 52.2 (CH), 51.3 (CH), 51.2 (C), 48.1 (C), 42.5 (CH$_2$), 41.7 (CH$_2$), 41.6 (CH$_2$), 41.3 (3xCH$_2$), 41.0 (CH$_2$), 36.5 (3xCH$_2$), 30.0 (CH), 29.3 (3xCH$_3$), 28.6 (3xCH$_3$), 24.7 (CH), 24.6 (CH), 24.4 (CH), 23.53 (CH$_3$), 23.47 (CH$_3$), 23.4 (CH$_3$), 22.2 (CH$_3$), 22.1 (2xCH$_3$); MS (ESI, MeOH): 782 (100, [M+H]$^+$).
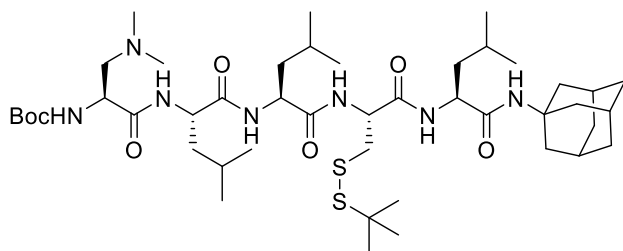
Compound 302 (0.9 g, 38%, colorless solid) was prepared from **301** (2.0 g, 2.6 mmol) and **270** (0.70 g, 3.0 mmol) following the general procedures A and

D. R_f (CH$_2$Cl$_2$/MeOH 15:1): 0.41; Mp: 227 – 228 °C (decomp); $[\alpha]_D^{20}$ –122 (c 1.00, CHCl$_3$);

IR (neat): 3272 (w), 3085 (w), 2911 (w), 1719 (w), 1630 (s), 1536 (m), 1456 (w), 1388 (w),

1363 (w), 1247 (w), 1165 (m), 1050 (w), 866 (w), 779 (w), 698 (w); ^{1}H NMR (300 MHz,

CDCl$_3$): 7.44 (d, $^3J_{H–H}$ = 5.6 Hz, 1H), 7.35 (d, $^3J_{H–H}$ = 6.6 Hz, 1H), 7.16 (s, 1H), 7.03 (d, $^3J_{H–H}$

= 8.2 Hz, 1H), 6.22 (s, 1H), 5.74 (s, 1H), 4.60 – 4.46 (m, 1H), 4.35 – 3.96 (m, 4H), 3.36 (dd,

$^2J_{H–H}$ = 13.4 Hz, $^3J_{H–H}$ = 3.5 Hz, 1H), 3.17 – 2.99 (m, 1H), 2.70 (dd, $^2J_{H–H}$ = 12.3 Hz, $^3J_{H–H}$ =

6.5 Hz, 1H), 2.52 (dd, $^2J_{H–H}$ = 12.3 Hz, $^3J_{H–H}$ = 9.0 Hz, 1H), 2.29 (s, 6H), 2.13 – 1.95 (m, 9H),

1.87 – 1.52 (m, 15H), 1.48 (s, 9H), 1.33 (s, 9H), 1.07 – 0.78 (m, 18H); ^{13}C NMR (75 MHz,

CDCl$_3$): 173.8 (C), 173.2 (C), 173.0 (C), 171.3 (C), 170.4 (C), 156.9 (C), 81.3 (C), 59.4 (CH$_2$),

54.2 (CH), 54.1 (CH), 53.6 (CH), 52.8 (CH), 51.8 (CH), 51.6 (C), 48.1 (C), 45.1 (2xCH$_3$), 41.2

(3xCH$_2$), 40.6 (CH$_2$), 40.2 (2xCH$_2$), 39.4 (CH$_2$), 36.5 (3xCH$_2$), 30.0 (CH), 29.6 (3xCH$_3$), 28.2

(3xCH$_3$), 25.2 (CH), 24.99 (CH), 24.96 (CH), 23.5 (CH$_3$), 23.03 (CH$_3$), 22.99 (CH$_3$), 21.7

(CH$_3$), 21.3 (CH$_3$), 21.1 (CH$_3$); MS (ESI, MeOH): 896 (100, [M+H]$^+$).
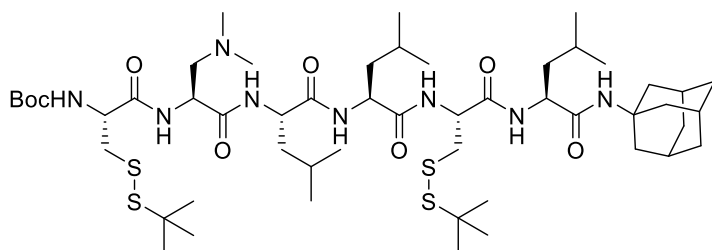
Compound 174 (420 mg, 40%, colorless solid) was prepared from **302** (861 mg, 0.961 mmol) and **271** (357 mg, 1.15 mmol)

following the general procedures A and D. R_f (CH$_2$Cl$_2$/MeOH 15:1): 0.49; Mp: 221 – 222 °C

(decomp); $[\alpha]_D^{20}$ –116 (c 1.00, CHCl$_3$); IR (neat): 3272 (w), 3082 (w), 2957 (w), 2911 (w),

1721 (w), 1630 (s), 1533 (m), 1455 (m), 1389 (w), 1363 (m), 1312 (w), 1275 (w), 1249 (w),

1216 (w), 1164 (m), 1047 (w), 1021 (w), 936 (w), 873 (w), 780 (w), 697 (m), ^{1}H NMR (400 MHz, CDCl$_3$): 7.77 – 7.43 (m, 3H), 7.26 – 7.22 (br s, 1H), 7.10 (d, $^3J_{H–H}$ = 8.0 Hz, 1H), 6.27 (s, 1H), 5.52 (d, $^3J_{H–H}$ = 4.0 Hz, 1H), 4.55 – 4.44 (m, 1H), 4.38 – 3.95 (m, 5H), 3.45 – 3.29 (m, 1H), 3.16 – 3.00 (m, 2H), 2.91 (dd, $^2J_{H–H}$ = 13.8, $^3J_{H–H}$ = 8.3 Hz, 1H), 2.82 – 2.57 (m, 2H), 2.27 (s, 6H), 2.10 – 1.92 (m, 9H), 1.88 – 1.57 (m, 15H), 1.51 (s, 9H), 1.40 – 1.26 (m, 18H), 1.07 – 0.74 (m, 18H); ^{13}C NMR (125 MHz, CDCl$_3$): 174.7 (C), 173.7 (C), 172.6 (C), 172.2 (C), 171.4 (C), 170.5 (C), 156.3 (C), 81.5 (C), 58.4 (CH$_2$), 55.0 (CH), 54.7 (CH), 54.4 (CH), 53.5 (CH), 53.2 (CH), 52.9 (CH), 51.8 (C), 49.0 (C), 48.0 (C), 45.2 (2xCH$_3$), 41.1 (3xCH$_2$), 40.6 (CH$_2$), 40.3 (CH$_2$), 40.1 (CH$_2$), 39.9 (CH$_2$), 39.7 (CH$_2$), 39.1 (CH$_2$), 36.5 (3xCH$_2$), 30.0 (CH), 29.9 (3xCH$_3$), 29.6 (3xCH$_3$), 28.2 (3xCH$_3$), 25.2 (CH), 24.9 (CH), 24.8 (CH), 23.5 (CH$_3$), 23.3 (CH$_3$), 23.1 (CH$_3$), 21.2 (CH$_3$), 21.03 (CH$_3$), 20.95 (CH$_3$); MS (ESI, MeOH): 1087 (100, [M+H]$^+$); HRMS (ESI, +ve) calcd for C$_{52}$H$_{94}$N$_8$O$_8$S$_4$ ([M+Na]$^+$): 1109.5970, found: 1109.5984.
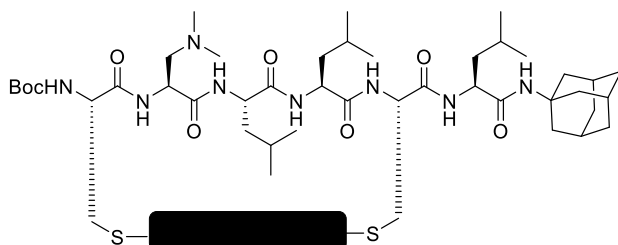
Compound 168 (12 mg, 4%, atropisomers not detectable, red solid) was prepared from **174** (200 mg, 0.184 mmol) following the general procedures F and G. R_f (CH$_2$Cl$_2$/MeOH 15:1): 0.40; Mp: 182 – 183 °C; UV-Vis (TFE): 520 (10.4), 373 (7.9), 294 (26.3); CD (TFE): 529 (–6.0), 377 (+7.8), 318 (–2.4), 299 (+3.6), 258 (–2.2), 211 (+23.5); IR (neat): 3292 (w), 2919 (w), 1649 (s), 1521 (m), 1438 (w), 1366 (w), 1311 (w), 1213 (m), 1160 (m), 1047 (w), 789 (w); ^{1}H NMR (400 MHz, CDCl$_3$): 9.57 (br, 1H), 8.87 (s, 1H), 8.83 (s, 1H), 6.76 (br s, 1H), 6.61 (d, $^3J_{H–H}$ = 9.5 Hz, 1H), 5.91 (br s, 1H), 5.81 (br s, 1H), 5.79 – 5.72 (m, 1H), 5.68 (s, 1H), 5.65 – 5.59 (m, 1H), 5.53 (br s, 1H), 5.21 – 5.01 (m, 1H), 4.95 – 4.85 (m, 1H), 4.39 – 4.23 (m, 2H), 4.22 – 4.09 (m, 1H), 4.09 – 3.76 (m, 4H), 3.72

– 3.43 (m, 1H), 3.35 – 3.12 (m, 5H), 3.03 – 2.85 (m, 1H), 2.80 – 2.62 (m, 1H), 2.33 – 2.19 (m, 8H), 2.10 – 2.07 (m, 2H), 2.02 – 1.98 (m, 8H),1.72 – 1.67 (m, 20H), 1.54 – 1.48 (m, 8H), 1.35 – 1.30 (m, 13H), 1.27 – 1.257 (m, 4H), 1.02 – 0.97 (m, 9H), 0.94 – 0.89 (m, 20H), 0.67 – 0.59 (m, 3H), 0.51 – 0.35 (m, 3H); ^{13}C NMR (100 MHz, CDCl$_3$): 173.0 (C), 172.7 (C), 172.5 (C), 170.3 (C), 169.5 (2xC), 169.0 (C), 168.3 (C), 163.9 (C), 162.9 (C), 162.4 (C), 161.8 (C), 154.2 (C), 143.4 (2xC), 129.9 (CH), 127.3 (CH), 126.1 (C). 125.8 (C), 125.2 (C), 124.9 (C), 123.7 (C), 119.6 (C), 80.3 (C), 58.4 (CH$_2$), 54.0 (2xCH), 53.4 (CH), 52.8 (CH), 52.1 (C), 52.1 (CH), 51.9 (2xCH), 48.9 (CH), 44.4 (2xCH$_3$), 41.5 (CH$_2$), 41.3 (CH$_2$), 41.1 (CH$_2$), 40.3 (CH$_2$), 40.1 (CH$_2$), 38.5 (CH$_2$), 37.8 (CH$_2$), 36.5 (CH$_2$), 36.3 (CH$_2$), 33.3 (CH$_2$), 32.3 (CH$_2$), 31.6 (CH$_2$), 31.5 (CH$_2$), 29.7 (CH$_2$), 29.53 (CH$_2$), 29.48 (CH$_2$), 29.4 (CH), 28.2 (3xCH$_3$), 28.0 (CH$_2$), 27.3 (CH$_2$), 26.8 (CH$_2$), 26.6 (CH$_2$), 25.9 (CH), 25.8 (CH), 24.9 (CH), 24.5 (CH), 24.4 (CH$_2$), 24.3 (CH$_2$), 23.82 (CH$_2$), 23.78 (CH$_2$), 23.5 (CH$_3$), 23.3 (CH$_3$), 23.2 (CH$_3$), 23.0 (CH$_3$), 22.6 (CH$_2$), 22.5 (CH$_3$), 22.20 (CH$_3$), 22.15 (CH$_3$), 22.0 (CH$_3$), 20.5 (CH$_3$), 14.1 (CH$_3$), 13.7 (CH$_3$); HPLC– MS: R_t = 3.12 min, 1568 (100, [M+H]$^+$); HRMS (ESI, +ve) calcd for C$_{82}$H$_{126}$N$_{12}$O$_{14}$S$_2$ ([M+H]$^+$): 1567.9031, found: 1567.9050.
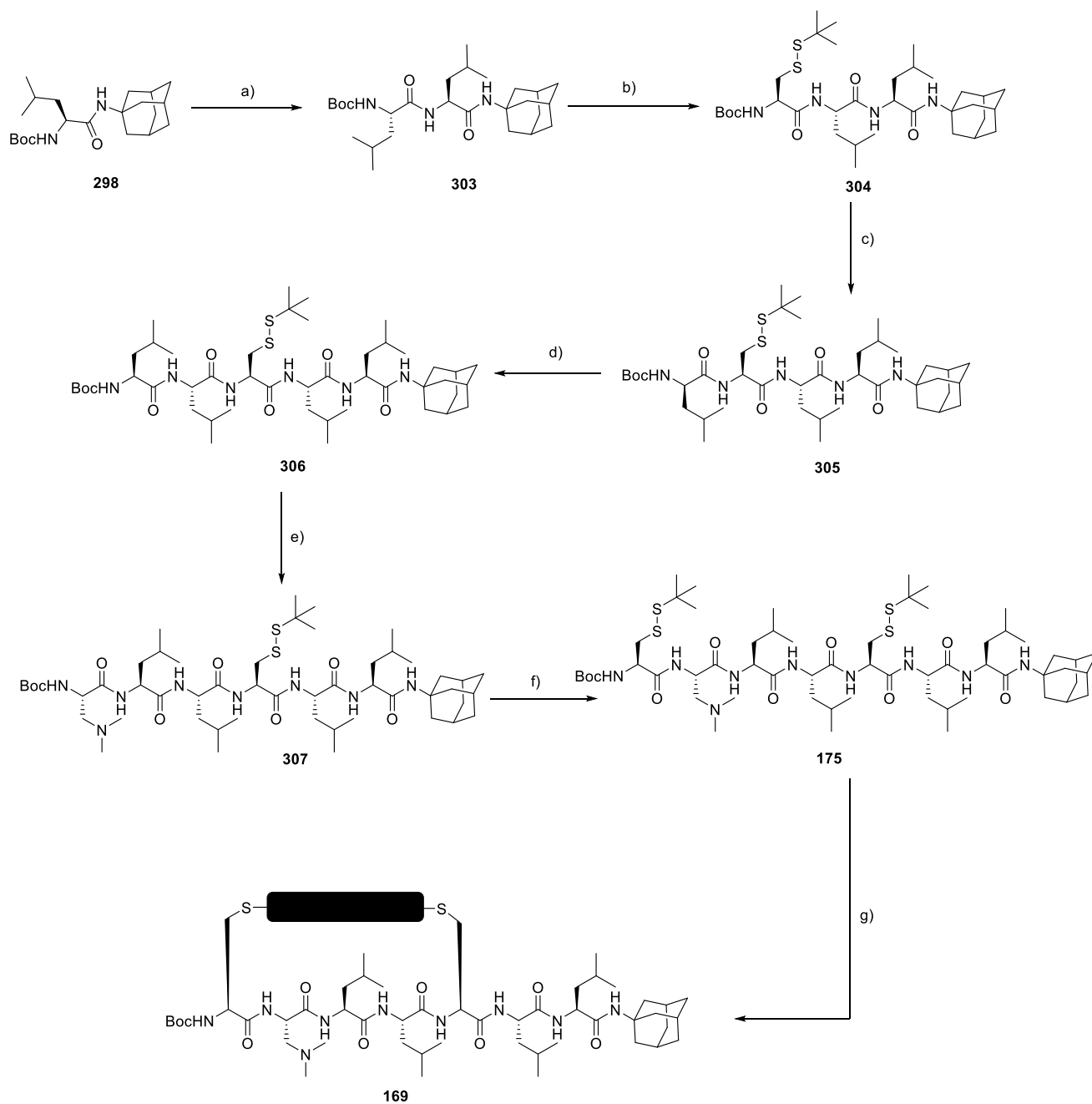
Scheme 19. (a) 1. TFA/CH$_2$Cl$_2$ 1:1, rt, 1 h; 2. Boc–L–Leu–OH, EDC, DMAP, DIPEA, CH$_2$Cl$_2$,

rt, overnight, 73%; (b) 1. TFA/CH$_2$Cl$_2$ 1:1, rt, 1 h; 2. **271**, EDC, DMAP, DIPEA, CH$_2$Cl$_2$, rt,

overnight, 71%; (c) 1. TFA/CH$_2$Cl$_2$ 1:1, rt, 1 h; 2. Boc–L–Leu–OH, EDC, DMAP, DIPEA,

CH$_2$Cl$_2$, rt, overnight, 65%; (d) 1. TFA/CH$_2$Cl$_2$ 1:1, rt, 1 h; 2. Boc–L–Leu–OH, EDC, DMAP,

DIPEA, CH$_2$Cl$_2$, rt, overnight, 73%; (e) 1. TFA/CH$_2$Cl$_2$ 1:1, rt, 1 h; 2. **270**, EDC, DMAP,

DIPEA, CH$_2$Cl$_2$, rt, overnight, 19%; (f) 1. TFA/CH$_2$Cl$_2$ 1:1, rt, 1 h; 2. **271**, EDC, DMAP,

DIPEA, CH₂Cl₂, rt, overnight, 44%; (g) 1. PBu₃, TEA, H₂O, TFE, rt, overnight; 2. **152**, TCEP·HCl, CH₃CN/buffer 3:1, 65 °C, overnight, 16%.
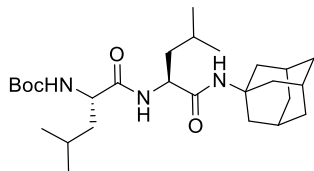
Compound 303 (2.6 g, 73%, colorless solid) was prepared from **298** (2.7 g, 7.4 mmol) and Boc–L–Leu–OH (2.1 g, 9.1 mmol) following the general procedures A and D. R_f (CH₂Cl₂/MeOH 25:1): 0.44; Mp: 165 – 166 °C; $[\alpha]_D^{20}$ –67.0 (*c* 1.00, CHCl₃); IR (neat): 3318 (w), 3079 (w), 2955 (w), 2909 (m), 2853 (w), 1692 (m), 1642 (s), 1523 (m), 1454 (w), 1389 (w), 1364 (m), 1344 (w), 1314 (w), 1292 (w), 1272 (w), 1240 (m), 1167 (s), 1119 (w), 1046 (w), 1023 (w), 953 (w), 875 (w), 780 (w), 624 (m); ¹H NMR (400 MHz, DMSO–d_6): 7.59 (d, $^3J_{H-H}$ = 8.6 Hz, 1H), 7.24 (s, 1H), 6.98 (d, $^3J_{H-H}$ = 8.3 Hz, 1H), 4.31 – 4.20 (m, 1H), 3.96 – 3.88 (m, 1H), 2.08 – 1.95 (m, 3H), 1.89 (d, $^3J_{H-H}$ = 2.9 Hz, 6H), 1.66 – 1.50 (m, 8H), 1.47 – 1.28 (m, 13H), 0.96 – 0.75 (m, 12H); ¹³C NMR (100 MHz, DMSO–d_6): 172.4 (C), 171.5 (C), 155.7 (C), 78.5 (C), 53.5 (CH), 51.7 (CH), 51.2 (C), 42.0 (CH₂), 41.4 (3xCH₂), 41.0 (CH₂), 36.5 (3xCH₂), 29.2 (CH), 28.6 (3xCH₃), 24.8 (CH), 24.6 (CH), 23.5 (CH₃), 23.3 (CH₃), 22.3 (CH₃), 22.2 (CH₃); MS (ESI, MeOH): 478 (100, [M+H]⁺).
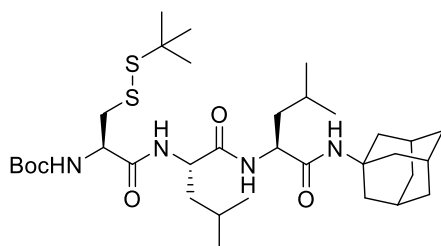
Compound 304 (2.2 g, 71%, colorless solid) was prepared from **303** (2.6 g, 5.4 mmol) and **271** (2.0 g, 6.5 mmol) following the general procedures A and D. R_f (CH₂Cl₂/MeOH 15:1): 0.60; Mp: 213 – 214 °C; $[\alpha]_D^{20}$ –44.8 (*c* 1.00, CHCl₃); IR (neat): 3276 (w), 3074 (w), 2909 (w), 2853 (w), 1720 (w), 1637 (s), 1527 (m), 1455 (w), 1389 (w), 1363 (m), 1313 (w), 1272 (w), 1246 (w), 1163 (s), 1047 (w), 1020 (w), 935 (w), 871 (w), 778 (w), 619 (w); ¹H NMR (400 MHz, DMSO–d_6): 7.97 (d, $^3J_{H-H}$ = 8.1 Hz, 1H), 7.68 (d, $^3J_{H-H}$ = 8.5 Hz, 1H), 7.15 (d, $^3J_{H-H}$ = 8.2 Hz, 1H), 7.09 (s, 1H),

4.31 – 4.07 (m, 3H), 3.06 – 2.84 (m, 2H), 2.06 – 1.93 (m, 3H), 1.87 (d, $^3J_{H–H}$ = 2.9 Hz, 6H), 1.66 – 1.47 (m, 8H), 1.47 – 1.32 (m, 13H), 1.28 (s, 9H), 0.93 – 0.74 (m, 12H); ^{13}C NMR (100 MHz, DMSO–d_6): 171.6 (C), 171.3 (C), 170.5 (C), 155.7 (C), 78.9 (C), 54.5 (CH), 51.9 (CH), 51.8 (CH), 51.2 (C), 48.1 (C), 42.8 (CH$_2$), 41.6 (CH$_2$), 41.3 (3xCH$_2$), 41.2 (CH$_2$), 36.5 (3xCH$_2$), 30.0 (CH), 29.3 (3xCH$_3$), 28.6 (3xCH$_3$), 24.6 (CH), 24.5 (CH), 23.49 (CH$_3$), 23.47 (CH$_3$), 22.22 (CH$_3$), 22.18 (CH$_3$); MS (ESI, MeOH): 669 (100, [M+H]$^+$).
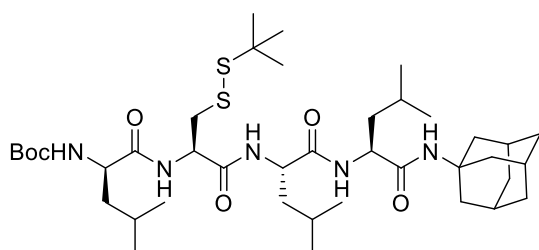
Compound 305 (1.7 g, 65%, colorless solid) was prepared from **304** (2.2 g, 3.3 mmol) and Boc–L–Leu–OH (0.93 g, 4.0 mmol) following the general procedures A and D. R_f (CH$_2$Cl$_2$/MeOH 15:1): 0.50; Mp: 223 – 224 ^{o}C; [α]$_D^{20}$ –101 (c 1.00, CHCl$_3$); IR (neat): 3279 (w), 3079 (w), 2957 (w), 2910 (w), 2869 (w), 1720 (w), 1634 (s), 1532 (m), 1455 (w), 1389 (w), 1363 (m), 1313 (w), 1248 (w), 1165 (m), 1046 (w), 1019 (w), 935 (w), 872 (w), 778 (w), 675 (w); ^{1}H NMR (400 MHz, DMSO–d_6): 8.16 – 8.01 (m, 2H), 7.59 (d, $^3J_{H–H}$ = 8.5 Hz, 1H), 7.08 (s, 1H), 6.99 (d, $^3J_{H–H}$ = 7.7 Hz, 1H), 4.58 – 4.44 (m, 1H), 4.32 – 4.10 (m, 2H), 4.01 – 3.86 (m, 1H), 3.10 (dd, $^2J_{H–H}$ = 12.9 Hz, $^3J_{H–H}$ = 5.5 Hz, 1H), 2.94 (dd, $^2J_{H–H}$ = 12.9 Hz, $^3J_{H–H}$ = 8.3 Hz, 1H), 2.06 – 1.95 (m, 3H), 1.89 (d, $^3J_{H–H}$ = 2.9 Hz, 6H), 1.72 – 1.49 (m, 9H), 1.49 – 1.33 (m, 15H), 1.29 (s, 9H), 0.94 – 0.75 (m, 18H); ^{13}C NMR (100 MHz, DMSO–d_6): 173.3 (C), 171.5 (C), 171.2 (C), 170.0 (C), 155.9 (C), 78.7 (C), 53.7 (CH), 52.7 (CH), 52.0 (CH), 51.9 (CH), 51.2 (C), 48.1 (C), 42.8 (CH$_2$), 41.6 (CH$_2$), 41.3 (3xCH$_2$), 41.2 (CH$_2$), 41.0 (CH$_2$), 36.5 (3xCH$_2$), 30.0 (CH), 29.3 (3xCH$_3$), 28.6 (3xCH$_3$), 24.7 (CH), 24.63 (CH), 24.56 (CH), 23.5 (CH$_3$), 23.4 (CH$_3$), 23.3 (CH$_3$), 22.2 (CH$_3$), 22.10 (CH$_3$), 22.06 (CH$_3$); MS (ESI, MeOH): 783 (100, [M+H]$^+$).
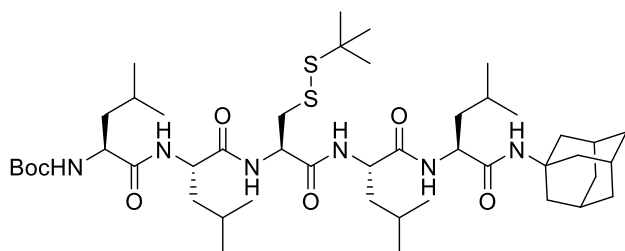
Compound 306 (1.4 g, 73%, colorless solid) was prepared from **305** (1.7 g, 2.2 mmol) and Boc–L–Leu–OH (0.60 g, 2.6 mmol) following the general

procedures A and D. R_f (CH$_2$Cl$_2$/MeOH 25:1): 0.34; Mp: 239 – 240 °C (decomp); $[\alpha]_D^{20}$ –138

(*c* 1.00, CHCl$_3$); IR (neat): 3281 (w), 3084 (w), 2957 (w), 2911 (w), 2869 (w), 1720 (w), 1690

(w), 1630 (s), 1532 (m), 1467 (w), 1389 (w), 1363 (m), 1313 (w), 1274 (w), 1248 (w), 1215

(w), 1164 (m), 1045 (w), 1018 (w), 936 (w), 873 (w), 778 (w), 689 (m), 621 (w); ^{1}H NMR (400

MHz, DMSO–d_6): 8.23 (d, $^3J_{H-H}$ = 7.7 Hz, 1H), 8.04 (d, $^3J_{H-H}$ = 8.1 Hz, 1H), 7.84 (d, $^3J_{H-H}$ =

7.9 Hz, 1H), 7.58 (d, $^3J_{H-H}$ = 8.5 Hz, 1H), 7.07 (s, 1H), 6.94 (d, $^3J_{H-H}$ = 8.2 Hz, 1H), 4.58 – 4.44

(m, 1H), 4.37 – 4.09 (m, 3H), 4.02 – 3.87 (m, 1H), 3.09 (dd, $^2J_{H-H}$ = 12.9 Hz, $^3J_{H-H}$ = 5.6 Hz,

1H), 2.91 (dd, $^2J_{H-H}$ = 12.9 Hz, $^3J_{H-H}$ = 8.4 Hz, 1H), 2.06 – 1.95 (m, 3H), 1.89 (d, $^3J_{H-H}$ = 3.3

Hz, 6H), 1.67 – 1.53 (m, 10H), 1.53 – 1.33 (m, 17H), 1.29 (s, 9H), 0.95 – 0.75 (m, 24H); ^{13}C

NMR (100 MHz, DMSO–d_6): 173.0 (C), 172.7 (C), 171.5 (C), 171.2 (C), 169.9 (C), 155.8 (C),

78.5 (C), 53.3 (CH), 52.8 (CH), 52.0 (CH), 51.9 (CH), 51.5 (CH), 51.2 (C), 48.1 (C), 42.5

(CH$_2$), 41.6 (CH$_2$), 41.5 (CH$_2$), 41.3 (3xCH$_2$), 40.9 (2xCH$_2$), 36.5 (3xCH$_2$), 30.0 (CH), 29.3

(3xCH$_3$), 28.6 (3xCH$_3$), 24.7 (CH), 24.62 (CH), 24.56 (CH), 24.4 (CH), 23.52 (CH$_3$), 23.49

(2xCH$_3$), 23.4 (CH$_3$), 22.2 (CH$_3$), 22.13 (2xCH$_3$), 22.06 (CH$_3$); MS (ESI, MeOH): 895 (100,

[M+H]$^+$).
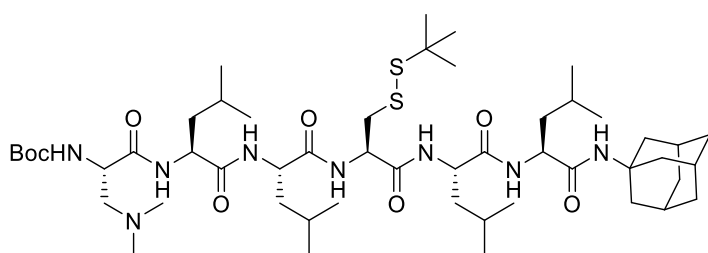
Compound 307 (0.5 g, 19%, colorless solid) was prepared from **306** (2.4 g, 2.7 mmol) and **270** (0.73 g, 3.1 mmol)

following the general procedures A and D. R_f (CH$_2$Cl$_2$/MeOH 15:1): 0.43; Mp: 227 – 228 °C

(decomp); $[\alpha]_D^{20}$ –124 (c 1.00, CHCl$_3$); IR (neat): 3273 (w), 3081 (w), 2956 (w), 2911 (w), 2868 (w), 1721 (w), 1692 (w), 1629 (s), 1534 (m), 1458 (m), 1388 (w), 1363 (m), 1276 (w), 1246 (w), 1166 (m), 1095 (w), 1050 (w), 1020 (w), 920 (w), 867 (w), 780 (w), 701 (m); ^{1}H NMR (300 MHz, CDCl$_3$): 7.63 – 7.45 (m, 2H), 7.22 (d, $^3J_{H-H}$ = 6.7 Hz, 1H), 7.13 (s, 1H), 7.05 (d, $^3J_{H-H}$ = 8.1 Hz, 1H), 6.28 (s, 1H), 5.77 (s, 1H), 4.49 – 4.34 (m, 1H), 4.33 – 4.17 (m, 2H), 4.13 – 3.94 (m, 3H), 3.32 (dd, $^2J_{H-H}$ = 13.4 Hz, $^3J_{H-H}$ = 3.0 Hz, 1H), 3.08 (dd, $^2J_{H-H}$ = 13.4 Hz, $^3J_{H-H}$ = 11.9 Hz, 1H), 2.73 (dd, $^2J_{H-H}$ = 12.3 Hz, $^3J_{H-H}$ = 6.1 Hz, 1H), 2.52 (dd, $^2J_{H-H}$ = 12.3 Hz, $^3J_{H-H}$ = 9.4 Hz, 1H), 2.29 (s, 6H), 2.14 – 1.95 (m, 9H), 1.92 – 1.53 (m, 18H), 1.48 (s, 9H), 1.34 (s, 9H), 1.06 – 0.79 (m, 24H); ^{13}C NMR (100 MHz, CDCl$_3$): 173.5 (C), 173.2 (C), 172.3 (C), 171.4 (C), 170.8 (C), 170.6 (C), 156.0 (C), 80.5 (C), 58.2 (CH$_2$), 53.5 (CH), 53.4 (CH), 53.1 (CH), 52.6 (CH), 52.5 (CH), 51.8 (CH), 50.7 (C), 47.1 (C), 44.1 (2xCH$_3$), 40.1 (3xCH$_2$), 39.3 (CH$_2$), 39.1 (CH$_2$), 38.5 (CH$_2$), 38.29 (CH$_2$), 38.26 (CH$_2$), 35.5 (3xCH$_2$), 29.0 (CH), 28.5 (3xCH$_3$), 27.2 (3xCH$_3$), 24.1 (2xCH), 23.89 (CH), 23.85 (CH), 22.5 (CH$_3$), 22.4 (CH$_3$), 22.0 (2xCH$_3$), 20.6 (CH$_3$), 20.2 (CH$_3$), 20.1 (CH$_3$), 19.9 (CH$_3$); MS (ESI, MeOH): 1009 (100, [M+H]$^+$).
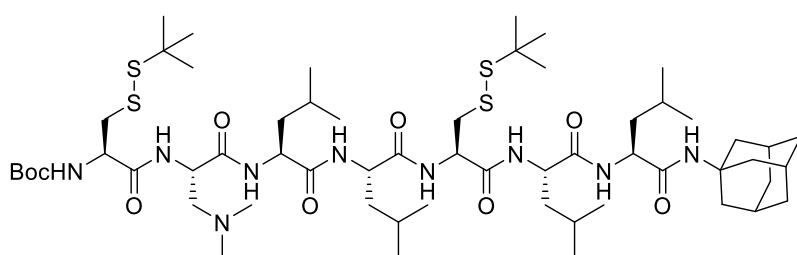
Compound 175 (260 mg, 44%, colorless solid) was prepared from **307** (498 mg, 0.494 mmol) and **271** (183 mg, 0.591 mmol) following the general procedures A and D. R_f (CH$_2$Cl$_2$/MeOH 15:1): 0.37; Mp: 234 – 235 °C (decomp); $[\alpha]_D^{20}$ –130 (c 1.00, CHCl$_3$); IR (neat): 3261 (w), 2926 (w), 1722 (w), 1629 (s), 1529 (m), 1362 (w), 1249 (w), 1163 (m), 1047 (w), 701 (w); ^{1}H NMR (400 MHz, CDCl$_3$): 7.77 – 7.53 (m, 3H), 7.44 (d, $^3J_{H-H}$ = 5.3 Hz, 1H), 7.29 (d, $^3J_{H-H}$ = 7.9 Hz, 1H), 7.10 (d, $^3J_{H-H}$ = 7.9 Hz, 1H), 6.31 (s, 1H), 5.56 (d, $^3J_{H-H}$ = 3.8 Hz, 1H), 4.47 – 4.16

(m, 5H), 4.10 – 3.91 (m, 2H), 3.32 (dd, $^2J_{H-H}$ = 13.3 Hz, $^3J_{H-H}$ = 2.9 Hz, 1H), 3.15 – 3.03 (m, 2H), 2.91 (dd, $^2J_{H-H}$ = 13.8 Hz, $^3J_{H-H}$ = 8.4 Hz, 1H), 2.81 – 2.57 (m, 2H), 2.27 (s, 6H), 2.10 – 1.96 (m, 9H), 1.87 – 1.55 (m, 18H), 1.45 (s, 9H), 1.40 – 1.27 (m, 18H), 1.04 – 0.82 (m, 24H); ^{13}C NMR (100 MHz, CDCl$_3$): 175.2 (C), 175.0 (C), 172.9 (C), 172.6 (C), 172.4 (C), 172.0 (C), 171.8 (C), 156.4 (C), 81.5 (C), 58.4 (CH$_2$), 55.1 (CH), 54.8 (CH), 54.6 (CH), 54.1 (CH), 53.6 (CH), 53.3 (CH), 53.0 (CH), 51.7 (C), 49.1 (C), 48.1 (C), 45.2 (2xCH$_3$), 41.1 (3xCH$_2$), 40.2 (CH$_2$), 40.0 (CH$_2$), 39.5 (CH$_2$), 39.3 (CH$_2$), 39.0 (CH$_2$), 36.5 (3xCH$_2$), 30.1 (CH), 29.9 (3xCH$_3$), 29.6 (3xCH$_3$), 28.2 (3xCH$_3$), 25.12 (CH), 25.07 (CH), 24.9 (CH), 24.8 (CH), 23.6 (CH$_3$), 23.4 (CH$_3$), 23.3 (CH$_3$), 23.1 (CH$_3$), 21.1 (CH$_3$), 21.0 (CH$_3$), 20.9 (2xCH$_3$); MS (ESI, MeOH): 1200 (100, [M+H]+); HRMS (ESI, +ve) calcd for C$_{58}$H$_{105}$N$_9$O$_9$S$_4$ ([M+Na]$^+$): 1222.6810, found: 1222.6827.
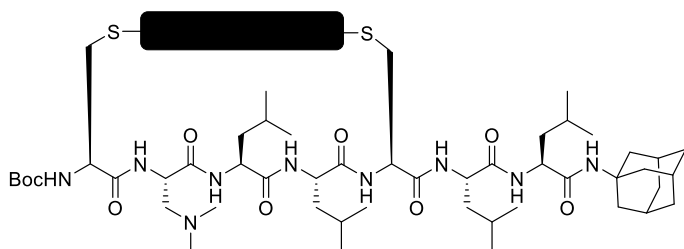
Compound 169 (46 mg, 16%, atropisomers not detectable, red solid) was prepared from **175** (200 mg, 0.167 mmol) following the general procedures F and G. R_f (CH$_2$Cl$_2$/MeOH 15:1): 0.40; Mp: 176 – 177 °C; UV-Vis (TFE): 520 (13.8), 373 (10.7), 295 (34.6); CD (TFE): 529 (–10.0), 377 (+12.9), 318 (–3.9), 299 (+5.0), 244 (–1.2), 209 (+34.4); IR (neat): 3294 (w), 2924 (w), 1645 (s), 1526 (m), 1440 (m), 1365 (w), 1313 (m), 1214 (m), 1160 (m); ^{1}H NMR (400 MHz, CDCl$_3$): 9.73 (s, 1H), 8.96 (s, 1H), 8.82 (s, 1H), 7.16 – 6.92 (m, 2H), 6.65 (s, 1H), 6.51 (s, 1H), 5.99 – 5.82 (m, 2H), 5.79 – 5.69 (m, 1H), 5.70 – 5.61 (m, 1H), 5.51 – 5.20 (m, 2H), 5.12 (d, $^3J_{H-H}$ = 8.5 Hz, 1H), 4.87 – 4.47 (m, 2H), 4.28 – 4.20 (m, 1H), 4.13 – 3.82 (m, 5H), 3.60 – 3.46 (m, 1H), 3.32 – 3.139 (m, 4H), 2.95 – 2.80 (m, 1H), 2.78 – 2.68 (m, 1H), 2.39 – 2.33 (m, 1H), 2.30 – 2.23 (m, 6H), 2.19 – 2.13 (m, 2H), 2.03 – 2.00 (m, 3H), 1.99 – 1.96 (m, 6H), 1.65 – 1.60 (m, 10H), 1.55 – 1.50 (m, 4H),

1.41 – 1.37 (m, 6H), 1.34 – 1.31 (m, 6H), 1.28 – 1.22 (m, 9H), 1.01 – 0.90 (m, 35H), 0.86 – 0.83 (m, 3H) , 0.61 – 0.52 (m, 3H) , 0.44 – 0.22 (m, 3H); ^{13}C NMR (125 MHz, CDCl$_3$): 173.1 (C), 172.6 (2xC), 172.3 (C), 171.7 (C), 170.8 (C), 169.5 (C), 168.9 (C), 168.3 (C), 163.6 (C), 163.0 (C), 162.6 (C), 161.7 (C), 154.1 (C), 142.8 (2xC), 129.8 (CH), 126.8 (CH), 126.1 (C), 125.8 (C), 125.5 (C), 125.1 (C), 123.6 (C), 119.0 (C), 80.2 (C), 58.5 (CH$_2$), 54.1 (CH), 53.8 (CH), 53.3 (CH), 52.5 (CH), 52.4 (CH), 52.3 (CH), 51.9 (C), 51.8 (CH), 51.7 (CH), 48.8 (CH), 44.5 (CH$_3$), 42.2 (CH$_3$), 41.3 (CH$_2$), 41.1 (CH$_2$), 40.3 (2xCH$_2$), 40.1 (CH$_2$), 38.6 (CH$_2$), 38.1 (CH$_2$), 37.6 (CH$_2$), 36.5 (3xCH$_2$), 36.4 (CH$_2$), 31.6 (CH$_2$), 31.4 (CH$_2$), 29.5 (CH$_2$), 29.4 (CH), 28.2 (3xCH$_3$), 27.4 (CH$_2$), 26.8 (CH$_2$), 26.6 (CH$_2$), 26.0 (CH), 25.7 (CH), 25.1 (CH), 24.8 (2xCH), 24.7 (CH), 24.4 (CH$_2$), 24.3 (CH$_2$), 23.81 (CH$_2$), 23.78 (CH$_2$), 23.6 (CH$_3$), 23.3 (2xCH$_3$), 23.1 (CH$_3$), 22.9 (CH$_3$, 2xCH$_3$), 22.6 (CH$_2$), 22.5 (CH$_2$), 22.4 (CH$_3$), 22.2 (CH$_3$), 21.9 (CH$_3$), 20.2 (CH$_3$), 14.1 (CH$_3$), 14.0 (CH$_3$), 13.7 (CH$_3$); HPLC–MS: R_t = 3.11 min, 1682 (100, [M+H]$^+$); HRMS (ESI, +ve) calcd for C$_{88}$H$_{137}$N$_{13}$O$_{15}$S$_2$ ([M+Na]$^+$): 1702.9691, found: 1702.9684.

5.2.3. Alkyl-Bridged PDIs

Compound 177 was synthesized as described previously.[236]

Compound 180 was synthesized as described previously.[237]
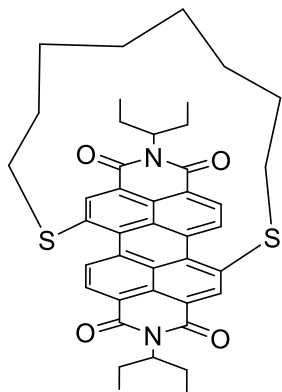
Compound 182. (17 mg, 17%, dark purple solid) was prepared from 1,8-Octanedithiol (27 µl, 0.15 mmol) following the general procedures G. The residue after work-up was purified by flash chromatography (CH$_2$Cl$_2$/pentane 4:1). R_f (CH$_2$Cl$_2$/pentane 4:1): 0.43; ^{1}H NMR (400 MHz, CDCl$_3$): 9.25 (d, $^3J_{H-H}$ = 8.0 Hz, 2H), 8.88 (s, 2H), 8.64 (d, $^3J_{H-H}$ = 8.0 Hz, 2H), 5.14 – 5.03 (m, 2H), 2.89 – 2.72 (m, 4H), 2.37 – 2.20 (m, 4H), 2.06 - 1.91 (m, 4H), 1.43 - 1.35 (m, 2H), 1.16 – 1.08 (m, 2H), 1.03 - 0.82 (m, 12H), 0.61 – 0.37 (m, 6H), 0.35 – 0.20 (m, 2H); ^{13}C NMR (125 MHz, CDCl$_3$): 164.5 (2xC), 163.5 (2xC), 138.4 (2xCH), 136.4 (2xC), 135.9 (2xC), 132.8 (2xC), 130.0 (2xCH), 128.6 (2xCH), 128.4 (2xC), 127.0 (2xC), 122.8 (2xC), 121.7 (2xC), 57.8 (2xCH), 36.0 (2xCH$_2$), 30.8 (2xCH$_2$), 28.4 (2xCH$_2$), 27.1 (2xCH$_2$), 25.1 (4xCH$_2$), 11.5 (4xCH$_3$); MS (MALDI-TOF): 704 ([M]$^+$). Two enantiomers of **182** were separated by preparative chiral HPLC using chiralpak ID column (CH$_2$Cl$_2$/n–hexane 1:1, 2 mL/min, rt; detection: 544 nm), **182a** (78% ee, R_t = 26.5 min), **182b** (95% ee, R_t = 28.6 min).
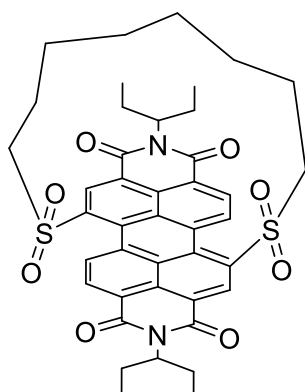
Compound 183. To a solution of **182** (18 mg, 25 µmol) in CH$_2$Cl$_2$ (1.2 ml), *m*-CPBA (64 mg, 0.27 mmol) was added. Reaction mixture was stirred at rt overnight. The reaction mixture was diluted with CH$_2$Cl$_2$, then washed with aqueous saturated solution of NaHCO$_3$ (3 times). The organic layer was dried over anhydrous Na$_2$SO$_4$, filtered and concentrated under vacuum. The residue was purified by PTLC (MeOH/CH$_2$Cl$_2$ 1:40) to yield desired product (9 mg, 45%) as a red solid. R_f (MeOH/CH$_2$Cl$_2$ 1:35): 0.74; Mp: 266 – 267 °C; IR (neat): 2931 (w), 1700 (m), 1658 (s), 1588 (m), 1459 (w), 1399 (w), 1384 (w), 1329 (m), 1299 (m), 1240

(m), 1203 (w), 1149 (w), 1124 (m), 1088 (w), 980 (w), 877 (w), 798 (w), 733 (w), 701 (w); ^{1}H NMR (400 MHz, CDCl$_3$): 9.52 (s, 2H), 9.37 (d, $^3J_{H-H}$ = 7.9 Hz, 2H), 8.87 (d, $^3J_{H-H}$ = 7.9 Hz, 2H), 5.15 -5.02 (m, 2H), 3.33 – 3.13 (m, 4H), 2.38 – 2.21 (m, 4H), 2.08 – 1.91 (m, 4H), 1.43 – 1.25 (m, 4H), 1.04 – 0.87 (m, 12H), 0.77 – 0.65 (m, 2H), 0.62 – 0.44 (m, 2H), 0.38 – 0.16 (m, 4H); ^{13}C NMR (100 MHz, CDCl$_3$): 163.1 (br, 4xC), 138.9 (2xC), 135.1 (2xCH), 134.0 (2xC), 132.3 (2xCH), 132.1 (2xCH), 131.6 (2xC), 128.8 (2xC), 127.9 (2xC), 124.6 (2xC), 123.6 (2xC), 58.4 (2xCH), 53.5 (2xCH$_2$), 27.5 (2xCH$_2$), 26.3 (2xCH$_2$), 25.0 (4xCH$_2$), 23.5 (2xCH$_2$), 11.4 (4xCH$_3$); MS (MALDI-TOF): 767 ([M]$^+$). **183a** and **183b** were synthesized by similar procedure from enantio-enriched **182a** and **182b**, respectively.

5.2.4.   PDI-Peptide Conjugates
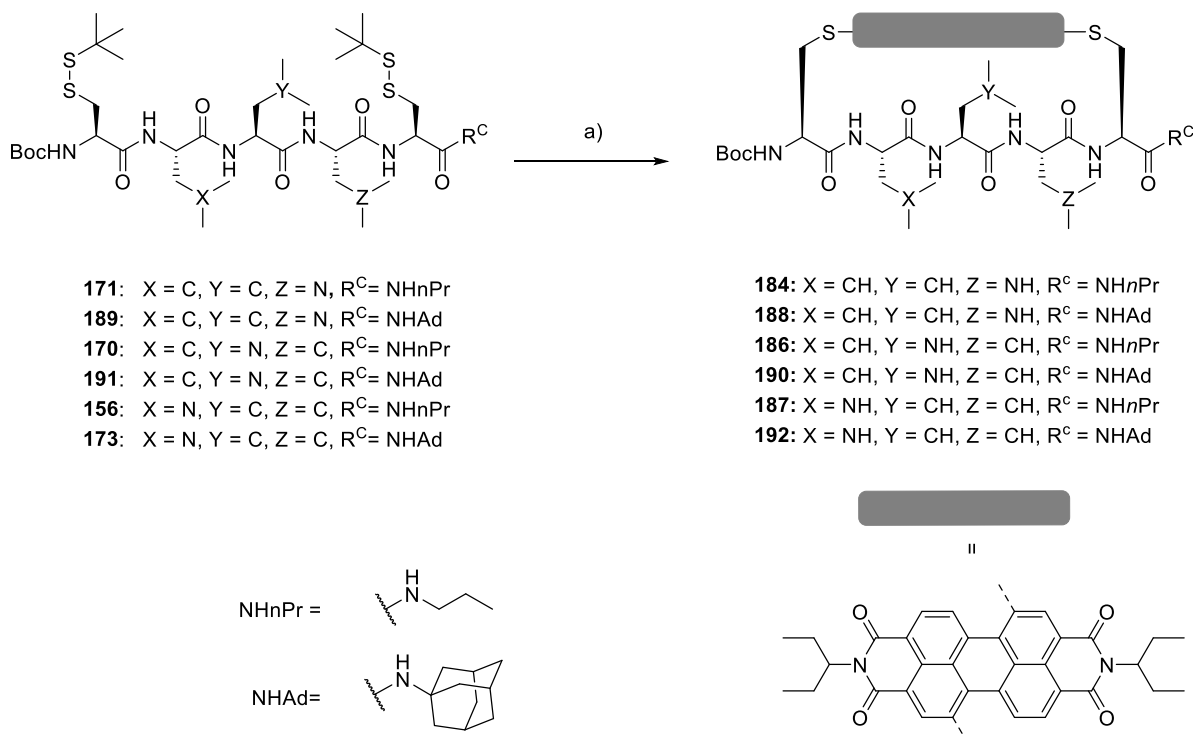
Scheme 20. (a) 1. PBu$_3$, TEA, H$_2$O, TFE, rt, overnight; 2. **180**, TCEP·HCl, CH$_3$CN/buffer 3:1, 65 °C, overnight, 10% (**184a**), 8% (**184b**), 19% (**188**), 1% (**186a**), 6% (**186b**), 9% (**190a**), 13% (**190b**), 4% (**187a**), 10% (**187b**), 9% (**192a**), 11% (**192b**).
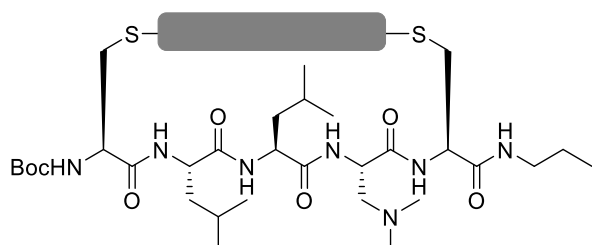
Compound 184. 184a (20 mg, 10%, dark purple solid) and **184b** (16 mg, 8%, dark red solid) was prepared from **171** (150 mg, 0.170 mmol) following the general procedures F and G. R_f (CH$_2$Cl$_2$/MeOH 15:1): 0.39 (**184a**), 0.38 (**184b**). **184a** and **184b** were separated using PTLC (CH$_2$Cl$_2$/MeOH 15:1). **184a.** Mp: 187 – 188 °C; CD (TFE): 598(+16.4), 477(+12.0), 427(-8.6), 376 (–9.7), 322 (–1.8), 238 (+19.2), 257 (-23.8); IR (neat): 3314 (w),

2929 (m), 1696 (m), 1658 (s), 1587 (m), 1529 (m), 1463 (m), 1399 (m), 1383 (m), 1326 (m), 1278 (m), 1242 (s), 1206 (m), 1156 (m), 1093 (m), 944 (w), 859 (w), 810 (w), 750 (w), 701 (w), 662 (w); ^{1}H NMR (400 MHz, CDCl$_3$): 9.89 (d, $^3J_{H-H}$ = 8.1 Hz, 1H), 9.13 (d, $^3J_{H-H}$ = 8.1 Hz, 1H), 8.82 (s, 1H), 8.79 (s, 1H), 8.65 (d, $^3J_{H-H}$ = 8.1 Hz, 1H), 8.51 (d, $^3J_{H-H}$ = 8.1 Hz, 1H), 7.04 (d, $^3J_{H-H}$ = 8.8 Hz, 1H), 6.72 – 6.60 (m, 2H), 6.32 (d, $^3J_{H-H}$ = 4.7 Hz, 1H), 5.71 (d, $^3J_{H-H}$ = 4.5 Hz, 1H), 5.65 (d, $^3J_{H-H}$ = 4.3 Hz, 1H), 5.22 – 5.15 (m, 1H), 5.13 – 5.02 (m, 2H), 4.24 (dd, $^2J_{H-H}$ = 15.3 Hz, $^3J_{H-H}$ = 2.5 Hz, 1H), 4.02 – 3.93 (m, 2H), 3.92 – 3.84 (m, 2H), 3.68 – 3.60 (m, 1H), 3.21 – 3.05 (m, 2H), 2.78 (dd, $^2J_{H-H}$ = 15.2 Hz, $^3J_{H-H}$ = 6.2 Hz, 1H), 2.34 – 2.19 (m, 4H), 2.15 (dd, $^2J_{H-H}$ = 9.1 Hz, $^3J_{H-H}$ = 4.8 Hz, 1H), 2.10 – 1.91 (m, 4H), 1.87 – 1.81 (m, 1H), 1.78 – 1.69 (m, 2H), 1.64 (s, 6H), 1.59 – 1.52 (m, 1H), 1.48 (s, 9H), 1.46 – 1.37 (m, 4H), 1.19 – 1.05 (m, 3H), 1.00 – 0.89 (m, 9H), 0.86 – 0.80 (m, 7H), 0.73 (d, $^3J_{H-H}$ = 6.5 Hz, 3H), 0.65 – 0.59 (m, 4H), 0.49 (d, $^3J_{H-H}$ = 6.5 Hz, 3H); ^{13}C NMR (125 MHz, CDCl$_3$): 173.1 (C), 171.8 (C), 170.8 (C), 170.2 (C), 168.5 (C), 164.0 (br, 3xC, deduced from HMBC), 156.4 (C), 140.7 (C), 137.8 (CH), 136.5 (C), 134.3 (C), 132.6 (C), 131.7 (CH), 131.4 (C), 130.3 (CH), 129.5 (C), 129.3 (C), 128.6 (2xCH), 128.12 (C), 128.07 (C), 125.8 (C), 125.1 (CH), 122.2 (C), 121.9 (2xC), 121.0 (C), 82.5 (C), 58.4 (CH$_2$), 57.9 (CH), 57.8 (CH), 54.5 (CH), 54.30 (CH), 54.26 (CH), 53.5 (CH), 52.4 (CH), 44.5 (2xCH$_3$), 41.9 (CH$_2$), 40.4 (CH$_2$), 39.0 (CH$_2$), 33.0 (CH$_2$), 30.3 (CH$_2$), 28.0 (3xCH$_3$), 25.0 (4xCH$_2$), 24.6 (CH), 24.3 (CH), 23.6 (CH$_3$), 23.0 (CH$_3$), 22.3 (CH$_2$), 21.7 (CH$_3$), 20.4 (CH$_3$), 11.8 (4xCH$_3$), 11.5 (CH$_3$); HRMS (ESI, +ve) calcd for C$_{65}$H$_{85}$N$_9$O$_{11}$S$_2$ ([M+H]$^+$): 1232.5884, found: 1232.5875.

184b. Mp: 190 – 191 ^{o}C; CD (TFE): 558 (-31.7), 364 (+8.6), 327 (+12.7), 290 (–28.7), 262 (+40.7), 222 (–27.7); IR (neat): 3302 (w), 2966 (w), 2874 (w), 1738 (w), 1696 (m), 1659 (s), 1586 (m), 1530 (m), 1457 (w), 1383 (m), 1327 (m), 1276 (w), 1237 (s), 1158 (m), 1093 (w), 943 (w), 844 (w), 809 (w), 750 (w), 700 (w), 662 (w); ^{1}H NMR (400 MHz, CDCl$_3$): 8.92 (s,

1H), 8.82 (s, 1H), 8.76 (d, $^3J_{\text{H–H}}$ = 7.9 Hz, 1H), 8.67 (d, $^3J_{\text{H–H}}$ = 7.9 Hz, 1H), 8.34 (d, $^3J_{\text{H–H}}$ = 7.9 Hz, 1H), 8.27 (d, $^3J_{\text{H–H}}$ = 7.9 Hz, 1H), 7.19 (d, $^3J_{\text{H–H}}$ = 9.4 Hz, 1H), 6.96 (dd, $^3J_{\text{H–H}}$ = 6.4 Hz, 4.8 Hz, 1H), 6.65 (d, $^3J_{\text{H–H}}$ = 4.1 Hz, 1H), 6.56 (d, $^3J_{\text{H–H}}$ = 4.5 Hz, 1H), 6.20 (d, $^3J_{\text{H–H}}$ = 4.6 Hz, 1H), 5.17 (d, $^3J_{\text{H–H}}$ = 3.8 Hz, 1H), 5.11 – 4.99 (m, 2H), 4.75 (dd, $^2J_{\text{H–H}}$ = 12.1 Hz, $^3J_{\text{H–H}}$ = 2.6 Hz, 1H), 4.66 – 4.57 (m, 1H), 4.23 – 4.15 (m, 1H), 3.92 – 3.83 (m, 1H), 3.70 – 3.63 (m, 1H), 3.54 (dd, $^2J_{\text{H–H}}$ = 15.7 Hz, $^3J_{\text{H–H}}$ = 2.1 Hz, 1H), 3.40 (dd, $^2J_{\text{H–H}}$ = 15.7, $^3J_{\text{H–H}}$ = 5.1 Hz, 1H), 3.35 – 3.25 (m, 1H), 3.19 – 3.09 (m, 1H), 3.09 – 3.00 (m, 1H), 2.32 – 2.13 (m, 4H), 2.07 – 1.87 (m, 5H), 1.79 – 1.73 (m, 1H), 1.60 – 1.50 (m, 9H), 1.49 – 1.42 (m, 3H), 1.40 – 1.31 (m, 10H), 1.12 – 1.02 (m, 2H), 1.01 – 0.90 (m, 10H), 0.87 (d, $^3J_{\text{H–H}}$ = 7.4 Hz, 3H), 0.83 (d, $^3J_{\text{H–H}}$ = 6.3 Hz, 3H), 0.80 – 0.75 (m, 1H), 0.75 – 0.67 (m, 6H), 0.53 (d, $^3J_{\text{H–H}}$ = 6.5 Hz, 3H), 0.11 – 0.02 (m, 1H); ^{13}C NMR (125 MHz, CDCl$_3$): 173.5 (C), 172.0 (C), 170.9 (C), 169.04 (C), 168.95 (C), 163.6 (br, 4xC, deduced from HMBC), 156.5 (C), 141.5 (C), 137.3 (C), 137.0 (CH), 136.8 (C), 134.3 (CH), 133.4 (C), 131.7 (C), 131.5 (CH), 131.3 (C), 130.7 (2xCH), 128.6 (CH), 127.1 (C), 126.8 (C), 126.4 (C), 125.2 (C), 123 (2xC), 122.1 (2xC), 82.2 (C), 58.6 (CH$_2$), 58.0 (CH), 57.9 (CH), 57.1 (CH), 54.4 (CH), 53.8 (CH), 53.7 (CH), 52.0 (CH), 44.6 (2xCH$_3$), 43.5 (CH$_2$), 42.1 (CH$_2$), 41.6 (CH$_2$), 38.9 (CH$_2$), 37.6 (CH$_2$), 28.0 (3xCH$_3$), 25.1 (2xCH$_2$), 25.0 (2xCH$_2$), 24.5 (CH), 24.2 (CH), 24.0 (CH$_3$), 23.1 (CH$_3$), 22.8 (CH$_3$), 22.2 (CH$_2$), 20.2 (CH$_3$), 11.5 (4xCH$_3$), 11.4 (CH$_3$); HRMS (ESI, +ve) calcd for C$_{65}$H$_{85}$N$_9$O$_{11}$S$_2$ ([M+H]$^+$): 1232.5884, found: 1232.5875.
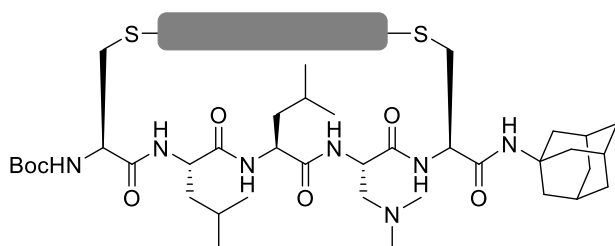
Compound 188 (mixture of 2 diastereomers 1:0.8, 39 mg, 19%, dark purple solid) was prepared from **189** (150 mg, 0.154 mmol) following the general procedures F and G. R_{f} (CH$_2$Cl$_2$/MeOH 15:1): 0.36 (**188a**), 0.35 (**188b**); IR (neat): 3294 (w), 2927 (w), 1740 (w), 1694

(m), 1655 (s), 1586 (m), 1526 (m), 1456 (m), 1398 (m), 1383 (m), 1366 (m), 1326 (m), 1239 (s), 1204 (m), 1163 (m), 1092 (w), 1050 (w), 926 (w), 857 (w), 809 (w), 750 (w), 700 (w), 665 (w), 608 (w); ^{1}H NMR (400 MHz, CDCl$_3$, nn/nn - isomers peaks): 9.91/8.76 (d, $^3J_{H-H}$ = 8.1 Hz, 1H), 9.03/8.67 (d, $^3J_{H-H}$ = 8.1 Hz, 1H), 8.92/8.83 (s, 1H), 8.83/8.79 (s, 1H), 8.65/8.37 (d, $^3J_{H-H}$ = 8.1 Hz, 1H), 8.50/8.30 (d, $^3J_{H-H}$ = 8.1 Hz, 1H), 7.25/7.19 (d, $^3J_{H-H}$ = 9.4 Hz, 1H), 6.66/6.59 (d, $^3J_{H-H}$ = 4.1/4.6 Hz, 1H), 6.28/6.46 (d, $^3J_{H-H}$ = 4.8/4.9 Hz, 1H), 6.02/6.34 (s, 1H), 5.71/6.22 (d, $^3J_{H-H}$ = 4.5/4.7 Hz, 1H), 5.55/5.10 (d, $^3J_{H-H}$ = 4.1 Hz, 1H), 5.17 – 5.00 (m, 2H), 4.27/4.67 (dd, $^2J_{H-H}$ = 15.2/12.1 Hz, $^3J_{H-H}$ = 1.9/2.6 Hz, 1H), 5.06 – 5.02/4.58 – 4.47 (m, 1H), 4.21 – 4.82 (m, 2H), 3.78 – 3.63 (m, 1H), 2.77/3.51 (dd, $^2J_{H-H}$ = 12.6/15.6 Hz, $^3J_{H-H}$ = 6.1/2.2 Hz, 1H), 3.98 – 3.84/3.38 (dd, $^2J_{H-H}$ = 15.5 Hz, $^3J_{H-H}$ = 5.1 Hz, 1H), 3.98 – 3.84/3.17 – 3.07 (m, 1H), 2.36 – 2.16 (m, 4H), 2.15 – 1.90 (m, 14H), 1.86 – 1.76 (m, 2H), 1.42 – 1.56 (m, 14H), 1.49/1.39 (s, 9H), 1.22 – 1.05 (m, 4H), 1.05 – 0.80 (m, 14H), 0.76 – 0.70 (m, 3H), 0.70 – 0.60 (m, 3H), 0.59 – 0.09 (m, 4H); ^{13}C NMR (125 MHz, CDCl$_3$, nn/nn - isomers peaks): 172.6/172.7 (C), 171.7/171.8 (C), 171.0/170.8 (C), 170.1/169.1 (C), 167.3/168.0 (C), 163.8 (br, 4xC, deduced from HMBC), 165.5 (C), 141.8/141.6 (C), 138.1/137.1 (CH), 137.5. (C), 136.62/136.59 (C), 134.5 (CH), 133.3 (C), 132.5 (C), 131.8 (CH), 131.39/131.36 (CH), 131.3 (C), 130.6 (C), 129.5/129.3 (C), 128.8/128.5 (CH), 128.14/128.0 (C), 127.2/126.9 (C), 126.6/125.5 (C), 125.2/125.1 (CH), 128.7/123.1 (C), 122.1 (C), 120.8 (C), 82.6/82.3 (C), 58.71/58.69 (CH$_2$), 58.1 (CH), 57.90/57.86 (CH), 57.1/54.6 (CH), 54.3/54.2 (CH), 54.1/53.8 (CH), 53.6/53.5 (CH), 52.54/42.57 (CH), 52.3/52.2 (C), 44.61/44.57 (2xCH$_3$), 43.5/42.1 (CH$_2$), 41.3/38.3 (3xCH$_2$), 41.1/38.9 (CH$_2$), 37.7/32.6 (CH$_2$), 36.54/36.48 (3xCH$_2$), 30.2/29.8 (CH$_2$), 29.6/29.5 (3xCH), 28.1/28.0 (3xCH$_3$), 25.1 (4xCH$_2$), 24.7/24.6 (CH), 24.41/24.37 (CH), 23.9/23.6 (CH$_3$), 23.1/23.0 (CH$_3$), 22.9/21.5 (CH$_3$), 20.4/20.3 (CH$_3$), 11.5 (4xCH$_3$); MS (ESI, MeOH): 1325 (100, [M+H]$^+$).
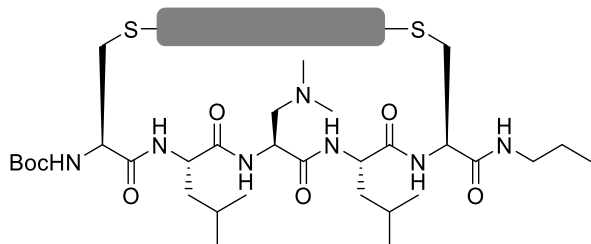
Compound 186. 186a (2 mg, 1%, dark purple solid) and **186b** (10 mg, 6%, dark red solid) was prepared from **170** (125 mg, 0.142 mmol) following the general procedures F and G. R_f (CH$_2$Cl$_2$/MeOH 15:1): 0.38 (**186a**), 0.37 (**186b**). **186a** and **186b** were separated using PTLC (CH$_2$Cl$_2$/MeOH 15:1). **186a.** Mp: 189 – 190 °C; CD (TFE): 590 (+26.0), 476 (+18.5), 426 (-12.0), 347 (–14.9), 322 (+27.6), 258 (–37.1), 216 (+27.8); IR (neat): 3294 (w), 2962 (w), 2930 (w), 2875 (w), 1695 (m), 1655 (s), 1585 (m), 1528 (m), 1461 (m), 1398 (m), 1383 (m), 1326 (m), 1239 (s), 1202 (m), 1162 (m), 1090 (w), 1054 (w), 919 (w), 843 (w), 798 (w), 750 (w), 699 (w); ^{1}H NMR (400 MHz, CDCl$_3$): 10.00 (d, $^3J_{H-H}$ = 8.1 Hz, 1H), 9.11 (d, $^3J_{H-H}$ = 8.1 Hz, 1H), 8.84 (s, 1H), 8.82 (s, 1H), 8.66 (d, $^3J_{H-H}$ = 8.1 Hz, 1H), 8.53 (d, $^3J_{H-H}$ = 8.1 Hz, 1H), 6.96 (d, $^3J_{H-H}$ = 8.8 Hz, 1H), 6.77 (d, $^3J_{H-H}$ = 3.4 Hz, 1H), 6.58 (t, $^3J_{H-H}$ = 5.6 Hz, 1H), 6.48 (d, $^3J_{H-H}$ = 6.1 Hz, 1H), 5.84 (d, $^3J_{H-H}$ = 3.5 Hz, 1H), 5.74 (d, $^3J_{H-H}$ = 5.6 Hz, 1H), 5.20 – 5.13 (m, 1H), 5.10 – 4.99 (m, 2H), 4.22 (dd, $^2J_{H-H}$ = 15.3 Hz, $^3J_{H-H}$ = 2.6 Hz, 1H), 4.00 (dd, $^2J_{H-H}$ = 15.3 Hz, $^3J_{H-H}$ = 5.1 Hz, 1H), 3.96 – 3.88 (m, 2H), 3.86 – 3.79 (m, 1H), 3.72 – 3.66 (m, 1H), 3.18 – 3.07 (m, 2H), 2.77 (dd, $^2J_{H-H}$ = 15.2 Hz, $^3J_{H-H}$ = 6.3 Hz, 1H), 2.47 – 2.32 (m, 2H), 2.32 – 2.16 (m, 4H), 2.06 (s, 6H), 2.03 – 1.94 (m, 4H), 1.50 (s, 9H), 1.46 – 1.36 (m, 3H), 1.11 – 1.05 (m, 3H), 0.97 – 0.93 (m, 6H), 0.88 – 0.79 (m, 10H), 0.75 – 0.71 (m, 1H), 0.66 (d, $^3J_{H-H}$ = 6.6 Hz, 3H), 0.59 (d, $^3J_{H-H}$ = 6.4 Hz, 3H), 0.49 (d, $^3J_{H-H}$ = 6.5 Hz, 3H), 0.21 – 0.08 (m, 4H); ^{13}C NMR (125 MHz, CDCl$_3$): 172.6 (C), 171.6 (C), 171.2 (C), 171.1 (C), 168.7 (C), 163.7 (br, 4xC, deduced from HMBC), 155.6 (C), 140.7 (C), 138.0 (CH), 136.6 (C), 134.4 (C), 132.5 (C), 131.9 (CH), 131.4 (C), 130.9 (CH), 129.33 (C), 129.30 (C), 128.8 (CH), 128.6 (CH), 128.1 (C), 128.0 (C), 125.9 (C), 125.2 (CH), 124.1 (2xC), 121.8 (C), 120.3 (C), 82.2 (C), 58.5 (CH$_2$), 58.0 (CH), 57.8 (CH), 54.5 (CH), 54.2 (CH), 53.32 (CH), 53.26 (CH), 52.8 (CH), 44.7 (2xCH$_3$), 41.8 (CH$_2$), 40.1 (CH$_2$), 38.5 (CH$_2$), 33.6 (CH$_2$), 30.7 (CH$_2$), 28.0 (3xCH$_3$), 25.04 (2xCH$_2$),

24.95 (2xCH$_2$),.24.5 (CH), 24.3 (CH), 23.4 (CH$_3$), 23.3 (CH$_3$), 22.5 (CH$_2$), 21.7 (CH$_3$), 19.9 (CH$_3$), 11.5 (5xCH$_3$); MS (ESI, MeOH): 1232 (100, [M+H]$^+$).

186b. Mp: 173 – 174 $^\text{o}$C; CD (TFE): 558 (-28.1), 366 (+9.4), 326 (+9.4), 289 (–28.6), 262 (+43.3), 222 (–32.8); IR (neat): 3309 (w), 2961 (w), 2928 (w), 2874 (w), 1693 (m), 1657 (s), 1585 (m), 1528 (m), 1461 (m), 1398 (m), 1383 (m), 1326 (m), 1240 (s), 1202 (w), 1162 (m), 1090 (w), 1050 (w), 923 (w), 844 (w), 809 (w), 798 (w), 750 (w), 700 (w), 664 (w), 609 (w); ^{1}H NMR (400 MHz, CDCl$_3$): 8.93 (s, 1H), 8.82 (s, 1H), 8.75 (d, $^3J_{\text{H–H}}$ = 8.0 Hz, 1H), 8.66 (d, $^3J_{\text{H–H}}$ = 8.0 Hz, 1H), 8.37 (d, $^3J_{\text{H–H}}$ = 8.0 Hz, 1H), 8.35 (d, $^3J_{\text{H–H}}$ = 8.0 Hz, 1H), 7.11 (d, $^3J_{\text{H–H}}$ = 9.2 Hz, 1H), 7.02 (d, $^3J_{\text{H–H}}$ = 3.4 Hz, 1H), 6.79 (t, $^3J_{\text{H–H}}$ = 5.6 Hz, 1H), 6.44 (d, $^3J_{\text{H–H}}$ = 5.6 Hz, 1H), 6.31 (d, $^3J_{\text{H–H}}$ = 3.8 Hz, 1H), 5.17 (d, $^3J_{\text{H–H}}$ = 6.0 Hz, 1H), 5.10 – 4.98 (m, 2H), 4.74 (dd, $^2J_{\text{H–H}}$ = 12.3, $^3J_{\text{H–H}}$ = 2.5 Hz, 1H), 4.66 – 4.56 (m, 1H), 4.22 – 4.14 (m, 1H), 3.85 – 3.75 (m, 1H), 3.70 – 3.62 (m, 1H), 3.58 (dd, $^2J_{\text{H–H}}$ = 15.0 Hz, $^3J_{\text{H–H}}$ = 2.7 Hz, 1H), 3.31 – 3.25 (m, 1H), 3.24 – 3.18 (m, 1H), 3.17 – 3.13 (m, 1H), 3.12 – 3.05 (m, 1H), 2.43 (dd, $^2J_{\text{H–H}}$ = 12.6 Hz, $^3J_{\text{H–H}}$ = 4.9 Hz, 1H), 2.32 (dd, $^2J_{\text{H–H}}$ = 12.6 Hz, $^3J_{\text{H–H}}$ = 9.8 Hz, 1H), 2.27 – 2.13 (m, 4H), 2.05 (s, 6H), 2.01 – 1.89 (m, 4H), 1.81 -1.80 (m, 1H), 1.69 – 1.64 (m, 1H), 1.55 – 1.47 (m, 2H), 1.42 (s, 9H), 1.16 – 1.06 (m, 2H), 0.99 – 0.91 (m, 9H), 0.88 – 0.83 (m, 6H), 0.71 (d, $^3J_{\text{H–H}}$ = 6.6 Hz, 3H), 0.59 (d, $^3J_{\text{H–H}}$ = 6.5 Hz, 3H), 0.52 (d, $^3J_{\text{H–H}}$ = 6.4 Hz, 3H), 0.40 – 0.29 (m, 1H), 0.25 – 0.13 (m, 4H); ^{13}C NMR (125 MHz, CDCl$_3$): 172.6 (C), 171.7 (C), 171.4 (C), 169.9 (C), 169.1 (C), 164.2 (br, 2xC, deduced from HMBC), 163.3 (br, 2xC, deduced from HMBC), 155.5 (C), 141.5 (C), 137.6 (CH), 137.2 (C), 136.4 (C), 134.7 (CH), 133.4 (C), 131.8 (C), 131.5 (CH), 131.5 (C), 130.7 (2xCH), 128.5 (CH), 127.2 (C), 126.9 (C), 126.5 (C), 125.1 (C), 123.3 (C), 122.8 (C), 122.3 (C), 121.8 (C), 81.9 (C), 58.1 (CH$_2$), 58.0 (CH), 57.9 (CH), 56.4 (CH), 54.3 (CH), 53.6 (CH), 53.1 (CH), 52.2 (CH), 44.8 (2xCH$_3$), 44.0 (CH$_2$), 42.1 (CH$_2$), 41.6 (CH$_2$), 38.4 (CH$_2$), 37.9 (CH$_2$), 28.0 (3xCH$_3$), 25.0 (4xCH$_2$), 24.9 (CH), 24.6 (CH$_3$), 23.6 (CH$_3$), 23.2

(CH$_3$), 22.8 (CH$_3$), 22.2 (CH$_2$), 20.4 (CH$_3$), 11.44 (4xCH$_3$), 11.40 (CH$_3$); MS (ESI, MeOH): 1232 (100, [M+H]$^+$).
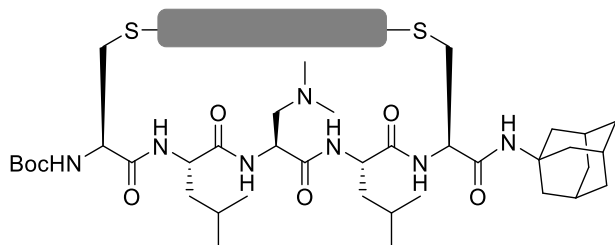
Compound 190. 190a (19 mg, 9%, dark purple solid) and **190b** (13 mg, 13%, dark red solid) was prepared from **191** (150 mg, 0.154 mmol) following the general procedures F and G. R_f (CH$_2$Cl$_2$/MeOH 15:1): 0.37 (**190a**), 0.34 (**190b**). **190a** and **190b** were separated using PTLC (CH$_2$Cl$_2$/MeOH 15:1) **190a.** Mp: 202 – 203 °C; CD (TFE): 585 (+34.3), 470 (+23.5), 423 (-18.0), 372 (–22.1), 322 (+36.2), 254 (–48.2), 216 (+35.8); IR (neat): 3322 (w), 2960 (w), 2910 (w), 1695 (m), 1657 (s), 1586 (m), 1525 (m), 1461 (m), 1398 (m), 1382 (m), 1325 (m), 1240 (s), 1205 (m), 1162 (m), 1092 (w), 1052 (w), 926 (w), 858 (w), 843 (w), 809 (w), 798 (w), 750 (w), 700 (w), 664 (w); ^{1}H NMR (400 MHz, CDCl$_3$): 10.02 (d, $^3J_{H-H}$ = 8.1 Hz, 1H), 9.01 (d, $^3J_{H-H}$ = 8.1 Hz, 1H), 8.85 (s, 1H), 8.83 (s, 1H), 8.68 (d, $^3J_{H-H}$ = 8.1 Hz, 1H), 8.53 (d, $^3J_{H-H}$ = 8.1 Hz, 1H), 7.22 (d, $^3J_{H-H}$ = 8.5 Hz, 1H), 6.73 (d, $^3J_{H-H}$ = 3.3 Hz, 1H), 6.42 (d, $^3J_{H-H}$ = 6.2 Hz, 1H), 5.92 (s, 1H), 5.79 – 5.73 (m, 2H), 5.15 – 5.02 (m, 3H), 4.26 (dd, $^2J_{H-H}$ = 15.1 Hz, $^3J_{H-H}$ = 2.1 Hz, 1H), 3.95 – 3.87 (m, 3H), 3.87 – 3.72 (m, 2H), 2.77 (dd, $^2J_{H-H}$ = 15.0 Hz, $^3J_{H-H}$ = 6.1 Hz, 1H), 2.52 – 2.35 (m, 2H), 2.34 – 2.18 (m, 4H), 2.07 (s, 6H), 2.01 – 1.94 (m, 12H), 1.63 – 1.56 (m, 8H), 1.51 (s, 9H), 1.08 – 0.71 (m, 17H), 0.66 (d, $^3J_{H-H}$ = 6.7 Hz, 3H), 0.60 (d, $^3J_{H-H}$ = 6.3 Hz, 3H), 0.47 (d, $^3J_{H-H}$ = 6.4 Hz, 3H), 0.21 – 0.10 (m, 4H); ^{13}C NMR (125 MHz, CDCl$_3$): 172.8 (C), 171.4 (C), 170.9 (C), 170.7 (C), 167.4 (C), 163.5 (br, 4xC, deduced from HMBC), 155.6 (C), 141.6 (C), 138.1 (CH), 136.7 (C), 134.4 (C), 132.3 (C), 131.8 (CH), 131.3 (C), 130.1 (CH), 129.3 (C), 129.2 (C), 128.9 (CH), 128.4 (2xCH), 128.1 (C), 127.8 (C), 125.6 (C), 125.1 (CH), 124.0 (C), 122.3 (C), 120.6 (C), 82.1 (C), 58.5 (CH$_2$), 57.9 (CH), 57.8 (CH), 54.3 (CH), 54.2 (CH), 53.4 (CH), 53.2 (CH), 52.8 (CH), 52.2 (C), 44.5

(2xCH$_3$), 40.8 (3xCH$_2$), 40.6 (CH$_2$), 38.7 (CH$_2$), 36.4 (3xCH$_2$), 33.2 (2xCH$_2$), 30.6 (CH$_2$), 29.4 (3xCH), 27.9 (3xCH$_3$), 25.1 (2xCH$_2$), 24.9 (2xCH$_2$), 24.5 (CH), 24.3 (CH), 23.4 (CH$_3$), 23.2 (CH$_3$), 21.3 (CH$_3$), 19.9 (CH$_3$), 11.5 (4xCH$_3$); MS (ESI, MeOH): 1325 (100, [M+H]$^+$).

190b. Mp: 201 – 202 ^{o}C; CD (TFE): 549 (-36.7), 366 (+11.7), 288 (-39.8), 262 (+55.2), 223 (–48.0); IR (neat): 3325 (w), 2958 (w), 2909 (w), 1695 (m), 1657 (s), 1586 (m), 1519 (m), 1459 (m), 1397 (m), 1383 (m), 1367 (m), 1326 (m), 1238 (s), 1203 (m), 1162 (m), 1092 (w), 1046 (w), 919 (w), 843 (w), 809 (w), 798 (w), 750 (w), 700 (w), 667 (w); ^{1}H NMR (400 MHz, CDCl$_3$): 8.92 (s, 1H), 8.83 (s, 1H), 8.75 (d, $^3J_{H-H}$ = 8.0 Hz, 1H), 8.67 (d, $^3J_{H-H}$ = 8.0 Hz, 1H), 8.47 – 8.40 (m, 2H), 7.11 (d, $^3J_{H-H}$ = 9.2 Hz, 1H), 6.98 (br s, 1H), 6.42 (br s, 1H), 6.32 (d, $^3J_{H-H}$ = 4.2 Hz, 1H), 6.19 (s, 1H), 5.13 – 5.01 (m, 2H), 4.97 (d, $^3J_{H-H}$ = 6.6 Hz, 1H), 4.60 (d, $^2J_{H-H}$ = 12.2 Hz, 1H), 4.57 – 4.48 (m, 1H), 4.23 – 4.16 (m, 1H), 3.94 – 3.82 (m, 1H), 3.69 – 3.62 (m, 1H), 3.54 (dd, $^2J_{H-H}$ = 15.0 Hz, $^3J_{H-H}$ = 3.0 Hz, 1H), 3.27 (dd, $^2J_{H-H}$ = 15.0 Hz, $^3J_{H-H}$ = 4.2 Hz, 1H), 3.21 – 3.10 (m, 1H), 2.43 (dd, $^2J_{H-H}$ = 12.7 Hz, $^3J_{H-H}$ = 5.5 Hz, 1H), 2.38 – 2.31 (m, 1H), 2.29 – 2.18 (m, 4H), 2.09 – 2.03 (m, 10H), 2.03 – 1.94 (m, 10H), 1.87 – 1.76 (m, 1H), 1.71 – 1.65 (m, 4H), 1.44 (s, 9H), 1.21 – 1.10 (m, 1H), 1.09 – 0.88 (m, 16H), 0.72 (d, $^3J_{H-H}$ = 6.6 Hz, 3H), 0.65 (d, $^3J_{H-H}$ = 6.5 Hz, 3H), 0.53 (d, $^3J_{H-H}$ = 5.8 Hz, 3H), 0.51 – 0.39 (m, 1H), 0.32 – 0.17 (m, 4H); ^{13}C NMR (125 MHz, CDCl$_3$): 172.4 (C), 171.2 (C), 170.9 (C), 169.7 (C), 167.1 (C), 163.8 (br, 4xC, deduced from HMBC), 155.3 (C), 141.5 (C), 137.7 (CH), 137.2 (C), 137.9 (C), 134.4 (CH), 133.1 (C), 131.9 (C), 131.5 (C), 131.3 (CH), 130.7 (CH), 130.4 (CH), 128.5 (CH), 127.3 (C), 127.0 (C), 126.7 (C), 125.1 (C). 123.1 (2xC), 122.0 (2xC), 81.9 (C), 58.1 (CH$_2$), 58.0 (CH), 57.9 (CH), 56.0 (CH), 54.2 (CH), 53.1 (CH), 52.6 (CH), 52.3 (CH), 44.8 (2xCH$_3$), 43.7 (CH$_2$), 41.7 (CH$_2$), 41.3 (3xCH$_2$), 38.3 (CH$_2$), 38.1 (CH$_2$), 36.4 (3xCH$_2$), 29.5 (3xCH), 28.0 (3xCH$_3$), 25.0 (4xCH$_2$), 24.9 (CH), 24.7 (CH), 23.3 (CH$_3$), 23.2 (CH$_3$), 22.8 (CH$_3$), 20.4 (CH$_3$), 11.4 (4xCH$_3$); MS (ESI, MeOH): 1325 (100, [M+H]$^+$).
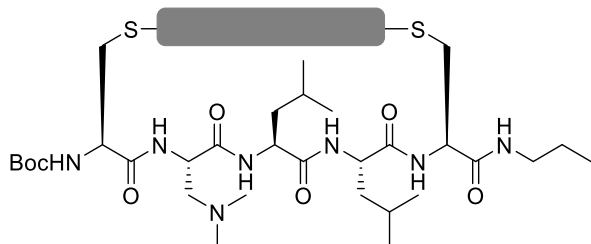
Compound 187. 187a (7 mg, 4%, dark purple solid) and **187b** (18 mg, 10%, dark red solid) was prepared from **156** (150 mg, 0.170 mmol) following the general procedures F and G. R_f (CH$_2$Cl$_2$/MeOH 15:1): 0.32 (**187a**), 0.31 (**187b**). **187a** and **187b** were separated using PTLC (CH$_2$Cl$_2$/MeOH 15:1) **187a.** Mp: 199 – 200 °C; CD (TFE): 592 (+23.2), 475 (+17.3), 426 (-10.5), 374 (–12.9), 322 (+26.0), 257 (–32.3), 216 (+30.4); IR (neat): 3313 (w), 2961 (w), 2934 (w), 2875 (w), 1694 (m), 1655 (s), 1586 (m), 1527 (m), 1460 (m), 1383 (m), 1325 (m), 1239 (s), 1205 (m), 1162 (m), 1091 (w), 924 (w), 844 (w), 809 (w), 750 (w), 700 (w), 663 (w); ^{1}H NMR (400 MHz, CDCl$_3$): 9.90 (d, $^3J_{H-H}$ = 8.1 Hz, 1H), 9.13 (d, $^3J_{H-H}$ = 8.1 Hz, 1H), 8.83 (s, 1H), 8.76 (s, 1H), 8.66 (d, $^3J_{H-H}$ = 8.1 Hz, 1H), 8.53 (d, $^3J_{H-H}$ = 8.1 Hz, 1H), 6.84 (d, $^3J_{H-H}$ = 4.8 Hz, 1H), 6.77 (d, $^3J_{H-H}$ = 6.0 Hz, 1H), 6.58 (d, $^3J_{H-H}$ = 8.9 Hz, 1H), 6.53 (t, $^3J_{H-H}$ = 5.6 Hz, 1H), 6.36 (d, $^3J_{H-H}$ = 6.2 Hz, 1H), 5.79 (d, $^3J_{H-H}$ = 4.6 Hz, 1H), 5.19 – 5.11 (m, 1H), 5.10 – 4.97 (m, 2H), 4.23 (dd, $^2J_{H-H}$ = 15.4 Hz, $^3J_{H-H}$ = 2.5 Hz, 1H), 4.05 – 3.98 (m, 1H), 3.94 (dd, $^2J_{H-H}$ = 15.2 Hz, $^3J_{H-H}$ = 1.7 Hz, 1H), 3.88 – 3.82 (m, 2H), 3.80 – 3.73 (m, 1H), 3.28 – 3.10 (m, 2H), 2.82 (dd, $^2J_{H-H}$ = 15.2 Hz, $^3J_{H-H}$ = 6.3 Hz, 1H), 2.29 – 2.11 (m, 6H), 2.07 – 1.94 (m, 4H), 1.90 (s, 6H), 1.70 – 1.61 (m, 2H), 1.49 – 1.41 (m, 12H), 1.38 – 1.29 (m, 2H), 1.19 (dd, $^2J_{H-H}$ = 13.9 Hz, $^3J_{H-H}$ = 6.2 Hz, 1H), 0.98 – 0.91 (m, 10H), 0.87 – 0.81 (m, 8H), 0.71 (d, $^3J_{H-H}$ = 6.4 Hz, 3H), 0.61 (d, $^3J_{H-H}$ = 5.9 Hz, 3H), 0.23 – 0.13 (m, 4H); ^{13}C NMR (125 MHz, CDCl$_3$): 173.3 (C), 172.5 (C), 172.1 (C), 170.9 (C), 168.5 (C), 164.6 (C), 163.3 (br, 3xC, deduced from HMBC), 156.3 (C), 140.6 (C), 138.1 (CH), 136.5 (C), 134.3 (C), 132.6 (C), 131.7 (CH), 131.1 (C), 130.4 (CH), 129.5 (C), 129.2 (C), 128.6 (CH), 128.4 (CH), 128.3 (C), 128.1 (C), 125.9 (C), 125.1 (CH), 123.9 (C), 122.5 (C), 120.9 (C), 82.2 (C), 58.1 (CH), 57.9 (CH), 57.0 (CH$_2$), 54.7 (CH), 54.3 (CH), 53.9 (CH), 53.1 (CH), 52.3 (CH), 46.9 (2xCH$_3$), 41.9 (CH$_2$), 39.4 (CH$_2$), 38.4 (CH$_2$), 32.9 (CH$_2$), 30.1 (CH$_2$), 28.0 (3xCH$_3$), 25.0 (4xCH$_2$), 24.40

(CH), 24.37 (CH), 23.3 (CH$_3$), 23.2 (CH$_3$), 22.3 (CH$_2$), 20.1 (CH$_3$), 20.0 (CH$_3$), 11.6 (5xCH$_3$);

MS (ESI, MeOH): 1232 (100, [M+H]$^+$).

187b. Mp: 182 – 183 ^{o}C; CD (TFE): 559 (-38.4), 365 (+10.1), 326 (+16.7), 289 (–34.4), 262 (+50.7), 222 (–37.4); IR (neat): 3310 (w), 2961 (w), 2931 (w), 2874 (w), 1693 (m), 1656 (s), 1585 (m), 1527 (m), 1461 (m), 1398 (m), 1383 (m), 1326 (m), 1239 (s), 1203 (m), 1162 (m), 1091 (w), 1054 (w), 955 (w), 923 (w), 843 (w), 809 (w), 798 (w), 750 (w), 700 (w), 672 (w);^{1}H NMR (400 MHz, CDCl$_3$): 8.95 (s, 1H), 8.82 (s, 1H), 8.75 (d, $^3J_{H–H}$ = 7.9 Hz, 1H), 8.67 (d, $^3J_{H–H}$ = 8.0 Hz, 1H), 8.35 (d, $^3J_{H–H}$ = 8.0 Hz, 1H), 8.26 (d, $^3J_{H–H}$ = 7.9 Hz, 1H), 7.08 (d, $^3J_{H–H}$ = 5.8 Hz, 1H), 6.92 (d, $^3J_{H–H}$ = 4.4 Hz, 1H), 6.88 (d, $^3J_{H–H}$ = 9.5 Hz, 1H), 6.84 (t, $^3J_{H–H}$ = 5.5 Hz, 1H), 6.38 (d, $^3J_{H–H}$ = 5.3 Hz, 1H), 5.38 (d, $^3J_{H–H}$ = 3.6 Hz, 1H), 5.14 – 4.96 (m, 2H), 4.79 (dd, $^2J_{H–H}$ = 12.3 Hz, $^3J_{H–H}$ = 2.6 Hz, 1H), 4.68 – 4.55 (m, 1H), 4.16 – 3.98 (m, 1H), 3.81 – 3.76 (m, 1H), 3.75 – 3.68 (m, 1H), 3.59 (dd, $^2J_{H–H}$ = 15.6 Hz, $^3J_{H–H}$ = 1.9 Hz, 1H), 3.37 (dd, $^2J_{H–H}$ = 15.6 Hz, $^3J_{H–H}$ = 5.1 Hz, 1H), 3.33 – 3.23 (m, 1H), 3.13 – 3.03 (m, 2H), 2.37 – 2.12 (m, 5H), 2.04 – 1.92 (m, 4H), 1.88 (s, 6H), 1.84 – 1.79 (m, 1H), 1.57 – 1.43 (m, 5H), 1.39 (s, 9H), 1.14 – 1.04 (m, 2H), 0.96 – 0.91 (m 9H), 0.88 – 0.81 (m, 9H), 0.78 – 0.65 (m, 4H), 0.55 (d, $^3J_{H–H}$ = 6.4 Hz, 3H), 0.29 – 0.15 (m, 4H); ^{13}C NMR (125 MHz, CDCl$_3$): 173.6 (C), 172.7 (C), 172.5 (C), 169.3 (C), 169.0 (C), 164.0 (br, 4xC, deduced from HMBC), 156.6 (C), 141.5 (C), 137.3 (C, CH – peaks overlap), 134.6 (CH), 133.6 (C), 131.8 (CH), 131.52 (C), 131.46 (C), 130.8 (CH), 130.5 (CH), 128.5 (CH), 127.1 (C), 126.8 (C), 126.4 (C), 123.6 (C), 122.6 (3xC), 121.9 (C), 81.8 (C), 57.9 (2xCH), 57.2 (CH), 56.8 (CH$_2$), 54.3 (CH), 53.8 (CH), 53.1 (CH), 52.0 (CH), 46.5 (2xCH$_3$), 44.0 (CH$_2$), 42.4 (CH$_2$), 41.7 (CH$_2$), 39.1 (CH$_2$), 38.4 (CH$_2$), 28.0 (3xCH$_3$), 25.1 (2xCH$_2$), 24.9 (2xCH$_2$), 24.8 (CH), 24.4 (CH), 23.1 (CH$_3$), 22.8 (CH$_3$), 22.2 (CH$_2$), 20.4 (CH$_3$), 20.2 (CH$_3$), 11.4 (5xCH$_3$); MS (ESI, MeOH): 1232 (100, [M+H]$^+$).
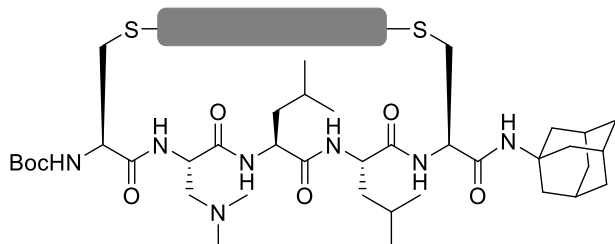
Compound 192. 192a (18 mg, 9%, dark purple solid) and **192b** (23 mg, 11%, dark red solid) was prepared from **173** (150 mg, 0.154 mmol) following the general procedures F and G. R_f (CH$_2$Cl$_2$/MeOH 15:1): 0.34 (**192a**), 0.32 (**192b**). **192a** and **192b** were separated using PTLC (CH$_2$Cl$_2$/MeOH 15:1). **192a.** Mp: 215 – 216 °C (decomp); CD (TFE): 596 (+20.4), 477 (+14.9), 427 (-10.8), 376 (–12.1), 323 (+24.2), 256 (–29.3), 217 (+20.6); IR (neat): 3316 (w), 2932 (w), 1831 (w), 1741 (m), 1696 (m), 1657 (s), 1586 (m), 1520 (m), 1453 (m), 1381 (m), 1326 (m), 1277 (m), 1237 (s), 1147 (s), 1093 (m), 944 (w), 843 (w), 798 (w), 751 (w), 700 (w), 662 (w); ^{1}H NMR (400 MHz, CDCl$_3$): 9.87 (d, $^3J_{H-H}$ = 8.1 Hz, 1H), 9.12 (d, $^3J_{H-H}$ = 8.1 Hz, 1H), 8.83 (s, 1H), 8.75 (s, 1H), 8.67 (d, $^3J_{H-H}$ = 8.1 Hz, 1H), 8.50 (d, $^3J_{H-H}$ = 8.1 Hz, 1H), 6.88 (d, $^3J_{H-H}$ = 8.6 Hz, 1H), 6.85 (d, $^3J_{H-H}$ = 4.6 Hz, 1H), 6.59 (d, $^3J_{H-H}$ = 6.1 Hz, 1H), 6.29 (d, $^3J_{H-H}$ = 6.3 Hz, 1H), 5.92 (s, 1H), 5.78 (d, $^3J_{H-H}$ = 4.6 Hz, 1H), 5.07 – 5.00 (m, 3H), 4.22 (dd, $^2J_{H-H}$ = 15.4 Hz, $^3J_{H-H}$ = 2.1 Hz, 1H), 3.99 – 3.90 (m, 2H), 3.89 – 3.1 (m, 4H), 2.81 (dd, $^2J_{H-H}$ = 15.2 Hz, $^3J_{H-H}$ = 6.4 Hz, 1H), 2.28 – 2.15 (m, 5H), 2.13 – 2.07 (m, 1H), 2.05 – 1.93 (m, 15H), 1.86 (s, 6H), 1.60 – 1.55 (m, 7H) 1.44 (s, 9H), 1.40 – 1.28 (m, 3H), 11.08 (dd, $^2J_{H-H}$ = 13.6 Hz, $^3J_{H-H}$ = 5.8 Hz, 1H), 0.99 – 0.91 (m, 10H), 0.82 (d, $^3J_{H-H}$ = 6.4 Hz, 3H), 0.68 (d, $^3J_{H-H}$ = 6.4 Hz, 3H), 0.59 (d, $^3J_{H-H}$ = 5.4 Hz, 3H), 0.22 – 0.14 (m, 4H); ^{13}C NMR (125 MHz, CDCl$_3$): 172.8 (C), 172.6 (C), 171.8 (C), 170.9 (C), 167.3 (C), 165.5 (C), 163.7 (br, 3xC, deduced from HMBC), 156.3 (C), 141.2 (C), 138.1 (CH), 136.5 (C), 134.4 (C), 132.5 (C), 131.8 (CH), 130.8 (C), 129.6 (C, CH – peaks overlap), 129.2 (C), 128.5 (CH), 128.22 (CH), 128.15 (C), 125.7 (C), 124.9 (CH), 123.9 (C), 122.4 (2xC), 121.2 (2xC), 82.2 (C), 58.0 (CH), 57.8 (CH), 57.1 (CH$_2$), 54.5 (CH), 54.4 (CH), 54.0 (CH), 52.9 (CH), 52.5 (CH), 52.4 (C), 46.8 (2xCH$_3$), 40.8 (3xCH$_2$), 39.1 (CH$_2$), 38.5 (CH$_2$), 36.5 (3xCH$_2$), 31.9 (CH$_2$), 30.0 (CH$_2$), 29.5 (3xCH), 28.0 (3xCH$_3$), 25.0 (4xCH$_2$), 24.4 (2xCH), 23.3 (CH$_3$), 23.2 (CH$_3$), 20.0 (CH$_3$), 19.9

(CH_3); 11.5 ($4xCH_3$); HRMS (ESI, +ve) calcd for $C_{72}H_{93}N_9O_{11}S_2$ ([M+H]$^+$): 1324.6509, found: 1324.6520.

192b. Mp: 211 – 212 ^{o}C (decomp); CD (TFE): 561 (-22.9), 367 (+6.2), 328 (+7.3), 291 (–20.5), 262 (+30.5), 221 (–22.9); IR (neat): 3291 (w), 2931 (w), 1694 (s), 1658 (s), 1586 (m), 1527 (m), 1513 (m), 1455 (w), 1383 (m), 1328 (m), 1277 (w), 1237 (s). 1205 (m), 1149 (s), 1092 (s), 945 (w), 843 (w), 798 (w), 751 (w), 700 (w), 663 (w); ^{1}H NMR (400 MHz, CDCl$_3$): 8.94 (s, 1H), 8.82 (s, 1H), 8.75 (d, $^3J_{H-H}$ = 8.0 Hz, 1H), 8.66 (d, $^3J_{H-H}$ = 8.0 Hz, 1H), 8.36 (d, $^3J_{H-H}$ = 8.0 Hz, 1H), 8.24 (d, $^3J_{H-H}$ = 8.0 Hz, 1H), 7.09 (d, $^3J_{H-H}$ = 5.9 Hz, 1H), 6.89 (d, $^3J_{H-H}$ = 9.5 Hz, 1H), 6.85 (d, $^3J_{H-H}$ = 4.8 Hz, 1H), 6.30 (d, $^3J_{H-H}$ = 5.7 Hz, 1H), 6.26 (s, 1H), 5.14 – 5.03 (m, 3H), 4.71 (dd, $^2J_{H-H}$ = 12.2 Hz, $^3J_{H-H}$ = 2.6 Hz, 1H), 4.58 – 4.51 (m, 1H), 4.08 – 4.04 (m, 1H), 3.87 – 3.80 (m, 1H), 3.79 – 3.72 (m, 1H), 3.53 (dd, $^2J_{H-H}$ = 15.5 Hz, $^3J_{H-H}$ = 2.0 Hz, 1H), 3.35 (dd, $^2J_{H-H}$ = 15.5 Hz, $^3J_{H-H}$ = 5.1 Hz, 1H), 3.13 – 3.03 (m, 1H), 2.30 – 2.15 (m, 3H), 2.06 – 2.01 (m, 11H), 1.89 (s, 6H), 1.67 – 1.57 (m, 13H), 1.56 – 1.45 (m, 3H), 1.39 (s, 9H), 1.33 - 1.28 (m, 1H), 1.24 – 1.18 (m, 1H), 1.00 – 0.89 (m, 11H), 0.83 (d, $^3J_{H-H}$ = 6.2 Hz, 3H), 0.71 (d, $^3J_{H-H}$ = 6.2 Hz, 3H), 0.54 (d, $^3J_{H-H}$ = 6.1 Hz, 3H), 0.25 – 0.13 (m, 4H); ^{13}C NMR (125 MHz, CDCl$_3$): 172.7 (C), 172.5 (C), 172.2 (C), 169.1 (C), 168.1 (C), 164.7 (C), 163.7 (br, 3xC, deduced from HMBC), 156.4 (C), 141.9 (C), 137.4 (C), 137.3 (CH), 136.9 (C), 134.5 (CH), 133.4 (C), 131.6 (CH), 131.54 (C), 131.47 (C), 130.6 (2xCH), 128.3 (CH), 127.1 (C), 126.7 (C), 126.5 (C), 125.0 (C), 123.5 (C), 122.7 (2xC), 121.7 (C), 81.9 (C), 57.9 (2xCH), 57.0 (CH), 56.7 (CH$_2$), 53.9 (CH), 53.5 (CH), 52.9 (CH), 52.4 (C), 52.0 (CH), 46.5 (2xCH$_3$), 44.0 (CH$_2$), 42.3 (CH$_2$), 41.2 (3xCH$_2$), 39.1 (CH$_2$), 38.3 (CH$_2$), 36.4 (3xCH$_2$), 29.5 (3xCH), 28.0 (3xCH$_3$), 25.2 (2xCH$_2$), 25.0 (2xCH$_2$), 24.8 (CH), 24.5 (CH), 23.1 (CH$_3$), 22.8 (CH$_3$), 20.3 (CH$_3$), 20.2 (CH$_3$), 11.5 (4xCH$_3$); HRMS (ESI, +ve) calcd for $C_{72}H_{93}N_9O_{11}S_2$ ([M+H]$^+$): 1324.6509, found: 1324.6520.

196: n = 0, m = 0, l = 1
198: n = 0, m = 1, l = 1
206: n = 2, m = 0, l = 1
207: n = 1, m = 0, l = 2

195: n = 0, m = 0, l = 1
197: n = 0, m = 1, l = 1
199: n = 2, m = 0, l = 1
200: n = 1, m = 0, l = 2
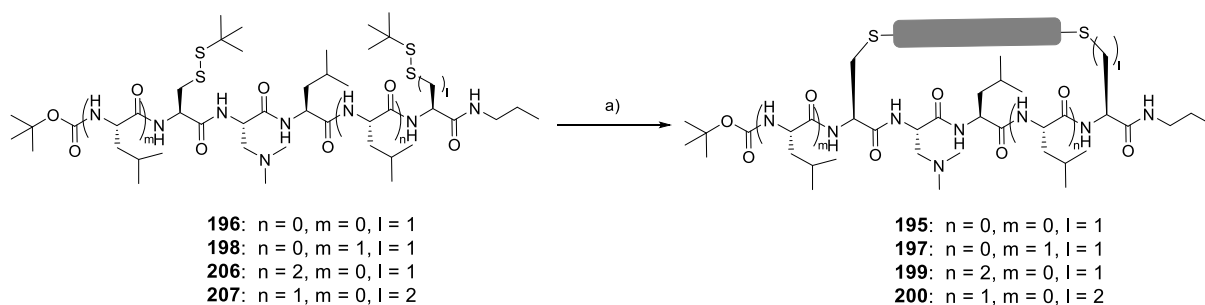
Scheme 21. (a) 1. PBu$_3$, TEA, H$_2$O, TFE, rt, overnight; 2. **180**, TCEP·HCl, CH$_3$CN/buffer 3:1, 65 °C, overnight, 19% (**195a**), 7% (**195b**), 5% (**197a**), 9% (**197b**), 8% (**199a**), 3% (**199b**), 10% (**200a**), 21% (**200b**).
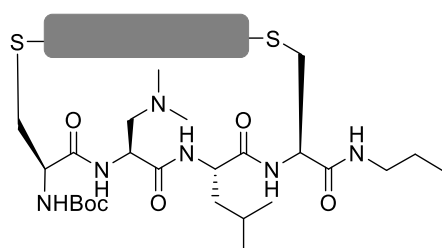
Compound 195. 195a (42 mg, 19%, dark red solid) and **195b** (15 mg, 7%, dark red solid) was prepared from **196** (150 mg, 0.195 mmol) following the general procedures F and G. R_f (CH$_2$Cl$_2$/MeOH 15:1): 0.31.

195a and **195b** were separated using chiral flash chromatography (Column: IF, Eluent CH$_2$Cl$_2$/MeOH gradient from 0% of MeOH to 3% of MeOH, flow rate: 7 ml/min) **195a.** Mp: 177 – 178 °C; CD (TFE): 555 (-28.7), 421 (+1.9), 365 (+12.0), 331 (–12.1), 299 (–18.8), 261 (+37.0), 223 (-42.0); IR (neat): 3307 (w), 2962 (w), 2932 (w), 2875 (w), 1695 (s), 1655 (s), 1585 (m), 1500 (m), 1460 (m), 1397 (m), 1383 (m), 1325 (s), 1240 (s), 1203 (m), 1163 (m), 1091 (w), 1046 (w), 917 (w), 856 (w), 843 (w), 809 (w), 798 (w), 750 (w), 732 (w), 700 (w); ^{1}H NMR (400 MHz, CDCl$_3$): 9.35 (br s, 1H), 8.99 (s, 1H), 8.94 (s, 1H), 8.81 (br s, 1H), 8.69 – 8.63 (m, 2H), 8.57 (d, $^3J_{H-H}$ = 8.2 Hz, 1H), 6.28 (br s, 1H), 6.22 – 6.10 (m, 2H), 5.12 – 5.05 (m, 2H), 4.95 (d, $^3J_{H-H}$ = 8.2 Hz, 1H), 4.69 – 4.55 (m, 1H), 4.07 – 3.90 (m, 3H), 3.65 – 3.57 (m, 1H), 3.41 – 3.31 (m, 1H), 3.30 – 3.22 (m, 1H), 3.09 – 3.00 (m, 3H), 2.83 – 2.66 (m, 1H), 2.33 – 2.22 (m, 4H), 2.11 (s, 6H), 2.01 - 1.93 (m, 4H), 1.76 – 1.67 (m, 1H), 1.49 – 1.44 (m, 1H), 1.35 (s, 9H), 1.30 – 1.24 (m, 2H), 0.99 – 0.93 (m, 12H), 0.86 (d, $^3J_{H-H}$ = 6.2 Hz, 3H), 0.79 (d,

$^3J_{H-H}$ = 6.3 Hz, 3H), 0.73 (t, $^3J_{H-H}$ = 7.4 Hz, 3H); ^{13}C NMR (125 MHz, CDCl$_3$): 172.3 (C),

171.2 (C), 169.9 (C), 169.0 (C), 163.8 (br, 4xC, deduced from HMBC), 154.8 (C), 136.2 (C),

136.0 (C), 135.0 (CH), 133.8 (CH), 132.8 (C), 132.6 (C), 130.0 (2xCH), 129.8 (CH), 129.3

(C), 128.7 (C), 127.9 (CH), 127.0 (C), 126.8 (C), 123.1 (3xC), 122.2 (2xC), 81.0 (C), 59.0

(CH$_2$), 58.01 (CH), 57.95 (CH), 53.1 (2xCH), 52.8 (CH), 49.2 (CH), 44.7 (2xCH$_3$), 41.5 (CH$_2$),

40.0 (CH$_2$), 37.0 (CH$_2$), 36.8 (CH$_2$), 28.3 (3xCH$_3$), 25.3 (2xCH$_2$), 25.2 (2xCH$_2$), 25.1 (CH),

22.7 (CH$_3$), 22.6 (CH$_3$), 22.2 (CH$_2$), 11.6 (4xCH$_3$), 11.4 (CH$_3$); MS (ESI, MeOH): 1120 (100,

[M+H]$^+$).

195b. Mp: 180 – 181 ^{o}C; CD (TFE): 553 (+27.0), 469 (+14.2), 409 (-3.4), 366 (–9.7), 292

(+26.1), 263 (–40.5), 229 (+30.0); IR (neat): 3330 (w), 2961 (w), 2875 (w), 1694 (s), 1657 (s),

1584 (m), 1499 (m), 1461 (m), 1383 (m), 1324 (s), 1240 (s), 1201 (m), 1163 (m), 1090 (w),

1024 (w), 919 (w), 843 (w), 798 (w), 750 (w), 699 (w); ^{1}H NMR (400 MHz, CDCl$_3$): 9.56 (br

s, 1H), 8.87 (br s, 1H), 8.78 (s, 1H), 8.74 (s, 1H), 8.65 (d, $^3J_{H-H}$ = 8.0 Hz, 1H), 8.61 (d, $^3J_{H-H}$ =

8.0 Hz, 1H), 7.02 (br s, 1H), 6.71 (br s, 1H), 6.56 (br s, 1H), 6.44 (br s, 1H), 5.48 (d, $^3J_{H-H}$ =

5.7 Hz, 1H), 5.10 – 5.02 (m, 2H), 4.47 – 4.33 (m, 1H), 4.04 - 3.91 (m, 1H), 3.86 - 3.71 (m, 1H),

3.69 – 3.60 (m, 1H), 3.57 – 3.46 (m, 1H), 3.41 – 3.29 (m, 1H), 3.29 – 3.02 (m, 3H), 2.94 – 2.81

(m, 1H), 2.61 – 2.46 (m, 1H), 2.44 – 2.33 (m, 1H), 2.29 – 2.19 (m, 4H), 2.05 (s, 6H), 2.00 –

1.93 (m, 4H), 1.86 – 1.76 (m, 1H), 1.54 – 1.44 (m, 4H), 1.41 (s, 9H), 0.99 – 0.89 (m, 15H),

0.80 (d, $^3J_{H-H}$ = 6.1 Hz, 3H), 0.69 (d, $^3J_{H-H}$ = 6.0 Hz, 3H); ^{13}C NMR (125 MHz, CDCl$_3$): 171.7

(C), 170.6 (C), 169.5 (C), 168.9 (C), 164.3 (br, 2xC), 163.3 (br,2xC), 155.2 (C), 137.5 (C),

137.1 (CH), 136.4 (C), 135.5 (CH), 134.7 (C), 133.5 (C), 133.1 (C), 132.3 (CH), 130.7 (2xCH),

129.5 (CH), 129.3 (C),, 128.7 (C), 127.3 (C), 126.8 (2xC), 123.3 (C), 122.3 (2xC), 121.2 (C),

81.0 (C), 57.9 (2xCH), 57.5 (CH$_2$), 54.5 (CH), 52.6 (2xCH), 50.8 (CH), 45.4 (2xCH$_3$), 41.4

(CH$_2$), 39.8 (CH$_2$), 39.1 (CH$_2$), 36.1 (CH$_2$), 28.2 (3xCH$_3$), 25.0 (4xCH$_2$), 24.5 (CH), 23.0

(CH$_3$), 22.5 (CH$_2$), 21.0 (CH$_3$), 11.5 (4xCH$_3$), 11.4 (CH$_3$); MS (ESI, MeOH): 1120 (100, [M+H]$^+$).
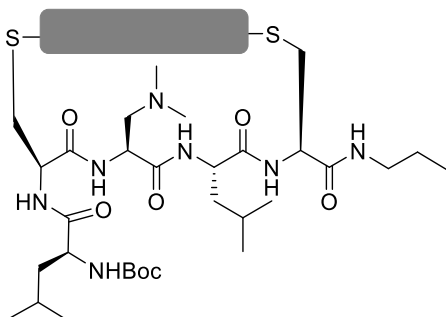
Compound 197. 197a (11 mg, 5%, dark red solid) and **197b** (19 mg, 9%, dark red solid) was prepared from **198** (150 mg, 0.170 mmol) following the general procedures F and G. R_f (CH$_2$Cl$_2$/MeOH 15:1): 0.29 (**197a**), 0.26 (**197b**). **a** and **b** were separated using PTLC (CH$_2$Cl$_2$/MeOH 15:1) **197a.** Mp: 168 – 169 °C; CD (TFE): 577 (+38.6), 476 (-17.9), 369 (-14.5), 293 (+48.8), 263 (–66.3), 230 (+48.2); IR (neat): 3315 (w), 2959 (w), 2930 (w), 2874 (w), 1694 (s), 1656 (s), 1585 (m), 1516 (m), 1461 (m), 1398 (m), 1383 (m), 1325 (s), 1241 (s), 1201 (m), 1163 (m), 1091 (w), 1046 (w), 921 (w), 856 (w), 810 (w), 798 (w), 750 (w), 698 (w), 663 (w); ^{1}H NMR (400 MHz, CDCl$_3$): 9.69 (d, $^3J_{H-H}$ = 8.0 Hz, 1H), 9.01 (d, $^3J_{H-H}$ = 8.0 Hz, 1H), 8.85 (s, 1H), 8.75 (s, 1H), 8.64 (d, $^3J_{H-H}$ = 8.0 Hz, 1H), 8.44 (d, $^3J_{H-H}$ = 8.0 Hz, 1H), 7.55 (d, $^3J_{H-H}$ = 3.4 Hz, 1H), 6.93 (d, $^3J_{H-H}$ = 3.9 Hz, 1H), 6.57 (d, $^3J_{H-H}$ = 5.7 Hz, 1H), 6.55 – 6.46 (m, 2H), 5.53 (d, $^3J_{H-H}$ = 4.0 Hz, 1H), 5.11 – 5.02 (m, 1H), 5.00 – 4.90 (m, 1H), 4.84 – 4.71 (m, 1H), 4.07 – 3.95 (m, 1H), 3.94 – 3.83 (m, 2H), 3.49 – 3.33 (m, 2H), 3.09 – 2.96 (m, 2H), 2.87 (dd, $^2J_{H-H}$ = 14.8 Hz, $^3J_{H-H}$ = 9.8 Hz, 1H), 2.73 – 2.65 (m, 1H), 2.65 – 2.57 (m, 1H), 2.36 – 2.21 (m, 4H), 2.17 – 2.10 (m, 1H), 2.05 (s, 6H), 2.02 – 1.90 (m, 3H), 1.70 (s, 9H), 1.67 – 1.56 (m, 3H), 1.44 – 1.37 (m, 3H), 1.34 – 1.29 (m, 2H), 1.19 – 1.12 (m, 1H), 0.98 – 0.78 (m, 28H); ^{13}C NMR (125 MHz, CDCl$_3$): 173.6 (C), 172.7 (C), 171.4 (C), 170.1 (C), 168.9 (C), 165.3 (2xC), 163.3 (2xC), 157.1 (C), 139.8 (C), 139.2 (CH), 138.5 (C), 137.3 (CH), 133.9 (C), 133.6 (C), 133.0 (C), 132.2 (C), 131.6 (CH), 129.6 (C), 129.2 (CH), 129.1 (CH), 128.9 (C), 128.2 (C), 127.6 (C), 126.3 (CH), 122.9 (2xC), 121.7 (2xC), 81.6 (C), 58.3 (CH$_2$), 57.9 (2xCH), 55.5 (CH), 54.3 (CH), 53.6 (CH), 52.3 (CH), 51.5 (C), 45.1 (2xCH$_3$),

41.5 (CH$_2$), 41.2 (CH$_2$), 40.9 (CH$_2$), 39.3 (CH$_2$), 37.9 (CH$_2$), 28.8 (3xCH$_3$), 25.2 (2xCH$_2$), 24.9 (2xCH$_2$), 24.8 (CH), 23.5 (CH), 22.8 (CH$_3$), 22.3 (CH$_2$), 21.8 (CH$_3$), 21.0 (2xCH$_3$), 11.6 (4xCH$_3$), 11.3 (CH$_3$); MS (ESI, MeOH): 1232 (100, [M+H]$^+$).

197b. Mp: 168 – 169 ^{o}C; CD (TFE): 570 (-23.7), 484 (–13.0), 370 (+11.2), 301 (–20.9), 263 (+39.6), 225 (–25.6); IR (neat): 3291 (w), 2960 (m), 2927 (m), 2874 (w), 1830 (w), 1694 (m), 1656 (s), 1586 (m), 1518 (m), 1459 (m), 1383 (m), 1326 (m), 1240 (m), 1202 (m), 1164 (m), 1092 (w), 918 (w), 842 (w), 798 (w), 750 (w); ^{1}H NMR (400 MHz, CDCl$_3$): 9.57 (d, $^3J_{H–H}$ = 5.1 Hz, 1H), 8.99 – 8.91 (m, 2H), 8.76 (d, $^3J_{H–H}$ = 5.1 Hz, 1H), 8.66 (d, $^3J_{H–H}$ = 8.0 Hz, 1H), 8.60 (d, $^3J_{H–H}$ = 8.0 Hz, 1H), 8.31 (br s, 1H), 6.80 (d, $^3J_{H–H}$ = 5.2 Hz, 1H), 6.25 (t, $^3J_{H–H}$ = 5.9 Hz, 1H), 6.13 (br s, 1H), 5.95 (d, $^3J_{H–H}$ = 7.9 Hz, 1H), 5.15 – 5.00 (m, 3H), 4.58 – 4.48 (m, 1H), 4.06 – 3.97 (m, 1H), 3.96 – 3.86 (m, 1H), 3.82 – 3.71 (m, 2H), 3.70 – 3.62 (m, 1H), 3.25 – 3.12 (m, 3H), 3.11 – 3.03 (m, 1H), 2.99 (dd, $^2J_{H–H}$ = 14.4 Hz, $^3J_{H–H}$ = 9.3 Hz, 1H), 2.34 – 2.20 (m, 5H), 2.15 (s, 6H), 2.01 – 1.89 (m, 6H), 1.67 – 1.53 (m, 3H), 1.48 (s, 9H), 1.41 – 1.32 (m, 3H), 1.22 – 1.14 (m, 1H), 0.96 – 0.83 (m, 24H), 0.74 (d, $^3J_{H–H}$ = 6.0 Hz, 3H); ^{13}C NMR (125 MHz, CDCl$_3$): 172.5 (C), 172.4 (C), 170.4 (C), 169.1 (C), 168.7 (C), 163.9 (br, 4xC), 155.9 (C), 136.5 (C), 135.3 (C), 135.1 (CH), 134.7 (C), 133.4 (C, CH – peaks overlap), 132.9 (C), 132.7 (C), 130.0 (2xCH), 129.7 (C), 128.9 (C), 128.8 (CH), 127.9 (CH), 127.1 (C), 126.7 (C), 123.2 (C), 122.4 (2xC), 121.8 (C), 80.5 (C), 59.1 (CH$_2$), 57.9 (CH), 57.8 (CH), 54.5 (CH), 52.9 (CH), 52.8 (CH), 51.6 (CH), 49.1 (CH), 44.6 (2xCH$_3$), 41.4 (CH$_2$), 40.6 (CH$_2$), 39.9 (CH$_2$), 37.8 (CH$_2$), 34.9 (CH$_2$), 28.4 (3xCH$_3$), 25.1 (2xCH$_2$), 25.0 (2xCH$_2$), 24.9 (CH), 24.7 (CH), 22.9 (CH$_3$), 22.7 (CH$_2$), 22.6 (CH$_3$), 22.1 (CH$_3$), 21.9 (CH$_3$), 11.5 (2xCH$_3$), 11.42 (CH$_3$), 11.38 (CH$_3$), 11.32 (CH$_3$); MS (ESI, MeOH): 1232 (100, [M+H]$^+$).
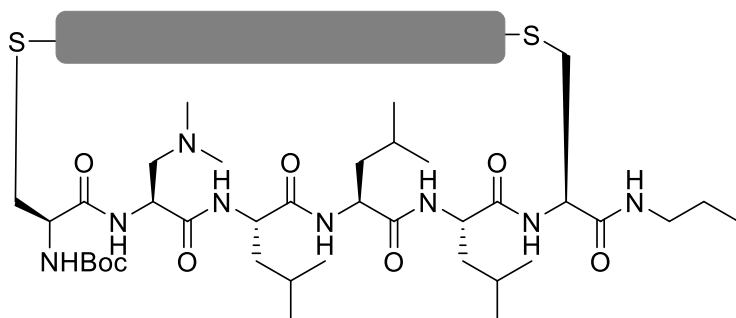
Compound 199. 199a (16 mg, 8%, dark red solid) and **199b** (7 mg, 3%, dark red solid) was prepared from **206** (150 mg, 0.151 mmol) following the general procedures F and G. R_f (CH$_2$Cl$_2$/MeOH 15:1): 0.33. **199a** and **199b** were separated using chiral flash chromatography (Column: IF, Eluent CH$_2$Cl$_2$/MeOH gradient from 0% of MeOH to 3% of MeOH, flow rate: 7 ml/min) **199a.** Mp: 194 – 195 ^{o}C; CD (TFE): 561 (-20.9), 471 (–7.2), 420 (+12.0), 367 (+21.8), 331 (-13.3), 301 (–8.7), 262 (+40.5), 222 (-33.2); IR (neat): 3318 (w), 2960 (w), 2875 (w), 1694 (s), 1652 (s), 1586 (m), 1515 (m), 1462 (m), 1383 (m), 1368 (m), 1325 (s), 1241 (s), 1206 (m), 1163 (m), 1091 (w), 1045 (w), 1020 (w), 920 (w), 843 (w), 809 (w), 750 (w), 698 (w), 666 (w), 611 (w); ^{1}H NMR (500 MHz, CDCl$_3$): 8.84 (s, 1H), 8.82 – 8.64 (m, 4H), 8.61 (d, $^3J_{H-H}$ = 8.1 Hz, 1H), 7.10 (d, $^3J_{H-H}$ = 9.4 Hz, 1H), 7.00 - 6.50 (m, 3H), 6.40 (br s, 1H), 6.14 – 5.87 (br s, 1H), 5.23 (br s, 1H), 5.13 – 4.98 (m, 2H), 4.83 – 4.49 (m, 2H), 4.26 – 4.06 (m, 1H), 4.06 – 3.84 (m, 3H), 3.84 – 3.60 (m, 1H), 3.41 – 3.18 (m, 3H), 3.16 – 3.02 (m, 1H), 2.97 – 2.70 (m, 1H), 2.53 – 2.06 (m, 11H), 2.03 – 1.88 (m, 4H), 1.81 – 1.68 (m, 1H), 1.59 – 1.46 (m, 4H), 1.40 (s, 9H), 1.37 – 1.31 (m, 3H), 1.23 – 1.08 (m, 3H), 0.97 – 0.88 (m, 15H), 0.84 (d, $^3J_{H-H}$ = 6.2 Hz, 3H), 0.78 (d, $^3J_{H-H}$ = 6.3 Hz, 3H), 0.74 (d, $^3J_{H-H}$ = 6.0 Hz, 3H), 0.59 (d, $^3J_{H-H}$ = 4.9 Hz, 3H), 0.55 (d, $^3J_{H-H}$ = 6.0 Hz, 3H), 0.31 – 0.01 (m, 3H); ^{13}C NMR (125 MHz, CDCl$_3$): 173.0 (2xC), 172.6 (C), 171.0 (C), 169.8 (C), 169.0 (C), 164.0 (4xC), 154.9 (C), 140.2 (C), 133.9 (CH), 133.4 (CH), 132.2 (C), 132.0 (C), 131.9 (C), 131.6 (CH), 130.1 (C), 129.8 (CH), 128.9 (2xCH), 128.5 (C), 127.8 (C), 126.4 (2xC), 125.4 (C), 122.7 (C), 122.4 (2xC), 121.9 (C), 80.8 (C), 60.6 (CH$_2$), 57.9 (CH), 57.7 (CH), 54.1 (CH), 54.0 (CH), 53.5 (CH), 52.9 (CH), 51.1 (CH), 50.1 (CH), 46.0 (2xCH$_3$), 41.6 (CH$_2$), 40.3 (CH$_2$), 39.5 (CH$_2$), 39.2 (2xCH$_2$), 35.1 (CH$_2$), 28.2 (3xCH$_3$), 25.1 (2xCH$_2$), 25.0 (CH$_2$), 24.9 (CH$_2$),

24.7 (CH), 24.6 (CH), 23.0 (CH), 22.7 (CH$_3$), 22.6 (CH$_3$), 22.4 (CH$_2$), 21.8 (CH$_3$), 21.0 (CH$_3$), 11.6 (4xCH$_3$), 11.4 (CH$_3$), 11.3 (CH$_3$), 11.2 (CH$_3$); MS (ESI, MeOH): 1346 (100, [M+H]$^+$);

199b. Mp: 183 – 184 $^\circ$C; CD (TFE): 544 (+21.2), 473 (+11.5), 422 (-3.2), 289 (+21.2), 263 (–31.7), 220 (+21.6); IR (neat): 3308 (w), 2958 (w), 2930 (w), 2874 (w), 1694 (s), 1656 (s), 1585 (m), 1525 (m), 1462 (m), 1382 (m), 1325 (s), 1240 (s), 1204 (m), 1163 (m), 1091 (w), 1045 (w), 918 (w), 843 (w), 798 (w), 750 (w), 730 (w), 700 (w), ^{1}H NMR (500 MHz, CDCl$_3$): 9.44 – 9.16 (m, 1H), 8.93 – 8.81 (m, 1H), 8.77 (s, 1H), 8.69 (d, $^3J_{H–H}$ = 7.4 Hz, 1H), 8.66 – 8.45 (m, 2H), 7.59 (br s, 1H), 7.08 (br s, 1H), 6.99 (br s, 1H), 6.81 – 6.52 (m, , 2H), 6.46 – 6.21 (m, 1H), 5.62 – 5.40 (m, 1H), 5.15 – 4.97 (m, 2H), 4.61 – 4.41 (m, 1H), 4.40 – 4.29 (m, 1H), 4.17 – 3.97 (m, 1H), 3.93 – 3.63 (m, 3H), 3.56 – 3.32 (m, 3H), 3.26 – 3.00 (m, 3H), 2.96 – 2.90 (m, 1H), 2.87 – 2.82 (m, 1H), 2.28 – 2.19 (m, 5H), 2.04 - 1.90 (m, 4H), 1.74 – 1.69 (m, 1H), 1.63 (s, 6H), 1.58 – 1.52 (m, 2H), 1.47 – 1.40 (m, 3H), 1.39 – 1.30 (m, 6H), 1.29 – 1.19 (m, 10H), 0.99 – 0.90 (m, 13H), 0.88 – 0.81 (m, 6H), 0.79 (d, $^3J_{H–H}$ = 6.1 Hz, 3H), 0.70 – 0.63 (m, 6H), 0.49 – 0.37 (m, 2H); ^{13}C NMR (125 MHz, CDCl$_3$): 172.9 (C), 172.3 (C), 172.1 (C), 171.2 (2xC), 169.3 (C), 167.4 (C), 163.9 (br, 4xC), 156.9 (C), 136.3 (C), 136.1 (C), 135.8 (C), 134.2 (C), 133.6 (C), 133.1 (C), 132.1 (C, CH – peaks overlap), 130.5 (2xCH), 130.1 (C), 129.2 (2xCH), 128.6 (C), 127.1 (C), 126.2 (CH), 123.5 (C), 122.3 (2xC), 121.6 (C) , 81.3 (C), 58.8 (CH$_2$), 57.9 (CH), 57.8 (CH), 56.7 (CH), 56.3 (CH), 54.1 (CH), 52.3 (CH), 51.4 (CH), 50.3 (CH), 45.7 (CH$_3$), 44.8 (CH$_3$), 41.5 (CH$_2$), 41.1 (CH$_2$), 39.4 (CH$_2$), 38.8 (CH$_2$), 37.9 (CH$_2$), 36.1 (CH$_2$), 28.07 (3xCH$_3$), 25.1 (2xCH$_2$), 25.0 (2xCH$_2$), 24.8 (CH), 24.6 (CH), 24.4 (CH), 23.1 (CH$_3$), 22.9 (CH$_3$), 22.6 (CH$_2$), 22.5 (CH$_3$), 21.5 (CH$_3$), 21.2 (CH$_3$), 21.0 (CH$_3$), 11.4 (5xCH$_3$); MS (ESI, MeOH): 1346 (100, [M+H]$^+$).
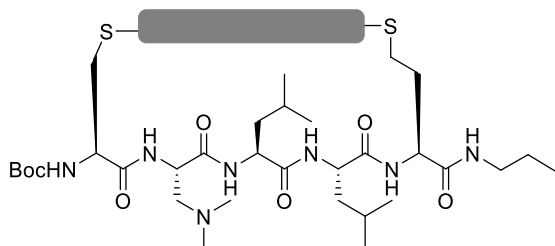
Compound 200. 200a (20 mg, 10%, dark purple solid) and **200b** (44 mg, 21%, dark red solid) was prepared from **207** (150 mg, 0.168 mmol) following the general procedures F and G. R_f (CH$_2$Cl$_2$/MeOH 15:1): 0.37. **200a** and **200b** were separated using chiral flash chromatography (Column: IF, Eluent CH$_2$Cl$_2$/MeOH gradient from 0% of MeOH to 3% of MeOH, flow rate: 7 ml/min) **200a.** Mp: 194 – 195 °C; CD (TFE): 580 (+21.0), 469 (+19.6), 421 (-11.3), 371 (–14.9), 326 (+28.9), 290 (+21.2), 264 (-27.6), 219 (+27.6); IR (neat): 3274 (w), 2958 (m), 2929 (m), 2872 (w), 1694 (m), 1633 (s), 1584 (m), 1527 (s), 1457 (m), 1382 (m), 1365 (m), 1323 (m), 1278 (m), 1239 (s), 1163 (s), 1092 (w), 1055 (w), 917 (w), 870 (w), 844 (w), 810 (w), 796 (w), 750 (w), 727 (w), 701 (w); ^{1}H NMR (400 MHz, CDCl$_3$): 10.01 (d, $^3J_{H-H}$ = 8.2 Hz, 1H), 9.49 (d, $^3J_{H-H}$ = 8.1 Hz, 1H), 8.81 (s, 1H), 8.76 (s, 1H), 8.69 (d, $^3J_{H-H}$ = 8.1 Hz, 1H), 8.55 (d, $^3J_{H-H}$ = 8.2 Hz, 1H), 7.09 – 7.04 (m, 2H), 6.58 (t, $^3J_{H-H}$ = 5.6 Hz, 1H), 6.54 (d, $^3J_{H-H}$ = 8.7 Hz, 1H), 6.34 (d, $^3J_{H-H}$ = 6.3 Hz, 1H), 5.86 (d, $^3J_{H-H}$ = 4.6 Hz, 1H), 5.11 – 4.98 (m, 2H), 4.96 – 4.86 (m, 1H), 3.99 (dd, $^2J_{H-H}$ = 15.2 Hz, $^3J_{H-H}$ = 1.9 Hz, 1H), 3.96 – 3.90 (m, 1H), 3.90 – 3.79 (m, 2H), 3.28 – 3.20 (m, 1H), 3.19 – 3.10 (m, 2H), 2.84 (dd, $^2J_{H-H}$ = 15.2 Hz, $^3J_{H-H}$ = 6.1 Hz, 1H), 2.59 – 2.44 (m, 1H), 2.32 – 2.15 (m, 7H), 2.15 – 2.03 (m, 1H), 2.03 – 1.86 (m, 10H), 1.56 – 1.44 (m, 14H), 1.05 – 0.83 (m, 21H), 0.74 (d, $^3J_{H-H}$ = 6.4 Hz, 3H), 0.58 (d, $^3J_{H-H}$ = 5.6 Hz, 3H), 0.31 – 0.20 (m, 1H), 0.11 (d, $^3J_{H-H}$ = 5.7 Hz, 3H); ^{13}C NMR (125 MHz, CDCl$_3$): 173.5 (C), 172.9 (C), 171.7 (C), 171.3 (C), 171.1 (C), 163.5 (br, 4xC, deduced from HMBC), 156.4 (C), 140.7 (C), 138.4 (CH), 137.4 (CH), 136.4 (C), 134.8 (C), 133.0 (C), 131.7 (CH), 131.2 (C), 129.62 (C), 129.59 (C), 129.4 (CH), 128.4 (C), 128.0 (C), 127.5 (C), 126.8 (CH), 125.1 (CH), 124.2 (C), 122.1 (C), 121.3 (2xC), 82.3 (C), 58.1 (CH), 57.8 (CH), 57.1 (CH$_2$), 54.8 (CH), 54.13 (CH), 54.07 (CH), 52.9 (CH), 50.4 (CH), 46.8 (2xCH$_3$), 41.2 (CH$_2$), 39.3 (CH$_2$), 38.2 (CH$_2$), 35.8 (CH$_2$), 30.3 (CH$_2$), 28.6 (CH$_2$), 28.0 (3xCH$_3$), 25.1 (2xCH$_2$), 24.9

(2xCH$_2$), 24.5 (2xCH), 23.3 (CH$_3$), 23.1 (CH$_3$), 22.4 (CH$_2$), 20.1 (CH$_3$), 19.9 (CH$_3$), 11.5 (4xCH$_3$), 11.2 (CH$_3$); (ESI, MeOH): 1247 (100, [M+H]$^+$).

200b. Mp: 188 – 189 ^{o}C; CD (TFE): 557 (-20.8), 423 (+3.6), 368 (+9.6), 301 (–23.9), 263 (+41.7), 225 (–20.5); IR (neat): 3310 (w), 2960 (w), 2875 (w), 1695 (m), 1657 (s), 1585 (m), 1518 (m), 1460 (m), 1398 (m), 1382 (m), 1325 (m), 1239 (s), 1203 (m), 1162 (m), 1091 (w), 1054 (w), 1021 (w), 916 (w), 843 (w), 810 (w), 797 (w), 750 (w), 730 (w), 700 (w), 667 (w), 609 (w); ^{1}H NMR (400 MHz, CDCl$_3$): 9.59 (d, $^3J_{H-H}$ = 8.1 Hz, 1H), 8.93 (s, 1H), 8.90 (s, 1H), 8.69 (d, $^3J_{H-H}$ = 8.0 Hz, 1H), 8.66 (d, $^3J_{H-H}$ = 8.0 Hz, 1H), 8.22 (d, $^3J_{H-H}$ = 8.0 Hz, 1H), 7.10 (d, $^3J_{H-H}$ = 5.6 Hz, 1H), 7.06 (d, $^3J_{H-H}$ = 4.8 Hz, 1H), 6.76 – 6.65 (m, 3H), 5.45 (d, $^3J_{H-H}$ = 3.6 Hz, 1H), 5.14 – 4.97 (m, 2H), 4.33 – 4.22 (m, 1H), 4.18 – 4.11 (m, 1H), 3.91 – 3.80 (m, 2H), 3.76 (dd, $^2J_{H-H}$ = 15.4 Hz, $^3J_{H-H}$ = 4.5 Hz, 1H), 3.59 (dd, $^2J_{H-H}$ = 15.4 Hz, $^3J_{H-H}$ = 2.4 Hz, 1H), 3.22 – 3.10 (m, 2H), 3.10 – 3.00 (m, 1H), 2.58 – 2.47 (m, 1H), 2.46 – 2.36 (m, 1H), 2.29 – 2.10 (m, 6H), 2.03 – 1.90 (m, 4H), 1.78 (s, 6H), 1.73 – 1.69 (m, 1H), 1.64 – 1.58 (m, 1H), 1.57 – 1.45 (m, 4H), 1.41 (s, 9H), 1.29 – 1.15 (m, 2H), 0.98 – 0.90 (m, 10H), 0.88 – 0.83 (m, 6H), 0.73 (d, $^3J_{H-H}$ = 6.5 Hz, 3H), 0.69 (d, $^3J_{H-H}$ = 6.2 Hz, 3H), 0.61 (d, $^3J_{H-H}$ = 6.5 Hz, 3H), 0.49 (dd, $^2J_{H-H}$ = 13.3 Hz, $^3J_{H-H}$ = 6.1 Hz, 1H); ^{13}C NMR (125 MHz, CDCl$_3$): 171.4 (C), 170.2 (C), 170.1 (C), 168.2 (C), 167.6 (C), 161.5 (br, 2xC, deduced from HMBC), 160.6 (br, 2xC, deduced from HMBC), 154.2 (C), 137.0 (C), 134.6 (2xCH), 133.7 (C), 133.4 (C), 130.2 (C), 130.0 (C), 129.1 (CH), 128.9 (C), 128.3 (CH), 126.8 (CH), 126.1 (C), 125.8 (C), 124.6 (C), 124.2 (CH), 124.0 (C), 120.4 (2xC), 119.8 (C), 118.8 (C), 79.5 (C), 55.49 (CH), 55.46 (CH), 54.5 (CH), 53.6 (CH$_2$), 51.8 (CH$_3$), 51.4 (CH$_3$), 51.3 (CH$_3$), 50.9 (CH$_3$), 43.9 (2xCH$_3$), 39.7 (CH$_2$), 38.9 (CH$_2$), 36.8 (CH$_2$), 35.9 (CH$_2$), 33.6 (CH$_2$), 28.7 (CH$_2$), 25.6 (3xCH$_3$), 22.6 (2xCH$_2$), 22.5 (2xCH$_2$), 22.4 (CH), 22.1 (CH), 20.8 (2xCH$_3$), 19.9 (CH$_2$), 17.9 (CH$_3$), 17.8 (CH$_3$), 9.1 (4xCH$_3$), 8.9 (CH$_3$); (ESI, MeOH): 1247 (100, [M+H]$^+$).
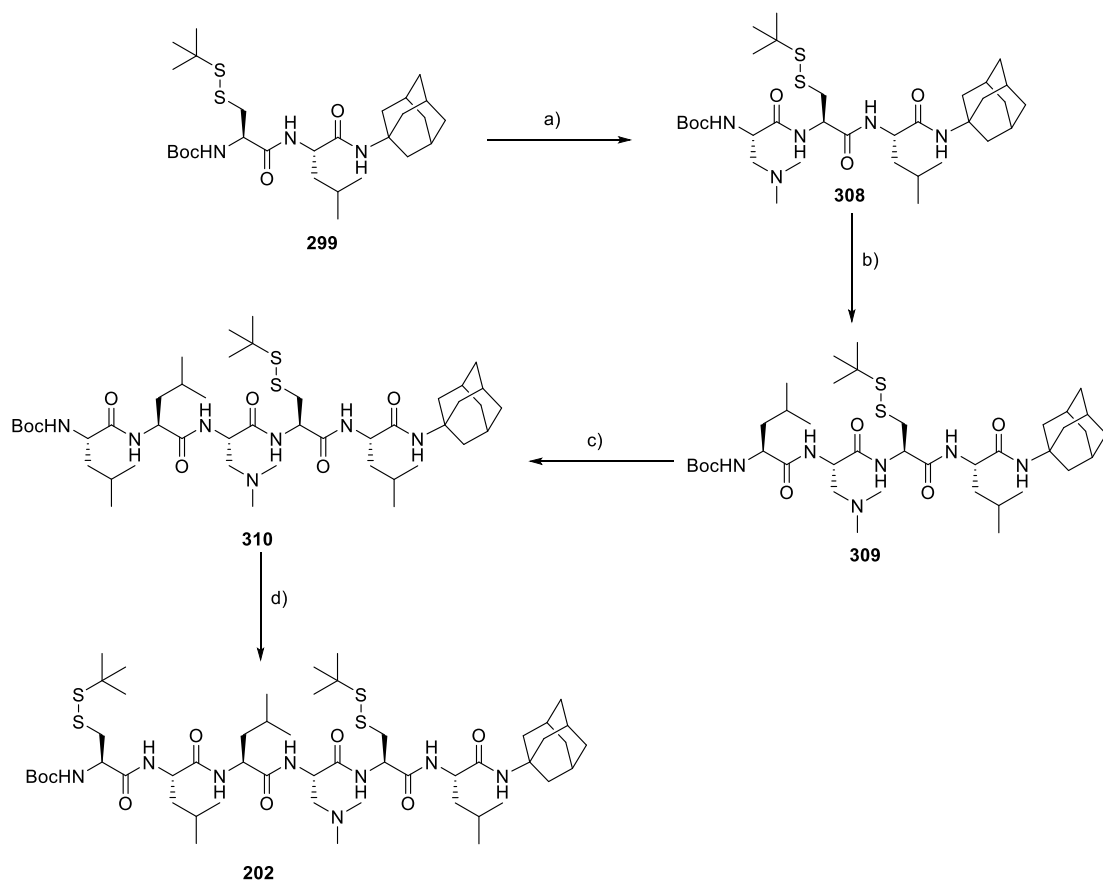
Scheme 22. (a) 1. TFA/CH$_2$Cl$_2$ 1:1, rt, 1 h; 2. **270**, EDC, DMAP, DIPEA, CH$_2$Cl$_2$, rt, overnight, 69%; (b) 1. TFA/CH$_2$Cl$_2$ 1:1, rt, 1 h; 2. Boc–L–Leu–OH, EDC, DMAP, DIPEA, CH$_2$Cl$_2$, rt, overnight, 90%; (c) 1. TFA/CH$_2$Cl$_2$ 1:1, rt, 1 h; 2. Boc–L–Leu–OH, EDC, DMAP, DIPEA, CH$_2$Cl$_2$, rt, overnight, 30%; (d) 1. TFA/CH$_2$Cl$_2$ 1:1, rt, 1 h; 2. Boc–L–Cys(StBu)–OH, EDC, DMAP, DIPEA, CH$_2$Cl$_2$, rt, overnight, 72%.
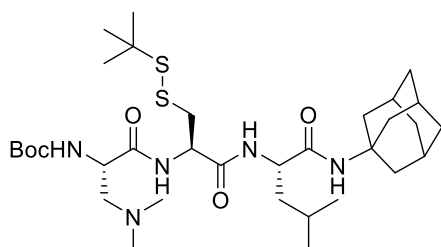
Compound 308 (910 mg, 69%, colorless solid) was prepared from **299** (1.1 g, 2.0 mmol) and **270** (0.6 g, 2.6 mmol) following the general procedures A and D. R_f (CH$_2$Cl$_2$/MeOH 15:1): 0.41; Mp: 224 – 225 °C (decomp); $[\alpha]_D^{20}$ –121 (c 1.00, CHCl$_3$); IR (neat): 3380 (w), 3277 (m), 3069 (w), 2967 (w), 2932 (w), 1707 (w), 1629 (s), 1529 (s), 1507 (s), 1454 (m), 1391 (w), 1363 (m), 1332 (w), 1247

(m), 1165 (s), 1050 (w), 1023 (w), 967 (w), 938 (w), 874 (w), 775 (w), 741 (w), 687 (w); ^{1}H NMR (300 MHz, CDCl$_3$): 8.31 (br s, 1H), 7.13 (d, $^{3}J_{H–H}$ = 8.6 Hz, 1H), 6.00 (s, 1H), 5.65 (br s, 1H), 4.73 – 4.58 (m, 1H), 4.44 – 4.30 (m, 1H), 4.10 – 3.98 (m, 1H), 3.32 (dd, $^{2}J_{H–H}$ = 13.8 Hz, $^{3}J_{H–H}$ = 5.9 Hz, 1H), 3.06 (dd, $^{2}J_{H–H}$ = 13.8 Hz, $^{2}J_{H–H}$ = 5.0 Hz, 1H), 2.72 – 2.48 (m, 2H), 2.33 (s, 6H), 2.11 – 2.03 (m, 3H), 2.01 (d, $^{3}J_{H–H}$ = 2.9 Hz, 6H), 1.87 – 1.75 (m, 1H), 1.71 – 1.60 (m, 7H), 1.58 – 1.52 (m, 1H), 1.49 (s, 9H), 1.36 (s, 9H), 0.96 – 0.87 (m, 6H); ^{13}C NMR (75 MHz, CDCl$_3$): 171.7 (C), 170.6 (C), 169.5 (C), 156.4 (C), 80.7 (C), 60.3 (CH$_2$), 54.1 (CH), 52.5 (2xCH), 52.0 (C), 48.8 (C), 45.2 (2xCH$_3$), 41.3 (3xCH$_2$), 41.2 (CH$_2$), 40.6 (CH$_2$), 36.4 (3xCH$_2$), 29.8 (3xCH), 29.5 (3xCH$_3$), 28.4 (3xCH$_3$), 24.8 (CH), 23.2 (CH$_3$), 21.6 (CH$_3$); MS (ESI, MeOH): 670 (100, [M+H]$^{+}$).
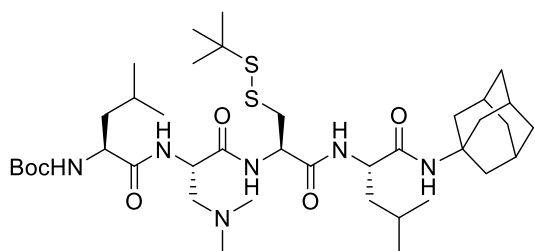
Compound 309 (960 mg, 90%, colorless solid) was prepared from **308** (910 mg, 1.36 mmol) and Boc–L–Leu–OH (377 mg, 1.63 mmol) following the general procedures A and D. R_f (CH$_2$Cl$_2$/MeOH 15:1): 0.49; Mp: 228 – 229 °C (decomp); [α]$_D^{20}$ –130 (c 1.00, CHCl$_3$); IR (neat): 3269 (m), 3083 (w), 2957 (m), 2871 (w), 1739 (s), 1630 (s), 1542 (m), 1503 (m), 1455 (m), 1405 (m), 1365 (s), 1216 (s), 1164 (s), 1048 (w), 1020 (w), 990 (w), 928 (w), 872 (w), 783 (w), 709 (w); ^{1}H NMR (400 MHz, CDCl$_3$): 7.85 (d, $^{3}J_{H–H}$ = 7.4 Hz, 1H), 7.34 (br s, 1H), 7.25 (br s, 1H), 6.07 (s, 1H), 4.96 (br s, 1H), 4.77 - 4.66 (m, 1H), 4.36 – 4.28 (m, 1H), 4.24 – 4.10 (m, 1H), 4.00 - 3.92 (m, 1H), 3.30 (dd, $^{2}J_{H–H}$ = 13.6 Hz, $^{3}J_{H–H}$ = 3.7 Hz, 1H), 3.01 (dd, $^{2}J_{H–H}$ = 13.6 Hz, $^{3}J_{H–H}$ = 9.6 Hz, 1H), 2.78 – 2.49 (m, 2H), 2.23 (s, 6H), 2.08 – 2.00 (m, 9H), 1.81 – 1.62 (m, 11H), 1.55– 1.45 (m, 10H), 1.34 (s, 9H), 0.98 (d, $^{3}J_{H–H}$ = 6.3 Hz, 3H), 0.95 (d, $^{3}J_{H–H}$ = 6.2 Hz, 3H), 0.93 (d, $^{3}J_{H–H}$ = 6.4 Hz, 3H), 0.88 (d, $^{3}J_{H–H}$ = 6.4 Hz, 3H); ^{13}C NMR (100 MHz, CDCl$_3$): 173.9 (C), 171.4 (C), 171.0 (C), 170.0 (C), 156.3 (C), 81.2 (C), 59.1 (CH$_2$),

54.5 (CH), 53.4 (CH), 52.8 (CH), 52.5 (CH), 51.8 (CH), 48.4 (C), 45.4 (2xCH$_3$), 41.2 (3xCH$_2$), 40.7 (2xCH$_2$), 40.3 (CH$_2$), 36.4 (3xCH$_2$), 29.9 (3xCH), 29.5 (3xCH$_3$), 28.4 (3xCH$_3$), 24.91 (CH), 24.86 (CH), 23.4 (CH$_3$), 23.0 (CH$_3$), 21.6 (CH$_3$), 21.4 (CH$_3$); MS (ESI, MeOH): 783 (100, [M+H]$^+$).
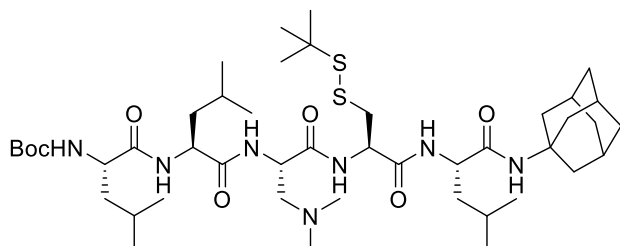
Compound 310 (332 mg, 30%, colorless solid) was prepared from **309** (960 mg, 1.23 mmol) and Boc–L–Leu–OH (340 mg, 1.47 mmol) following the general procedures A and D. R_f (CH$_2$Cl$_2$/MeOH 15:1): 0.39; Mp: 228 – 229 °C (decomp); [α]$_D^{20}$ –143 (*c* 1.00, CHCl$_3$); IR (neat): 3288 (m), 3085 (w), 2955 (m), 2910 (m), 2869 (w), 1720 (w), 1631 (s), 1531 (s), 1456 (m), 1389 (w), 1364 (m), 1313 (w), 1273 (w), 1247 (m), 1166 (m), 1104 (w), 1045 (w), 1022 (w), 955 (w), 874 (w), 814 (w), 789 (w), 692 (w); ^{1}H NMR (500 MHz, CDCl$_3$): 7.80 (d, $^3J_{H–H}$ = 6.8 Hz, 1H), 7.31 (br s, 1H), 7.19 (d, $^3J_{H–H}$ = 8.1 Hz, 1H), 6.81 (br s, 1H), 6.10 (s, 1H), 4.89 (d, $^3J_{H–H}$ = 7.0 Hz, 1H), 4.67 – 4.61 (m, 1H), 4.31 – 4.25 (m, 1H), 4.25 – 4.05 (m, 3H), 3.31 (dd, $^2J_{H–H}$ = 13.7 Hz, $^3J_{H–H}$ = 3.7 Hz, 1H), 3.10 (dd, $^2J_{H–H}$ = 13.7 Hz, $^3J_{H–H}$ = 10.2 Hz, 1H), 2.89 – 2.52 (m, 2H), 2.29 (s, 6H), 2.09 – 2.01 (m, 9H), 1.81 – 1.77 (m, 3H), 1.73 – 1.62 (m, 12H), 1.58 – 1.51 (m, 1H), 1.46 (s, 9H), 1.34 (s, 9H), 1.00 – 0.96 (m, 9H), 0.94 – 0.91 (m, 6H), 0.87 (d, $^3J_{H–H}$ = 6.5 Hz, 3H); ^{13}C NMR (125MHz, CDCl$_3$): 174.3 (C), 173.4 (C), 171.1 (C), 170.2 (C), 156.2 (C), 80.9 (C), 58.9 (CH$_2$), 54.0 (CH), 53.5 (CH), 53.1 (CH), 52.9 (CH), 52.6 (CH), 51.8 (C), 48.3 (C), 45.3 (2xCH$_3$), 41.2 (3xCH$_2$), 40.9 (CH$_2$), 40.2 (2xCH$_2$), 40.1 (CH$_2$), 36.5 (3xCH$_2$), 29.9 (3xCH), 29.5 (3xCH$_3$), 28.3 (3xCH$_3$), 24.9 (CH), 24.8 (2xCH), 23.4 (CH$_3$), 23.02 (CH$_3$), 22.99 (CH$_3$), 21.9 (CH$_3$), 21.5 (CH$_3$), 21.4 (CH$_3$); MS (ESI, MeOH): 897 (100, [M+H]$^+$).
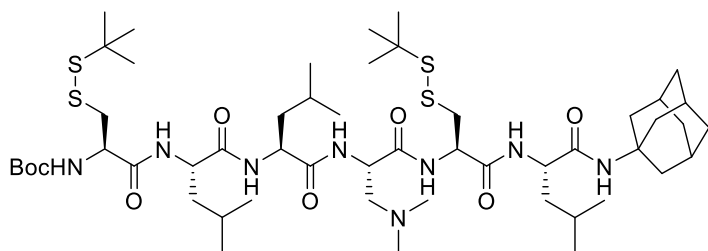
Compound 202 (269 mg, 72%, colorless solid) was prepared from **310** (310 mg, 0.346 mmol) and Boc–L–Cys(StBu)–OH (128 mg, 0.414 mmol) following the general procedures A and D. R_f (CH$_2$Cl$_2$/MeOH 15:1): 0.32; Mp: 219 – 220 °C (decomp); $[\alpha]_D^{20}$ –90.2 (*c* 0.50, DMSO); IR (neat): 3271 (m), 3082 (w), 2957 (m), 2910 (m), 1627 (s), 1531 (s), 1456 (m), 1388 (m), 1362 (m), 1312 (m), 1275 (m), 1217 (m), 1164 (m), 1046 (w), 873 (w), 781 (w), 702 (w); ^{1}H NMR (400 MHz, DMSO-d$_6$): 8.41 (d, $^3J_{\text{H–H}}$ = 7.6Hz, 1H), 8.12 – 7.90 (m, 1H), 7.84 (d, $^3J_{\text{H–H}}$ = 8.2 Hz, 1H), 7.73 (d, $^3J_{\text{H–H}}$ = 7.3 Hz, 1H), 7.68 (d, $^3J_{\text{H–H}}$ = 7.9Hz, 1H), 7.07 (br s, 1H), 6.88 (s, 1H), 4.55 – 4.25 (m, 4H), 4.23 – 4.09 (m, 2H), 3.21 – 3.08 (m, 2H), 3.07 – 2.82 (m, 4H), 2.48 – 2.29 (m, 2H), 2.18 (s, 6H), 2.02 – 1.96 (m, 3H), 1.90 (d, $^3J_{\text{H–H}}$ = 3.0 Hz, 6H), 1.66 – 1.55 (m, 9H), 1.50 – 1.44 (m, 4H), 1.38 (s, 9H), 1.30 – 1.27 (m, 18H), 0.89 – 0.78 (m, 18H); ^{13}C NMR (100 MHz, DMSO-d$_6$): 172.31 (C), 172.25 (C), 171.3 (C), 171.0 (C), 169.5 (C), 150.7 (C), 79.0 (C), 60.8 (CH$_2$), 54.8 (CH), 54.6 (CH), 53.1 (CH), 52.2 (CH), 51.5 (CH), 51.4 (CH), 51.3 (C), 48.2 (C), 48.1 (C), 45.8 (2xCH$_3$), 43.0 (CH$_2$), 42.9 (CH$_2$), 42.5 (CH$_2$), 41.4 (3xCH$_2$), 41.3 (CH$_2$), 40.9 (CH$_2$), 36.5 (3xCH$_2$), 30.1 (6xCH$_3$), 29.3 (3xCH), 28.6 (3xCH$_3$), 24.7 (CH), 24.52 (CH), 24.48 (CH), 23.5 (2xCH$_3$), 22.2 (CH$_3$), 22.14 (CH$_3$), 22.11 (CH$_3$), 22.04 (CH$_3$);MS (ESI, MeOH): 1088 (100, [M+H]$^+$).

Scheme 23. (a) 1. TFA/CH₂Cl₂ 1:1, rt, 1 h; 2. **270**, EDC, DMAP, DIPEA, CH₂Cl₂, rt, overnight, 56%; (b) 1. TFA/CH₂Cl₂ 1:1, rt, 1 h; 2. Boc–L–Leu–OH, EDC, DMAP, DIPEA, CH₂Cl₂, rt, overnight, 61%; (c) 1. TFA/CH₂Cl₂ 1:1, rt, 1 h; 2. Boc–L–Cys(StBu)–OH, EDC, DMAP, DIPEA, CH₂Cl₂, rt, overnight, 72%.

Compound 311 (599 mg, 56%, colorless solid) was prepared from **300** (910 mg, 1.36 mmol) and **270** (377 mg, 1.63 mmol) following the general procedures A and D. R_f (CH₂Cl₂/MeOH 15:1): 0.36; Mp: 210 – 211 °C (decomp); $[\alpha]_D^{20}$ –135 (*c* 1.00, CHCl₃); IR (neat): 3264 (w), 3087 (w), 2957 (w), 2931 (w), 1714 (w), 1630 (s), 1544 (m), 1456 (w), 1388 (w), 1364 (w), 1278 (w), 1251 (w), 1212 (w), 1163 (m), 1067 (w), 949 (w), 872 (w), 815 (w), 780 (w), 709 (w), 606 (w); ¹H NMR (400 MHz, CDCl₃): 7.91 (br s, 1H), 7.32 (d, $^3J_{H-H}$ = 5.7 Hz, 1H), 7.05 (d, $^3J_{H-H}$ = 8.3 Hz, 1H), 6.08 (s, 1H), 5.67 (br s, 1H), 4.72 – 4.61 (m, 1H), 4.34 – 4.26 (m, 1H), 4.24 – 4.16 (m, 1H), 4.11 – 3.93 (m, 1H), 3.26 (dd, $^2J_{H-H}$ = 13.7 Hz, $^3J_{H-H}$ = 4.4 Hz, 1H), 3.06 (dd, $^2J_{H-H}$ = 13.7 Hz, $^3J_{H-H}$ = 9.0 Hz, 1H), 2.88 – 2.54 (m, 1H), 2.37 (s, 6H), 2.10

– 2.01 (m, 9H), 1.79 – 1.61 (m, 12H), 1.46 (s, 9H), 1.35 (s, 9H), 0.99 (d, $^3J_{H-H}$ = 6.3 Hz, 3H),

0.96 (d, $^3J_{H-H}$ = 4.5 Hz, 3H), 0.94 (d, $^3J_{H-H}$ = 4.7 Hz, 3H), 0.89 (d, $^3J_{H-H}$ = 6.4 Hz, 3H); ^{13}C

NMR (100 MHz, CDCl$_3$): 172.3 (2xC), 170.9 (C), 170.0 (C), 156.6 (C), 81.1 (C), 59.9 (CH$_2$),

53.9 (CH), 53.2 (CH), 52.7 (CH), 52.3 (CH), 51.9 (C), 48.5 (C), 44.9 (2xCH$_3$), 41.2 (3xCH$_2$),

40.6 (CH$_2$), 40.4 (CH$_2$), 40.1 (CH$_2$), 36.4 (3xCH$_2$), 29.9 (3xCH), 29.5 (3xCH$_3$), 28.3 (3xCH$_3$),

25.2 (CH), 24.9 (CH), 23.4 (CH$_2$), 23.0 (CH$_2$), 21.7 (CH$_2$), 21.4 (CH$_2$); MS (ESI, MeOH): 783

(100, [M+H]$^+$).
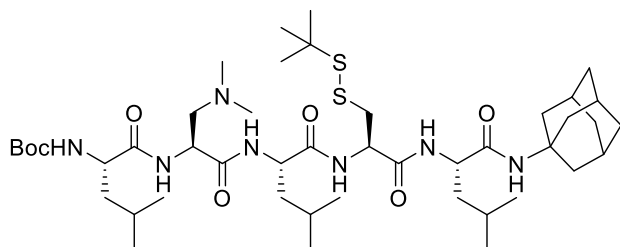
Compound 312 (415 mg, 61%, colorless solid) was prepared from **311** (599 mg, 0.765 mmol) and Boc–L–Leu–OH (212 mg, 0.917 mmol)

following the general procedures A and D. R_f (CH$_2$Cl$_2$/MeOH 15:1): 0.41; Mp: 217 – 218 ºC

(decomp); [α]$_D^{20}$ –140 (c 1.00, CHCl$_3$); IR (neat): 3283 (w), 3070 (w), 2956 (w), 2911 (w),

2869 (w), 1719 (w), 1631 (s), 1528 (m), 1455 (w), 1388 (w), 1363 (w), 1313 (w), 1274 (w),

1249 (w), 1165 (m), 1103 (w). 1044 (w), 952 (w), 873 (w), 814 (w), 779 (w), 694 (w); ^{1}H NMR

(400 MHz, CDCl$_3$): 7.64 (br s, 1H), 7.51 (d, $^3J_{H-H}$ = 6.6 Hz, 1H), 7.45 (br s, 1H), 7.00 (d, $^3J_{H-H}$ = 8.4 Hz, 1H), 6.21 (s, 1H), 5.03 (br s, 1H), 4.62 – 4.54 (m, 1H), 4.33 – 4.22 (m, 1H), 4.22 –

4.15 (m, 1H), 4.13 – 3.98 (m, 2H), 3.35 (dd, $^2J_{H-H}$ = 13.5 Hz, $^3J_{H-H}$ = 3.6 Hz, 1H), 3.08 (dd,

$^2J_{H-H}$ = 13.5 Hz, $^3J_{H-H}$ = 11.3 Hz, 1H), 2.83 – 2.50 (m, 2H), 2.22 (s, 6H), 2.07 – 2.02 (m, 9H),

1.81 – 1.60 (m, 15H), 1.47 (s, 9H), 1.33 (s, 9H), 1.01 – 0.96 (m, 9H), 0.94 – 0.90 (m, 6H), 0.87

(d, $^3J_{H-H}$ = 6.5 Hz, 3H); ^{13}C NMR (100MHz, CDCl$_3$): 174.4 (C), 173.2 (C), 172.6 (C), 171.2

(C), 170.5 (C), 156.4 (C), 81.1 (C), 58.7 (CH$_2$), 54.8 (CH), 54.1 (CH), 53.6 (CH), 53.2 (CH),

53.0 (CH), 52.8 (CH), 51.8 (C), 47.9 (C), 41.1 (3xCH$_2$), 40.6 (CH$_2$), 40.3 (CH$_2$), 40.2 (CH$_2$),

39.6 (CH$_2$), 36.5 (3xCH$_2$), 30.0 (3xCH), 29.5 (3xCH$_3$), 28.2 (3xCH$_3$), 25.0 (CH), 24.89 (CH),

24.85 (CH), 23.4 (CH$_3$), 23.1 (CH$_3$), 23.0 (CH$_3$), 21.6 (CH$_3$), 21.3 (CH$_3$), 21.1 (CH$_3$); MS (ESI,

MeOH): 897 (100, [M+H]$^+$).
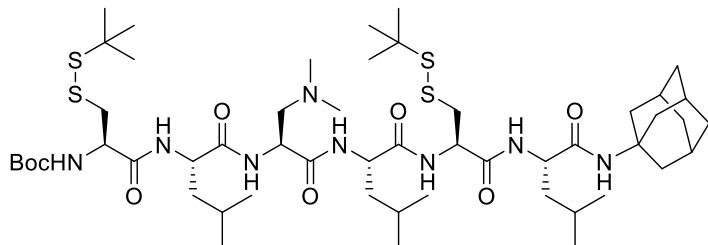
Compound 204 (349 mg, 72%, colorless solid) was prepared from **312** (400 mg, 0.446 mmol) and Boc–L–Cys(StBu)–OH (166

mg, 0.536 mmol) following the general procedures A and B. R_f (CH$_2$Cl$_2$/MeOH 15:1): 0.35;

Mp: 225 – 226 °C (decomp); $[\alpha]_\text{D}^{20}$ –83.4 (c 0.50, DMSO); IR (neat): 3270 (m), 3087 (w), 2957

(m), 2911 (m), 2866 (w), 1721 (w), 1690 (w), 1629 (s), 1531 (s), 1456 (m), 1388 (w), 1362

(m), 1312 (w), 1275 (w), 1217 (w), 1164 (m), 1047 (w), 935 (w), 873 (w), 781 (w), 701 (w);[1]H

NMR (500 MHz, CDCl$_3$): 7.55 (d, $^3J_\text{H–H}$ = 5.8 Hz, 1H), 7.45 (d, $^3J_\text{H–H}$ = 6.5 Hz, 1H), 7.31 (br

s, 1H), 7.04 (d, $^3J_\text{H–H}$ = 8.2 Hz, 1H), 6.91 (br s, 1H), 6.23 (s, 1H), 5.30 (br s, 1H), 4.60 – 4.52

(m, 1H), 4.51 – 4.41 (m, 1H), 4.29 – 4.23 (m, 1H), 4.21 – 4.13 (m, 2H), 4.11 – 3.99 (m, 1H),

3.37 (dd, $^2J_\text{H–H}$ = 13.3 Hz, $^3J_\text{H–H}$ = 3.5 Hz, 1H), 3.16 – 3.03 (m, 2H), 3.03 – 2.88 (m, 1H), 2.78

– 2.44 (m, 2H), 2.23 (s, 6H), 2.07 – 1.98 (m, 9H), 1.81 – 1.59 (m, 15H), 1.48 (s, 9H), 1.36 (s,

9H), 1.33 (s, 9H), 1.03 – 0.98 (m, 6H), 0.96 (d, $^3J_\text{H–H}$ = 6.0 Hz, 3H), 0.94 – 0.90 (m, 6H), 0.87

(d, $^3J_\text{H–H}$ = 6.4 Hz, 3H); ^{13}C NMR (125MHz, CDCl$_3$): 173.6 (C), 173.4 (C), 172.2 (C). 171.3

(C), 170.6 (C), 155.9 (C), 81.4 (C), 58.7 (CH$_2$), 54.6 (CH), 54.2 (CH), 54.1 (CH), 53.8 (CH),

53.6 (CH), 52.9 (CH), 51.8 (C), 48.9 (C), 47.9 (C), 45.0 (2xCH$_3$), 41.1 (3xCH$_2$), 40.6 (CH$_2$),

40.3 (2xCH$_2$), 39.9 (CH$_2$), 39.3 (CH$_2$), 36.5 (3xCH$_2$), 30.0 (3xCH), 29.8 (3xCH$_3$), 29.6

(3xCH$_3$), 28.2 (3xCH$_3$), 25.1 (CH), 25.0 (CH), 24.9 (CH), 23.5 (CH$_3$), 23.3 (CH$_3$), 23.1 (CH$_3$),

21.4 (CH$_3$), 21.2 (CH$_3$), 21.0 (CH$_3$); MS (ESI, MeOH): 1088 (100, [M+H]$^+$).

202: X = C, Y = C, Z = N
204: X = C, Y = N, Z = C
174: X = N, Y = C, Z = C

201: X = C, Y = C, Z = N
203: X = C, Y = N, Z = C
205: X = N, Y = C, Z = C
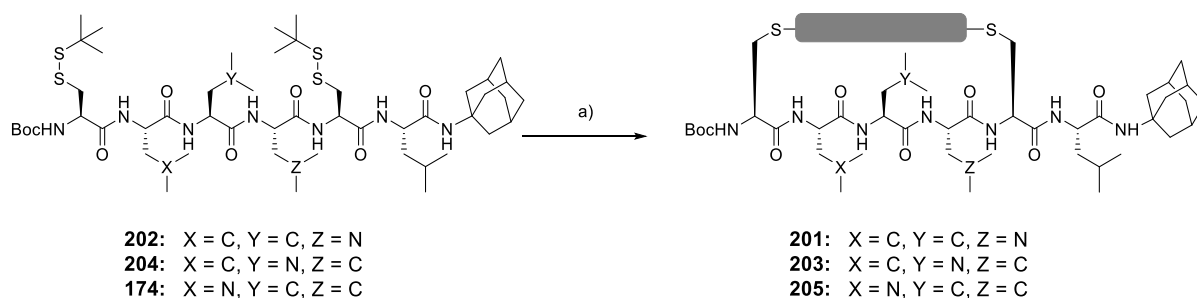
Scheme 24. (a) 1. PBu_3, TEA, H_2O, TFE, rt, overnight; 2. **180**, TCEP·HCl, CH_3CN/buffer 3:1, 65 °C, overnight, 4% (**201a**), 3% (**201b**), 15% (**203a**), 23% (**203b**), 15% (**205a**), 17% (**205b**).
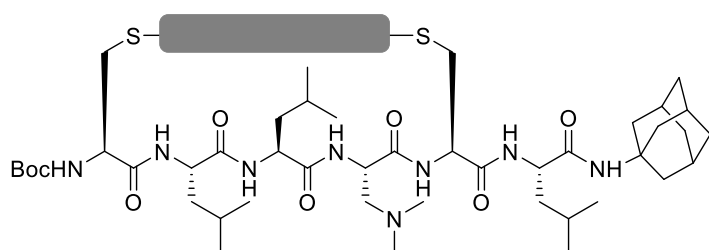
Compound 201. 201a (7 mg, 4%, dark purple solid) and **201b** (5 mg, 3%, dark red solid) was prepared from **202** (150 mg, 0.138 mmol) following the general procedures F and G. R_f (CH_2Cl_2/MeOH 15:1): 0.31. **201a** and **201b** were separated using chiral flash chromatography (Column: IF, Eluent CH_2Cl_2/MeOH gradient from 0% of MeOH to 3% of MeOH, flow rate: 7 ml/min) **201a.** Mp: 192 – 193 °C; CD (TFE): 575 (+22.4), 470 (+15.8), 423 (-10.0), 372 (−10.8), 322 (+22.5), 258 (−35.6), 222 (+15.1); IR (neat): 3323 (w), 2957 (m), 2930 (m), 1695 (m), 1658 (s), 1586 (m), 1524 (m), 1462 (m), 1398 (m), 1325 (m), 1240 (s), 1205 (m), 1162 (m), 1092 (w), 1054 (w), 917 (w), 858 (w), 810 (w), 798 (w), 750 (w), 730 (w), 700 (w), 666 (w); ^{1}H NMR (500 MHz, CDCl$_3$): 9.86 (d, $^3J_{H-H}$ = 8.1 Hz, 1H), 9.49 (d, $^3J_{H-H}$ = 8.1 Hz, 1H), 8.82 (s, 1H), 8.79 (s, 1H), 8.65 (d, $^3J_{H-H}$ = 8.1 Hz, 1H), 8.53 (d, $^3J_{H-H}$ = 8.1 Hz, 1H), 7.02 (d, $^3J_{H-H}$ = 9.1 Hz, 1H), 6.90 (d, $^3J_{H-H}$ = 8.1 Hz, 1H), 6.70 (d, $^3J_{H-H}$ = 3.9 Hz, 1H), 6.31 (d, $^3J_{H-H}$ = 4.3 Hz, 1H), 5.93 (s, 1H), 5.72 (d, $^3J_{H-H}$ = 4.2 Hz, 1H), 5.70 (d, $^3J_{H-H}$ = 4.5 Hz, 1H), 5.30 – 5.23 (m, 1H), 5.14 – 5.00 (m, 2H), 4.35 – 4.24 (m, 1H), 4.01 – 3.95 (m, 3H), 3.91 (dd, $^2J_{H-H}$ = 15.2 Hz, $^3J_{H-H}$ = 2.0 Hz, 1H), 3.88 – 3.82(m, 1H), 3.65 – 3.57 (m, 1H), 2.79 (dd, $^2J_{H-H}$= 15.2 Hz, $^3J_{H-H}$ = 6.2 Hz, 1H), 2.30 –

2.17 (m, 5H), 2.07 – 2.03 (m, 3H), 2.01 – 1.93 (m, 9H), 1.89 – 1.84 (m, 1H), 1.69 – 1.59 (m, 19H), 1.48 (s, 9H), 1.42 – 1.33 (m, 3H), 1.23 – 1.16 (m, 1H), 1.12 – 1.06 (m, 1H), 1.01 – 0.89 (m, 10H), 0.84 (d, $^3J_{H-H}$ = 6.5 Hz, 3H), 0.81 (d, $^3J_{H-H}$ = 6.5 Hz, 3H), 0.76 (d, $^3J_{H-H}$ = 6.5 Hz, 3H), 0.74 (d, $^3J_{H-H}$ = 6.6 Hz, 3H), 0.63 (d, $^3J_{H-H}$ = 6.7 Hz, 3H), 0.61 – 0.56 (m, 1H), 0.48 (d, $^3J_{H-H}$ = 6.5 Hz, 3H); ^{13}C NMR (125 MHz, CDCl$_3$): 173.3 (C), 172.0 (C), 170.8 (C), 170.5 (C), 170.2 (C), 169.1 (C), 163.8 (br, 4xC, deduced from HMBC), 156.4 (C), 139.3 (C), 137.8 (CH), 136.3 (C), 134.4 (C), 132.9 (C), 131.9 (2xCH), 129.6 (C), 129.4 (C), 129.0 (CH), 128.5 (C), 128.12 (2xC), 128.07 (CH), 126.4 (C), 125.3 (CH), 123.7 (C), 122.2 (2xC), 121.2 (C), 82.6 (C), 58.2 (CH$_2$), 58.0 (CH), 57.9 (CH), 54.59 (CH), 54.56 (CH), 54.3 (CH), 53.4 (CH), 53.3 (CH), 53.2 (CH), 51.8 (C), 44.5 (2xCH$_3$), 41.3 (3xCH$_2$), 40.4 (CH$_2$), 40.2 (CH$_2$), 39.2 (CH$_2$), 36.4 (3xCH$_2$), 32.8 (CH$_2$), 30.3 (CH$_2$), 29.7 (CH$_2$), 29.5 (3xCH), 28.0 (3xCH$_3$), 25.0 (4xCH$_2$), 24.6 (CH), 24.3 (2xCH), 23.5 (CH$_3$), 23.0 (CH$_3$), 22.7 (CH$_3$), 22.2 (CH$_3$), 21.7 (CH$_3$), 20.7 (CH$_3$), 11.6 (4xCH$_3$); MS (ESI, MeOH): 1438 (100, [M+H]$^+$).

201b. Mp: 194 – 195 °C; CD (TFE): 546 (-44.6), 361 (+12.0), 325 (+20.7), 288 (–43.9), 262 (+62.1), 224 (–46.9); IR (neat): 3297 (w), 2959 (m), 2926 (m), 1696 (m), 1658 (s), 1585 (m), 1526 (m), 1458 (m), 1399 (m), 1383 (m), 1367 (m), 1326 (m), 1239 (s), 1204 (m), 1163 (m), 1092 (m), 1050 (w), 919 (w), 843 (w), 809 (w), 798 (w), 750 (w), 700 (w), 607 (w); ^{1}H NMR (400 MHz, CDCl$_3$): 8.93 (s, 1H), 8.82 (s, 1H), 8.75 (d, $^3J_{H-H}$ = 7.9 Hz, 1H), 8.70 (d, $^3J_{H-H}$ = 7.9 Hz, 1H), 8.33 (d, $^3J_{H-H}$ = 7.9 Hz, 1H), 8.28 (d, $^3J_{H-H}$ = 7.9 Hz, 1H), 7.16 – 7.10 (m, 2H), 6.67 (d, $^3J_{H-H}$ = 3.8 Hz, 1H), 6.56 (d, $^3J_{H-H}$ = 3.7 Hz, 1H), 6.17 (d, $^3J_{H-H}$ = 4.5 Hz, 1H), 6.00 (s, 1H), 5.18 – 4.99 (m, 3H), 4.66 (dd, $^2J_{H-H}$ = 12.1 Hz, $^3J_{H-H}$ = 2.3 Hz, 1H), 4.59 – 4.48 (m, 1H), 4.38 – 4.27 (m, 1H), 4.25 – 4.18 (m, 1H), 3.86 – 3.75 (m, 1H), 3.70 – 3.38 (m, 3H), 3.19 – 3.09 (m, 1H), 2.32 – 2.16 (m, 4H), 2.06 – 2.02 (m, 4H), 2.01 - 1.93 (m, 9H), 1.90 – 1.81 (m, 1H), 1.78 – 1.72 (m, 2H), 1.68 – 1.65 (m, 4H), 1.57 (s, 6H), 1.50 – 1.44 (m, 3H), 1.39 (s, 9H), 1.05 –

0.88 (m, 18H), 0.86 – 0.81 (m, 8H), 0.79 – 0.61 (m, 8H), 0.53 (d, $^3J_{H-H}$ = 6.5 Hz, 3H), 0.08 - -0.02 (m, 1H); ^{13}C NMR (125 MHz, CDCl$_3$): 173.7 (C), 172.1 (C), 171.5 (C), 171.0 (C), 169.0 (C), 168.9 (C), 163.8 (br, 4xC, deduced from HMBC), 156.5 (C), 140.9 (C), 137.2 (2xC), 137 (CH), 134.6 (CH), 131.6 (CH), 131.3 (C), 130.9 (CH), 130.4 (CH), 128.8 (CH), 127.0 (C), 126.9 (C), 126.4 (C), 125.3 (C), 123.2 (br, 2xC), 122.2 (br, 4xC), 82.3 (C), 58.6 (CH$_2$), 58.1 (CH), 57.9 (CH), 57.1 (CH), 54.6 (CH), 54.1 (CH), 53.6 (CH), 53.1 (CH), 53.0 (CH), 51.7 (C), 44.6 (2xCH$_3$), 43.6 (CH$_2$) , 41.3 (CH$_2$), 41.2 (CH$_2$), 41.1 (3xCH$_2$), 40.3 (CH$_2$), 39.0 (CH$_2$), 37.7 (CH$_2$), 36.4 (3xCH$_2$), 29.5 (3xCH), 27.9 (3xCH$_3$), 25.1 (2xCH$_2$), 25.0 (2xCH$_2$), 24.6 (2xCH), 24.4 (CH), 24.1 (CH$_3$), 23.5 (CH$_3$), 23.1 (CH$_3$), 22.7 (CH$_3$), 21.6 (CH$_3$), 20.4 (CH$_3$), 11.5 (2xCH$_3$), 11.4 (2xCH$_3$); MS (ESI, MeOH): 1438 (100, [M+H]$^+$).
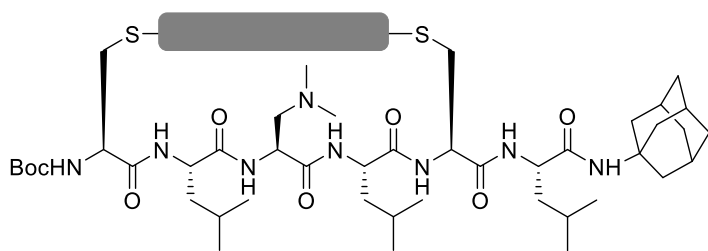
Compound 203. 203a (29 mg, 15%, dark purple solid) and **203b** (45 mg, 23%, dark red solid) was prepared from **204** (150 mg, 0.138 mmol) following the general procedures F and G. R_f (CH$_2$Cl$_2$/MeOH 15:1): 0.42 (**203a**), 0.39 (**203b**). **203a** and **203b** were separated using chiral flash chromatography (Column: IF, Eluent CH$_2$Cl$_2$/MeOH gradient from 0% of MeOH to 3% of MeOH, flow rate: 7 ml/min) **203a.** Mp: 186 – 187 °C; CD (TFE): 577 (+22.2), 468 (+15.5), 421 (-9.5), 371 (–11.5), 321 (+23.4), 258 (–33.0), 219 (+14.1); IR (neat): 3293 (w), 2958 (m), 2911 (m), 2874 (m), 1693 (m), 1656 (s), 1586 (m), 1524 (m), 1460 (m), 1398 (m), 1381 (m), 1324 (m), 1239 (s), 1205 (m), 1162 (m), 1092 (w), 1053 (w), 917 (w), 858 (w), 810 (w), 798 (w), 750 (w), 730 (w), 701 (w); ^{1}H NMR (500 MHz, CDCl$_3$): 9.98 (d, $^3J_{H-H}$ = 8.1 Hz, 1H), 9.35 (d, $^3J_{H-H}$ = 8.1 Hz, 1H), 8.83 (s, 1H), 8.81 (s, 1H), 8.66 (d, $^3J_{H-H}$ = 8.2 Hz, 1H), 8.54 (d, $^3J_{H-H}$ = 8.1 Hz, 1H), 7.00 (d, $^3J_{H-H}$ = 9.1 Hz, 1H), 6.87 (d, $^3J_{H-H}$ = 8.3 Hz, 1H), 6.79 (d, $^3J_{H-H}$ = 3.3 Hz, 1H), 6.47 (d, $^3J_{H-}$

H = 6.0 Hz, 1H), 5.91 (d, $^3J_{H-H}$ = 3.5 Hz, 1H), 5.80 (s, 1H), 5.73 (d, $^3J_{H-H}$ = 5.4 Hz, 1H), 5.28 – 5.21 (m, 1H), 5.11 – 5.00 (m, 2H), 4.33 – 4.25 (m, 1H), 4.09 – 3.97 (m, 2H), 3.97 – 3.88 (m, 2H), 3.85 – 3.78 (m, 1H), 3.78 – 3.72 (m, 1H), 2.78 (dd, $^2J_{H-H}$ = 15.2 Hz, $^3J_{H-H}$ = 6.2 Hz, 1H), 2.45 – 2.15 (m, 7H), 2.06 (s, 6H), 2.06 – 2.02 (m, 5H), 1.98 – 1.94 (m, 8H), 1.76 (s, 3H), 1.70 – 1.66 (m, 1H), 1.60 – 1.55 (m, 1H), 1.50 (s, 9H), 1.46 – 1.34 (m, 1H), 1.34 – 1.25 (m, 2H), 1.17 – 1.08 (m, 1H), 1.03 – 0.85 (m, 15H), 0.82 (d, $^3J_{H-H}$ = 6.5 Hz, 3H), 0.78 (d, $^3J_{H-H}$ = 6.5 Hz, 3H), 0.76 – 0.71 (m, 2H), 0.67 (d, $^3J_{H-H}$ = 6.6 Hz, 3H), 0.59 (d, $^3J_{H-H}$ = 6.4 Hz, 3H), 0.49 (d, $^3J_{H-H}$ = 6.5 Hz, 3H), 0.23 – 0.09 (m, 4H); ^{13}C NMR (125 MHz, CDCl$_3$):171.6 (C), 170.6 (C), 170.3 (C), 170.1 (C), 169.2 (C), 168.2 (C), 162.7 (br, 4xC, deduced from HMBC), 154.5 (C), 138.4 (C), 136.9 (CH), 135.4 (C), 133.4 (C), 131.7 (C), 130.7 (2xCH), 128.42 (C), 128.37 (C), 128.0 (CH), , 127.4 (C), 127.3 (CH), 127.1 (C), 125.3 (C), 124.3 (CH), 123.0 (C), 121.4 (C), 120.9 (C), 120.1 (C), 81.1 (C), 57.5 (CH$_2$), 57.0 (CH), 56.8 (CH), 53.7 (CH), 53.2 (CH), 52.3 (2xCH), 52.2 (CH), 52.1 (CH), 50.8 (C), 43.7 (2xCH$_3$), 40.3 (3xCH$_2$), 39.3 (CH$_2$), 38.9 (CH$_2$), 37.4 (CH$_2$), 35.4 (3xCH$_2$), 32.4 (CH$_2$), 29.6 (CH$_2$), 28.4 (3xCH$_3$), 26.9 (3xCH), 23.9 (4xCH$_2$), 23.4 (2xCH), 23.3 (CH), 22.4 (CH$_3$), 22.3 (CH$_3$), 21.8 (CH$_3$), 21.2 (CH$_3$), 20.9 (CH$_3$), 18.9 (CH$_3$); 10.5 (4xCH$_3$); MS (ESI, MeOH): 1438 (100, [M+H]$^+$).

203b. Mp: 197 – 198 °C; CD (TFE): 546 (-47.5), 363 (+13.1), 325 (+17.1), 288 (–49.6), 262 (+71.5), 222 (–56.8); IR (neat): 3315 (w), 2960 (w), 2910 (w), 2874 (w), 1695 (m), 1657 (s), 1586 (m), 1524 (m), 1461 (m), 1398 (m), 1384 (m), 1367 (m), 1326 (m), 1240 (s), 1204 (m), 1162 (m), 1092 (w), 1049 (w), 916 (w), 844 (w), 809 (w), 798 (w), 749 (w), 730 (w), 700 (w), 666 (w); ^{1}H NMR (500 MHz, CDCl$_3$): 8.93 (s, 1H), 8.83 (s, 1H), 8.74 (d, $^3J_{H-H}$ = 8.0 Hz, 1H), 8.70 (d, $^3J_{H-H}$ = 8.0 Hz, 1H), 8.35 (d, $^3J_{H-H}$ = 8.0 Hz, 2H), 7.07 (d, $^3J_{H-H}$ = 8.5 Hz, 1H), 7.04 (d, $^3J_{H-H}$ = 5.0 Hz, 1H), 6.97 (d, $^3J_{H-H}$ = 8.2 Hz, 1H), 6.50 (d, $^3J_{H-H}$ = 5.0 Hz, 1H), 6.28 (d, $^3J_{H-H}$ = 3.8 Hz, 1H), 5.95 (s, 1H), 5.11 – 4.99 (m, 3H), 4.71 – 4.62 (m, 1H), 4.58 – 4.50 (m, 1H), 4.33

– 4.25 (m, 1H), 4.24 – 4.17 (m, 1H), 3.77 – 3.70 (m, 1H), 3.65 – 3.53 (m, 2H), 3.31 (dd, $^2J_{\text{H–H}}$ = 15.1 Hz, $^3J_{\text{H–H}}$ = 4.4 Hz, 1H), 3.22 – 3.10 (m, 1H), 2.39 (dd, $^2J_{\text{H–H}}$ = 12.6 Hz, $^3J_{\text{H–H}}$ = 4.8 Hz, 1H), 2.34 – 2.15 (m, 6H), 2.13 – 2.02 (m, 10H), 2.02 – 1.87 (m, 10H), 1.78 – 1.65 (m, 4H), 1.61 – 1.53 (m, 3H), 1.43 (s, 9H), 1.16 – 1.05 (m, 3H), 1.03 – 0.86 (m, 17H), 0.83 (d, $^3J_{\text{H–H}}$ = 6.6 Hz, 3H), 0.74 (d, $^3J_{\text{H–H}}$ = 6.6 Hz, 3H), 0.60 (d, $^3J_{\text{H–H}}$ = 6.5 Hz, 3H), 0.52 (d, $^3J_{\text{H–H}}$ = 6.5 Hz, 3H), 0.37 – 0.32 (m, 1H), 0.30 – 0.22 (m, 1H), 0.19 (d, $^3J_{\text{H–H}}$ = 6.5 Hz, 3H); ^{13}C NMR (125 MHz, CDCl$_3$): 171.0 (C), 169.6 (C), 169.3 (C), 168.6 (C), 167.6 (C), 166.6 (C), 161.9 (br, 4xC, deduced from HMBC), 153.1 (C), 138.6 (C), 135.3 (CH), 134.7 (C), 134.2 (C), 132.7 (CH), 131.3 (C), 129.32 (C), 129.25 (C), 129.2 (C), 128.7 (2xCH), 128.1 (CH), 126.3 (CH), 124.8 (C), 124.7 (C), 124.1 (C), 121.1 (C), 120.6 (C), 119.5 (C), 79.7 (C), 55.83 (CH$_2$), 55.77 (CH), 55.6 (CH), 54.1 (CH), 52.0 (CH), 51.8 (CH), 51.0 (CH), 50.8 (CH), 50.6 (CH), 49.4 (C), 42.4 (2xCH$_3$), 41.7 (CH$_2$), 38.9 (CH$_2$), 38.8 (3xCH$_2$), 37.8 (CH$_2$), 36.2 (CH$_2$), 35.6 (CH$_2$), 34.1 (3xCH$_2$), 27.2 (3xCH), 25.7 (3xCH$_3$), 22.7 (4xCH$_2$), 22.5 (CH), 22.3 (CH), 22.2 (CH), 21.4 (CH$_3$), 21.2 (CH$_3$), 20.8 (CH$_3$), 20.5 (CH$_3$), 19.1 (CH$_3$), 18.2 (CH$_3$), 9.1 (4xCH$_3$); MS (ESI, MeOH): 1438 (100, [M+H]$^+$).
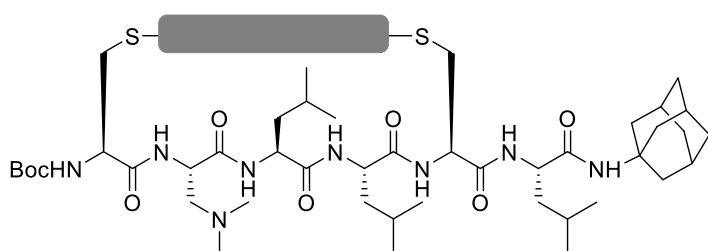
Compound 205. 205a (39 mg, 15%, dark red solid) and **205b** (45 mg, 17%, dark purple solid) was prepared from **174** (200 mg, 0.184 mmol) following the general procedures F and G. R_f (CH$_2$Cl$_2$/MeOH 15:1): 0.36. **205a** and **205b** were separated using chiral flash chromatography (Column: IF, Eluent CH$_2$Cl$_2$/IPA 150:1, flow rate: 5 ml/min). **205a.** Mp: 210 – 211 ºC (decomp); CD (TFE): 558 (-36.6), 365 (+9.6), 326 (+15.0), 290 (–31.4), 262 (+49.7), 223 (–33.1); IR (neat): 3312 (w), 2934 (w), 1694 (m), 1658 (s), 1586 (m), 1527 (m), 1456 (w), 1383 (m), 1328 (m), 1277 (m), 1237 (s), 1151

(s), 1093 (w), 944 (w), 843 (w), 810 (w), 750 (w), 700 (w), 662 (w); ^{1}H NMR (400 MHz, CDCl$_3$): 9.91 (d, $^3J_{H-H}$ = 8.2 Hz, 1H), 9.24 (d, $^3J_{H-H}$ = 8.1 Hz, 1H), 8.84 (s, 1H), 8.75 (s, 1H), 8.67 (d, $^3J_{H-H}$ = 8.2 Hz, 1H), 8.54 (d, $^3J_{H-H}$ = 8.1 Hz, 1H), 6.91 (d, $^3J_{H-H}$ = 4.3 Hz, 1H), 6.87 (d, $^3J_{H-H}$ = 7.9 Hz, 1H), 6.77 (d, $^3J_{H-H}$ = 6.0 Hz, 1H), 6.64 (d, $^3J_{H-H}$ = 8.9 Hz, 1H), 6.32 (d, $^3J_{H-H}$ = 6.0 Hz, 1H), 5.88 (s, 1H), 5.79 (d, $^3J_{H-H}$ = 4.5 Hz, 1H), 5.28 – 5.21 (m, 1H), 5.08 – 5.00 (m, 2H), 4.35 – 4.27 (m, 1H), 4.10 – 4.04 (m, 2H), 3.98 – 3.91 (m, 1H), 3.89 – 3.80 (m, 2H), 3.78 – 3.70 (m, 1H), 2.83 (dd, $^2J_{H-H}$ = 15.2 Hz, $^3J_{H-H}$ = 6.3 Hz, 1H), 2.31 – 2.10 (m, 7H), 2.05 – 2.01 (m, 4H), 1.98 – 1.96 (m, 6H), 1.90 (s, 6H), 1.74 – 1.68 (m, 2H), 1.62 – 1.59 (m, 10H), 1.45 (s, 9H), 1.41 – 1.28 (m, 3H), 1.22 – 1.18 (m, 1H), 0.97 – 0.90 (m, 11H), 0.88 – 0.83 (m, 8H), 0.80 (d, $^3J_{H-H}$ = 6.4 Hz, 3H), 0.71 (d, $^3J_{H-H}$ = 6.5 Hz, 3H), 0.61 (d, $^3J_{H-H}$ = 5.8 Hz, 3H), 0.21 (d, $^3J_{H-H}$ = 6.0 Hz, 3H), 0.19 – 0.13 (m, 1H); ^{13}C NMR (125 MHz, CDCl$_3$): 173.1 (C), 172.5 (C), 172.3 (C), 171.0 (C), 170.4 (C), 169.1 (C), 163.4 (br, 4xC, deduced from HMBC), 156.3 (C), 139.7 (C), 138.2 (CH), 136.4 (C), 134.3 (C), 132.7 (C), 131.6 (CH), 131.3 (C), 130.7 (CH), 129.6 (C), 129.3 (C), 128.9 (CH), 128.5 (C), 128.14 (CH), 128.1 (C), 126.1 (CH), 125.1 (C), 123.9 (C), 122.6 (C), 121.7 (C), 121.2 (C), 82.3 (C), 58.1 (CH), 57.9 (CH), 57.0 (CH$_2$), 54.7 (CH), 54.3 (CH), 54.2 (CH), 53.3 (CH), 53.1 (CH), 52.7 (CH), 51.8 (C), 46.9 (2xCH$_3$), 41.3 (3xCH$_2$), 40.2 (CH$_2$), 39.5 (CH$_2$), 38.4 (CH$_2$), 36.4 (3xCH$_2$), 33.0 (CH$_2$), 30.1 (CH$_2$), 29.5 (3xCH), 28.0 (3xCH$_3$), 25.0 (4xCH$_2$), 24.43 (2xCH), 24.40 (CH), 23.3 (CH$_3$), 23.2 (CH$_3$), 23.1 (CH$_3$), 22.3 (CH$_3$), 20.3 (CH$_3$), 19.9 (CH$_3$), 11.6 (4xCH$_3$); MS (ESI, MeOH): 1438 (100, [M+H]$^+$).

205b. Mp: 205 – 206 °C (decomp); CD (TFE): 586 (+20.2), 474 (+15.5), 425 (-9.7), 375 (–11.1), 321 (+23.8), 256 (–30.2), 218 (+18.7); IR (neat): 3312 (w), 2961 (w), 1740 (w), 1696 (m), 1658 (s), 1586 (m), 1518 (m), 1459 (w), 1381 (m), 1326 (m), 1277 (m), 1238 (s), 1148 (s), 1094 (m), 943 (w), 798 (w), 751 (w), 700 (w), 662 (w); ^{1}H NMR (400 MHz, CDCl$_3$): 8.95 (s, 1H), 8.82 (s, 1H), 8.74 (d, $^3J_{H-H}$ = 7.9 Hz, 1H), 8.69 (d, $^3J_{H-H}$ = 7.9 Hz, 1H), 8.33 (d, $^3J_{H-H}$

= 7.9 Hz, 1H), 8.25 (d, $^3J_{H–H}$ = 7.9 Hz, 1H), 7.05 (d, $^3J_{H–H}$ = 5.8 Hz, 1H), 7.00 (d, $^3J_{H–H}$ = 8.2 Hz, 1H), 6.94 (d, $^3J_{H–H}$ = 4.1 Hz, 1H), 6.82 (d, $^3J_{H–H}$ = 8.7 Hz, 1H), 6.41 (d, $^3J_{H–H}$ = 4.7 Hz, 1H), 6.00 (s, 1H), 5.23 (d, $^3J_{H–H}$ = 3.7 Hz, 1H), 5.15 – 5.01 (m, 2H), 4.68 (dd, $^2J_{H–H}$ = 12.3 Hz, $^3J_{H–H}$ = 2.2 Hz, 1H), 4.59 – 4.50 (m, 1H), 4.36 – 4.26 (m, 1H), 4.11 – 4.05 (m, 1H), 3.75 – 3.68 (m, 1H), 3.67 – 3.62 (m, 1H), 3.59 (dd, $^2J_{H–H}$ = 15.5 Hz, $^3J_{H–H}$ = 1.9 Hz, 1H), 3.39 (dd, $^2J_{H–H}$ = 15.5 Hz, $^3J_{H–H}$ = 5.0 Hz, 1H), 3.15 – 3.06 (m, 1H), 2.33 – 2.17 (m, 4H), 2.07 – 2.02 (m, 4H), 2.01 - 1.98 (m, 9H), 1.88 (s, 6H), 1.84 – 1.78 (m, 1H), 1.77 – 1.73 (m, 1H), 1.72 – 1.66 (m, 3H), 1.64 – 1.59 (m, 8H), 1.52 – 1.47 (m, 1H), 1.39 (s, 9H), 1.37 – 1.30 (m, 1H), 1.15 – 1.07 (m, 1H), 1.04 – 0.90 (m, 15H), 0.85 – 0.81 (m, 7H), 0.69 (d, $^3J_{H–H}$ = 6.5 Hz, 3H), 0.55 (d, $^3J_{H–H}$ = 6.5 Hz, 3H), 0.36 – 0.25 (m, 1H), 0.19 (d, $^3J_{H–H}$ = 6.6 Hz, 3H); ^{13}C NMR (125 MHz, CDCl$_3$): 173.9 (C), 173.4 (C), 172.6 (C), 171.0 (C), 169.3 (C), 168.9 (C), 164.7 (C), 163.7(br, 3xC, deduced from HMBC), 156.5 (C), 140.9 (C), 137.3 (C, CH – peaks overlap), 137.1 (C), 134.8 (CH), 131.7 (CH), 131.6 (C), 131.3 (C), 131.1 (CH), 130.4 (CH), 128.5 (CH), 127.0 (C), 126.8 (C), 126.3 (C), 123.7 (C), 122.7 (2xC), 121.9 (C), 81.9 (C), 58.0 (CH), 57.9 (CH), 57.1 (CH), 56.9 (CH$_2$), 54.4 (CH), 54.2 (CH), 53.2 (CH), 53.1 (CH), 53.1 (CH), 51.8 (C), 46.5 (2xCH$_3$), 44.0 (CH$_2$), 41.4 (CH$_2$), 41.1 (3xCH$_2$), 40.5 (CH$_2$), 39.3 (CH$_2$), 38.6 (CH$_2$), 36.4 (3xCH$_2$), 29.5 (3xCH), 28.0 (3xCH$_3$), 25.1 (4xCH$_2$), 24.8 (CH), 24.6 (CH), 24.3 (CH), 23.5 (CH$_3$), 23.2 (CH$_3$), 22.7 (CH$_3$), 21.7 (CH$_3$), 20.5 (CH$_3$), 20.4 (CH$_3$); 11.5 (4xCH$_3$); MS (ESI, MeOH): 1438 (100, [M+H]$^+$).

5.2.5.   Additives
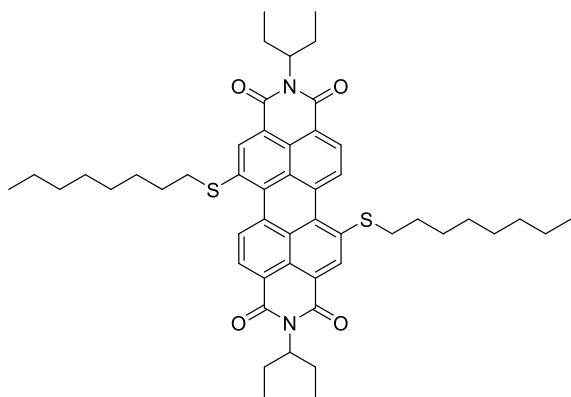
Compound 194. To a solution of **180** (50 mg, 0.07 mmol) in THF (16 ml) were added 1-octanethiol (38 μl, 0.21 mmol), K_2CO_3 (30 mg, 0.21 mmol) and 18-crown-6-ether (57 mg, 0.21 mmol). Reaction mixture was stirred at rt overnight under N_2 atmosphere. The solvent was removed under vacuum. The residue was purified by flash chromatography (CH$_2$Cl$_2$/pentane 1:1) to yield desired product (50 mg, 84%) as a purple solid. R_f (CH$_2$Cl$_2$/pentane 1:1): 0.37; Mp: 187 – 188 °C; IR (neat): 2959 (w), 2924 (m), 2852 (w), 1741 (w), 1696 (m), 1656 (s), 1585 (m), 1551 (w), 1503 (w), 1458 (w), 1369 (m), 1380 (m), 1348 (w), 1322 (s), 1238 (s), 1208 (m), 1164 (w), 1143 (w), 1096 (w), 988 (w), 913 (w), 867 (w), 842 (w), 803 (w), 749 (w), 699 (w), 628 (w); ^{1}H NMR (400 MHz, CDCl$_3$): 8.86 (d, $^3J_{H–H}$ = 8.0 Hz, 2H), 8.78 (s, 2H), 8.67 (d, $^3J_{H–H}$ = 8.0 Hz, 2H), 5.14 – 5.04 (m, 2H), 3.22 (t, $^3J_{H–H}$ = 7.4 Hz, 4H), 2.37 – 2.21 (m, 4H), 2.05 – 1.90 (m, 4H), 1.77 – 1.64 (m, 4H), 1.50 – 1.38 (m, 4H), 1.30 – 1.21 (m, 16H), 0.95 (t, $^3J_{H–H}$ = 7.4 Hz, 12H), 0.90 – 0.80 (m, 6H); ^{13}C NMR (125 MHz, CDCl$_3$): 162.0 (2xC), 161.3 (2xC), 136.1 (2xC), 130.2 (2xC), 130.0 (2xC), 128.5 (2xCH), 126.5 (4xCH), 126.0 (2xC), 123.2 (2xC), 119.8 (2xC), 119.2 (2xC), 55.2 (2xCH), 33.5 (2xCH$_2$), 29.3 (2xCH$_2$), 26.6 (4xCH$_2$), 26.4 (2xCH$_2$), 26.0 (2xCH$_2$), 22.6 (4xCH$_2$), 20.1 (2xCH$_2$), 11.6 (2xCH$_3$), 8.9 (4xCH$_3$); MS (MALDI-TOF): 818 ([M]$^+$).
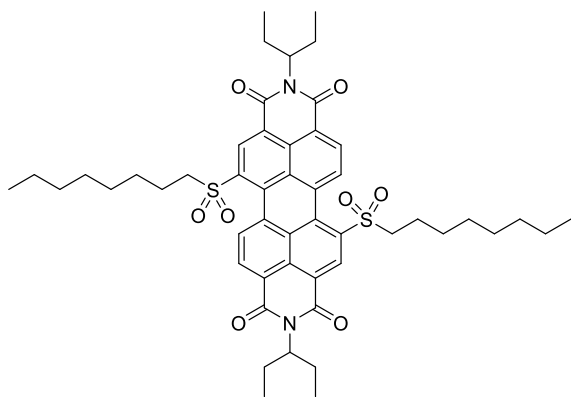
Compound 193. To a solution of **194** (40 mg, 49 μmol) in CH_2Cl_2 (2.0 ml), *m*-CPBA (60 mg, 0.25 mmol) was added. Reaction mixture was stirred at rt overnight. The reaction mixture was diluted with CH_2Cl_2, then washed with aqueous saturated solution of $NaHCO_3$ (3 times). The organic layer was dried over anhydrous Na_2SO_4, filtered and concentrated under vacuum. The residue was purified by flash chromatography (MeOH/CH_2Cl_2 1:100) to yield desired product (37 mg, 86%) as a red solid. R_f (MeOH/CH_2Cl_2 1:100): 0.19; Mp: 107 – 108 °C; IR (neat): 2927 (w), 2857 (w), 1699 (m), 1658 (s), 1589 (m), 1458 (w), 1401 (w), 1386 (w), 1330 (s), 1305 (s), 1242 (s), 1204 (w), 1150 (w), 1127 (m), 1090 (w), 983 (w), 916 (w), 878 (w), 848 (w), 811 (w), 798 (w), 770 (w), 748 (w), 721 (w), 700 (w), 661 (w); ^{1}H NMR (400 MHz, CDCl$_3$): 9.19 (s, 2H), 9.03 (d, $^3J_{H-H}$ = 7.9 Hz, 2H), 8.82 (d, $^3J_{H-H}$ = 7.9 Hz, 2H), 5.15 – 5.01 (m, 2H), 3.52 – 3.39 (m, 4H), 2.35 – 2.18 (m, 4H), 2.15 – 1.89 (m, 4H), 1.81 – 1.67 (m, 4H), 1.44 – 1.32 (m, 4H), 1.29 – 1.16 (m, 16H), 0.94 (t, $^3J_{H-H}$ = 7.4 Hz, 12H), 0.84 (t, $^3J_{H-H}$ = 6.9 Hz, 6H); ^{13}C NMR (100 MHz, CDCl$_3$): 163.1 (4xC), 139.1 (2xC), 135.8 (2xCH), 134.3 (2xC), 131.8 (2xCH), 131.5 (2xC), 130.0 (2xCH), 128.4 (2xC), 128.0 (2xC), 124.2 (2xC), 123.3 (2xC), 58.3 (2xCH), 55.4 (2xCH$_2$), 31.6 (2xCH$_2$), 28.83 (2xCH$_2$), 28.77 (2xCH$_2$), 28.2 (2xCH$_2$), 25.0 (4xCH$_2$), 22.5 (2xCH$_2$), 22.4 (2xCH$_2$), 14.0 (2xCH$_3$), 11.3 (4xCH$_3$); MS (MALDI-TOF): 883 ([M+H$^+$]$^+$).

5.2.6.   Thiol-Mediated Uptake Inhibitors

5.2.6.1. Thiosulfonate Derivatives

5.2.6.1.1. 5-Membered Cyclic Thiosulfonate Derivatives
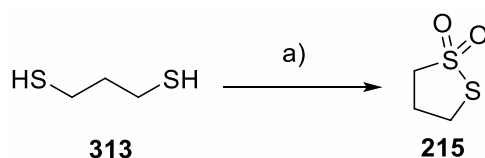
Scheme 25. (a) H_2O_2, 0 °C to rt, overnight, 39%.
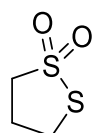
Compound 215 (537 mg, 39%, colorless oil) was synthesized from **313** (1.0 ml, 9.96 mmol) and 30% aqueous solution of H_2O_2 (3.6 ml, 34 mmol) in AcOH (22 ml) following general procedure J. R_f (CH_2Cl_2): 0.24; IR (neat): 3000 (w), 2943 (w), 2857 (w), 1436 (w), 1409 (w), 1298 (s), 1270 (m), 1210 (w), 1151 (m), 1118 (s), 1028 (w), 994 (w), 909 (w), 873 (w), 844 (w), 733 (w), 699 (m), 660 (w); ^{1}H NMR (400 MHz, CDCl$_3$): 3.73 (t, $^3J_{H-H}$ = 6.5 Hz, 2H), 3.43 (t, $^3J_{H-H}$ = 7.0 Hz, 2H), 2.66 – 2.58 (m, 2H); ^{13}C NMR (100 MHz, CDCl$_3$): 8.3 (CH$_2$), 36.8 (CH$_2$), 25.0 (CH$_2$); MS (ESI, CHCl$_3$): 156 (100, [M+NH$_4$]$^+$).
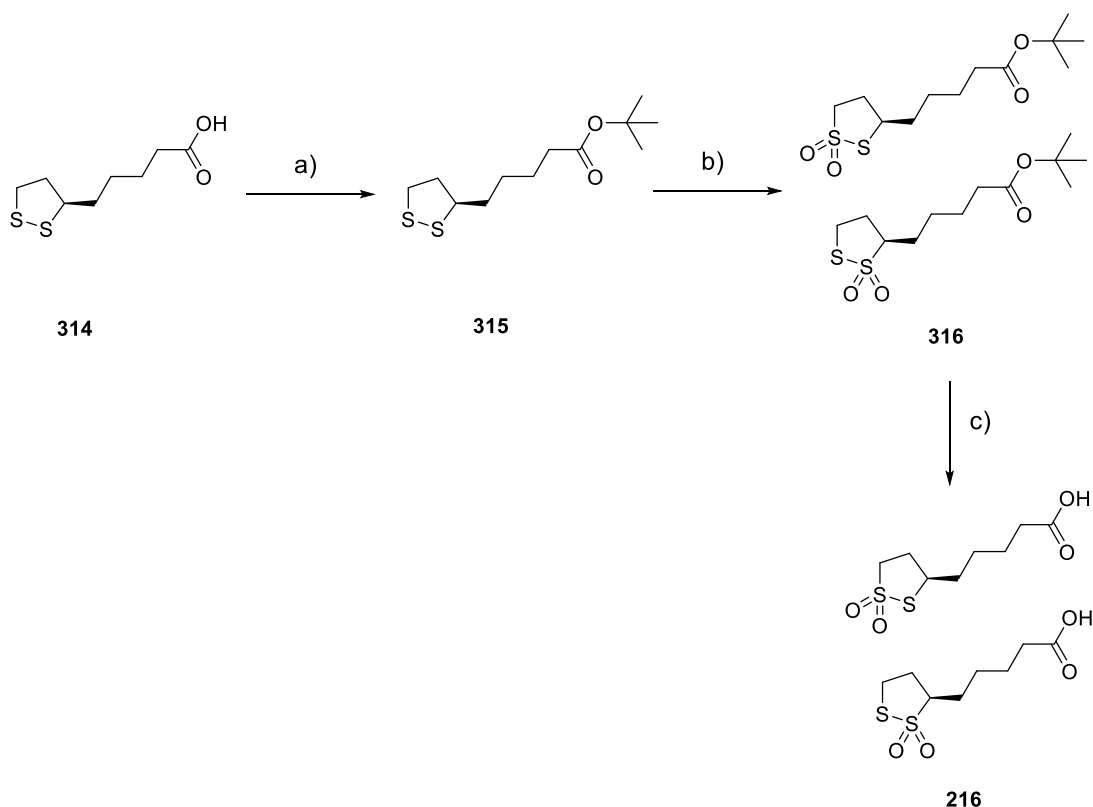
Scheme 26. (a) *t*-BuOH, EDC, DMAP, CH$_2$Cl$_2$, rt, overnight, 50%; (b) *m*-CPBA, rt, 2 d, 31%; (c) TFA/CH$_2$Cl$_2$ 1:1, rt, 4 h, 71%.
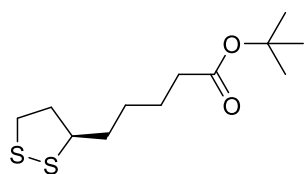
Compound 315. To a solution of *t*-BuOH (691 μl, 7.27 mmol) in CH$_2$Cl$_2$ (10.0 ml), DMAP (355 mg, 2.91 mmol) was added, followed by **314** (500 mg, 2.42 mmol) and EDC (575 mg, 2.91 mmol). The reaction mixture was stirred at rt overnight. The reaction mixture was diluted with CH$_2$Cl$_2$, then washed with 10% aqueous solution of citric acid, water, saturated solution of NaHCO$_3$ and brine. The organic layer was dried over anhydrous Na$_2$SO$_4$ and filtered. The solvent was removed under vacuum. The residue was purified by column chromatography (CH$_2$Cl$_2$) to yield desired product (321 mg, 50%, yellow oil). R_f (CH$_2$Cl$_2$): 0.63; IR (neat): 2974 (w), 2929 (w), 2859 (w), 1724 (s), 1456 (w), 1391 (w), 1366 (m), 1253 (m), 1149 (s), 946 (w), 917 (w), 846 (w), 755 (w), 677 (w), 640 (w); ^{1}H NMR (400 MHz, CDCl$_3$): 3.65 – 3.53 (m,

1H), 3.26 – 3.03 (m, 2H), 2.55 – 2.42 (m, 1H), 2.24 (t, $^3J_{H-H}$ = 7.4 Hz, 2H), 1.99 – 1.87 (m, 1H), 1.81 – 1.57 (m, 4H), 1.56 – 1.38 (m, 11H); ^{13}C NMR (100 MHz, CDCl$_3$): 172.9 (C), 80.1 (C), 56.4 (CH), 40.2 (CH$_2$), 38.5 (CH$_2$), 35.4 (CH$_2$), 34.7 (CH$_2$), 28.7 (CH$_2$), 28.1 (3xCH$_3$), 24.8 (CH$_2$); MS (ESI, CHCl$_3$): 207 (10, [M-tBu+H]$^+$), 263 (1, [M+H]$^+$).
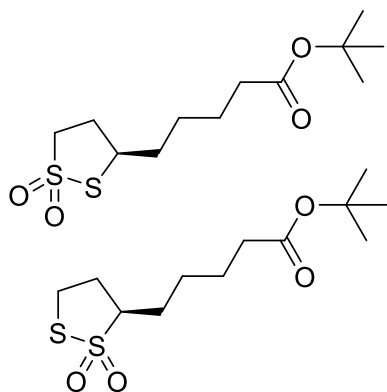
Compound 316. To a solution of **315** (321 mg, 1.22 mmol) in CH$_2$Cl$_2$ (15 ml), *m*-CPBA (754 mg, 3.05 mmol) was added. The reaction mixture was stirred at rt for 2 days. The reaction mixture was diluted with CH$_2$Cl$_2$ and washed with aqueous solution of NaHCO$_3$ (3 times). The organic layer was dried over anhydrous Na$_2$SO$_4$ and filtered. The solvent was removed under vacuum. The residue was purified by flash chromatography (CH$_2$Cl$_2$/MeOH 40:1) to yield desired products (113 mg, mixture of 2 regioisomers 46:54, 31%, colorless oil). R_f (CH$_2$Cl$_2$/MeOH 25:1): 0.60; IR (neat): 2934 (w), 2869 (w), 1724 (s), 1458 (w), 1367 (m), 1308 (s), 1262 (m), 1153 (s), 1130 (s), 944 (w), 847 (w), 709 (w), 671 (w); ^{1}H NMR (400 MHz, CD$_3$OD, nn/nn- regioisomers peaks): 4.36 – 4.24/3.50 – 3.41 (m, 1H), 3.72 – 3.51 (m, 2H), 2.75 – 2.65 (m, 1H), 2.29 – 2.12 (m, 3H), 2.00 – 1.35 (m, 15H); ^{13}C NMR (100 MHz, CD$_3$OD, nn/nn- regioisomers peaks): 173.3 (C), 80.14/80.11 (C), 68.6/55.5 (CH), 59.5/32.9 (CH$_2$), 35.9/31.2 (CH$_2$), 34.62/34.58 (CH$_2$), 30.5/25.9 (CH$_2$), 27.3/27.2 (CH$_2$), 27.0 (3xCH$_3$), 24.4/24.3 (CH$_2$); MS (ESI, MeOH): 239 (98, [M-tBu+H]$^+$), 312 (41, [M+NH$_4$]$^+$).
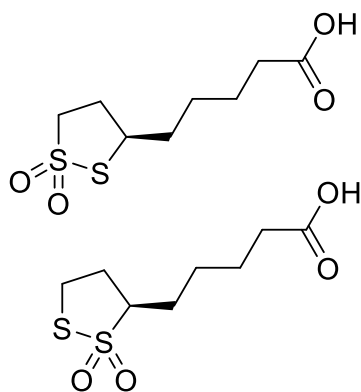
Compound 216. 316 (113 mg, 0.384 mmol) was dissolved in a mixture of CH_2Cl_2/TFA 1:1 (1.2 ml). The reaction mixture was stirred at rt for 4 h. The solvent was removed under vacuum. The residue was purified by flash chromatography (CH_2Cl_2/MeOH/AcOH 96.9:3:0.1) to yield desired products (65 mg, mixture of 2 regioisomers 46:54, 71%, colorless oil). R_f (CH_2Cl_2/MeOH/AcOH 91.9:8:0.1): 0.53; IR (neat): 2937 (w), 2869 (w), 2612 (br), 2232 (br), 2082 (w), 1695 (s), 1460 (w), 1436 (w), 1406 (w), 1299 (s), 1267 (m), 1228 (w), 1207 (w), 1176 (w), 1122 (s), 1053 (w), 1024 (w), 932 (w), 855 (w), 791 (w), 732 (w), 706 (w), 671 (m), 655 (w), 604 (w); ^{1}H NMR (400 MHz, CD$_3$OD, nn/nn- regioisomers peaks): 4.35 – 4.24/3.50 – 3.42 (m, 1H), 3.72 – 3.50 (m, 2H), 2.76 – 2.64 (m, 1H), 2.36 – 2.28 (m, 2H), 2.28 – 2.13(m, 1H), 2.00 – 1.33 (m, 6H); ^{13}C NMR (100 MHz, CD$_3$OD, nn/nn- regioisomers peaks): 175.81/175.79 (C), 68.7/55.6 (CH), 59.4/32.9 (CH$_2$), 35.9/31.2 (CH$_2$), 33.14/33.04 (CH$_2$), 30.4/26.3 (CH$_2$), 27.23/27.21 (CH$_2$), 24.3/24.2 (CH$_2$); MS (ESI, MeOH): 256 (100, [M+NH$_4$]$^+$), 494 (59, [2M+NH$_4$]$^+$), 239 (20, [M+H]$^+$).
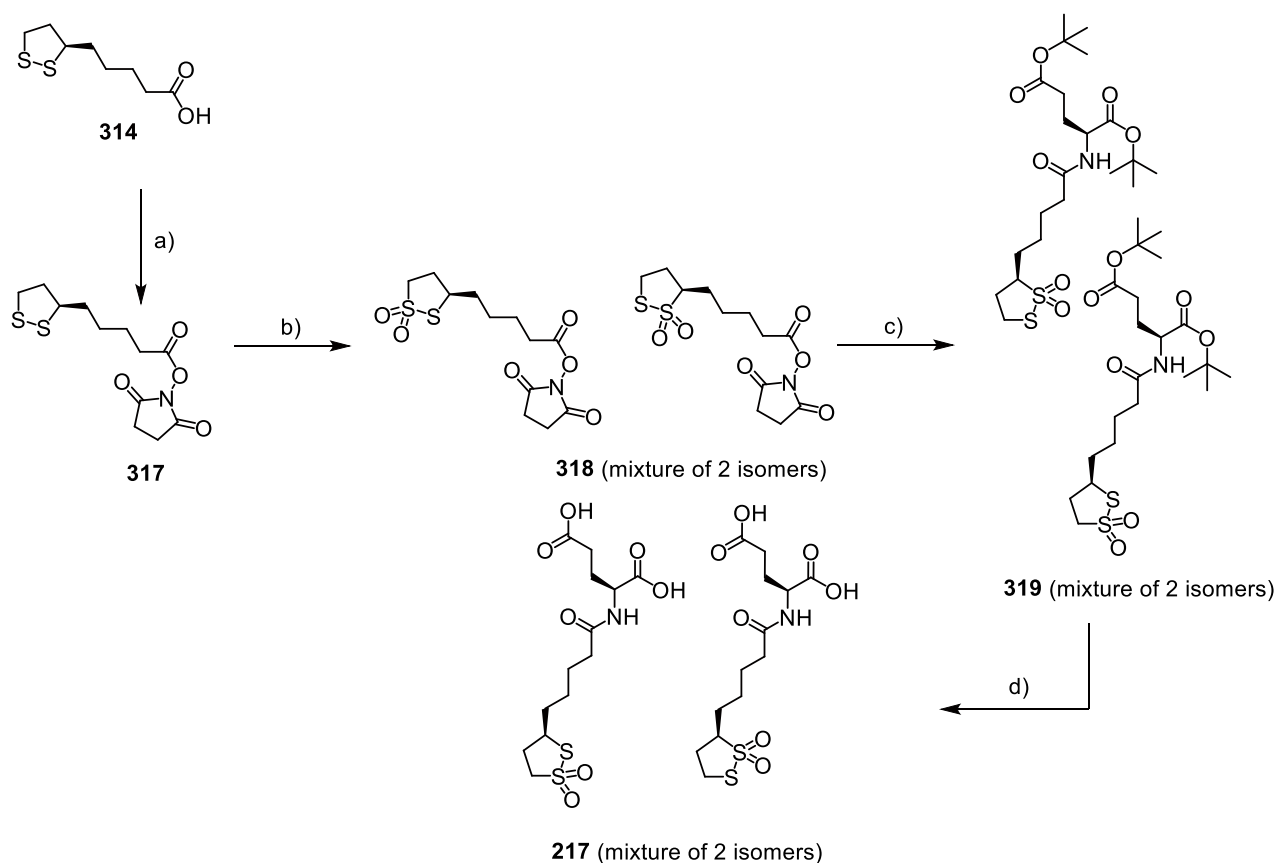
Scheme 27. (a) *N*-Hydroxysuccinimide, EDC, CH$_2$Cl$_2$, rt, overnight, 68%; (b) *m*-CPBA, rt, 24 h, 48%; (b) L-Glutamic acid di-*tert*-butyl ester hydrochloride, TEA, CH$_2$Cl$_2$, rt, overnight, 51%; (c) TFA/DCM 1:1, rt, 24 h, 100%.
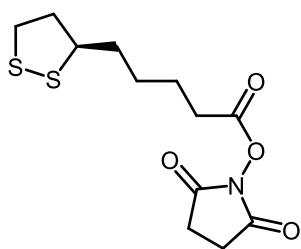
Compound 317. To a solution of (*R*)-α-lipoic acid **314** (1.0 g, 4.8 mmol) in CH$_2$Cl$_2$ (30 mL), *N*-Hydroxysuccinimide (0.6 g, 4.8 mmol) was added, followed by the addition of EDC (1.1 g, 5.3 mmol). The reaction mixture was stirred at rt overnight. Then the mixture was diluted with CH$_2$Cl$_2$, washed with water 3 times. The organic layer was dried over anhydrous Na$_2$SO$_4$ and concentrated in vacuo. The residue was purified by flash chromatography to yield desired product as a yellow solid (1.3 g, 68%). R_f (CH$_2$Cl$_2$): 0.23. Spectroscopic data were consistent with those reported in literature.[232]
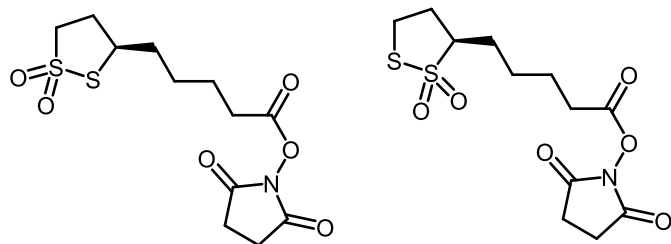
Compound 318. To a solution of **317** (68 mg, 0.22 mmol) in CH_2Cl_2 (2.0 mL), was added *m*-CPBA (128 mg, 0.556 mmol). The resulting mixture was stirred at rt for 24 h. The reaction mixture was diluted with CH_2Cl_2, washed with saturated aqueous solution of $NaHCO_3$ 3 times. The organic layer was dried over anhydrous Na_2SO_4. The solvent was removed under vacuum. The residue was purified by flash chromatography (CH_2Cl_2/MeOH 18:1) to yield desired product as a colorless oil (36 mg, 48%, mixture of 2 isomers). R_f (CH_2Cl_2/MeOH 15:1): 0.47; IR (neat): 2941 (w), 1812 (w), 1782 (w), 1734 (s), 1430 (w), 1362 (w), 1302 (m), 1206 (m), 1127 (m), 1068 (m), 995 (w), 814 (w), 708 (w), 650 (w); ^{1}H NMR (500 MHz, CDCl$_3$, nn/nn-55:45 isomeric peaks, some isomeric peaks overlap): 4.23 – 4.16/3.39 – 3.31 (m, 1H), 3.66 – 3.41 (m, 2H), 2.83 (s, 4H), 2.73 – 2.57 (m, 3H), 2.36 – 2.18 (m, 1H), 1.74 – 1.69/2.10 – 1.99 (m, 1H), 1.95 – 1.86 (m, 1H), 1.84 – 1.76 (m, 2H), 1.66 – 1.45 (m, 2H); ^{13}C NMR (100 MHz, CDCl$_3$, nn/nn isomeric peaks, some isomeric peaks could not be assigned due to overlap in ^{1}H NMR): 169.2/168.3 (C), 68.6/55.0 (CH), 59.6/35.9 (CH$_2$), 33.27 (CH$_2$), 31.2 (CH$_2$), 30.63 (CH$_2$), 30.57 (CH$_2$), 30.2 (CH$_2$), 27.3 (CH$_2$), 27.0 (CH$_2$), 25.9 (CH$_2$), 25.6 (CH$_2$), 24.3/24.1 (CH$_2$); HPLC–MS: R_t = 1.89 min, 336 (100, [M+H]$^+$) (Eluent: CH$_3$CN + 0.1% TFA/water 0.1% TFA gradient from 5:95 to 95:5); MS (ESI, MeOH): 336 (100, [M+H]$^+$).
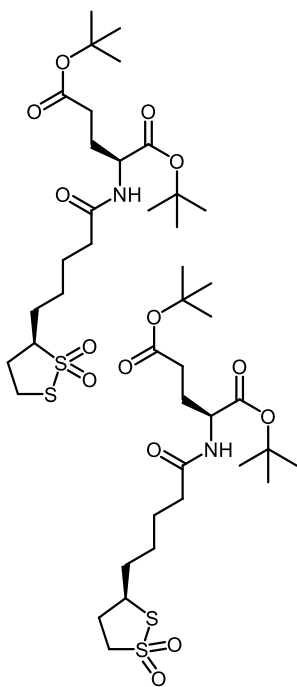
Compound 319. To a solution of **318** (36 mg, 0.11 mmol) in CH_2Cl_2 (150 µL), was added glutamic acid di-*tert*-butyl ester hydrochloride (26 mg, 0.13 mmol), followed by TEA (21 µL, 0.17 mmol). The reaction mixture was kept stirring at rt overnight. The reaction mixture was diluted with CH_2Cl_2, washed with 10% aqueous solution of citric acid, water, saturated solution of $NaHCO_3$ and brine. The organic layer was dried over anhydrous Na_2SO_4. Then the solvent was removed *in vacuo*. The residue was purified by flash chromatography (CH_2Cl_2/MeOH 25:1) to yield the desired product as a colorless oil (26 mg, 51%, mixture of 2 isomers). R_f (CH_2Cl_2/MeOH 25:1): 0.49; IR (neat): 3307 (w), 2977 (w), 2929 (w), 1728 (m), 1652 (m), 1539 (w), 1455 (w), 1368 (w), 1305 (m), 1255 (m), 1152 (s), 1130 (s), 965 (w), 846 (w), 752 (w), 709 (w), 673 (w); ^{1}H NMR (400 MHz, CDCl$_3$, nn/nn-55:45 isomeric peaks, some isomeric peaks overlap): 6.21 (d, $^3J_{H-H}$ = 8.1 Hz, 1H), 4.50 – 4.43 (m, 1H), 4.25 – 4.15/3.41 – 3.32 (m, 1H), 3.67 – 3.42 (m, 2H), 2.74 – 2.63 (m, 1H), 2.40 – 2.18 (m, 5H), 2.16 – 2.01 (m, 2H), 1.98 – 1.83 (m, 2H), 1.79 – 1.64 (m, 3H), 1.63 – 1.52 (m, 1H), 1.48 (s, 9H), 1.45 (s, 9H); ^{13}C NMR (100 MHz, CDCl$_3$, nn/nn isomeric peaks, some isomeric peaks could not be assigned due to overlap in ^{1}H NMR): 172.37/172.35 (C), 172.22/172.18 (C), 171.24/171.21 (C), 82.4/82.3 (C), 80.84/80.82 (C), 68.7/55.2 (CH), 59.6/36.2 (CH$_2$), 52.3 (CH), , 35.9/35.8 (CH$_2$), 33.2 (CH$_2$), 31.6 (CH$_2$), 31.3 (CH$_2$), 30.2 (CH$_2$), 28.1 (6xCH$_3$), 28.0 (6xCH$_3$), 27.6 (CH$_2$), 27.5 (CH$_2$), 27.5 (CH$_2$), 26.4 (CH$_2$), 25.0/24.9 (CH$_2$); HPLC–MS: R_t = 2.68 min, 368 (100, [M-2*t*-Bu+H]$^+$), 424 (33, [M-*t*-Bu+H]$^+$), 480 (18, [M+H]$^+$) (Eluent: CH$_3$CN + 0.1% TFA/water 0.1% TFA gradient from 5:95 to 95:5); MS (ESI, MeOH): 480 (100, [M+H]$^+$).
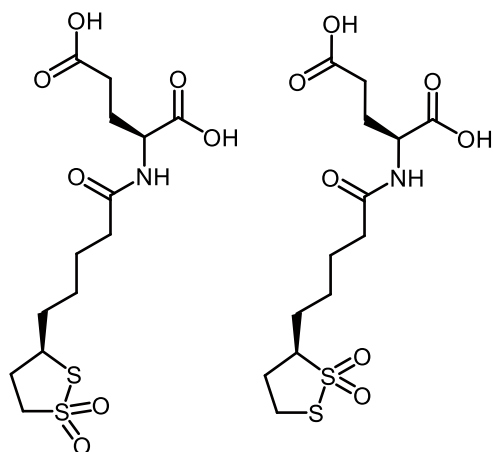
Compound 217 (20 mg, 100%, colorless oil, mixture of 2 isomers) was prepared from **319** (26 mg, 0.05 mmol) following the general procedure A. Crude product was purified by reversed phase flash column chromatography (Eluent: H_2O + 0.1% TFA/CH_3CN + 0.1% TFA gradient from 95:5 to 40:60). IR (neat): 3340 (w), 2936 (w), 2507 (w), 1719 (s), 1628 (m), 1548 (w), 1444 (w), 1413 (w), 1296 (m), 1208 (m), 1174 (m), 1124 (s), 1025 (w), 784 (w), 709 (w), 672 (w); ^{1}H NMR (400 MHz, CD_3OD, nn/nn-55:45 isomeric peaks, some isomeric peaks overlap): 4.45 – 4.37 (m, 1H), 4.34 – 4.24/3.48 – 3.41 (m, 1H), 3.72 – 3.50 (m, 2H), 2.78 – 2.64 (m, 1H), 2.44 – 2.34 (m, 2H), 2.32 – 2.13 (m, 4H), 2.01 – 1.75 (m, 3H), 1.71 – 1.40 (m, 4H); ^{13}C NMR (100 MHz, CD_3OD, nn/nn isomeric peaks, some isomeric peaks could not be assigned due to overlap in ^{1}H NMR): 178.8 (C), 178.6 (C), 177.49/177.47 (C), 72.6/59.5 (CH), 63.3/39.8 (CH_2), 55.48/55.46 (CH), 38.9/38.8 (CH_2), 36.9 (CH_2), 35.1 (CH_2), 34.2 (CH_2), 33.8 (CH_2), 31.03/31.02 (CH_2), 30.33/30.31 (CH_2), 29.9 (CH_2), 29.0/28.9 (CH_2); HPLC–MS: R_t = 1.36 min, 368 (100, [M+H]$^+$) (Eluent: CH_3CN + 0.1% TFA/water 0.1% TFA gradient from 5:95 to 95:5).

5.2.6.1.2.   6-Membered Cyclic Thiosulfonate Derivatives

5.2.6.1.2.1.   Monocyclic Derivatives
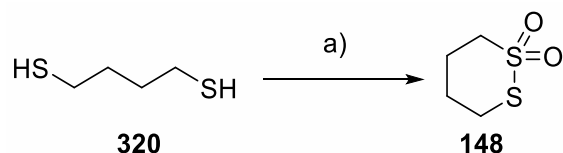
Scheme 28. (a) H_2O_2, 0 °C to rt, overnight, 20%.
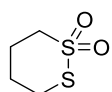
Compound 148. (45 mg, 20%, colorless solid) was synthesized from **306** (184 mg, 1.51 mmol) and 30% aqueous solution of H_2O_2 (538 μl, 5.29 mmol) in AcOH (1.5 ml) following general procedure J. R_f (CH_2Cl_2): 0.49. Spectroscopic data were consistent with those reported in literature.[173]
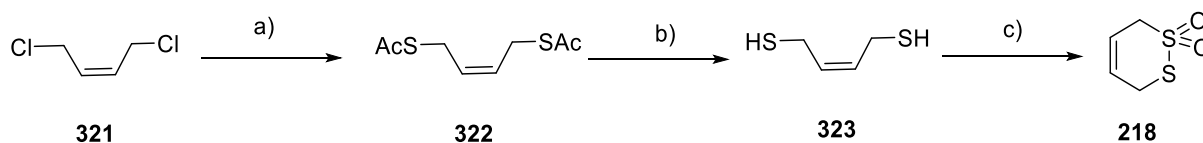
Scheme 29. (a) KSAc, 18-crown-6-ether, DMF, rt, under N_2, overnight, 58%; (b) 1.25 M HCl in MeOH, rt, under N_2, 4 h, 61%; (c) H_2O_2, 0 °C to rt, overnight, 5%.
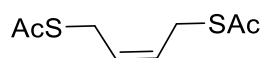
Compound 322. (1.7 g, 58%, colorless oil) was synthesized from **321** (1.5 ml, 14 mmol) following general procedure H. R_f (CH_2Cl_2): 0.44. Spectroscopic data were consistent with those reported in literature.[239]
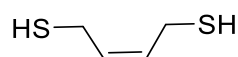
Compound 323. (180 mg, 61%, smelly colorless oil) was synthesized from **322** (500 mg, 2.45 mmol) following general procedure I. Spectroscopic data were consistent with those reported in literature.[239]
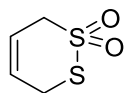
Compound 218. (16 mg, 5%, pale yellow oil) was synthesized from **323** (252 mg, 2.10 mmol) in 4.5 ml AcOH following general procedure J. R_f (CH₂Cl₂): 0.33; IR (neat): 2940 (w), 2905 (w), 1660 (w), 1413 (w), 1392 (w), 1295 (s), 1253 (m), 1201 (w), 1147 (m), 1115 (s), 1004 (w), 971 (w), 905 (w), 873 (w), 830 (m), 735 (s), 644 (s); ^{1}H NMR (400 MHz, CDCl₃): 6.19 – 6.00 (m, 1H), 5.91 – 5.68 (m, 1H), 4.02 – 3.91 (m, 4H); ^{13}C NMR (100 MHz, CDCl₃): 123.8 (CH), 122.9 (CH), 57.0 (CH₂), 34.5 (CH₂); MS (ESI, CHCl₃): 339 (20, [M+K]$^+$).
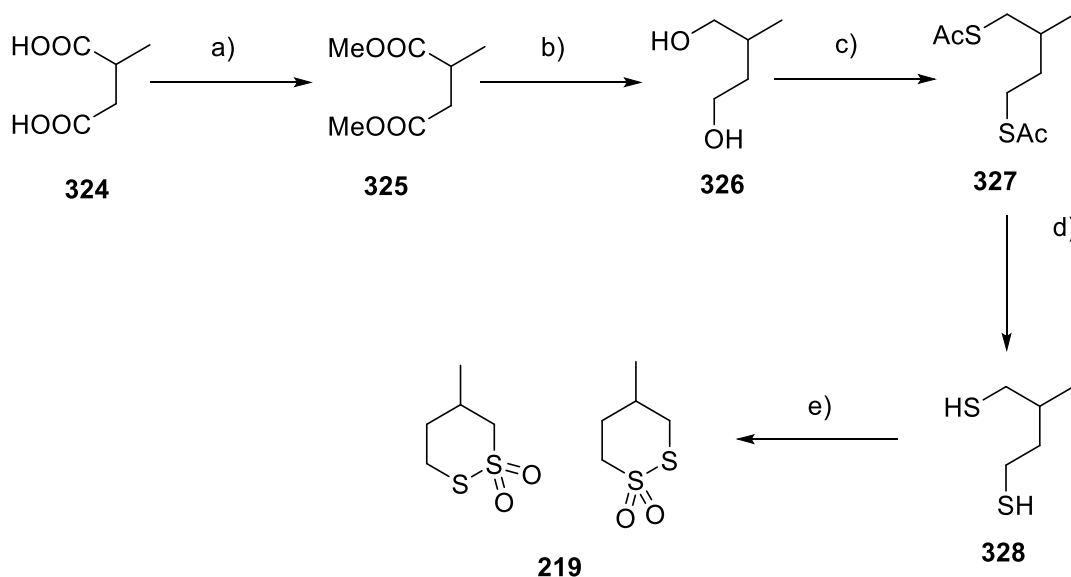
Scheme 30. (a) SOCl₂, MeOH, 0 °C to rt, under N₂, overnight, 97%; (b) LiAlH₄, dry THF, 0 °C to rt, 3 h, 82%; (c) PPh₃, DIAD, HSAc, dry THF, 0 °C to rt, under N₂, 17 h, 43%; (d) 1.25 M HCl in MeOH, rt, under N₂, 4 h, 59%; (f) H₂O₂, 0 °C to rt, overnight, 46%.
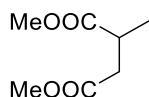
Compound 325. To a solution of **324** (5.0 g, 38 mmol) in MeOH (60 ml) under N₂ at 0 °C, SOCl₂ (8.3 ml, 114 mmol) was added dropwise. The reaction mixture was warmed up to rt and kept stirring overnight. The solvent was removed under vacuum. The residue was dissolved in CH₂Cl₂. The organic layer was washed with

saturated aqueous solution of NaHCO$_3$ and brine. The organic layer was dried over anhydrous Na$_2$SO$_4$. The solvent was removed under vacuum to yield desired product as a colorless oil (5.9 g, racemic, 97%). Spectroscopic data were consistent with those reported in literature.[240]
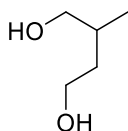
Compound 326. To a suspension of LiAlH$_4$ (2.1 g, 55 mmol) in dry THF (150 ml) under N$_2$, at 0 °C, a solution of **325** (3.0 g, 19 mmol) in dry THF (50 ml) was added dropwise. The reaction mixture was stirred at 0 °C for 1 h, then at rt for another 2 h. Then 2.2 ml of water was added dropwise to the reaction mixture at 0 °C, followed by 2.2 ml of 15% aqueous solution of NaOH and 6.6 ml of water. The reaction mixture was kept stirring at rt for 1 h. Then the mixture was filtered. The solid was washed several times with CH$_2$Cl$_2$. The filtrates were combined and the solvents were removed under vacuum. The residue was purified by flash chromatography (EtOAc) to yield the desired product as a colorless oil. R_f (EtOAc): 0.45. Spectroscopic data were consistent with those reported in literature.[241]
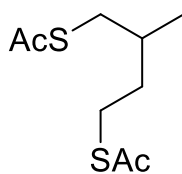
Compound 327. To a solution of PPh$_3$ (6.0 g, 23 mmol) in dry THF (70 ml) under N$_2$ at 0 °C, DIAD (3.6 ml, 23 mmol) was added dropwise. The reaction mixture was stirred at 0 °C for 20 min. Then a solution of **326** (1.0 g, 9.6 mmol) in dry THF (29 ml) was added, followed by HSAc (1.6 ml, 23 mmol). The reaction mixture was stirred at 0 oC for 1 h, then at rt for 16 h. The solvent was removed under vacuum. The residue was purified by column chromatography (CH$_2$Cl$_2$) to yield the desired product (913 mg, 43%, colorless oil). R_f (CH$_2$Cl$_2$): 0.47; IR (neat): 2963 (w), 2928 (w), 1691 (s), 1425 (w), 1378 (w), 1354 (w), 1135 (m), 1108 (m), 958 (m), 750 (w), 627 (m); ^{1}H NMR (400 MHz, CDCl$_3$): 3.04 – 2.74 (m, 4H), 2.34 (s, 3H), 2.33 (s, 3H), 1.82 – 1.72 (m, 1H), 1.72 – 1.61 (m, 1H), 1.51 – 1.41 (m, 1H), 0.98 (d, $^3J_{H-H}$ = 6.7 Hz, 3H); ^{13}C NMR (100 MHz, CDCl$_3$): 195.8

(C), 195.7 (C), 35.5 (CH$_2$), 35.4 (CH$_2$), 32.8 (CH), 30.7 (CH$_3$), 30.6 (CH$_3$), 26.8 (CH$_2$), 18.8 (CH$_3$).
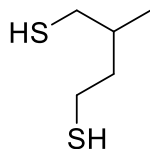
Compound 328 (332 mg, 59%, smelly colorless oil) was synthesized from **327** (913 mg, 4.14 mmol) following general procedure I. R_f (pentane/CH$_2$Cl$_2$ 9:1): 0.27; IR (neat): 2958 (s), 2924 (s), 2872 (w), 2551 (w), 1457 (m), 1432 (m), 1377 (m), 1336 (w), 1305 (w), 1283 (m), 1256 (w), 1162 (w), 1089 (w), 930 (w), 885 (w), 828 (w), 707 (m), 669 (w); ^{1}H NMR (400 MHz, CDCl$_3$): 2.71 – 2.36 (m, 4H), 1.88 – 1.73 (m, 2H), 1.66 – 1.45 (m, 1H), 1.37 (t, $^3J_{H-H}$ = 7.7 Hz, 1H), 1.29 (t, $^3J_{H-H}$ = 8.2 Hz, 1H), 1.01 (d, $^3J_{H-H}$ = 6.6 Hz, 3H); ^{13}C NMR (100 MHz, CDCl$_3$): 39.5 (CH$_2$), 34.8 (CH), 31.2 (CH$_2$), 22.3 (CH$_2$), 18.2 (CH$_3$).
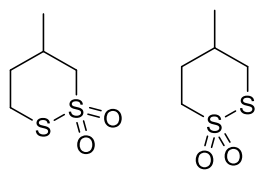
Compound 219 (mixture of 2 regioisomers 3:2, 112 mg, 46%, colorless oil) was synthesized from **328** (200 mg, 1.47 mmol) and H$_2$O$_2$ (524 μl, 5.15 mmol) in AcOH (2.5 ml) following general procedure J. R_f (CH$_2$Cl$_2$): 0.44; IR (neat): 2964 (w), 2928 (w), 2878 (w), 1457 (w). 1418 (w), 1401 (w), 1381 (w), 1345 (w), 1313 (s), 1292 (s), 1243 (w), 1202 (w), 1126 (s), 1067 (w), 1046 (w), 1022 (w), 990 (w), 945 (w), 890 (m), 849 (w), 778 (m), 734 (w), 713 (m), 674 (w), 650 (w), 617 (w); ^{1}H NMR (400 MHz, CDCl$_3$, nn/nn - regioisomers peaks): 3.57 – 3.02 (m, 4H), 2.60 – 2.45/2.24 – 2.11 (m, 1H), 2.34 – 2.10/1.68 – 1.50 (m, 2H), 1.14/1.12 (d, $^3J_{H-H}$ = 6.3 Hz/6.8 Hz, 3H); ^{13}C NMR (125 MHz, CDCl$_3$, nn/nn- regioisomers peaks): 65.8/58.6 (CH$_2$), 41.1/34.2 (CH$_2$), 33.62/33.58 (CH$_2$), 33.3/30.7 (CH), 21.8/20.2 (CH$_3$); MS (ESI, CHCl$_3$): 184 (100, [M+NH$_4$]$^+$).
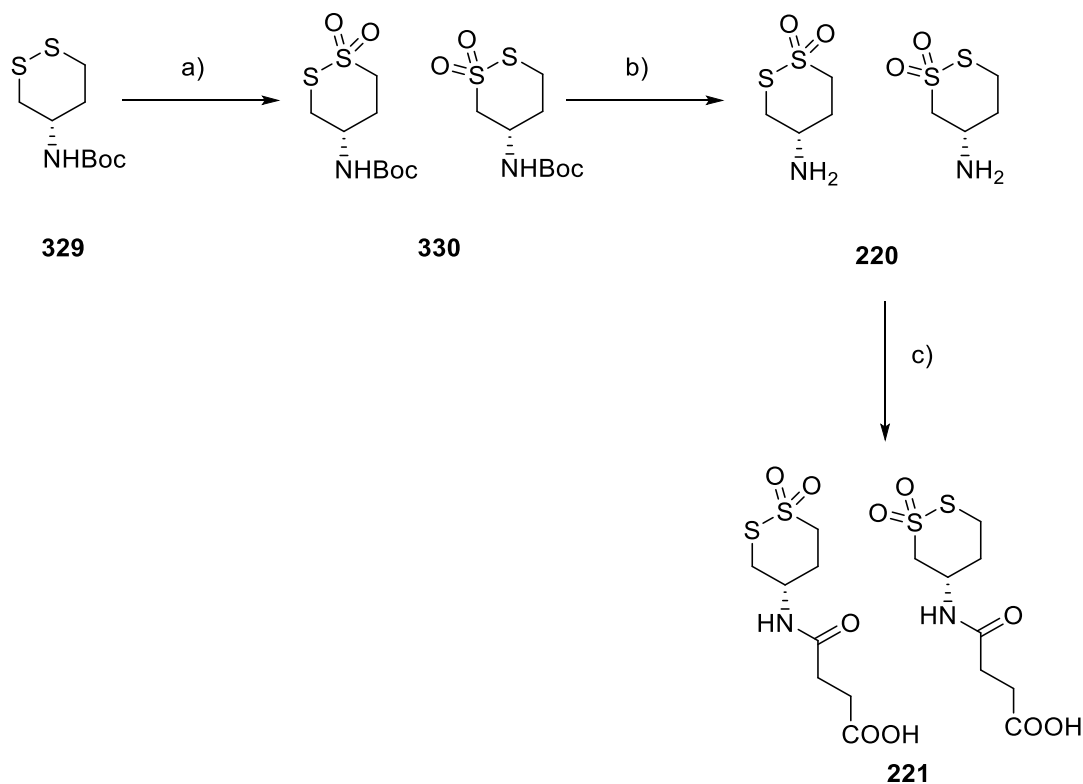
Scheme 31. (a) *m*-CPBA, CH$_2$Cl$_2$, rt, 2 d, 32%; (b) 1.25 M HCl in MeOH, rt, overnight, 81%; (c) succinic anhydride, TEA, CH$_2$Cl$_2$, rt, overnight, 59%.

Compound 329 was synthesized and purified according to procedures described in literature.[242]
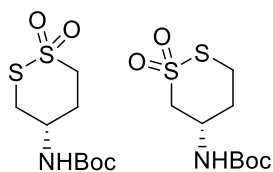
Compound 330. To a solution of **329** (150 mg, 0.637 mmol) in CH$_2$Cl$_2$ (6.0 ml), *m*-CPBA (393 mg, 1.59 mmol) was added. The reaction mixture was stirred at rt for 2 days. The reaction mixture was diluted with CH$_2$Cl$_2$, then washed with saturated aqueous solution of NaHCO$_3$ (3 times). The organic layer was dried over anhydrous Na$_2$SO$_4$. The solvent was removed under vacuum. The residue was purified by flash chromatography (CH$_2$Cl$_2$/MeOH 18:1) to yield desired product (mixture of 2 regioiomers 9:1, 54 mg, 32%, colorless solid). R_f (CH$_2$Cl$_2$/MeOH 15:1):

0.61; IR (neat): 3344 (w), 2981 (w), 2941 (w), 1681 (s), 1519 (s), 1461 (w), 1415 (w), 1392 (w), 1367 (w), 1305 (s), 1258 (m), 1226 (w), 1167 (m), 1128 (s), 1054 (m), 1013 (m), 894 (w), 876 (w), 856 (w), 804 (w), 782 (w), 746 (w), 715 (m), 631 (w); ^{1}H NMR (400 MHz, DMSO-d_6, nn/nn - regioisomers peaks): 7.35 – 7.20 (m, 1H), 3.95 – 3.80/4.02 – 3.95(m, 1H), 3.77 – 3.62/3.48 – 3.40 (m, 2H), 3.33 – 3.10 (m, 2H, partially overlaps with water peaks, deduced by HSQC and HMBC), 2.28 – 2.13/2.28 – 2.13 and 1.77 – 1.62 (m, 2H), 1.38 (s, 9H); ^{13}C NMR (125 MHz, DMSO-d_6, nn/nn - regioisomers peaks): 155.2/154.7 (C), 78.9/19.0 (C), 58.5/63.8 (CH$_2$), 45.7/48.9 (CH), 38.4/32.1 (CH$_2$), 31.3/32.0 (CH$_2$), 28.6 (CH$_3$); MS (ESI, MeOH): 168 (100, [M+H-Boc]$^+$), 285 (100, [M+NH$_4$]$^+$), 268 (25, [M+H]$^+$).
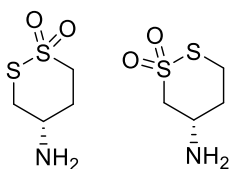
Compound 220. 330 (33 mg, 0.12 mmol) was dissolved in 1.25 M solution of HCl in MeOH (3.0 ml). The reaction mixture was stirred at rt overnight. The solvent was removed under vacuum. The residue was purified by preparative HPLC (eluent: CH$_3$CN + 0.1% TFA/ H$_2$O + 0.1% TFA gradient from 0% CH$_3$CN + 0.1% TFA to 1% (the first 7 min), then 1% to 95%). Fractions contained product were lyophilized to yield desired product (28 mg – TFA salt, anion was exchanged during purification, mixture of 2 regioiomers 9:1, 81%, colorless, very hydroscopic solid). IR (neat): 2934 (br), 1779 (w), 1666 (m), 1531 (w), 1432 (w), 1381 (w), 1325 (w), 1303 (w), 1165 (s), 1128 (s), 1033 (w), 997 (w), 969 (w), 895 (w), 839 (w), 796 (w), 720 (m), 705 (m), 632 (w); ^{1}H NMR (400 MHz, DMSO-d_6, nn/nn - regioisomers peaks): 8.48 (s, 3H), 3.91 – 3.63 (m, 3H), 3.53 – 3.43/3.27 – 3.18 (m, 2H, partially overlaps with water peaks, deduced by HSQC and HMBC), 2.42 – 2.21/1.94 – 1.80 (m, 2H), ^{13}C NMR (125 MHz, DMSO-d_6, nn/nn - regioisomers peaks): 158.84 (q, $^2J_{CF}$ = 32.8 Hz, C, TFA anion), 117.18 (q, $^1J_{CF}$ = 297.2 Hz, C, TFA anion), 57.5/61.2 (CH$_2$), 45.8/48.8 (CH), 36.4/31.8 (CH$_2$), 29.7/29.5 (CH$_2$); MS (ESI, MeOH): 168 (100, [M+H]$^+$).
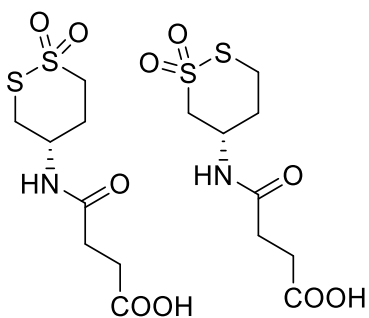
Compound 221. To a solution of **220** (39 mg, 0.24 mmol) in CH_2Cl_2 (2.0 ml), TEA (99 μl, 0.71 mmol) was added, followed by succinic anhydride (28 mg, 0.28 mmol). The reaction mixture was stirred at rt overnight. The solvent was removed under vacuum. The residue was purified by preparative HPLC (eluent: CH_3CN + 0.1% TFA/ H_2O + 0.1% TFA gradient from 0% CH_3CN + 0.1% TFA to 1% (the first 7 min), then 1% to 95%). Fractions contained product were lyophilized to yield desired product (37 mg, mixture of 2 regioiomers 9:1, 59%, colorless, very hydroscopic solid). IR (neat): 3282 (w), 2929 (br), 2550 (br), 1701 (s), 1671 (w), 1623 (s), 1556 (s), 1436 (w), 1408 (w), 1376 (w), 1320 (m), 1297 (s), 1252 (m), 1229 (m), 1196 (w), 1172 (m), 1122 (s), 1094 (w), 1023 (w), 997 (w), 956 (w), 929 (w), 895 (w), 837 (w), 806 (w), 762 (w), 739 (w), 716 (m), 648 (w); ^1H NMR (400 MHz, DMSO-d_6, nn/nn - regioisomers peaks): 12.05 (br, 1H), 8.17 (d, $^3J_{HH}$ = 7.4 Hz, 1H), 4.21 – 4.11/4.35 – 4.22 (m, 1H), 3.84 – 3.62 (m, 2H), 3.52 – 3.01 (m, 1H), 3.33 – 3.16 (m, 2H), 2.46 – 2.15 and 1.80 – 1.68 (m, 6H); ^{13}C NMR (125 MHz, DMSO-d_6, nn/nn - regioisomers peaks): 174.22/174.18 (C), 171.3/170.8 (C), 58.0/63.4 (CH_2), 43.6/47.4 (CH), 38.4/46.2 (CH_2), 31.1/32.2 (CH_2), 30.5/31.6 (CH_2), 29.5/29.4 (CH_2); MS (ESI, MeOH): 290 (100, [M+Na]$^+$).

5.2.6.1.2.2. Bicyclic Derivatives
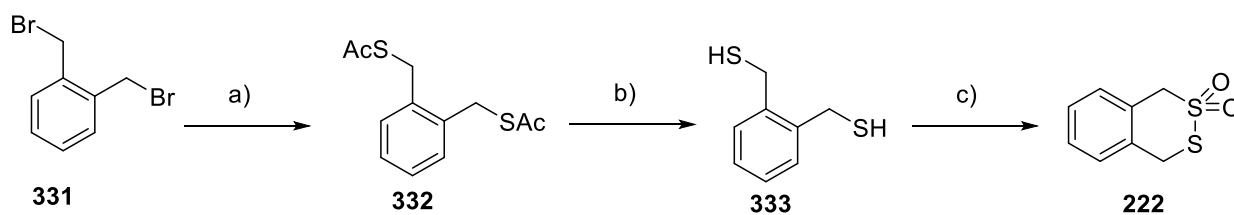
Scheme 32. (a) KSAc, 18-crown-6-ether, DMF, rt, under N_2, overnight, 89%; (b) 1.25 M HCl in MeOH, rt, under N_2, 4 h, 82%; (c) H_2O_2, 0 °C to rt, overnight, 31%.
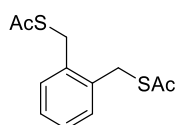
Compound 332 (428 mg, 89%, red brown oil) was synthesized from **331** (500 mg, 1.89 mmol) following general procedure H. R_f (CH_2Cl_2): 0.47. Spectroscopic data were consistent with those reported in in literature.[243]
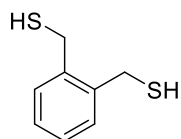
Compound 333 (235 mg, 82%, smelly brown oil) was synthesized from **332** (428 mg, 1.68 mmol) following general procedure I. R_f (pentane/CH_2Cl_2 1:1): 0.62. Spectroscopic data were consistent with those reported in literature.[243]
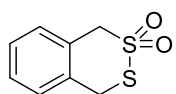
Compound 222 (86.0 mg, 31%, colorless solid) was synthesized from **333** (235 mg, 1.38 mmol) following general procedure J. R_f (pentane/CH_2Cl_2 4:1): 0.35. Spectroscopic data were consistent with those reported in in literature.[244]
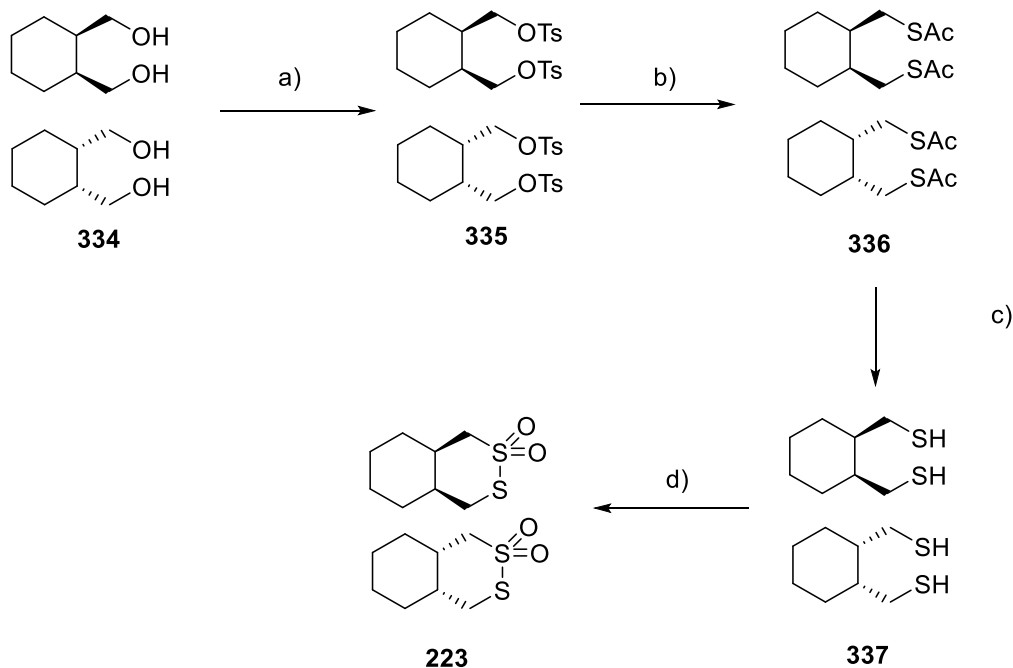
Scheme 33. (a) TsCl, pyridine/CHCl$_3$, rt, 0 °C to rt, overnight, 67%; (b) KSAc, 18-crown-6-ether, DMF, rt, under N$_2$, overnight, 80%; (c) 1.25 M HCl in MeOH, rt, under N$_2$, 4 h, 91%; (d) H$_2$O$_2$, 0 °C to rt, overnight, 30%.

Compound 335 (racemic) was synthesized and purified according to procedures described in literature.[245]
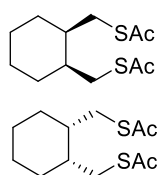
Compound 336 (484 mg, 80%, yellow oil) was synthesized from **335** (1.05 g, 2.32 mmol) following general procedure H. R_f (CH$_2$Cl$_2$/pentane 3:1): 0.36; IR (neat): 2926 (m), 2857 (w), 1690 (s), 1450 (w), 1419 (w), 1354 (w), 1255 (w), 1135 (m), 1109 (m), 957 (m), 746 (w), 666 (w), 930 (m); ^{1}H NMR (400 MHz, CDCl$_3$): 3.04 – 2.81 (m, 4H), 2.34 (s, 6H), 1.88 – 1.79 (m, 2H), 1.61 – 1.43 (m, 6H), 1.41 – 1.25 (m, 2H); ^{13}C NMR (100 MHz, CDCl$_3$): 195.8 (C), 39.1 (CH), 30.6 (CH$_3$), 29.7 (CH$_2$), 28.0 (CH$_2$), 23.1 (CH$_2$).
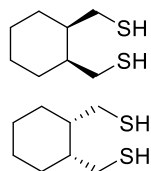
Compound 337 (299 mg, 91%, colorless oil) was synthesized from **3336** (484 mg, 1.86 mmol) following general procedure I. R_f (CH$_2$Cl$_2$/pentane 1:9): 0.47. Spectroscopic data were consistent with those reported in literature.[246]
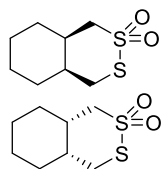
Compound 223 (106 mg, 30%, colorless solid) was synthesized from **337** (299 mg, 1.70 mmol) following general procedure J. R_f (CH$_2$Cl$_2$/pentane 4:1): 0.44; Mp: 94 – 95 °C; IR (neat): 2983 (w), 2930 (s), 2860 (m), 1451 (w), 1415 (w), 1397 (w), 1371 (w), 1346 (w), 1302 (s), 1247 (m), 1167 (w), 1125 (s), 1051 (m), 978 (w), 953 (w), 926 (w), 907 (w), 888 (w), 817 (m), 778 (m), 660 (w), 629 (w); ^{1}H NMR (400 MHz, CDCl$_3$): 3.80 – 3.54 (m, 2H), 3.17 – 2.88 (m, 2H), 2.79 – 2.67 (m, 1H), 2.18 – 2.02 (m, 1H), 1.99 – 1.78 (m, 2H), 1.78 – 1.51 (m, 4H), 1.50 – 1.09 (m, 4H); ^{13}C NMR (100 MHz, CDCl$_3$): 59.1 (CH$_2$), 41.2 (CH), 36.9 (CH), 34.0 (CH$_2$), 31.9 (CH$_2$), 25.3 (CH$_2$), 24.3 (CH$_2$), 20.5 (CH$_2$); MS (ESI, CHCl$_3$): 430 (100, [2M+NH$_4$]$^+$), 224 (67, [M+NH$_4$]$^+$).
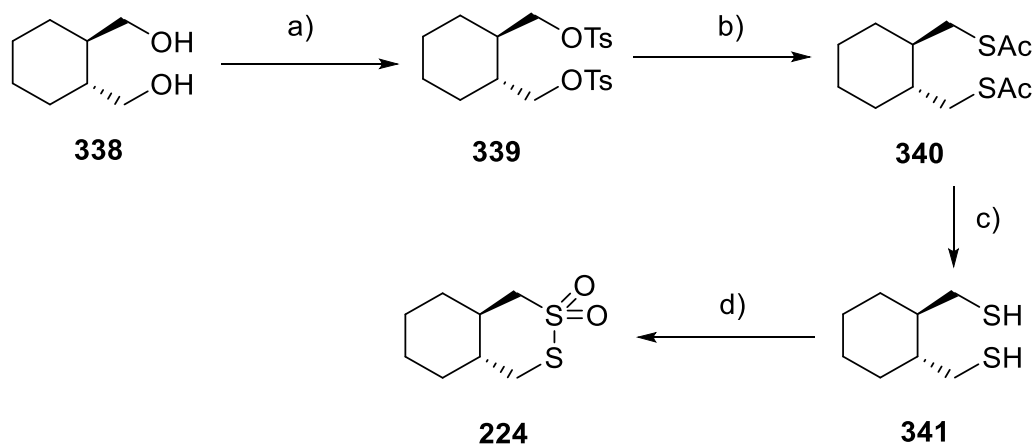
Scheme 34. (a) TsCl, pyridine, 0 °C to rt, overnight, 68%; (b) KSAc, 18-crown-6-ether, DMF, rt, under N$_2$, overnight, 72%; (c) 1.25 M HCl in MeOH, rt, under N$_2$, 4 h, 54%; (d) H$_2$O$_2$, 0 °C to rt, overnight, 34%.

Compound 339 was synthesized and purified according to procedures described in in literature.[247]
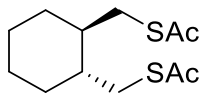
Compound 340 (496 mg, 72%, yellow oil) was synthesized from **339** (1.20 g, 2.65 mmol) following general procedure H. R_f (CH$_2$Cl$_2$/pentane 3:1): 0.31; IR (neat): 2925 (m), 2854 (w), 1691 (s), 1446 (w), 1424 (w), 1354 (w), 1303 (w), 1135 (m), 1108 (w), 954 (w), 740 (w), 670 (w), 628 (w); ^{1}H NMR (400 MHz, CDCl$_3$): 3.25 (m, 2H), 2.87 – 2.72 (m, 2H), 2.35 (s, 6H), 1.88 – 1.74 (m, 2H), 1.72 – 1.62 (m, 2H), 1.46 – 1.36 (m, 2H), 1.27 – 1.15 (m, 2H), 1.10 – 0.95 (m, 2H). ^{13}C NMR (100 MHz, CDCl$_3$): 195.7 (C), 41.1 (CH), 33.1 (CH$_2$), 31.3 (CH$_2$), 30.7 (CH$_3$), 25.6 (CH$_2$).
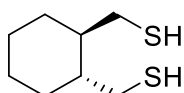
Compound 341 (180 mg, 54%, colorless oil) was synthesized from **340** (496 mg, 1.90 mmol) following general procedure I. R_f (CH$_2$Cl$_2$/pentane 1:9): 0.26. Spectroscopic data were consistent with those reported in in literature.[246]
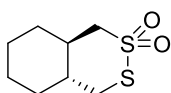
Compound 224 (71 mg, 34%, colorless solid) was synthesized from **341** (180 mg, 1.02 mmol) following general procedure J. R_f (CH$_2$Cl$_2$/pentane 4:1): 0.53; Mp: 80 – 81 ºC; IR (neat): 2954 (w), 2921 (m), 2854 (w), 1445 (w), 1398 (w), 1368 (w), 1332 (w), 1302 (m), 1286 (m), 1236 (w), 1209 (w), 1178 (w), 1253 (w), 1110 (s), 1074 (m), 953 (w), 929 (w), 887 (w), 837 (w), 814 (w), 775 (m), 711 (w); ^{1}H NMR (400 MHz, CDCl$_3$): 3.30 (m, 1H), 3.23 – 3.13 (m, 2H), 2.88 (m, 1H), 2.24 – 2.07 (m, 1H), 1.96 – 1.74 (m, 3H), 1.74 – 1.52 (m, 2H), 1.43 – 1.09 (m, 4H).; ^{13}C NMR (100 MHz, CDCl$_3$): 64.6 (CH$_2$), 42.3 (CH), 41.9 (CH), 39.9 (CH$_2$), 33.4 (CH$_2$), 32.0 (CH$_2$), 26.1 (CH$_2$), 24.9 (CH$_2$); MS (ESI, CHCl$_3$): 207 (100, [M+H]$^+$).
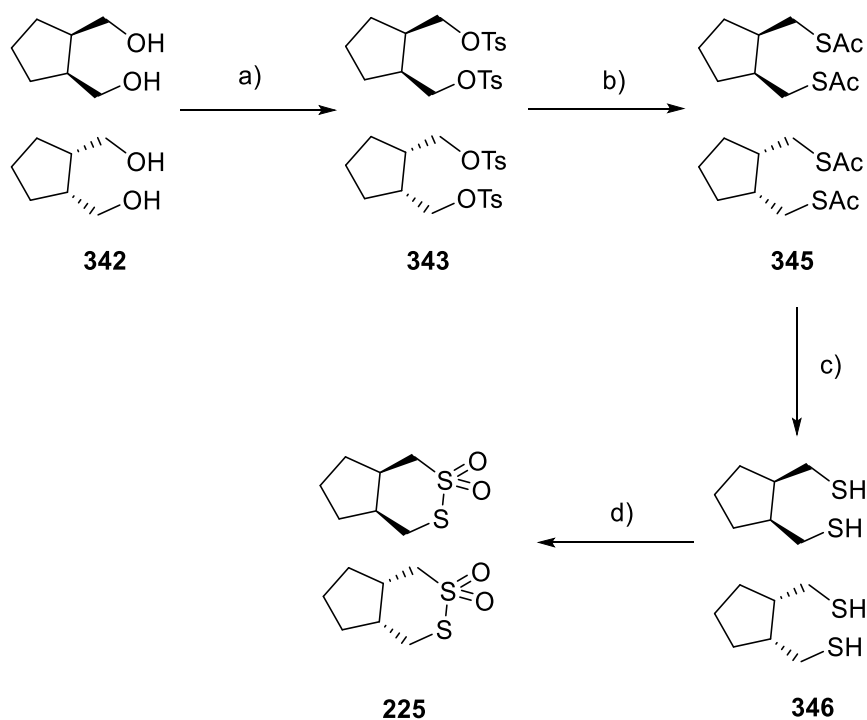
Scheme 35. (a) TsCl, pyridine/CHCl$_3$, 0 °C to rt, overnight, 66%; (b) KSAc, 18-crown-6-ether, DMF, rt, under N$_2$, overnight, 72%; (c) 1.25 M HCl in MeOH, rt, under N$_2$, 4 h, 54%; (d) H$_2$O$_2$, 0 °C to rt, overnight, 34%.

Compound 342 (racemic) was synthesized and purified according to procedures described in in literature.[248]
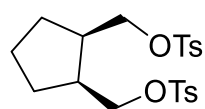
Compound 343 (533 mg, 66%, colorless solid) was synthesized from **342** (241 mg, 1.85 mmol) following general procedure K. R_f (CH$_2$Cl$_2$): 0.33; Mp: 137 − 138 °C; IR (neat): 2961 (w), 1598 (w), 1494 (w), 1455 (w), 1360 (s), 1308 (w), 1293 (w), 1175 (s), 1121 (w), 1097 (w), 1020 (w), 950 (s), 815 (m), 786 (w), 666 (m); ^{1}H NMR (400 MHz, CDCl$_3$): 7.88 − 7.70 (m, 4H), 7.46 − 7.33 (m, 4H), 4.06 − 3.82 (m, 4H), 2.47 (s, 6H), 2.36 − 2.27 (m, 2H), 1.86 − 1.71 (m, 2H), 1.70 − 1.60 (m, 1H), 1.56 − 1.49 (m, 1H), 1.47 − 1.26 (m, 2H); ^{13}C NMR (100 MHz,

CDCl$_3$): 142.4 (2xC), 130.4 (2xC), 127.5 (4xCH), 125.4 (4xCH), 68.0 (2xCH$_2$), 37.9 (2xCH),

25.8 (2xCH$_2$), 20.5 (CH$_2$), 19.2 (2xCH$_3$); MS (ESI, CHCl$_3$): 456 (82, [M+NH$_4$]$^+$).
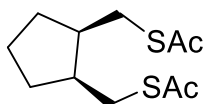
Compound 345 (141 mg, 51%, yellow oil) was synthesized from **343** (533 mg, 1.22 mmol) following general procedure H. R_f (CH$_2$Cl$_2$/pentane 3:1): 0.36; ^{1}H NMR (400 MHz, CDCl$_3$): 3.00 (m, 2H), 2.90 – 2.75 (m, 2H), 2.35 (s, 6H), 2.20 – 2.09 (m, 2H), 1.87 – 1.75 (m,

2H), 1.75 – 1.67 (m, 1H), 1.67 – 1.56 (m, 1H), 1.52 – 1.40 (m, 2H); ^{13}C NMR (100 MHz,

CDCl$_3$): 195.8 (2xC), 42.4 (2xCH), 30.6 (2xCH$_3$), 30.2 (2xCH$_2$), 29.7 (2xCH$_2$), 22.2 (CH$_2$).
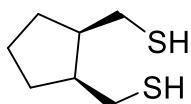
Compound 346 (39 mg, 38%, colorless oil) was synthesized from **345** (154 mg, 0.625 mmol) following general procedure I. R_f (CH$_2$Cl$_2$/pentane 1:1): 0.61; ^{1}H NMR (400 MHz, CDCl$_3$): 2.69 – 2.55 (m, 2H), 2.49 – 2.27 (m, 2H), 2.22 – 2.03 (m, 2H), 1.96 – 1.76 (m, 2H), 1.76 – 1.59 (m, 2H),

1.59 – 1.44 (m, 2H), 1.35 (t, $^3J_{H-H}$ = 7.5 Hz, 2H); ^{13}C NMR (100 MHz, CDCl$_3$): 46.1 (2xCH),

29.9 (2xCH$_2$), 24.9 (2xCH$_2$), 22.3 (CH$_2$).
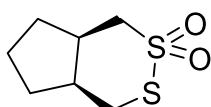
Compound 225 (25 mg, 56%, colorless oil) was synthesized from **346** (39 mg, 0.240 mmol) in 300 μl AcOH following general procedure J. R_f (CH$_2$Cl$_2$/pentane 4:1): 0.33; IR (neat): 2967 (w), 2946 (w), 2923 (w), 2876 (w), 1460 (w), 1421 (w), 1400 (w), 1362 (w), 1305 (s), 1264 (m),
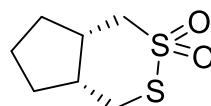
1215 (w), 1172 (w), 1135 (m), 1113 (s), 1035 (w), 1014 (w), 985 (w), 962 (w), 927 (w), 887

(w), 874 (w), 844 (w), 794 (m), 671 (w), 614 (w); ^{1}H NMR (400 MHz, CDCl$_3$): 3.81 (m, 1H),

3.29 – 3.14 (m, 3H), 2.90 – 2.79 (m, 1H), 2.39 – 2.23 (m, 1H), 2.04 – 1.86 (m, 2H), 1.86 – 1.70

(m, 3H), 1.64 – 1.55 (m, 1H); ^{13}C NMR (100 MHz, CDCl$_3$): 58.8 (CH$_2$), 41.4 (CH), 36.8 (CH$_2$),

36.1 (CH), 30.9 (2xCH$_2$), 25.5 (2xCH$_2$), 21.35 (CH$_2$); MS (ESI, CHCl$_3$): 215 (20, [M+Na]$^+$).
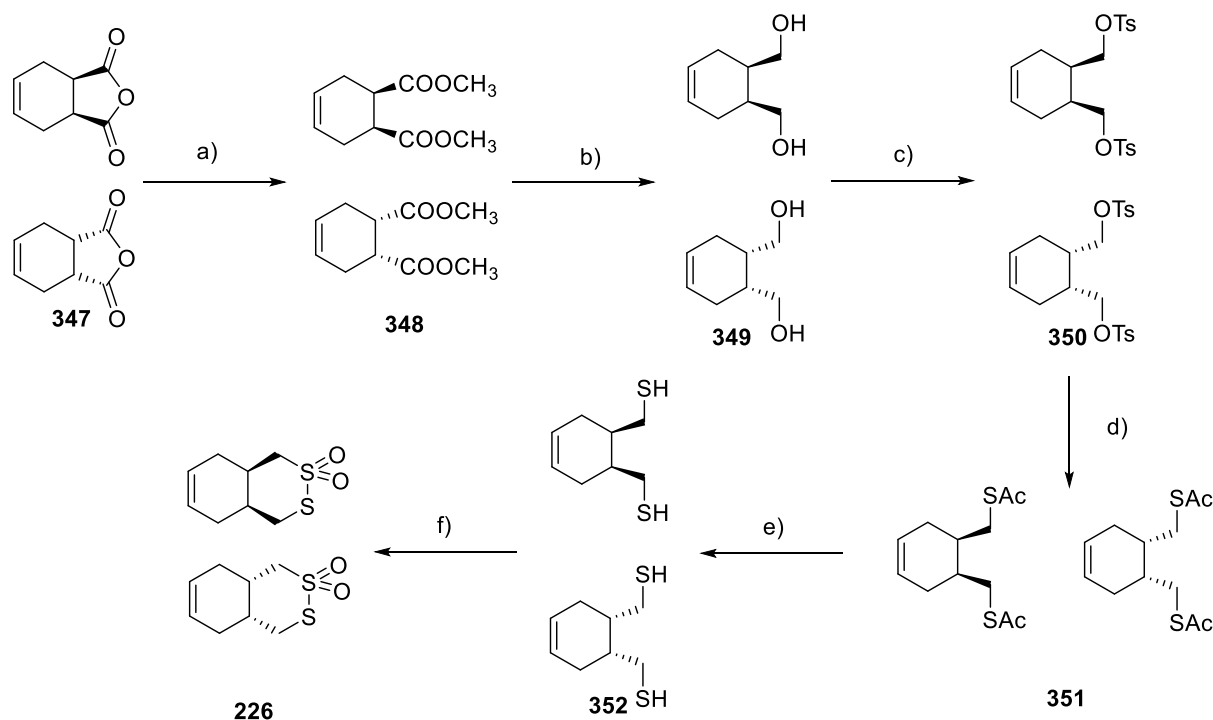
Scheme 36. (a) H$_2$SO$_4$, MeOH, reflux, under N$_2$, overnight, 91%; (b) LiAlH$_4$, dry THF, 0 °C

to reflux, 1.5 h, 81%; (c) TsCl, pyridine, 0 °C to rt, overnight, 100%; (d) KSAc, 18-crown-6-

ether, DMF, rt, under N$_2$, overnight, 45%; (e) 1.25 M HCl in MeOH, rt, under N$_2$, 4 h, 76%;

(f) H$_2$O$_2$, 0 °C to rt, overnight, 7%.

Compound 348 (racemic) was synthesized and purified according to procedures described

previously in literature.[249]

Compound 349 (racemic) was synthesized and purified according to procedures described

previously in literature.[250]

Compound 350 (racemic) was synthesized and purified according to procedures described previously in literature.[251]
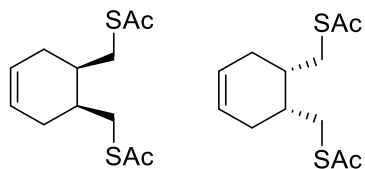
Compound 351 (582 mg, 45%, colorless oil) was synthesized from **350** (1.3 g, 5.03 mmol) following general procedure H. R_f (CH$_2$Cl$_2$): 0.46; IR (neat): 3026 (w), 2973 (w), 2906 (w), 2840 (w), 1690 (s), 1426 (w), 1354 (w), 1134 (m), 1108 (m), 959 (m), 753 (w), 663 (w), 628 (m); ^{1}H NMR (400 MHz, CDCl$_3$): 5.76 – 5.41 (m, 2H), 3.01 (m, 2H), 2.82 (m, 2H), 2.34 (s, 6H), 2.24 – 2.02 (m, 2H), 2.02 – 1.78 (m, 4H); ^{13}C NMR (100 MHz, CDCl$_3$): 195.7 (2xC), 125.2 (2xCH), 36.7 (2xCH), 30.6 (2xCH$_3$), 29.9 (2xCH$_2$), 28.7 (2xCH$_2$); MS (ESI, CHCl$_3$): 175 (38, [M-2Ac+3H]$^+$).
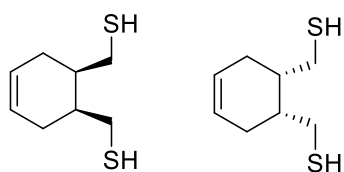
Compound 352 (299 mg, 76%, smelly colorless oil) was synthesized from **351** (582 mg, 2.25 mmol) following general procedure I. R_f (pentane/CH$_2$Cl$_2$ 9:1): 0.34; IR (neat): 3339 (br), 2931 (s), 2856 (w), 2538 (m), 1742 (br), 1445 (w), 1343 (w), 1316 (w), 1217 (w), 1119 (w), 1019 (w), 713 (w); ^{1}H NMR (400 MHz, CDCl$_3$): 5.67 – 5.58 (m, 2H), 2.64 – 2.36 (m, 4H), 2.33 – 2.14 (m, 2H), 2.13 – 1.95 (m, 4H), 1.34 (t, $^3J_{H-H}$ = 10.6 Hz, 2H); ^{13}C NMR (100 MHz, CDCl$_3$): 125.3 (2xCH), 39.8 (2xCH), 28.2 (2xCH$_2$), 25.0 (2xCH$_2$).
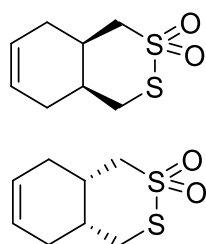
Compound 226 (25 mg, 7%, colorless oil) was synthesized from **352** (299 mg, 1.72 mmol) and H$_2$O$_2$ (876 µl, 8.60 mmol) in AcOH (4.0 ml) following general procedure J. R_f (CH$_2$Cl$_2$): 0.49; IR (neat): 3033 (w), 2973 (w), 2916 (w), 2881 (w), 2846 (w), 1655 (w), 1443 (w), 1417 (w), 1397 (w), 1374 (w), 1325 (w), 1303 (s), 1245 (w), 1222 (w), 1197 (w), 1180 (w), 1163 (w),

1120 (s), 1052 (w), 1027 (w), 985 (w), 955 (w), 935 (w), 898 (w), 863 (w), 817 (w), 767 (w), 744 (w), 671 (m), 653 (m); ^{1}H NMR (400 MHz, CDCl$_3$): 5.78 – 5.71 (m, 1H), 5.68 – 5.61 (m, 1H), 3.84 – 3.74 (m, 1H), 3.54 – 3.43 (m, 1H), 3.17 – 2.98 (m, 2H), 2.95 – 2.83 (m, 1H), 2.78 – 2.66 (m, 1H), 2.63 – 2.53 (m, 1H), 2.49 – 2.37 (m, 1H), 2.12 – 1.96 (m, 1H), 1.94 – 1.77 (m, 1H); ^{13}C NMR (100 MHz, CDCl$_3$): 125.2 (CH), 123.3 (CH), 60.1 (CH$_2$), 40.2 (CH$_2$), 34.7 (CH), 31.6 (CH$_2$), 30.0 (CH), 23.5 (CH$_2$); MS (ESI, CHCl$_3$): 222 (100, [M+NH$_4$]$^+$).

5.2.6.1.2.3. Dimeric Derivatives
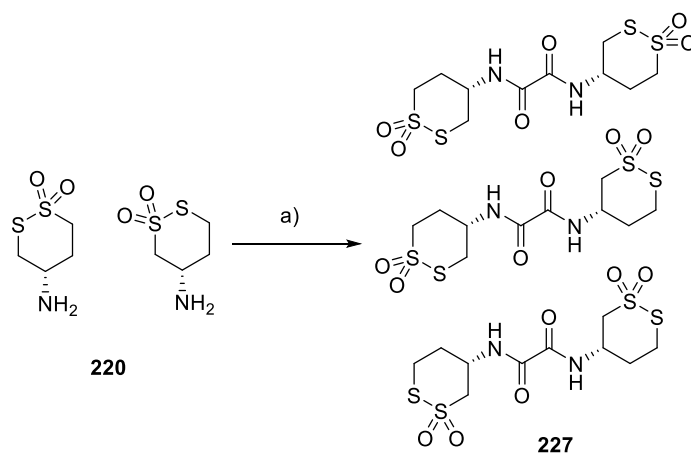
Scheme 37. (a) oxalyl chloride, TEA, DMF, 0 °C to rt, overnight, 53%;
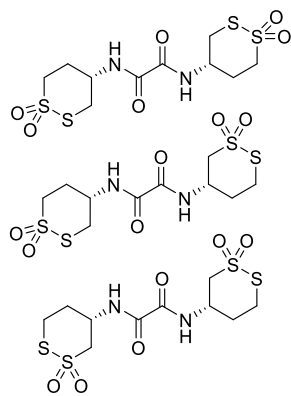
Compound 227. To a solution of **220** (50 mg, 0.30 mmol) in DMF (1.5 ml) at 0 °C, TEA (125 μl, 0.898 mmol) was added, followed by oxalyl chloride (13 μl, 0.15 mmol) dropwise. The reaction mixture was stirred at rt overnight. Then solvent was removed under vacuum. The residue was purified by reversed phase chromatography (eluent: CH$_3$CN + 0.1% TFA/ H$_2$O +

0.1% TFA gradient from 10% CH$_3$CN + 0.1% TFA to 80%). Fractions contained product were lyophilized to yield desired product (31 mg, mixture of 3 regioiomers 81: 18:1, 53%, colorless solid); IR (neat): 3323 (w), 3086 (w), 2998 (w), 2935 (w), 1699 (m), 1549 (m), 1451 (w), 1421 (w), 1406 (w), 1317 (m), 1290 (m), 1242 (w), 1159 (s), 1123 (s), 897 (m), 856 (w), 808 (w), 775 (w), 720 (m), 677 (w), 610 (w); ^{1}H NMR (400 MHz, DMSO-d_6, nn/nn/nn - regioisomers peaks): 9.73 – 9.56 (m, 2H), 4.35 – 4.24/4.42 – 4.35 (m, 2H), 3.95 – 3.66 (m, 4H), , 3.55 – 3.19 (m, 4H), 2.45 – 2.22/1.93 – 1.77 (m, 4H); ^{13}C NMR (125 MHz, DMSO-d_6, nn/nn - regioisomers peaks): 155.6/155.3 (2xC), 58.6/62.5 (2xCH$_2$), 45.7/48.0 (2xCH), 37.2/32.1 (2xCH$_2$), 30.6/31.1 (2xCH$_2$); MS (ESI, MeOH): 281 (100, [2M+3Na]$^{2+}$).
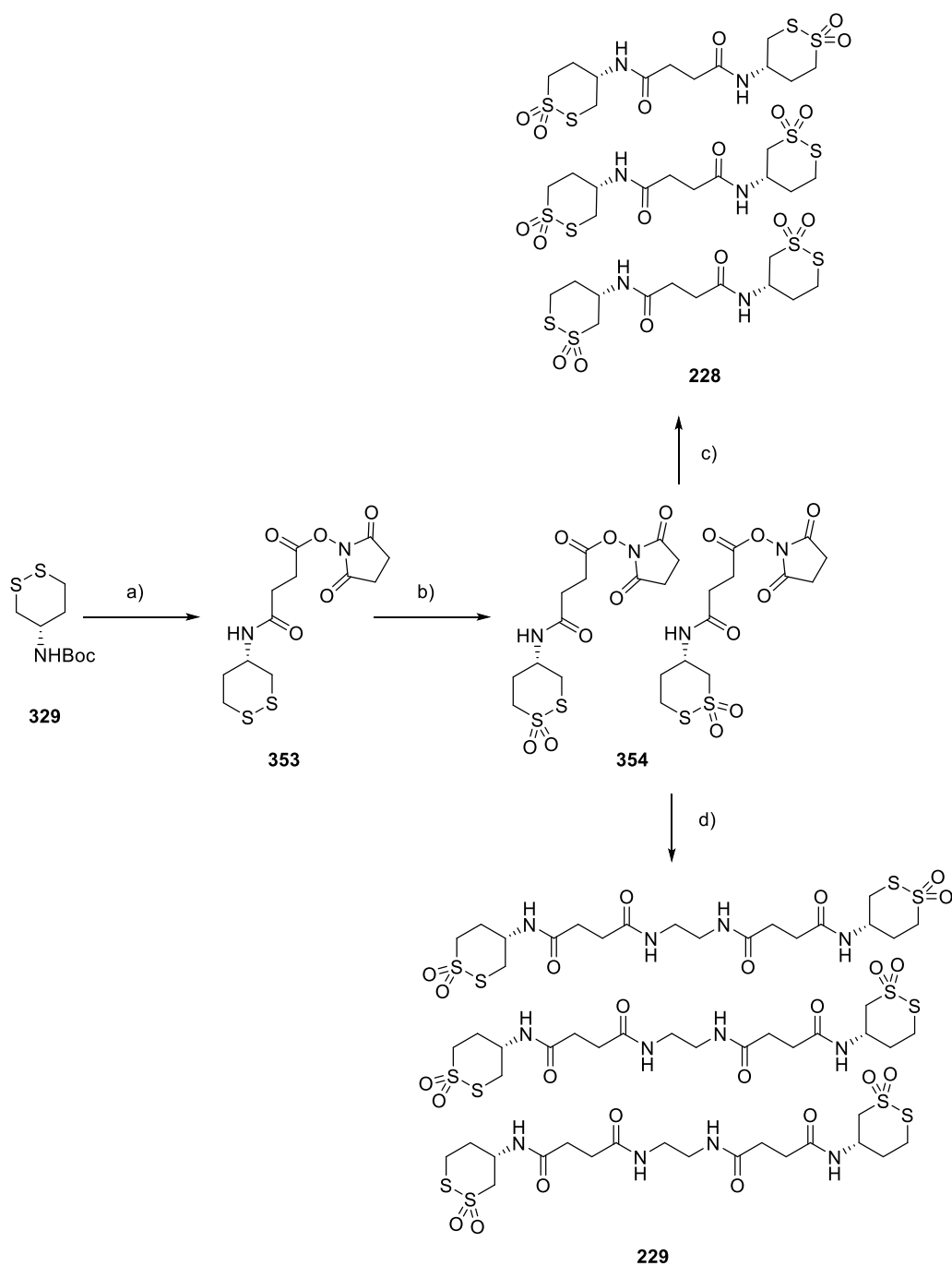
Scheme 38. (a) 1. TFA:CH₂Cl₂ 1:1, rt, overnight; 2. Succinic anhydride, TEA, CH₂Cl₂, rt, overnight; 3. *N*-Hydroxysuccinimide, EDC, CH₂Cl₂, rt, overnight, 33%; (b) *m*-CPBA, CH₂Cl₂, rt, 2 d, 51%; (c) oxalyl chloride, TEA, DMF, 0 °C to rt, overnight, 53%; (d), ethane-1,2-diamine, TEA, DMF, rt, overnight, 35%.
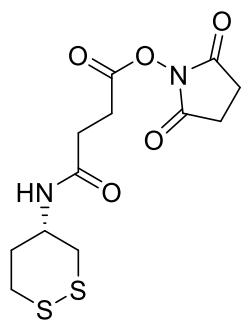
Compound 353. 329 (150 mg, 0.637 mmol) was dissolved in a mixture of TFA: CH_2Cl_2 (1:1) (3.0ml). The reaction mixture was stirred at rt overnight. Then the solvent was removed under vacuum. The residue was dissolved in CH_2Cl_2 (2.0 ml). To the resulting mixture, TEA (267 μl, 1.91 mmol) was added, followed by succinic anhydride (77 mg, 0.77 mmol). The reaction mixture was stirred at rt overnight. The solvent was removed under vacuum. The residue was dissolved in CH_2Cl_2 (3.0 ml). To the reaction mixture, *N*-Hydroxysuccinimide (88 mg, 0.76 mmol) was added, followed by EDC (151 mg, 0.76 mmol). The reaction mixture was stirred at rt overnight. The reaction mixture was diluted with CH_2Cl_2. The organic layer was washed with H_2O, saturated solution of $NaHCO_3$ and brine. The organic layer was dried over anhydrous Na_2SO_4. The solvent was removed under vacuum. The residue was purified by flash chromatography (CH_2Cl_2/MeOH 25:1) to yield desired product (69 mg, 33%, colorless solid). R_f (CH_2Cl_2/MeOH 25:1): 0.31; Mp: 137 – 138 °C; $[\alpha]_D^{20}$ -0.637 (*c* 1.00, CHCl$_3$); IR (neat): 3357 (w), 2916 (w), 1793 (m), 1730 (s), 1652 (s), 1513 (s), 1435 (w), 1114 (w), 1367 (m), 1293 (w), 1248 (w), 1198 (s), 1101 (m), 1077 (s), 1047 (m), 988 (w), 954 (w), 898 (w), 880 (w), 865 (w), 814 (w), 755 (w), 742 (w), 641 (m); ^{1}H NMR (400 MHz, DMSO-d_6): 8.14 (d, $^3J_{H–H}$ = 7.8 Hz, 1H), 3.89 – 3.74 (m, 1H), 3.11 – 3.02 (m, 1H), 2.98 – 2.82 (m, 4H), 2.79 (s, 4H), 2.66 – 2.55 (m, 1H), 2.47 – 2.41 (m, 2H), 2.10 – 2.00 (m, 1H), 1.72 – 1.56 (m, 1H); ^{13}C NMR (100 MHz, DMSO-d_6): 170.6 (C), 169.3 (C), 169.0 (C), 47.4 (CH), 37.4 (CH_2), 33.9 (2xCH_2), 29.8 (CH_2), 26.4 (CH_2), 25.9 (CH_2); MS (ESI, MeOH): 333 (63, [M+H]$^+$).
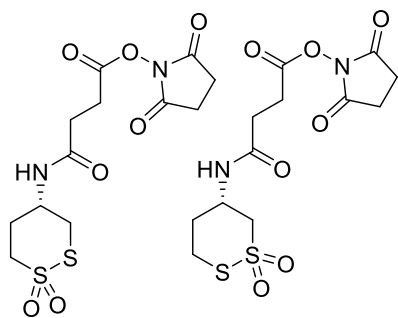
Compound 354. To a solution of **353** (69 mg, 0.21 mmol) in CH₂Cl₂ (6.0 ml), *m*-CPBA (128 mg, 0.525 mmol) was added. The reaction mixture was stirred at rt for 2 days. The reaction mixture was diluted with CH₂Cl₂, then washed with saturated aqueous solution of NaHCO₃ (3 times). The organic layer was dried over anhydrous Na₂SO₄. The solvent was removed under vacuum. The residue (38 mg, 51%, colorless solid) was used for the next step without purification.
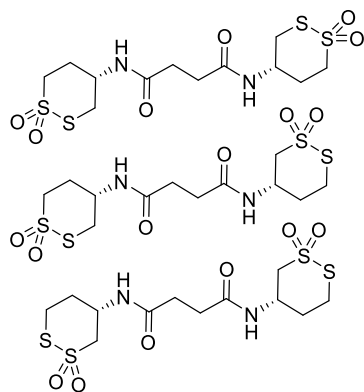
Compound 228. To a solution of **354** (44 mg, 0.27 mmol) in DMF (1.5 ml), TEA (37 μl, 0.27 mmol) was added, followed by **220** (98 mg, 0.27 mmol). The reaction mixture was stirred at rt overnight. The solvent was removed under vacuum. The residue was purified by reversed phase chromatography (eluent: CH₃CN + 0.1% TFA/ H₂O + 0.1% TFA gradient from 5% CH₃CN + 0.1% TFA to 95%). Fractions contained product were lyophilized to yield desired product (39 mg, mixture of 3 regioiomers 77: 17:6, 53%, colorless solid). IR (neat): 3276 (br), 3055 (br), 2930 (w), 1647 (s), 1530 (s), 1413 (w), 1368 (w), 1315 (s), 1293 (s), 1255 (w), 1234 (w), 1201 (m), 1169 (m), 1122 (s), 1048 (w), 1026 (w), 1003 (w), 895 (w), 826 (w), 799 (w), 717 (m), 669 (w), 634 (w); ¹H NMR (400 MHz, DMSO-*d₆*, nn/nn/nn - regioisomers peaks): 8.25 – 8.13 (m, 2H), 4.22 – 4.10/4.55 – 4.41 and 4.33 – 4.22/ 4.33 – 4.22 (m, 2H), 4.06 – 3.43 (m, 4H), 2.44 – 2.20/2.62 – 2.56 (m, 4H), 2.29 – 2.15/1.80 – 1.66 (m, 4H); ¹³C NMR (125 MHz, DMSO-*d₆*, nn/nn/nn - regioisomers peaks): 169.4/175.6, 168.8/169.4 (2xC), 55.9/61.3, 58.2/58.9 (2xCH₂), 41.4/46.0, 45.2/44.1 (2xCH),

36.3/30.0, 29.4/32.6 (2xCH$_2$), 29.0/26.4, 25.9/26.3 (2xCH$_2$), 28.9/28.2, 26.3/26.7 (2xCH$_2$); MS (ESI, MeOH): 417 (100, [M+H]$^+$).
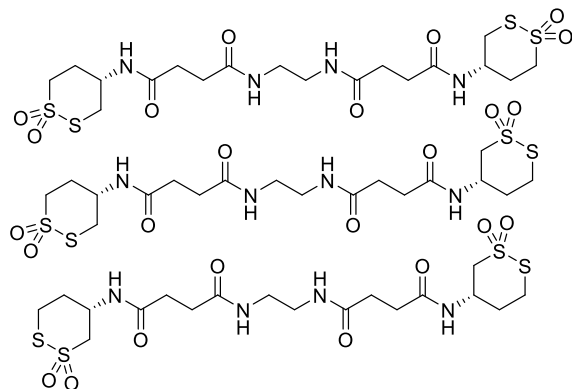
Compound 229. To a solution of **354** (38 mg, 0.10 mmol) in CH$_2$Cl$_2$ (1.0 ml), ethane-1,2-diamine (3.5 μl, 0.050 mmol) was added. The reaction mixture was stirred at rt overnight. The solvent was removed under vacuum. The residue was purified by preparative HPLC (eluent: CH$_3$CN + 0.1% TFA/ H$_2$O + 0.1% TFA gradient from 0% CH$_3$CN + 0.1% TFA to 1% (the first 7 min), then 1% to 95%). Fractions contained product were lyophilized to yield desired product (7 mg, mixture of 3 regioiomers 71:25:4, 24%, colorless solid). IR (neat): 3309 (w), 3081 (w), 2933 (w), 1634 (s), 1533 (s), 1423 (w), 1353 (w), 1314 (m), 1294 (m), 1237 (w), 1203 (w), 1167 (w), 1127 (s), 948 (w), 896 (w), 800 (w), 718 (w), 656 (w); ^{1}H NMR (400 MHz, DMSO-d_6, nn/nn/nn - regioisomers peaks): 8.17 (d, $^3J_{\text{H–H}}$ = 7.6 Hz, 2H), 7.96 – 7.72 (m, 2H), 4.21 – 4.11/4.57 – 4.42, 4.35 – 4.21/4.35 – 4,21 (m, 2H), 3.83 – 3.17 (m, 8H), 3.13 – 3.97 (m, 4H), 2.38 – 1.93, 2.62 – 2.57, 1.82 – 1.64 (m, 12H); ^{13}C NMR (125 MHz, DMSO-d_6, nn/nn/nn - regioisomers peaks): 171.83/171.78, 177.7 (2xC), 171.7/171.1, 177.6 (2xC), 58.0/63.4, 60.3/61.0 (2xCH$_2$), 43.6/ 48.12, 47.34/48.09 (2xCH), 38.8/38.4 (2xCH$_2$), 30.0/32.6, 29.4/30.3 (2xCH$_2$), 29.0/28.8, 28.2/27.6 (2xCH$_2$), 28.9 (2xCH$_2$), 26.4/26.3, 25.9/26.7 (2xCH$_2$); MS (ESI, MeOH): 581 (100, [M+Na]$^+$), 559 (100, [M+H]$^+$) .

5.2.6.1.3. 7 and 8-Membered Cyclic Thiosulfonates
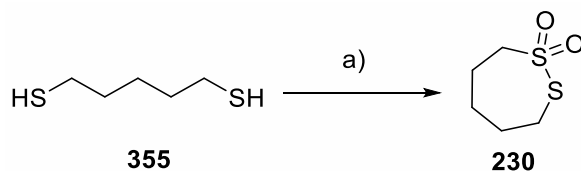
Scheme 39. (a) H_2O_2, 0 °C to rt, overnight, 4%.
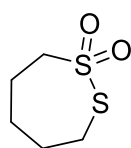
Compound 220 (17 mg, 4%, colorless oil) was synthesized from **355** (300 μl, 2.34 mmol) and 30% aqueous solution of H_2O_2 (799 μl, 8.19 mmol) in AcOH (220 ml) following general procedure J. R_f (CH_2Cl_2): 0.53; IR (neat): 2932 (m), 2859 (w), 1448 (m), 1402 (w), 1338 (m), 1315 (s), 1291 (s), 1224 (w), 1208 (w), 1173 (w), 1115 (s), 1042 (m), 960 (w), 929 (w), 832 (m), 784 (w), 736 (w), 695 (s), 656 (w); ^1H NMR (400 MHz, $CDCl_3$): 3.59 – 3.40 (m, 2H), 3.36 – 3.17 (m, 2H), 2.12 – 1.90 (m, 6H); ^{13}C NMR (100 MHz, $CDCl_3$): 65.7 (CH_2), 34.2 (CH_2), 30.3 (CH_2), 24.6 (CH_2), 22.3 (CH_2); MS (ESI, $CHCl_3$): 184 (100, $[M+NH_4]^+$).
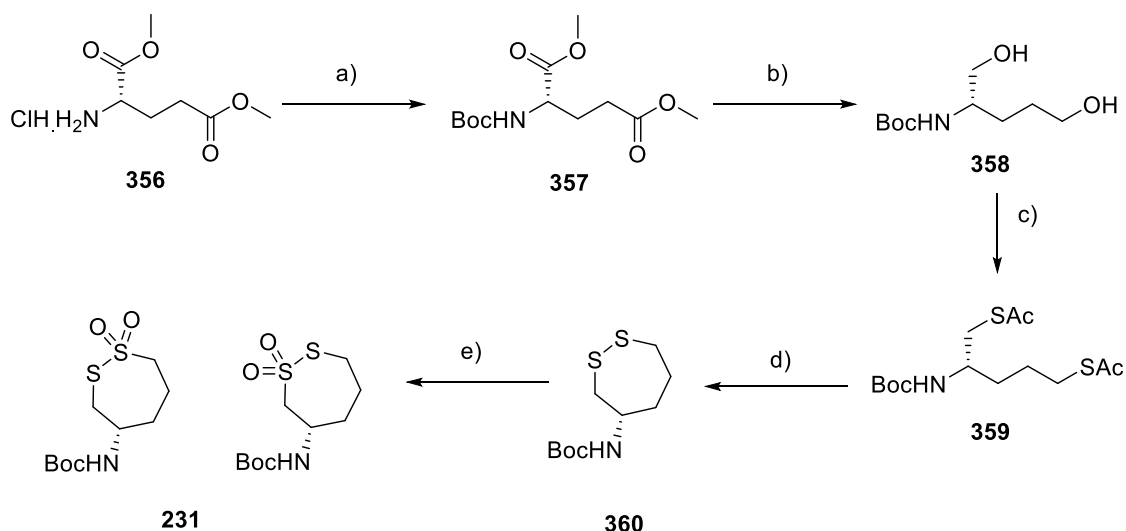
Scheme 40. (a) Boc$_2$O, NaHCO$_3$, CH$_2$Cl$_2$/H$_2$O, 60 °C, 4 h, 96%; (b) LiAlH$_4$, dry THF, rt, 4 h, 36%; (c) PPh$_3$, DIAD, HSAc, 0 °C to rt, 17 h, 57%; (d) KOH, air, MeOH, rt, overnight, 15%; (d) *m*-CPBA, rt, overnight, 17%.
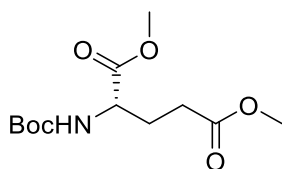
Compound 357. To a mixture of CH$_2$Cl$_2$ (150 ml) and H$_2$O (100 ml), NaHCO$_3$ (4.2 g, 50 mmol) was added, followed by **356** (8.0 g, 38 mmol) and Boc$_2$O (9.8 g, 45 mmol). The reaction mixture was heated at 60 °C for 4 h. The reaction mixture was cooled to rt. The organic layer was separated, dried over anhydrous Na$_2$SO$_4$. The solvent was removed under vacuum. The residue was purified by flash chromatography (CH$_2$Cl$_2$/MeOH 40:1) to yield desired product (10 g, 96%, colorless oil). R_f (CH$_2$Cl$_2$/MeOH 25:1): 0.34. Spectroscopic data were consistent with those reported in literature.[252]
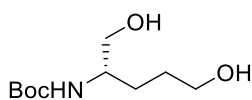
Compound 358. To a suspension of LiAlH$_4$ (2.5 g, 66 mmol) in dry THF (200 ml) at 0 °C, under N$_2$, a solution of **357** (6.0 g, 22 mmol) in dry THF (100 ml) was added dropwise. The reaction mixture was warmed up to rt

and stirred for 3 h. To the reaction mixture, H_2O (1.0 ml) was added, followed by 15% aqueous solution of NaOH (1.0 ml) and H_2O (2.0 ml) at 0 °C to quench the excess of $LiAlH_4$. The reaction mixture was filtered. The precipitate was washed with CH_2Cl_2. The filtrates were combined and dried over anhydrous Na_2SO_4. The residue was purified by flash chromatography (EtOAc) to yield the desired product (1.7 g, 36%, colorless oil). R_f (EtOAc): 0.27. Spectroscopic data were consistent with those reported in literature.[253]
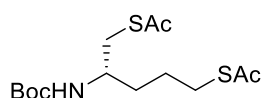
Compound 359. To a solution of PPh_3 (2.0 g, 7.6 mmol) in dry THF (30 ml) at 0 °C, under N_2, DIAD (1.5 ml, 7.6 mmol) was added dropwise. The reaction mixture was stirred at 0 °C for 20 min. To the reaction mixture, a solution of **358** (0.7 g, 3.2 mmol) in dry THF (12 ml) was added, followed by HSAc (0.6 ml, 7.6 mmol). The reaction mixture was stirred at 0 °C for 1 h, then at rt for 16 h. The solvent was removed under vacuum. The residue was purified by flash chromatography (EtOAc/pentane 1:4) to yield the desired product (0.6 g, 57%, colorless oil). R_f (EtOAc/pentane 1:4): 0.32; $[\alpha]_D^{20}$ -17.0 (c 1.00, $CHCl_3$); IR (neat): 3360 (w), 2984 (w), 2937 (w), 1685 (s), 1519 (s), 1454 (w), 1395 (w), 1371 (w), 1353 (w), 1298 (w), 1281 (w), 1245 (m), 1167 (m), 1130 (s), 1101 (m), 1051 (m), 1026 (w), 954 (m), 872 (w), 761 (w), 744 (w), 716 (w), 658 (w), 620 (s); ^1H NMR (400 MHz, $CDCl_3$): 4.48 (d, $^3J_{H-H}$ = 8.0 Hz, 1H), 3.80 – 3.65 (m, 1H), 3.08 (dd, $^2J_{H-H}$ = 13.9 Hz, $^3J_{H-H}$ = 4.9 Hz, 1H), 2.98 (dd, $^3J_{H-H}$ = 13.9 Hz, $^3J_{H-H}$ =7.2 Hz, 1H), 2.91 – 2.83 (m, 2H), 2.35 (s, 3H), 2.33 (s, 3H), 1.71 – 1.51 (m, 4H), 1.43 (s, 9H); ^{1}C NMR (100 MHz, $CDCl_3$): 195.8 (C), 195.6 (C), 155.5 (C), 79.5 (C), 50.2 (CH), 33.9 (CH_2), 33.4 (CH_2), 30.63 (CH_3), 30.58 (CH_3), 28.7 (CH_2), 28.4 (3xCH_3), 26.2 (CH_2); MS (ESI, $CHCl_3$): 236 (50, $[M-Boc+H]^+$).
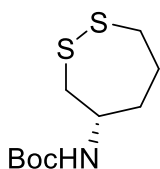
Compound 360. To a solution of **359** (504 mg, 1.5 mmol) in MeOH (50 ml), KOH (340 mg, 6.07 mmol) was added. A stream of air was bubbled through the solution. The reaction mixture was stirred at rt overnight. The solvent was removed under vacuum. The residue was loaded onto silica-gel and purified by flash chromatography (EtOAc/pentane gradient from 3% EtOAc to 25%) to yield the desired product (55 mg, 15%, colorless solid). R_f (EtOAc/pentane 1:9): 0.51; Mp: 110 – 111 °C; $[\alpha]_D^{20}$ -37.4 (*c* 1.00, CHCl$_3$); IR (neat): 3362 (m), 2981 (w), 2935 (w), 2907 (w), 1676 (s), 1512 (s), 1443 (w), 1402 (w), 1388 (w), 1365 (w), 1344 (w), 1303 (m), 1278 (m), 1231 (m), 1160 (s), 1045 (m), 999 (m), 929 (w), 863 (w), 825 (w), 780 (w), 750 (w), 622 (w); ^{1}H NMR (400 MHz, DMSO-*d$_6$*): 6.87 (d, $^3J_{H-H}$ = 8.0 Hz, 1H), 3.61 – 3.49 (m, 1H), 2.92 (dd, $^2J_{H-H}$ = 13.6 Hz, $^3J_{H-H}$ = 4.7 Hz, 1H), 2.79 (dt, $^2J_{H-H}$ = 12.6 Hz, $^3J_{H-H}$ = 4.6 Hz, 1H), 2.60 – 2.50 (m, 1H), 2.46 (dd, $^2J_{H-H}$ = 13.6 Hz, $^3J_{H-H}$ = 9.9 Hz, 1H), 2.11 – 1.97 (m, 1H), 1.80 – 1.56 (m, 3H), 1.24 (s, 9H); ^{13}C NMR (100 MHz, DMSO-*d$_6$*): 155.1 (C), 78.3 (C), 53.5 (CH), 44.6 (CH$_2$), 36.4 (CH$_2$), 33.3 (CH$_2$), 28.7 (3xCH$_3$), 24.9 (CH$_2$).
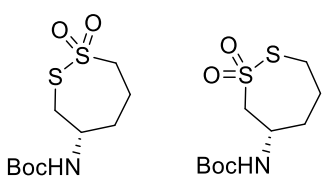
Compound 231. To a solution of **360** (149 mg, 0.597 mmol) in CH$_2$Cl$_2$ (6.0 ml), *m*-CPBA (368 mg, 1.49 mmol) was added. The reaction mixture was stirred at rt overnight. The reaction mixture was diluted with CH$_2$Cl$_2$, then washed with saturated aqueous solution of NaHCO$_3$ (3 times). The organic layer was dried over anhydrous Na$_2$SO$_4$. The solvent was removed under vacuum. The residue was purified by flash chromatography (CH$_2$Cl$_2$/MeOH 40:1) to yield the desired product (29 mg, mixture of 2 regioisomers 9:1, 17%, colorless solid). R_f (CH$_2$Cl$_2$/MeOH 40:1): 0.42, 0.31; IR (neat): 3364 (w), 2977 (w), 2934 (w), 1688 (s), 1509 (m), 1451 (w), 1392 (w), 1366 (w), 1316 (s), 1248 (m), 1163 (s), 1120 (s), 1050

(m), 1025 (m), 1008 (m), 951 (w), 866 (w), 848 (w), 825 (w), 781 (w), 721 (w), 699 (w), 617 (w); ^{1}H NMR (400 MHz, DMSO-d_6, nn/nn - regioisomers peaks): 7.23/7.10 (d, $^3J_{H-H}$ = 7.4 Hz, 1H), 3.97 – 3.86/3.83 – 3.75 (m, 1H), 3.62 – 3.48 (m, 2H), [3.44 (dd, $^2J_{H-H}$ = 15.7 Hz, $^3J_{H-H}$ = 5.3 Hz, 1H), 3.18 (dd, $^2J_{H-H}$ = 15.7 Hz, $^3J_{H-H}$ =6.6 Hz, 1H)]/3.29 – 3.24 (m, 2H), 2.17 – 1.92 (m, 2H), 1.87 – 1.66 (m, 2H), 1.37 (s, 9H); ^{13}C NMR (125 MHz, DMSO-d_6, nn/nn - regioisomers peaks): 155.1/155.0 (C), 78.5/18.9 (C), 65.6/68.7 (CH$_2$), 51.7/47.2 (CH), 38.2/35.0 (CH$_2$), 31.3/33.4 (CH$_2$), 28.7 (3xCH$_3$), 18.6/27.6 (CH$_2$); MS (ESI, MeOH): 299 (100, [M+NH$_4$]$^+$).
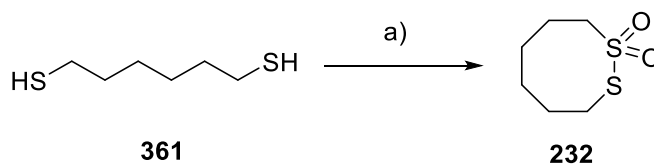
Scheme 41. (a) H$_2$O$_2$, 0 ^{o}C to rt, overnight, 1%.
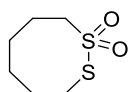
Compound 232 (3 mg, 1%, colorless oil) was synthesized from **361** (300 μl, 1.96 mmol) and 30% aqueous solution of H$_2$O$_2$ (701 μl, 6.86 mmol) in AcOH (196 ml) following general procedure J. R_f (CH$_2$Cl$_2$): 0.50; IR (neat): 2935 (m), 2859 (w), 1458 (w), 1409 (w), 1365 (w), 1309 (s), 1254 (w), 1229 (w), 1121 (s), 1058 (m), 959 (w), 762 (m), 726 (m), 692 (w), 621 (w); ^{1}H NMR (400 MHz, CDCl$_3$): 3.66 – 3.53 (m, 2H), 3.45 – 3.34 (m, 2H), 2.22 – 2.08 (m, 2H), 1.98 – 1.84 (m, 4H), 1.84 – 1.72 (m, 2H); ^{13}C NMR (125 MHz, CDCl$_3$): 61.6 (CH$_2$), 33.7 (CH$_2$), 25.2 (CH$_2$), 21.9 (CH$_2$), 20.8 (CH$_2$), 20.2 (CH$_2$); MS (ESI, CHCl$_3$): 198 (74, [M+NH$_4$]$^+$).

5.2.6.2. Disulfide Bridged γ-turn Peptides
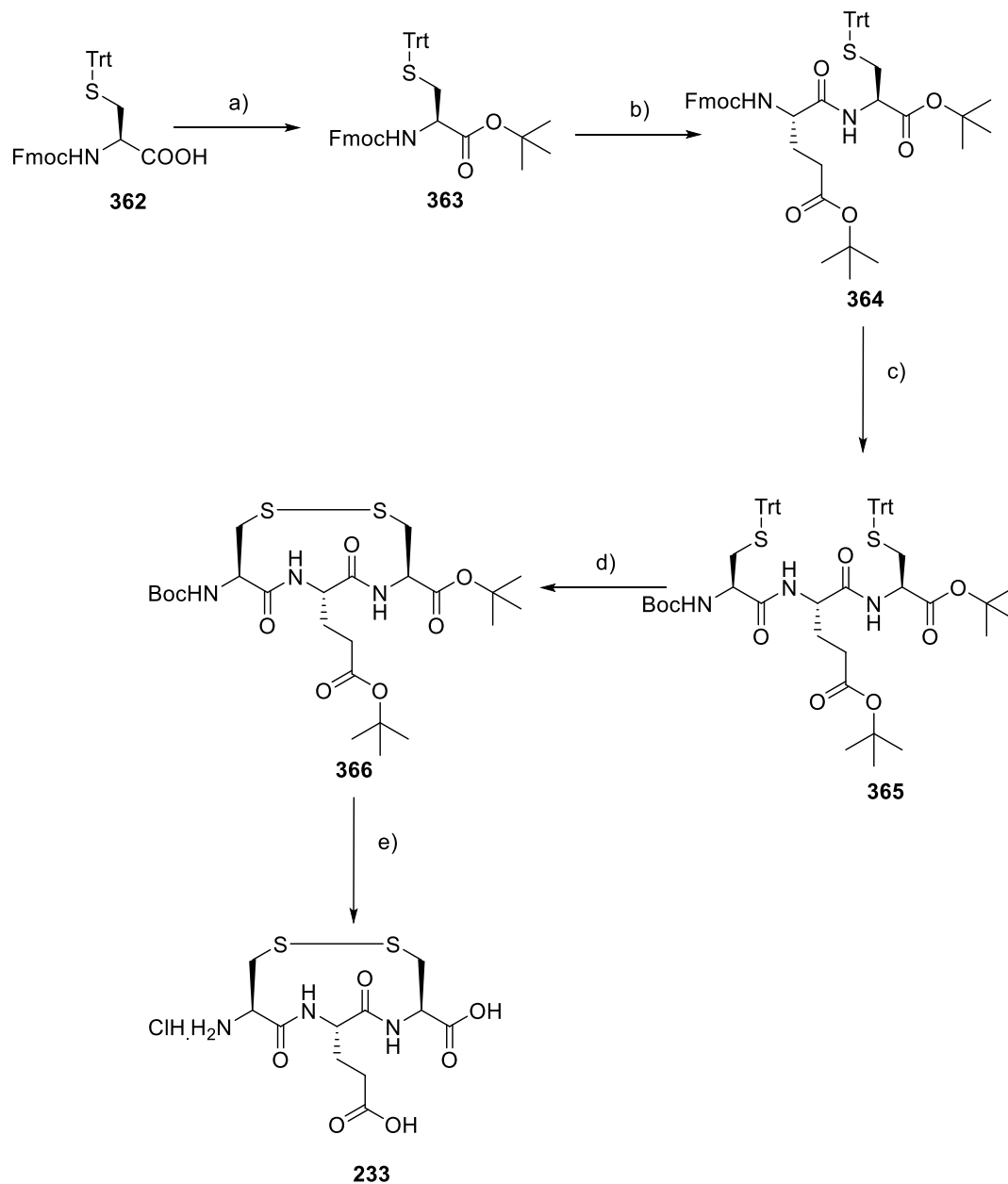
Scheme 42. (a) *t*-Butyl-2,2,2-Trichloroacetimidate, BF$_3$.Et$_2$O, CH$_2$Cl$_2$, 4 h, 30%; (b) 1. Et$_2$NH/CH$_2$Cl$_2$ 1:1, rt, 1 h; 2. Fmoc-L-Glu(tBu)-OH, EDC, DMAP, CH$_2$Cl$_2$, rt, overnight, 74%; (c) 1. Et$_2$NH/CH$_2$Cl$_2$ 1:1, rt, 1 h; 2. Boc-L-Cys(Trt)-OH, EDC, DMAP, CH$_2$Cl$_2$, rt, overnight, 80%; (d) I$_2$, MeOH, 55%; (e) HCl gas, EtOAc, 1 h, 93%.

Compound 363 was synthesized as described in reference.[254]
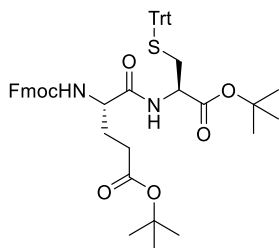
Compound 364 (813 mg, 74%, colorless solid) was prepared from **363** (852 mg, 1.3 mmol) and Fmoc-L-Glu(tBu)-OH (678 mg, 1.6 mmol) following the general procedures B and D. R_f (CH$_2$Cl$_2$/MeOH 25:1): 0.63; Mp: 76 – 77 °C; [α]$_D^{20}$ +6 (*c* 1.00, CHCl$_3$); IR (neat): 3324 (w), 2978 (w), 1726 (m), 1669 (m), 1494 (m), 1447 (w), 1392 (w), 1367 (w), 1246 (m), 1150 (s), 1081 (w), 1049 (w), 845 (w), 740 (s), 700 (s), 620 (w); ^{1}H NMR (400 MHz, CDCl$_3$): 7.77 (d, $^3J_{H-H}$ = 8.0 Hz, 2H), 7.67 – 7.53 (m, 2H), 7.43 – 7.38 (m, 8H), 7.33 – 7.28 (m, 4H), 7.26 – 7.24 (m, 2H), 7.22 – 7.17 (m, 3H), 6.69 (d, $^3J_{H-H}$ = 7.7 Hz, 1H), 5.74 (d, $^3J_{H-H}$ = 7.7 Hz, 1H), 4.48 – 4.43 (m, 1H), 4.39 (d, $^3J_{H-H}$ = 7.2 Hz, 2H), 4.28 – 4.19 (m, 2H), 2.66 (dd, $^2J_{H-H}$ = 12.1, $^3J_{H-H}$ = 5.8 Hz, 1H), 2.52 (dd, $^2J_{H-H}$ = 12.1, $^3J_{H-H}$ = 4.5 Hz, 1H), 2.48 – 2.31 (m, 2H), 2.15 – 2.04 (m, 1H), 2.00 – 1.86 (m, 1H), 1.46 – 1.42 (m, 18H); ^{13}C NMR (100 MHz, CDCl$_3$):172.9 (C), 170.7 (C), 168.9 (C), 156.1 (C), 144.3 (3xC), 144.0 (4xC), 129.5 (6xCH), 128.0 (6xCH), 127.7 (3xCH), 127.1 (2xCH), 126.8 (2xCH), 125.20 (2xCH), 125.17 (2xCH), 120.0 (2xCH), 82.7 (C), 81.0 (C), 67.1 (CH$_2$), 66.7 (C), 54.1 (CH), 51.8 (CH), 47.2 (CH), 33.8 (CH$_2$), 31.6 (CH$_2$), 28.5 (CH$_2$), 28.1 (3xCH$_3$), 27.94 (3xCH$_3$); MS (MALDI-TOF): 850 ([M+Na]$^+$).
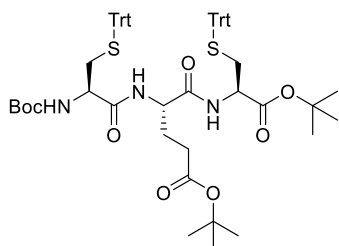
Compound 365 (279 mg, 80%, colorless solid) was prepared from **364** (275 mg, 0.33 mmol) and Boc-L-Cys(Trt)-OH (185 mg, 0.40 mmol) following the general procedures B and D. R$_f$ (CH$_2$Cl$_2$/MeOH 25:1): 0.49; Mp: 91 – 92 °C; [α]$_D^{20}$ +7 (*c* 1.00, CHCl$_3$); IR (neat): 3324 (w), 2979 (w), 2931 (w), 1716 (m), 1660 (m), 1596 (w), 1490 (m), 1445 (w), 1392 (w), 1367 (w), 1318 (w), 1249 (w), 1219 (w), 1152 (s), 1083 (w), 1034 (w), 846 (w), 743 (s), 699 (s), 619 (w); ^{1}H NMR (400 MHz, CDCl$_3$):7.31 – 7.22 (m, 12H), 7.17 – 7.10 (m, 12H), 7.09 – 7.02 (m, 6H), 6.79 (d, $^3J_{H-H}$ = 7.4 Hz, 1H), 6.54 (d, $^3J_{H-H}$ = 7.9 Hz, 1H),

4.63 (d, $^3J_{H-H}$ = 7.5 Hz, 1H), 4.26 – 4.14 (m, 2H), 3.77 – 3.60 (m, 1H), 2.69 – 2.57 (m, 1H),

2.49 (dd, $^2J_{H-H}$ = 12.3 Hz, $^3J_{H-H}$ = 6.2 Hz, 1H), 2.39 (dd, $^2J_{H-H}$ = 12.9 Hz, $^3J_{H-H}$ = 5.0 Hz, 1H),

2.33 (dd, $^2J_{H-H}$ = 12.3 Hz, $^3J_{H-H}$ = 4.7 Hz, 1H), 2.29 – 2.13 (m, 1H), 1.97 – 1.85 (m, 1H), 1.77

– 1.65 (m, 1H), 1.33 – 1.19 (m, 27H); ^{13}C NMR (100 MHz, CDCl$_3$): 172.9 (C), 170.3 (C),

170.2 (C), 168.9 (C), 155.4 (C), 144.40 (3xC), 144.37 (3xC), 129.6 (6xCH), 129.5 (6xCH),

128.1 (6xCH), 128.0 (6xCH), 126.9 (3xCH), 126.8 (3xCH), 82.4 (2xC), 80.8 (C), 80.3 (C),

67.2 (CH$_2$), 66.8 (CH$_2$), 53.6 (CH), 52.4 (CH), 51.9 (CH), 33.7 (CH$_2$), 31.5 (CH$_2$), 28.3

(3xCH$_3$), 28.1 (3xCH$_3$), 27.9 (3xCH$_3$); MS (MALDI-TOF): 1073 ([M+Na]$^+$).
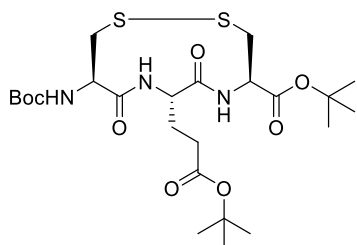
Compound 366 (119 mg, 55%, colorless solid) was prepared from **365** (400 mg, 0.38 mmol) following the general procedure E. R$_f$ (CH$_2$Cl$_2$/MeOH 25:1): 0.24; Mp: 90 – 91 °C; [α]$_D^{20}$ +5 (*c* 1.00, CHCl$_3$); IR (neat): 3315 (w), 3060 (w), 1662 (m), 1493 (m), 1446 (m), 1368 (w), 1319 (w), 1246 (m), 1153 (s), 1081 (w), 1034 (m), 845 (w), 740 (s), 700 (s), 619 (w); ^{1}H NMR (400 MHz, CDCl$_3$): 7.41 (br, 1H), 6.87 (br, 1H), 5.56 (br, 1H), 4.93 – 4.52 (br, 2H), 4.30 (br, 1H), 3.66 – 3.13 (m, 3H), 2.90 (br, 1H), 2.52 – 2.40 (m, 1H), 2.38 – 2.29 (m, 1H), 2.26 – 1.98 (m, 2H), 1.48 (s, 9H), 1.46 – 1.42 (m, 18H); ^{13}C NMR (125 MHz, CDCl$_3$): 172.7 (C), 171.9 (C), 170.4 (C), 168.2 (C), 154.6 (C), 83.3 (C), 81.1 (C), 80.3 (C), 538 (CH), 53.2 (CH), 52.3 (CH), 44.5 (CH$_2$), 41.5 (CH$_2$), 31.6 (CH$_2$), 28.3 (3xCH$_3$), 28.1 (3xCH$_3$), 28.0 (3xCH$_3$), 23.4 (CH$_2$); HPLC–MS: R_t = 2.17 min, 564 (100, [M+H]$^+$) (Eluent: CH$_3$CN + 0.1% TFA/water 0.1% TFA gradient from 30:70 to 95:5); MS (ESI, CHCl$_3$): 564 (100, [M+H]$^+$).
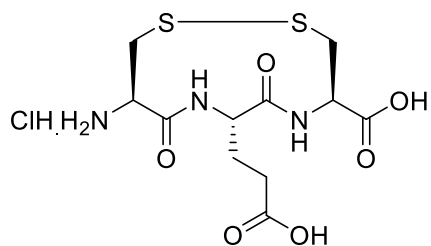
Compound 233 (76 mg, 93%, colorless solid) was prepared from **366** (119 mg, 0.21 mmol) following the general procedure C. Mp: 230 – 231 °C (decomp); $[\alpha]_D^{20}$ -43 (*c* 0.50, MeOH); IR (neat): 2938 (m), 1669 (s), 1544 (m), 1409 (m), 1241 (m), 1190 (m), 1045 (w), 967 (w), 941 (w), 840 (w), 655 (w), 615 (w); ^{1}H NMR (500 MHz, methanol-d$_4$): 4.84 – 4.68 (m, 2H), 4.39 – 4.00 (br, 1H), 3.68 – 2.74 (br, 4H), 2.59 – 2.42 (m, 2H), 2.30 – 2.13 (m, 1H), 2.08 – 1.93 (m, 1H); ^{13}C NMR (125 MHz, methanol-d4): 173.42 (C), 173.37 (C), 170.6 (C), 169.7 (C), 52.9 (CH), 52.2 (CH), 52.0 (CH, conformer), 51.4 (CH), 40.4 (2xCH$_2$), 29.40 (CH$_2$), 29.37 (CH$_2$, conformer), 23.2 (CH$_2$), 23.1 (CH$_2$, conformer); HRMS (ESI, +ve) calcd for C$_{11}$H$_{17}$N$_3$O$_6$S$_2$ ([M+H]$^+$): 352.0632, found: 352.0615.
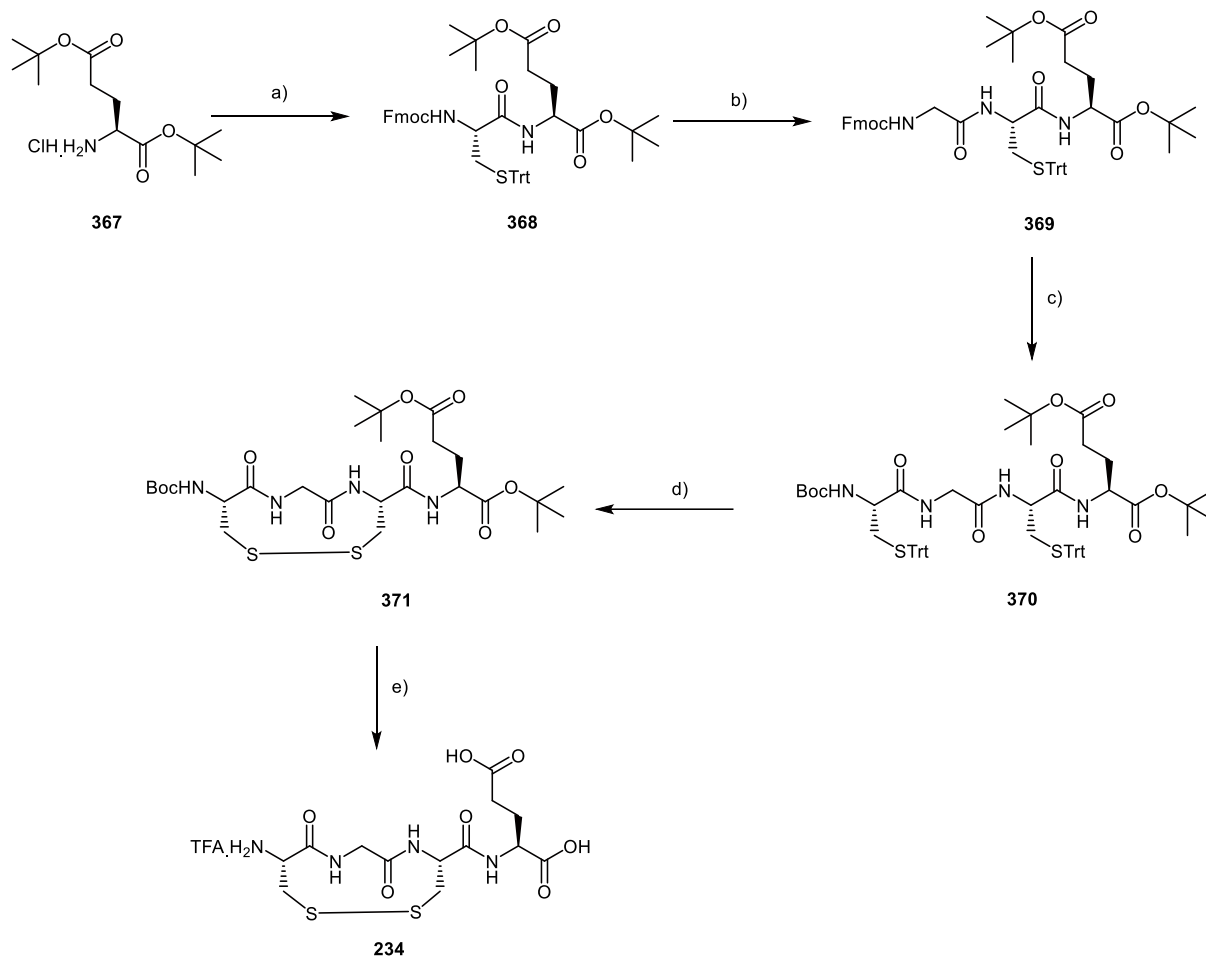
Scheme 43. (a) Fmoc-L-Cys(Trt)-OH, EDC, DMAP, CH$_2$Cl$_2$, rt, overnight, 66%; (b) 1. Et$_2$NH/CH$_2$Cl$_2$ 1:1, rt, 1 h; 2. Fmoc-Gly-OH, EDC, DMAP, CH$_2$Cl$_2$, rt, overnight, 47%; (c) 1. Et$_2$NH/CH$_2$Cl$_2$ 1:1, rt, 1 h; 2. Boc-L-Cys(*t*-Bu)-OH, EDC, DMAP, CH$_2$Cl$_2$, rt, overnight, 75%; (d) I$_2$, MeOH, rt, 4 h, 77%; (e) TFA/DCM 1:1, rt, overnight, 92%.
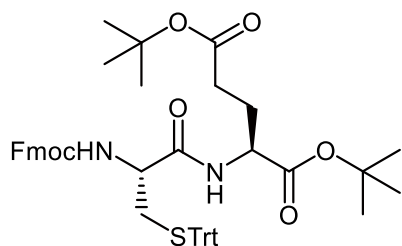
Compound 368 (468 mg, 66%, colorless solid) was prepared from **367** (303 mg, 1.02 mmol) and Fmoc-L-Cys(*t*-Bu)-OH (500 mg, 0.854 mmol) following the general procedure D. R_f (CH$_2$Cl$_2$/MeOH 25:1): 0.71; Mp: 71 – 72 °C; $[\alpha]_D^{20}$ +15 (*c* 1.00, CHCl$_3$); IR (neat): 3318 (w), 2924 (m), 2855 (w), 1726 (s), 1673 (m), 1493 (m), 1448 (m), 1367 (w), 1250 (m), 1149 (s), 1079 (w), 1035 (w), 845 (w), 740 (s),

700 (s), 619 (w); ^{1}H NMR (400 MHz, CDCl$_3$): 7.80 – 7.72 (m, 2H), 7.63 – 7.55 (m, 2H), 7.43 – 7.36 (m, 8H), 7.30 – 7.27 (m, 5H), 7.26 – 7.25 (m, 1H), 7.23 – 7.18 (m, 3H), 6.46 (d, $^3J_{H-H}$ = 7.7 Hz, 1H), 5.03 (d, $^3J_{H-H}$ = 8.1 Hz, 1H), 4.45 – 4.31 (m, 3H), 4.27 – 4.16 (m, 1H), 3.92 – 3.78 (m, 1H), 2.74 (dd, $^2J_{H-H}$ = 12.9 Hz, $^3J_{H-H}$ = 7.3 Hz, 1H), 2.57 (dd, $^2J_{H-H}$ = 12.9, $^3J_{H-H}$ = 5.3 Hz, 1H), 2.33 – 2.16 (m, 2H), 2.14 – 2.05 (m, 1H), 1.92 – 1.81 (m, 1H), 1.45 – 1.38 (m, 18H); ^{13}C NMR (100 MHz, CDCl$_3$): 172.1 (C), 170.3 (C), 169.7 (C), 155.8 (C), 144.3 (3xC), 143.7 (2xC), 141.3 (2xC), 129.6 (6xCH), 128.1 (6xCH), 127.7 (3xCH), 127.1 (2xCH), 126.9 (2xCH), 125.1 (2xCH), 120.0 (2xCH), 82.4 (C), 80.6 (C), 67.3 (C), 67.1 (CH$_2$), 54.0 (CH), 52.4 (CH), 47.1 (CH), 34.0 (CH$_2$), 31.4 (CH$_2$), 28.1 (3xCH$_3$), 27.9 (3xCH$_3$), 27.7 (CH$_2$); MS (MALDI-TOF): 865 ([M+K]$^+$).
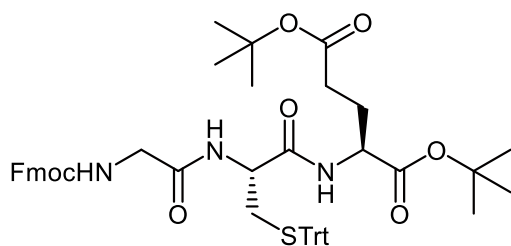
Compound 369 (1.0 g, 47%, colorless solid) was prepared from **368** (2.0 g, 2.4 mmol) and Fmoc-Gly-OH (0.9 g, 2.9 mmol) following the general procedures B and D. R_f (CH$_2$Cl$_2$/MeOH 25:1): 0.47; Mp: 110 – 111 °C; [α]$_D^{20}$ +7 (c 1.00, CHCl$_3$); IR (neat): 3283 (w), 2978 (w), 1725 (w), 1646 (s), 1531 (m), 1444 (w), 1392 (w), 1368 (w), 1335 (w), 1246 (m), 1149 (s), 1096 (w), 1050 (w), 845 (w), 741 (s), 704 (m), 671 (w); ^{1}H NMR (400 MHz, CDCl$_3$): 7.79 – 7.73 (m, 2H), 7.60 – 7.55 (m, 2H), 7.46 – 7.37 (m, 8H), 7.32 – 7.26 (m, 8H), 7.23 – 7.17 (m, 3H), 6.53 (d, $^3J_{H-H}$ = 7.7 Hz, 1H), 6.15 (d, $^3J_{H-H}$ = 7.7 Hz, 1H), 5.37 (br, 1H), 4.44 – 4.33 (m, 3H), 4.24 – 4.18 (m, 1H), 4.17 – 4.09 (m, 1H), 3.83 – 3.77 (m, 2H), 2.81 (dd, $^2J_{H-H}$ = 13.1 Hz, $^3J_{H-H}$ = 6.9 Hz, 1H), 2.57 (dd, $^2J_{H-H}$ = 13.1 Hz, $^3J_{H-H}$ = 5.7 Hz, 1H), 2.33 – 2.15 (m, 2H), 2.15 – 2.00 (m, 1H), 1.97 – 1.84 (m, 1H), 1.43 (s, 9H), 1.41 (s, 9H); ^{13}C NMR (125 MHz, CDCl$_3$): 169.8 (C), 167.8 (C), 166.9 (C), 166.2 (C), 153.0 (C), 141.9 (3xC), 141.3 (2xC), 138.9 (2xC), 127.1 (6xCH), 125.7 (6xCH), 125.3 (3xCH), 124.7 (2xCH), 124.5 (2xCH), 122.7 (2xCH),

117.6 (2xCH), 80.0 (C), 78.4 (C), 64.9 (CH$_2$), 50.1 (CH), 49.7 (CH), 44.7 (CH), 42.0 (CH$_2$), 30.9 (CH$_2$), 29.0 (CH$_2$), 25.6 (3xCH$_3$), 25.5 (3xCH$_3$), 25.1 (CH$_2$); MS (MALDI-TOF): 907 ([M+Na]$^+$).
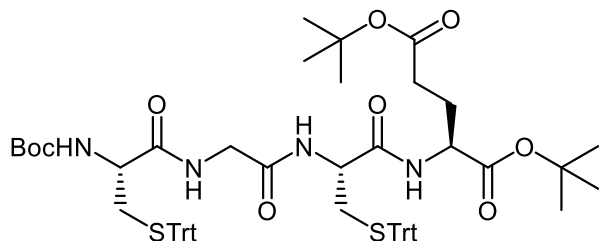
Compound 370 (0.9 g, 75%, colorless solid) was prepared from **369** (1.0 g, 1.1 mmol) and Boc-L-Cys(Trt)-OH (0.6 g, 1.3 mmol) following the general procedures B and D. R_f (CH$_2$Cl$_2$/MeOH 25:1): 0.34; Mp: 194 – 195 °C (decomp); [α]$_D^{20}$ +9 (c 1.00, CHCl$_3$); IR (neat): 3298 (w), 2977 (w), 1723 (m), 1644 (m), 1491 (m), 1445 (w), 1391 (w), 1367 (w), 1249 (w), 1152 (s), 1082 (w), 1033 (w), 846 (w), 743 (s), 699 (w), 619 (w); ^{1}H NMR (400 MHz, CDCl$_3$): 7.45 – 7.38 (m, 12H), 7.34 – 7.27 (m, 12H), 7.25 – 7.19 (m, 6H), 6.69 – 6.53 (m, 2H), 6.37 (br, 1H), 4.88 (br, 1H), 4.38 – 4.30 (m, 1H), 4.07 – 4.00 (m, 1H), 3.90 – 3.65 (m, 3H), 2.80 – 2.53 (m, 4H), 2.28 – 2.12 (m, 2H), 2.10 – 1.99 (m, 1H), 1.95 – 1.78 (m 1H), 1.45 – 1.38 (m, 27H); ^{13}C NMR (125 MHz, CDCl$_3$): 172.3 (C), 171.2 (C), 170.4 (C), 169.3 (C), 168.2 (C), 155.7 (C), 144.4 (3xC), 144.3 (3xC), 129.61 (6xCH), 129.55 (6xCH), 128.13 (6xCH), 128.07 (6xCH), 127.0 (3xCH), 126.9 (3xCH), 82.2 (C), 80.7 (C), 80.6 (C), 67.4 (C), 67.3 (C), 53.8 (CH), 52.4 (CH), 52.3 (CH), 43.3 (CH$_2$), 33.4 (CH$_2$), 33.2 (CH$_2$), 31.5 (CH$_2$), 28.3 (3xCH$_3$), 28.1 (3xCH$_3$), 28.0 (CH$_3$), 27.5 (CH$_2$); MS (MALDI-TOF): 1130 ([M+Na]$^+$).
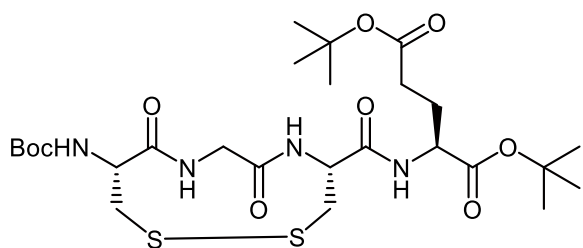
Compound 371 (190 mg, 77%, colorless solid) was prepared from **370** (440 mg, 0.397 mmol) following the general procedure E R_f (CH$_2$Cl$_2$/MeOH 25:1):

0.16; Mp: 125 – 126 °C; $[\alpha]_D^{20}$-57 (c 1.00, CHCl$_3$); IR (neat): 3313 (w), 2979 (w), 2935 (w), 1721 (m), 1655 (s), 1517 (m), 1454 (w), 1409 (w), 1367 (w), 1327 (w), 1246 (m), 1151 (s), 1048 (w), 1021 (w), 846 (w), 752 (w), 665 (w), 616 (w); ^{1}H NMR (400 MHz, CDCl$_3$): 8.05 – 7.73 (m, 2H), 7.17 (d, $^3J_{H–H}$ = 7.8 Hz, 1H), 5.68 (br, 1H), 5.25 – 4.81 (br, 1H), 4.61 – 4.39 (m, 2H), 4.33 – 3.98 (br, 1H), 3.91 – 3.71 (br, 1H), 3.62 – 3.51 (br, 1H), 3.43 – 3.25 (br, 2H), 3.11 – 2.94 (br, 1H), 2.42 – 2.23 (m, 2H), 2.17 – 2.06 (m, 1H), 2.01 – 1.88 (m, 1H), 1.46 (s, 9H), 1.45 – 1.42 (m, 18H); ^{13}C NMR (100 MHz, CDCl3): 172.7 (C), 172.4 (C), 170.6 (C), 168.8 (2xC), 154.9 (C), 82.5 (C), 81.0 (C), 80.9 (C), 55.5 (CH), 52.5 (2xCH), 45.5(CH$_2$), 45.2 (CH$_2$), 31.6 (CH$_2$), 28.3 (3xCH$_3$), 28.1 (3xCH$_3$), 28.0 (3xCH$_3$), 27.7 (CH$_2$); HPLC–MS: R_t = 1.91 min, 621 (100, [M+H]$^+$) (Eluent: CH$_3$CN + 0.1% TFA/water 0.1% TFA gradient from 30:70 to 95:5); MS (ESI, CHCl$_3$): 620 (100, [M+H]$^+$).
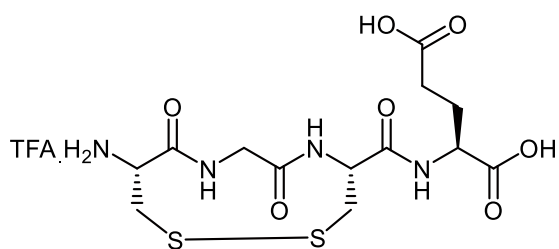
Compound 234 (83 mg, 92%, colorless solid) was prepared from **371** (190 mg, 0.306 mmol) following the general procedure A. Crude product was purified by HILIC flash column chromatography (Eluent: H$_2$O + 0.1% TFA/CH$_3$CN + 0.1% TFA gradient from 5:95 to 95:5). Mp: 213 – 214 °C (decomp); $[\alpha]_D^{20}$ -104 (c 0.50, DMSO); IR (neat): 3313 (w), 2970 (w), 1665 (s), 1530 (m), 1409 (w), 1201 (m), 839 (w), 800 (w), 723 (w), 665 (w); ^{1}H NMR (400 MHz, CD$_3$OD): 4.74 – 4.30 (m, 3H), 4.24 – 3.80 (br, 1H), 3.55 – 3.37 (m, 3H), 3.26 - 2.69 (br, 1H), 2.50 – 2.29 (m, 2H), 2.27 – 2.13 (m, 1H), 2.04 – 1.88 (m, 1H); ^{13}C NMR (125 MHz, CD$_3$OD): 177.2 (C), 175.3 (C), 172.8 (C), 172 (C), 170.2 (C), 55.5 (CH), 54.1 (CH), 53.8 (CH), 46.6 (CH$_2$), 43.9 (2xCH$_2$), 32.0 (CH$_2$), 28.6 (CH$_2$); HRMS (ESI, +ve) calcd for C$_{13}$H$_{20}$N$_4$O$_7$S$_2$ ([M+H]$^+$): 409.0847, found: 409.0846.
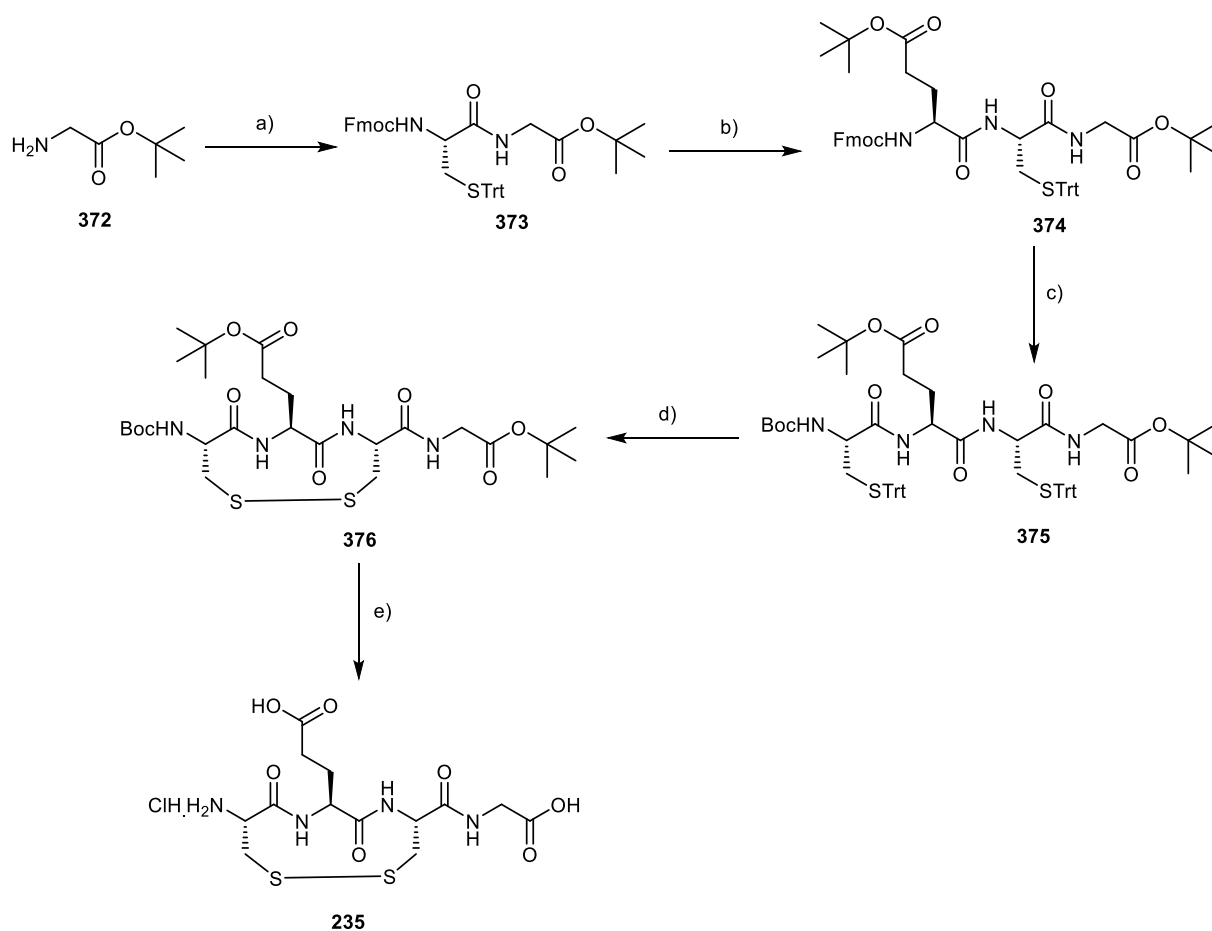
Scheme 44. (a) Fmoc-L-Cys(Trt)-OH, EDC, DMAP, CH$_2$Cl$_2$, rt, overnight, 84%; (b) 1. Et$_2$NH/CH$_2$Cl$_2$ 1:1, rt, 1 h; 2. Fmoc-L-Glu(t-Bu)-OH, EDC, DMAP, CH$_2$Cl$_2$, rt, overnight, 52%; (c) 1. Et$_2$NH/CH$_2$Cl$_2$ 1:1, rt, 1 h; 2. Boc-L-Cys(t-Bu)-OH, EDC, DMAP, CH$_2$Cl$_2$, rt, overnight, 67%; (d) I$_2$, MeOH, 4 h, rt, 39%; (e) HCl gas, EtOAc, rt, 1 h, 96%.
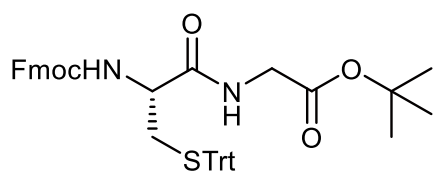
Compound 373 (0.9 g, 84%, colorless solid) was prepared from **372** (0.2 g, 1.5 mmol) and Fmoc-L-Cys(Trt)-OH (1.1 g, 1.8 mmol) following the general procedure D. R_f (CH$_2$Cl$_2$/MeOH 25:1): 0.68. Spectroscopic data were consistent with those reported in literature.[248]
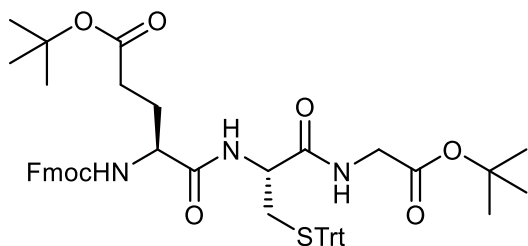
Compound 374 (1.0 g, 52%, colorless solid) was prepared from **373** (1.5 g, 2.1 mmol) and Fmoc-L-Glu(*t*-Bu)-OH (1.1 g, 2.5 mmol) following the general procedures B and D. R_f (CH$_2$Cl$_2$/MeOH 25:1): 0.46; Mp: 99 – 100 °C; $[\alpha]_D^{20}$ -2 (*c* 1.00, CHCl$_3$); IR (neat): 3288 (w), 2877 (w), 1725 (m), 1650 (m), 1515 (w), 1446 (w), 1367 (w), 1226 (m), 1152 (s), 1082 (w), 1036 (w), 841 (w), 740 (m), 700 (m), 620 (w); ^{1}H NMR (400 MHz, CDCl$_3$): 7.77 (d, $^3J_{H-H}$ = 7.5 Hz, 2H), 7.61 – 7.57 (m, 2H), 7.44 – 7.38 (m, 8H), 7.32 – 7.27 (m, 4H), 7.26 – 7.24 (m, 2H), 7.21 – 7.16 (m, 3H), 6.70 (br, 1H), 6.61 (d, $^3J_{H-H}$ = 8.0 Hz, 1H), 5.99 (d, $^3J_{H-H}$ = 6.6 Hz, 1H), 4.45 – 4.31 (m, 2H), 4.24 – 4.07 (m, 3H), 3.99 – 3.86 (m, 1H), 3.81 – 3.69 (m, 1H), 2.89 – 2.75 (m, 1H), 2.61 (dd, $^2J_{H-H}$ = 13.0 Hz, $^3J_{H-H}$ = 5.2 Hz, 1H), 2.51 – 2.27 (m, 2H), 2.14 – 2.02 (m, 1H), 1.99 – 1.86 (m, 1H), 1.46 – 1.39 (m, 18H); ^{13}C NMR (100 MHz, CDCl$_3$): 173.3 (C), 171.2 (C), 169.6 (C), 156.5 (C), 144.4 (3xC), 143.7 (2xC), 141.3 (2xC), 129.6 (6xCH), 128.1 (6xCH), 127.8 (3xCH), 127.1 (2xCH), 126.9 (2xCH), 125.2 (2xCH), 120.0 (2xCH), 82.1 (C), 81.3 (C), 67.3 (CH$_2$), 65.2 (C), 55.0 (CH), 53.5 (CH), 52.2 (CH), 47.1 (CH), 42.1 (CH$_2$), 33.3 (CH$_2$), 31.8 (CH$_2$), 28.1 (3xCH$_3$), 28.0 (3xCH$_3$), 27.5 (CH$_2$); MS (MALDI-TOF): 922 ([M+K]$^+$).
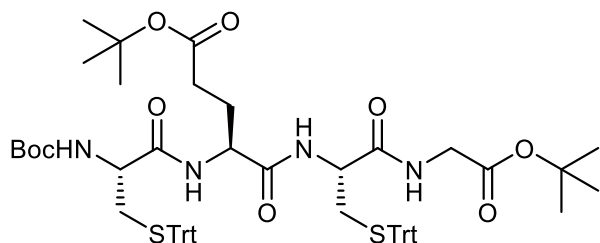
Compound 375 (831 mg, 67%, colorless solid) was prepared from **374** (987 mg, 1.12 mmol) and Boc-L-Cys(Trt)-OH (622 mg, 1.34 mmol) following the general procedures B and D. R_f (CH$_2$Cl$_2$/MeOH 25:1): 0.44; Mp: 174 – 175 °C (decomp); $[\alpha]_D^{20}$ +3 (*c* 1.00, CHCl$_3$); IR (neat): 3286 (w), 2977 (w), 2929 (w), 1717 (m), 1645 (m), 1491 (m), 1445 (w), 1391 (w), 1367 (w), 1247 (w), 1153 (s), 1034 (w), 846 (w), 743 (s), 699 (s), 675 (w),

619 (w); ^{1}H NMR (400 MHz, CDCl$_3$): 7.49 (d, $^3J_{H-H}$ = 5.9 Hz, 1H), 7.42 – 7.36 (m, 12H), 7.32 – 7.26 (m, 8H), 7.26 – 7.23 (m, 4H), 7.23 – 7.16 (m, 6H), 6.89 (d, $^3J_{H-H}$ = 8.3 Hz, 1H), 6.76 (br, 1H), 4.85 (d, $^3J_{H-H}$ = 6.1 Hz, 1H), 4.23 – 4.13 (m, 1H), 4.08 – 3.98 (m, 1H), 3.89 – 3.78 (m, 2H), 3.77 – 3.68 (m, 1H), 2.78 – 2.64 (m, 3H), 2.53 (dd, $^2J_{H-H}$ = 12.9 Hz, $^3J_{H-H}$ = 4.8 Hz, 1H), 2.47 – 2.37 (m, 1H), 2.35 – 2.24 (m, 1H), 2.08 – 1.98 (m, 1H), 1.98 – 1.86 (m, 1H), 1.45 – 1.41 (m, 18H), 1.40 (s, 9H); ^{13}C NMR (100 MHz, CDCl$_3$): 173.7 (C), 171.4 (C), 170.8 (C), 169.7 (C), 168.4 (C), 155.8 (C), 144.6 (3xC), 144.2 (3xC), 129.6 (6xCH), 129.5 (6xCH), 128.2 (6xCH), 128.0 (6xCH), 127.0 (3xCH), 126.8 (3xCH), 81.8 (C), 81.2 (C), 80.7 (C), 67.30 (C), 67.28 (C), 54.4 (CH), 53.9 (CH), 52.8 (CH), 42.1 (CH$_2$), 33.3 (CH$_2$), 33.1 (CH$_2$), 31.8 (CH$_2$), 28.3 (3xCH$_3$), 28.1 (6xCH$_3$), 26.5 (CH$_2$); MS (MALDI-TOF): 1130 ([M+Na]$^+$).
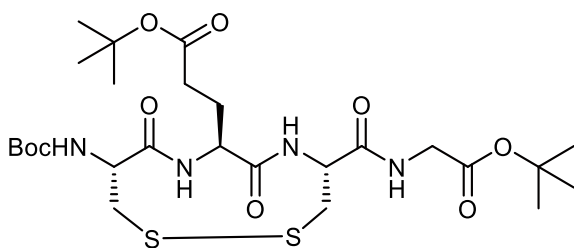
Compound 376 (122 mg, 39%, colorless solid) was prepared from **375** (557 mg, 0.503 mmol) following the general procedure E. R_f (CH$_2$Cl$_2$/MeOH 25:1): 0.24; Mp: 158 – 159 ^{o}C; [α]$_D^{20}$ -2 (*c* 1.00, CHCl$_3$); IR (neat): 3213 (w), 2977 (w), 1660 (s), 1516 (m), 1367 (m), 1248 (m), 1153 (s), 1052 (w), 847 (w), 754 (w); ^{1}H NMR (400 MHz, CDCl$_3$): 7.96 – 7.64 (m, 2H), 7.11 (br, 1H), 5.56 (br, 1H), 4.80 – 4.62 (m, 1H), 4.62 – 4.50 (m, 1H), 4.50 – 4.35 (m, 1H), 4.02 – 3.86 (m, 2H), 3.68 – 3.10 (br, 3H), 3.09 – 2.79 (m, 1H), 2.51 – 2.33 (m, 2H), 2.21 – 1.99 (m, 2H), 1.46 (s, 9H), 1.44 – 1.42 (m, 18H); ^{13}C NMR (100 MHz, CDCl$_3$): 173.1 (C), 172.4 (C), 169.1 (2xC), 168.5 (C), 154.7 (C), 82.3 (C), 81.4 (C), 80.4 (C), 54.5 (CH), 53.4 (CH), 52.9 (CH), 44.7 (2xCH$_2$), 42.0 (CH$_2$), 31.7 (CH$_2$), 28.3 (3xCH$_3$), 28.09 (3xCH$_3$), 28.07 (3xCH$_3$), 23.7 (CH$_2$); HPLC–MS: R_t = 1.96 min, 1241 (100, [2M+H]$^+$) (Eluent: CH$_3$CN + 0.1 %TFA/water 0.1% TFA gradient from 30:70 to 95:5); MS (ESI, MeOH): 620 (100, [M+H]$^+$).
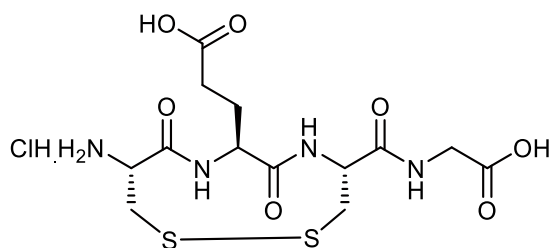
Compound 235 (84 mg, 96%, colorless solid) was prepared from **376** (122 mg, 0.197 mmol) following the general procedure C. Mp: 234 – 235 °C (decomp); $[\alpha]_D^{20}$ -51 (*c* 0.50, MeOH); IR (neat): 2938 (m), 1658 (s), 1531 (m), 1408 (m), 1208 (m), 1039 (w), 855 (w), 664 (w); ^{1}H NMR (500 MHz, CD$_3$OD):

4.72 – 4.30 (m, 2H), 4.12 (m, 1H), 3.97 – 3.76 (m, 2H), 3.68 – 3.26 (m, 2H), 3.19 – 2.71 (m, 2H), 2.45 – 2.28 (m, 2H), 2.19 – 2.05 (m, 1H), 1.96 – 1.83 (m, 1H); ^{13}C NMR (125 MHz, CD$_3$OD): 173.5 (C), 171.3 (C), 170.3 (C), 170.2 (C), 169.0 (C), 53.0 (CH), 52.6 (CH), 52.2 (CH), 40.5 (2xCH$_2$), 40.4 (CH$_2$), 29.4 (CH$_2$), 23.0 (CH$_2$); HRMS (ESI, +ve) calcd for C$_{13}$H$_{20}$N$_4$O$_7$S$_2$ ([M+H]$^+$): 409.0847, found: 409.0846.

Note: Peaks broadening in NMR spectra caused by the presence of conformers as describing for similar compounds in literature.[255–258]

5.2.6.3. Heteroaromatic Sulfones
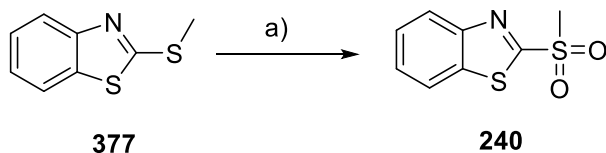
Scheme 45. (a) *m*-CPBA, CH$_2$Cl$_2$, rt, 2 h, 82%.
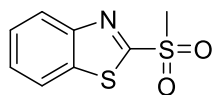
Compound 240. To a solution of **377** (0.8 g, 4.4 mmol), *m*-CPBA (2.1 g, 9.2 mmol) was added. The reaction mixture was stirred at rt for 2 h. The reaction mixture was diluted with CH_2Cl_2 and washed with saturated aqueous solution of $NaHCO_3$ 3 times. The organic layer was dried over anhydrous Na_2SO_4. The solvent was removed in vacuo. The residue was purified by flash chromatography (CH_2Cl_2) to yield desired product (0.8 g, 82%). R_f (CH_2Cl_2): 0.41. Spectroscopic data were consistent with those reported in literature.[176]
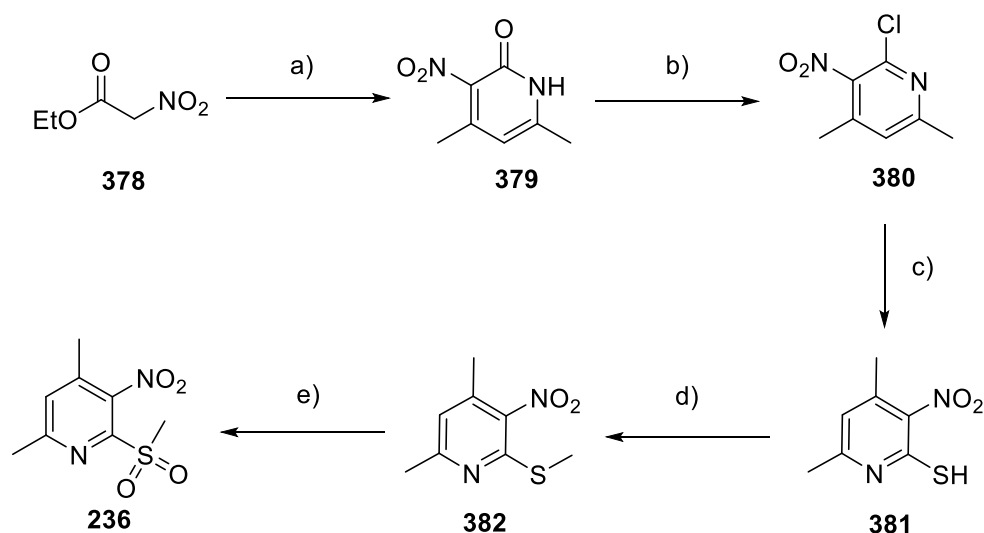
Scheme 46. (a) 1. NH_4OH, 3 d, rt; 2. 2,4-Pentanedione, AcOH, pyridine, H_2O, rt, 7 d, 22%; (b) $POCl_3$, reflux, 3 h, 60%; (c) thiourea, EtOH/IPA 1:1, reflux, overnight, 40%; (d) CH_3I, TEA, CH_2Cl_2, rt, 10 min, 100%; (e) *m*-CPBA, CH_2Cl_2, 2 h, 60%.

Compound 379 was synthesized as described previously in literature.[259]

Compound 380 was synthesized as described in previously in literature.[259]

Compound 381 was synthesized as described in previously in literature.[259]
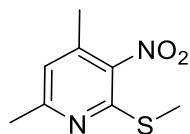
Compound 382. To a suspension of **381** (370 mg, 2.01 mmol) in 2.5 ml of CH_2Cl_2, a solution of CH_3I (186 μl, 3.02 mmol) in 660 μl of CH_2Cl_2 was added, followed by a solution of TEA (420 μl, 3.02 mmol) in 660 μl of CH_2Cl_2. After becoming clear, the reaction mixture was kept stirring at rt for 10 min. Then reaction mixture was diluted with CH_2Cl_2, washed with water, brine, and dried over anhydrous Na_2SO_4. The solvent was removed in vacuo. The residue was purified by flash chromatography (CH_2Cl_2/pentane 1:3) to yield desired product (398 mg, 100%). R_f (CH_2Cl_2/pentane 1:3): 0.42. Spectroscopic data were consistent with those reported in literature.[259]
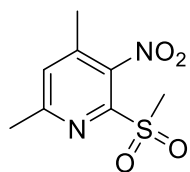
Compound 236. To a solution of **382** (419 mg, 2.11 mmol), *m*-CPBA (1.0 g, 4.4 mmol) was added. The reaction mixture was stirred at rt for 2 h. The reaction mixture was diluted with CH_2Cl_2 and washed with saturated aqueous solution of $NaHCO_3$ 3 times. The organic layer was dried over anhydrous Na_2SO_4. The solvent was removed in vacuo. The residue was purified by flash chromatography (Gradient from CH_2Cl_2/MeOH 60:1 to CH_2Cl_2/MeOH 25:1) to yield desired product (290 mg, 60%). R_f (CH_2Cl_2/MeOH 25:1): 0.72. Spectroscopic data were consistent with those reported in literature.[259]
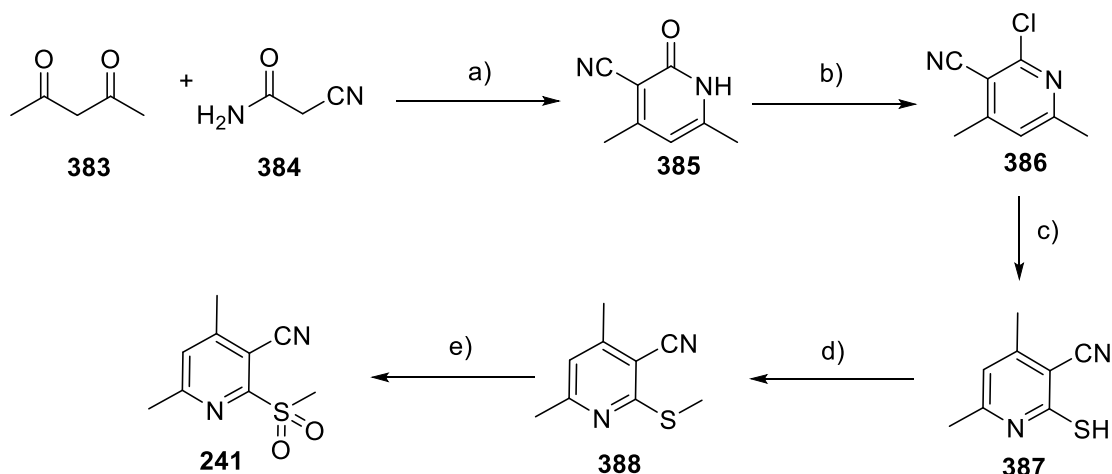
Scheme 47. (a) K_2CO_3, EtOH, rt, overnight, 70%; (b) $POCl_3$, reflux, 3 h, 88%; (c) thiourea, EtOH/IPA 1:1, reflux, overnight, 85%; (d) CH_3I, TEA, CH_2Cl_2, rt, 10 min, 92%; (e) *m*-CPBA, CH_2Cl_2, 2 h, 46%.

Compound 385 was synthesized as described previously in literature.[259]

Compound 386 was synthesized as described previously in literature.[259]

Compound 387 was synthesized as described previously in literature.[259]
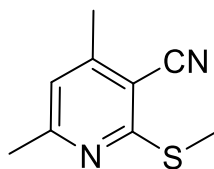
Compound 388. To a suspension of **387** (1.0 g, 6.1 mmol) in 6.0 ml of CH_2Cl_2, a solution of CH_3I (563 µl, 9.15 mmol) in 2.0 ml of CH_2Cl_2 was added, followed by a solution of TEA (1.3 ml, 9.2 mmol) in 2.0 ml of CH_2Cl_2. After becoming clear, the reaction mixture was kept stirring at rt for 10 min. Then reaction mixture was diluted with CH_2Cl_2, washed with water, brine, and dried over anhydrous Na_2SO_4. The solvent was removed in vacuo. The residue was purified by flash chromatography

(CH$_2$Cl$_2$/pentane 1:1) to yield desired product as a white solid (1.0 g, 92%). R$_f$ (CH$_2$Cl$_2$/pentane 1:1): 0.39. Spectroscopic data were consistent with those reported in literature.[259]
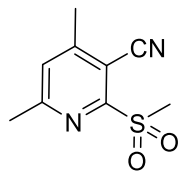
Compound 241 To a solution of **388** (609 mg, 3.42 mmol), *m*-CPBA (1.7 g, 7.2 mmol) was added. The reaction mixture was stirred at rt for 2 h. The reaction mixture was diluted with CH$_2$Cl$_2$ and washed with saturated aqueous solution of NaHCO$_3$ 3 times. The organic layer was dried over anhydrous Na$_2$SO$_4$. The solvent was removed in vacuo. The residue was purified by flash chromatography (CH$_2$Cl$_2$/MeOH 30:1) to yield desired product (334 mg, 46%). R$_f$ (CH$_2$Cl$_2$/MeOH 25:1): 0.47. Spectroscopic data were consistent with those reported in literature.[259]
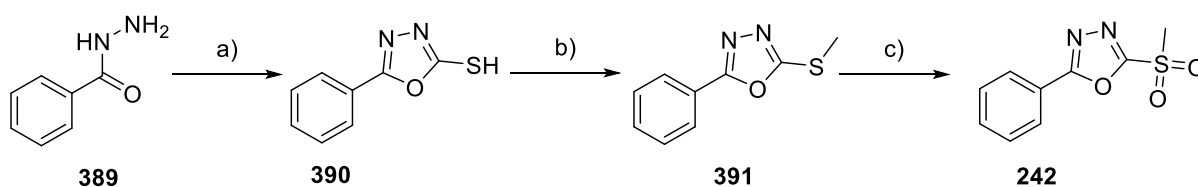
Scheme 48. (a) CS$_2$, KOH, EtOH/H$_2$O, 50 °C, 6 h, 50%; (b) CH$_3$I, TEA, THF, rt, 2 h, 57%; (c) KMnO$_4$, AcOH, rt, 20 min, 71%.

Compound 390 was synthesized as described previously in literature.[260]

Compound 391 was synthesized as described previously in literature.[176]

Compound 242 was synthesized as described previously in literature.[261]
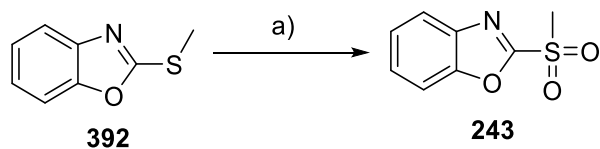
Scheme 49. (a) m-CPBA, CH$_2$Cl$_2$, rt, 2 h, 63%.

Compound 243 was synthesized as described previously in literature.[176]
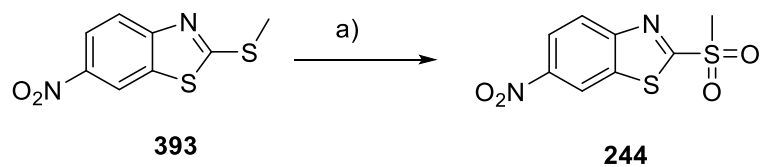
Scheme 50. (a) m-CPBA, CH$_2$Cl$_2$, rt, overnight, 77%.

Compound 393 was synthesized as described previously in literature.[262]

Compound 244 was synthesized as described previously in literature.[176]

5.2.6.4. Other Inhibitors

394 → a) → **395** → b) → **245**
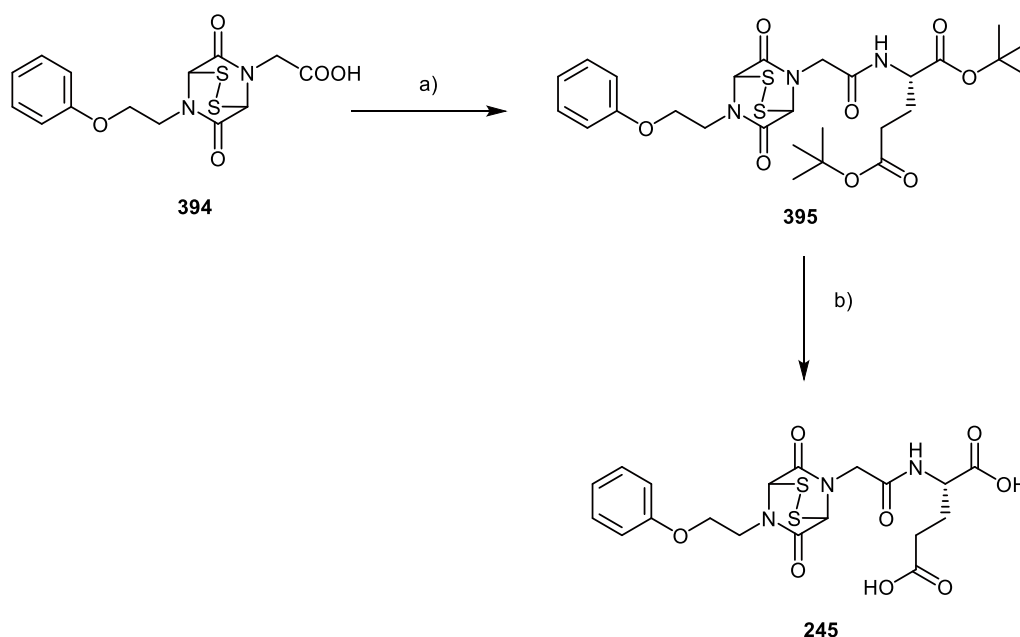
Scheme 51. (a) L-Glutamic acid di-*tert*-butyl ester hydrochloride, EDC, TEA, CH$_2$Cl$_2$, rt, overnight, 71%; (b) TFA/CH$_2$Cl$_2$ (1:1), rt, 1 h, 91%.

Compound 394 was synthesized as described previously in literature.[165]
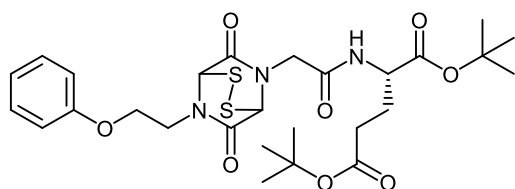
Compound 395. To a solution of **394** (30 mg, 0.08 mmol) in CH$_2$Cl$_2$ (800 µL), L-Glutamic acid di-*tert*-butyl ester hydrochloride (22 mg, 0.11 mmol), EDC (22 mg, 0.11 mmol) and TEA (3.0 µl, 0.04 mmol) were added. The reaction mixture was stirred at rt overnight. The solvent was removed under vacuum. The residue was purified by reversed phase flash column chromatography (Eluent: H$_2$O + 0.1% TFA/CH$_3$CN + 0.1% TFA gradient from 80:20 to 5:95) to yield desired product as a colorless solid (36 mg, 71%, mixture of 2 diastereomers (1:1)). Mp: 54 – 55 °C; IR (neat): 3324 (w), 2981 (w), 2935 (w), 1688 (s), 1600 (w), 1535 (w), 1497 (w), 1441 (w), 1414 (w), 1393 (w), 1368 (w), 1299 (w), 1225 (m), 1148 (s), 1082 (w), 1033 (w), 953 (w), 907 (w), 844 (w), 813 (w), 787 (w), 754

(w), 692 (w), 673 (w), 615 (w); ^{1}H NMR (400 MHz, CDCl$_3$, nn/nn-50:50 diastereomeric peaks, some peaks overlap): 7.31 – 7.26 (m, 2H), 7.01 – 6.95 (m, 1H), 6.94 – 6.88 (m, 2H), 6.77 – 6.64 (m, 1H), 5.78/5.76 (s, 1H), 5.55/5.54 (s, 1H), 4.48 – 4.43 (m, 1H), 4.36 – 4.08 (m, 4H), 4.03 – 3.87 (m, 2H), 2.38 – 2.20 (m, 2H), 2.15 – 2.03 (m, 1H), 1.95 – 1.76 (m, 1H), 1.48 – 1.46 (m, 9H), 1.44 – 1.42 (m, 9H); ^{13}C NMR (100 MHz, CDCl$_3$, nn/nn-diastereomeric peaks): 172.3/172.2 (C), 170.5/170.3 (C), 166.5/166.4 (C), 164.0/163.8 (C), 163.3/163.2 (C), 157.9 (C), 129.6 (2xCH), 121.6 (CH), 114.6/114.5 (2xCH), 82.8 (C), 81.01/80.96 (C), 66.4/66.3 (CH), 66.2/66.1 (CH$_2$), 66.0/65.9 (CH), 52.7/52.6 (CH), 47.7/47.0 (CH$_2$), 44.33/44.31 (CH$_2$), 31.4/31.2 (CH$_2$), 28.10/28.06 (3xCH$_3$), 27.99/27.96 (3xCH$_3$), 27.40/27.37 (CH$_2$); HPLC–MS: R_t = 2.94 min, 484 (100, [M-2t-Bu+H]$^+$), 540 (15, [M-t-Bu+H]$^+$), 596 (10, [M+H]$^+$) (Eluent: CH$_3$CN + 0.1%TFA/ H$_2$O + 0.1%TFA gradient from 5:95 to 95:5); MS (ESI, MeOH): 484 (100, [M-2t-Bu+H]$^+$).
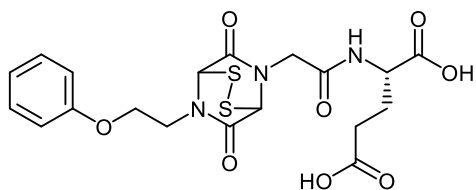
Compound 245. 395 (36.0 mg, 0.063 mmol) was dissolved in CH$_2$Cl$_2$/TFA (1.0 mL: 1.0 mL). The reaction mixture was stirred at rt for 1 h. The solvents were removed under vacuum. The residue was purified by reversed phase flash column chromatography (Eluent: H$_2$O + 0.1% TFA/CH$_3$CN + 0.1% TFA gradient from 95:5 to 30:70) to yield desired product as a colorless solid (28.0 mg, 91%, mixture of 2 diastereomers). Mp: 181 – 182 ºC (decomp.); IR (neat): 3304 (br), 2988 (br), 2608 (br), 1677 (s), 1599 (m), 1544 (m), 1493 (m), 1442 (m), 1412 (m), 1363 (w), 1336 (w), 1298 (w), 1227 (s), 1191 (s), 1175 (s), 1082 (w), 1033 (w), 953 (w), 906 (w), 815 (w), 788 (w), 755 (m), 691 (w), 673 (w), 914 (w); ^{1}H NMR (400 MHz, CD$_3$OD, nn/nn-50:50 diastereomeric peaks, some peaks overlap): 7.32 – 7.18 (m, 2H), 7.05 – 6.85 (m, 3H), 5.97/5.97 (s, 1H), 5.81/5.81 (s, 1H), 4.59 – 4.36 (m, 2H), 4.28 – 4.12 (m, 2H), 4.10 – 3.83 (m, 3H), 2.48 – 2.31 (m, 2H), 2.23 – 2.11

(m, 1H), 2.03 – 1.86 (m, 1H); ^{13}C NMR (125 MHz, CD$_3$OD, nn/nn-50:50 diastereomeric peaks, some peaks overlap): 175.1/174.9 (C); 173.6/173.3 (C); 167.9/167.8 (C), 164.66/164.65 (C), 164.44/164.41, 158.5 (C), 129.1 (2xCH), 120.8 (CH), 114.4 (2xCH), 65.91/65.90 (CH), 65.75/65.73 (CH), 65.5 (CH$_2$), 52.0 (CH), 45.11/45.14 (CH$_2$), 43.8 (CH$_2$), 29.8 (CH$_2$), 26.72/26.65 (CH$_2$); HPLC–MS: R_t = 1.91 min, 484 (100, [M+H]$^+$) (Eluent: CH$_3$CN + 0.1% TFA/water 0.1% TFA gradient from 5:95 to 95:5); MS (ESI, MeOH): 484 (100, [M+H]$^+$).
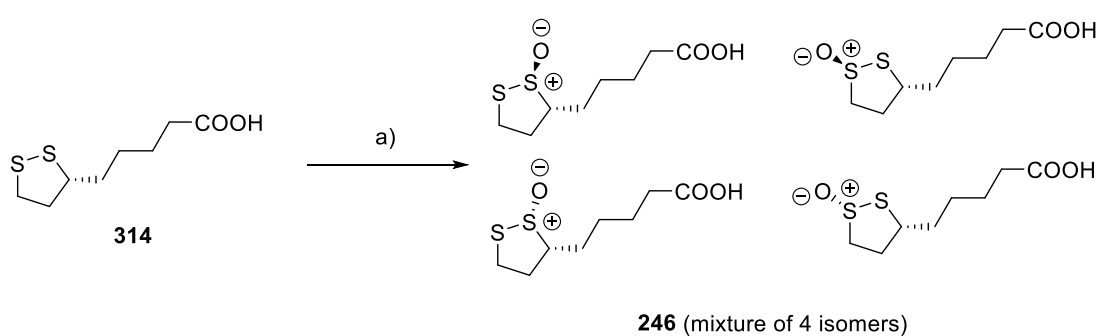
Scheme 52. (a) H$_2$O$_2$ (30% in H$_2$O), acetone, rt, 24 h, 39%.

Compound 246 was synthesized as described in reference.[172]
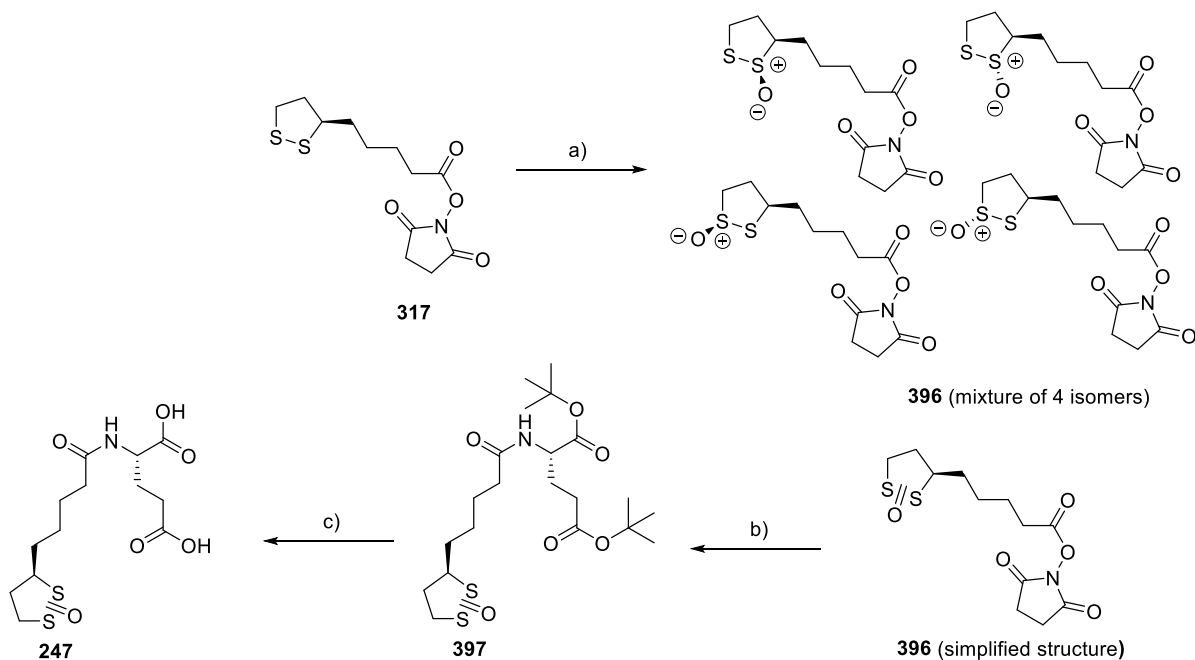
Scheme 53. (a) H₂O₂ (30% aqueous solution), acetone, rt, 1 d, 60%; (b) HCl.NH₂-Glu(2xOtBu), TEA, CH₂Cl₂, rt, overnight, 75%; (c) TFA/DCM 1:1, rt, 24 h, 93%.
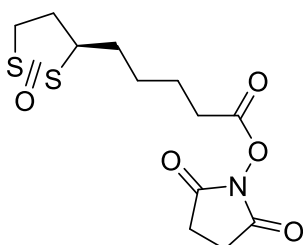
Compound 396. To a solution of **317** (195 mg, 0.643 mmol) in acetone (1.2 ml), was added H₂O₂ (30 % aqueous solution) (148 µl, 0.707 mmol). The reaction mixture was kept stirring at rt for 1 day. Then the reaction mixture was diluted with CH₂Cl₂. The resulting solution was dried over anhydrous Na₂SO₄. The solvents were removed *in vacuo*. The residue was purified by flash chromatography (CH₂Cl₂/MeOH 18:1) to yield desired product as a colorless oil (123 mg, 60%, mixture of 4 isomers 33:34:28:5). R_f (CH₂Cl₂/MeOH 15:1): 0.34; IR (neat): 2937 (w), 2862 (w), 1811 (w), 1781 (w), 1732 (s), 1430 (w), 1363 (w), 1302 (w), 1254 (w), 1204 (m), 1127 (w), 1066 (s), 995 (w), 814 (w), 649 (w); ¹H NMR (400 MHz, CDCl₃, nn/nn-isomeric peaks, some peaks overlap): 4.23 – 4.14/3.95 – 2.85/3.76 – 3.71/3.65 – 3.60 (m, 1H), 3.71 – 3.66/3.50 – 3.43/3.59 – 3.54/ 3.30 – 3.26 (m, 1H), 3.37 – 2.88 (m, 2H), 2.82 (s, 4H), 2.76 – 2.51 (m, 3H), 2.08 – 1.83 (m, 1H), 1.82 – 1.72 (m, 2H), 1.70 – 1.30 (m,

3H); ^{13}C NMR (100 MHz, CDCl$_3$, nn/nn-isomeric peaks, some peaks overlap): 169.21/169.18 (2xC), 168.4/168.3/168.2 (C), 77.6/75.2/57.8/55.2 (CH), 62.7/61.6/37.0/36.7 (CH$_2$), 36.1/35.4/33.9/33.7 (CH$_2$), 35.30/35.0/27.7/27.5 (CH$_2$), 30.69/30.67/30.65/30.60 (CH$_2$), 28.5/27.0/26.7/26.6 (CH$_2$), 25.6 (2xCH$_2$), 24.4/24.3/24.2/20.6 (CH$_2$); HPLC–MS: R_t = 1.71 min, 320 (100, [M+H]+) (Eluent: CH$_3$CN + 0.1%TFA/water 0.1%TFA gradient from 5:95 to 95:5); MS (ESI, MeOH): 320 (100, [M+H]$^+$).
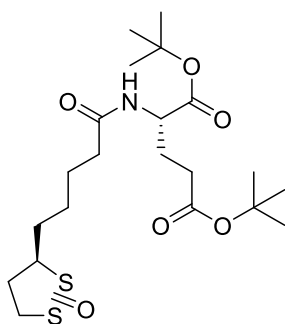
Compound 397. To a solution of **396** (91 mg, 0.28 mmol) in CH$_2$Cl$_2$ (300 µl), was added HCl.NH$_2$-Glu(2xOtBu) (68 mg, 0.34 mmol), followed by TEA (57 µl, 0.42 mmol). The reaction mixture was kept stirring at rt overnight. The reaction mixture was diluted with CH$_2$Cl$_2$, washed with 10% aqueous solution of citric acid, water, saturated solution of NaHCO$_3$ and brine. The organic layer was dried over anhydrous Na$_2$SO$_4$. Then the solvent was removed *in vacuo*. The residue was purified by flash chromatography (CH$_2$Cl$_2$/MeOH 25:1) to yield the desired product as a colorless oil (99 mg, 75%, mixture of 4 isomers 33:34:28:5). R_f (CH$_2$Cl$_2$/MeOH 25:1): 0.17; IR (neat): 3299 (w), 2977 (w), 2932 (w), 1727 (m), 1652 (m), 1534 (w), 1453 (w), 1367 (m), 1253 (m), 1150 (s), 1076 (m), 967 (w), 846 (w), 788 (w), 751 (w), 623 (w), ^{1}H NMR (400 MHz, CDCl$_3$, nn/nn-isomeric peaks, some peaks overlap): 6.31 – 6.18 (m, 1H), 4.53 – 4.40 (m, 1H), 4.23 – 4.13/3.96 – 3.86/3.76 – 3.67 (m, 1H), 3.64 – 2.79 (m, 3H), 2.74 – 2.50 (m, 1H), 2.38 – 2.18 (m, 4H), 2.17 – 1.57 (m, 6H), 1.54 – 1.21 (m, 20H); ^{13}C NMR (125 MHz, CDCl$_3$, nn/nn-isomeric peaks, some peaks overlap): 172.40/172.38/172.36 (C), 172.34/172.32/172.22 (C), 171.26/171.24/171.23 (C), 82.31/82.28/82.26 (C), 80.81/80.80/80.77 (C), 77.8/75.3/57.9/55.4 (CH), 62.7/61.6/37.0/36.6 (CH$_2$), 52.24/52.21 (CH), 36.26/36.06/36.05/35.91 (CH$_2$), 35.88/35.7/35.3/35.0 (CH$_2$), 31.6 (CH$_2$), 29.0/33.9/33.8 (CH$_2$), 28.1 (3xCH$_3$), 28.0 (3xCH$_3$),

27.6/27.53/27.50 (CH$_2$), 27.3/27.1/26.8 (CH$_2$), 25.2/25.11/25.07/25.0 (CH$_2$).;HPLC–MS: R_t = 2.52 min, 352 (100, [M-2tBu+H]$^+$), 408 (65, [M-tBu+H]$^+$), 464 (42, [M+H]$^+$) (Eluent: CH$_3$CN + 0.1%TFA/water 0.1%TFA gradient from 5:95 to 95:5); MS (ESI, MeOH): 464 (100, [M+H]$^+$).
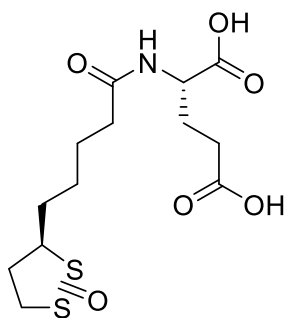
Compound 247 (24 mg, 93 %, colorless oil, mixture of 4 isomers 33:34:28:5) was prepared from **397** (34 mg, 73 μmol) following the general procedure A, purified by reversed-phase flash column chromatography (Eluent: H$_2$O + 0.1% TFA/CH$_3$CN + 0.1% TFA gradient from 95:5 to 40:60). IR (neat): 3291 (w), 2931 (w), 2862 (w), 1729 (s), 1644 (m), 1536 (m), 1438 (w), 1412 (w), 1378 (w), 1202 (m), 1083 (m), 1035 (m), 784 (w), 640 (w); ^{1}H NMR (400 MHz, CD$_3$OD, nn/nn-isomeric peaks, some peaks overlap): 4.48 – 4.38 (m, 1H), 4.31 – 4.20/4.09 – 3.93 (m, 1H), 3.84 – 3.55 (m, 1H), 3.53 – 3.33 (m, 1H), 3.24 – 2.48 (m, 3H), 2.45 – 2.35 (m, 2H), 2.34 – 2.24 (m, 2H), 2.23 – 2.06 (m, 2H), 2.01 – 1.81 (m, 2H), 1.76 – 1.32 (m, 5H); ^{13}C NMR (125 MHz, CD$_3$OD, nn/nn-isomeric peaks, some peaks overlap): 174.9 (C), 174.7/174.64/174.61/174.2 (C), 173.53/173.52/170.2 (C), 78.2/75.4/58.4/58/0 (CH), 62.6/61.4/36.8/36.5 (CH$_2$), 51.5 (CH), 35.9/35.1/35.0 (CH$_2$), 34.91/34.87/34.84/34.5 (CH$_2$), 33.5/33.1/29.0/28.5 (CH$_2$), 29.9 (CH$_2$), 27.63/27.59/26.72/26.68 (CH$_2$), 26.4/26.3/25.4 (CH$_2$), 25.2/25.1/25.04/24.98 (CH$_2$); HPLC–MS: R_t = 1.27 min, 352 (100, [M+H]+) (Eluent: CH$_3$CN + 0.1%TFA/water 0.1%TFA gradient from 5:95 to 95:5).
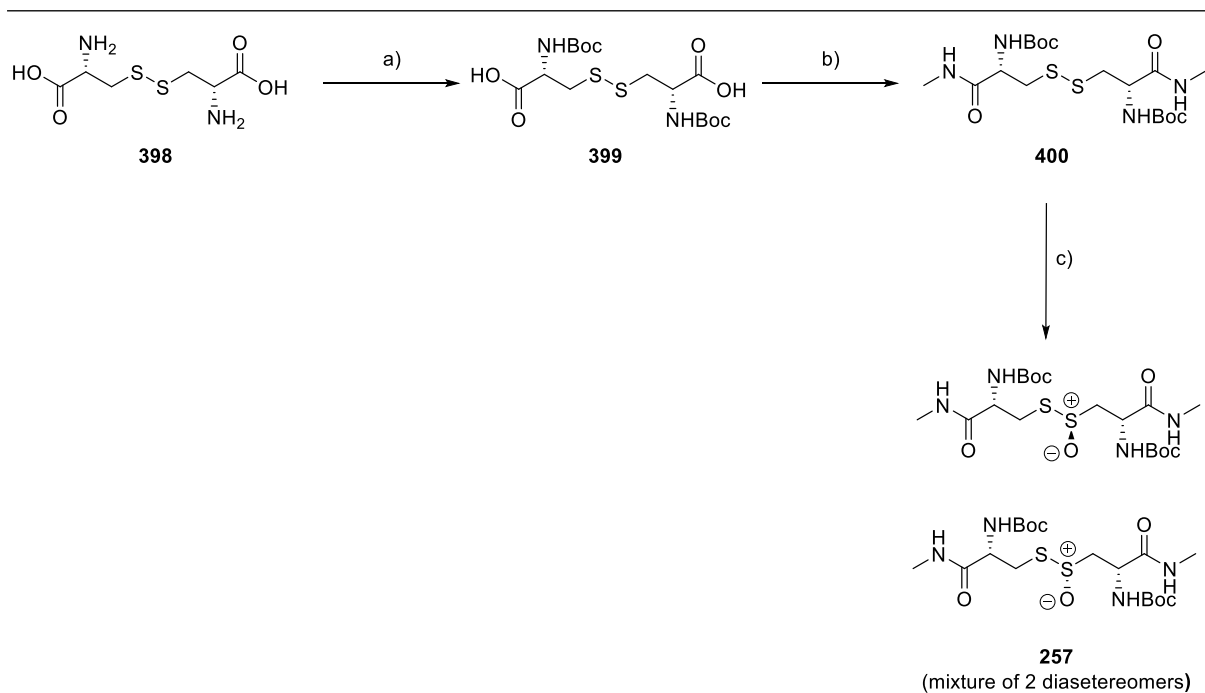
Scheme 54. (a) Boc₂O, TEA, H₂O, rt, 4 h, 94%; (b) isobutyl chloroformate, CH₃NH₂ (2 M solution in THF), THF, 0 °C to rt, 24 h, 48%; (c) *m*-CPBA, CH₂Cl₂, rt, 0 °C, 1 h, 23%.

Compound 399 was synthesized as described previously in literature.[263]

Compound 400 was synthesized as described previously in literature.[264]
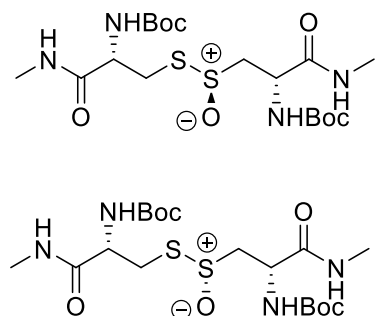
Compound 257. To a suspension of **400** (250 mg, 0.536 mmol) in CH₂Cl₂ (11.0 ml) at 0 °C, was added *m*-CPBA (132 mg, 0.574 mmol). Reaction mixture was stirred at 0 °C for 1 h, then warmed up to rt. The reaction mixture was diluted with CH₂Cl₂, and washed with saturated aqueous solution of NaHCO₃ 3 times. The organic layer was dried over anhydrous Na₂SO₄, filtered and concentrated under vacuum. The residue was purified by flash chromatography

(CH$_2$Cl$_2$/MeOH 15:1) to yield desired product as a colorless solid (60 mg, 23%, mixture of 2 diastereomers). R_f (CH$_2$Cl$_2$/MeOH 15:1): 0.19; IR (neat): 3324 (m), 2977 (w), 1687 (m), 1652 (s), 1521 (s), 1412 (w), 1366 (m), 1320 (m), 1250 (m), 1163 (s), 1065 (m), 1047 (m), 1023 (m), 870 (w), 779 (w), 648 (w); ^{1}H NMR (400 MHz, CDCl$_3$): 7.53 – 6.90 (m, 2H), 6.08 – 5.64 (m, 2H), 4.81 – 4.38 (m, 2H), 3.87 – 3.31 (m, 4H), 2.82 – 2.74 (m, 6H), 1.46 – 1.33 (m, 18H); ^{13}C NMR (100 MHz, CDCl$_3$, nn/nn-diastereomeric peaks):170.9 (C), 169.7/169.1 (C), 156.1 (C), 155.4 (C), 81.0/80.8 (C), 80.3 (C), 65.4/41.8 (CH$_2$), 54.8 (CH), 54.4/49.8 (CH), 47.2 (CH$_2$), 28.4 (3xCH$_3$), 28.3 (3xCH$_3$), 26.3/26.2 (CH$_3$), 26.0 (CH$_3$); HPLC–MS: R_t = 1.93 min, 483 (100, [M+H]$^+$) (Eluent: CH$_3$CN + 0.1%TFA/water 0.1%TFA gradient from 5:95 to 95:5); MS (ESI, MeOH): 483 (100, [M+H]$^+$).
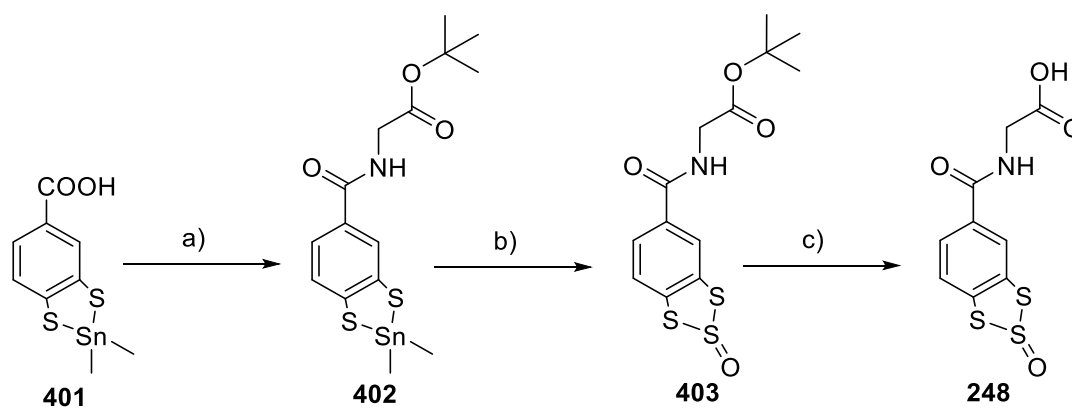
Scheme 55. (a) *t*-butyl glycinate, EDC, CH$_2$Cl$_2$, rt, overnight, 67%; (b) SOCl$_2$, dry THF, -60 °C to -10 °C, 23%; (c) TFA/CH$_2$Cl$_2$ (1:1), 45%.

Compound 401 was synthesized as described previously in literature.[165]
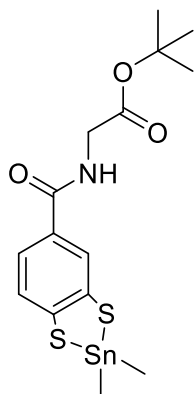
Compound 402. To a solution of **401** (50.0 mg, 0.150 mmol) in CH_2Cl_2 (1.5 ml) was added *t*-butyl glycinate (24.0 mg, 0.183 mmol), followed by EDC (36.0 mg, 0.183 mmol). The reaction mixture was stirred at rt overnight, then diluted with CH_2Cl_2. The reaction mixture was washed with 10% aqueous solution of citric acid, water, saturated aqueous solution of $NaHCO_3$ and brine. The organic layer was dried over anhydrous Na_2SO_4. The solvent was removed under vacuum. The residue (45.0 mg, 67%) was used for the next step without further purification.
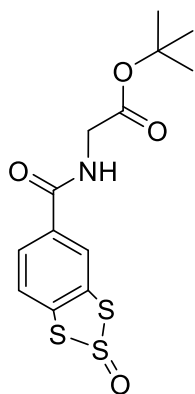
Compound 403. To a solution of **402** (45.0 mg, 0.100 mmol) in dry THF (774 µl) at -60 °C, was added $SOCl_2$ (10.0 µl, 0.140 mmol). The reaction mixture was slowly warm up to -10 °C in 4 h. Then bi-distilled water (387 µl) was added to the reaction mixture to quench the excess of $SOCl_2$. The reaction mixture was extracted using CH_2Cl_2. The organic layer was dried over anhydrous Na_2SO_4, filtered and concentrated under vacuum. The residue was purified by reversed-phase flash column chromatography (Eluent: H_2O + 0.1% TFA/CH_3CN + 0.1% TFA gradient from 90:10 to 20:80). Fractions contained product were lyophilized to yield the designed product as a colorless solid (8.0 mg, 23%). Mp: 76 – 77 °C; IR (neat): 3321 (w), 2981 (w), 2937 (w), 1739 (m), 1642 (m), 1582 (w), 1530 (m), 1454 (w), 1403 (w), 1394 (w), 1367 (m), 1315 (w), 1227 (s), 1152 (s), 1115 (s), 1032 (w), 1009 (w), 944 (w), 896 (w), 842 (w), 752 (m), 699 (w); ^1H NMR (400 MHz, $CDCl_3$): 8.09 (dd, $^4J_{H–H}$ = 1.7, 0.5 Hz, 1H), 7.77 (dd, $^3J_{H–H}$ = 8.3, $^4J_{H–H}$ = 1.7 Hz, 1H), 7.67 (dd, $^3J_{H–H}$ = 8.3, $^4J_{H–H}$ = 0.5 Hz, 1H), 6.66 (br, 1H), 4.15 (d, $^3J_{H–H}$ = 4.8 Hz, 2H), 1.52 (s, 9H); ^{13}C NMR (100 MHz, $CDCl_3$): 169.0 (C), 165.5 (C), 139.6 (C), 137.0 (C), 133.4 (C), 125.9 (CH), 124.6 (CH), 123.7 (CH), 83.0 (C), 42.7 (CH_2), 28.1 (3xCH_3); HPLC–MS: R_t = 2.29 min, 290 (100, [M-tBu+H+]), 290

(100, [M-tBu+H+]), 691 (28, [2M+H+]), 346 (10, [M+H+]) (Eluent: CH_3CN + 0.1%TFA/water 0.1%TFA gradient from 95:5 to 95:5); MS (ESI, $CHCl_3$): 290 (100, [M-tBu+H+]), 691 (55, [2M+H+]), 346 (28, [M+H+]).
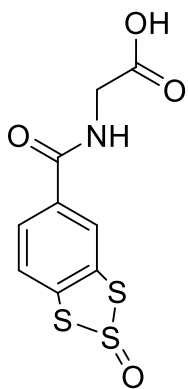
Compound 248. (3.0 mg, 45%, colorless solid) was synthesized from **403** (8.0 mg, 23 µmol) followed general procedure A. Product was purified by reversed-phase flash column chromatography (Eluent: H_2O + 0.1% TFA/CH_3CN + 0.1% TFA gradient from 95:5 to 30:70). Mp: 112 – 113 °C (decomp.); IR (neat): 3319 (br), 3076 (br), 1723 (m), 1638 (m), 1583 (m), 1531 (m), 1453 (w), 1406 (w), 1312 (w), 1199 (m), 1111 (s), 1030 (w0, 1007 (w), 890 (w), 830 (w), 752 (w), 681 (w), 625 (w); ^1H NMR (400 MHz, methanol-d4): 8.90 (br, 1H), 8.17 (d, $^4J_{H-H}$ = 1.7 Hz, 1H), 7.88 (dd, $^3J_{H-H}$ = 8.3, $^4J_{H-H}$ = 1.7 Hz, 1H), 7.80 (d, $^3J_{H-H}$ = 8.3 Hz, 1H), 4.10 (s, 2H); ^{13}C NMR (125 MHz, methanol-d4):171.6 (C), 167.3 (C), 139.8 (C), 136.8 (C), 133.3 (C), 126.0 (CH), 124.2 (CH), 123.3 (C), 40.9 (CH_2); HPLC–MS: R_t = 1.51 min, 290 (100, [M +H+]) (Eluent: CH_3CN + 0.1%TFA/water 0.1%TFA gradient from 95:5 to 95:5); MS (ESI, $CHCl_3$): 290 (100, [M+H+]).
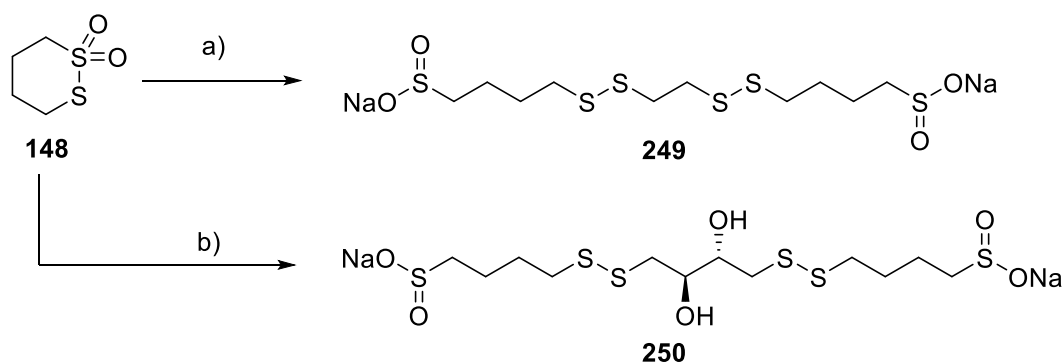
Scheme 56. (a) ethane-1,2-dithiol, Na, MeOH, 0 °C to rt, under N_2, 42%; (a) DTT, Na, MeOH, 0 °C to rt, under N_2, 69%.

Compound 249 was synthesized and purified according to procedures described previously in literature.[265]

Compound 250 was synthesized and purified according to procedures described previously in literature.[266]

Compound 251 was synthesized and purified according to procedures described previously in literature.[267]

Compound 252 was synthesized and purified according to procedures described previously in literature.[267]

Compound 253 was synthesized and purified according to procedures described previously in literature.[225]

Compound 254 was synthesized and purified according to procedures described previously in literature.[225]

Compound 255 was synthesized and purified according to procedures described previously in literature.[269]
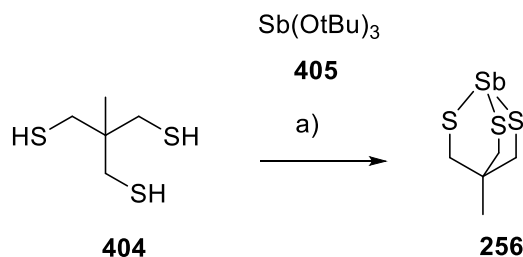
Scheme 57. (a) anhydrous hexane, rt, 58%

Compound 404 was synthesized and purified according to procedures described previously in literature.[268]

Compound 405 was synthesized and purified according to procedures described previously in literature.[270]

Compound 256. To a solution of **404** (100 mg, 0.594 mmol) in anhydrous hexane (1.2 ml), a solution of **405** (108 mg, 0.592 mmol) in anhydrous hexane (3.0 ml) was added while stirring. A white precipitate formed immediately. The solid was filtered and washed with excess amount of anhydrous hexane. The colorless solid was dried under vacuum to yield desired product (99 mg, 58%).^{1}H NMR (400 MHz, DMSO-d_6): 2.97 (s, 6H), 0.98 (s, 3H); ^{13}C NMR (100 MHz, DMSO-d_6): 35.3 (C), 33.8 (CH$_3$), 32.8 (3xCH$_2$).

5.2.7.   Fluorescently-Labelled Thiosulfonate

Compound 259 (racemic) was synthesized and purified according to procedures described previously in literature. [271]
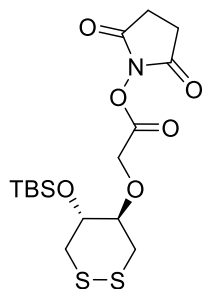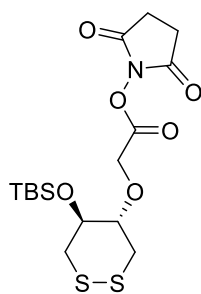
Compound 260. To a solution of *N*-Hydroxysuccinimide (68 mg, 0.59 mmol) in CH_2Cl_2 (6 ml), **259** (191 mg, 0.589 mmol) was added, followed by EDC (151 mg, 0.764 mmol). The reaction mixture was stirred at rt overnight. The reaction mixture was diluted with CH_2Cl_2, then washed with water. The organic layer was dried over anhydrous Na_2SO_4. The solvent was removed under vacuum. The residue was purified by flash chromatography (CH_2Cl_2) to yield desired product (71 mg, 29%, colorless solid). R_f (CH_2Cl_2): 0.35; Mp: 83 – 84 °C; IR (neat): 2949 (w), 2930 (w), 2857 (w), 1825 (w), 1785 (w), 1737 (s), 1469 (w), 1426 (w), 1381 (w), 1358 (w), 1323 (w), 1297 (w), 1253 (w), 1203 (m), 1148 (w), 1065 (s), 1029 (w), 1000 (w), 953 (w), 884 (w), 852 (m), 838 (m), 814 (w), 777 (m), 751 (w), 731 (w), 669 (w), 644 (w), 615 (w); ^{1}H NMR (400 MHz, $CDCl_3$): 4.72 – 4.49 (m, 2H), 3.79 – 3.68 (m, 1H), 3.50 – 3.26 (m, 2H), 3.05 – 2.92 (m, 3H), 2.85 (s, 4H), 0.91 (s, 9H), 0.11 (s, 3H), 0.10 (s, 3H); ^{13}C NMR (100 MHz, $CDCl_3$): 168.7 (2xC), 166.4 (C), 84.4 (CH), 76.6 (CH), 67.4 (CH_2), 42.2 (CH_2), 39.1 (CH_2), 25.8 (3xCH_3), 25.6 (2xCH_2), 17.9 (C), -4.7 (CH_3), -4.8 (CH_3).
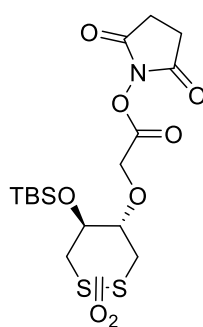
Compound 261. To a solution of **260** (631 mg, 1.50 mmol) in CH_2Cl_2 (16 ml), *m*-CPBA (861 mg, 3.75 mmol) was added. The reaction mixture was stirred at rt for 2 d. The reaction mixture was diluted with CH_2Cl_2, washed with saturated aqueous solution of $NaHCO_3$ (3 times). The organic layer was dried over anhydrous Na_2SO_4. The solvent was removed. The residue (321 mg, 47%, colorless solid) was used for the next step without further purification.

Compound 262 was synthesized and purified according to procedures described previously in literature.[272]
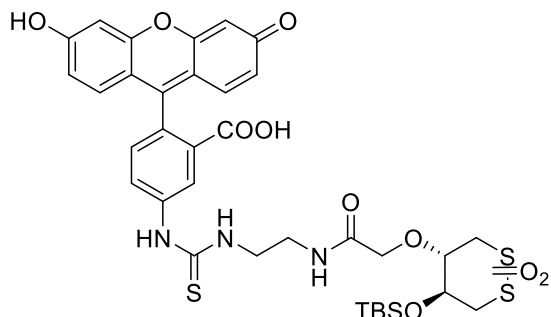
Compound 263 To a solution of **261** (57 mg, 0.13 mmol) in DMF (1.5 ml), **262** (56 mg, 0.13 mmol) was added. The reaction mixture was stirred at rt for 4 h. The solvent was removed under vacuum. The residue was purified by reversed phase chromatography (eluent: CH_3CN + 0.1% TFA/ H_2O + 0.1% TFA gradient from 10% CH_3CN + 0.1% TFA to 90%). Fractions contained product were lyophilized to yield desired product (30 mg, mixture of 2 regioiomers 3:2, 31%, yellow solid). IR (neat): 3291 (br), 2932 (w), 2858 (w), 2614 (br), 1721 (w), 1635 (m), 1595 (s), 1540 (s), 1456 (m), 1384 (m), 1313 (s), 1255 (s), 1202 (s), 1114 (s), 995 (w), 918 (w), 889 (w), 838 (m), 780 (m), 719 (w), 669 (w); ^{1}H NMR (500 MHz, CD_3OD, nn/nn- regioisomers peaks): 8.13 (s, 1H), 7.78 – 7.69 (m, 1H), 7.14 – 7.08 (m, 1H), 6.89 (br s, 2H), 6.78 (br s, 2H), 6.64 (br s, 2H), 4.27 – 4.23/4.01-3.96 (m, 1H), 3.85 – 3.45 (m, 6H), 3.41 – 3.00 (m, 3H), 0.79 – 0.75 (m, 9H), 0.01 - -0.02 (m, 6H); ^{13}C NMR (125 MHz, CD_3OD, nn/nn- regioisomers peaks): 182.1 (C), 171.2/171.1 (C), 168.5 (2xC), 163.9 (C), 159.5 (C), 159.2 (C), 155.3 (C), 141.2 (C), 130.5 (2xCH), 129.0 (CH), 126.6 (CH), 121.4 (CH), 119.1 (2xC), 116.8 (2xC), 115.0 (2xCH), 112.6 (C), 102.0 (2xCH), 79.8/77.7 (CH), 71.0/67.6 (CH), 69.2/68.9 (CH_2), 63.4/58.9 (CH_2), 43.4/43.3 (CH_2), 39.1/38.8 (CH_2), 31.8/36.1 (CH_2), 24.78/24.82 (3xCH_3), 17.43/17.37 (2xC), -6.0/-6.2 (CH_3), -6.0/-6.1 (CH_3); HPLC-MS: R_t =2.69 (1st regioisomer), 2.74 (2nd regioisomer), 788 (100, [M+H]+).
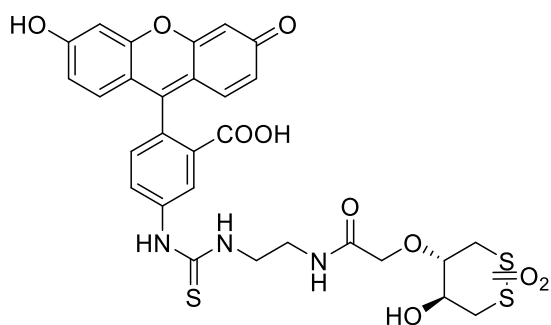
Compound 258. 263 (13 mg, 17 μmol) was dissolved in 1.25 M solution of HCl in MeOH (2.0 ml). The reaction mixture was stirred at rt for 1 h. The solvent was removed under vacuum. The residue was purified by reversed phase chromatography (eluent: CH$_3$CN + 0.1% TFA/ H$_2$O + 0.1% TFA gradient from 10% CH$_3$CN + 0.1% TFA to 90%). Fractions contained product were lyophilized to yield desired product (3.7 mg, mixture of 2 regioiomers, 33%, yellow solid). IR (neat): 3256 (br), 2925 (br), 1639 (m), 1601 (m), 1541 (m), 1451 (w), 1312 (m), 1176 (s), 1117 (s), 916 (w), 836 (w), 797 (w), 719 (w); ^{1}H NMR (400 MHz, CD$_3$OD): 8.51 – 8.35 (br m, 1H), 8.35 – 8.20 (m, 1H), 7.88 (d, $^3J_{H–H}$ = 8.0 Hz, 1H), 7.93 – 7.81 (m, 1H), 7.13 – 6.97 (m, 2H), 6.90 (s, 2H), 6.83 – 6.67 (m, 2H), 4.33 –3.69 (m, 4H), 3.69 – 3.40 (m, 7H), 3.69 – 3.40 (m, 4H), 3.28 – 3.19 (m, 1H); ^{13}C NMR (125 MHz, CD$_3$OD, nn/nn- regioisomers peaks): 181.9 (C), 171.8/171.6 (C), 168.6 (2xC), 159.5 (C), 159.2 (C), 154.9 (C), 141.1 (C), 130.4 (2xCH), 129.4/128.8 (CH), 126.4 (CH), 121.1 (CH), 116.8 (2xC), 114.8 (2xCH), 112.6 (C), 102.0 (2xCH), 80.5/80.0 (CH), 69.7 (CH), 68.8/68.6 (CH$_2$), 64.5/61.0 (CH$_2$), 43.6 (CH$_2$), 38.4 (CH$_2$), 34.9/31.8 (CH$_2$); HPLC-MS: R_t =1.97, 674 (100, [M+H]+).

5.3. Catalyst Evaluation

5.3.1. NDI-Peptide Conjugates

Chemoselectivity Studies

Solutions comprising substrates **42** (200 mM) and **44** (2000 mM) and desired catalyst (20 mol%, i.e. 40 mM) were prepared in CD_2Cl_2 and stirred at 20 °C. ^{1}H NMR spectra of the mixture in $CDCl_3$ were recorded at different times after the start of the reaction until the reaction was completed. Integrals assigned to the protons alpha to the nitro group of the addition product **46** (δ 3.07) and the CH_3 group of the decarboxylation product **47** (δ 2.38) were compared to the combined integration of all $-OCH_3$ protons (from δ 3.85 to 3.78) present in the substrates and products. Addition/decarboxylation ratio A/D for the MAHT reaction was determined from the ratio of concentration of addition product to concentration of decarboxylation product measured at the end of each reaction using equation (1).

$$A/D = \frac{\int \text{Addition}}{\int \text{Decarboxylation}} \times \frac{H_D}{H_A} \qquad (1)$$

here $H_A = 2.0$ and $H_D = 3.0$ for integrals measured at δ 3.07 and 2.38.

The selectivity values A/D obtained were reported in Table 1.

For better comparison between catalysts, we noticed that changes at high A/D are overappreciated compared to changes at low A/D, and that they should be calibrated against a general standard such as TEA because intrinsic A/D_0 values also depend strongly on conditions. We thus propose here to use qAD, the log of the measured A/D minus the log of the intrinsic A/D_0 with TEA. The obtained qAD values were reported in Table 1.
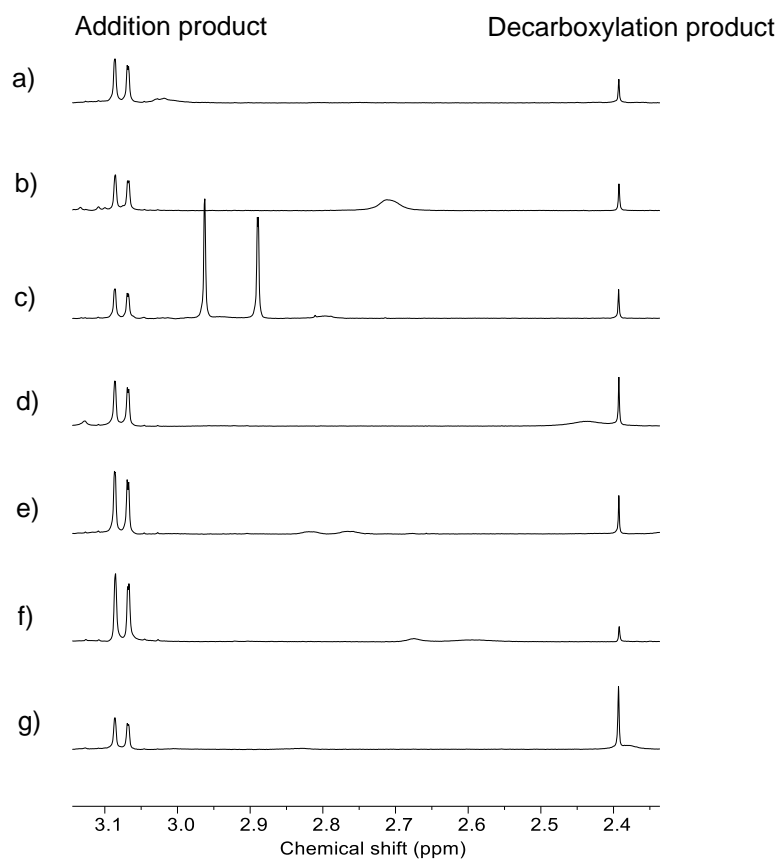
Figure 81. Representative ^{1}H NMR data of the reaction of substrate **42** (200 mM) and **44** (2000 mM) with catalyst **159a** (a), **159b** (b), **171** (c), **160** (d), **170** (e), **158** (f) and **156** (g) (40 mM) in CD_2Cl_2 at 20 °C.
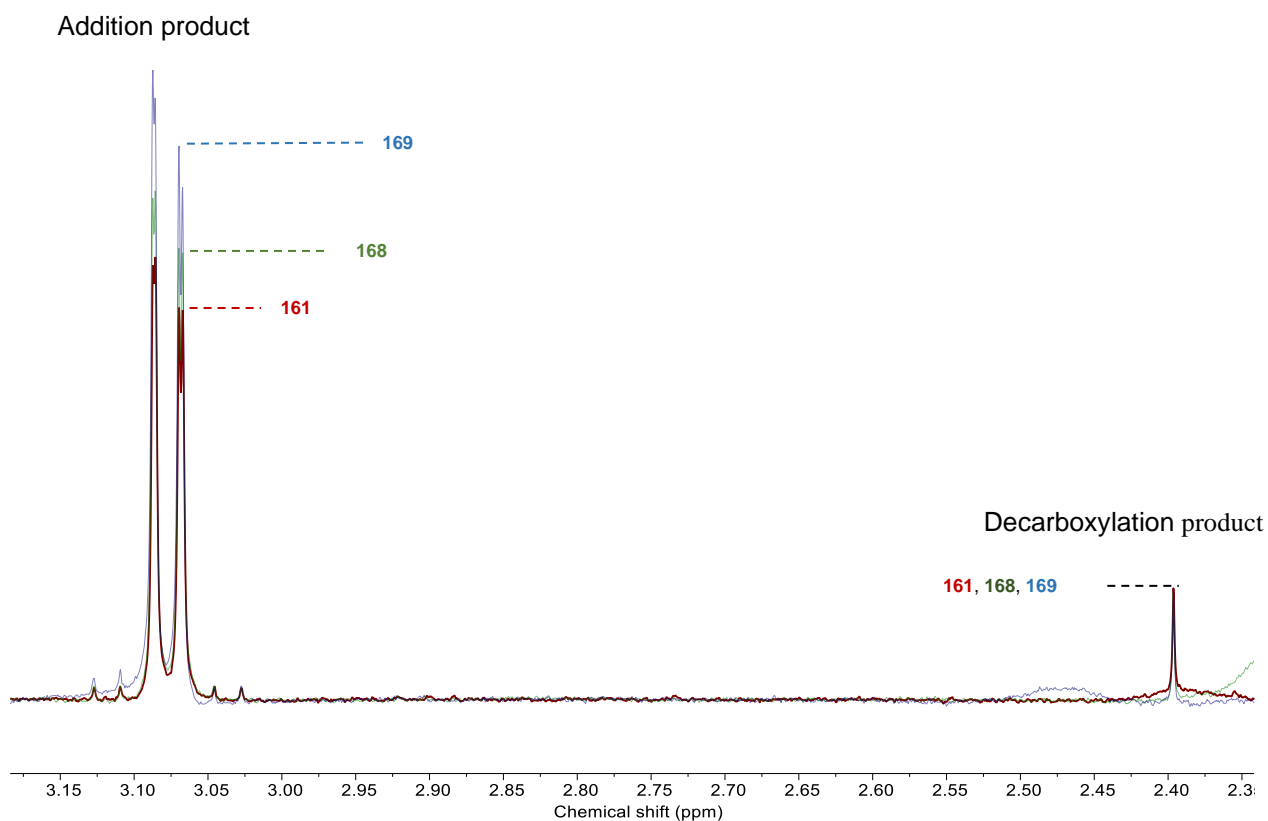
Figure 82. Representative ^{1}H NMR data of the reaction of substrate **42** (200 mM) and **44** (2000 mM) with catalyst **161** (maroon), **168** (green) and **169** (blue) (40 mM) in CD_2Cl_2 at 20 °C after normalizing against the integration of decarboxylation product.

Enantioselectivity Studies

Enantiomeric ratio of product **46** was determined using previously reported conditions.[54] (i.e., column: CHIRALPAK ID, 250 mm x 4.6 mm, Daicel; mobile phase: *n*–hexane/i–PrOH 60:40, 0.5 mL/min, 25 °C; detection: 207 nm). The retention times found for the two enantiomers of **46** were consistent with the ones reported in the literature (Figures 83). The enantiomeric ratios obtained were reported in Table 1.
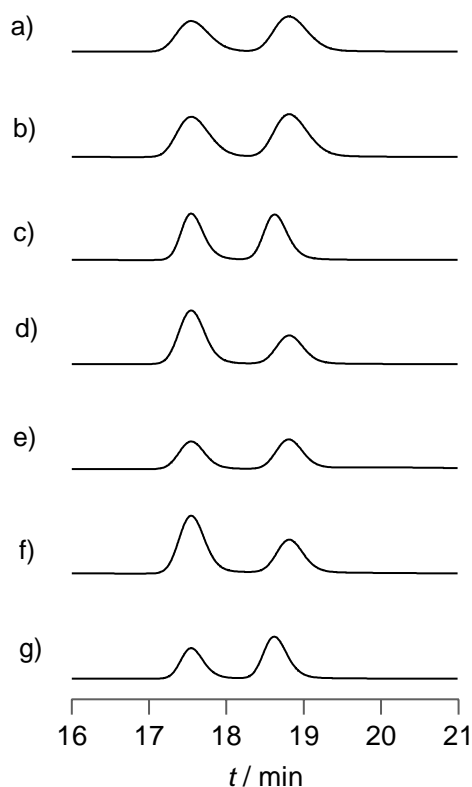
Figure 83. Representative chiral HPLC chromatograms obtained using chiralpak ID column (*n*–hexane/i–PrOH 60:40, 0.5 mL/min, 25 °C; detection: 207 nm) of the addition product **46**, obtained using catalyst **159a** (a), **159b** (b), **171** (c), **160** (d), **170** (e), **158** (f) and **156** (g) (40 mM) in CD_2Cl_2 at 20 °C.

Kinetic Studies

Concentration of **46** and **47** were plotted against the time and the initial velocities v_{ini} were extracted from the slopes of the linear fit of the plot (Figure 51). Rate constants k_{app} could be calculated using equation (2).

$$k_{app} = v_{ini} / ([\mathbf{41}]_0 [\mathbf{42}]_0) \qquad (2)$$

Then the rate enhancements k_{rel} were calculated using equation (3).

$$k_{rel} = k_{app}(1) / k_{app}(2) \tag{3}$$

Changes in activation energy were determined by equation (4).

$$\Delta E_a = - RT \ln k_{rel} \tag{4}$$

Finally, selective catalysis of a disfavored reaction $\Delta\Delta E_a$ were approximated by equation (5).

$$\Delta\Delta E_a = \Delta E_a^A - \Delta E_a^D \tag{5}$$

in which ΔE_a^A and ΔE_a^D are changes in activation energy of addition reaction and decarboxylation reactions.

The values obtained were reported in Table 2.
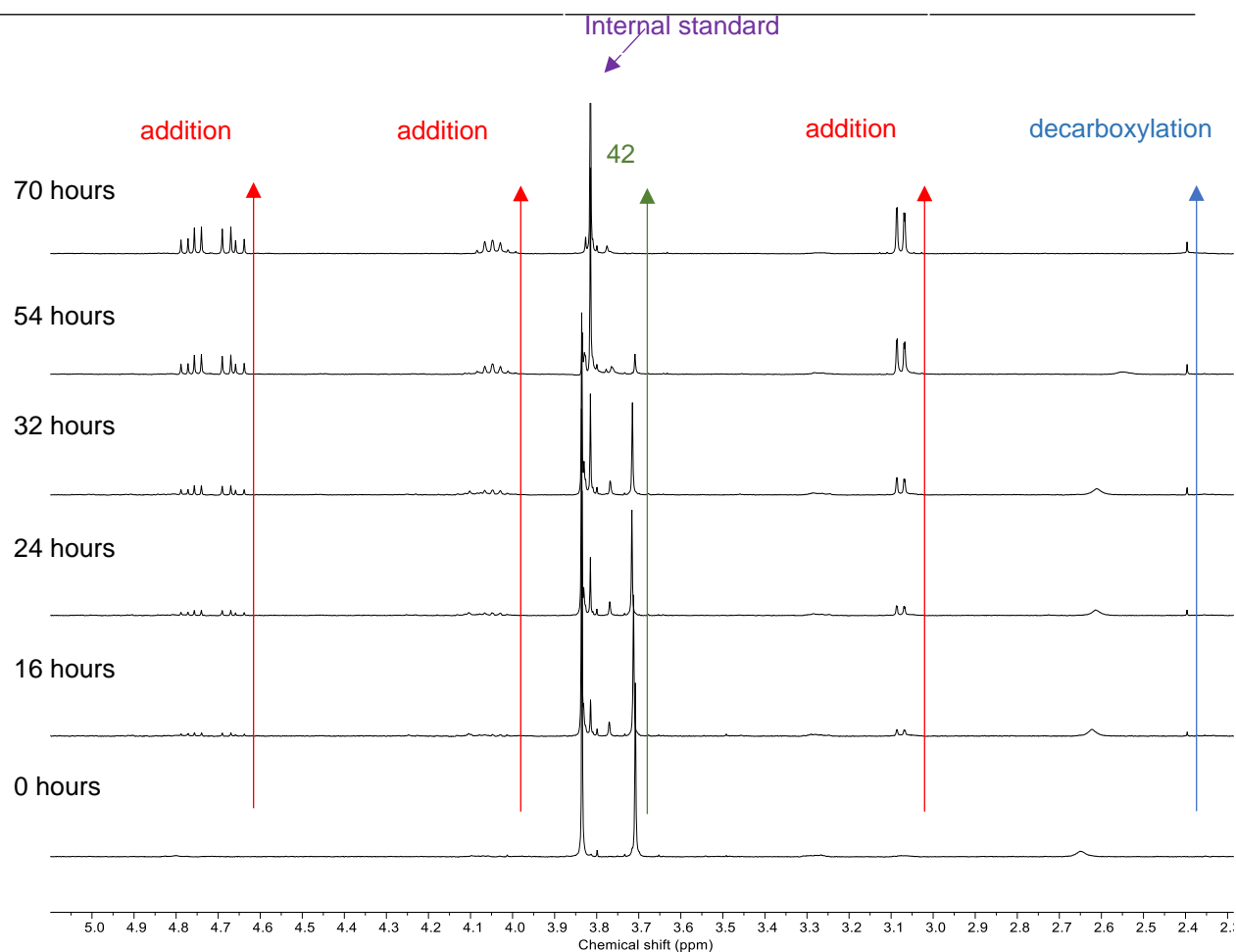
Figure 84. ^{1}H NMR spectra of a mixture of **42** (200 mM), **44** (2 M) and catalyst **161** (40 mM) in CD_2Cl_2 at 20 °C diluted in $CDCl_3$ as an example. The red arrows show the formation of addition product, the blue one shows the decarboxylation and the green one shows the consumption of substrate **42**. Methoxyl group is used as an internal standard (purple arrow).

5.3.2. PDI-Peptide Conjugates

Chemoselectivity

Catalyst evaluation was done as described for NDI-peptide conjugates. In the case of catalytic reaction with addition of additive, solutions comprising substrates **42** (200 mM) and **44** (2000 mM), desired catalyst (20 mol%, i.e. 40 mM) and additive **193** (100 mM) were prepared in CD$_2$Cl$_2$ and stirred at 20 ºC. ^{1}H NMR spectra of the mixture in CDCl$_3$ were recorded at different times after the start of the reaction until the reaction was completed. Addition/decarboxylation ratio A/D and qAD for the MAHT reaction were determined as described in previous section. The values obtained were reported in Table 3.
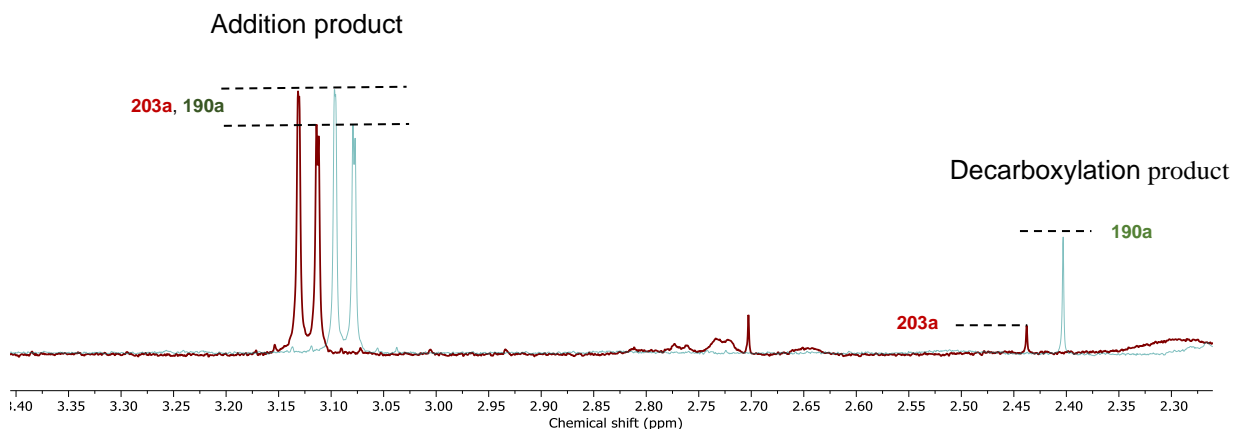
Figure 85. Representative ^{1}H NMR data of the reaction of substrate **42** (200 mM) and **44** (2000 mM) with catalyst **203a** (maroon), **190a** (green) (40 mM) in CD$_2$Cl$_2$ at 20 °C after normalizing against the integration of addition product (Spectra of **203a** was aligned upfield to make easily visible)

Enantioselectivity

Enantiomeric ratio of product **46** was determined using previously reported conditions as described in previous section. The enantiomeric ratios obtained were reported in Table 3.
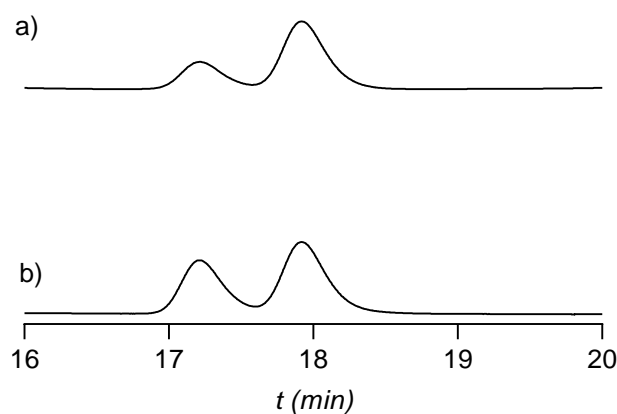
Figure 86. Representative chiral HPLC chromatograms obtained using chiralpak ID column (*n*–hexane/i–PrOH 60:40, 0.5 mL/min, 25 °C; detection: 207 nm) of the addition product **46**, obtained using catalyst **203a** (a), **190a** (b), (40 mM) in CD_2Cl_2 at 20 °C.

Kinetic Studies

Concentration of **42** were plotted against the time and the initial velocities v_{ini} were extracted from the slopes of the linear fit of the plot (Figure 87, Figure 88). The obtained data is reported in the graphs of Figure 69.
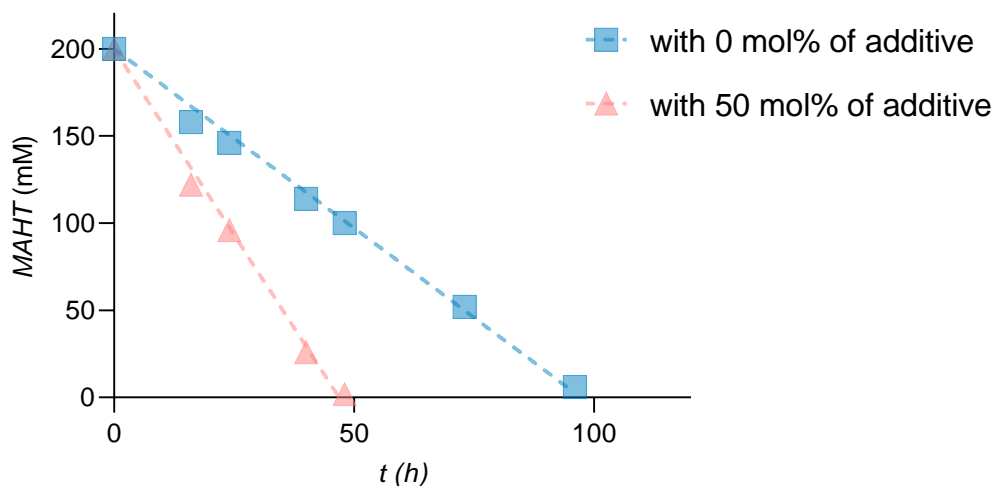
Figure 87. Concentration of **42** in MAHT reaction catalyzed by **190a** (40 mM) without the addition of additive (square) and with the addition of additive **193** (100 mM, 50 mol%) (triangle) in CD_2Cl_2 at 20 °C as an example.
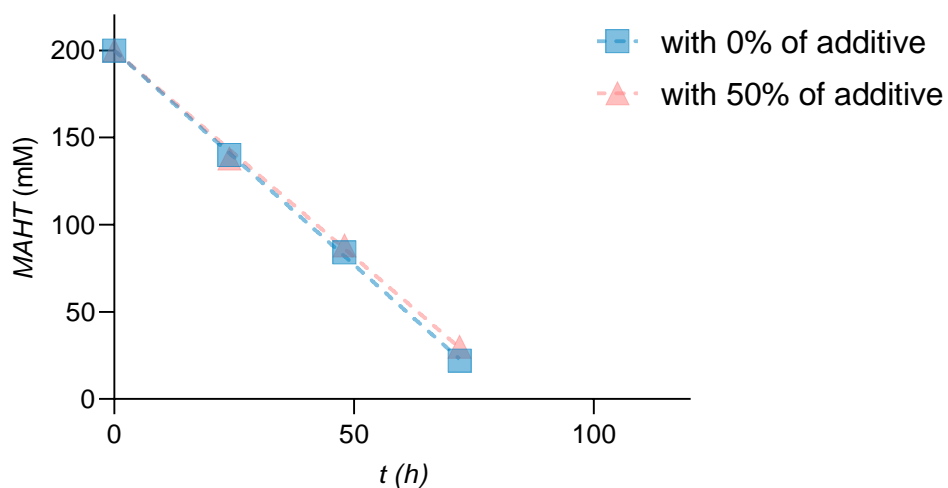
Figure 88. Concentration of **42** in MAHT reaction catalyzed by **191** (40 mM) without the addition of additive (square) and with the addition of additive **193** (100 mM, 50 mol%) (triangle) in CD_2Cl_2 at 20 °C as an example.
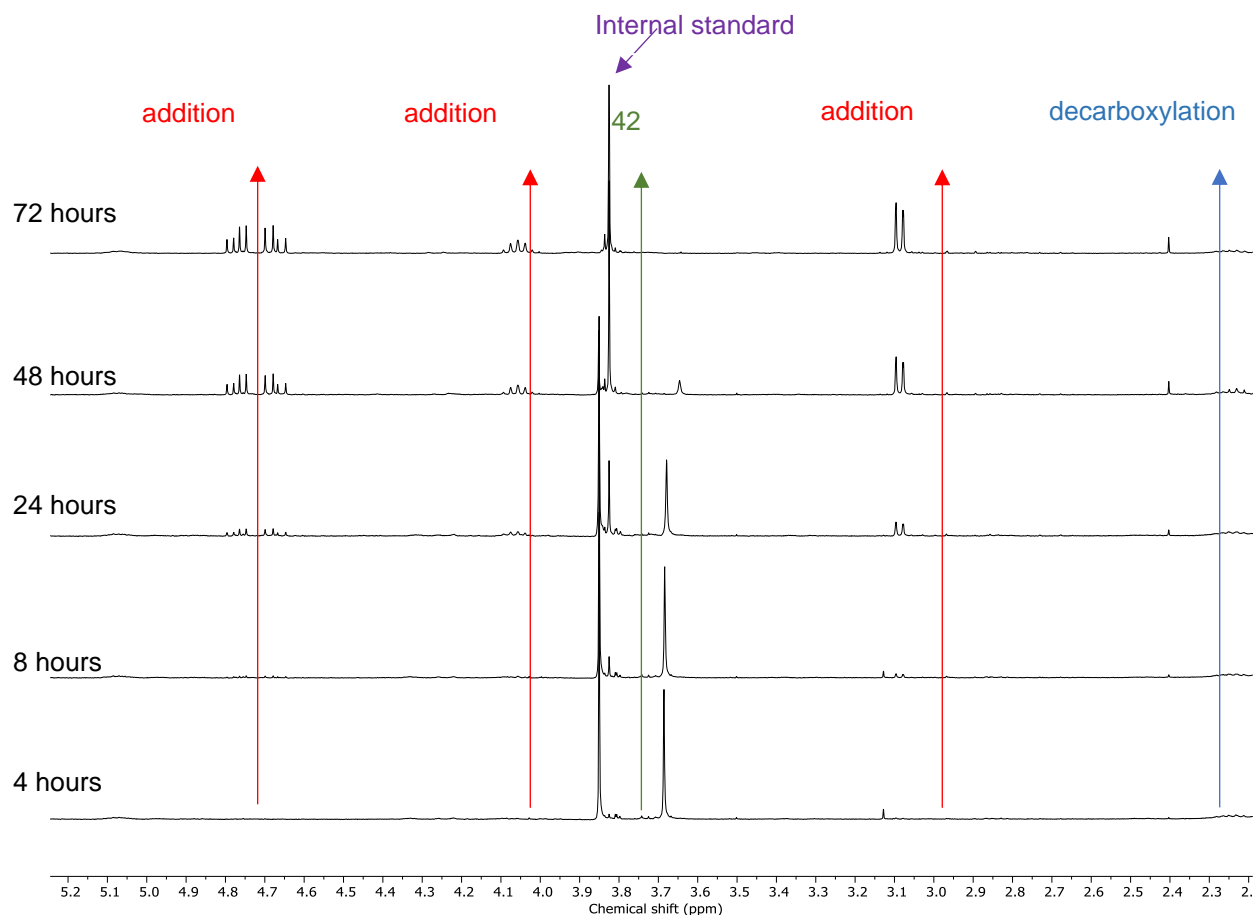
Figure 89. ^{1}H NMR spectra of a mixture of **42** (200 mM), **44** (2000 mM) and catalyst **188** (40 mM) in CD$_2$Cl$_2$ at 20 °C diluted in CDCl$_3$ as an example. The red arrows show the formation of addition product, the blue one shows the decarboxylation and the green one shows the consumption of substrate **42**. Methoxyl group is used as an internal standard (purple arrow).

5.4.   List of Structures

5.4.1.   Anion-π Catalysts

156

158

173

161

171

159

189

162

170

160

191

163

196

164

198

172

206

165

207

166

297

167

174

168

175

169

182

183

193

184

188

186

190

187

192

195

197

199

200

201

202

203

204

205
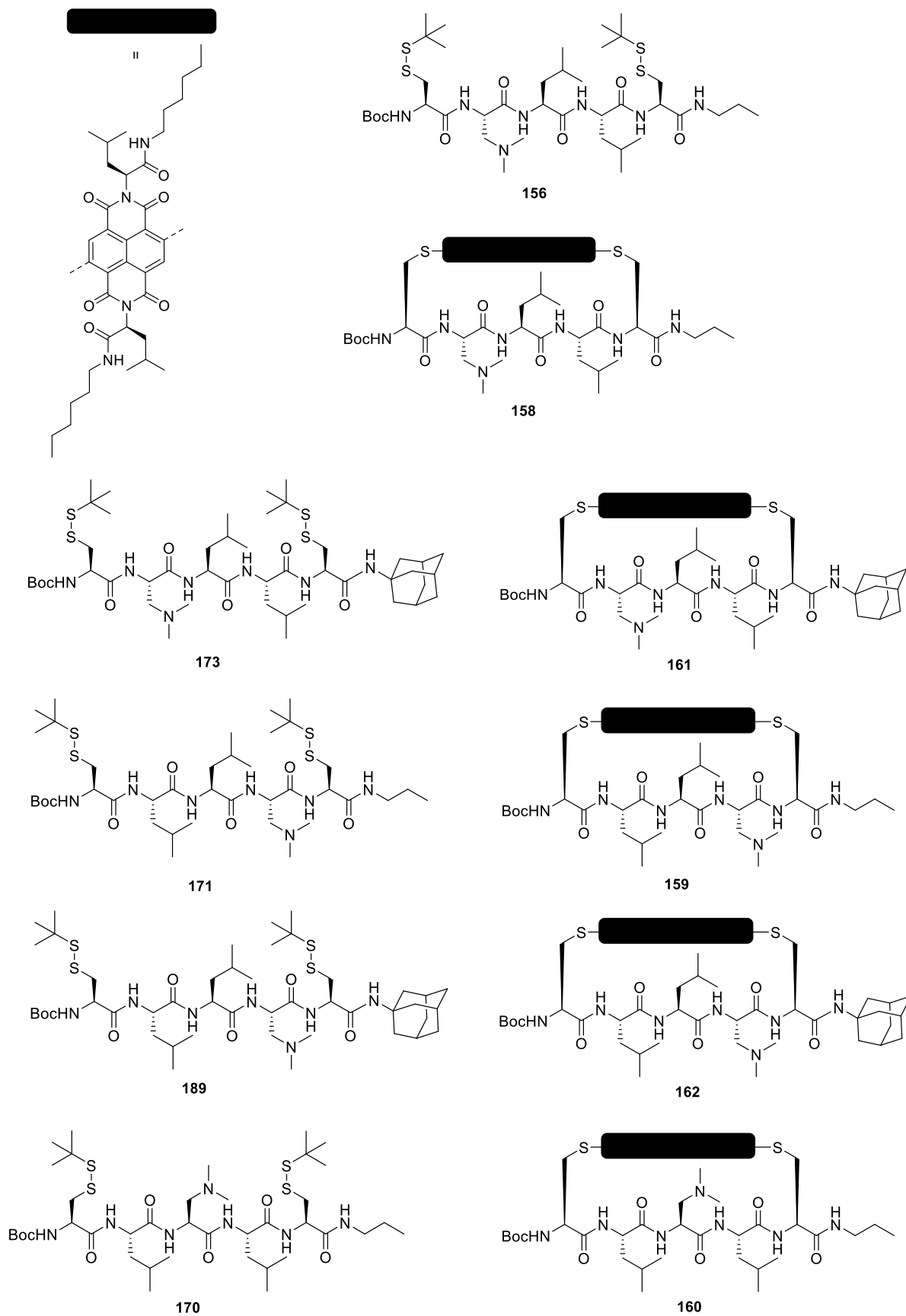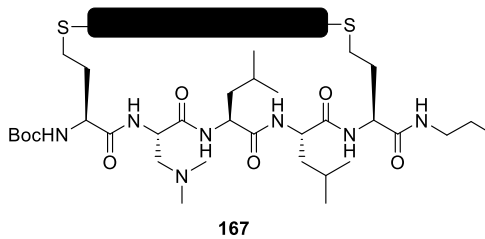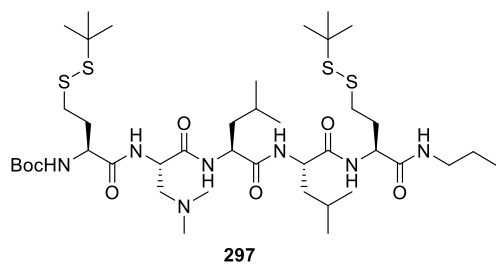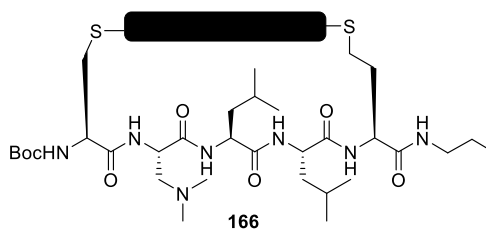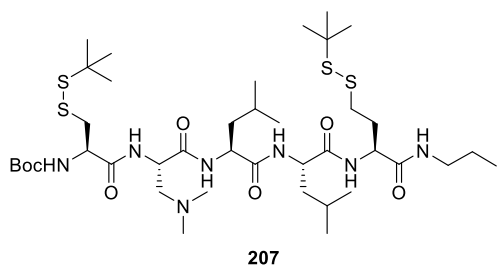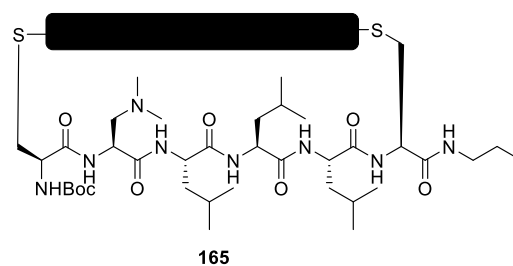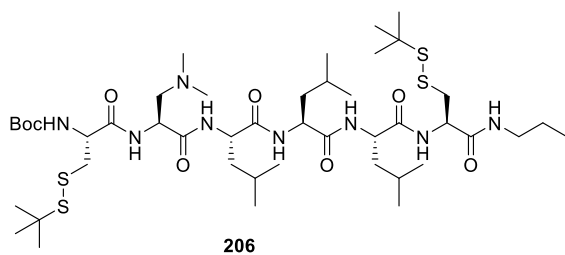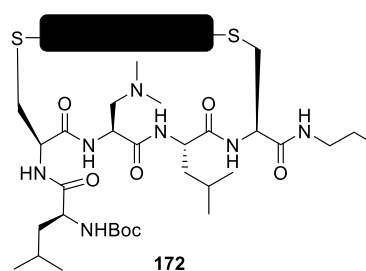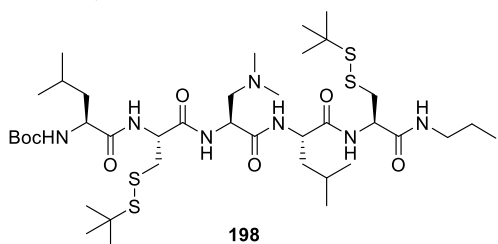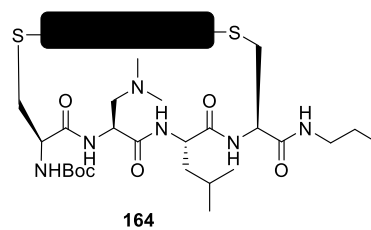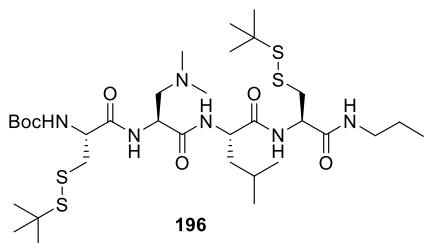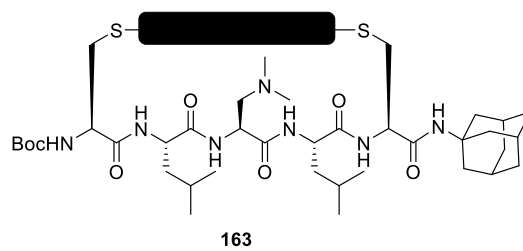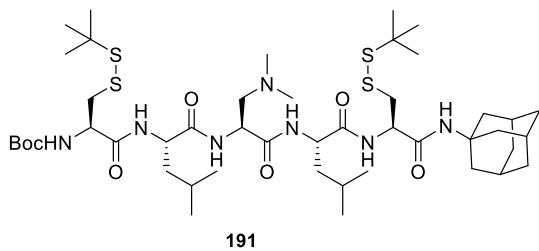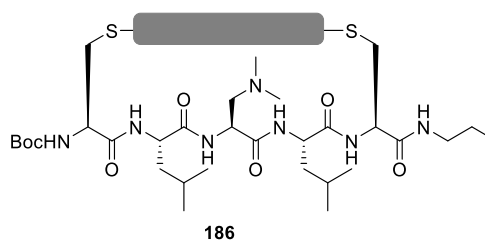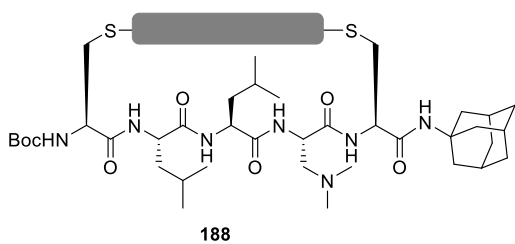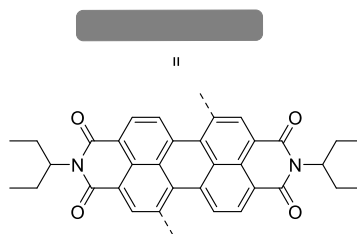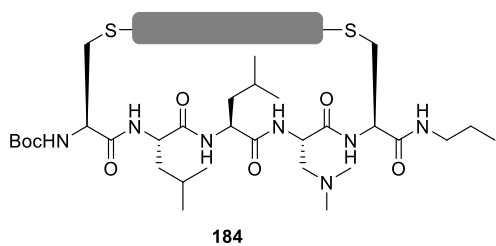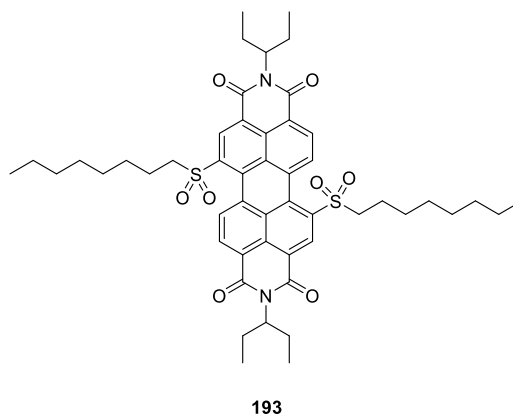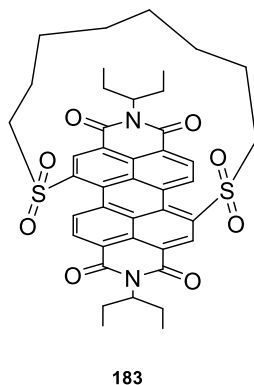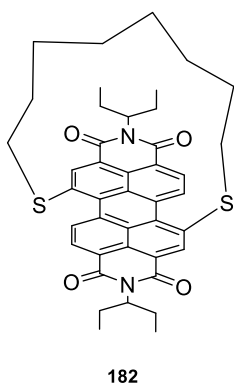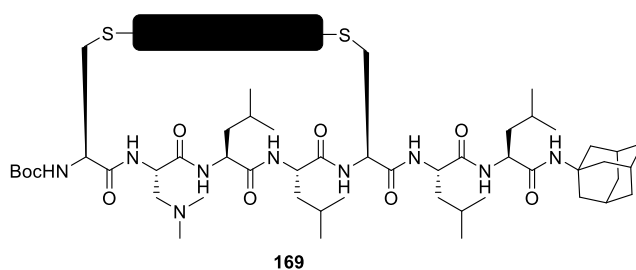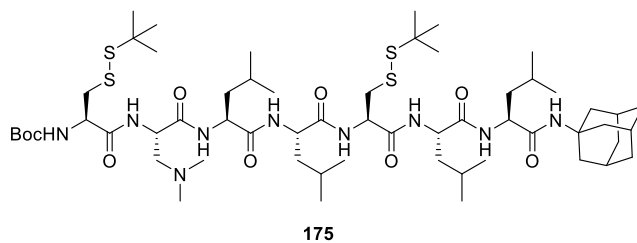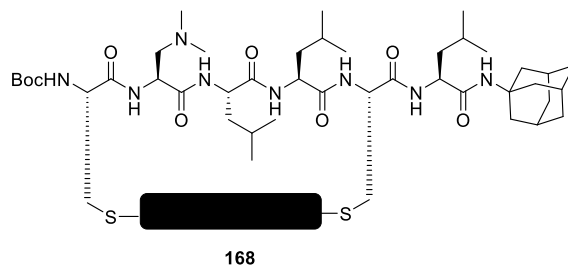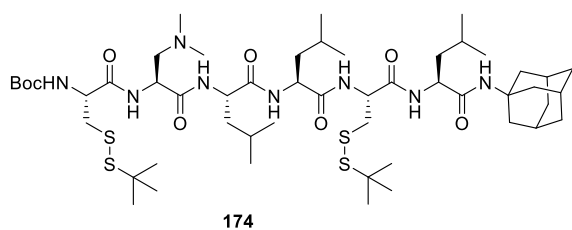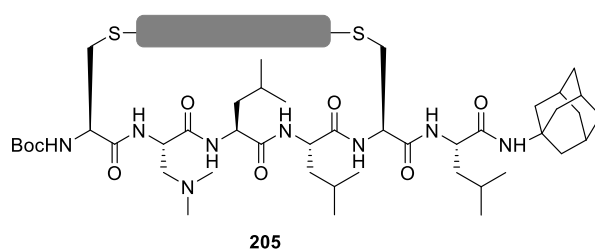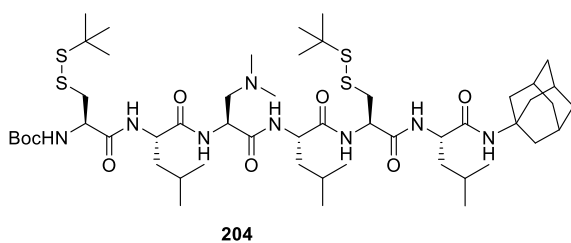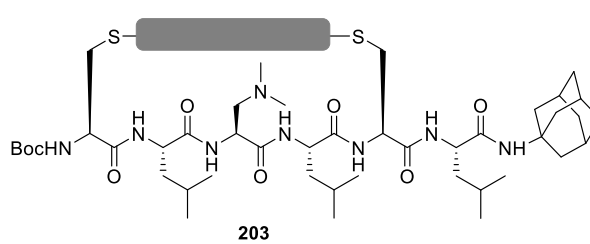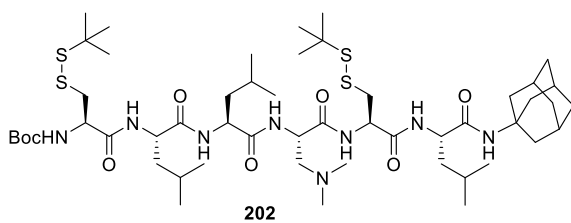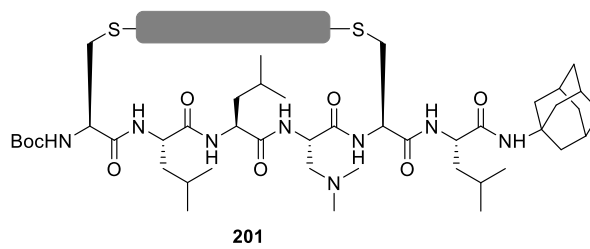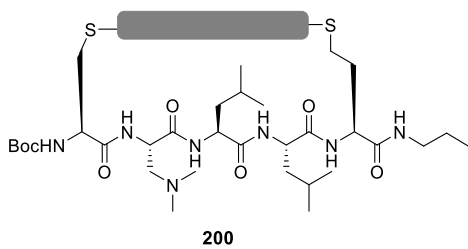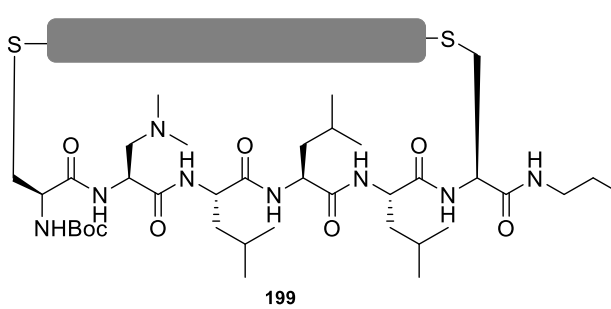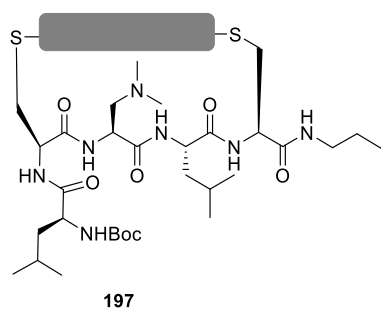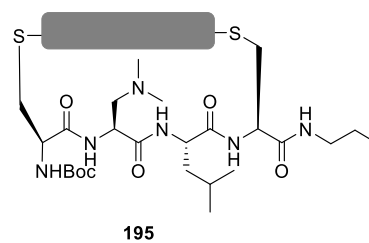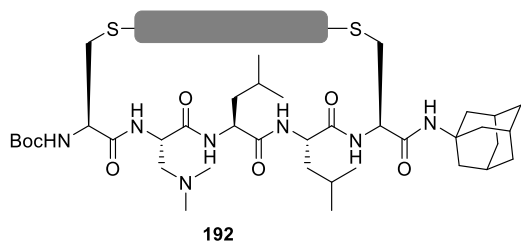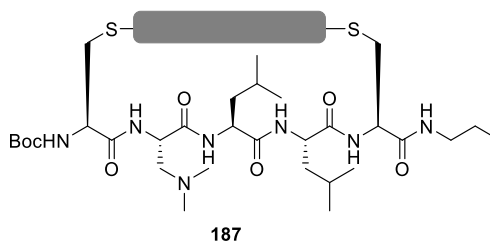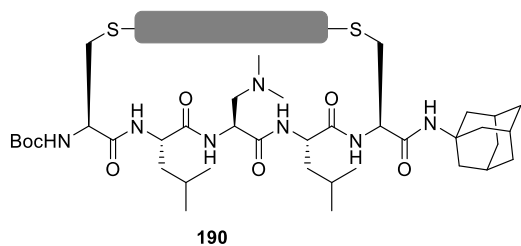
5.4.2. Thiol-Mediated Uptake Inhibitors

215
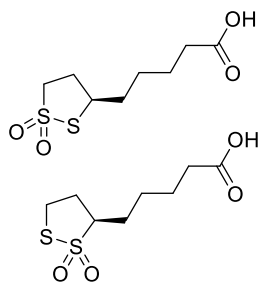
216 *(mixture of regioisomers)*
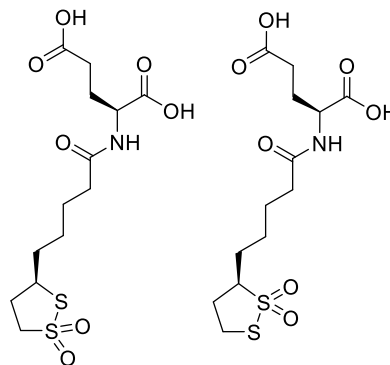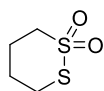
217 *(mixture of regioisomers)*

148
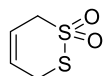
218
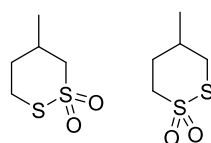
219 *(mixture of regioisomers and enantiomers)*

220 *(mixture of regioisomers)*
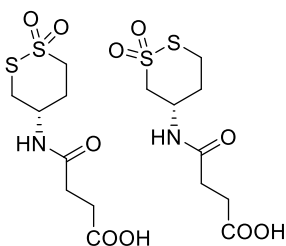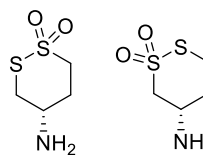
221 *(mixture of regioisomers)*

222
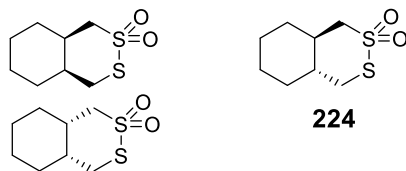
223 *(mixture of diastereomers)*

224
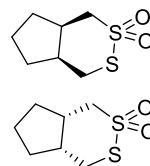
225 *(mixture of diastereomers)*
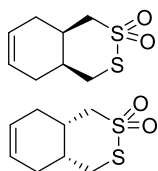
226 *(mixture of diastereomers)*
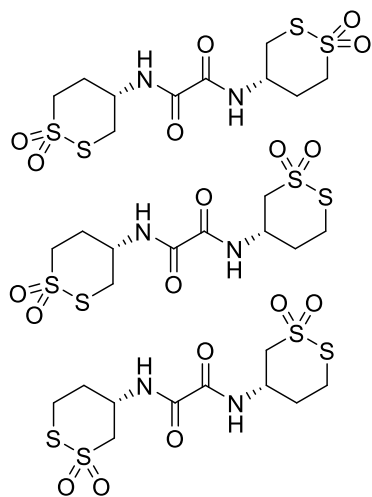
227 *(mixture of regioisomers)*
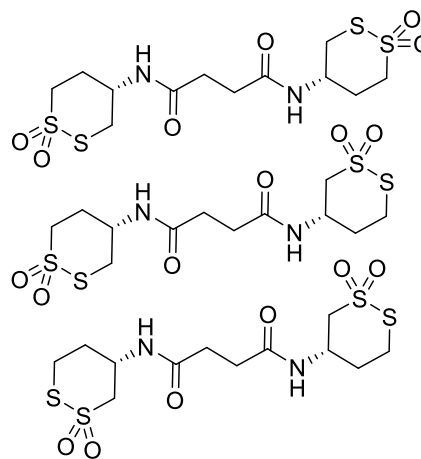
228 *(mixture of regioisomers)*
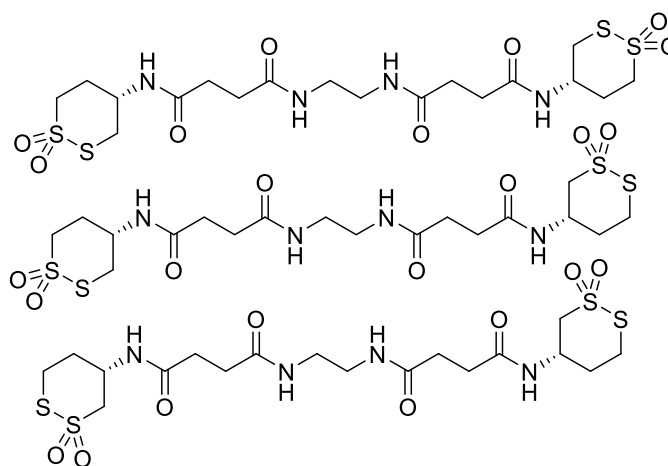
229 *(mixture of regioisomers)*

230
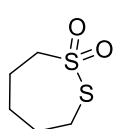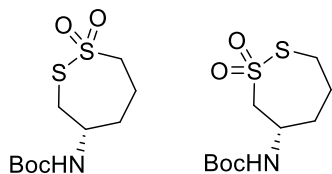
231 *(mixture of regioisomers)*
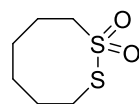
232
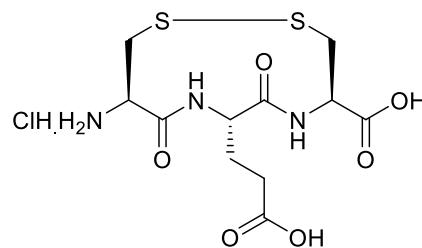
233
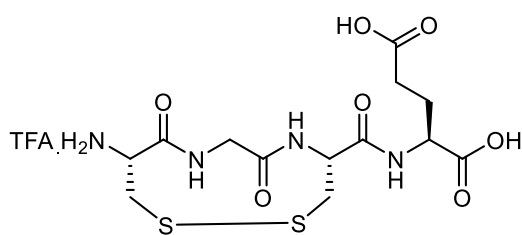
234
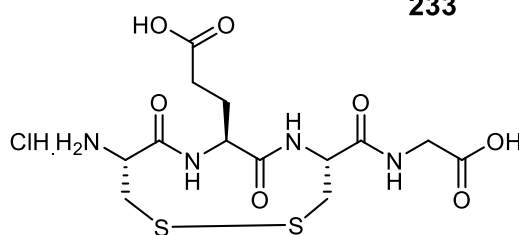
235
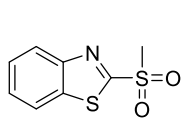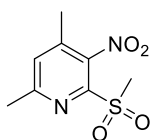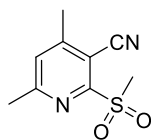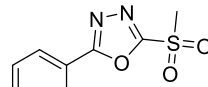
240 **236** **241** **242**
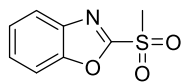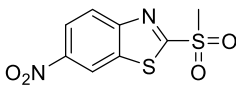
243 **244**
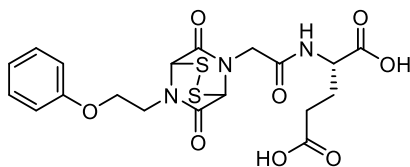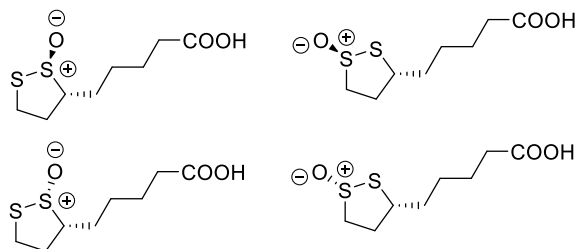
245 **246** (mixture of 4 isomers)
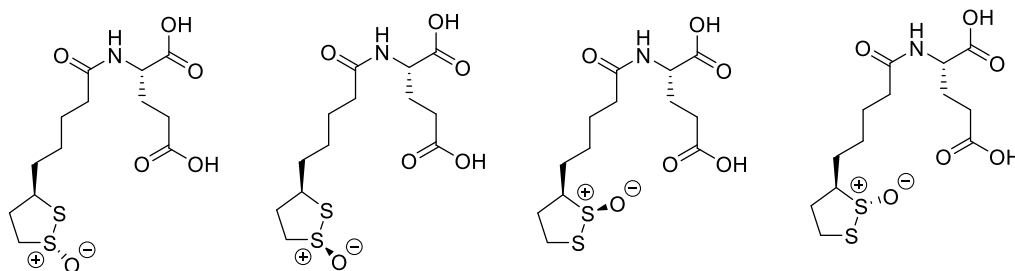
247 (mixture of 4 isomers)
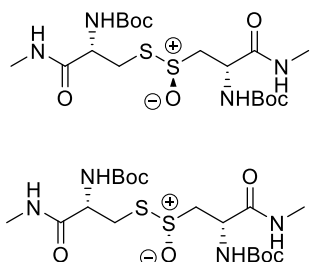
257 (mixture of 2 diastereomers) **248**

249

250

251 **252** **253** **254**

255 **256**
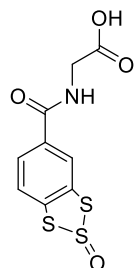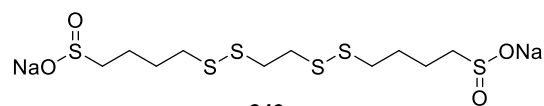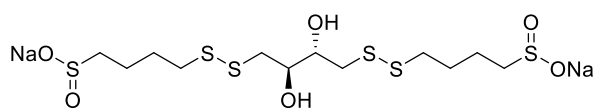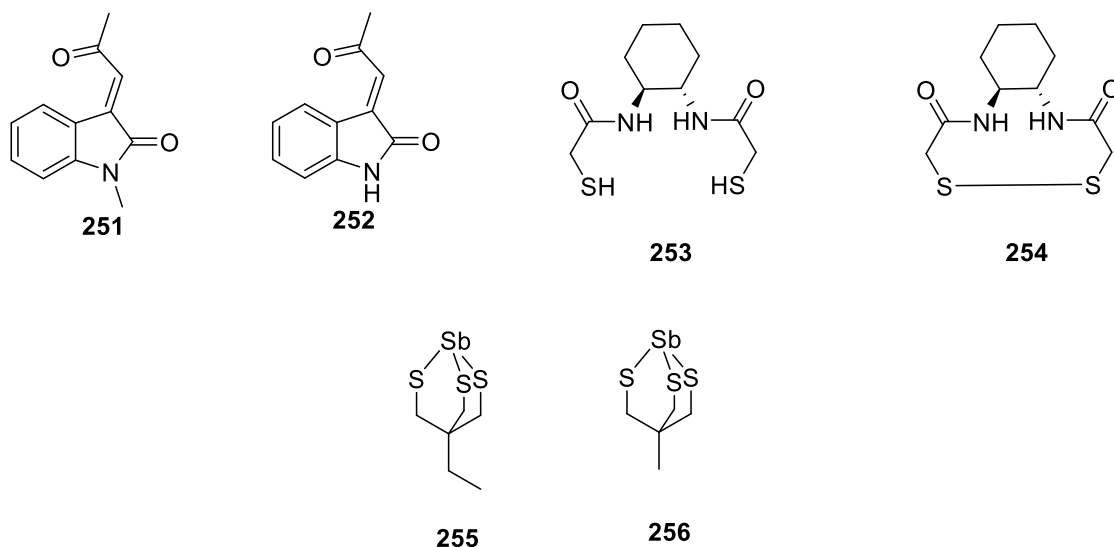
5.5.   Abbreviation

4F-2CN	2,3,5,6-tetrafluoroterephthalonitrile
Aib	2-Aminoisobutyric acid
AcOH	Acetic acid
AspA	Asparagusic acid
B	(Buckinghams)
Boc	*tert*–Butyloxycarbonyl
Boc₂O	Di-*tert*-butyl dicarbonate
Boc–L–Ala–OH	N_α–(*tert*–Butyloxycarbonyl)–L–Alanine
Boc–L–Dap–OH	N_α–(*tert*–Butyloxycarbonyl)–L–2,3–Diaminopropionic acid
Boc–L–Leu–OH	N_α–(*tert*–Butyloxycarbonyl)–L–Leucine
Boc-L-Cys(Trt)-OH	N_α–(*tert*–Butyloxycarbonyl)–S-trityl-L–Cysteine
BMC	(±)-trans-1,2-bis(2-mercaptoacetamido)cyclohexane
BINAP	2,2′-Bis(diphenylphosphino)-1,1′-binaphthalene
BPS	Benzopolysulfane

c	Concentration
CD	Circular Dichroism
CKAP4	Cytosekeleton-associated protein 4
CLIC1	Chloride intracellular channel protein 1
CPDs	Cell-penetrating poly(disulfide)s
CPPs	Cell-penetrating peptides
DBH	1,3–Dibromo–5,5–dimethylhydantoin
DBU	1,8-Diazabicyclo[5.4.0]undec-7-ene
decomp	Decomposed
DFS	Decafluoro-diphenylsulfone
DIAD	Diisopropyl azodicarboxylate
DIPEA	*N*,*N*–Diisopropylethylamine
DiSeL	Diseleno lipoic acid
DMAP	4– (Dimethylamino)pyridine
DMF	*N*,*N*-Dimethylformamide
DMSO	Dimethyl Sulfoxide
DNA	Deoxyribonucleic acid
DT	Diphtheria toxin
DTNB	5,5-dithio-bis(2-nitrobenzoic acid)
DTT	1,4-dithiothreitol
E_a	Activation Energy
ee	Enantiomeric excess
EDC	*N*–(3–Dimethylaminopropyl)–*N*′–ethylcarbodiimide hydrochloride
EGFR	Epidermal Growth Factor Receptor

eq	Equivalents
er	Enantiomeric ratio
ESI-MS	Electrospray-Ionization Mass Spectrometry
Et$_2$NH	Diethylamine
Et$_2$O	Diethyl ether
EtOAc	Ethyl acetate
ETP	Epidithiodiketopiperazine
Fmoc-L-Cys(Trt)-OH	*N*-(9-Fluorenylmethoxycarbonyl)-S-trityl-L-cysteine
Fmoc-L-Glu(tBu)-OH	*N*-(9-Fluorenylmethoxycarbonyl)-L-glutamic acid 5-*tert*-butyl ester
Fmoc-Gly-OH	*N*-(9-Fluorenylmethoxycarbonyl)-glycine
GAPDH	Glyceraldehyde 3-phosphate dehydrogenase
GSH	Glutathione
h	Hours
HAT(CN)$_6$	1,4,5,8,9,12-hexaazatriphenylene-hexacarbonitrile
HIV	Human immunodeficiency viruses
HPLC	High-Performance Liquid Chromatography
HRMS	High Resolution Mass Spectrometry
HSAc	Thioacetic acid
IPA	Isopropanol
KSAc	Potassium thioacetate
LiAlH$_4$	Lithium aluminum hydride
MAHT	Malonic Acid Half Thioester
m-CPBA	3-Chloroperbenzoic acid

MeOH	Methanol
min	Minutes
Mp	Melting Point
MSBT	Methylsulfonyl benzothiazole
NDA	1,4,5,8–Naphthalenetetracarboxylic dianhydride
NDI	Naphthalenediimide
NMR	Nuclear Magnetic Resonance
PBu_3	Tri–n–butylphosphine
PDA	Perylene-3,4,9,10-tetracarboxylic dianhydride
PDI	Perylenediimide
PDIases	Protein Disulfide Isomerases
PEA	Phosphatodylethanolamine
PEG	Polyethylene glycol
PPIs	Protein-protein interactions
RNA	Ribonucleic acid
RI	Reactive intermediates
rt	Room temperature
SCARB1	Scavenger receptor class B member 1
SIN	Sindbis virus
SOD1	Cu/Zn-superoxide dismutase
t	Time
tBu	$tert$–Butyl
TCEP·HCl	Tris(2–carboxyethyl)phosphine hydrochloride
TEA	Triethylamine
TFA	Trifluoroacetic acid

TFE	2,2,2–Trifluoroethanol
TFRC	Transferrin receptor protein 1
THF	Tetrahydrofurane
TRIS	Tris(hydroxymethyl)aminomethane
TS	Transition State
Ts	Tosylate
TsCl	*p*-Toluenesulfonyl chloride
UHP	Urea hydrogen peroxide
UV	Ultra Violet
VAPA	Vesicle-associated membrane protein-associated protein A
Vis	Visible
μW	Microwave

BIBLIOGRAPHY

(1) Scheiner, S. Understanding noncovalent bonds and their controlling forces. *J. Chem. Phys.* **2020**, *153*, 140901.

(2) Jeffrey, G.; Saenger, W. *Hydrogen Bonding in Biological Structures*; Springer: Berlin, **1991**.

(3) Kollman, P. Chapter 2: Non-covalent forces of importance in biochemistry. *The Chemistry of Enzyme Action*; New Comprehensive Biochemistry; Elsevier, **1984**; 55–71.

(4) Yamauchi, O. Noncovalent interactions in biocomplexes. *Physical Sciences Reviews* **2016**, 20160001.

(5) Renslo, A. *The organic chemistry of medicinal agents*; McGraw-Hill Education, **2016**.

(6) Hiraoka, K.; Mizuse, S.; Yamabe, S. High-symmetric structure of the gas-phase cluster ions $X^- \cdots C_6F_6$ (X = Cl, Br, and I). *The Journal of Physical Chemistry* **1987**, *91*, 5294-5297.

(7) Giese, M.; Albrecht, M.; Rissanen, K. Experimental investigation of anion-π interactions—applications and biochemical relevance. *Chem. Commun.* **2016**, *52*, 1778–1795.

(8) Schneider, H.-J.; Werner, F.; Blatter, T. Attractive interactions between negative charges and polarizable aryl parts of host–guest systems. *J. Phys. Org. Chem.* **1993**, *6*, 590–594.

(9) Quiñonero, D.; Carolina Garau, C.; Rotger, C.; Frontera, A.; Ballester, P.; Costa, A.; Deyà, P. M. Anion–π interactions: Do they exist? *Angew. Chem. Int. Ed.* **2002**, *41*, 3389–3392.

(10) Mascal, M.; Armstrong, A.; Bartberger, M. D. Anion-aromatic bonding: a case for anion recognition by π-acidic rings. *J. Am. Chem. Soc.* **2002**, *124*, 6274–6276.

(11) Alkorta, I.; Rozas, I.; Elguero, J. Interaction of anions with perfluoro aromatic compounds. *J. Am. Chem. Soc.* **2002**, *124*, 8593–8598.

(12) Zhao, Y.; Cotelle, Y.; Le Liu; López-Andarias, J.; Bornhof, A.-B.; Akamatsu, M.; Sakai, N.; Matile, S. The emergence of anion-π catalysis. *Acc. Chem. Res.* **2018**, *51*, 2255–2263.

(13) Hay, B. P.; Custelcean, R. Anion−π interactions in crystal structures: commonplace or extraordinary? *Crystal Growth & Design* **2009**, *9*, 2539–2545.

(14) Gomila, R. M.; Frontera, A. Chapter 5. Anion–π catalysis. *Noncovalent Interactions in Catalysis*; Royal Society of Chemistry: Cambridge, **2019**; 122–136.

(15) Bauzá, A.; Mooibroek, T. J.; Frontera, A. The bright future of unconventional σ/π-hole interactions. *Chemphyschem* **2015**, *16*, 2496–2517.

(16) Frontera, A.; Gamez, P.; Mascal, M.; Mooibroek, T. J.; Reedijk, J. Putting anion-π interactions into perspective. *Angew. Chem. Int. Ed.* **2011**, *50*, 9564–9583.

(17) Wang, H.; Wang, W.; Jin, W. J. σ-Hole bond vs π-Hole bond: A comparison based on halogen bond. *Chem. Rev.* **2016**, *116*, 5072–5104.

(18) Garau, C.; Frontera, A.; Quiñonero, D.; Ballester, P.; Costa, A.; Deyà, P. M. A topological analysis of the electron density in anion-π interactions. *Chemphyschem* **2003**, *4*, 1344–1348.

(19) Garau, C.; Quiñonero, D.; Frontera, A.; Ballester, P.; Costa, A.; Deyà, P. M. Dual binding mode of s-triazine to anions and cations. *Org. Lett.* **2003**, *5*, 2227–2229.

(20) Garau, C.; Quiñonero, D.; Frontera, A.; Ballester, P.; Costa, A.; Deyà, P. M. Anion–π interactions: must the aromatic ring be electron-deficient? *New J. Chem.* **2003**, *27*, 211–214.

(21) Garau, C.; Frontera, A.; Quiñonero, D.; Ballester, P.; Costa, A.; Deyà, P. M. Cation-π vs anion-π interactions: a complete π-orbital analysis. *Chem. Phys. Lett.* **2004**, *399*, 220–225.

(22) Garau, C.; Frontera, A.; Quiñonero, D.; Ballester, P.; Costa, A.; Deyà, P. M. Cation−π versus anion−π interactions: Energetic, charge transfer, and aromatic aspects. *J. Phys. Chem. A* **2004**, *108*, 9423–9427.

(23) Alkorta, I.; Quiñonero, D.; Garau, C.; Frontera, A.; Elguero, J.; Deyà, P. M. Dual cation and anion acceptor molecules. The case of the (η^6-C$_6$H$_6$)(η^6C$_6$F$_6$)Cr(0) complex. *J. Phys. Chem. A* **2007**, *111*, 3137–3142.

(24) Anstöter, C. S.; Rogers, J. P.; Verlet, J. R. R. Spectroscopic determination of an anion-π bond strength. *J. Am. Chem. Soc.* **2019**, *141*, 6132–6135.

(25) Gorteau, V.; Bollot, G.; Mareda, J.; Perez-Velasco, A.; Matile, S. Rigid oligonaphthalenediimide rods as transmembrane anion-π slides. *J. Am. Chem. Soc.* **2006**, *128*, 14788–14789.

(26) Perez-Velasco, A.; Gorteau, V.; Matile, S. Rigid oligoperylenediimide rods: anion- π slides with photosynthetic activity. *Angew. Chem. Int. Ed.* **2008**, *47*, 921–923.

(27) Wang, D.-X.; Zheng, Q.-Y.; Wang, Q.-Q.; Wang, M.-X. Halide recognition by tetraoxacalix[2]arene[2]triazine receptors: concurrent noncovalent halide-π and lone-pair-π interactions in host-halide-water ternary complexes. *Angew. Chem. Int. Ed.* **2008**, *47*, 7485–7488.

(28) Wang, D.-X.; Wang, M.-X. Anion-π interactions: generality, binding strength, and structure. *J. Am. Chem. Soc.* **2013**, *135*, 892–897.

(29) Wang, D.-X.; Wang, Q.-Q.; Han, Y.; Wang, Y.; Huang, Z.-T.; Wang, M.-X. Versatile anion-π interactions between halides and a conformationally rigid bis(tetraoxacalix[2]arene[2]triazine) cage and their directing effect on molecular assembly. *Chemistry* **2010**, *16*, 13053–13057.

(30) Wang, X.-D.; Li, S.; Ao, Y.-F.; Wang, Q.-Q.; Huang, Z.-T.; Wang, D.-X. Oxacalix[2]arene[2]triazine based ion-pair transporters. *Org. Biomol. Chem.* **2016**, *14*, 330–334.

(31) Huang, W.-L.; Wang, X.-D.; Li, S.; Zhang, R.; Ao, Y.-F.; Tang, J.; Wang, Q.-Q.; Wang, D.-X. Anion transporters based on noncovalent balance including anion-π, hydrogen, and halogen bonding. *J. Org. Chem.* **2019**, *84*, 8859–8869.

(32) Huang, W.-L.; Wang, X.-D.; Ao, Y.-F.; Wang, Q.-Q.; Wang, D.-X. Artificial chloride-selective channel: Shape and function mimic of the ClC channel selective pore. *J. Am. Chem. Soc.* **2020**, *142*, 13273–13277.

(33) Schneebeli, S. T.; Frasconi, M.; Liu, Z.; Wu, Y.; Gardner, D. M.; Strutt, N. L.; Cheng, C.; Carmieli, R.; Wasielewski, M. R.; Stoddart, J. F. Electron sharing and anion-π recognition in molecular triangular prisms. *Angew. Chem. Int. Ed.* **2013**, *52*, 13100–13104.

(34) Han, B.; Lu, J.; Kochi, J. K. Anion recognitions via cocrystallizations with organic π-acids in the efficient self-assembly of nanoscopic one-dimensional molecular chains (wires). *Crystal Growth & Design* **2008**, *8*, 1327–1334.

(35) Chifotides, H. T.; Schottel, B. L.; Dunbar, K. R. The π-accepting arene HAT(CN)$_6$ as a halide receptor through charge transfer: multisite anion interactions and self-assembly in solution and the solid state. *Angew. Chem. Int. Ed.* **2010**, *49*, 7202–7207.

(36) He, Q.; Han, Y.; Wang, Y.; Huang, Z.-T.; Wang, D.-X. Size-regulable vesicles based on anion-π interactions. *Chemistry* **2014**, *20*, 7486–7491.

(37) Tuo, D.-H.; Liu, W.; Wang, X.-Y.; Wang, X.-D.; Ao, Y.-F.; Wang, Q.-Q.; Li, Z.-Y.; Wang, D.-X. Toward anion-π interactions directed self-assembly with predesigned dual macrocyclic receptors and dianions. *J. Am. Chem. Soc.* **2019**, *141*, 1118–1125.

(38) Zhao, Y.; Domoto, Y.; Orentas, E.; Beuchat, C.; Emery, D.; Mareda, J.; Sakai, N.; Matile, S. Catalysis with anion-π interactions. *Angew. Chem. Int. Ed.* **2013**, *52*, 9940–9943.

(39) Zhao, Y.; Beuchat, C.; Domoto, Y.; Gajewy, J.; Wilson, A.; Mareda, J.; Sakai, N.; Matile, S. Anion-π catalysis. *J. Am. Chem. Soc.* **2014**, *136*, 2101–2111.

(40) Zhao, Y.; Sakai, N.; Matile, S. Enolate chemistry with anion-π interactions. *Nat. Commun.* **2014**, *5*, 3911.

(41) Zhao, Y.; Cotelle, Y.; Avestro, A.-J.; Sakai, N.; Matile, S. Asymmetric anion-π catalysis: Enamine addition to nitroolefins on π-acidic surfaces. *J. Am. Chem. Soc.* **2015**, *137*, 11582–11585.

(42) Duschmalé, J.; Wiest, J.; Wiesner, M.; Wennemers, H. Effects of internal and external carboxylic acids on the reaction pathway of organocatalytic 1,4-addition reactions between aldehydes and nitroolefins. *Chem. Sci.* **2013**, *4*, 1312.

(43) Wiesner, M.; Revell, J. D.; Wennemers, H. Tripeptides as efficient asymmetric catalysts for 1,4-addition reactions of aldehydes to nitroolefins—a rational approach. *Angew. Chem. Int. Ed.* **2008**, *47*, 1871–1874.

(44) Akamatsu, M.; Matile, S. Expanded chiral surfaces for asymmetric anion–π catalysis. *Synlett* **2016**, *27*, 1041–1046.

(45) Wang, C.; Miros, F. N.; Mareda, J.; Sakai, N.; Matile, S. Asymmetric anion-π catalysis on perylenediimides. *Angew. Chem. Int. Ed.* **2016**, *55*, 14422–14426.

(46) Zhao, Y.; Benz, S.; Sakai, N.; Matile, S. Selective acceleration of disfavored enolate addition reactions by anion-π interactions. *Chem. Sci.* **2015**, *6*, 6219–6223.

(47) Liu, L.; Cotelle, Y.; Bornhof, A.-B.; Besnard, C.; Sakai, N.; Matile, S. Anion-π catalysis of Diels-Alder reactions. *Angew. Chem. Int. Ed.* **2017**, *56*, 13066–13069.

(48) Zhang, X.; Hao, X.; Le Liu; Pham, A.-T.; López-Andarias, J.; Frontera, A.; Sakai, N.; Matile, S. Primary anion-π catalysis and autocatalysis. *J. Am. Chem. Soc.* **2018**, *140*, 17867–17871.

(49) Paraja, M.; Matile, S. Primary anion-π catalysis of epoxide-opening ether cyclization into rings of different sizes: Access to new reactivity. *Angew. Chem. Int. Ed.* **2020**, *59*, 6273–6277.

(50) Paraja, M.; Hao, X.; Matile, S. Polyether natural product inspired cascade cyclizations: Autocatalysis on π-acidic aromatic surfaces. *Angew. Chem. Int. Ed.* **2020**, *59*, 15093–15097.

(51) Liu, L.; Cotelle, Y.; Avestro, A.-J.; Sakai, N.; Matile, S. Asymmetric anion-π catalysis of iminium/nitroaldol cascades to form cyclohexane rings with five stereogenic centers directly on π-acidic surfaces. *J. Am. Chem. Soc.* **2016**, *138*, 7876–7879.

(52) Liu, L.; Cotelle, Y.; Klehr, J.; Sakai, N.; Ward, T. R.; Matile, S. Anion-π catalysis: bicyclic products with four contiguous stereogenic centers from otherwise elusive diastereospecific domino reactions on π-acidic surfaces. *Chem. Sci.* **2017**, *8*, 3770–3774.

(53) Cotelle, Y.; Benz, S.; Avestro, A.-J.; Ward, T. R.; Sakai, N.; Matile, S. Anion-π catalysis of enolate chemistry: rigidified leonard turns as a general motif to run reactions on aromatic surfaces. *Angew. Chem. Int. Ed.* **2016**, *55*, 4275–4279.

(54) Wang, C.; Matile, S. Anion-π catalysts with axial chirality. *Chemistry* **2017**, *23*, 11955–11960.

(55) Cotelle, Y.; Lebrun, V.; Sakai, N.; Ward, T. R.; Matile, S. Anion-π enzymes. *ACS Cent. Sci.* **2016**, *2*, 388–393.

(56) Akamatsu, M.; Sakai, N.; Matile, S. Electric-field-assisted anion-π catalysis. *J. Am. Chem. Soc.* **2017**, *139*, 6558–6561.

(57) López-Andarias, J.; Frontera, A.; Matile, S. Anion-π catalysis on fullerenes. *J. Am. Chem. Soc.* **2017**, *139*, 13296–13299.

(58) López-Andarias, J.; Bauzá, A.; Sakai, N.; Frontera, A.; Matile, S. Remote control of anion-π catalysis on fullerene-centered catalytic triads. *Angew. Chem. Int. Ed.* **2018**, *57*, 10883–10887.

(59) Bornhof, A.-B.; Vázquez-Nakagawa, M.; Rodríguez-Pérez, L.; Ángeles Herranz, M.; Sakai, N.; Martín, N.; Matile, S.; López-Andarias, J. Anion-π catalysis on carbon nanotubes. *Angew. Chem. Int. Ed.* **2019**, *58*, 16097–16100.

(60) Luo, N.; Ao, Y.-F.; Wang, D.-X.; Wang, Q.-Q. Exploiting anion-π interactions for efficient and selective catalysis with chiral molecular cages. *Angew. Chem. Int. Ed.* DOI: 10.1002/anie.202106509.

(61) Lau, Y. H.; Andrade, P. de; Wu, Y.; Spring, D. R. Peptide stapling techniques based on different macrocyclisation chemistries. *Chem. Soc. Rev.* **2015**, *44*, 91–102.

(62) Ali, A. M.; Atmaj, J.; Oosterwijk, N.; Groves, M. R.; Dömling, A. Stapled peptides inhibitors: A new window for targeting drug discovery. *Comput. Struct. Biotechnol. J* **2019**, *17*, 263–281.

(63) Li, X.; Chen, S.; Zhang, W.-D.; Hu, H.-G. Stapled helical peptides bearing different anchoring residues. *Chem. Rev.* **2020**, *120*, 10079–10144.

(64) Spokoyny, A. M.; Zou, Y.; Ling, J. J.; Yu, H.; Lin, Y.-S.; Pentelute, B. L. A perfluoroaryl-Cysteine S$_N$Ar chemistry approach to unprotected peptide stapling. *J. Am. Chem. Soc.* **2013**, *135*, 5946–5949.

(65) Fairlie, D. P.; Dantas de Araujo, A. Review stapling peptides using Cysteine crosslinking. *Biopolymers* **2016**, *106*, 843–852.

(66) Fadzen, C. M.; Wolfe, J. M.; Cho, C.-F.; Chiocca, E. A.; Lawler, S. E.; Pentelute, B. L. Perfluoroarene-based peptide macrocycles to enhance penetration across the blood-brain barrier. *J. Am. Chem. Soc.* **2017**, *139*, 15628–15631.

(67) Thabault, L.; Brisson, L.; Brustenga, C.; Martinez Gache, S. A.; Prévost, J. R. C.; Kozlova, A.; Spillier, Q.; Liberelle, M.; Benyahia, Z.; Messens, J.*;* Copetti, T.; Sonveaux, P.; Frédérick, R. Interrogating the lactate dehydrogenase tetramerization site using (stapled) peptides. *J. Med. Chem.* **2020**, *63*, 4628–4643.

(68) Verhoork, S. J. M.; Jennings, C. E.; Rozatian, N.; Reeks, J.; Meng, J.; Corlett, E. K.; Bunglawala, F.; Noble, M. E. M.; Leach, A. G.; Coxon, C. R. Tuning the binding affinity and selectivity of perfluoroaryl-stapled peptides by cysteine-editing. *Chemistry* **2019**, *25*, 177–182.

(69) Kalhor-Monfared, S.; Jafari, M. R.; Patterson, J. T.; Kitov, P. I.; Dwyer, J. J.; Nuss, J. M.; Derda, R. Rapid biocompatible macrocyclization of peptides with decafluoro-diphenylsulfone. *Chem. Sci.* **2016**, *7*, 3785–3790.

(70) Liu, W.; Zheng, Y.; Kong, X.; Heinis, C.; Zhao, Y.; Wu, C. Precisely regulated and efficient locking of linear peptides into stable multicyclic topologies through a one-pot reaction. *Angew. Chem. Int. Ed.* **2017**, *56*, 4458–4463.

(71) Grison, C. M.; Burslem, G. M.; Miles, J. A.; Pilsl, L. K. A.; Yeo, D. J.; Imani, Z.; Warriner, S. L.; Webb, M. E.; Wilson, A. J. Double quick, double click reversible peptide "stapling". *Chem. Sci.* **2017**, *8*, 5166–5171.

(72) Tucker, M. J.; Courter, J. R.; Chen, J.; Atasoylu, O.; Smith, A. B.; Hochstrasser, R. M. Tetrazine phototriggers: probes for peptide dynamics. *Angew. Chem. Int. Ed.* **2010**, *49*, 3612–3616.

(73) Tucker, M. J.; Abdo, M.; Courter, J. R.; Chen, J.; Smith, A. B.; Hochstrasser, R. M. Di-Cysteine S,S-Tetrazine: A potential ultra-fast photochemical trigger to explore the early events of peptide/protein folding. *J. Photochem. Photobiol. A Chem.* **2012**, *234*, 156–163.

(74) Brown, S. P.; Smith, A. B. Peptide/protein stapling and unstapling: introduction of s-tetrazine, photochemical release, and regeneration of the peptide/protein. *J. Am. Chem. Soc.* **2015**, *137*, 4034–4037.

(75) Jarvo, E. R.; Miller, S. J. Amino acids and peptides as asymmetric organocatalysts. *Tetrahedron* **2002**, *58*, 2481–2495.

(76) Davie, E. A. C.; Mennen, S. M.; Xu, Y.; Miller, S. J. Asymmetric catalysis mediated by synthetic peptides. *Chem. Rev.* **2007**, *107*, 5759–5812.

(77) Freund, M.; Tsogoeva, S. B. Peptides for asymmetric catalysis. *Catalytic Methods in Asymmetric Synthesis*; John Wiley & Sons, Inc: Hoboken, NJ, USA, **2011**; 529–578.

(78) Gruttadauria, M.; Giacalone, F., Eds. *Catalytic Methods in Asymmetric Synthesis*; John Wiley & Sons, Inc: Hoboken, NJ, USA, **2011**.

(79) Wennemers, H. Asymmetric catalysis with peptides. *Chem. Commun.* **2011**, *47*, 12036–12041.

(80) Zozulia, O.; Dolan, M. A.; Korendovych, I. V. Catalytic peptide assemblies. *Chem. Soc. Rev.* **2018**, *47*, 3621–3639.

(81) Metrano, A. J.; Miller, S. J. Peptide-based catalysts reach the outer sphere through remote desymmetrization and atroposelectivity. *Acc. Chem. Res.* **2019**, *52*, 199–215.

(82) Metrano, A. J.; Chinn, A. J.; Shugrue, C. R.; Stone, E. A.; Kim, B.; Miller, S. J. Asymmetric catalysis mediated by synthetic peptides, version 2.0: Expansion of scope and mechanisms. *Chem. Rev.* **2020**, *120*, 11479–11615.

(83) Yamagata, N.; Demizu, Y.; Sato, Y.; Doi, M.; Tanaka, M.; Nagasawa, K.; Okuda, H.; Kurihara, M. Design of a stabilized short helical peptide and its application to catalytic enantioselective epoxidation of (*E*)-chalcone. *Tetrahedron Lett.* **2011**, *52*, 798–801.

(84) Rokade, B. V.; Guiry, P. J. Axially chiral P,N-ligands: Some recent twists and turns. *ACS Catal.* **2018**, *8*, 624–643.

(85) Rickhaus, M.; Mayor, M.; Juríček, M. Strain-induced helical chirality in polyaromatic systems. *Chem. Soc. Rev.* **2016**, *45*, 1542–1556.

(86) Rickhaus, M.; Mayor, M.; Juríček, M. Chirality in curved polyaromatic systems. *Chem. Soc. Rev.* **2017**, *46*, 1643–1660.

(87) Shen, Y.; Chen, C.-F. Helicenes: synthesis and applications. *Chem. Rev.* **2012**, *112*, 1463–1535.

(88) Narcis, M. J.; Takenaka, N. Helical-chiral small molecules in asymmetric catalysis. *Eur. J. Org. Chem.* **2014**, *2014*, 21–34.

(89) Hasan, M.; Borovkov, V. Helicene-based chiral auxiliaries and chirogenesis. *Symmetry* **2018**, *10*, 10.

(90) Gingras, M. One hundred years of helicene chemistry. Part 3: applications and properties of carbohelicenes. *Chem. Soc. Rev.* **2013**, *42*, 1051–1095.

(91) Pascal, R. A. Twisted acenes. *Chem. Rev.* **2006**, *106*, 4809–4819.

(92) Bedi, A.; Gidron, O. The consequences of twisting nanocarbons: Lessons from tethered twisted acenes. *Acc. Chem. Res.* **2019**, *52*, 2482–2490.

(93) Chen, Z.; Baumeister, U.; Tschierske, C.; Würthner, F. Effect of core twisting on self-assembly and optical properties of perylene bisimide dyes in solution and columnar liquid crystalline phases. *Chemistry* **2007**, *13*, 450–465.

(94) Chang, C.-W.; Chien, F.-Y.; Hu, J.-W.; Tsai, H.-Y.; Chen, K.-Y. 1,6-Diaminoperylene bisimide with a highly twisted perylene core. *J. Chem. Sci.* **2017**, *129*, 149–156.

(95) Osswald, P.; Würthner, F. Conformational effects of bay substituents on optical, electrochemical and dynamic properties of perylene bisimides: macrocyclic derivatives as effective probes. *Chemistry* **2007**, *13*, 7395–7409.

(96) Jones, B. A.; Ahrens, M. J.; Yoon, M.-H.; Facchetti, A.; Marks, T. J.; Wasielewski, M. R. High-mobility air-stable n-type semiconductors with processing versatility: dicyanoperylene-3,4:9,10-bis(dicarboximides). *Angew. Chem. Int. Ed.* **2004**, *43*, 6363–6366.

(97) Würthner, F. Bay-substituted perylene bisimides: Twisted fluorophores for supramolecular chemistry. *Pure Appl. Chem.* **2006**, *78*, 2341–2349.

(98) Osswald, P.; Würthner, F. Effects of bay substituents on the racemization barriers of perylene bisimides: resolution of atropo-enantiomers. *J. Am. Chem. Soc.* **2007**, *129*, 14319–14326.

(99) Wang, W.; Han, J. J., Wang, L.-Q.; Li, L.-S.; Shaw, W. J.; Li, A. D. Q. Dynamic π−π stacked molecular assemblies emit from green to red colors. *Nano Letters* **2003**, *3,* 455–458.

(100) Nowak-Król, A.; Röhr, M. I. S.; Schmidt, D.; Würthner, F. A crystalline π-stack containing five stereoisomers: insights into conformational isomorphism, chirality inversion, and disorder. *Angew. Chem. Int. Ed.* **2017**, *56*, 11774–11778.

(101) Wang, W.; Shaller, A. D.; Li, A. D. Q. Twisted perylene stereodimers reveal chiral molecular assembly codes. *J. Am. Chem. Soc.* **2008**, *130*, 8271–8279.

(102) Shaller, A. D.; Wang, W.; Gan, H.; Li, A. D. Q. Tunable molecular assembly codes direct reaction pathways. *Angew. Chem. Int. Ed.* **2008**, *47*, 7705–7709.

(103) Bhosale, S. V.; Al Kobaisi, M.; Jadhav, R. W.; Morajkar, P. P.; Jones, L. A.; George, S. Naphthalene diimides: perspectives and promise. Chemical Society reviews [Online early access]. DOI: 10.1039/d0cs00239a. Published Online: Jul. 26, 2021.

(104) Diac, A.; Matache, M.; Grosu, I.; Hădade, N. D. Naphthalenediimide - A Unique Motif in Macrocyclic and Interlocked Supramolecular Structures. Adv. Synth. Catal. 2018, 360, 817–845.

(105) Kobaisi, M. A.; Bhosale, S. V.; Latham, K.; Raynor, A. M.; Bhosale, S. V. Functional Naphthalene Diimides: Synthesis, Properties, and Applications. Chemical reviews 2016, 116, 11685–11796.

(106) Chen, G.; Lean, J. T.; Alcalá, M.; Mallouk, T. E. Modular synthesis of pi-acceptor cyclophanes derived from 1,4,5,8-naphthalenetetracarboxylic diimide and 1,5-dinitronaphthalene. The Journal of organic chemistry 2001, 66, 3027–3034.

(107) Chen, Y.; Li, T.; Li, J.; Cheng, S.; Wang, J.; Verma, C.; Zhao, Y.; Wu, C. Stabilization of peptides against proteolysis through disulfide-bridged conjugation with synthetic

(108) Osswald, P.; Leusser, D.; Stalke, D.; Würthner, F. Perylene bisimide based macrocycles: effective probes for the assessment of conformational effects on optical properties. *Angew. Chem. Int. Ed.* **2004**, *44*, 250–253.

(109) Osswald, P.; Reichert, M.; Bringmann, G.; Würthner, F. Perylene bisimide atropisomers: synthesis, resolution, and stereochemical assignment. *J. Org. Chem.* **2007**, *72*, 3403–3411.

(110) Safont-Sempere, M. M.; Osswald, P.; Radacki, K.; Würthner, F. Chiral self-recognition and self-discrimination of strapped perylene bisimides by pi-stacking dimerization. *Chemistry* **2010**, *16*, 7380–7384.

(111) Safont-Sempere, M. M.; Stepanenko, V.; Lehmann, M.; Würthner, F. Impact of core chirality on mesophase properties of perylene bisimides. *J. Mater. Chem.* **2011**, *21*, 7201-7209.

(112) Safont-Sempere, M. M.; Osswald, P.; Stolte, M.; Grüne, M.; Renz, M.; Kaupp, M.; Radacki, K.; Braunschweig, H.; Würthner, F. Impact of molecular flexibility on binding strength and self-sorting of chiral π-surfaces. *J. Am. Chem. Soc.* **2011**, *133*, 9580–9591.

(113) Weh, M.; Rühe, J.; Herbert, B.; Krause, A.-M.; Würthner, F. Deracemization of carbohelicenes by a chiral perylene bisimide cyclophane template catalyst. *Angew. Chem. Int. Ed.* **2021**, 60, 15323-15327.

(114) Xie, Z.; Würthner, F. Perylene bisimides with rigid 2,2'-biphenol bridges at bay area as conjugated chiral platforms. *Org. Lett.* **2010**, *12*, 3204–3207.

(115) Ball, M.; Fowler, B.; Li, P.; Joyce, L. A.; Li, F.; Liu, T.; Paley, D.; Zhong, Y.; Li, H.; Xiao, S.*;* Ng, F.; Steigerwald, M. L.; Nuckolls, C. Chiral conjugated corrals. *J. Am. Chem. Soc.* **2015**, *137*, 9982–9987.

(116) Mosquera, J.; García, I.; Liz-Marzán, L. M. Cellular uptake of nanoparticles versus small molecules: A matter of size. *Acc. Chem. Res.* **2018**, *51*, 2305–2313.

(117) Cournia, Z.; Allen, T. W.; Andricioaei, I.; Antonny, B.; Baum, D.; Brannigan, G.; Buchete, N.-V.; Deckman, J. T.; Delemotte, L.; Del Val, C.*;* Friedman, R.; Gkeka, P.; Hege, H.-C.; Hénin, J.; Kasimova, M. A.; Kolocouris, A.; Klein, M. L.; Khalid, S.; Lemieux, M. J.; Lindow, N.; Roy, M.; Selent, J.; Tarek, M.; Tofoleanu, F.; Vanni, S.; Urban, S.; Wales, D. J.;

Smith, J. C.; Bondar, A.-N. Membrane protein structure, function, and dynamics: A perspective from experiments and theory. *J. Membr. Biol.* **2015**, *248*, 611–640.

(118) Vinothkumar, K. R.; Henderson, R. Structures of membrane proteins. *Q. Rev. Biophys.* **2010**, *43*, 65–158.

(119) Almeida, J. G.; Preto, A. J.; Koukos, P. I.; Bonvin, A. M. J. J.; Moreira, I. S. Membrane proteins structures: A review on computational modeling tools. *Biochim. Biophys. Acta Biomembr.* **2017**, *1859*, 2021–2039.

(120) Torres, A. G.; Gait, M. J. Exploiting cell surface thiols to enhance cellular uptake. *Trends Biotechnol.* **2012**, *30*, 185–190.

(121) Hogg, P. J. Disulfide bonds as switches for protein function. *Trends BioChem. Sci.* **2003**, *28*, 210–214.

(122) Ryser, H. J.; Mandel, R.; Ghani, F. Cell surface sulfhydryls are required for the cytotoxicity of diphtheria toxin but not of ricin in Chinese hamster ovary cells. *J. Biol. Chem.* **1991**, *266*, 18439–18442.

(123) Lavillette, D.; Barbouche, R.; Yao, Y.; Boson, B.; Cosset, F.-L.; Jones, I. M.; Fenouillet, E. Significant redox insensitivity of the functions of the SARS-CoV spike glycoprotein: comparison with HIV envelope. *J. Biol. Chem.* **2006**, *281*, 9200–9204.

(124) Jain, S.; McGinnes, L. W.; Morrison, T. G. Thiol/disulfide exchange is required for membrane fusion directed by the Newcastle disease virus fusion protein. *J. Virol.* **2007**, *81*, 2328–2339.

(125) Glomb-Reinmund, S.; Kielian, M. The role of low pH and disulfide shuffling in the entry and fusion of Semliki Forest virus and Sindbis virus. *Virology* **1998**, *248*, 372–381.

(126) Gallagher, T. M. Murine coronavirus membrane fusion is blocked by modification of thiols buried within the spike protein. *J. Virol.* **1996**, *70*, 4683–4690.

(127) Fenouillet, E.; Barbouche, R.; Jones, I. M. Cell entry by enveloped viruses: redox considerations for HIV and SARS-coronavirus. *Antioxid. Redox. Signal* **2007**, *9*, 1009–1034.

(128) Wallin, M.; Löving, R.; Ekström, M.; Li, K.; Garoff, H. Kinetic analyses of the surface-transmembrane disulfide bond isomerization-controlled fusion activation pathway in moloney Murine Leukemia virus. *J. Virol.* **2005**, *79*, 13856−13864.

(129) Kichler, A.; Remy, J.-S.; Behr, J.-P.; Schuber, F. Targeted transfection of human hepatoma cells with a combination of lipospermine and neo-galactolipids. *Journal of Liposome Research* **1995**, *5*, 735-745.

(130) Abell, B. A.; Brown, D. T. Sindbis virus membrane fusion is mediated by reduction of glycoprotein disulfide bridges at the cell surface. *J. Virol.* **1993**, *67*, 5496–5501.

(131) Laurent, Q.; Martinent, R.; Lim, B.; Pham, A.-T.; Kato, T.; López-Andarias, J.; Sakai, N.; Matile, S. Thiol-mediated uptake. *JACS Au* **2021**, *1,* 710–728.

(132) Cheng, Y.; Pham, A.-T.; Kato, T.; Lim, B.; Moreau, D.; López-Andarias, J.; Zong, L.; Sakai, N.; Matile, S. Inhibitors of thiol-mediated uptake. *Chem. Sci.* **2021**, *12*, 626–631.

(133) Abegg, D.; Gasparini, G.; Hoch, D. G.; Shuster, A.; Bartolami, E.; Matile, S.; Adibekian, A. strained cyclic disulfides enable cellular uptake by reacting with the Transferrin receptor. *J. Am. Chem. Soc.* **2017**, *139*, 231–238.

(134) Gasparini, G.; Sargsyan, G.; Bang, E.-K.; Sakai, N.; Matile, S. Ring tension applied to thiol-mediated cellular uptake. *Angew. Chem. Int. Ed.* **2015**, *54*, 7328–7331.

(135) Laurent, Q.; Sakai, N.; Matile, S. The opening of 1,2-dithiolanes and 1,2-diselenolanes: Regioselectivity, rearrangements, and consequences for poly(disulfide)s, cellular uptake and pyruvate dehydrogenase complexes. *Helv. Chim. Acta* **2019**, *102*, e1800209.

(136) Chuard, N.; Poblador-Bahamonde, A. I.; Zong, L.; Bartolami, E.; Hildebrandt, J.; Weigand, W.; Sakai, N.; Matile, S. Diselenolane-mediated cellular uptake. *Chem. Sci.* **2018**, *9*, 1860–1866.

(137) Ryser, H. J.-P.; Flückiger, R. Keynote review: Progress in targeting HIV-1 entry. *Drug Discovery Today* **2005**, *10*, 1085–1094.

(138) Markovic, I.; Pulyaeva, H.; Sokoloff, A.; Chernomordik, L. V. Membrane fusion mediated by baculovirus gp64 involves assembly of stable gp64 trimers into multiprotein aggregates. *J. Cell. Biol.* **1998**, *143*, 1155–1166.

(139) Pinter, A.; Kopelman, R.; Li, Z.; Kayman, S. C.; Sanders, D. A. Localization of the labile disulfide bond between SU and TM of the murine leukemia virus envelope protein complex to a highly conserved CWLC motif in SU that resembles the active-site sequence of thiol-disulfide exchange enzymes. *J. Virol.* **1997**, *71*, 8073–8077.

(140) Faaberg, K. S.; Even, C.; Palmer, G. A.; Plagemann, P. G. Disulfide bonds between two envelope proteins of lactate dehydrogenase-elevating virus are essential for viral infectivity. *J. Virol.* **1995**, *69*, 613–617.

(141) Abou-Jaoudé, G.; Sureau, C. Entry of hepatitis delta virus requires the conserved Cysteine residues of the hepatitis B virus envelope protein antigenic loop and is blocked by inhibitors of thiol-disulfide exchange. *J. Virol.* **2007**, *81*, 13057–13066.

(142) Wagner, P. L.; Waldor, M. K. Bacteriophage control of bacterial virulence. *Infect. Immun.* **2002**, *70*, 3985–3993.

(143) Shafiee, F.; Aucoin, M. G.; Jahanian-Najafabadi, A. Targeted Diphtheria toxin-based therapy: a review article. *Front. Microbiol.* **2019**, *10*, 2340.

(144) Lim, B.; Cheng, Y.; Kato, T.; Pham, A.-T.; Le Du, E.; Mishra, A. K.; Grinhagena, E.; Moreau, D.; Sakai, N.; Waser, J.*;* Matile, S. Inhibition of thiol-mediated uptake with irreversible covalent inhibitors. *Helv. Chim. Acta.* **2021**, *104*, e2100085.

(145) Feener, E. P.; Shen, W. C.; Ryser, H. J. Cleavage of disulfide bonds in endocytosed macromolecules. A processing not associated with lysosomes or endosomes. *J. Biol. Chem.* **1990**, *265*, 18780–18785.

(146) Kichler, A.; Remy, J. S.; Boussif, O.; Frisch, B.; Boeckler, C. Efficient gene delivery with neutral complexes of lipospermine and thiol-reactive phospholipids. *Biochem. Biophys. Res. Commun.* **1995**, *209*, 444-450.

(147) Aubry, S.; Burlina, F.; Dupont, E.; Delaroche, D.; Joliot, A.; Lavielle, S.; Chassaing, G.; Sagan, S. Cell-surface thiols affect cell entry of disulfide-conjugated peptides. *FASEB J,* **2009**, *23*, 2956–2967.

(148) Gasparini, G.; Bang, E.-K.; Molinard, G.; Tulumello, D. V.; Ward, S.; Kelley, S. O.; Roux, A.; Sakai, N.; Matile, S. Cellular uptake of substrate-initiated cell-penetrating poly(disulfide)s. *J. Am. Chem. Soc.* **2014**, *136*, 6069–6074.

(149) Morelli, P.; Bartolami, E.; Sakai, N.; Matile, S. Glycosylated cell-penetrating poly(disulfide)s: multifunctional cellular uptake at high solubility. *Helv. Chim. Acta* **2018**, *101*, e1700266.

(150) Morelli, P.; Martin-Benlloch, X.; Tessier, R.; Waser, J.; Sakai, N.; Matile, S. Ethynyl benziodoxolones: functional terminators for cell-penetrating poly(disulfide)s. *Polym. Chem.* **2016**, *7*, 3465–3470.

(151) Morelli, P.; Matile, S. Sidechain engineering in cell-penetrating poly(disulfide)s. *Helv. Chim. Acta* **2017**, *100*, e1600370.

(152) Gasparini, G.; Matile, S. Protein delivery with cell-penetrating poly(disulfide)s. *Chem. Commun.* **2015**, *51*, 17160–17162.

(153) Okamoto, Y.; Kojima, R.; Schwizer, F.; Bartolami, E.; Heinisch, T.; Matile, S.; Fussenegger, M.; Ward, T. R. A cell-penetrating artificial metalloenzyme regulates a gene switch in a designer mammalian cell. *Nat. Commun.* **2018**, *9*, 1943.

(154) Derivery, E.; Bartolami, E.; Matile, S.; Gonzalez-Gaitan, M. Efficient delivery of quantum dots into the cytosol of cells using cell-penetrating poly(disulfide)s. *J. Am. Chem. Soc.* **2017**, *139*, 10172–10175.

(155) Yuan, P.; Zhang, H.; Qian, L.; Mao, X.; Du, S.; Yu, C.; Peng, B.; Yao, S. Q. Intracellular delivery of functional native antibodies under hypoxic conditions by using a biodegradable silica nanoquencher. *Angew. Chem. Int. Ed.* **2017**, *56*, 12481–12485.

(156) Yuan, P.; Mao, X.; Wu, X.; Liew, S. S.; Li, L.; Yao, S. Q. Mitochondria-targeting, intracellular delivery of native proteins using biodegradable silica nanoparticles. *Angew. Chem. Int. Ed.* **2019**, *58*, 7657–7661.

(157) Yuan, P.; Mao, X.; Chong, K. C.; Fu, J.; Pan, S.; Wu, S.; Yu, C.; Yao, S. Q. Simultaneous imaging of Endogenous Survivin mRNA and on-demand drug release in live cells by using a mesoporous silica nanoquencher. *Small* **2017**, *13*, 1700569.

(158) Yu, C.; Qian, L.; Ge, J.; Fu, J.; Yuan, P.; Yao, S. C. L.; Yao, S. Q. Cell-penetrating poly(disulfide) assisted intracellular delivery of mesoporous silica nanoparticles for inhibition of miR-21 function and detection of subsequent therapeutic effects. *Angew. Chem. Int. Ed.* **2016**, *55*, 9272–9276.

(159) Qian, L.; Fu, J.; Yuan, P.; Du, S.; Huang, W.; Li, L.; Yao, S. Q. Intracellular delivery of native proteins facilitated by cell-penetrating poly(disulfide)s. *Angew. Chem. Int. Ed.* **2018**, *57*, 1532–1536.

(160) Fu, J.; Yu, C.; Li, L.; Yao, S. Q. Intracellular delivery of functional proteins and native drugs by cell-penetrating poly(disulfide)s. *J. Am. Chem. Soc.* **2015**, *137*, 12153–12160.

(161) Zong, L.; Bartolami, E.; Abegg, D.; Adibekian, A.; Sakai, N.; Matile, S. Epidithiodiketopiperazines: strain-promoted thiol-mediated cellular uptake at the highest tension. *ACS Cent. Sci.* **2017**, *3*, 449–453.

(162) Bartolami, E.; Basagiannis, D.; Zong, L.; Martinent, R.; Okamoto, Y.; Laurent, Q.; Ward, T. R.; Gonzalez-Gaitan, M.; Sakai, N.; Matile, S. Diselenolane-mediated cellular uptake: efficient cytosolic delivery of probes, peptides, proteins, artificial metalloenzymes and protein-coated quantum dots. *Chemistry* **2019**, *25*, 4047–4051.

(163) Li, T.; Gao, W.; Liang, J.; Zha, M.; Chen, Y.; Zhao, Y.; Wu, C. BisCysteine-bearing peptide probes to reveal extracellular thiol-disulfide exchange reactions promoting cellular uptake. *Anal. Chem.* **2017**, *89*, 8501–8508.

(164) Meng, X.; Li, T.; Zhao, Y.; Wu, C. CXC-mediated cellular uptake of miniproteins: forsaking "arginine magic". *ACS Chem. Biol.* **2018**, *13*, 3078–3086.

(165) Cheng, Y.; Zong, L.; López-Andarias, J.; Bartolami, E.; Okamoto, Y.; Ward, T. R.; Sakai, N.; Matile, S. Cell-penetrating dynamic-covalent Benzopolysulfane networks. *Angew. Chem. Int. Ed.* **2019**, *58*, 9522–9526.

(166) López-Andarias, J.; Saarbach, J.; Moreau, D.; Cheng, Y.; Derivery, E.; Laurent, Q.; González-Gaitán, M.; Winssinger, N.; Sakai, N.; Matile, S. Cell-penetrating Streptavidin: A general tool for bifunctional delivery with spatiotemporal control, mediated by transport systems such as adaptive Benzopolysulfane networks. *J. Am. Chem. Soc.* **2020**, *142*, 4784–4792.

(167) Chuard, N.; Gasparini, G.; Moreau, D.; Lörcher, S.; Palivan, C.; Meier, W.; Sakai, N.; Matile, S. Strain-promoted thiol-mediated cellular uptake of giant substrates: Liposomes and polymersomes. *Angew. Chem. Int. Ed.* **2017**, *56*, 2947–2950.

(168) Martinent, R.; Du, D.; López-Andarias, J.; Sakai, N.; Matile, S. Oligomers of cyclic oligochalcogenides for enhanced cellular uptake. *Chembiochem* **2021**, *22*, 253–259.

(169) Peng, H.; Chen, W.; Cheng, Y.; Hakuna, L.; Strongin, R.; Wang, B. Thiol reactive probes and chemosensors. *Sensors* **2012**, *12*, 15907–15946.

(170) Wang, K.; Peng, H.; Wang, B. Recent advances in thiol and sulfide reactive probes. *J. Cell. Biochem.* **2014**, *115*, 1007–1022.

(171) Hoch, D. G.; Abegg, D.; Adibekian, A. Cysteine-reactive probes and their use in chemical proteomics. *Chem. Commun.* **2018**, *54*, 4501–4512.

(172) Donnelly, D. P.; Dowgiallo, M. G.; Salisbury, J. P.; Aluri, K. C.; Iyengar, S.; Chaudhari, M.; Mathew, M.; Miele, I.; Auclair, J. R.; Lopez, S. A.*;* Manetsch, R.; Agar, J. N. Cyclic thiosulfinates and cyclic disulfides selectively cross-link thiols while avoiding modification of lone thiols. *J. Am. Chem. Soc.* **2018**, *140*, 7377–7380.

(173) Ferreira, R. B.; Law, M. E.; Jahn, S. C.; Davis, B. J.; Heldermon, C. D.; Reinhard, M.; Castellano, R. K.; Law, B. K. Novel agents that downregulate EGFR, HER2, and HER3 in parallel. *Oncotarget* **2015**, *6*, 10445–10459.

(174) Zhang, D.; Devarie-Baez, N. O.; Li, Q.; Lancaster, J. R.; Xian, M. Methylsulfonyl benzothiazole (MSBT): a selective protein thiol blocking reagent. *Org. Lett.* **2012**, *14*, 3396–3399.

(175) Toda, N.; Asano, S.; Barbas, C. F. Rapid, stable, chemoselective labeling of thiols with Julia-Kocieński-like reagents: a serum-stable alternative to maleimide-based protein conjugation. *Angew. Chem. Int. Ed.* **2013**, *52*, 12592–12596.

(176) Motiwala, H. F.; Kuo, Y.-H.; Stinger, B. L.; Palfey, B. A.; Martin, B. R. Tunable heteroaromatic sulfones enhance in-cell cysteine profiling. *J. Am. Chem. Soc.* **2020**, *142*, 1801–1810.

(177) Kim, D.; Tarakeshwar, P.; Kim, K. S. Theoretical investigations of anion−π interactions: The role of anions and the nature of π systems. *J. Phys. Chem. A* **2004**, *108*, 1250–1258.

(178) Le Liu; Matile, S. Anion-π transaminase mimics. *Supramol. Chem.* **2017**, *29*, 702–706.

(179) Zhang, X.; Le Liu; López-Andarias, J.; Wang, C.; Sakai, N.; Matile, S. Anion- π catalysis: focus on nonadjacent stereocenters. *Helv. Chim. Acta* **2018**, *101*, e1700288.

(180) Hao, X.; Li, T.-R.; Chen, H.; Gini, A.; Zhang, X.; Rosset, S.; Mazet, C.; Tiefenbacher, K.; Matile, S. Bioinspired ether cyclizations within a π-basic capsule compared to autocatalysis on π-acidic surfaces and pnictogen-bonding catalysts. *Chemistry* DOI: 10.1002/chem.202101548.

(181) Araujo, A. D.; Hoang, H. N.; Kok, W. M.; Diness, F.; Gupta, P.; Hill, T. A.; Driver, R. W.; Price, D. A.; Liras, S.; Fairlie, D. P. Comparative α-helicity of cyclic pentapeptides in water. *Angew. Chem. Int. Ed.* **2014**, *53*, 6965–6969.

(182) Nakamura, T.; Shioya, N.; Shimoaka, T.; Nishikubo, R.; Hasegawa, T.; Saeki, A.; Murata, Y.; Murdey, R.; Wakamiya, A. Molecular orientation change in naphthalene diimide thin films induced by removal of thermally cleavable substituents. *Chem. Mater.* **2019**, *31*, 1729–1737.

(183) Brändén, C.-I.; Tooze, J. *Introduction to protein structure*, 2nd ed.; Garland Pub: New York, **1999**.

(184) Nagano, M.; Doi, M.; Kurihara, M.; Suemune, H.; Tanaka, M. Stabilized α-helix-catalyzed enantioselective epoxidation of α,β-unsaturated ketones. *Org. Lett.* **2010**, *12*, 3564–3566.

(185) Miros, F. N.; Zhao, Y.; Sargsyan, G.; Pupier, M.; Besnard, C.; Beuchat, C.; Mareda, J.; Sakai, N.; Matile, S. Enolate stabilization by anion-π interactions: deuterium exchange in malonate dilactones on π-acidic surfaces. *Chemistry* **2016**, *22*, 2648–2657.

(186) Nick Pace, C.; Martin Scholtz, J. A Helix propensity scale based on experimental studies of peptides and proteins. *Biophys. J.* **1998**, *75*, 422–427.

(187) Chou, P. Y.; Fasman, G. D. Empirical Predictions of Protein Conformation. *Ann. Rev. Biochem.* **1978**, *47*, 251-276.

(188) Altmann, R.; Etzlstorfer, C.; Falk, H. Chiroptical properties and absolute configurations of the hypericin chromophore propeller enantiomers. *Monatsh. Chem.* **1997**, *128*, 785–793.

(189) Bornhof, A.-B.; Bauzá, A.; Aster, A.; Pupier, M.; Frontera, A.; Vauthey, E.; Sakai, N.; Matile, S. Synergistic anion-(π) n-π catalysis on π-stacked foldamers. *J. Am. Chem. Soc.* **2018**, *140*, 4884–4892.

(190) Lubkoll, J.; Wennemers, H. Mimicry of polyketide synthases—enantioselective 1,4-addition reactions of malonic acid half-thioesters to nitroolefins. *Angew. Chem. Int. Ed.* **2007**, *46*, 6841–6844.

(191) Bae, H. Y.; Some, S.; Lee, J. H.; Kim, J.-Y.; Song, M. J.; Lee, S.; Zhang, Y. J.; Song, C. E. Organocatalytic enantioselective michael-addition of malonic acid half-thioesters to β-nitroolefins: From mimicry of polyketide synthases to scalable synthesis of γ-amino acids. *Adv. Synth. Catal.* **2011**, *353*, 3196–3202.

(192) Hill, A. M. The biosynthesis, molecular genetics and enzymology of the polyketide-derived metabolites. *Nat. Prod. Rep.* **2006**, *23*, 256–320.

(193) Staunton, J.; Weissman, K. J. Polyketide biosynthesis: a millennium review. *Nat. Prod. Rep.* **2001**, *18*, 380–416.

(194) Jez, J. M.; Austin, M. B.; Ferrer, J.-L.; Bowman, M. E.; Schröder, J.; Noel, J. P. Structural control of polyketide formation in plant-specific polyketide synthases. *Chem. Biol.* **2000**, *7*, 919–930.

(195) Pham, A.-T.; Matile, S. Peptide Stapling with Anion-π Catalysts. *Chem. Asian. J.* **2020**, *15*, 1562–1566.

(196) Duan, Y.; Xu, X.; Li, Y.; Peng, Q. Recent development of perylene diimide-based small molecular non-fullerene acceptors in organic solar cells. *Chin. Chem. Lett.* **2017**, *28*, 2105–2115.

(197) Kozma, E.; Catellani, M. Perylene diimides based materials for organic solar cells. *Dyes Pigm.* **2013**, *98*, 160–179.

(198) Liu, Z.; Wu, Y.; Zhang, Q.; Gao, X. Non-fullerene small molecule acceptors based on perylene diimides. *J. Mater. Chem. A* **2016**, *4*, 17604–17622.

(199) Nowak-Król, A.; Shoyama, K.; Stolte, M.; Würthner, F. Naphthalene and perylene diimides - better alternatives to fullerenes for organic electronics? *Chem. Commun.* **2018**, *54*, 13763–13772.

(200) Nowak-Król, A.; Würthner, F. Progress in the synthesis of perylene bisimide dyes. *Org. Chem. Front.* **2019**, *6*, 1272–1318.

(201) Würthner, F. Perylene bisimide dyes as versatile building blocks for functional supramolecular architectures. *Chem. Commun.* **2004**, 1564–1579.

(202) Würthner, F.; Saha-Möller, C. R.; Fimmel, B.; Ogi, S.; Leowanawat, P.; Schmidt, D. Perylene bisimide dye assemblies as archetype functional supramolecular materials. *Chem. Rev.* **2016**, *116*, 962–1052.

(203) Zhan, C.; D. Q. Li, A. Perylene diimide: versatile building blocks for molecular self-assemblies, folding motifs, and reaction-directing codes. *Curr. Org. Chem.* **2011**, *15*, 1314–1339.

(204) Yang, Y.; Mannion, M. R.; Dawe, L. N.; Kraml, C. M.; Pascal, R. A.; Bodwell, G. J. Synthesis, crystal structure, and resolution of [10](1,6)pyrenophane: an inherently chiral [n]cyclophane. *J. Org. Chem.* **2012**, *77*, 57–67.

(205) Nandaluru, P. R.; Dongare, P.; Kraml, C. M.; Pascal, R. A.; Dawe, L. N.; Thompson, D. W.; Bodwell, G. J. Concise, aromatization-based approach to an elaborate C2-symmetric pyrenophane. *Chem. Commun.* **2012**, *48*, 7747–7749.

(206) Menning, S.; Krämer, M.; Coombs, B. A.; Rominger, F.; Beeby, A.; Dreuw, A.; Bunz, U. H. F. Twisted tethered tolanes: unanticipated long-lived phosphorescence at 77 K. *J. Am. Chem. Soc.* **2013**, *135*, 2160–2163.

(207) Bedi, A.; Shimon, L. J. W.; Gidron, O. Helically locked tethered twistacenes. *J. Am. Chem. Soc.* **2018**, *140*, 8086–8090.

(208) Bedi, A.; Gidron, O. Chiroptical properties of twisted acenes: Experimental and computational study. *Chemistry* **2019**, *25*, 3279–3285.

(209) Würthner, F.; Osswald, P.; Schmidt, R.; Kaiser, T. E.; Mansikkamäki, H.; Könemann, M. Synthesis and optical and electrochemical properties of core-fluorinated perylene bisimides. *Org. Lett.* **2006**, *8*, 3765–3768.

(210) Wannere, C. S.; Schleyer, P. V. R. How do ring currents affect ^{1}H NMR chemical shifts? *Org. Lett.* **2003**, *5*, 605–608.

(211) Rule, G. S.; Hitchens, T. K. *Fundamentals of protein NMR spectroscopy*; Springer: Dordrecht, **2006**.

(212) Caballero, D.; Määttä, J.; Zhou, A. Q.; Sammalkorpi, M.; O'Hern, C. S.; Regan, L. Intrinsic α-helical and β-sheet conformational preferences: a computational case study of alanine. *Protein. Sci.* **2014**, *23*, 970–980.

(213) Haimov, B.; Srebnik, S. A closer look into the α-helix basin. *Sci. Rep.* **2016**, *6*, 38341.

(214) Milorey, B.; Schweitzer-Stenner, R.; Andrews, B.; Schwalbe, H.; Urbanc, B. Short peptides as predictors for the structure of polyarginine sequences in disordered proteins. *Biophys. J.* **2021**, *120*, 662–676.

(215) Würthner, F.; Saha-Möller, C. R.; Fimmel, B.; Ogi, S.; Leowanawat, P.; Schmidt, D. Perylene bisimide dye assemblies as archetype functional supramolecular materials. *Chem. Rev.* **2016**, *116*, 962–1052.

(216) Chen, Z.; Lohr, A.; Saha-Möller, C. R.; Würthner, F. Self-assembled pi-stacks of functional dyes in solution: structural and thermodynamic features. *Chem. Soc. Rev.* **2009**, *38*, 564–584.

(217) Würthner, F.; Chen, Z.; Hoeben, F. J. M.; Osswald, P.; You, C.-C.; Jonkheijm, P.; Herrikhuyzen, J. V.; Schenning, A. P. H. J.; van der Schoot, P. P. A. M.; Meijer, E. W.*;* Berkers, E. H. A.; Meskers, S. C. J.; Janssen, R. A. Supramolecular p-n-heterojunctions by co-self-

organization of oligo(p-phenylene vinylene) and perylene bisimide dyes. *J. Am. Chem. Soc.* **2004**, *126*, 10611–10618.

(218) Wang, W.; Wang, L.; Palmer, B. J.; Exarhos, G. J.; Li, A. D. Q. Cyclization and catenation directed by molecular self-assembly. *J. Am. Chem. Soc.* **2006**, *128*, 11150–11159.

(219) Wang, W.; Shaller, A. D.; Li, A. D. Q. Twisted perylene stereodimers reveal chiral molecular assembly codes. *J. Am. Chem. Soc.* **2008**, *130*, 8271–8279.

(220) Xie, Z.; Stepanenko, V.; Radacki, K.; Würthner, F. Chiral J-aggregates of atropo-enantiomeric perylene bisimides and their self-sorting behavior. *Chemistry* **2012**, *18*, 7060–7070.

 (221) Chuard, N.; Gasparini, G.; Roux, A.; Sakai, N.; Matile, S. Cell-penetrating poly(disulfide)s: the dependence of activity, depolymerization kinetics and intracellular localization on their length. *Org. Biomol. Chem.* **2015**, *13*, 64–67.

(222) Zhang, R. M.; Snyder, G. H. Dependence of formation of small disulfide loops in two-Cysteine peptides on the number and types of intervening amino acids. *J. Biol. Chem.* **1989**, *264*, 18472–18479.

(223) Lee, A. H. F.; Chen, J.; Liu, D.; Leung, T. Y. C.; Chan, A. S. C.; Li, T. Acid-promoted DNA-cleaving activities and total synthesis of Varacin C. *J. Am. Chem. Soc.* **2002**, *124*, 13972–13973.

(224) Macpherson, L. J.; Dubin, A. E.; Evans, M. J.; Marr, F.; Schultz, P. G.; Cravatt, B. F.; Patapoutian, A. Noxious compounds activate TRPA1 ion channels through covalent modification of Cysteines. *Nature* **2007**, *445*, 541–545.

(225) Woycechowsky, K. J.; Wittrup, K. D.; Raines, R. T. A small-molecule catalyst of protein folding in vitro and in vivo. *Chem. Biol.* **1999**, *6*, 871–879.

(226) Stoll, R. S.; Hecht, S. Artificial light-gated catalyst systems. *Angew. Chem. Int. Ed.* **2010**, *49*, 5054–5075.

(227) Dorel, R.; Feringa, B. L. Photoswitchable catalysis based on the isomerisation of double bonds. *Chem. Commun.* **2019**, *55*, 6477–6486.

(228) Brouwer, A. M.; Frochot, C.; Gatti, F. G.; Leigh, D. A.; Mottier, L.; Paolucci, F.; Roffia, S.; Wurpel, G. W. Photoinduction of fast, reversible translational motion in a hydrogen-bonded molecular shuttle. *Science* **2001**, *291*, 2124–2128.

(229) Bottari, G.; Leigh, D. A.; Pérez, E. M. Chiroptical switching in a bistable molecular shuttle. *J. Am. Chem. Soc.* **2003**, *125*, 13360–13361.

(230) Altieri, A.; Gatti, F. G.; Kay, E. R.; Leigh, D. A.; Martel, D.; Paolucci, F.; Slawin, A. M. Z.; Wong, J. K. Y. Electrochemically switchable hydrogen-bonded molecular shuttles. *J. Am. Chem. Soc.* **2003**, *125*, 8644–8654.

(231) Fioravanti, G.; Haraszkiewicz, N.; Kay, E. R.; Mendoza, S. M.; Bruno, C.; Marcaccio, M.; Wiering, P. G.; Paolucci, F.; Rudolf, P.; Brouwer, A. M.*;* Leigh, D. A. Three state redox-active molecular shuttle that switches in solution and on a surface. *J. Am. Chem. Soc.* **2008**, *130*, 2593–2601.

(232) Sasikumar, M.; Suseela, Y. V.; Govindaraju, T. Dibromohydantoin: a convenient brominating reagent for 1,4,5,8-naphthalenetetracarboxylic dianhydride. *Asian J. Org. Chem.* **2013**, *2*, 779–785.

(233) Lee, S.; Hua, Y.; Flood, A. H. β-Sheet-like hydrogen bonds interlock the helical turns of a photoswitchable foldamer to enhance the binding and release of chloride. *J. Org. Chem.* **2014**, *79*, 8383–8396.

(234) Tanaka, T.; Wagner, A. M.; Warner, J. B.; Wang, Y. J.; Petersson, E. J. Expressed protein ligation at methionine: N-terminal attachment of Homocysteine, ligation, and masking. *Angew. Chem. Int. Ed.* **2013**, *52*, 6210–6213.

(235) Y. Wang, D. Li, J. Lin, K. Wei, Organocatalytic asymmetric Michael addition of aldehydes and ketones to nitroalkenes catalyzed by adamantoyl L-prolinamide. *RSC Adv.* **2015**, *5*, 5863–5874.

(236) Yang, W.; Zhao, J.; Sonn, C.; Escudero, D.; Karatay, A.; Yaglioglu, H. G.; Küçüköz, B.; Hayvali, M.; Li, C.; Jacquemin, D. Efficient intersystem crossing in heavy-atom-free perylenebisimide derivatives. *J. Phys. Chem. C* **2016**, *120*, 10162–10175.

(237) Rajasingh, P.; Cohen, R.; Shirman, E.; Shimon, L. J. W.; Rybtchinski, B. Selective bromination of perylene diimides under mild conditions. *J. Org. Chem.* **2007**, *72*, 5973–5979.

(238) Du, Y.; Xia, L.; Jo, A.; Davis, R. M.; Bissel, P.; Ehrich, M. F.; Kingston, D. G. I. Synthesis and evaluation of Doxorubicin-loaded gold nanoparticles for tumor-targeted drug delivery. *Bioconjug. Chem.* **2018**, *29*, 420–430.

(239) Shimizu, H.; Watanabe, H.; Mizuno, M.; Kataoka, T.; Hori, M. Synthesis and properties of novel medium-sized heterocyclic compounds containing two sulfur atoms in the ring and synthetic approaches to conjugated cyclic disulfonium ylides. *Heterocycles* **2001**, *54*, 139–150.

(240) Hall, M.; Stueckler, C.; Hauer, B.; Stuermer, R.; Friedrich, T.; Breuer, M.; Kroutil, W.; Faber, K. Asymmetric bioreduction of activated C=C bonds using Zymomonas mobilis NCR Enoate Reductase and Old Yellow Enzymes OYE 1–3 from yeasts. *Eur. J. Org. Chem.* **2008**, *2008*, 1511–1516.

(241) Casas, F.; Trincado, M.; Rodriguez-Lugo, R.; Baneerje, D.; Grützmacher, H. A Diaminopropane diolefin Ru(0) complex catalyzes hydrogenation and dehydrogenation reactions. *ChemCatChem* **2019**, *11*, 5241–5251.

(242) Lukesh, J. C.; Palte, M. J.; Raines, R. T. A potent, versatile disulfide-reducing agent from aspartic acid. *J. Am. Chem. Soc.* **2012**, *134*, 4057–4059.

(243) Johnson, M. Novel prodrugs of dithiol mucolytic agents. PCT/US2016/029729, **2016**.

(244) Singh, P. K.; Field, L.; Sweetman, B. J. Organic disulfides and related substances. Cyclic di- and trisulfides based on 1,4-dithiols. *Phosphorus and Sulfur and the Related Elements* **1988**, *39*, 61–71.

(245) Jones, G. B.; Wright, J. M.; Plourde, G. W.; Hynd, G.; Huber, R. S.; Mathews, J. E. A Direct and stereocontrolled route to conjugated enediynes. *J. Am. Chem. Soc.* **2000**, *122*, 1937–1944.

(246) Houk, J.; Whitesides, G. M. Structure-reactivity relations for thiol-disulfide interchange. *J. Am. Chem. Soc.* **1987**, *109*, 6825–6836.

(247) Samuel, C. J. Deazetation of a bicyclic azo compound: resolution of a stereochemical ambiguity and conformational analysis of a biradical. *J. Chem. Soc. Perkin Trans 1* **1989**, 1259–1265.

(248) Wang, Y.; Hu, X.; Morales-Rivera, C. A.; Li, G.-X.; Huang, X.; He, G.; Liu, P.; Chen, G. Epimerization of tertiary carbon centers via reversible radical cleavage of unactivated C(sp^3)-H Bonds. *J. Am. Chem. Soc.* **2018**, *140*, 9678–9684.

(249) Fuchs, M.; Fürstner, A. trans-Hydrogenation: application to a concise and scalable synthesis of Brefeldin A. *Angew. Chem. Int. Ed.* **2015**, *54*, 3978–3982.

(250) Bouhadir, K. H.; Aleiwe, B. A.; Fares, F. A. Facile preparation of the tosylhydrazone derivatives of a series of racemic trans-3,4-substituted cyclopentanones. *Molecules* **2011**, *17*, 1–14.

(251) Nagasawa, S.; Sasano, Y.; Iwabuchi, Y. Synthesis of 1,3-cycloalkadienes from cycloalkenes: Unprecedented reactivity of oxoammonium salts. *Angew. Chem. Int. Ed.* **2016**, *55*, 13189–13194.

(252) Wang, H.; He, S.; Deng, W.; Zhang, Y.; Li, G.; Sun, J.; Zhao, W.; Guo, Y.; Yin, Z.; Li, D.*;* Shang, L. Comprehensive Insights into the catalytic mechanism of middle east respiratory

syndrome 3C-like protease and severe acute respiratory syndrome 3C-like protease. *ACS Catal.* **2020**, *10*, 5871–5890.

(253) Suhartono, M.; Schneider, A. E.; Durner, G.; Gobel, M. W. Synthetic aromatic amino acids from a negishi cross-coupling reaction. *Synthesis* **2010**, *2*, 293–303.

(254) Haag, T.; Hughes, R. A.; Ritter, G; Schmidt, R. R. Carbohydrate-Based VEGF Inhibitors. *Eur. J. Org. Chem.* **2007**, 36, 6016-6033.

(255) Ma, Y.; Wu, C. Revisiting the complexation between DNA and polyethylenimine - when and where -S-S- linked PEI is cleaved inside the cell. *J. Mater. Chem. B* **2014**, *2*, 3282–3291.

(256) Cacciatore, I.; Di Stefano, A.; Duprè, S.; Morera, E.; Pinnen, F.; Spirito, A. Synthesis and biological evaluation of the disulfide form of the glutathione analogue γ-(l-glutamyl)-l-cysteinyl-l-aspartyl-l-cysteine. *Bioorg. Chem.* **2003**, *31*, 109–121.

(257) Kishore, R.; Balaram, P. Stabilization of γ-turn conformations in peptides by disulfide bridging. *Biopolymers* **1985**, *24*, 2041–2043.

(258) Schmidt, B.; Lindman, S.; Tong, W.; Lindeberg, G.; Godoll, A.; Lai, Z.; Thornwall, M.; Synnergren, B.; Nilsson, A.; Welch, C. J.*;* Sohtell, M.; Westerlund, C.; Nyberg, F.; Karlén, A.; Hallberg, A. Design, synthesis, and biological activities of four Angiotensin ii receptor ligands with γ-turn mimetics replacing amino acid residues 3-5. *J. Med. Chem.* **1997**, *40*, 903–919.

(259) Zambaldo, C.; Vinogradova, E. V.; Qi, X.; Iaconelli, J.; Suciu, R. M.; Koh, M.; Senkane, K.; Chadwick, S. R.; Sanchez, B. B.; Chen, J. S.*;* Chatterjee, A. K.; Liu, P.; Schultz, P. G.; Cravatt, B. F.; Bollong, M. J. 2-Sulfonylpyridines as tunable, cysteine-reactive electrophiles. *J. Am. Chem. Soc.* **2020**, *142*, 8972–8979.

(260) Azizian, H.; Esmailnejad, A.; Fathi Vavsari, V.; Mahernia, S.; Amanlou, M.; Balalaie, S. Pantoprazole derivatives: Synthesis, urease inhibition assay and in silico molecular modeling studies. *ChemistrySelect* **2020**, *5*, 4580–4587.

(261) Kalia, D.; Pawar, S. P.; Thopate, J. S. Stable and rapid thiol bioconjugation by light-triggered thiomaleimide ring hydrolysis. *Angew. Chem. Int. Ed.* **2017**, *56*, 1885–1889.

(262) Söderström, M.; Zamaratski, E.; Odell, L. R. BF 3 ·SMe 2 for Thiomethylation, Nitro reduction and tandem reduction/SMe insertion of nitrogen heterocycles. *Eur. J. Org. Chem.* **2019**, *2019*, 5402–5408.

(263) Demeter, O.; Kormos, A.; Koehler, C.; Mező, G.; Németh, K.; Kozma, E.; Takács, L. B.; Lemke, E. A.; Kele, P. Bisazide cyanine dyes as fluorogenic probes for bis-cyclooctynylated peptide tags and as fluorogenic cross-linkers of cyclooctynylated proteins. *Bioconjug. Chem.* **2017**, *28*, 1552–1559.

(264) Agnihotri, G.; Crall, B. M.; Lewis, T. C.; Day, T. P.; Balakrishna, R.; Warshakoon, H. J.; Malladi, S. S.; David, S. A. Structure-activity relationships in toll-like receptor 2-agonists leading to simplified monoacyl lipopeptides. *J. Med. Chem.* **2011**, *54*, 8148–8160.

(265) Harrison, R. Sulphonamide compounds that modulate chemokine receptor acwity (CCR4). PCT/SE2004/000850.

(266) Macke, J. D.; Field, L. Sulfinic acids and related compounds. Synthesis and properties of some α, ω-alkylenebis(dithioalkane-sulfinates). *Phosphorous and Sulfur and the Related Elements* **1988**, *37*, 27–33.

(267) Nagle, A. A.; Reddy, S. A.; Bertrand, H.; Tajima, H.; Dang, T.-M.; Wong, S.-C.; Hayes, J. D.; Wells, G.; Chew, E.-H. 3-(2-oxoethylidene)indolin-2-one derivatives activate Nrf2 and inhibit NF-κB: potential candidates for chemoprevention. *ChemMedChem* **2014**, *9*, 1763–1774.

(268) C. Kolomyjec/J. Whelan/B. Bosnich. Biological analogs. Synthesis of vicinal trimercapto ligands. *Inorg. Chem.* **1983**, *22*, 2343–2345.

(269) Moaven, S.; Watson, B. T.; Thompson, S. B.; Lyons, V. J.; Unruh, D. K.; Casadonte, D. J.; Pappas, D.; Cozzolino, A. F. Self-assembly of reversed bilayer vesicles through pnictogen

bonding: water-stable supramolecular nanocontainers for organic solvents. *Chem. Sci.* **2020**, *11*, 4374–4380.

(270) Moaven, S.; Yu, J.; Yasin, J.; Unruh, D. K.; Cozzolino, A. F. Precise Steric Control over 2D versus 3D Self-Assembly of Antimony(III) alkoxide cages through strong secondary bonding interactions. *Inorg. Chem.* **2017**, *56*, 8372–8380.

(271) Calandra, N. A.; Cheng, Y. L.; Kocak, K. A.; Miller, J. S. Total synthesis of Spiruchostatin A via chemoselective macrocyclization using an accessible enantiomerically pure latent thioester. *Org. Lett.* **2009**, *11*, 1971–1974.

(272) Wende, C.; Kulak, N. Fluorophore ATCUN complexes: combining agent and probe for oxidative DNA cleavage. *Chem. Commun.* **2015**, *51*, 12395–12398.